UNIVERSITÉ DE TOURS

ÉCOLE DOCTORALE : SSBCV

Physiologie de la Reproduction et des Comportements
INRAE, Université de Tours, UMR85, 37380 Nouzilly
Équipe Interactions Cellulaires et Fertilité

THÈSE présentée par :

Coline MAHÉ

soutenue le : **23 Mars 2023**

pour obtenir le grade de : **Docteur de l'université de Tours**
Discipline/ Spécialité : Sciences de la vie/biologie de la reproduction

Migration spermatique dans les voies génitales femelles : interactions fonctionnelles chez le bovin

THÈSE dirigée par :
Mme SAINT-DIZIER Marie Professeure des Universités, Université de Tours

RAPPORTEURS :
M ARNOULT Christophe Directeur de Recherches, CNRS, Université Grenoble Alpes
Mme LABBÉ Catherine Directrice de Recherches, INRAE Rennes

JURY : *(directeurs, rapporteurs, examinateurs)*
Mme SAINT-DIZIER Marie Professeure des Universités, Université de Tours
M ARNOULT Christophe Directeur de Recherches, CNRS, Université Grenoble Alpes
Mme LABBÉ Catherine Directrice de Recherches, INRAE Rennes
M MOREAU Thierry Professeur des Universités, Université de Tours
M SAEZ Fabrice Maître de conférences, HDR, Université Clermont Auvergne
M GUYONNET Benoît Chargé d'ingénierie, Union Evolution, Noyal-sur-Vilaine

INVITES :
M MERMILLOD Pascal Ingénieur de recherche, HDR, INRAE Nouzilly

Remerciements

Cette thèse a été réalisée sous la direction de Marie Saint-Dizier au sein de l'équipe Interactions Cellulaires et Fertilité (ICF) de l'unité Physiologie de la Reproduction et des Comportements (PRC) à l'INRAE de Nouzilly et grâce au soutien financier de l'INRAE et de la région centre Val de Loire.

Arrivée au bout de ces trois années et demie de thèse passées à vitesse grand V, je pense à tous ceux qui m'ont accompagné, supporté et aidé. Tout ce travail n'aurait jamais été possible sans vous.

Je voudrais tout d'abord remercier les membres du jury d'avoir accepté d'évaluer ce travail, Christophe Arnoult et Catherine Labbé en tant que rapporteurs, Fabrice Saez, Benoît Guyonnet, et Thierry Moreau en tant qu'examinateurs et Pascal Mermillod en tant qu'invité.

Un travail de thèse n'est rien sans sa directrice et je voudrais dire un grand merci au professeure Marie Saint-Dizier. Merci pour ta confiance et tes conseils tout au long de ces trois années. Je me souviendrais de tes corrections (souvent toutes de rouges vêtues) et je retiendrais grâce à toi que l'oviducte, c'est vachement bien.

Merci également aux membres de mon comité de thèse, Christophe Arnoult et Sophie Rehault-Godbert, d'avoir donné de leur temps et de précieux conseils pour mener à bien ce projet.

Merci à Monsieur Mermillod, le grand sage de l'équipe, qui mange à midi pile et arrive toujours à débloquer des situations à l'aide de ses conseils avisés.

Un énorme merci à Guillaume Tsikis, sans qui je n'aurai jamais appris les bases et réussi à faire de superbes western blots. Merci d'être toujours disponible, pour ton aide très précieuse sans laquelle ces beaux résultats n'auraient pas pu voir le jour.

Un (très) grand merci à Karine Reynaud, ma grande dame. Merci pour ta perpétuelle joie de vivre et pour le tri des beaux rêves. Ton écoute et ta capacité à imprimer des chansons (pas très recommandables) dans ma tête resteront gravés dans ma mémoire.

Merci à Barbara Schmaltz alias Babou. Tu nous as quitté en cours de route, mais je n'oublierai jamais ta constante envie de m'aider et ton légendaire « c'est dégueulasse » du vendredi matin !

Merci à Ludivine Laffont alias Lulu. Malgré ton arrivée en cours de route, j'ai le sentiment que tu as toujours été là. Merci infiniment d'avoir été mon double pendant ces derniers mois.

Un énorme merci à Benoît Marteau, Thierry Delpuech et surtout à Albert Arnould alias la flèche bleue pour ces nombreux allers-retours aux abattoirs. Vous êtes la base de tout ce travail et sans vous cette thèse n'aurait simplement pas eu lieu.

Merci à Jennifer Schoen et Aleksandra Maria Zlotkowska, nos acolytes allemande et polonaise. Jennifer, merci pour ses réunions très enrichissantes, qui ont grandement contribué à tout ce travail et bien sûr à ta bonne humeur perpétuelle !

Cette thèse n'aurait jamais été possible sans les plateformes d'analyse. Merci à Paulo Marcelo de la plateforme ICAP à Amiens pour les analyses protéomiques des fluides utérins. Merci à Charles Pineau, Emmanuelle Com et Régis Lavigne de la plateforme PROTIM à Rennes pour les analyses protéomiques des fluides d'oviductes et des protéines d'interaction. Je remercie également la plateforme PIC et plus particulièrement Marie-Claire Blache et Maryse Meurisse pour la formation et l'utilisation du microscope confocal. Merci à Thierry Meylheuc de la plateforme MIMA2 de l'INRAE de Jouy en Josas pour les magnifiques images réalisées en microscopie électronique à balayage. Enfin, je remercie Valérie Labas, Ana Paula Teixeira et Daniel Tomas de la plateforme PIXANIM pour la formation et l'utilisation des logiciels de traitement de données protéomiques.

Je tiens à remercier tous les membres du service technique, du magasin et du secrétariat, Barbara Corbière, Pascal Tondereau, Jean-Noël Couet, Chantal Flon, Patrick Trezy, Sophie Mary, Ghislaine Ploux, pour votre travail qui m'ont rendu la vie tellement plus facile ! Un spécial merci à Gaël Ramé, toujours en première ligne quand on a besoin de lui ! Merci aussi à Anne Mychak et Sophie Picard qui ont été présentes et m'ont suivie pendant ma mésaventure de la perte partielle d'un doigt.

Merci à tous les membres de l'équipe Interactions Cellulaires et Fertilité, ma famille d'accueil pendant cette thèse : Marie Saint-Dizier, Pascal Mermillod, Xavier Druart, Nadine Gérard, Guillaume Tsikis, Karine Reynaud, Ludivine Laffont, Isabelle Grasseau, Yann Locatelli, Florence Guignot, Anaïs Carvalho, Veronique Demattei, Hsiu-Lien Lin, Théo Prudhomme et Lorraine Schmaltz.

Je remercie également toutes les personnes de l'équipe BINGO et en particulier Sébastien Elis, sans qui le séjour à Bologne aurait été beaucoup moins fun et Peggy Jarrier Gaillard, pour son écoute et son côté maternel.

Merci à Valérie et Ana Paula de m'avoir accueillie dans leur cercle pixanimien et pour ces pauses café matinales et post-prandiales toujours emplies de rires !

Un grand merci à tous les stagiaires et compatriotes thésards. Merci à Lolo, ma petite cochonne préférée. Merci à Thanya pour son aide précieuse lors des ateliers dissection du vendredi. Merci à Charlotte et son expertise en termes de cliquage et d'introduction. Merci aussi à Maoui, LE meilleur stagiaire de tous les temps. Merci aussi à Mr Bourdon et son légendaire caramel au beurre salé et Ophélie Bernardi, ma première camarade de bureau.

Un spécial merci à l'illustre et vieux docteur Banliat, deuxième thésard préféré de Marie après moi et son soutien dogmatique.

A mes co-thésardes du début, Ophélie et Claire, un énorme merci ! Le trio infernal est finalement venu à bout de ces thèses !!! Merci de m'avoir supportée et d'avoir été là tout simplement.

A mes co-thésardes de fin. Flo alias bactos, la psychologue sous Wilson et ses tentatives infructueuses de contamination par des bactéries existantes et inconnues. Merci à l'autre Marie de ma vie, alias ma deuxième boule et une femme incroyable. Si je devais résumer ma thèse aujourd'hui, c'est d'abord une rencontre, la nôtre, puis des crashs à répétition, des « Et bah c'est bien ! », devenue une expression somme toute classique et en conclusion je dirai que ça fait extrêmement réfléchir.

Merci à Dani, la personne la plus gentille du multivers et de la galaxie. Ces trois années et demie avec toi ont été pauvres en millions d'euros mais riches en gentillesse, en desserts et surtout, en tarte au citron meringuée.

Merci à Mimi, mon petit flamant rose, ma handballeuse de l'extrême. Merci d'avoir veillé sur moi, dans les bons comme dans les mauvais moments (comme une certaine soirée aux urgences), et merci pour tes petits mots qui ont magnifiquement décoré mon bureau et mes écrans.

À mes copines de prépa, Paupau, Aurélie et Aline, merci infiniment pour ces escapades annuelles aux quatre coins de Paris et de la Loire. Le quatuor mythique des faidherbardes ne cessera d'exister !

À mes copines de lycée, Alex et Camilia, mes deux infirmières personnelles, un énorme merci ! Après plus de 10 ans d'amitié, vous remplissez toujours ma vie d'amour et d'étrons !

À mes copines d'école, Lisa et Marine, merci car vous êtes les lumières qui m'ont apporté la connaissance. Merci à ma copine Lisa, ma mouche tse tse, mon âme sœur, je t'aime tout simplement. Si on revenait 5 ans en avance, jamais je n'aurais cru trouver mon flocon des neiges. Finalement, on n'aura pas arrêté la thèse et ça c'est une bénédiction. Merci à Maine, une personne de quaeulité grâce à qui j'ai pu garder espoir tout au long de ma thèse. Malgré la distance, la cordonnerie a toujours su être présente (comme par hasard) de par ses fêtes au terter, son approvisionnement en biscuit rose, champagne et diverses gâteries en tout genre.

Enfin, un énorme merci à ma famille. Merci à mes parents, ma bichette et mon père, sans qui je ne serais jamais arrivée là où je suis. Je ne les remercierai jamais assez pour leur présence, patience et soutien inconditionnel durant toutes ces années. Merci à mes grands-parents, mamée et papou, d'avoir toujours été là pour moi mais aussi pour ces moments hebdomadaires au téléphone booster de moral. Merci aussi à Marjorie alias sale laide, tu pourras m'appeler docteur nounouille désormais ! Enfin, merci à Maéna, Alex et Tom, sur qui je pourrai toujours compter.

Table des matières

Résumé **7**

Abstract **9**

Liste des publications et communications **11**

Liste des tableaux **14**

Liste des figures **15**

Liste des annexes **16**

Liste des abréviations **17**

Contexte général **18**

Étude bibliographique **20**

1. Sécrétions des voies génitales femelles : média des interactions mâle-femelle en période péri-conceptionnelle **20**

1.1. Anatomie fonctionnelle de l'utérus et de l'oviducte 20
1.1.1. Anatomie et histologie de l'utérus et de l'oviducte de vache 20
1.1.2. Variations physiologiques de l'utérus et de l'oviducte de vache au cours du cycle estrien 23
1.1.3. Mécanismes de sécrétion luminale des cellules épithéliales utérines et oviductales 26

1.2. Régulation des protéomes luminaux de l'utérus et l'oviducte 29
1.2.1. Abondance et fonctions prédites des protéines luminales de l'utérus et l'oviducte 29
1.2.2. Facteurs de régulation des protéomes luminaux de l'utérus et de l'oviducte 33

2. Migration et acquisition de la capacité fécondante des spermatozoïdes dans les voies génitales femelles **40**

2.1. Migration des spermatozoïdes jusqu'au site de fécondation 40
2.1.1. Migration à travers le cervix et l'utérus 41
2.1.2. Migration à travers la jonction-utéro tubaire et l'oviducte..... 43

2.2. Capacitation des spermatozoïdes et facteurs de régulation mâles et femelles..... 46
2.2.1. Mécanismes de la capacitation 46
2.2.2. Modulation de la capacitation par les protéines du plasma séminal et les facteurs femelles 47

3. Interactions entre les spermatozoïdes et l'oviducte : ticket pour une fécondation réussie **52**

3.1. Interactions spermatozoïdes-oviducte et facteurs de régulation 52

3.2. Modèles d'étude des interactions spermatozoïdes-oviducte 68

Questions de recherche et démarche scientifique **72**

Étude expérimentale **76**

1. Dynamique des protéomes luminaux traversés par les spermatozoïdes pendant la période péri-conceptionnelle chez le bovin **76**

1.1. Protéome luminal de l'utérus et variations en fonction du stade péri-ovulatoire et du côté de l'ovulation 76

1.2. Protéome luminal de l'oviducte et variations en fonction de la région anatomique, du stade péri-ovulatoire et du côté de l'ovulation 91

2. Protéome d'interaction des spermatozoïdes pendant leur migration dans l'oviducte en période péri-conceptionnelle chez le bovin **109**

3. Effets des interactions avec le fluide d'oviducte sur la liaison des spermatozoïdes au réservoir **137**

Discussion et perspectives **180**

1. Les spermatozoïdes traversent un environnement protéique changeant au cours de leur migration jusqu'au site de fécondation **181**

1.1. De l'utérus à l'oviducte : les protéines luminales varient en fonction du stade péri-ovulatoire et de la proximité de l'ovaire ovulant 181

1.2. De l'isthme à l'ampoule : les protéines interagissant avec les spermatozoïdes varient en fonction de la région anatomique et du stade péri-ovulatoire 185

2. L'interaction des spermatozoïdes avec le fluide d'oviducte modifie leur physiologie et leur capacité à se lier au réservoir spermatique **188**

2.1. L'isthme et l'ampoule modulent différemment la physiologie des spermatozoïdes mais ces différences sont discrètes 188

2.2. Les sécrétions de l'oviducte ont un effet majeur sur la liaison des spermatozoïdes au réservoir 189

3. Perspectives **195**

3.1. Raffiner le modèle de réservoir *in vitro* 195

3.2. Comprendre les mécanismes d'interaction avec les protéines luminales du tractus femelle 195

3.3. Mieux comprendre les mécanismes d'inhibition de la liaison aux cellules par le fluide d'oviducte 196

Conclusion générale **198**

Bibliographie **199**

Annexes **216**

Résumé

Chez le bovin, la réussite de l'insémination artificielle est conditionnée par la migration des spermatozoïdes dans les voies génitales femelles jusqu'au site de la fécondation. Au cours de cette migration, les spermatozoïdes interagissent avec les fluides issus des cellules épithéliales luminales et peuvent se lier à ces cellules, notamment dans la première partie de l'oviducte, pour former un « réservoir spermatique ». Ce réservoir est impliqué dans la survie des spz avant l'ovulation et leur sélection pour la fécondation. Cependant, la composition moléculaire des milieux successivement traversés par les spermatozoïdes pendant la période péri-conceptionnelle et le rôle de ces interactions pour la fécondation ont été peu étudiés. De plus, les modèles *in vitro* utilisés pour étudier le réservoir sont éloignés de l'environnement *in vivo* ou techniquement difficiles à reproduire. Notre hypothèse est que les spermatozoïdes interagissent de manière dynamique avec les protéines luminales des voies génitales femelles, ces interactions modulant à la fois leur liaison au réservoir et l'acquisition de leur fécondance. Nos objectifs sont donc de déterminer (1) la composition protéique des milieux femelles traversés par les spermatozoïdes ; (2) les protéines interagissant avec les spermatozoïdes dans l'oviducte ; (3) les effets de ces interactions sur la physiologie et la liaison des spermatozoïdes aux cellules épithéliales de l'oviducte à l'aide d'un nouveau modèle de réservoir spermatique.

Le premier chapitre est consacré à la caractérisation par spectrométrie de masse des protéomes luminaux de l'utérus et l'oviducte bovin et leurs variations en fonction du stade péri-ovulatoire, de la proximité de l'ovaire ovulant et de la région anatomique. Dans les cornes utérines, plus de 1200 protéines ont été identifiées, dont l'albumine, des protéines du complément et la myosine 9 parmi les plus abondantes. Une trentaine de ces protéines seulement varient en abondance entre stades et en fonction de la proximité de l'ovaire ovulant. Dans l'oviducte, plus de 3500 protéines ont été identifiées, dont l'oviductine, des protéines de chocs thermiques et la myosine 9 parmi les plus abondantes. La région (ampoule et isthme), s'est avérée être le facteur ayant le plus d'impact sur l'abondance des protéines, suivi de la proximité de l'ovaire ovulant et du stade.

Le second chapitre se focalise sur l'identification des protéines luminales de l'oviducte interagissant avec les spermatozoïdes et de leur variation en fonction de la région et du stade péri-ovulatoire. Par une approche quantitative en spectrométrie de masse, 245 protéines d'interaction ont été identifiées, dont des myosines et l'oviductine parmi les plus abondantes. Au total, 31% de ces protéines diffèrent entre région et stade du cycle, révélant des interactions très dynamiques au cours de la migration spermatique. Les effets des fluides sur la viabilité, la mobilité et la fécondance des spermatozoïdes étaient également modulé par la région et le stade. De plus, l'abondance de ces protéines sur les spermatozoïdes n'est pas corrélée à leur abondance initiale dans les fluides, suggérant des mécanismes spécifiques d'interaction variant suivant l'état physiologique des spermatozoïdes et la composition du fluide traversé.

Enfin, le troisième chapitre présente un nouveau modèle in vitro de réservoir spermatique à partir de sphéroïdes de cellules épithéliales d'isthme et les effets du fluide d'oviducte sur la liaison des spermatozoïdes aux sphéroïdes. Le modèle de sphéroïdes est facilement manipulable, reproductible et présente des interactions entre spz et cellules épithéliales ciliées à l'image de celles décrites in vivo dans l'oviducte. En utilisant ce modèle, nous avons montré que le fluide tubaire inhibe la liaison des spermatozoïdes aux cellules épithéliales sans modifier leur mobilité ni leur viabilité. Les mécanismes impliqués dans cet effet seraient médiés par des N-glycanes portées par les glycoprotéines du fluide et certains glycosaminoglycanes comme le sulfate d'héparane.

Ces résultats ouvrent le pas vers l'amélioration des milieux utilisés pour conserver, sélectionner et utiliser les spermatozoïdes en insémination animale, pour la fécondation *in vitro* et la conservation de la biodiversité animale.

Abstract

In cattle, successful artificial insemination depends on the migration of spermatozoa through the female genital tract to the site of fertilization. During this migration, the spermatozoa interact with fluids from the luminal epithelial cells and can bind to these cells, especially in the first part of the oviduct, to form a "sperm reservoir". This reservoir is involved in sperm survival before ovulation and their selection for fertilization. However, the molecular composition of the environments successively crossed by spermatozoa during the periconceptional period and the role of these interactions for fertilization have been little studied. Moreover, the *in vitro* models used to study the reservoir are not like the *in vivo* environment or technically difficult to reproduce. Our hypothesis is that spermatozoa interact dynamically with luminal proteins in the female tract, these interactions modulating both their binding to the reservoir and their acquisition of fertilizing ability. Our objectives are therefore to determine (1) the protein composition of the female environments crossed by spermatozoa; (2) the proteins interacting with spermatozoa in the oviduct; and (3) the effects of these interactions on sperm physiology and binding to oviduct epithelial cells using a novel model of sperm reservoir.

The first chapter is devoted to the characterization by mass spectrometry of the luminal proteomes of the bovine uterus and oviduct and their variations according to the periovulatory stage, the proximity of the ovulating ovary and the anatomical region (ampulla and isthmus). In the uterine horns, more than 1200 proteins have been identified, with albumin, complement proteins and myosin 9 among the most abundant. Only about thirty of these proteins vary in abundance between stages and according to the proximity of the ovulating ovary. In the oviduct, more than 3500 proteins have been identified, with oviductin, heat shock proteins and myosin 9 among the most abundant. The region was found to be the factor with the greatest impact on protein abundance, followed by the proximity to the ovulating ovary and stage of cycle.

The second chapter focuses on the identification of oviduct luminal proteins interacting with spermatozoa and their variation according to region and periovulatory stage. Using a quantitative mass spectrometry approach, 245 interacting proteins were identified, with myosins and oviductin among the most abundant. Overall, 31% of these proteins differed between region and stage of the cycle, revealing highly dynamic interactions during sperm migration. The effects of fluids on sperm viability, motility and fertility were also modulated by the region and stage. Moreover, the abundance of these proteins on spermatozoa is not correlated with their initial abundance in fluids, suggesting specific mechanisms of interaction varying according to the physiological state of the spermatozoa and the composition of the fluid.

Finally, the third chapter presents a new *in vitro* model of sperm reservoir from isthmus epithelial cell spheroids and the effects of oviduct fluid on sperm binding to spheroids. The spheroid model is easily manipulated, reproducible, and exhibits interactions between spermatozoa and cilia of epithelial cells that mimic those described *in vivo* in the oviduct. Using this model, we have shown that the tubal fluid inhibits sperm binding to epithelial cells without modifying their mobility or viability. The mechanisms involved in this effect may be mediated by N-glycans carried by the fluid glycoproteins and some glycosaminoglycans like heparan sulfate.

These results open the way to the improvement of media used to conserve, select and use spz in animal insemination, *in vitro* fertilization and animal biodiversity conservation.

Liste des publications et communications

Publications dans des revues internationales à comité de lecture

➔ **Articles de recherche**

Mahé C, Lavigne R, Com E, Pineau C, Locatelli Y, Zlotkowska AM, Almiñana C, Tsikis G, Mermillod P, Schoen J and Saint-Dizier M (2022) Spatiotemporal profiling of the bovine oviduct fluid proteome around the time of ovulation. *Scientific Reports* **12** 4135. https://doi.org/10.1038/s41598-022-07929-3.

Mahé C, Marcelo P, Tsikis G, Tomas D, Labas V and Saint-Dizier M (2023) The bovine uterine fluid proteome is more impacted by the stage of the estrous cycle than the proximity of the ovulating ovary in the periconception period. *Theriogenology* **198** 332–343. https://doi.org/10.1016/j.theriogenology.2023.01.006.

Mahé C, Lavigne R, Com E, Pineau C, Zlotkowska AM, Guillaume T, Mermillod P, Schoen J and Saint-Dizier M (2023) The sperm-interacting proteome in the bovine isthmus and ampulla during the periovulatory period. *Journal of Animal Science and Biotechnology* **14** 30. https://doi.org/10.1186/s40104-022-00811-2.

Mahé C, Pranomphon T, Reynaud K, Laffont L, Meylheuc T, Schoen J, Mermillod P, and Saint-Dizier M (2023) Sperm-fluid-cell interplays in the bovine oviduct: glycoprotein N-glycans and glycosaminoglycans modulate sperm binding to the reservoir (en preparation).

➔ **Chapitres d'ouvrage**

Mahé C, Laffont L, Pranomphon T, Schmaltz L, Reynaud K, Mermillod P, and Saint-Dizier M (2023) Assessment of sperm binding capacity in the oviduct reservoir using an *in vitro* model of epithelial spheroids in cattle. *Methods in Molecular Biology, Spermatology: Methods and Protocols* (soumis sur invitation en janvier 2023 ; annexe 1).

➔ **Articles de synthèse**

Saint-Dizier M, Mahé C, Reynaud K, Tsikis G, Mermillod P, Druart X (2020) Sperm interactions with the female reproductive tract: a key for successful fertilization in mammals. *Molecular and Cellular Endocrinology* **516** 110956. https://doi.org/10.1016/j.mce.2020.110956 (annexe 2).

Mahé C, Zlotkowska AM, Reynaud K, Tsikis G, Mermillod P, Druart X, Schoen J and Saint-Dizier M (2021) Sperm migration, selection, survival, and fertilizing ability in the mammalian oviduct. *Biology of Reproduction* **105** 317–331. https://doi.org/10.1093/biolre/ioab105.

Communications dans des congrès internationaux

Mahé C, Lavigne R, Com E, Pineau C, Zlotkowska AM, Tsikis G, Mermillod P, Schoen J, Saint-Dizier M (2022) Spatiotemporal regulation of sperm-interacting proteins in the bovine oviduct fluid. *International Congress on Animal Reproduction (ICAR), Bologne, Italie, 26-30 Juin 2022*, poster (annexe 3).

Mahé C, Karine Reynaud, Ludivine Laffont, Pascal Mermillod, Marie Saint-Dizier. (2022) Role of secreted proteins and heparan sulfate on sperm binding to oviduct epithelial cells in cattle. *Association of Embryo Technology in Europe (AETE), Utrecht, Pays-Bas, 15-16 Sept 2022*, communication orale et poster (annexe 4).

Publications lors de collaboration au cours de la thèse

Mahé C, Gatien J, Desnoes O, Le Bourhis D, Mermillod P, Salvetti P and Saint-Dizier M (2021) Metabolomic analysis of oviduct fluid on day 3 post-estrus in Holstein heifers. *Reproductive Biology* **21** 100512 . https://doi.org/10.1016/j.repbio.2021.100512 (annexe 5).

Banliat C*, Mahé C*, Lavigne R, Com E, Pineau C, Labas V, Guyonnet B, Mermillod P and Saint-Dizier M (2022a) Dynamic changes in the proteome of early bovine embryos developed in vivo. *Frontiers in Cell and Developmental Biology* **10** 863700. https://doi.org/10.3389/fcell.2022.863700.*co-premiers auteurs (annexe 6).

Banliat C*, Mahé C*, Lavigne R, Com E, Pineau C, Labas V, Guyonnet B, Mermillod P and Saint-Dizier M (2022b) The proteomic analysis of bovine embryos developed in vivo or in vitro reveals the contribution of the maternal environment to early embryo. *BMC Genomics* **23** 839. https://doi.org/10.1186/s12864-022-09076-5. *co-premiers auteurs (annexe 7).

Communications lors de collaboration au cours de la thèse

Banliat C, Mahé C, Lavigne R, Com E, Pineau C, Labas V, Guyonnet B, Mermillod P and Saint-Dizier M (2022) What does the mother bring to the early embryo? Proteomic comparison of bovine embryos produced in vivo or in vitro. *International Congress on Animal Reproduction (ICAR), Bologne, Italie, 26-30 Juin 2022*, poster.

Banliat C, Mahé C, Lavigne R, Com E, Pineau C, Labas V, Guyonnet B, Mermillod P and Saint-Dizier M (2022) What does the mother bring to the early embryo? Proteomic comparison of bovine embryos produced in vivo or in vitro. *Association of Embryo Technology in Europe (AETE), Utrecht, Pays-Bas, 15-16 Sept 2022*, poster.

Liste des tableaux

Tableau 1 : Protéines majoritaires, voies de sécrétion et fonctions prédites des protéomes des fluides utérins et oviductaux chez les mammifères d'intérêt agronomique. 32

Tableau 2 : Facteurs de régulation de l'expression génique et protéomique dans les cellules épithéliales utérines et oviductales de mammifères. 38

Tableau 3 : Facteurs de régulation des protéines luminales solubles et intra-vésiculaires dans l'utérus et l'oviducte. 39

Liste des figures

Figure 1 : Anatomie de l'utérus et de l'oviducte bovin. 22

Figure 2 : Morphologie de l'ovaire bovin au cours du cycle estrien et pendant la période péri-conceptionnelle. 24

Figure 3 : Voies de sécrétion des cellules épithéliales utérines et oviductales. 28

Figure 4 : Proportion et morphologie des spermatozoïdes dans les voies génitales femelles. 42

Figure 5 : Mécanisme de la capacitation du spermatozoïde bovin. 49

Figure 6 : Avantages et inconvénients des modèles de culture cellulaire utilisés in vitro pour étudier les interactions entre les spermatozoïdes et l'oviducte. 70

Figure 7 : Description de la démarche scientifique. 75

Figure 8 : Schéma récapitulatif de l'étude du protéome luminal de l'utérus en fonction du stade péri-ovulatoire et de la proximité de l'ovaire ovulant. 78

Figure 9 : Schéma récapitulatif de l'étude du protéome luminal de l'oviducte en fonction de la région, du stade péri-ovulatoire et de la proximité de l'ovaire ovulant. 93

Figure 10 : Schéma récapitulatif de l'étude des protéines interagissant avec les spermatozoïdes dans l'oviducte en période péri-conceptionnelle. 112

Figure 11 : Effets des fluides d'isthme et d'ampoule péri-ovulatoires sur la mobilité des spermatozoïdes. 135

Figure 12 : Effets des fluides d'isthme et d'ampoule péri-ovulatoires sur la viabilité, la fluidité membranaire et la réaction acrosomique des spermatozoïdes. 136

Figure 13 : Schéma récapitulatif de l'étude de l'effet du fluide d'oviducte et de ses composants sur la liaison des spermatozoïdes au réservoir modélisé in vitro par des sphéroïdes de cellules épithéliales d'isthme. 141

Figure 14 : Effets de l'annexine A1, de l'albumine, de la progestérone et effet libérateur du fluide d'oviducte sur la liaison des spermatozoïdes aux sphéroïdes. 179

Figure 15 : Illustration des résultats et hypothèses sur les interactions fonctionnelles entre les spermatozoïdes et l'environnement maternel en période péri-conceptionnelle. 194

Liste des annexes

Annexe 1 : chapitre d'ouvrage : « Assessment of sperm binding capacity in the oviduct reservoir using an in vitro model of epithelial spheroids in cattle » 216

Annexe 2 : revue : « Sperm interactions with the female reproductive tract: a key for successful fertilization in mammals »..... 235

Annexe 3 : communication (poster) : « Spatiotemporal regulation of sperm-interacting proteins in the bovine oviduct fluid », International Congress on Animal Reproduction (ICAR), 2022 250

Annexe 4 : communication (orale et poster) : « Role of secreted proteins and heparan sulfate on sperm binding to oviduct epithelial cells in cattle », Association of Embryo Technology in Europe (AETE), 2022 252

Annexe 5 : article de recherche (collaboration au cours de la thèse) : « Metabolomic analysis of oviduct fluid on day 3 post-estrus in Holstein heifers » 254

Annexe 6 : article de recherche (collaboration au cours de la thèse) : « Dynamic changes in the proteome of early bovine embryos developed *in vivo* »..... 259

Annexe 7 : article de recherche (collaboration au cours de la thèse) : « The proteomic analysis of bovine embryos developed in vivo or in vitro reveals the contribution of the maternal environment to early embryo» 276

Liste des abréviations

BSP	Binder of sperm protein
CASA	Computer assisted sperm analysis
CEO	Cellules épithéliales d'oviducte
CEU	Cellules épithéliales d'utérus
FIV	Fécondation *in vitro*
FO	Fluide oviductal
FU	Fluide utérin
GAG	Glycosaminoglycanes
GDE	Gènes différentiellement exprimés
HDL	Lipoprotéines à haute densité
HSP	Protéine de choc thermique ou heat shock protein
IA	Insémination artificielle
JUT	Jonction utéro-tubaire
NanoLC-MS/MS	Nanochromatographie liquide couplé à la spectrométrie de masse en tandem
oEV	Vésicules extracellulaires issues des sécrétions oviductales
OVGP1	Oviductine
PDA/E	Protéines différentiellement abondantes/exprimées
Péri-ov	Phase péri-ovulatoire
Post-ov	Stade post-ovulatoire
Pre-ov	Stade pré-ovulatoire
Spz	Spermatozoïdes
uEV	Vésicules extracellulaires issues des sécrétions utérines

Contexte général

L'insémination artificielle (IA) en élevage bovin est aujourd'hui communément utilisée et permet depuis plus de 60 ans un progrès génétique des troupeaux tout en évitant la diffusion de maladies sexuellement transmissibles. Cette technique s'est développée grâce à la cryoconservation, et plus récemment du tri sexé de la semence. En élevage bovin laitier, 80% des femelles sont inséminées, contre 33% en élevage allaitant (données 2021 de l'institut de l'élevage Idele). Néanmoins, chez certaines races, la durée moyenne entre deux vêlages s'allonge depuis plusieurs années, en partie due à un déclin des performances de reproduction. Chez la Prim'Holstein, le taux de réussite en première insémination (taux de non-retour en chaleur 90 jours après insémination) n'est que de 45%, contre 60% chez les génisses (bilan des inséminations animales 2020, Idele). Ces freins à la réussite de l'IA découlent en partie de la période fertile courte de la vache, de 12 à 24 h tous les 21 jours, et de la difficulté à détecter cette période (les chaleurs) par l'éleveur. De plus, la durée de survie limitée des spermatozoïdes (spz) dans les voies génitales femelles impose d'inséminer entre 4 à 16 h après le début des chaleurs pour une fertilité optimale (Diskin, 2018). Les mécanismes de migration et de survie des spermatozoïdes dans les voies génitales femelles, notamment dans l'oviducte, sont très mal connus, lié à l'inaccessibilité des oviductes du vivant de l'animal. Mieux connaitre ces mécanismes permettrait d'imaginer des façons innovantes d'allonger la durée de survie des spz, de faciliter leur migration jusqu'au site de la fécondation, ceci afin de faciliter les pratiques d'IA et d'en améliorer les résultats.

La production d'embryons via la fécondation *in vitro* (FIV) est de plus en plus utilisée en élevage bovin pour valoriser le potentiel génétique de certaines femelles (Ferré *et al.*, 2020). Les embryons sont produits à partir d'ovocytes collectés par ponction folliculaire échoguidée (ou ovum pick-up) sur des femelles de haute valeur génétique puis maturés *in vitro* et inséminés avec de la semence cryoconservée. Cependant, les résultats sont hétérogènes et la proportion d'embryons atteignant le stade blastocyste ne s'élève en moyenne qu'à 20 à 40% (Rizos *et al.*, 2008). De plus, les embryons produits *in vitro* sont de qualité inférieure en termes de morphologie, composition lipidique, expression génique et capacité à résister à la congélation par rapport à leurs homologues conçus *in vivo* (Rizos *et al.*, 2002; Gad *et al.*, 2012).

Les taux de gestation mais aussi de vêlage après transfert d'embryons produits *in vitro* sont en moyenne 10 à 40% plus faibles qu'avec des embryons conçus *in vivo* (Ealy *et al.*, 2019). Ces différences sont en partie dues à la qualité inférieure des ovocytes (Sirard and Blondin, 1996; Caetano *et al.*, 2022), mais aussi de la faible sélection des spermatozoïdes utilisés en FIV. En effet, *in vitro*, en moyenne 50% des spermatozoïdes sont sélectionnés après centrifugation sur Percoll ou swim-up avant incubation avec les ovocytes, tandis qu'*in vivo*, il est estimé que moins de 1% des spermatozoïdes entre dans l'oviducte, où a lieu la fécondation (Heyman and Levasseur, 1981; Parrish *et al.*, 1995). Néanmoins, très peu d'études se sont intéressées à ces étapes de sélection *in vivo*.

Explorer les processus de migration et de stockage des spermatozoïdes par les voies génitales femelles est donc un enjeu majeur de connaissances en biologie de la reproduction. C'est aussi un enjeu important pour optimiser les performances de reproduction et d'amélioration génétique des élevages bovins.

Étude bibliographique

Comprendre le processus de migration des spermatozoïdes dans voies génitales femelles signifie d'abord comprendre la nature du microenvironnement dans lequel progressent ces spermatozoïdes jusqu'au site de la fécondation. Les lumières utérine et oviductale sont décrites dans la première partie de cette étude bibliographique. Ces environnements femelles vont coordonner l'acquisition progressive de la capacité fécondante des spermatozoïdes (ou capacitation), aboutissant à une sous-population de spermatozoïdes aptes à féconder dans la deuxième partie de l'oviducte, l'ampoule. Les mécanismes de cette capacitation et de la migration spermatique sont résumés dans la deuxième partie de cette synthèse bibliographique. Enfin, dans une troisième et dernière partie, les interactions cellulaires et moléculaires entre l'environnement femelle (majoritairement l'oviducte) et les spermatozoïdes, ainsi que leurs effets sur la physiologie spermatique, sont présentés.

1. Sécrétions des voies génitales femelles : média des interactions mâle-femelle en période péri-conceptionnelle

Après saillie ou insémination, les spermatozoïdes traversent l'utérus puis l'oviducte, lui-même divisé en deux régions, l'isthme puis l'ampoule. La physiologie de ces deux organes des voies génitales femelles changent en fonction de l'environnement endocrinien au cours du cycle estrien, en particulier en période péri-ovulatoire. La première partie de cette étude bibliographique est consacrée à l'exploration anatomique, histologique et moléculaire de la lumière de ces voies génitales femelles.

1.1. Anatomie fonctionnelle de l'utérus et de l'oviducte

1.1.1. Anatomie et histologie de l'utérus et de l'oviducte de vache

La lumière de l'utérus est le premier environnement femelle traversé par les spermatozoïdes. L'utérus est constitué d'un corps très court (3-4 cm) qui se subdivise en deux cornes de 35 - 45 cm de long (Barone, 2001) (Figure 1A page 22).

Le diamètre externe des cornes utérines est de 3 - 4 cm en partie caudale pour se réduire à seulement 5 - 6 mm au niveau de la jonction utéro-tubaire (JUT) (Barone, 2001).

L'oviducte a un diamètre externe beaucoup plus réduit, de 3 à 8 mm en moyenne : il est le siège de la capacitation (acquisition du pouvoir fécondant des gamètes mâles ; cf partie 2.2), de la fécondation et des premiers stades du développement embryonnaire. De l'ovaire à la JUT, l'oviducte est constitué d'un infundibulum, qui capte l'ovocyte à l'ovulation puis est divisé en deux régions anatomiques : l'ampoule, lieu de la fécondation, puis l'isthme, lieu de stockage et de capacitation des spermatozoïdes puis du développement embryonnaire précoce (Avilés *et al.*, 2010; Coy *et al.*, 2012) (Figure 1A page 22). Ces deux régions ont des origines embryonnaires distinctes (Ford *et al.*, 2021). La vache étant une espèce mono-ovulante, la corne utérine et l'oviducte du côté de l'ovulation sont qualifiées d'ipsilatérales et ceux opposé à l'ovulation, de controlatérales.

Les tissus utérin et oviductal sont constitués de l'extérieur vers l'intérieur d'une couche séreuse (respectivement périmétrium et mésosalpinx), d'une musculaire (myomètre et myosalpinx) et d'une muqueuse (respectivement endomètre et endosalpinx) (Figure 1B et 1C page 22). Dans l'espèce bovine, l'endomètre est parsemée d'une centaine de caroncules, où s'établissent les interactions placentaires lors de la gestation (Kumro *et al.*, 2020; Nabors, 2021). L'endosalpinx lui est caractérisé par de nombreux replis muqueux, de plus en plus complexes de l'isthme vers l'ampoule (Yániz *et al.*, 2000). Les muqueuses utérine et oviductale sont tapissées d'un épithélium pseudo-stratifié composé de cellules ciliées et non ciliées, appelées cellules sécrétrices (Barone, 2001; Ito *et al.*, 2016).

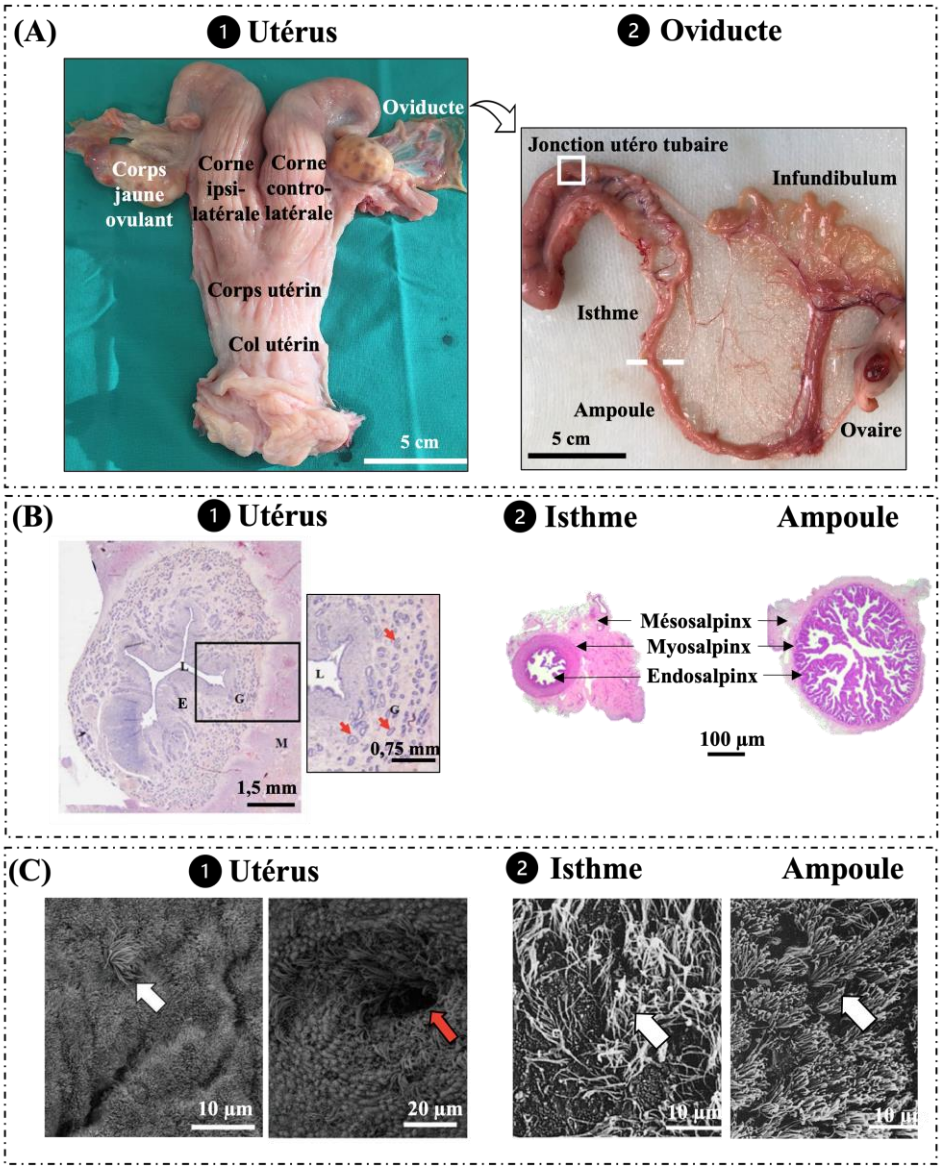

Figure 1 : Anatomie de l'utérus et de l'oviducte bovin.

(A) 1. L'utérus bovin se décompose en un col, un corps, et deux cornes utérines.

2. L'oviducte comprend un isthme, une ampoule et un infundibulum recouvrant l'ovaire (ici avec un corps jaune récent) (Photo : K. Reynaud).

(B) 1. Coupe transversale de corne utérine (M = le myomètre ; E = l'endomètre ; G = l'endomètre glandulaire ; L = la lumière) (Kumro *et al.*, 2020).

2. Coupe transversale des deux régions de l'oviducte (Cerny *et al.*, 2015).

(C) 1. Images en microscopie électronique à balayage de la surface de l'épithélium bovin utérin composé de cellules non ciliées et ciliées (flèche blanche) parsemé d'invaginations appelées glandes (flèche rouge) (Kumro *et al.*, 2020).

2. Images en microscopie électronique à balayage de la surface de l'épithélium d'oviducte bovin composé de cellules non ciliées et ciliées (flèche blanche) (Abe and Oikawa, 1993).

1.1.2. Variations physiologiques de l'utérus et de l'oviducte de vache au cours du cycle estrien

Description du cycle estrien et concentration en stéroïdes ovariens

Le cycle estrien de la vache dure en moyenne 21 jours et se décompose en trois phases (Figure 2 page 24) (Ireland *et al.*, 1980) : 1/ la phase folliculaire, aussi appelée pré-ovulatoire, au cours de laquelle a lieu l'estrus (ou chaleurs). L'ovaire présente un *corpus albicans* et un follicule pré-ovulatoire entre 11 et 20 mm de diamètre. La concentration en progestérone dans le plasma circulant est indétectable tandis que celle en estradiol est élevée (autour de 5-10 pg/mL) (Kanchev *et al.*, 1976); 2/ la phase post-ovulatoire, qui est le début de la phase lutéale et définie dans ce manuscrit comme les 4-5 premiers jours suivant l'ovulation : l'ovaire présente un corps jaune hémorragique ou de couleur rouge et de diamètre inférieur à 1 cm ; 3/ le reste de la phase lutéale, entre 5 à 18 jours après l'ovulation avec un ovaire présentant un corps jaune (de couleur orange-brune à jaune) d'environ 2 cm de diamètre. Pendant la phase lutéale, la concentration plasmatique en progestérone augmente pour atteindre un plateau (autour de 6 à 10 ng/mL) tandis que celle en estradiol est indétectable (Glencross *et al.*, 1973). La période péri-conceptionnelle débute au moment de l'estrus, soit 2 - 3 jours avant l'ovulation, et s'achève au moment de l'entrée de l'embryon dans l'utérus (4 - 5 jours après l'ovulation), soit une période de 6 à 8 jours au cours du cycle estrien de la vache.

La progestérone et l'estradiol sont aussi présents dans les sécrétions de l'appareil reproducteur autour du moment de l'ovulation, mais leurs concentrations dans les sécrétions utérines n'ont pas été encore rapportées. Néanmoins, la progestérone a été mesurée dans l'endomètre bovin de la corne ipsilatérale à l'ovulation, où sa concentration était deux à quatre fois plus élevée 2 à 5 jours post-ovulation comparés aux autres jours du cycle estrien (Kowalik *et al.*, 2019). Dans le fluide d'oviducte, les concentrations de ces deux hormones ont été évaluées chez le bovin (Lamy *et al.*, 2016a), le porcin (Ballester *et al.*, 2014) et l'équin (Nelis *et al.*, 2016) avec des variations au cours du cycle et notamment pendant la période péri-ovulatoire. Dans l'oviducte bovin ipsilatérale à l'ovulation, la concentration en progestérone augmente de la phase pré-ovulatoire (6 ng/mL) à la phase post-ovulatoire (57 ng/mL) pour atteindre un maximum en milieu de phase lutéale (120 ng/mL) (Lamy *et al.*, 2016a). L'œstradiol a quant à lui une concentration plus élevée en période pré-ovulatoire (291 pg/mL) comparé aux autres périodes du cycle (< 120 pg/mL) dans les deux oviductes de vache (Lamy *et al.*, 2016a).

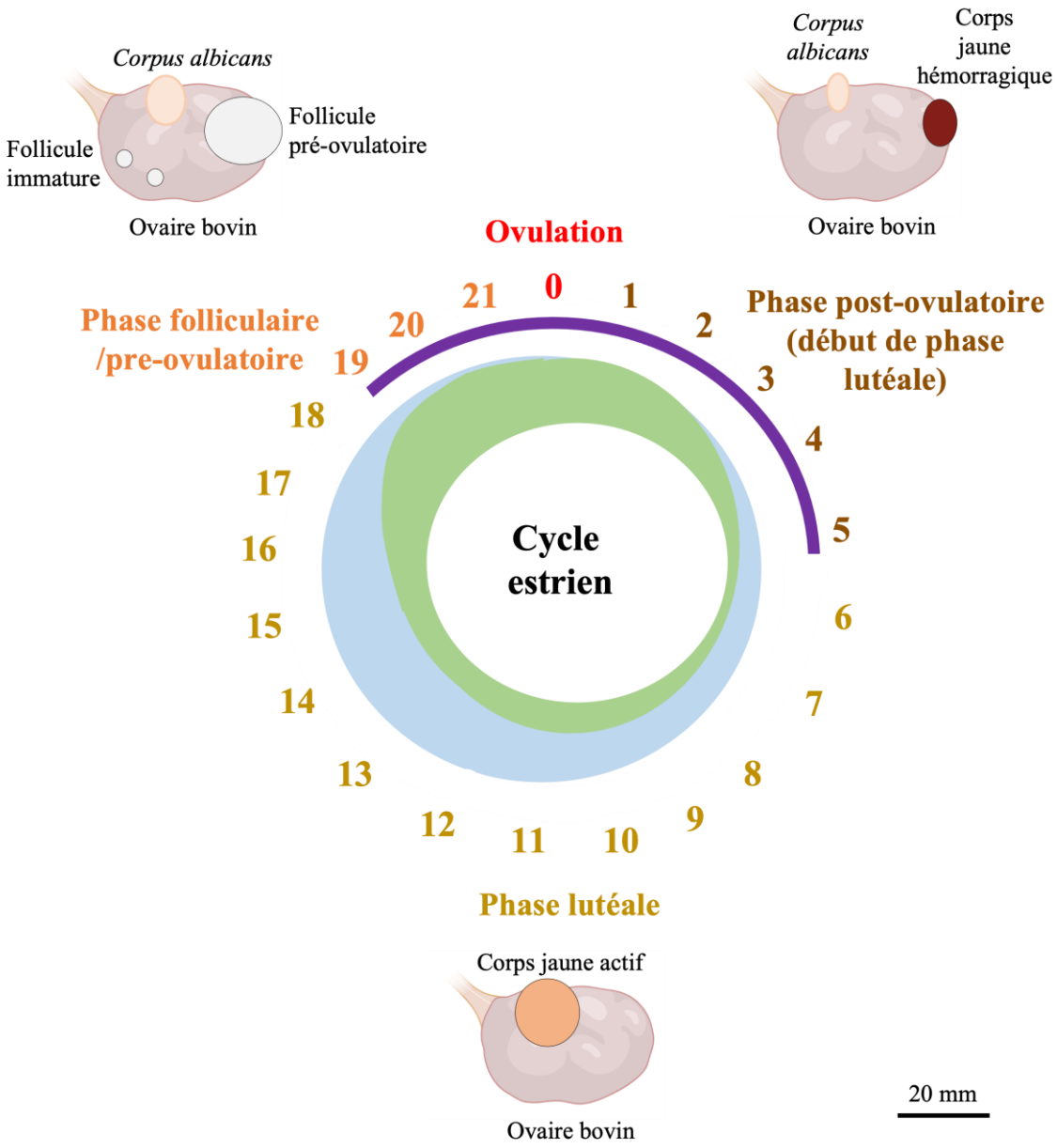

Figure 2 : Morphologie de l'ovaire bovin au cours du cycle estrien et pendant la période péri-conceptionnelle.

Le cycle estrien de la vache dure en moyenne 21 jours et se décompose en phase : 1/ folliculaire ou pré-ovulatoire avec un ovaire présentant un *corpus albicans* et un follicule de 11 à 20 mm de diamètre. La concentration en progestérone (en bleu) dans le plasma circulant est indétectable tandis que celle en estradiol (en vert) est élevée ; 2/ post-ovulatoire ou début de la phase lutéale, de 0 à 5 jours après l'ovulation avec un ovaire présentant un corps jaune hémorragique ; 3/ le reste de la phase lutéale, de 5 à 18 après l'ovulation avec un ovaire présentant un corps jaune actif. La concentration en progestérone augmente pour atteindre un plateau tandis que celle en estradiol est indétectable. La période péri-conceptionnelle dure 6-8 jours (en violet) (Ireland *et al.*, 1980).

Régulation de la morphologie de l'utérus et de l'oviducte au cours du cycle

Au cours du cycle estrien, l'utérus et l'oviducte subissent des changements morphologiques et fonctionnels. Dans l'utérus, l'amplitude et la durée des contractions du myomètre augmentent juste avant l'ovulation et diminuent après, induisant un tonus utérin et une pression intra-luminale maximaux en période péri-ovulatoire (Rodriguez-Martinez *et al.*, 1987). De plus, chez le bovin, les pourcentages de cellules épithéliales en prolifération et apoptotiques augmentent pendant la phase péri-ovulatoire comparé à la phase lutéale (Arai *et al.*, 2013). Enfin, de l'estrus vers le milieu de la phase lutéale chez la vache, la proportion de cellules ciliées augmente dans l'épithélium caronculaire et diminue dans l'épithélium inter-caronculaire (Kumro *et al.*, 2020).

Dans l'oviducte, au niveau du myosalpinx, la fréquence et l'amplitude des contractions sont minimales pendant la phase lutéale, augmentent 3 à 5 jours avant l'estrus puis diminuent 3 à 5 jours après l'estrus (Bennett *et al.*, 1988). De plus, une plus forte activité musculaire a été observée dans l'oviducte ipsilatérale à l'ovulation par rapport au côté opposé (Bennett *et al.*, 1988). L'épithélium de l'oviducte est également soumis à un remodelage au cours du cycle estrien, qui est particulièrement visible dans l'ampoule (Abe and Oikawa, 1993; Sostaric *et al.*, 2008; Ito *et al.*, 2016). Dans cette région en phase péri-ovulatoire, la hauteur épithéliale, la proportion de cellule ciliées et l'activité sécrétoire augmentent tandis qu'en phase lutéale, l'épithélium subit une réduction de la hauteur cellulaire et une déciliation marquée (Abe and Oikawa, 1993; Sostaric *et al.*, 2008; Ito *et al.*, 2020). En revanche, peu ou aucun changement n'a été observé dans l'isthme au cours du cycle et en fonction de la proximité de l'ovaire ovulant (Abe and Oikawa, 1993; Ito *et al.*, 2016; Gonella-Diaza *et al.*, 2017).

1.1.3. Mécanismes de sécrétion luminale des cellules épithéliales utérines et oviductales

Mécanisme de sécrétion

Les fluides dans les lumières de l'utérus et de l'oviducte proviennent de sécrétions *de novo* des cellules de l'épithélium mais aussi d'ultrafiltrat du plasma circulant et de potentiels apports dans l'oviducte du follicule pré-ovulatoire au moment de l'ovulation (Leese *et al.*, 2001; Saint-Dizier *et al.*, 2020). Chez la vache, le volume du fluide utérin peut atteindre 400 µL (Velazquez *et al.*, 2010) mais se restreint dans l'oviducte à maximum 10 µL dans l'isthme et 50 µL dans l'ampoule (données du laboratoire). Ces fluides contiennent des mélanges complexes de macromolécules comme les protéines, glycoprotéines, protéoglycanes et glycosaminoglycanes (GAG), mais aussi des ions, hormones stéroïdiennes, lipides et petits métabolites (Saint-Dizier *et al.*, 2020).

Les protéines sont des composants majeurs des fluides utérins (FU) et oviductaux (FO) et peuvent être sécrétées dans la lumière de manière conventionnelle ou par des voies de sécrétion non classiques (Rabouille, 2017) (Figure 3 page 28). Les protéines possédant un peptide signal côté N-terminal sont classiquement sécrétées via des granules de sécrétion passant par le réticulum endoplasmique et l'appareil de Golgi. En revanche, certaines protéines sont sécrétées en contournant cette machinerie classique via trois principales voies dites « non-conventionnelles » : (1) la translocation directe du réticulum endoplasmique à la membrane plasmique sans passer par le Golgi via des transporteurs membranaires, (2) la fusion d'organelles cytoplasmiques comme les phagosomes ou lysosomes avec la membrane plasmique, et (3) les vésicules extracellulaires (EV).

Les protéines des fluides utérins et oviductaux, mais aussi des petits ARN et de l'ADN, peuvent en effet être encapsulées dans des exosomes (40 - 100 nm) et des microvésicules (100-1000 nm), appartenant à la famille des EV (Martin-DeLeon, 2016; Almiñana *et al.*, 2017; van Niel *et al.*, 2018; Hamdi *et al.*, 2021). Les exosomes se forment par bourgeonnement interne d'endosomes ou corps multivésiculaires, fusionnant ensuite avec la membrane plasmique pour les libérer dans le milieu extracellulaire, alors que les microvésicules sont formées par le bourgeonnement direct de la membrane plasmique (Martin-DeLeon, 2016; van Niel *et al.*, 2018).

Durant le processus de mort cellulaire, la cellule peut également relarguer des composants dans des corps apoptotiques (500 nm – 2 µm) (Battistelli and Falcieri, 2020). Ces vésicules ont été décrites dans les sécrétions utérines (uEV) et oviductales (oEV) chez plusieurs mammifères dont la vache (Franchi *et al.*, 2019; Hamdi *et al.*, 2021), la jument (Almiñana *et al.*, 2021; Lange-Consiglio *et al.*, 2022) et la femme (Bathala *et al.*, 2018; Rai *et al.*, 2021). Chez la vache, la concentration en EV dans les fluides a été évaluée par NTA (*nanoparticle tracker analysis*) à 60 milliards par mL pour les uEV et 2 milliards par mL pour les oEV (Almiñana *et al.*, 2018; Hamdi *et al.*, 2021).

Prédiction des voies de sécrétion des protéines dans les fluides utérin et oviductal

Dans quelques rares études, les voies de sécrétion des protéines identifiées dans le fluide utérin ou oviductal ont été prédites par des outils bio-informatiques. La proportion de protéines présentant un peptide signal (voie conventionnelle) est généralement déterminée via le logiciel en ligne SignalP et celle sécrétées par des voies non conventionnelles via Outcyte.

L'analyse bio-informatique des protéines identifiées dans le fluide utérin de vache gestante a révélé qu'en moyenne 62% des protéines étaient d'origine cytoplasmique et 9 % d'origine membranaire (Aranciaga *et al.*, 2021). Cette importante proportion de protéines intracellulaires pourrait être dû à la méthode de collecte du fluide par flushing, récupérant les cellules desquamées dans la lumière, mais aussi à la sécrétion par des voies non conventionnelles précédemment évoquées. Le renouvellement constant de l'épithélium des voies génitales peut entraîner un relargage de protéines intracellulaires dans la lumière (Arai *et al.*, 2013). Dans le fluide utérin de vache gestante, une étude a estimé la proportion de protéines sécrétées de manière classique via un peptide signal à seulement 14% (Aranciaga *et al.*, 2021). Parmi les voies non conventionnelles, les uEV ont été identifiées comme cargos pour la sécrétion protéique dans le fluide utérin chez la vache et la jument (Kusama *et al.*, 2018; Almiñana *et al.*, 2021).

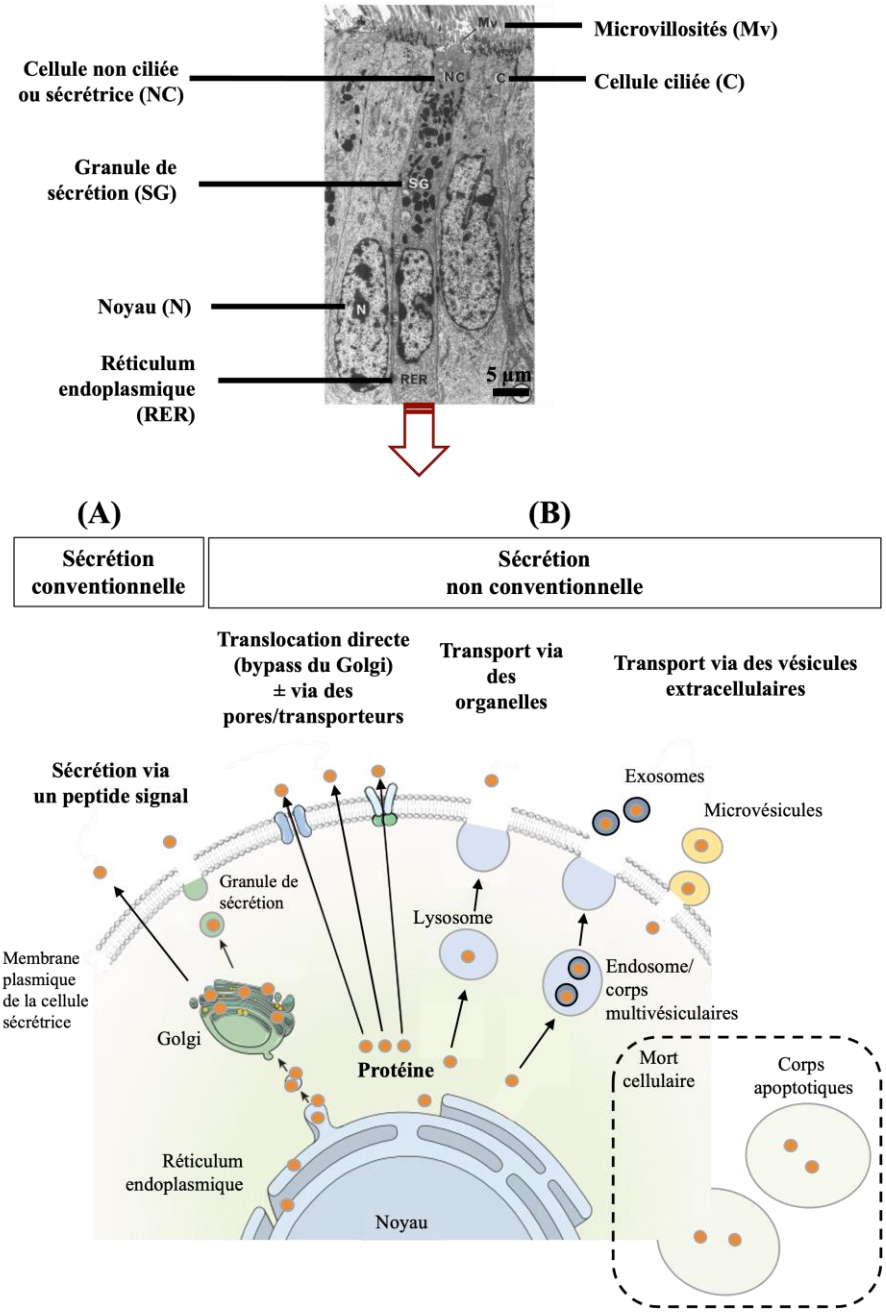

Figure 3 : Voies de sécrétion des cellules épithéliales utérines et oviductales.

Les cellules sécrétrices de l'épithélium (ici en microscopie électronique à balayage) tapissant les voies génitales femelles sécrètent les protéines des fluides via plusieurs voies de sécrétion : (**A**) voies de sécrétion classique via le réticulum endoplasmique et l'appareil de Golgi (via un peptide signal) (**B**) voies de sécrétion non conventionnelles : (i) translocation directe du réticulum à la membrane plasmique sans passer par le Golgi via des pores ou des transporteurs membranaire ; (ii) fusion d'organelles cytoplasmiques ; (iii) les vésicules extracellulaires (exosomes, microvésicules). Lorsque la cellule entre en apoptose, elle peut aussi libérer des corps apoptotiques (Eriksen *et al.*, 1994; Rabouille, 2017; van Niel *et al.*, 2018; Battistelli and Falcieri, 2020).

Concernant les voies de sécrétion du protéome oviductal, une première étude évalue à 14 % la proportion de protéines du fluide possédant un peptide signal, sécrétées de manière conventionnelle via la machinerie du réticulum endoplasmique/Golgi (Gegenfurtner *et al.*, 2019). Par ailleurs, les protéomes des oEV ont été récemment analysés par spectrométrie de masse chez la truie (Laezer *et al.*, 2020), la chatte (Ferraz *et al.*, 2019) et la vache (Almiñana *et al.*, 2017). Dans l'espèce bovine, des protéines abondamment présentes dans le FO, comme l'oviductine (OVGP1), une glycoprotéine spécifique de l'oviducte, les annexines A1 et A2 et la protéine de choc thermique (HSP) A8, sont également retrouvées parmi les plus abondantes dans les oEV (Almiñana *et al.*, 2018). Concernant les rôles possibles de ces protéines, une analyse *in silico* a montré que 20% des protéines identifiées dans les oEV sont impliquées dans des processus métaboliques et cellulaires, dont 58% dans la communication cellule-cellule (Almiñana *et al.*, 2017). En particulier, 21 protéines identifiées, dont des protéines chaperonnes et l'oviductine, avaient des rôles prédits dans l'interaction spermatozoïdes-zone pellucide (Almiñana *et al.*, 2018).

1.2. Régulation des protéomes luminaux de l'utérus et l'oviducte

1.2.1. Abondance et fonctions prédites des protéines luminales de l'utérus et l'oviducte

Les protéines sont des composants majeurs des fluides dans les voies génitales femelles. Dans le fluide utérin, les concentrations protéiques rapportées dans la littérature varient entre 71 et 93 mg/mL chez la vache (Alavi-Shoushtari *et al.*, 2006), entre 14 et 59 mg/mL chez la jument (Tunón *et al.*, 1998) et entre 37 et 53 mg/mL chez la brebis (Iritani *et al.*, 1974). Dans l'oviducte, leur concentration moyenne atteint 50 à 70 mg/mL chez la vache (données du laboratoire), varie entre 25 et 40 mg/mL chez la jument (Engle *et al.*, 1984) et entre 12 et 16 mg/mL chez la brebis (Restall and Wales, 1966) (Tableau 1 page 32). Les protéines issues de ces fluides sont formées de chaînes polypeptidiques qui peuvent porter des chaînes sucrées sur leur asparagine, appelées N-glycanes et/ou sur leur sérine/thréonine, appelées O-glycanes (Eichler, 2019).

La glycosylation est la modification post-traductionnelle la plus fréquente des protéines et la majorité des protéines sécrétées sont probablement des glycoprotéines (Eichler, 2019). Néanmoins, la proportion de protéines glycosylées dans les fluides utérin et oviductal, y compris celles issues de voies de sécrétion non conventionnelles, n'a pas été évaluée.

Avec l'émergence de la spectrométrie de masse à haute résolution, la nature des protéines présentes dans les fluides de l'appareil reproducteur commence à être mieux connue. La nano-chromatographie liquide couplé à de la spectrométrie de masse en tandem (NanoLC-MS/MS) est la technique la plus utilisée pour étudier ces molécules. La particularité de cette technique est la profondeur d'analyse car elle permet, après digestion enzymatique et séparation par chromatographie, d'analyser tous les peptides obtenus. Comparé à l'immunohistochimie ou au western-blot, cette approche permet d'identifier et de quantifier de manière exhaustive et non ciblée les protéines.

Protéome luminale de l'utérus

Les protéines du fluide utérin ont été analysées par LC-MS/MS au cours du cycle chez la jument (Khan *et al.*, 2020) et la brebis (Soleilhavoup *et al.*, 2016), et pendant la gestation chez la truie (He *et al.*, 2022) et la vache (Gegenfurtner *et al.*, 2020; Aranciaga *et al.*, 2021) (Tableau 1 page 32). Dans ces études, les protéines ont été majoritairement extraites de flushs prélevés en post-mortem (Soleilhavoup *et al.*, 2016; Gegenfurtner *et al.*, 2020; Khan *et al.*, 2020; He *et al.*, 2022). Chez le bovin, jusqu'à 1737 protéines ont été identifiée dans le FU. L'albumine, la lactoferrine, des protéines du complément, mais aussi les protéines de choc thermique HSPAA1, AB1, A8 ont été identifiées parmi les protéines les plus abondantes du FU bovin dans toutes les études (Forde *et al.*, 2014; Gegenfurtner *et al.*, 2020; Aranciaga *et al.*, 2021).

Les fonctions des protéines identifiées ont été prédites via des outils bioinformatiques comme PANTHER (Protein analysis through evolutionary relationships) ou via la base de données DAVID (Database for Annotation, Visualization and Integrated Discovery). L'analyse fonctionnelle du protéome utérin a mis en évidence des rôles dans des processus métaboliques (glucide, énergétique, acide aminé), immunitaires et dans la réponse à un stress/stimulus (Faulkner *et al.*, 2013; Forde *et al.*, 2014; Gegenfurtner *et al.*, 2020; Aranciaga *et al.*, 2021).

Les protéines du fluide utérin seraient particulièrement impliquées dans la réponse immunitaire aux cellules étrangères que sont les spermatozoïdes. Chez le bovin, la co-incubation d'explants d'épithélium utérin avec des spermatozoïdes enclenche l'expression génique et protéique de cytokines pro-inflammatoires et de protéines du complément (Elweza *et al.*, 2018; Akthar *et al.*, 2020). L'addition de ces protéines dans le milieu sécrété par les cellules épithéliales utérines augmente la proportion de spermatozoïdes phagocytés par les cellules immunitaires (Elweza *et al.*, 2018).

Protéome luminal de l'oviducte

Le protéome du fluide d'oviducte a été étudié par LC-MS/MS pendant la période péri-ovulatoire chez la jument (Fernández-Hernández *et al.*, 2021) et au cours du cycle chez la brebis (Soleilhavoup *et al.*, 2016) et la vache (Lamy *et al.*, 2016b) (Tableau 1 page 32). Les protéines quantifiées parmi les plus abondantes dans le FO incluent les myosines 9, 14, l'OVGP1, les annexines A1, A2 ou encore les protéines de choc thermique HSPA5 et A8 (Lamy *et al.*, 2016b; Papp *et al.*, 2019). Comme pour l'utérus, les fluides sont très majoritairement prélevés par des flushs post-mortem sur des oviductes collectés en abattoir, donc après la saignée. Une étude récente chez le bovin rapporte une analyse protéomique du FO après flush *in vivo* effectué par guidage endoscopique : dans ce cas, les sous-unités alpha et béta de l'hémoglobine sont parmi les protéines les plus abondantes (Papp *et al.*, 2019) .

Après analyse bio-informatique, les protéines du FO ont majoritairement des propriétés de liaison et sont impliquées dans des processus métaboliques, catalytiques et cellulaires (Pillai *et al.*, 2017; Papp *et al.*, 2019). Par ailleurs, 7% d'entre elles sont impliquées dans des fonctions de reproduction. Parmi elles, l'oviductine, une glycoprotéine spécifique de l'oviducte, agit positivement sur la viabilité, la motilité des spermatozoïdes de buffle (Choudhary *et al.*, 2017) et d'humain (Zhao *et al.*, 2016) mais aussi dans le contrôle de la polyspermie *in vitro* chez les porcins et bovins (Coy *et al.*, 2008). Chez le bovin, d'autres protéines comme HSPA8 ont également des effets positifs sur la viabilité des spermatozoïdes et diminue la polyspermie *in vitro* (Elliott *et al.*, 2009).

Tableau 1 : Protéines majoritaires, voies de sécrétion et fonctions prédites des protéomes des fluides utérins et oviductaux chez les mammifères d'intérêt agronomique.

FO = Fluide oviductal ; FU = Fluide utérin

	Fluide étudié	Espèce	Résultat	Référence
Concentration protéique dans les fluides	FU	Bovin	71 - 93 mg/mL	Alavi-Shoushtari *et al.*, 2006
		Équin	14 - 59 mg/mL	Tunón *et al.*, 1998
		Ovins	37 – 53 mg/mL	Iritani *et al.*, 1974
	FO	Bovin	50 - 70 mg/mL	Données du laboratoire
		Équin	25 - 40 mg/mL	Engle *et al.*, 1984
		Ovin	12 - 16 mg/mL	Restall and Wales, 1966
Période d'étude du protéome	FU	Équin	Phases folliculaire/estrus et lutéale	Khan *et al.*, 2020
		Ovin		Soleilhavoup *et al.*, 2016
		Porcin	Jour 9, 12, 15 de la gestation	He *et al.*, 2022
		Bovin	Jour 19 de la gestation	Gegenfurtner *et al.*, 2020
			Jour 7 de la gestation	Aranciaga *et al.*, 2021
	FO	Équin	Phase péri-ovulatoire	Fernández-Hernández *et al.*, 2021
		Ovin	Phases folliculaire/estrus et lutéale	Soleilhavoup *et al.*, 2016
		Bovin	Phases pré-, post-ovulatoire et lutéale	Lamy *et al.*, 2016
Protéines majoritaires	FU	Bovin	Albumine, protéines du complément, lactoferrine, protéines de choc thermique HSPAA1, AB1, A8	Aranciaga *et al.*, 2021 ; Forde *et al.*, 2014
	FO		Oviductine, myosines 9,14, annexines A1, A2, HSPA5, A8	Lamy *et al.*, 2016; Papp *et al.*, 2019
Voies de sécrétion prédites	FU	Bovin	14% sécrétées de manière conventionnelle et 12% par des voies non conventionnelles	Aranciaga *et al.*, 2021
	FO		14 % de manière conventionnelle via un peptide signal	Gegenfurtner *et al.*, 2019
Fonctions majeures prédites	FU	Bovin	Processus métaboliques ; système immunitaire ; réponse à un stress/stimulus	Aranciaga *et al.*, 2021 ; Faulkner *et al.*, 2013; Forde *et al.*, 2014; Gegenfurtner *et al.*, 2019
	FO		Liaison ; processus métaboliques, catalytiques et cellulaires ; reproduction	Pillai *et al.*, 2017; Papp *et al.*, 2019

1.2.2. Facteurs de régulation des protéomes luminaux de l'utérus et de l'oviducte

Les approches à grande échelle de type « omique » ont permis de mettre en évidence des variations d'abondance des transcrits et des protéines exprimées dans les cellules épithéliales de l'utérus (CEU) et l'oviducte (CEO), et des protéines sécrétées dans les fluides de ces organes. Les facteurs de variation étudiés comprennent essentiellement la région anatomique du tractus, le stade du cycle dans une région donnée, et chez les espèces mono-ovulantes, la proximité de l'ovaire ovulant au cours du cycle. Les facteurs de régulation et leurs effets sur l'abondance des transcrits et protéines exprimées dans les cellules épithéliales de l'utérus et de l'oviducte sont résumés dans le tableau 2 page 38. Les facteurs de régulation et leurs effets sur l'abondance des protéines présentes dans les fluides utérins et oviductaux sont résumés dans le tableau 3 page 39.

Région anatomique de l'appareil génital

De façon étonnante, très peu d'études ont comparé les compositions des sécrétions utérines et oviductales. Chez les mammifères, une seule étude a comparé les protéomes luminaux de l'utérus et de l'oviducte chez la brebis (Soleilhavoup *et al.*, 2016). Seule une série d'études issues du même laboratoire a permis de mettre en évidence des concentrations différentielles en ions, acides aminés et métabolites énergétiques entre FO et FU en début de phase lutéale chez la vache (Hugentobler *et al.*, 2007a, b, 2008).

Dans l'oviducte, bien que l'isthme et l'ampoule diffèrent du point de vue anatomique et fonctionnel, aucune étude n'a comparé le contenu protéique de ces deux régions. Pourtant, dans une analyse multifactorielle du transcriptome des CEO bovin, la région (isthme vs. ampoule) a été rapportée comme le facteur le plus discriminant comparé à la proximité de l'ovaire ovulant (ipsi- vs. controlatérale) et au statut physiologique des génisses (cyclique vs. gestante) au jour 3 post-estrus (Maillo *et al.*, 2016). En effet, aucun gène n'était différentiellement exprimé entre les deux oviductes dans une région donnée, ni en fonction de la présence d'un embryon (génisses gestantes) ou d'un ovocyte (génisses cyclées), alors que plus de 4000 gènes ont été identifiées comme différentiellement exprimés entre l'isthme et l'ampoule des génisses gestantes (Maillo *et al.*, 2016).

Dans deux autres études portant sur le transcriptome des CEO bovin, le nombre de transcrits différentiellement exprimés entre stades ou entre côtés était différent en fonction de la région considérée (Cerny *et al.*, 2015; Locatelli *et al.*, 2019), ce qui suggère des différences importantes de régulation d'expression génique entre les deux régions. Par exemple, 14 fois plus de gènes différentiellement exprimés ont été identifiés dans l'isthme comparé à l'ampoule lorsque les deux côtés étaient comparés par séquençage des ARN (Locatelli *et al.*, 2019). De plus, chez la vache, quelques gènes candidats analysés par RT-qPCR ont été détectés comme différentiellement exprimés entre régions. Par exemple, le transcrit d'OVGP1 a été quantifié à des niveaux 10 à 14 fois plus élevés dans l'ampoule que dans l'isthme au cours du cycle chez le zébu (Gonella-Diaza *et al.*, 2015). A l'inverse, le transcrit codant pour le récepteur nucléaire à la progesterone a été détecté à des niveaux deux fois plus élevés dans l'isthme que dans l'ampoule de l'oviducte bovin pendant la période post-ovulatoire (Saint-Dizier *et al.*, 2012).

Dans les tissus, des différences d'abondance protéique ont été mises en évidence entre régions de l'oviducte, mais uniquement par des approches candidates. Par exemple, chez la chienne, la protéine OVGP1 a été détectée à des niveaux 4 à 5 fois plus élevés dans l'isthme que dans l'ampoule pendant la période post-ovulatoire où a lieu l'expulsion de l'ovocyte (Saint-Dizier *et al.*, 2014).

Des gradients de concentrations luminales pourraient donc exister entre ampoule et isthme pour différents composants du fluide oviductal. Les glycosaminoglycanes (GAG) sont des macromolécules (de poids moléculaire compris entre 5 et 100 kDa) présents dans les matrices extracellulaires et les fluides biologiques et sont constitués de chaînes polyglucidiques souvent associées à des protéines (protéoglycanes). Chez la vache, la concentration en GAG sulfatés dans le FO a été mesurée à des niveaux plus élevés dans l'ampoule (74 µg/mL) que dans l'isthme (43 µg/mL) (Bergqvist *et al.*, 2005; Bergqvist and Rodríguez-Martínez, 2006). Dans le FO de truie en revanche, aucune différence entre l'isthme et l'ampoule n'a été détecté pour les concentration de GAG sulfatés et d'acide hyaluronique (seul GAG non sulfaté) (Tienthai *et al.*, 2000). De plus, quelques métabolites et acides aminés comme la glycine, le lactate et l'alanine ont été mesurés avec des concentrations trois fois plus importantes dans l'ampoule que dans l'isthme bovin (Rodríguez-Alonso *et al.*, 2020).

Stade du cycle

De nombreuses études transcriptomiques et protéomiques ont mis en évidence l'impact du stade du cycle et de son environnement endocrinien spécifique sur les variations d'expression et de sécrétion luminale dans l'épithélium de l'utérus ou de l'oviducte. Dans l'endomètre bovin, une analyse en microarray a mis en évidence 269 gènes différentiellement exprimés entre 0, 4, 12 et 18 jours après l'estrus (Mitko *et al.,* 2008). Dans l'endomètre de jument, 377 gènes différentiellement exprimés ont été mis en évidence entre stades du cycle par la technique de séquençage ARN (Rudolf Vegas *et al.,* 2021). Chez la truie, entre les jours 9 et 12 du cycle, 59 protéines de l'endomètre, dont l'albumine et l'annexine A4, voyaient leur abondance varier de manière significative (Jalali *et al.,* 2015). Dans l'oviducte de génisses entre l'estrus (phase folliculaire) induit et la phase lutéale (11-12 jours plus tard), 1563 gènes étaient différentiellement exprimés dans l'ampoule et 1758 dans l'isthme (Cerny *et al.,* 2015). Chez la truie, entre le jour de l'ovulation et la phase lutéale (3 à 18 jours post-ovulation), de 423 à 2343 gènes différentiellement exprimés ont été identifiés (Jang *et al.*, 2022). Dans une étude protéomique, 78 protéines étaient différentiellement exprimées par les cellules épithéliales d'oviductes de truie entre les phases folliculaire et lutéale (Seytanoglu *et al.*, 2008).

Des modifications importantes des abondances protéiques quantifiées par MS dans les fluides sont également rapportées. Dans l'utérus entre les phases folliculaire et lutéale du cycle, 6% des protéines du FU de jument étaient différentiellement abondantes (Maloney *et al.*, 2019) et 39% dans celui de brebis (Soleilhavoup *et al.*, 2016). Chez la vache, le protéome utérin a été décrit uniquement entre les jours 7 et 13 de la phase lutéale avec 5% de protéines différentiellement abondantes entre ces deux stades (Mullen *et al.*, 2012). De plus, 2% des protéines dans les uEV variaient en abondance entre la phase folliculaire et lutéale chez le bovin (Piibor *et al.*, 2022). Pour l'oviducte, l'analyse protéomique du FO bovin a identifié entre 4 et 20% de protéines différentiellement abondantes au cours du cycle (Lamy *et al.*, 2016b). En particulier, 17% et 14% des protéines du FO étaient différentiellement abondantes entre les stades pré- et post-ovulatoire chez la vache et la jument respectivement (Lamy *et al.*, 2016b; Fernández-Hernández *et al.,* 2021). Des protéines comme les annexines A1, A2 étaient plus abondantes avant l'ovulation tandis que des protéines de chocs thermiques (HSPA5, 8, AB1) étaient plus abondantes après l'ovulation (Lamy *et al.*, 2016b). Chez la brebis, l'analyse protéomique du FO a mis en évidence une proportion similaire de protéines différentielles (29%) entre l'estrus et la phase lutéale du cycle (Soleilhavoup *et al.*, 2016).

De plus, 51% des protéines dans les oEV variaient en abondance entre les jours 1 et 20 du cycle chez le bovin (Almiñana *et al.*, 2018). Les GAG varient également dans le FO au cours du cycle. La concentration en GAG est plus importante pendant l'estrus que la phase lutéale dans le FO de chienne et de vache (Kawakami *et al.*, 2000; Bergqvist *et al.*, 2005) alors qu'aucune variation n'a été identifiée au cours du cycle chez la truie et la brebis (Lee *et al.*, 1986; Tienthai *et al.*, 2000).

Hormis les macromolécules, quelques études se sont également intéressées aux variations en abondance des métabolites (Hugentobler *et al.*, 2008; Lamy *et al.*, 2018; Tríbulo *et al.*, 2019) dans les sécrétions génitales au cours du cycle. Une analyse du FU bovin a permis d'identifier 34% de métabolites différentiellement abondants au cours de la phase lutéale dont la leucine et la taurine, plus abondants au jour 7 qu'au jour 0 (Tríbulo et al., 2019). L'ajout de ces deux métabolites dans le milieu de culture embryonnaire améliore la viabilité et le développement au stade blastocyste comparé à une condition dépourvue de métabolites (Ealy *et al.*, 1992; González *et al.*, 2012). Dans le FO bovin, 36% des métabolites identifiés variaient en concentration en fonction du stade du cycle comme la glycine, le lactate et le pyruvate (Lamy *et al.*, 2018), décrits comme sources énergétiques de la capacitation chez les mammifères (Ferramosca and Zara, 2014). L'analyse lipidomique du FO bovin a mis en évidence jusqu'à 127 masses différentielles entre les phases péri-ovulatoires et lutéale du cycle, dont 32% différentielles entre les stades pré- et post-ovulatoire (Banliat *et al.*, 2019).

Proximité de l'ovaire ovulant au cours du cycle

Chez les espèces mono-ovulantes comme la vache, la jument ou la femme, des différences d'expression de gènes ont été mises en évidence en comparant les deux cornes utérines. Chez des génisses entre 5 et 16 jours après l'estrus, 217 transcrits ont été identifiés comme différentiellement exprimés entre la corne portant l'ovaire ayant ovulé et la corne controlatérale (Sánchez *et al.*, 2019). Dans l'oviducte de brebis, 4 des 14 gènes analysés par RT-qPCR, dont le gène *ESR1* codant pour le récepteur aux estrogènes ERα, avaient une expression différentielle en fonction de la proximité de l'ovaire ovulant 6 jours après l'ovulation (Graña-Baumgartner *et al.*, 2020). Chez le bovin, des données contradictoires ont été obtenus sur les différences d'expression génique entre oviductes ipsi- et contro-latéraux à l'ovulation. L'analyse transcriptomique d'oviductes de génisses 3 jours après l'estrus a montré 192 gènes différentiellement exprimés entre les deux côtés dans l'ampoule et 2583 dans l'isthme (Locatelli *et al.*, 2019).

Néanmoins, une autre étude par micro-array n'a identifié aucun effet de la proximité de l'ovaire ovulant sur le transcriptome d'oviductes de génisses cycliques 3 jours post-estrus (Maillo *et al.*, 2016).

La proximité de l'ovaire ovulant a également un impact sur les composants des fluides. Chez le bovin, au jour 7 et 15 du cycle aucune différence n'a été identifié entre les protéomes luminaux des cornes utérines ipsi- et controlatérales (Faulkner *et al.*, 2013). En revanche, 10 à 24 % des protéines identifiées dans les sécrétions oviductales en période pré- et post-ovulatoire différaient en abondance entre l'oviducte ipsi- et controlatéral à l'ovulation (Lamy *et al.*, 2016b). Chez la jument, 4 jours après l'ovulation, 7% des protéines identifiées dans le FO étaient différentiellement abondantes entre les deux oviductes (Smits *et al.*, 2017). Ces différences de contenu protéomique des fluides sont probablement en partie liées aux différences hormonales entre les deux côtés. Aucune donnée sur les concentrations hormonales dans les deux cornes utérines n'est disponible à ce jour. Cependant dans les oviductes bovins, la progestérone a été mesurée par chromatographie gazeuse couplée à la spectrométrie de masse à des niveaux quatre à seize fois plus élevées côté ipsilatérale (de 50 à 150 ng/mL) que controlatérale (autour de 20 ng/mL) pendant tout le cycle (Lamy *et al.*, 2016a). Chez la jument en période post-ovulatoire, la progestérone a été mesurée à des concentrations cent fois plus importante dans l'oviducte ipsilatéral comparé à celui controlatéral à l'ovulation (Nelis *et al.*, 2016). En revanche pour l'œstradiol, aucune différence notoire n'a été observée entre les deux oviductes à la fois chez la vache et la jument (Lamy *et al.*, 2016a; Nelis *et al.*, 2016). Par ailleurs, les concentrations de quelques protéines différentiellement abondantes entre côtés étaient corrélées positivement ou négativement avec les concentrations intra-oviductales de progestérone chez la vache (Lamy *et al.*, 2016b).

D'autres molécules dans le FO ont des abondances différentielles en fonction de la proximité de l'ovaire ovulant. Chez le bovin, la concentration en GAG sulfatés est plus importante côté ipsi- (74 mg/L) que controlatéral (43 mg/L) (Bergqvist and Rodríguez-Martínez, 2006). De plus, chez cette même espèce, 13% (5/39) des métabolites quantifiés dans le FO sont différentiellement abondants entre côtés tout au long du cycle (Lamy *et al.*, 2018).

Tableau 2 : Facteurs de régulation de l'expression génique et protéomique dans les cellules épithéliales utérines et oviductales de mammifères.

CEO = cellules épithéliales oviductales ; CEU = cellules épithéliales utérines ; GDE = génes différentiellement exprimés ; PDE = protéines différentiellement exprimées

Facteur de régulation	Cellules étudiées	Espèce	Résultats	Référence
Stade du cycle	CEU	Équin	377 GDE entre les jours 10 et 13 du cycle	Rudolf Vegas *et al.*, 2021
		Bovin	269 GDE entre les jours 0, 4, 12 et 18 du cycle	Mitko *et al.*, 2008
		Porcin	59 PDE entre les jours 9 et 12 du cycle	Jalil *et al.*, 2015
	CEO	Bovin	1563 et 1758 GDE entre stades folliculaire et lutéale respectivement dans l'ampoule et l'isthme	Cerny *et al.*, 2015
		Porcin	423 à 2343 GDE entre les jours 0 et 3-18 du cycle	Jang *et al.*, 2022
		Porcin	78 PDE entre phases folliculaire et lutéale	Seytanoglu *et al.*, 2008
Proximité de l'ovaire ovulant	CEU	Bovin	14 à 217 GDE entre les deux cornes 5 à 16 jours après l'estrus	Sánchez *et al.*, 2019
		Ovin	4 à 14 GDE entre les deux cornes dont le récepteur aux estrogènes *ESR1*, 6 jours post-ovulation	Graña-Baumgartner *et al.*, 2020
	CEO	Bovin	2583 GDE entre les deux oviductes dans l'isthme et 192 dans l'ampoule, 3 jours post-ovulation,	Locatelli *et al.*, 2019
			Pas de GDE entre les deux oviductes 3 jours post-estrus	Maillo *et al.*, 2016
Région anatomique	CEO	Bovin	2287 GDE entre ampoule et isthme de génisses gestantes (embryon au stade 8 cellules)	Maillo *et al.*, 2016

Tableau 3 : Facteurs de régulation des protéines luminales solubles et intra-vésiculaires dans l'utérus et l'oviducte.

FO = fluide oviductal ; FU = fluide utérin ; PDA = protéines différentiellement abondantes

Facteur de régulation	Fluide étudié	Espèce	Résultats	Référence
Stade du cycle	FU	Equin	6 % de PDA entre les phases folliculaire et lutéale	Maloney *et al.*, 2019
		Ovin	38,5% de PDA entre l'estrus et la phase lutéale	Soleilhavoup *et al.*, 2016
		Bovin	5% (34/707) de PDA entre J7 et J13 post-estrus	Mullen *et al.*, 2012
			5% (41/2587) de PDA dans les uEV entre la phase folliculaire et lutéale	Piibor *et al.*, 2022
	FO	Equin	14% de PDA entre stades péri-ovulatoires	Fernández-Hernández *et al.*, 2021
		Bovin	4-20% de PDA entre stades dont 17% entre stades péri-ovulatoires	Lamy *et al.*, 2016b
		Ovin	29 % de PDA entre l'estrus et la phase lutéale	Soleilhavoup *et al.*, 2016
		Bovin	51 % de PDA dans les oEV du jour 1 au jour 20 du cycle	Alminana *et al.*, 2018
Proximité de l'ovaire ovulant	FU	Bovin	Pas de PDA entre les deux cornes au jour 7 et 15 du cycle	Faulkner *et al.*, 2013
	FO	Bovin	10 et 24 % de PDA entre les deux oviductes en période péri-ovulatoire	Lamy *et al.*, 2016b
		Equin	7% de PDA entre les deux oviductes au jour 4 du cycle	Smits *et al.*, 2017
Région anatomique de l'oviducte	FO	Bovin	OVGP1 détectée 4 à 5 fois plus dans l'isthme que dans l'ampoule en post-ovulatoire	Saint-Dizier *et al.*, 2014

En résumé de cette première partie de synthèse bibliographique, la majorité des études sur la composition des fluides génitaux femelles portent sur l'oviducte de la femelle cyclée et l'utérus de la femelle gestante. Ces études montrent que les transcrits dans les cellules oviductales et utérines, et les protéines dans la lumière de l'oviducte varient en abondance en fonction du stade du cycle et de la proximité de l'ovaire ovulant. En revanche, la géographie précise des protéines rencontrées successivement par les spermatozoïdes depuis l'utérus jusqu'à l'ampoule de l'oviducte n'a pas été explorée. De plus, les périodes pré- et post-ovulatoires, au cours desquelles les spermatozoïdes puis les embryons ont probablement des besoins différents, ont rarement été comparées. Ces données permettent de décrire la régulation des composants, et surtout des protéines, des fluides mais l'analyse fonctionnelle de ces protéines régulées reste pour l'instant uniquement prédictive. Le rôle de cette régulation dans la capacitation des spermatozoïdes, la fécondation et le développement embryonnaire reste à découvrir. Néanmoins, ces données constituent une base ouvrant le pas vers l'amélioration de la physiologie des spermatozoïdes et de l'embryon.

2. Migration et acquisition de la capacité fécondante des spermatozoïdes dans les voies génitales femelles

Après avoir décrit l'environnement femelle traversé par les spermatozoïdes au cours de leur migration, cette partie se focalise sur la migration et la capacitation des spermatozoïdes ayant lieu dans cet environnement, et dont les mécanismes sont modulés à la fois par des protéines du plasma séminal et les propriétés physico-chimiques des fluides traversés.

2.1. Migration des spermatozoïdes jusqu'au site de fécondation

Dans les voies génitales femelles, les spermatozoïdes de mammifères doivent parcourir une distance correspondant à environ 10 000 fois leur taille (65-75 cm pour 75-80 µm chez le bovin) : pour un humain, cela correspondrait à une course de 18 km. Mais 99% des spermatozoïdes n'atteignent pas l'oviducte, où a lieu la fécondation. Cette proportion est le fruit d'études souvent anciennes de comptage *ex vivo* des spermatozoïdes sur des coupes histologiques ou des frottis après insémination artificielle (synthétisées en Figure 4 page 42). Cette technique très couteuse nécessite l'abattage post-insémination d'un grand nombre de femelles. De nouvelles méthodes d'imagerie *in vivo* voient donc le jour comme

l'endomicroscopie confocale à fluorescence (technologie Cellvizio®). Cette technique semi-quantitative a permis de suivre la progression des spermatozoïdes préalablement colorés par un fluorochrome jusqu'en haut des cornes utérines chez la brebis (Druart et al. 2009) et la vache (Saint-Dizier *et al.*, 2016).

En revanche, les méthodes d'exploration de la migration spermatique dans l'oviducte sont toujours réalisées par de l'imagerie *ex vivo*, c'est-à-dire après insémination, sacrifice de l'animal et collecte des oviductes pour observer les spz à travers la paroi ou après ouverture (La Spina *et al.*, 2016; Wang and Larina, 2018). La souris, dont la paroi très fine des oviductes est transparente, est le modèle le plus utilisé pour ces études.

2.1.1. Migration à travers le cervix et l'utérus

Chez la plupart des mammifères, les spermatozoïdes sont déposés dans la partie caudale du vagin : le col de l'utérus constitue la première barrière physique de la migration spermatique. Chez la brebis, 24 h après l'accouplement, en moyenne un spz sur 27 000 est capable de franchir le col (Hawk *et al.*, 1978; Holt and Fazeli, 2015). Chez le bovin, sur 2 milliards de spz inséminés et 300 millions récupérés dans tout le tractus, de une à vingt-quatre heure(s) après insémination, 58 à 77 % des spermatozoïdes étaient dans le vagin pour seulement 22 à 26 % dans le col et 1 à 15 % dans l'utérus (Figure 4A page 42) (Dobrowolski and Hafez, 1970).

De plus, 70 à 100 % des spermatozoïdes anormaux, immobiles et/ou morts ne passent pas à travers le mucus cervical après insémination ou accouplement chez le rat (Bedford and Yanagimachi, 1992), le mouton (Mattner and Braden, 1969) et *ex vivo* chez l'homme (Katz *et al.*, 1990). Ce mucus, sécrétée par les cellules bordant le col, est très visqueux et représente un véritable piège pour les spermatozoïdes anormaux (Katz *et al.*, 1990; Suarez and Pacey, 2006).

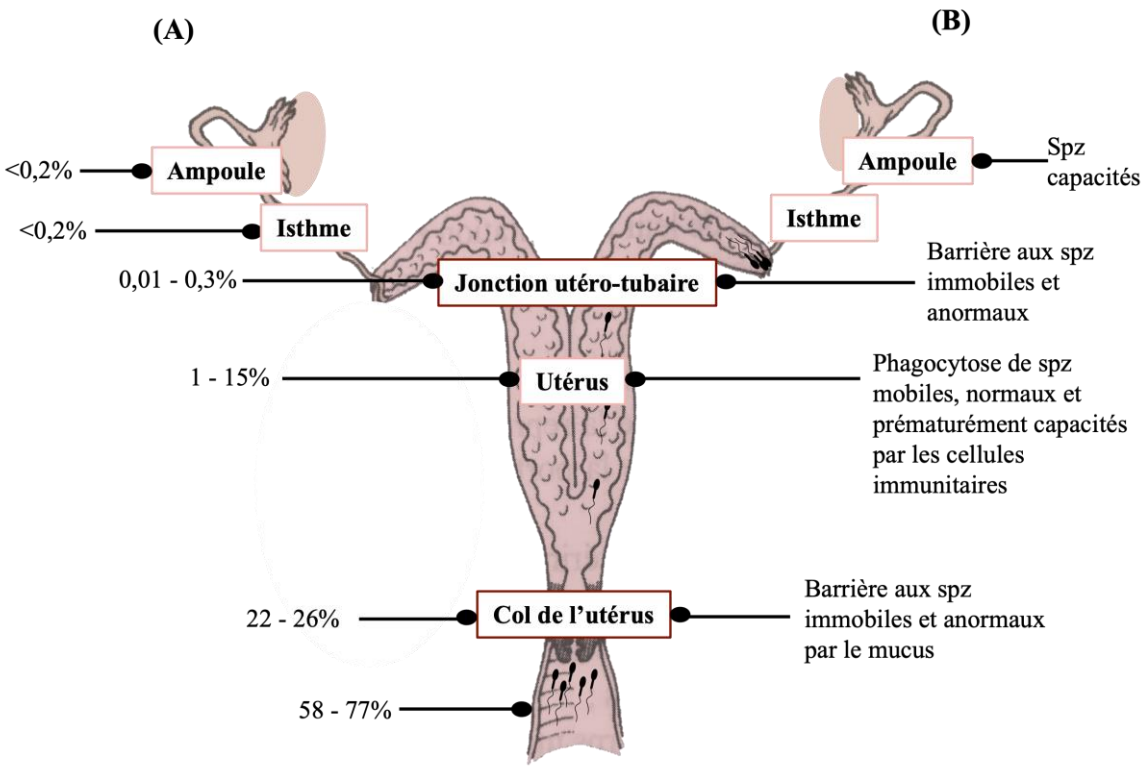

Figure 4 : Proportion et morphologie des spermatozoïdes dans les voies génitales femelles.

(**A**) Proportion de spermatozoïdes (spz) comptés 1 à 24 h après insémination avec deux milliards de spermatozoïdes éjaculés chez le bovin (Dobrowolski and Hafez, 1970).

(B) Morphologie des spermatozoïdes dans les voies génitales femelles (Mattner, 1968; Mattner and Braden, 1969; Baker and Degen, 1972; Krzanowska, 1974; Gaddum-Rosse, 1981; Heyman and Levasseur, 1981; Katz *et al.*, 1990; Bedford and Yanagimachi, 1992; García-Vázquez *et al.*, 2015; La Spina *et al.*, 2016; Muro *et al.*, 2016).

Après avoir franchi le col, les spermatozoïdes sont soumis à la réponse inflammatoire utérine. De manière similaire à des agents pathogènes, les spz provoquent une entrée massive de cellules immunitaires dans la lumière utérine (Mattner, 1968) et leurs interactions avec les cellules épithéliales utérines accentuent cette réponse via la production de cytokines pro-inflammatoires (Elweza *et al.*, 2018). Les granulocytes ou polynucléaires neutrophiles sont la première ligne de défense immunitaire de l'utérus : ces cellules interagissent directement avec les spz ou via des pièges extracellulaires afin de les phagocyter (Wrenzycki, 2022). Les polynucléaires neutrophiles se lient à des spermatozoïdes viables et mobiles *in vitro* chez le porc (Taylor *et al.*, 2008) et le cheval (Troedsson *et al.*, 2005). Chez l'humain, les polynucléaires neutrophiles phagocytent également des spermatozoïdes viables et mobiles mais préférentiellement des spermatozoïdes capacités (Oren-Benaroya *et al.*, 2007). Les cellules immunitaires présentes dans l'utérus permettraient donc d'éliminer, entre autres, des spermatozoïdes prématurément capacités. (Figure 4B page 42).

2.1.2. Migration à travers la jonction-utéro tubaire et l'oviducte

Migration des spermatozoïdes à travers la jonction utéro-tubaire

Après leur migration utérine, les spermatozoïdes sont massivement retenus au niveau de la jonction utéro-tubaire (Druart *et al.*, 2009). Chez la brebis, 4 h après insémination intra-utérine, un gradient croissant de spermatozoïdes de la base des cornes utérines jusqu'à la JUT a été observé, suivi d'une diminution significative du nombre de spermatozoïdes dans les oviductes (Druart *et al.*, 2009). Chez la truie et la brebis, il est estimé que seulement 1 spz sur 10 millions est capable de traverser la JUT (First *et al.*, 1968; Hawk *et al.*, 1978). Chez le bovin, 18 h après l'accouplement, 20 000 spermatozoïdes ont été comptés dans la JUT pour seulement 2 000 dans l'isthme (Heyman and Levasseur, 1981). Plus globalement, 0,01 à 0,3 % des spz comptés dans la totalité du tractus bovin se trouvaient au niveau de la JUT (Dobrowolski and Hafez, 1970) (Figure 4B page 42).

La JUT est aussi une barrière pour les spermatozoïdes présentant des anomalies morphologiques. Chez la truie, 24 h après insémination, 98 % des spermatozoïdes récupérés dans la JUT ne présentaient aucune anomalie morphologique, contre 70 % dans le reflux utérin (García-Vázquez *et al.*, 2015).

De plus, chez le porcin, le rat, la souris et le hamster, seuls des spermatozoïdes vivants (Baker and Degen, 1972), mobiles (Gaddum-Rosse, 1981), non capacités (Shalgi *et al.*, 1992; Muro *et al.*, 2016) et morphologiquement normaux (Krzanowska, 1974) ont été retrouvés dans la première partie de l'oviducte (Figure 4B page 42).

Les caractéristiques physiologiques de la JUT font d'elle la deuxième barrière physique après le col, avec une réduction drastique du diamètre utérin et des nombreux replis muqueux envahissant sa lumière décrient chez plusieurs mammifères dont la vache (Yániz *et al.*, 2000; Barone, 2001; Suarez and Pacey, 2006). La migration à travers la JUT semble être aussi régie par des interactions moléculaires via les protéines de surface des spermatozoïdes. Chez la souris mâle, les KO d'*Adam3* et de quelques gènes cibles comme *Adam1a,2* ou *Calr3* entrainant l'absence ou la mauvaise expression de la protéine ADAM3 à la surface des spz, empêchent totalement leur passage à travers la JUT de femelles non mutées (Fujihara *et al.*, 2018; Xiong *et al.*, 2019). Les spz issus d'autres souris mâles mutants pour des gènes non reliés à la protéine ADAM3 sont également incapable de traverser la JUT, suggérant des mécanismes à la fois dépendants et indépendants d'ADAM3 pour le franchissement de la JUT chez cette espèce (les gènes sont décrits en détails dans la partie 3.1 page 52) (Fujihara *et al.*, 2018; Xiong *et al.*, 2019). Les molécules côté femelle impliquées dans ces interactions au sein de la JUT restent inconnues. L'existence de tels « passeports » moléculaires pour le franchissement de la JUT chez les espèces d'élevage n'est aujourd'hui pas connue. Par ailleurs, sa morphologie étant très variables entre mammifères, le mécanisme du passage des spz à travers la JUT peut être différent d'une espèce à l'autre (Suarez, 2006). Cette traversée est plus simple chez l'humain que chez d'autres espèces comme la vache, la truie et la souris, complexifiée par la présence de nombreux replis muqueux. En particulier chez la souris, la JUT constitue une véritable porte, qui s'ouvre juste après l'accouplement et se ferme environ une heure plus tard, laissant aux spz une très courte fenêtre de temps pour atteindre l'oviducte (Suarez, 2006).

Migration des spermatozoïdes dans l'oviducte

Dans l'oviducte, un gradient décroissant de spermatozoïdes de la JUT vers l'ampoule a été observé après observation de coupes histologiques post-mortem chez le bovin (Heyman and Levasseur, 1981), chez l'ovin après hystérectomie et flush (Sumransap *et al.*, 2007; Tummaruk *et al.*, 2007), et chez la souris par de l'imagerie *ex vivo* à travers la paroi oviductale (La Spina *et al.*, 2016). Après insémination chez la brebis, 0,3% des spz comptés dans l'ensemble du tractus se trouvaient dans l'isthme et 0,1% dans l'ampoule (Quinlivan and Robinson, 1969). En particulier, 18 h après l'accouplement chez la vache, 2000 spz ont été comptés dans la partie caudale de l'isthme pour seulement 10 dans l'ampoule, lieu de la fécondation (Heyman and Levasseur, 1981).

Cette diminution du nombre de spz dans l'oviducte s'accompagne de modifications de leur physiologie. Chez la souris, l'imagerie *ex vivo* couplé à de l'immunocytochimie a permis de suivre l'état de l'acrosome des spz dans l'oviducte (La Spina *et al.*, 2016). Quatre heures après l'accouplement, la totalité des spz observés dans la partie caudale de l'isthme avaient un acrosome intact tandis que 50% avaient réagi dans la partie crâniale de l'isthme (proche de l'ampoule) et 95% des spz observés dans l'ampoule étaient dépourvu de leur acrosome (La Spina *et al.*, 2016). Ces données récentes ont remis en question le dogme selon lequel les spz font leur réaction acrosomique (fusion de la membrane plasmique et de la membrane externe de l'acrosome du spz) au contact de la zone pellucide des ovocytes. De telles données *ex vivo* ne sont disponibles que chez la souris.

2.2. Capacitation des spermatozoïdes et facteurs de régulation mâles et femelles

2.2.1. Mécanismes de la capacitation

La capacitation correspond à l'ensemble des modifications cellulaires et moléculaires des spermatozoïdes leur permettant de faire leur réaction acrosomique et fusionner avec l'ovocyte. Décrite pour la première fois dans les années 50 chez le rat et le lapin, la capacitation est associée à des changements membranaires et métaboliques (Austin, 1951; Chang, 1951; Leemans *et al.*, 2019). Même si les mécanismes de la capacitation ne sont pas totalement élucidés, il est clair que les transporteurs d'ions présents à la surface des spz en sont des acteurs majeurs (Wang *et al.*, 2021) (Figure 5 page 49).

La genèse de la capacitation démarre par un efflux de cholestérol, provoquant une fluidité membranaire et une augmentation du pH intracellulaire (Wang *et al.*, 2021). Cette alcalinisation entraîne à la fois un efflux d'ions potassium et une entrée massive d'ions calcium dans les spermatozoïdes (Navarro *et al.*, 2007). Ces ions calciques ont un rôle central dans la capacitation et leur entrée est dépendante de canaux spécifiques nommés CATSPER (sperm-specific, Ca^{2+}-permeable, pH-dependent channels), codé par des gènes (*Catsper* 1 à 4) dont les séquences sont très conservées chez les mammifères (Johnson *et al.*, 2017).

Principalement retrouvés au niveau du flagelle, ces canaux calciques jouent un rôle important dans les changements de mobilité du spz associés à la capacitation : l'hyperactivation, qui se traduit par des battements flagellaires asymétriques de grande amplitude et nécessaire à la progression des spz dans des milieux visqueux tels que le fluide d'oviducte (riche en glycoprotéines comme l'OVGP1 et en GAG) et le cumulus (riche en acide hyaluronique) entourant l'ovocyte (Johnson *et al.*, 2017; Rahban and Nef, 2020). Chez le bovin, l'inhibition pharmacologique des canaux CATSPER par le dihydrochloride ou par un anticorps contre CATSPER 1 diminue la proportion de spermatozoïdes hyperactivés (Johnson *et al.*, 2017; Romero-Aguirregomezcorta *et al.*, 2019). L'entrée de calcium active la phosphorylation des tyrosines des protéines du spermatozoïdes via la production d'AMP cyclique et la protéine kinase A (Visconti *et al.*, 1995).

L'entrée de calcium au niveau de la tête ainsi que l'augmentation de la fluidité membranaire est nécessaire à la réaction acrosomique, pré-requis pour atteindre l'espace périvitellin sous la zone pellucide et fusionner avec la membrane de l'ovocyte (Visconti *et al.*, 2002).

2.2.2. Modulation de la capacitation par les protéines du plasma séminal et les facteurs femelles

Modulation de la capacitation par les protéines du plasma séminal

Des protéines présentes spécifiquement dans le plasma séminal peuvent moduler la capacitation des spermatozoïdes. C'est le cas des Binder of Sperm Proteins (BSPs) qui ont des rôles bénéfiques connus dans la capacitation chez le bovin (Thérien *et al.*, 1998, 1999), le porcin (Lusignan *et al.*, 2007) et l'humain (Plante *et al.*, 2014). Au cours de l'éjaculation, ces protéines quantifiées en grande abondance dans le plasma séminal de plusieurs mammifères se lient directement via des sites de liaison aux phospholipides sur toute la surface des spermatozoïdes (Barrios, 2005; Plante *et al.*, 2016; Druart and de Graaf, 2018). Les BSPs possèdent une structure très conservée décomposée en deux domaines fibronectine de type II précédés d'un domaine N-terminal (Plante *et al.*, 2016). Elles ont été pour la première fois décrites dans le plasma séminal de taureau et se décomposent en trois protéines : BSP1 (anciennement PDC-109 ou BSPA1/A2), BSP3 (anciennement BSPA3) et BSP5 (anciennement BSP30 kDa). Leurs homologues ont également été identifiés dans le plasma séminal d'autres mammifères dont le verrat (BSP1), l'étalon (BSP1 et 2) et le buffle (BSP1) (Plante and Manjunath, 2014). Le domaine N-terminal permet aux BSP 1, 3 et 5 d'interagir avec des facteurs capacitants de l'oviducte comme les GAG et les lipoprotéines à haute densité (HDL) (Manjunath *et al.*, 1989; Chandonnet *et al.*, 1990; Thérien *et al.*, 1997, 2005). Ces interactions faciliteraient l'efflux de cholestérol et la déstabilisation membranaire et donc la capacitation dans l'oviducte. En accord avec cette hypothèse, l'incubation successive de spz avec des BSPs puis des HDL augmente la proportion de spz ayant réalisé leur réaction acrosomique comparé à des spz incubés uniquement avec des HDL, soulignant l'effet capacitant des BSPs (Thérien *et al.*, 1997). Les BSPs peuvent aussi avoir des effets décapacitants, pouvant freiner une capacitation prématurée chez certaines espèces (Leemans *et al.*, 2019). Par exemple, chez le bélier, dans des conditions capacitantes *in vitro*, BSP5 maintient la stabilité membranaire des spz tandis que BSP1 induit un efflux de cholestérol et une phosphorylation des tyrosines (Pini *et al.*, 2018).

D'autres protéines du plasma séminal ont des effets contrastés sur la capacitation. Chez la souris, une protéine de la famille des inhibiteurs de protéases, SERPIN2 (Serpin family E member 2), interagit avec le spz et inhibe la capacitation induite par l'albumine (Lu *et al.*, 2011). Chez l'humain, CD38, extraite du plasma séminal, induit la phosphorylation des tyrosines et la réaction acrosomique en interagissant avec CD31 sur le spz (Kim *et al.*, 2015).

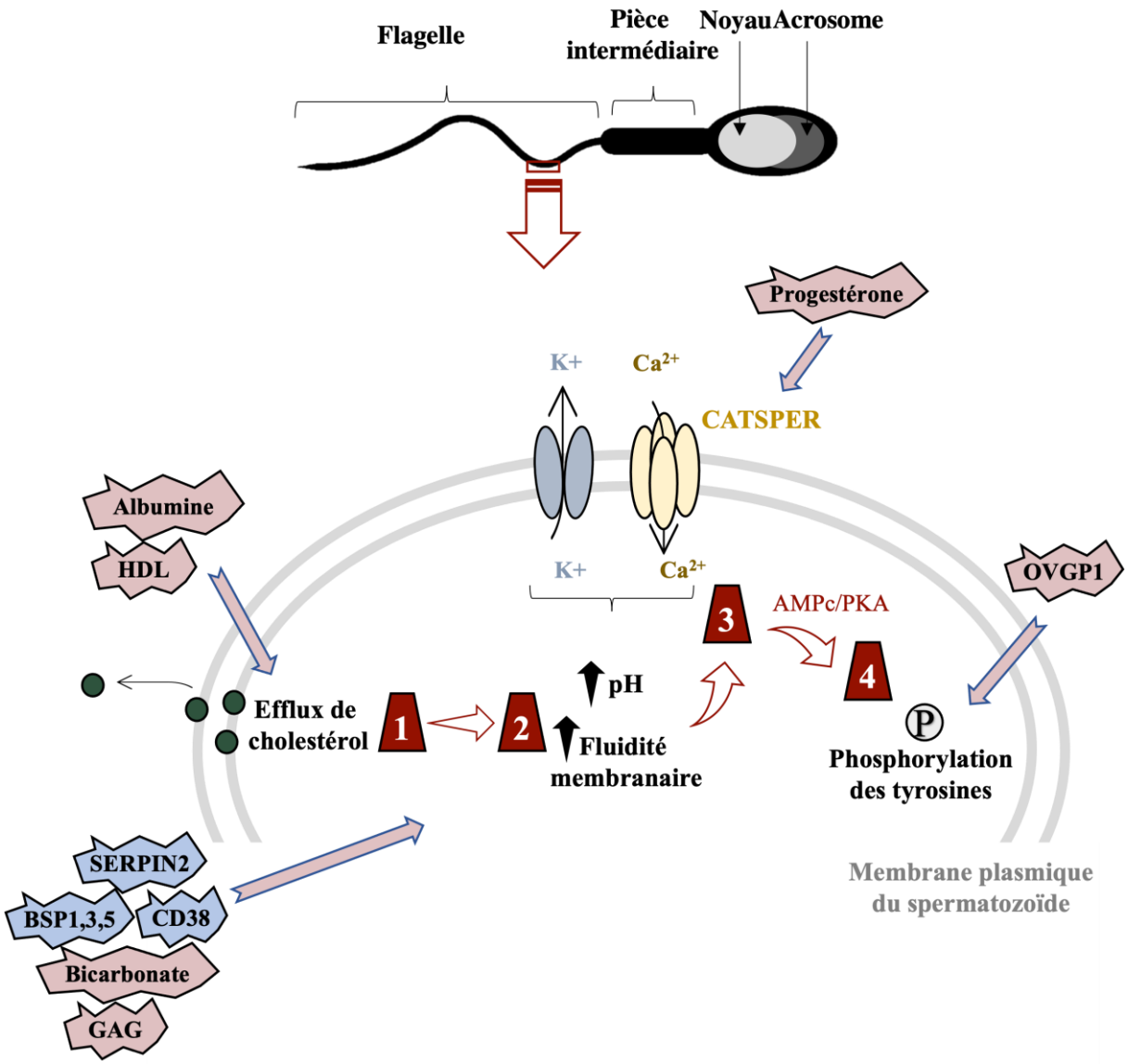

Figure 5 : Mécanisme de la capacitation du spermatozoïde bovin.

Un efflux de cholestérol (1) entraine une augmentation de la fluidité membranaire et une augmentation du pH intracellulaire (2). Cette alcalinisation entraîne un efflux d'ion potassium et une entrée massive de calcium via l'activation des canaux CATSPER (3). L'augmentation du calcium intracellulaire aboutit à la phosphorylation des tyrosines via la production d'AMP cyclique (AMPc) et l'activation de la protéine kinase A (PKA) (4). Des molécules présentes dans les sécrétions femelles (en rose : progestérone, glycosaminoglycanes (GAG), ions bicarbonate, albumine, HDL, OVGP1) et dans le plasma séminal (en bleu : SERPIN2, BSPs, CD38) modulent la capacitation.

Modulation de la capacitation par les facteurs femelles

In vivo, la capacitation se déroule lors de la migration dans les différentes parties des voies génitales femelles. Des études chez la truie comparant la proportion d'ovocytes fécondés après insémination classique dans l'utérus ou directement dans l'isthme ont montré que la majeure partie de la capacitation se déroule dans l'oviducte mais débute dans l'utérus, avec un effet synergique entre les deux organes (Hunter and Hall, 1974).

In vitro, la liaison des spermatozoïdes à des monocouches de cellules épithéliales d'oviducte permet de réguler leur capacitation. Chez le cheval, après 30 min de co-incubation, le calcium intracellulaire est deux fois plus important au sein des spermatozoïdes libres comparés aux spermatozoïdes liés aux cellules (Dobrinski, 1996). De plus, chez le porc, 59% des spermatozoïdes libres possèdent une phosphorylation sur les tyrosines de leurs protéines contre seulement 3% dans des spermatozoïdes liés aux cellules (López-Úbeda *et al.*, 2017). L'attachement des spermatozoïdes aux cellules d'oviducte empêcherait donc une capacitation prématurée des spermatozoïdes et maintiendrait cet état jusqu'à leur libération.

Des résultats obtenus *in vitro* suggèrent que de nombreux ions présents dans le fluide oviductal modulent la capacitation *in vivo*. Une des étapes essentielles de la capacitation est l'influx d'ions bicarbonate. Le pH plus élevé de l'oviducte comparé à celui de l'utérus suggère une plus grande concentration d'ions bicarbonate dans l'oviducte, qui sont probablement des acteurs majeurs dans le déclenchement de la capacitation (Hugentobler *et al.*, 2004). Hormis les flux de bicarbonate, l'augmentation des niveaux calciques intracellulaires via les canaux CATSPER est également un évènement central de la capacitation. Les canaux CATSPER possèdent des récepteurs à la progestérone et celle-ci a été mesurée dans le fluide oviductal bovin à des concentrations allant de 10 à 100 ng/mL (Lamy *et al.*, 2016a). *In vitro*, des concentrations physiologiques de progestérone augmentent le calcium intracellulaire des spz en agissant directement sur les canaux CATSPER des spz de taureau (Romero-Aguirregomezcorta *et al.*, 2019) et de verrat (Machado *et al.*, 2019) (Figure 5 page 49).

Les protéines du fluide d'oviducte seraient également impliquées dans la capacitation. Chez le bovin, l'albumine est une des protéines les plus abondantes dans les sécrétions utérines et oviductales (Lamy *et al.,* 2016b; Aranciaga *et al.,* 2021) et agit en tant qu'accepteur de cholestérol (Ehrenwald *et al.*, 1990).

Le même rôle a été décrit pour les HDL, dont la concentration a été mesurée dans le FO de vache, mais pas encore dans le FU (Ehrenwald *et al.*, 1990). Enfin, l'oviductine interagit avec le spz, comme démontré par immunomarquage chez le bovin, l'humain et l'hamster (King and Killian, 1994; Yang *et al.*, 2015; Zhao *et al.*, 2016). L'oviductine recombinante augmente *in vitro* la phosphorylation des tyrosines des protéines spermatiques chez l'hamster et l'humain comparés aux témoins (Saccary *et al.*, 2013; Zhao *et al.*, 2016). OVGP1 promeut également la capacitation *in vitro* des spz de buffles (Choudhary *et al.*, 2017).

Les glycosaminoglycanes (GAG) sont d'autres macromolécules présentes dans le FO modulant probablement la capacitation. Outre l'acide hyaluronique, les GAG sont tous sulfatés et incluent les sulfates d'héparane, de chondroïtine, de dermatane et de kératane. Peu d'études ont été réalisées sur la composition en GAG dans le FO de mammifères. Une seule étude est disponible chez le bovin, indiquant des proportions s'élevant à 39 % d'acide hyaluronique, 26 % de sulfate d'héparane, 12% de sulfate de chondroïtine et 23 % d'autres GAG sulfatés (Lee and Ax, 1984). *In vitro*, des fractions purifiées de GAG sulfatés extraites de fluides folliculaires bovins stimulent la réaction acrosomique induite par la lysophosphatidylcholine comparé aux spz témoins (Thérien *et al.*, 2005). De plus, l'héparine, un GAG sulfaté très souvent utilisé *in vitro*, induit également la capacitation chez le taureau (Parrish *et al.*, 1988) et l'étalon (Varner *et al.*, 1993). L'hypothèse est que son homologue dans l'oviducte, le sulfate d'héparane, très proche chimiquement, soit le facteur capacitant des spz bovins *in vivo* (Parrish *et al.*, 1989).

En résumé de cette deuxième partie, la proportion et la morphologie des spermatozoïdes sont modifiées pendant leur migration dans les voies génitales femelles, aboutissant à une infime proportion d'entre eux au niveau du site de fécondation dans l'ampoule de l'oviducte. Cette migration dépend de la qualité initiale des spermatozoïdes en termes de mobilité et de morphologie, mais aussi d'interactions avec les cellules immunitaires de l'utérus et de nombreuses molécules, en particulier des protéines et glycosaminoglycanes présentes dans la lumière de l'oviducte. Ces interactions mènent à la capacitation, phénomène complexe acquis surtout dans l'oviducte et modulée par les protéines du plasma séminal et les cellules et sécrétions femelles.

3. Interactions entre les spermatozoïdes et l'oviducte : ticket pour une fécondation réussie

Les mécanismes de migration et de capacitation des spermatozoïdes dans les voies génitales femelles ont souligné le rôle central de l'oviducte. Mais la réussite de la fécondation dépend aussi de la survie des spermatozoïdes « élites » avant l'ovulation, puis de leur migration au bon moment (juste après l'ovulation) au bon endroit (ampoule de l'oviducte) et dans le bon état physiologique (capacité) jusqu'à l'ovocyte. Cette dernière partie est donc consacré aux interactions moléculaires et cellulaires entre les spermatozoïdes et l'environnement tubaire participant à l'orchestration complexe de ces événements.

3.1. Interactions spermatozoïdes-oviducte et facteurs de régulation

Les spermatozoïdes qui ont franchi l'utérus s'apprête à entamer la dernière étape de leur voyage pour atteindre le site de fécondation : l'oviducte. Dans cet environnement, les spermatozoïdes sont en contact permanent avec les sécrétions successives des différentes régions traversées. La revue ci-jointe présente six facteurs femelles régulant la migration, la survie et la capacitation des spermatozoïdes dans l'oviducte :

(i) La jonction utéro-tubaire, véritable barrière physique pour les spermatozoïdes ;

(ii) La liaison des spermatozoïdes à la surface des cellules épithéliales de l'oviducte, qui prolonge leur viabilité et favorise la fécondation monospermique. Dans l'isthme, cette liaison forme un réservoir, constituant une salle d'attente et de triage des spermatozoïdes pendant la période péri-ovulatoire ;

(iii) Les contractions de l'oviducte qui participent à la progression des spermatozoïdes vers le lieu de la fécondation dans l'ampoule ;

(iv) Les deux régions anatomiques, l'isthme et l'ampoule, qui modulent différemment la physiologie des spermatozoïdes et leurs interactions avec les cellules épithéliales ;

(v) Le moment de l'ovulation, qui coordonne les interactions cellulaires et la capacitation des spermatozoïdes ;

(vi) Les hormones stéroïdiennes, qui régulent la libération des spermatozoïdes des cellules épithéliales et facilitent la capacitation.

Biology of Reproduction, 2021, 1–15
doi:10.1093/biolre/ioab105
Review

Review

Sperm migration, selection, survival, and fertilizing ability in the mammalian oviduct†

Coline Mahé[1,*], Aleksandra Maria Zlotkowska[2], Karine Reynaud[1], Guillaume Tsikis[1], Pascal Mermillod[1], Xavier Druart[1], Jennifer Schoen[2] and Marie Saint-Dizier[1,3]

[1]CNRS, IFCE, INRAE, Université de Tours, PRC, Nouzilly, France, [2]Institute of Reproductive Biology, Leibniz Institute for Farm Animal Biology, FBN, Dummerstorf, Germany and [3]Tours University, Faculty of Sciences and Techniques, Agrosciences Department, Tours, France

***Correspondence**: CNRS, IFCE, INRAE, Université de Tours, PRC, Nouzilly 37380, France. Tel: +33-2-4742-7381; E-mail: coline.mahe@inrae.fr

†Grant support: This work was funded by INRAE and ANR, grant number 18-CE92-0049 "DIALOG."

Received 28 January 2021; Revised 28 April 2021; Accepted 21 May 2021

Abstract

In vitro fertilization (IVF) gives rise to embryos in a number of mammalian species and is currently widely used for assisted reproduction in humans and for genetic purposes in cattle. However, the rate of polyspermy is generally higher in vitro than in vivo and IVF remains ineffective in some domestic species like pigs and horses, highlighting the importance of the female reproductive tract for gamete quality and fertilization. In this review, the way the female environment modulates sperm selective migration, survival, and acquisition of fertilizing ability in the oviduct is being considered under six aspects: (1) the utero-tubal junction that selects a sperm sub-population entering the oviduct; (2) the presence of sperm binding sites on luminal epithelial cells in the oviduct, which prolong sperm viability and plays a role in limiting polyspermic fertilization; (3) the contractions of the oviduct, which promote sperm migration toward the site of fertilization in the ampulla; (4) the regions of the oviduct, which play different roles in regulating sperm physiology and interactions with oviduct epithelial cells; (5) the time of ovulation, and (6) the steroid hormonal environment which regulates sperm release from the luminal epithelial cells and facilitates capacitation in a finely orchestrated manner.

Summary sentence

Summary sentence After mating or insemination, the region-specific and hormonally regulated morphology and secretions of the utero-tubal junction and oviduct lead to the selection of a limited sub-population of top quality spermatozoa at the site of fertilization.

© The Author(s) 2021. Published by Oxford University Press on behalf of Society for the Study of Reproduction. All rights reserved.
For permissions, please e-mail: journals.permissions@oup.com
This is an Open Access article distributed under the terms of the Creative Commons Attribution Non-Commercial License (http://creativecommons.org/licenses/by-nc/4.0/), which permits non-commercial re-use, distribution, and reproduction in any medium, provided the original work is properly cited. For commercial re-use, please contact journals.permissions@oup.com

Graphical Abstract

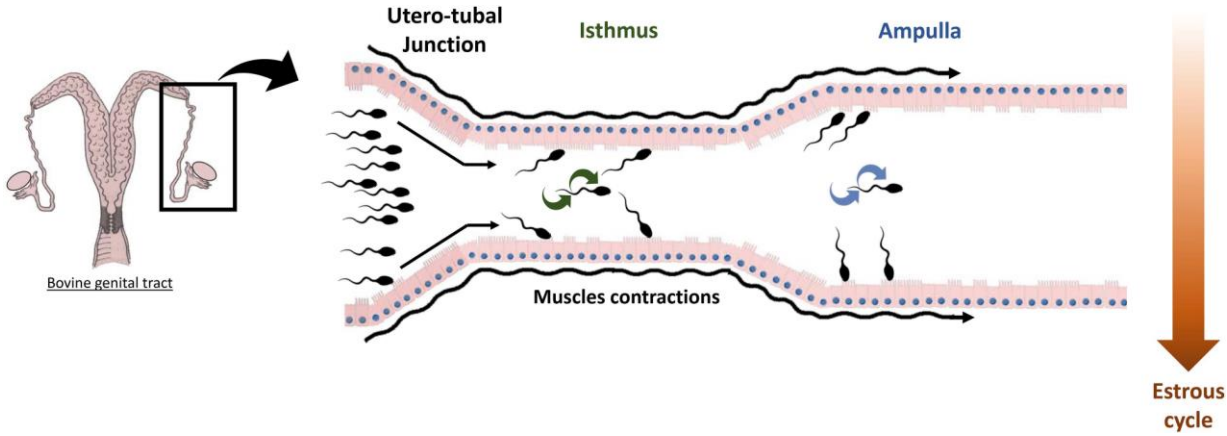

Key words: oviduct, spermatozoa, capacitation, sperm migration, fallopian tube, fertilization.

Introduction

Although sperm capacitation and fertilization can occur in vitro, comparisons between data from in vitro and in vivo demonstrated the important role played by the maternal environment in successful monospermic fertilization. In vivo, only 13% of porcine fertilized oocytes are polyspermic [1–3], whereas polyspermic rates after in vitro fertilization (IVF) reach up to 75% in pigs [4, 5], 45% in cattle, and 30% in humans [6]. Moreover, more than 30% of in vitro produced embryos may present chromosomal abnormalities compared with an average of 15% in vivo in cattle [7, 8]. In horses and dogs, IVF remains unsuccessful despite many attempts made to improve both oocyte quality and sperm ability to fertilize [9, 10]. The comprehension of how the oviduct microenvironment affects gamete quality and that of underlying mechanisms are thus useful to improve assisted reproduction technologies and fertility. In mammals, the ability of the female reproductive tract to support sperm survival and storage relies on the binding of spermatozoa to the epithelium of the oviduct [11]. The understanding of the mechanisms supporting sperm storage in vivo may help to prolong sperm lifespan and to improve sperm quality outside the female body. This could also help to develop methods to improve sperm storage in vivo, in particular after insemination in farm animals. This might reduce the use of hormones to synchronize estrus (and induce ovulation just after insemination) or the time dedicated to detect natural estrus before insemination.

Although oocyte quality and fertilization have been investigated in numerous studies, only few studies focused on the effect of the maternal environment on sperm quality. The use of chemically defined efficient media for sperm capacitation in the IVF process and the success of intra-cytoplasmic sperm injection probably led us to underestimate the role of the female tract in selecting high-quality sperm and promoting sperm viability and fertilizing ability. Indeed, sperm migration in the female genital tract is a highly selective process. From millions of spermatozoa deposited in the vagina or uterus, only hundreds cross the utero-tubal junction (UTJ) and reach the oviduct [12, 13]. For this subpopulation of spermatozoa, major steps remain to be accomplished in the oviduct: migrate toward the oocyte and acquire fertilizing ability in a complex process of membrane destabilization and changes in motility, named capacitation [14], and to survive for sometimes hours to days up to the time of ovulation. During their journey through the oviduct, spermatozoa undergo many interactions with luminal epithelial cells and secreted components of oviductal cells such as proteins and extracellular vesicles take place. Those interactions represent crucial steps not only to enable fertilization but also to reduce the number of spermatozoa reaching the site of fertilization. In this review, six female modulators of sperm migration, survival and/or capacitation in the oviduct were individually considered: (1) the UTJ, (2) sperm binding sites on epithelial cells, (3) the presence of region-specific (ampulla vs. isthmus) promoters of capacitation, (4) the contractions of the oviduct, (5) the time of ovulation and (6) steroid hormonal environment. For each of those items, sperm migration and interactions with female fluids components and epithelial cells as well as the effects of these interactions on sperm physiology are reviewed. A particular attention is given to farm animals, in view of the large amount of data acquired in those species and the economic significance of reproductive biotechnologies and fertility in the livestock industry.

The UTJ selects a sperm sub-population to enter the oviduct

After uterine migration, spermatozoa are massively retained in the UTJ, which can be considered as the second major selective barrier beyond the cervix. In cows, the UTJ is characterized by a drastic restriction of the uterine diameter and by the presence of mucosal folds filling the lumen and forming impasses rather than channels to the isthmus, the lower part of the oviduct [15]. In sheep, 4 hours after insemination, increasing numbers of spermatozoa were observed from the base of the uterine horns to the UTJ but a sharp decline was seen in the oviducts [16]. More precisely, 42% of inseminated ram spermatozoa were found at the top of the uterine horn but only 0.5% in the isthmus [17, 18]. In cows, 18 h after mating, up to 20 000 spermatozoa were counted in the UTJ but only 2000 in the isthmus [12]. A large majority of spermatozoa reaching the UTJ are normal. In pigs, 98% of spermatozoa recovered from the UTJ lumen 24 h

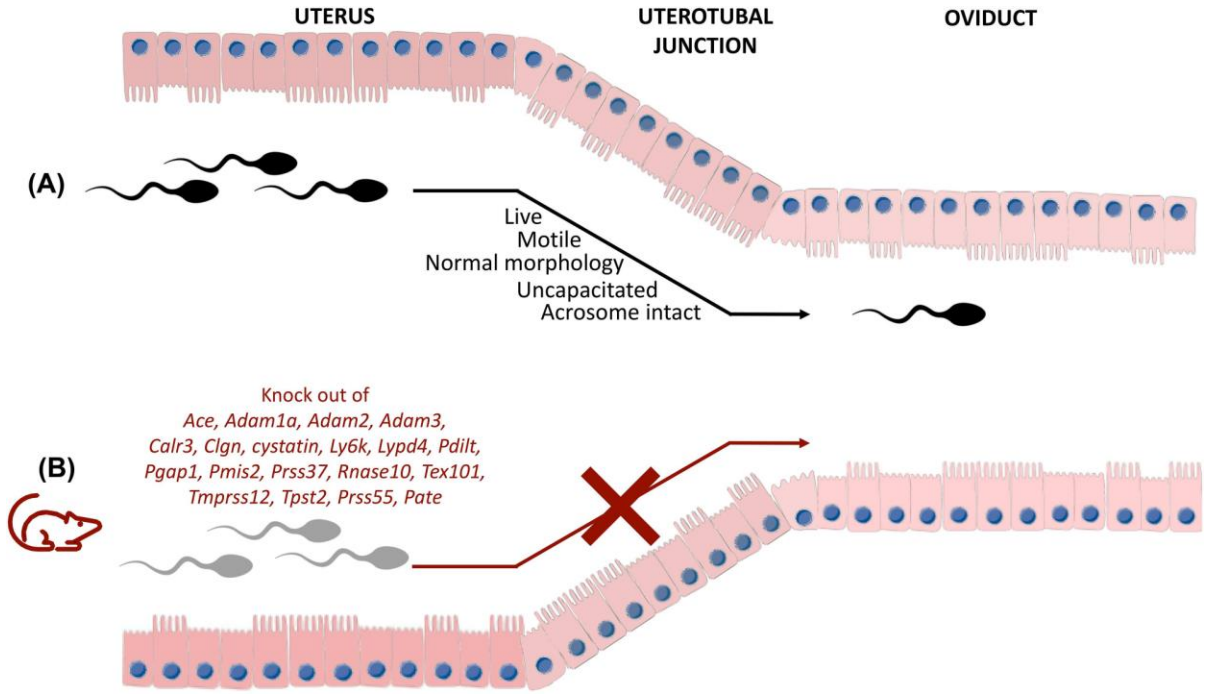

Figure 1. Sperm selection by the utero-tubal junction (UTJ) in mammals. (A) The UTJ reduces the number of spermatozoa reaching the oviduct [16–18] and selects a sub-population of live boar spermatozoa [20], motile rat spermatozoa [21], acrosome-intact mouse spermatozoa [22], uncapacitated hamster spermatozoa, and morphologically normal mouse spermatozoa [24]. (B) Thanks to KO models, a list of genes required for sperm passage through the UTJ was identified in mice [25–30].

after insemination were found to be morphologically normal compared with 70% in the uterine backflow [19]. The UTJ drastically reduces the number of sperm entering the oviduct and also operates as a selective barrier for sperm. In pigs, rats, mice, and hamsters, only live [20], motile [21], acrosome intact [22], uncapacitated [23], and morphologically normal [24] spermatozoa were found in the lower part of the oviduct. In farm animals, the mechanisms underlying the selective role of the UTJ are still largely unknown. However, the use of knock out (KO) mouse models allowed the identification of more than 15 genes necessary for sperm passage through the UTJ, including one coding for A Disintegrin and Metalloproteinase (*Adam*) 3, a glycosylated membrane protein normally present on the surface of spermatozoa, as well as several genes coding for proteins interacting with ADAM3 or required for the maturation of ADAM3 on sperm membrane [25–27] (Figure 1). However, whether ADAM3 interacts with specific proteins on luminal cells in the UTJ and how these interactions may allow sperm passage into the oviduct are still unknown. Furthermore, other genes required for sperm migration into the oviduct in mice, including *Ly6k*, *Pgap1*, and *Lypd4*, do not interfere with ADAM3 maturation on sperm, indicating that there are still unknown mechanisms that operate independently of *Adam3* [28–30].

Proteins on luminal cells in the UTJ and how these interactions may allow sperm passage into the oviduct are still unknown. Furthermore, other genes required for sperm migration into the oviduct in mice, including *Ly6k*, *Pgap1*, and *Lypd4*, do not interfere with ADAM3 maturation on sperm, indicating that there are still unknown mechanisms that operate independently of *Adam3* [28–30].

Spermatozoa bind to oviduct epithelial cells in the sperm reservoir

Sperm binding sites in the oviduct

The oviduct epithelium consists of ciliated and non-ciliated cells [31] and it is well established that spermatozoa bind preferentially to ciliated cells [32–34] (Figure 2). Sperm binding to oviduct epithelial cells (OECs) is reportedly mediated by proteins identified by protein affinity using purified sperm proteins and identification by mass spectrometry or immunohistochemistry [35, 36] or competition binding assays [37]. Sperm receptors identified on OECs include annexins A1, A2, A4, and A5 in cattle [35] and annexin A2 in pigs [36]; heat shock protein 5 (HSPA5) (also known as GRP78) in humans [38] and cattle [38], HSPA8 in cattle [39, 40] and pigs [40], HSP60 in cattle [41] and humans [42], and E-cadherin [43] and fibronectin [37] in cattle (Figure 3). Fibronectin was demonstrated to bind specifically to the integrin $\alpha 5\beta 1$ on bull sperm membrane [37]. Other proteins that coat sperm surface during maturation in the epididymis or at ejaculation were shown to be involved in the formation of the sperm reservoir: the binder of sperm proteins (BSPs) 1, 3, and 5 in cattle [44, 45], beta-defensin 126 (DEFB126) in macaque [46], and spermadhesin AQN1 [47] and lactadherin [48] in pigs. The use of a glycan array in pigs and cattle revealed that carbohydrates are primary species-specific components allowing sperm binding to the oviduct epithelium: boar sperm bind to the (6-Sialylated) N-acetyllactosamine and the Lewis X motifs, whereas bull sperm preferentially bind to the Lewis A motif [49]. Sialylated lactosamine was also abundantly observed on the apical side of OECs in pigs

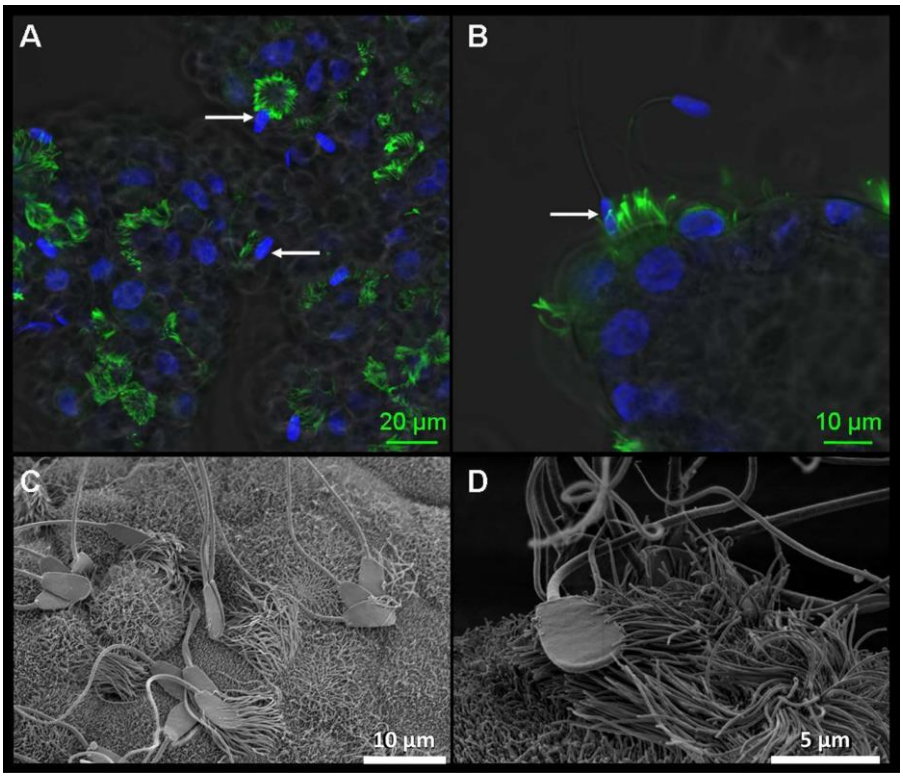

Figure 2. Confocal and scanning electron microscopy images of bull sperm interacting with bovine oviduct epithelial cells. Bovine oviduct epithelial spheroids were co-incubated with frozen–thawed bull sperm in vitro. (A) Nuclei of oviduct epithelial cells and spermatozoa (white arrows) are stained with Hoechst (blue, DNA) and cilia are immunolocalized using an anti-acetylated tubulin antibody (green, cilia). (B) Higher magnification showing sperm head (white arrow) interacting with cilia at the cell surface. (C, D) Scanning electron microscopy pictures showing tight interactions between bull sperm heads and epithelial ciliated cells.

[50]. Those sperm-binding glycans are probably linked to membrane glycoproteins present on OEC cilia; however, their exact link with sperm protein receptors reported above remains to be clarified.

Except for some bat species capable of storing sperm for months during hibernation, sperm storage in the tract of most mammalian females lasts generally no more than 2 days [11]. There is evidence from the observation of oviducts after mating or insemination that the main sites for sperm binding are located in the caudal part of the isthmus, as reported in cattle [12], rabbits [51], pigs [17, 18], and hamsters [52]. However, the surgical infusion of sperm through the ampulla ostium (or infundibulum) of heifers showed that spermatozoa became attached to epithelial cells in both the ampulla and isthmus, suggesting that the sperm reservoir is located in the isthmus because it is the first region encountered by sperm beyond the UTJ [32]. Some in vitro data demonstrated a higher number of spermatozoa bound to OECs recovered from the isthmus than from the ampulla [53–55]. However, most studies reported equivalent densities of sperm binding sites on oviductal explants and monolayers from both the ampulla and isthmus in cats [56], cattle [32], pigs [34, 57], and sheep [58]. In vivo, frequent detachments and reattachments of spermatozoa were observed in the isthmus but also in the ampulla of inseminated mice during contractions of the oviduct [59]. Therefore, sperm binding to OECs is not restricted to the caudal isthmus and may support important physiological functions in the remaining segments of the oviduct. Whether these successive binding and release from luminal epithelial cells occur throughout the oviduct in domestic mammals is currently not known.

Prerequisite to bind to OECs and impact on sperm physiology

After crossing the UTJ, only a sub-population of spermatozoa of high quality seem able to bind to oviduct luminal epithelial cells. In vitro studies showed that only viable [60], uncapacitated [61–63], and acrosome-intact [64, 65] spermatozoa bound to OECs in humans, pigs, horses, and cattle (Figure 3). It has been proposed that this selected subpopulation forms a "functional sperm reservoir" able to provide motile and capacitated spermatozoa at the time of ovulation [66]. Accordingly, binding to OECs in vitro maintained sperm viability and motility up to 24 h in pigs [34, 67], cattle [41, 64, 68], and humans [69, 70]. Furthermore, sperm attached to OECs had lower levels of membrane and acrosome disruption and also less chromatin abnormalities compared with unattached sperm in humans [60] cattle [64], pigs [57], and horse [61]. Thus, biding to OECs may be considered as a selective process for sperm. However, little is known about the local female factors regulating sperm binding to OECs. In particular, the proteins involved in sperm binding to the apical side of OECs are also present in the oviductal fluid (OF) and expected to compete with sperm binding sites on the cells. This binding competition may also play a role in sperm release from OECs at the time of ovulation (see section, The time of ovulation regulates sperm interactions with oviductal cells and capacitation).

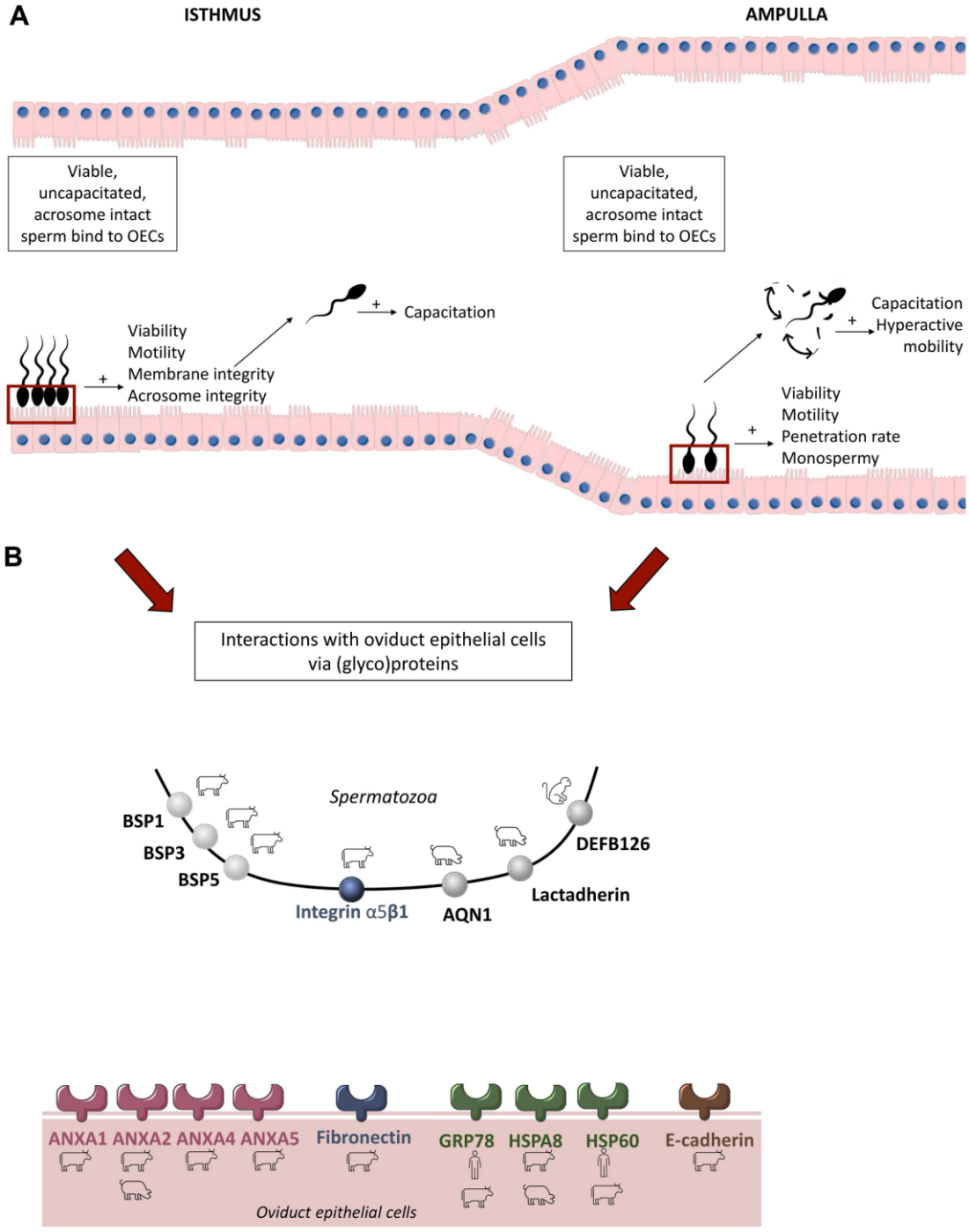

Figure 3. Mechanisms involved in sperm interactions with oviductal epithelial cells (OECs) and functional consequences on sperm physiology. After crossing the utero-tubal junction, a sub-population of sperm [60–65] is able to bind to OECs of the isthmus, forming a sperm reservoir [12, 17, 18, 41, 67], and also of the ampulla close to the fertilization site [32, 34, 56–58]. Binding to OECs maintains sperm viability [34, 41, 64, 67–70], membrane, and acrosome integrity [57, 60, 61, 64] and increases the rates of oocyte penetration and monospermy in vitro [68, 73–75] especially in the ampulla [112]. Subsequent release of spermatozoa from OECs induced sperm capacitation and hyperactive motility [74, 104–106, 109]. The insert below indicates the proteins on sperm head (up dark line) [37, 44–47] and on the apical side of OECs (down pink rectangle) [35–43] identified as playing a role in sperm binding to OECs.

Impact of sperm binding to OECs on fertilization

The surgical removal of the isthmus promoted polyspermy in pigs and rabbits [1, 2], leading to the hypothesis that the binding of spermatozoa to the isthmus followed by their progressive release around the time of ovulation provide a small population of spermatozoa around the oocyte(s) in a way that precludes polyspermy

[71, 72]. Accordingly, the pre-incubation of spermatozoa with OECs reduced polyspermy and increased IVF rates in pigs compared with no OECs [73]. Similarly in cattle, the pre-incubation of bull sperm with OECs maintained sperm fertilizing capacity for 30 h [68] and when co-incubated with in vitro matured oocytes, increased cleavage and blastocysts rates compared with the control group with no pre-incubation with OECs [74]. Recently, the use of an oviduct-on-a-chip system was also shown to improve monospermic fertilization in cattle [75] (Figure 3).

The contractions of the oviduct promote sperm progression toward the ampulla

Spermatozoa in the oviduct are submitted to contractions assumed to help their progression toward the ampulla. The injection of ink directly in the isthmus of mice highlighted an upward fluid flow created by isthmic contractions toward the ampulla [76]. After insemination, the chemical inhibition of oviductal contractions reduced the number of spermatozoa able to migrate through the isthmus in mice [77] and rabbits [78] and decreased the fertilization rate by 27% compared with untreated controls in mice [76, 77]. The number of spermatozoa in the ampulla was slightly reduced by the inhibition of contractions but to a lesser extent than in the isthmus [77], supporting the idea that oviductal contractions are required for sperm to migrate through the isthmus but that other factors like sperm motility may be more important for migration through the ampulla. In addition, live-cell imaging of mouse oviducts ex vivo revealed that sperm detach from both the isthmus and ampulla during strong contractions of the oviduct, suggesting that contractions of the oviduct may help sperm to successively bind and then be released from luminal epithelial cells in their progression toward the fertilization site [59].

Few studies examined the endocrine and local regulation of oviductal contractions. Oxytocin and prostaglandins are hormones with well-described roles in uterine contractions at the time of parturition [79, 80]. Their roles in sperm migration in the female genital tract have been little explored. The administration of oxytocin to women during the follicular phase of cycle was reported to amplify the uterine contractions and increase the transport of labeled particles toward the ipsilateral fallopian tube [81–83]. Nanomolar concentrations of prostaglandins E2 and F2α were detected in the oviduct of cows around the time of ovulation [84, 85] but further investigations are needed to understand their role in oviductal contractions and sperm transport.

Regions of the oviduct play different roles in regulating sperm physiology and interactions with OECs

Region-specific promoters of capacitation in the OF

Capacitation involves several mechanisms including membrane the efflux of membrane cholesterol, changes in intracellular concentrations of Ca^{2+} and Zn^{2+}, an increase in intracellular pH, and protein tyrosine phosphorylation. These changes prepare spermatozoa to undergo the acrosome reaction (AR) and fertilize an egg [14]. Another characteristic of capacitation is the change in the flagellar movements toward higher amplitude and asymmetrical beating, called hyperactivated motility [14]. There is evidence that sperm encounter region-specific changes in their capacitation status when progressing through the oviduct but with species-specific patterns (Figure 4). As observed by in vivo imaging in mice, most sperm undergo capacitation and the AR during their passage from the isthmus to the ampulla [86, 87]. This observation let to reconsider the former widely accepted concept that the zona pellucida of the oocyte causes the AR in vivo. Although the thinness and transparency of the mouse oviduct allow live-cell imaging of spermatozoa (with fluorescent acrosomes) within the oviductal lumen, most studies in domestic mammals used in vitro incubation of spermatozoa with OF (collected by oviduct cannulation), oviductal flushings (oEVs) or epithelial cells collected post-mortem, thus far from in vivo conditions. Ejaculated bull sperm incubated with ampullary OF fertilized more oocytes [88] and promoted a higher rate of monospermic fertilization [89] than sperm treated with isthmic OF. In another study in cattle, more oocytes were fertilized when sperm were pre-incubated in isthmic OF and oocytes in ampullary OF than if both gametes were incubated in ampullary OF [90], supporting the idea that sperm passage through the isthmus may be beneficial for in vivo fertilization. However, in rabbits [91] and sheep [92], when sperm were directly injected into the ampulla via surgical or intra-peritoneal insemination, fertilization still occurred (up to 100% of oocytes were fertilized) questioning the exact role of the isthmus in selecting spermatozoa for fertilization.

The OF is a complex mixture of molecules [93] among which proteins appear to play important modulating roles on sperm functions. There is evidence that in vitro OF-extracted proteins promote the viability and delay the AR of bull sperm in vitro [94]. Moreover, some proteins highly abundant or specifically present in the OF including oviductin (OVGP1), annexin A1, HSPA5, and myosin 9 interact with the sperm surface, at least in vitro [38, 95–97], but the functional roles of these interactions need to be clarified. To date, few studies examined the region-specific effect of the OF proteins on sperm. In buffalos, proteins extracted from the isthmic flushings maintained higher post-thaw sperm viability, motility, and acrosomal integrity than proteins from the ampullary flushings, suggesting a protective effect of isthmic flushings on cryopreserved sperm [98]. Sperm interactions with specific proteins in the ampulla and isthmus might explain region-specific effects of the OF on sperm. Bull spermatozoa incubated with biotinylated OF and subsequent western blot of sperm membrane proteins revealed no difference between ampullary and isthmic protein signals that associate with bull spermatozoa [99]. It is worth noting that several sperm-interacting proteins identified in the OF have also been identified in extracellular vesicles isolated from oEVs, also called oviductosomes [97, 100]. These oEVs have been recently reported to modulate sperm physiology via interactions with sperm membrane in cats [101], cattle [102], and pigs [103]. Furthermore, oEVs isolated from isthmic and ampullary flushings were both able to interact with bull sperm membrane [102]. In particular, oEVs from the ampulla induced a higher Ca^{2+} influx in sperm compared with oEVs from the isthmus [102], suggesting that oEVs may be involved in the regional effect of the oviduct on sperm capacitation. However, the concentrations of oEVs used in these experiments may not reflect the in vivo situation.

Region-specific modulation of sperm interactions with oviductal cells

There is evidence from in vitro studies in cattle that binding followed by progesterone- or heparin-induced release from OECs triggers rapid sperm membrane remodeling, hyperactivated motility, increase in intracellular Ca^{2+} and tyrosine phosphorylation, all associated with capacitation [74, 104–106]. However, it is still not known whether the binding to isthmic and/or ampullary cells is a

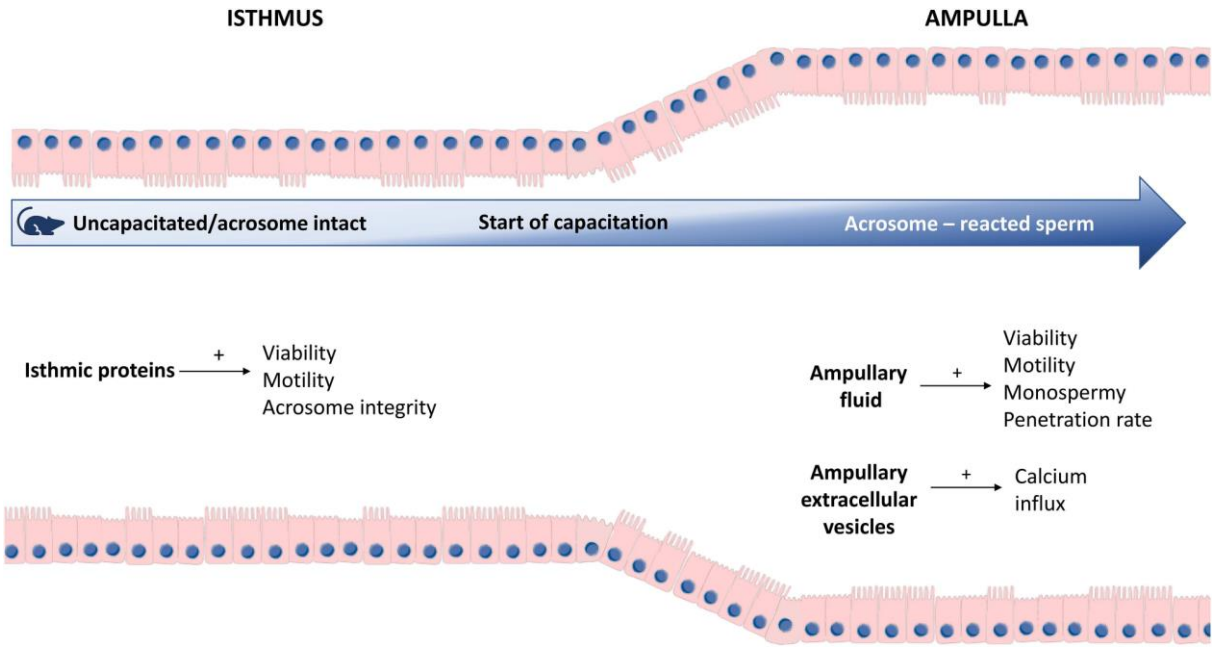

Figure 4. Region-specific effects of the oviductal fluid, proteins, and extracellular vesicles on sperm capacitation and fertilizing ability. In vivo observation in mice closely analyzes the functions of the lower and upper isthmus on sperm capacitation [86, 87], whereas in cattle, the effect of proteins purified from the isthmic OF were shown to have beneficial effect on sperm viability [98]. The ampulla stimulates capacitation [102], monospermy [89], and fertilization rate [88].

prerequisite for in vivo fertilization. Furthermore, the mechanisms of sperm detachment may differ depending on the oviductal region and proximity to the oocyte. In cattle, heparin-like GAGs are present in high abundance in the OF before ovulation [107] and heparin-binding sites are present on the BSP proteins covering the spermatozoa at ejaculation [108]. The addition of heparin to a bovine sperm-OECs co-culture was sufficient to release all sperm from isthmic but not ampullary cells; in the ampulla, an additional induction of sperm hyperactivated motility was necessary to release bull spermatozoa [109]. This suggests that sperm binding may be stronger in the ampulla than in the isthmus. In addition, the proportion of bull sperm exhibiting hyperactivated motility in vitro was higher in the presence of oviduct explants from the ampulla than from the isthmus [110]. Moreover, for the optimization of cryopreservation media in cattle, the addition of proteins from OECs apical membrane was shown to better maintain post-thaw sperm membrane integrity when using isthmic rather than ampullary cells [111]. In sheep, the penetration of oocytes and monospermic fertilization were promoted by the addition of ampullary but not isthmic OECs to the fertilization medium [112]. Taken together, these data indicate that at least in ruminants, the micro-environment of the ampulla may be more capacitating, whereas that of the isthmus may be more conducive to sperm survival.

The time of ovulation regulates sperm interactions with oviductal cells and capacitation

Sperm interactions with oviductal epithelial cells related to ovulation time

The role of the time of ovulation on sperm binding to OECs has also been studied in vitro but with a lack of consistency among studies and species. In cattle, pigs, and horses, sperm binding to oviduct explants was not affected by the time relative to ovulation (pre-ovulatory vs. post-ovulatory) at which the tissues were collected [32, 55, 57]. However, in one study in cattle, a higher number of sperm bound to pre-ovulatory compared with post-ovulatory oviduct explants [33]. Moreover, sperm were found to bind preferentially to oviduct explants from the follicular (or pre-ovulatory) phase compared with the luteal phase of cycle in horses [55]. Unexpectedly in sheep, more sperm bound to OECs from the luteal phase rather than those from the follicular phase of cycle after only 1 hour of co-incubation, whereas after 24 h, an opposite pattern was observed [58]. To our knowledge, only one study in pigs evaluated the capacity of sperm to bind in vivo to the epithelium of UTJ and oviduct out of the periovulatory period [113]. Surprisingly, sperm were found more numerous in the UTJ and oviduct when the intrauterine insemination was performed at mid-luteal than at pre- or post-ovulatory phases of the cycle [113]. However, a higher rate of sperm presented abnormalities or was damaged at the luteal phase, suggesting that this stage did not offer a suitable environment for the maintenance of sperm viability in the oviduct [113]. The oviducts being inaccessible in vivo by current techniques of imaging, the timing of sperm release from the isthmic sperm reservoir related to the time of ovulation was studied after the synchronization or monitoring of ovulation and subsequent collection of oviducts by surgery or post-mortem. A redistribution of spermatozoa from the isthmus toward the ampulla around ovulation time was observed in several mammals including the macaque [114], mouse [59], rabbit [51], and hamster [115]. In pigs, the proportion of sperm in the caudal isthmus was more important at the pre-ovulatory phase, whereas around the time of ovulation, an increasing number of spermatozoa were found in the upper isthmus [13]. In cattle, several compounds increasing in concentrations around the time of ovulation in the OF, including the steroid hormone progesterone, [74], heparin-like sulfated GAGs [109], fibronectin [37], and anandamide [116] have been shown

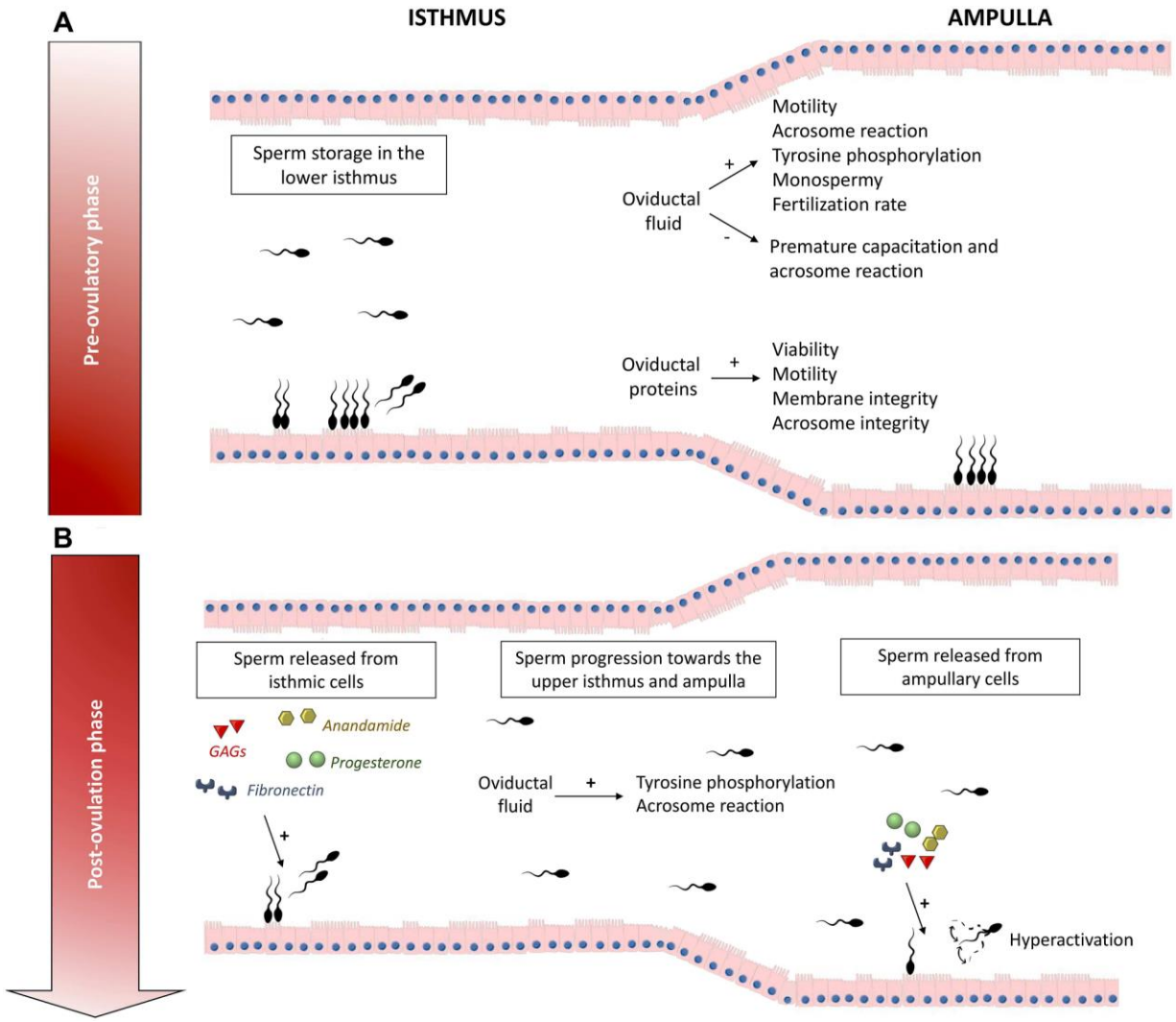

Figure 5. Summarized effects of ovulation time on sperm storage, interactions with luminal epithelial cells, and capacitation in the oviduct. The pre-ovulatory OF [4, 5, 33, 93, 113–115] and its proteins [123] display mostly beneficial effects on sperm physiology and fertilizing ability. Around the time of ovulation, spermatozoa are progressively released from OECs [51, 59, 114, 115] via the action of chemical compounds, including progesterone [37, 74, 109, 116] rising in concentrations in the OF at ovulation time and thanks to sperm hyperactivated motility [109]. The post-ovulatory OF usually promotes capacitation and acrosome reaction [4, 5, 33, 93, 113–115].

to induce sperm release from OECs in vitro and were proposed as sperm releasing factors from the sperm reservoir acting alone or in combination (Figure 5).

Sperm capacitation related to ovulation time

The co-incubation of sperm with OF collected at different times in the cycle has been used to study the regulatory effect of ovulation on sperm physiology. In cattle, the motility, viability [117], tyrosine phosphorylation, and AR [118] of cryopreserved bull sperm were promoted by OF from the follicular/pre-ovulatory phase compared with OF from the luteal phase of the cycle. However, in the same species, another study pointed out that the peri-ovulatory (non-luteal) OF reduced overall sperm motility compared with the luteal OF in vitro [88]. In addition, samples of periovulatory and luteal oviduct fluid samples induced similar rates of ARs in fresh bull sperm [88]. It is likely that these discrepancies are due to differences in pre-capacitation status between cryopreserved and fresh sperm as well as the various sources of OF (cannulation vs. post-mortem collection) used for co-incubation.

In pigs, fresh sperm incubated for 3 h with peri-ovulatory OF (combination of late follicular and early luteal phases) displayed reduced tyrosine phosphorylation levels and protein kinase A activity during capacitation compared with OF from the late luteal phase of cycle [5]. In addition, the peri-ovulatory OF displayed an inhibitory effect on sperm ARs which was not observed with the luteal OF [5]. Differential effects of the OF on sperm physiology were also detected between closer stages around ovulation time (pre vs. post-ovulatory) [119, 120]. A 5-min incubation of frozen–thawed boar sperm with OF collected just before ovulation was sufficient to increase significantly the proportion of motile sperm, whereas the post-ovulatory OF did not affect sperm motility [119]. In cattle,

after 2 h of co-incubation, the proportion of viable sperm with destabilized membrane or acrosome reacted were higher with OF from late follicular compared with OF from early luteal stages [120]. Furthermore, after only 15 to 30 min of incubation, the percentage of tyrosine-phosphorylated sperm was higher in OF collected before rather than after ovulation, and this difference was still visible after 1 h of incubation [119]. These data suggest that at least in pigs and cattle, acute changes in the oviductal environment occur around the time of ovulation in the oviductal environment that may rapidly change sperm motility and process of capacitation.

The OF was also reported to differentially promote sperm fertilizing ability according to the time relative to ovulation. In cattle, the percentage of fertilized oocytes was greater after 5 h of co-incubation with non-luteal rather than luteal ampullary OF [88]. In pigs, polyspermy is a frequent issue during IVF. In this species, the addition of OF from follicular or early luteal, but not from the late luteal phase, to the IVF medium promoted monospermic fertilization [5]. A favorable effect of the pre-ovulatory OF on the oocyte contributes to this result as the pre-incubation of pig oocytes in peri-ovulatory OF was reported to increase the hardening of the zona pellucida, leading to a reduction of polyspermy and improvement of IVF outcomes in pigs [4, 121].

The horse is another species for which an efficient IVF protocol still needs to be developed. In this species, the pre-incubation of sperm with porcine pre-ovulatory OF succeeded in obtaining oocyte penetration rates between 4 and 12% compared with no penetration at all with post-ovulatory OF [122], showing stage-specific effects on sperm capacitation under heterospecific conditions.

Proteins in the OF may play important roles in the regulation of sperm functions depending on the stage in the estrous cycle. In this regard, proteins extracted from buffalo OF at estrus (pre-ovulatory phase of cycle) maintained higher post-thaw sperm viability, motility, acrosome, and membrane integrity compared with proteins collected at the luteal phase of cycle [123]. Using mass spectrometry, we recently identified 27 sperm-interacting proteins following incubation of bull sperm with OF collected either before or after ovulation, and during the luteal phase of cycle [97]. Among those proteins, eight interacted with sperm only at the post-ovulatory and luteal but not at the pre-ovulatory phases of cycle. Furthermore, 14 proteins were shared between stages but with variable abundance on sperm: this protein abundance was on average twice higher during the luteal phase than at post-ovulatory phase of cycle, and again twice higher at the post-ovulatory than at the pre-ovulatory phase of cycle [97]. On the other hand, only one protein, the oviduct-specific glycoprotein 1 or OVGP1, was more abundant on sperm at the pre-ovulatory than at other phases of cycle. This suggests that ovulation triggers changes in sperm-OF protein interactions that may modulate the time-specific release of sperm from the oviductal reservoir as well as the initiation of sperm capacitation.

Steroid hormones locally regulate sperm migration, capacitation, and release from the oviduct reservoir

Sperm exposure and receptivity to steroid hormones in the oviduct

In most mammals, the circulating concentrations of estrogens, in particular of estradiol (E2), are elevated during the pre-ovulatory period and drop after ovulation, whereas the levels of progesterone (P4) rise locally in the pre-ovulatory follicle after the Luteinizing Hormone (LH) peak and become detectable in the circulating blood a few days after ovulation [124]. Ovarian steroid hormones diffuse locally and may be transported by vascular transfer to various parts of the genital tract [125]. In vivo, both P4 and E2 are present in the OF around the time of ovulation but at species-specific concentrations. Nanomolar concentrations of P4 were found in the OF ipsilateral to ovulation in mares [126] and cows [127] and in both oviducts of sows [4] around the time of ovulation. Levels of E2 in the OF were highest at the pre-ovulatory stage and measured at picomolar concentrations in cows [127] and sows [4], and at nanomolar concentrations in mares [126]. In monovular species such as cattle and horses, steroid hormones were also found at much higher levels in the side of ovulation than in the contralateral side [126, 127], showing that there is an important diffusion of steroid hormones from the ovary to the proximal oviduct. Therefore, although little is known about the biological activity of steroid hormones in the OF, spermatozoa may be exposed to relatively high concentrations of P4 and E2 during their migration in the oviduct. Atypical P4 receptors were detected in acrosomal and equatorial regions of sperm head as well as in the midpiece of sperm in pigs [128] and sheep [129], suggesting a non-genomic effect of this hormone on spermatozoa. Moreover, estrogen receptors were identified on sperm acrosomal region, midpiece, and tail in humans [130], pigs [131], and mice [132].

Sperm migration according to the steroid hormonal environment

Experiments conducted by Hunter *et al*. in pigs [3, 133] provided evidence that P4 plays a role in sperm transport toward the site of fertilization. The surgical microinjection of nanomolar concentrations of exogenous P4 or of P4-rich follicular fluid into the isthmus of inseminated gilts significantly increased the number of sperm around the oocytes and the rate of polyspermy compared with control animals [3, 133]. It was suggested that P4 inhibits oviductal contractions and enlarged the oviductal lumen, leading to less selective sperm migration. More recently, P4 was proposed as a chemoattractant for sperm cells in vivo. The cumulus cells surrounding the oocyte produce and secrete P4 [134, 135]. Co-incubation of rabbit sperm with oocyte-cumulus complexes (COCs) revealed that sperm migrate preferentially toward the cumulus cells [136]. In addition, the suppression of P4 action inhibited sperm chemoattractive response [136]. Similarly, human spermatozoa subjected to a picomolar gradient of P4 orient themselves toward the highest concentration of P4 [137, 138]. Moreover, a higher percentage of capacitated sperm with intact DNA and low levels of oxidative stress were found among human spermatozoa oriented toward the P4 gradient compared with non-attracted sperm [139], suggesting that P4 positive chemotaxis selects a subpopulation of high-quality spermatozoa. The chemotactic response of human sperm toward this hormone was optimal at P4 picomolar concentrations (1–100 pM), but a small population of sperm was also able to chemotactically respond to higher P4 levels up to 1 µM [138]. To our knowledge, the concentration of P4 in the human OF has not been reported to date. However, since P4 was measured in the OF of several mammals at nanomolar concentrations [4, 126, 127], the existence of a sperm chemotaxis toward picomolar levels of P4 in vivo remains questionable.

Sperm physiology according to the steroid hormonal environment

The effects of physiological (i.e. intra-oviductal) concentrations of P4 and E2 on spermatozoa were studied in various mammals (Figure 6).

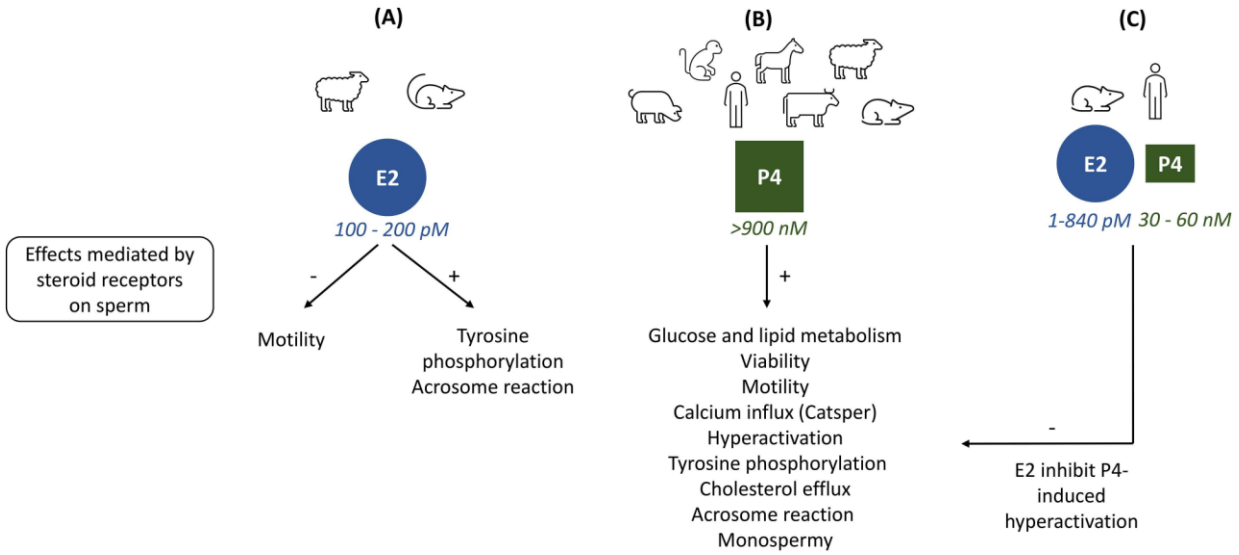

Figure 6. Effects of intra-oviductal concentrations of 17β-estradiol (E2) and progesterone (P4) on sperm physiology in vitro. (A) Treatment with picomolar concentrations of E2 inhibits sperm motility in sheep [129], promotes capacitation in mice [132], and acrosome reaction in sheep [129]. (B) Nanomolar concentrations of P4 found after ovulation have beneficial effect on sperm capacitation in pigs [4, 128, 142, 145], human [140, 143, 144, 148], cattle [105], sheep [129], in horse [129], in macaques [147], and in hamster [141]. (C) A suppressive effect of picomolar levels of E2 on P4-induced hyperactivation was reported in hamster [149, 150] and humans [148].

Exposure of boar sperm to P4 concentrations ranging from 10 to 100 nM was reported to rapidly enhance sperm viability and sperm glucose and lipid metabolism compared with untreated controls [128]. In addition, P4 at 50 nM was found to stimulate within 30 min the progressive motility of human sperm after cryopreservation [140], suggesting a significant role of P4 on sperm motility. Accordingly, sperm hyperactivated motility was shown to be promoted by nanomolar concentrations of P4 in cattle [105] and hamster [141]. The depletion of extracellular calcium in the medium or the inhibition of the sperm-specific calcium channels CatSper (Cation channel of Sperm) suppressed the promoting effect of P4 on sperm hyperactivated motility, indicating that the P4-mediated hyperactive motility relies on calcium influx via CatSper [105, 142]. Furthermore, in several mammals including pigs, sheep, and humans, P4 up to 900 nM in concentrations induced calcium influx [142–144], cholesterol efflux [128], and tyrosine phosphorylation [128, 129, 145], indicating a promoting role of P4 on sperm capacitation. P4 was also shown to promote AR in several mammals including pigs [128, 145], horse [146], sheep [129], macaque [147], and humans [148]. In pigs, the addition of P4 at concentrations found in the pre-ovulatory OF (8 nM) in the fertilization medium was shown to favor monospermic fertilization compared with the control group [4].

The reported effects of intra-oviductal concentrations of E2 on sperm physiology were less numerous and consistent. Exposure to picomolar concentrations of E2 had no effect on sperm motility in hamster [149] but reduced total sperm motility in sheep [129] compared with controls. At 200 pM, E2 promoted tyrosine phosphorylation on sperm head in mice [132]. Incubation of ram sperm with 100 pM of E2 increased the percentage of acrosome reacted sperm compared with controls [129]. This suggests positive but species-specific effects of E2 on mammalian sperm capacitation. Furthermore, in vitro studies reported a suppressive effect of E2 on P4 action on sperm. For instance, in hamster, the addition of picomolar concentrations of E2 to an incubation medium containing nanomolar concentrations of P4 inhibited sperm hyperactivation compared with P4 alone [148–150] (Figure 6). As both hormones are present at the fertilization site in vivo, the combined effects of E2 and P4 at physiological concentrations on sperm capacitation require further investigation.

Sperm interactions with oviductal cells according to the steroid hormonal environment

Domestic mammalian females become receptive to mating during estrus, in parallel with increasing picomolar concentrations of E2 in the oviduct lumen [4, 126, 127]. Accordingly, hormonal treatment of porcine OECs with physiological concentrations of P4 and E2 mimicking the estrous phase of the cycle led to an increase in sperm binding to OECs compared with a simulated luteal phase of the cycle [151]. Some studies examined the specific effects of steroid hormones on sperm-oviduct interactions, with divergent results among species (Figure 7). In pigs, a 48-h pre-exposure of OEC explants to 100 ng/mL (i.e. 367 nM) of E2 did not affect numbers of sperm bound and released from oviductal cells over time [152]. However, another study reported a rapid increase in the number of spermatozoa bound to oviductal explants after the addition of 70 pg/mL (257 pM) of E2 to the incubation medium [34], suggesting that E2 may promote the ability of OECs to bind sperm cells in a short-term manner. On the other hand, in cattle, a pretreatment of OECs monolayers with 100 pg/mL or 100 ng/mL of E2 temporally reduced the numbers of sperm able to bind to OECs compared with untreated controls but this effect lasted no more than 1 h [74] (Figure 7). These data suggest that E2, although highly present in the OF before ovulation, may not have a strong impact on sperm binding to the sperm reservoir.

Once spermatozoa bind to OECs in the isthmus in vivo, a progressive release of sperm has been observed around the time of

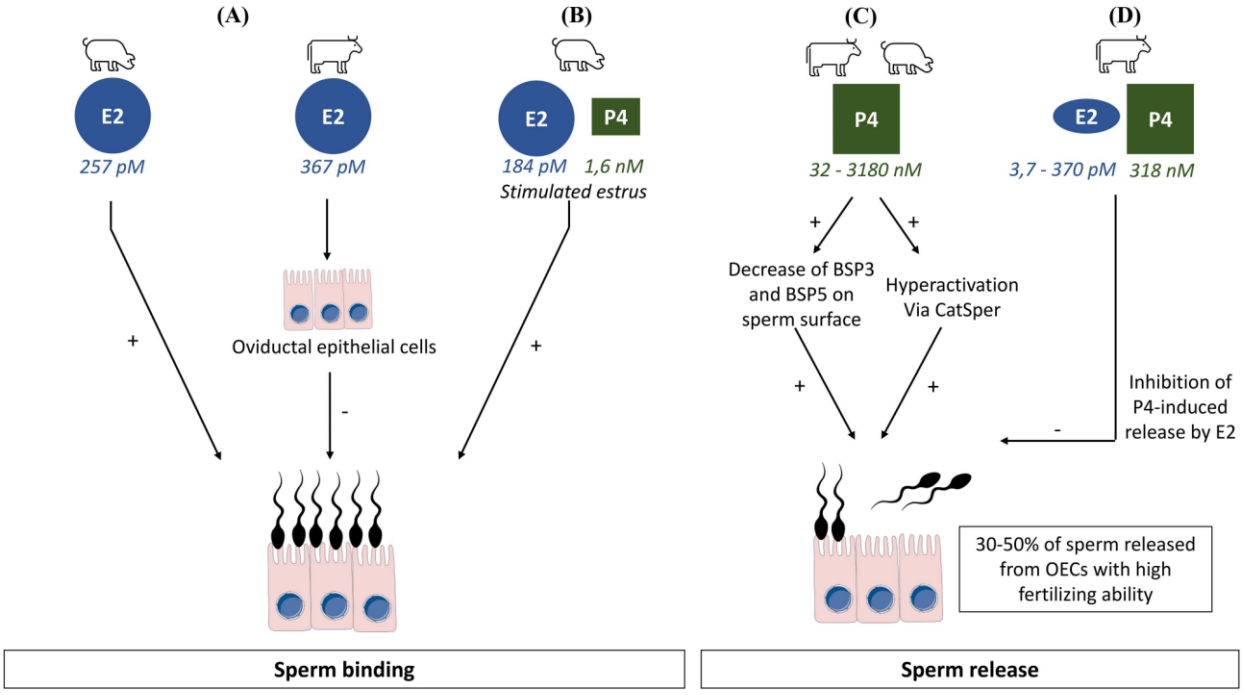

Figure 7. Regulation of sperm interactions with oviductal epithelial cells (OECs) by physiological concentrations of 17β-estradiol (E2) and progesterone (P4). (A) Treatment with E2 shortly increases in pigs [34] or reduces in cattle [74] the ability of OECs to bind spermatozoa. (B) Pretreatment of OECs with P4 and E2 at concentrations mimicking estrus promotes sperm binding in pigs [151]. (C) Nanomolar concentrations of P4 induce sperm release from OECs in cattle [25, 74, 104, 105] and pigs [142]. (D) E2 has no direct effect on sperm release but inhibits P4-induced release in cattle [74] .

ovulation in vivo [66, 153]. Therefore, it is assumed that sperm release from isthmic cells occurs in parallel with increasing local concentrations of P4. A specific role of P4 on sperm release from OECs was recently shown in the bovine [74, 105] and porcine [142] species. The addition of nanomolar concentrations of P4 to co-cultures induced the release of 30–50% of bull sperm [74] and around 50% of boar sperm bound to oviductal cells [142]. It was shown that P4 increases sperm intracellular calcium levels and induces hyperactivated motility at the time of sperm detachment from OECs within minutes in cattle [105] and pigs [142]. In addition, P4 was shown to induce an increase in sperm membrane fluidity and significant changes in bull sperm lipidomic and proteomic composition at the time of sperm release from bovine OEC monolayers [104]. Among those proteomic changes, a significant decrease in the abundance of BSPs 3 and 5, two seminal proteins involved in sperm binding to OECs and capacitation, were demonstrated [25, 104]. In this regard, the sperm population collected after the sequential binding to OEC and subsequent P4-induced release displayed higher fertilizing ability than controls in cattle [74]. Therefore, P4 seems to play important roles in the induction of sperm release from OECs at ovulation time, which in turn induces sperm hyperactivated motility and capacitation leading to improved fertilizing ability.

Although E2 showed no direct effect on bull sperm release from bovine OEC monolayers, this hormone was shown to inhibit the P4-mediated release of sperm from OECs in a dose-dependent manner [74]. Thus, it is likely that both P4 and E2 regulate sperm release from the sperm reservoir around the time of ovulation. It is to note that in pigs and cattle, up to 70% of spermatozoa remained bound to OECs after the action of physiological concentrations of P4 in vitro [74, 142], suggesting that only a subpopulation of sperm are P4-responsive and able to be released from the sperm reservoir toward the oocyte.

Conclusion

After uterine migration, spermatozoa are sequentially exposed to the UTJ, isthmus, and ampulla, each region having specific properties in terms of contractions, ability to bind sperm, and molecular secretions. The mice KO models have provided valuable data on requirements for sperm to enter the oviduct, yet, a more precise anatomical and molecular characterization of the UTJ and of its selective role on sperm progression is still needed in domestic mammals. The behavior of spermatozoa within the oviduct has become clearer in mice thanks to ex vivo live-cell imaging but these pictures are rather scarce in domestic species. Therefore, the exact roles played by each part of the oviduct in the selection of a subpopulation of top quality spermatozoa around the oocyte still remain to be elucidated. Sperm are also exposed to time-specific changes during their journey. Recent data demonstrated important changes in the oviductal miroenvironment triggered by ovulation, which in turn may regulate sperm lifespan and ability to fertilize. However, it is still difficult to figure what is really going on in the isthmus when spermatozoa enter the oviduct either days before or just after ovulation. Because of the limited access to oviducts in live animals, in vitro studies were mostly used to dissect sperm-oviduct interactions. We pointed out multiple discrepancies between studies, which could

be due to the partial loss of the morphological and molecular characteristics of OECs in vitro. More physiological models able to mimic the oviduct microenvironment throughout the estrous cycle are being developed and will be helpful to proceed further on those unsolved questions.

Acknowledgments

We are grateful to Marc Chodkiewicz for the critical reading of this paper. We thank Maryse Meurisse and Marie-Claire Blache from the imaging platform PIC (INRAe, Nouzilly, France) and Thierry Meylheuc from the imaging facility MIMA2 (INRAe, Jouy-en-Josas, France) for their help with confocal and scanning electronic microscopy images. MSD thanks the CNRS for full-time delegation in the PRC Unit.

Conflict of interest: The authors declare no conflict of interest.

References

1. Hunter RH, Léglise PC. Polyspermic fertilization following tubal surgery in pigs, with particular reference to the rôle of the isthmus. *J Reprod Fertil* 1971; **24**:233–246.
2. Hunter RH, Léglise PC. Tubal surgery in the rabbit: fertilization and polyspermy after resection of the isthmus. *Am J Anat* 1971; **132**:45–52.
3. Hunter RHF. Local action of progesterone leading to polyspermic fertilization in pigs. *Reproduction* 1972; **31**:433–444.
4. Ballester L, Romero-Aguirregomezcorta J, Soriano-Úbeda C, Matás C, Romar R, Coy P. Timing of oviductal fluid collection, steroid concentrations, and sperm preservation method affect porcine in vitro fertilization efficiency. *Fertil Steril* 2014; **102**:1762–1768.e1.
5. Zapata-Carmona H, Soriano-Úbeda C, París-Oller E, Matás C. Periovulatory oviductal fluid decreases sperm protein kinase A activity, tyrosine phosphorylation, and in vitro fertilization in pig. *Andrology* 2019; **8**:756–768.
6. Coy P, Avilés M. What controls polyspermy in mammals, the oviduct or the oocyte? *Biol Rev* 2009; **85**:593–605.
7. Yao T, Suzuki R, Furuta N, Suzuki Y, Kabe K, Tokoro M, Sugawara A, Yajima A, Nagasawa T, Matoba S, Yamagata K, Sugimura S. Live-cell imaging of nuclear–chromosomal dynamics in bovine in vitro fertilised embryos. *Sci Rep* 2018; **8**:7460.
8. Viuff D, Rickords L, Offenberg H, Hyttel P, Avery B, Greve T, Olsaker I, Williams JL, Callesen H, Thomsen PD. A high proportion of bovine blastocysts produced in vitro are Mixoploid. *Biol Reprod* 1999; **60**:1273–1278.
9. Morris LHA. The development of in vitro embryo production in the horse. *Equine Vet J* 2018; **50**:712–720.
10. Chastant-Maillard S, Chebrout M, Thoumire S, Saint-Dizier M, Chodkiewicz M, Reynaud K. Embryo biotechnology in the dog: a review. *Reprod Fertil Dev* 2010; **22**:1049.
11. Holt WV, Fazeli A. Sperm storage in the female reproductive tract. *Annu Rev Anim Biosci* 2016; **4**:291–310.
12. Heyman Y, Levasseur. Transport des spermatozoïdes dans les voies génitales. In: *L'utérus de la vache. Anatomie, Physiologie, Pathologie*. 1981; **5**:121–133.
13. Mburu JN, Einarsson S, Lundeheim N, Rodriguez-Martinez H. Distribution, number and membrane integrity of spermatozoa in the pig oviduct in relation to spontaneous ovulation. *Anim Reprod Sci* 1996; **45**:109–121.
14. Leemans B, Stout TAE, De Schauwer C, Heras S, Nelis H, Hoogewijs M, Van Soom A, Gadella BM. Update on mammalian sperm capacitation: How much does the horse differ from other species? *Reprod Camb Engl* 2019; **157**:R181–R197.
15. Suarez SS. Regulation of sperm storage and movement in the mammalian oviduct. *Int J Dev Biol* 2008; **52**:455–462.
16. Druart X, Cognié J, Baril G, Clément F, Dacheux J-L, Gatti J-L. In vivo imaging of in situ motility of fresh and liquid stored ram spermatozoa in the ewe genital tract. *Reproduction* 2009; **138**:45–53.
17. Sumransap P, Tummaruk P, Kunavongkrit A. Sperm distribution in the reproductive tract of sows after intrauterine insemination. *Reprod Domest Anim* 2007; **42**:113–117.
18. Tummaruk P, Sumransap P, Techakumphu M, Kunavongkrit A. Distribution of spermatozoa and embryos in the female reproductive tract after unilateral deep intra uterine insemination in the pig. *Reprod Domest Anim* 2007; **42**:603–609.
19. García-Vázquez FA, Hernández-Caravaca I, Matás C, Soriano-Úbeda C, Abril-Sánchez S, Izquierdo-Rico MJ. Morphological study of boar sperm during their passage through the female genital tract. *J Reprod Dev* 2015; **61**:407–413.
20. Baker RD, Degen AA. Transport of live and dead boar spermatozoa within the reproductive tract of gilts. *Reproduction* 1972; **28**:369–377.
21. Gaddum-Rosse P. Some observations on sperm transport through the uterotubal junction of the rat. *Am J Anat* 1981; **160**:333–341.
22. Muro Y, Hasuwa H, Isotani A, Miyata H, Yamagata K, Ikawa M, Yanagimachi R, Okabe M. Behavior of mouse spermatozoa in the female reproductive tract from soon after mating to the beginning of Fertilization. *Biol Reprod* 2016; **94**:80.
23. Shalgi R, Smith TT, Yanagimachi R. A quantitative comparison of the passage of capacitated and uncapacitated hamster spermatozoa through the uterotubal junction. *Biol Reprod* 1992; **46**:419–424.
24. Krzanowska H. The passage of abnormal spermatozoa through the uterotubal junction of the mouse. *Reproduction* 1974; **38**:81–90.
25. Saint-Dizier M, Mahé C, Reynaud K, Tsikis G, Mermillod P, Druart X. Sperm interactions with the female reproductive tract: a key for successful fertilization in mammals. *Mol Cell Endocrinol* 2020; **516**:110956.
26. Fujihara Y, Miyata H, Ikawa M. Factors controlling sperm migration through the oviduct revealed by gene-modified mouse models. *Exp Anim* 2018; **67**:91–104.
27. Larasati T, Noda T, Fujihara Y, Shimada K, Tobita T, Yu Z, Matzuk MM, Ikawa M. Tmprss12 is required for sperm motility and uterotubal junction migration in mice. *Biol Reprod* 2020; **103**:254–263.
28. Fujihara Y, Okabe M, Ikawa M. GPI-anchored protein complex, LY6K/TEX101, is required for sperm migration into the oviduct and male fertility in Mice. *Biol Reprod* 2014; **90**:60.
29. Fujihara Y, Noda T, Kobayashi K, Oji A, Kobayashi S, Matsumura T, Larasati T, Oura S, Kojima-Kita K, Yu Z, Matzuk MM, Ikawa M. Identification of multiple male reproductive tract-specific proteins that regulate sperm migration through the oviduct in mice. *Proc Natl Acad Sci* 2019; **116**:18498–18506.
30. Ueda Y, Yamaguchi R, Ikawa M, Okabe M, Morii E, Maeda Y, Kinoshita T. PGAP1 knock-out mice show otocephaly and male infertility. *J Biol Chem* 2007; **282**:30373–30380.
31. Abe H. The mammalian oviductal epithelium: regional variations in cytological and functional aspects of the oviductal secretory cells. *Histol Histopathol* 1996; **11**:743–768.
32. Lefebvre R, Chenoweth PJ, Drost M, LeClear CT, MacCubbin M, Dutton JT, Suarez SS. Characterization of the oviductal sperm reservoir in cattle. *Biol Reprod* 1995; **53**:1066–1074.
33. Sostaric E, Dieleman SJ, van de Lest CHA, Colenbrander B, Vos PLAM, Garcia-Gil N, Gadella BM. Sperm binding properties and secretory activity of the bovine oviduct immediately before and after ovulation. *Mol Reprod Dev* 2008; **75**:60–74.
34. Suarez S, Redfern K, Raynor P, Martin F, Phillips D. Attachment of boar sperm to mucosal explants of oviduct in vitro: possible role in formation of a sperm reservoir. *Biol Reprod* 1991; **44**:998–1004.
35. Ignotz GG, Cho MY, Suarez SS. Annexins are candidate oviductal receptors for bovine sperm surface proteins and thus may serve to hold bovine sperm in the oviductal Reservoir. *Biol Reprod* 2007; **77**:906–913.
36. Teijeiro JM, Ignotz GG, Marini PE. Annexin A2 is involved in pig (*Sus scrofa*)sperm-oviduct interaction. *Mol Reprod Dev* 2009; **76**:334–341.

37. Osycka-Salut CE, Castellano L, Fornes D, Beltrame JS, Alonso CAI, Jawerbaum A, Franchi A, Díaz ES, Perez Martinez S. Fibronectin from oviductal cells fluctuates during the estrous cycle and contributes to sperm-oviduct interaction in cattle. *J Cell Biochem* 2017; **118**:4095–4108.
38. Marín-Briggiler CI, González-Echeverría MF, Munuce MJ, Ghersevich S, Caille AM, Hellman U, Corrigall VM, Vazquez-Levin MH. Glucose-regulated protein 78 (Grp78/BiP) is secreted by human oviduct epithelial cells and the recombinant protein modulates sperm–zona pellucida binding. *Fertil Steril* 2010; **93**:1574–1584.
39. Holt WV, Del Valle I, Fazeli A. Heat shock protein A8 stabilizes the bull sperm plasma membrane during cryopreservation: effects of breed, protein concentration, and mode of use. *Theriogenology* 2015; **84**:693–701.
40. Elliott RMA, Lloyd RE, Fazeli A, Sostaric E, Georgiou AS, Satake N, Watson PF, Holt WV. Effects of HSPA8, an evolutionarily conserved oviductal protein, on boar and bull spermatozoa. *Reproduction* 2009; **137**:191–203.
41. Boilard M, Reyes-Moreno C, Lachance C, Massicotte L, Bailey JL, Sirard M-A, Leclerc P. Localization of the chaperone proteins GRP78 and HSP60 on the luminal surface of bovine oviduct epithelial cells and their association with spermatozoa. *Biol Reprod* 2004; **71**:1879–1889.
42. Lachance C, Bailey JL, Leclerc P. Expression of Hsp60 and Grp78 in the human endometrium and oviduct, and their effect on sperm functions. *Hum Reprod* 2007; **22**:2606–2614.
43. Caballero JN, Gervasi MG, Veiga MF, Dalvit GC, Perez-Martínez S, Cetica PD, Vazquez-Levin MH. Epithelial cadherin is present in bovine oviduct epithelial cells and gametes, and is involved in fertilization-related events. *Theriogenology* 2014; **81**:1189–1206.
44. Gwathmey TM, Ignotz GG, Suarez SS. PDC-109 (BSP-A1/A2) promotes bull sperm binding to oviductal epithelium in vitro and may be involved in forming the oviductal sperm reservoir. *Biol Reprod* 2003; **69**:809–815.
45. Gwathmey TM, Ignotz GG, Mueller JL, Manjunath P, Suarez SS. Bovine seminal plasma proteins PDC-109, BSP-A3, and BSP-30-kDa share functional roles in storing sperm in the oviduct. *Biol Reprod* 2006; **75**: 501–507.
46. Tollner TL, Yudin AI, Tarantal AF, Treece CA, Overstreet JW, Cherr GN. Beta-Defensin 126 on the surface of macaque sperm mediates attachment of sperm to oviductal Epithelia. *Biol Reprod* 2008; **78**: 400–412.
47. Ekhlasi-Hundrieser M, Gohr K, Wagner A, Tsolova M, Petrunkina A, Töpfer-Petersen E. Spermadhesin AQN1 is a candidate receptor molecule involved in the formation of the oviductal sperm reservoir in the Pig. *Biol Reprod* 2005; **73**:536–545.
48. Silva E, Frost D, Li L, Bovin N, Miller DJ. Lactadherin is a candidate oviduct Lewis X trisaccharide receptor on porcine spermatozoa. *Andrology* 2017; **5**:589–597.
49. Miller DJ. Review: The epic journey of sperm through the female reproductive tract. *Animal* 2018; **12**:s110–s120.
50. Kadirvel G, Machado SA, Korneli C, Collins E, Miller P, Bess KN, Aoki K, Tiemeyer M, Bovin N, Miller DJ. Porcine sperm bind to specific 6-Sialylated biantennary glycans to form the oviduct Reservoir. *Biol Reprod* 2012; **87**:6.
51. Overstreet JW, Cooper GW, Katz DF. Sperm transport in the reproductive tract of the female rabbit: II. The sustained phase of transport. *Biol Reprod* 1978; **19**:115–132.
52. Ito M, Smith TT, Yanagimachi R. Effect of ovulation on sperm transport in the hamster oviduct. *J Reprod Fertil* 1991; **93**:157–163.
53. Baillie HS, Pacey AA, Warren MA, Scudamore IW, Barratt CL. Greater numbers of human spermatozoa associate with endosalpingeal cells derived from the isthmus compared with those from the ampulla. *Hum Reprod* 1997; **12**:1985–1992.
54. Raychoudhury SS, Suarez SS. Porcine sperm binding to oviductal explants in culture. *Theriogenology* 1991; **36**:1059–1070.
55. Thomas PG, Ball BA, Brinsko SP. Interaction of equine spermatozoa with oviduct epithelial cell explants is affected by estrous cycle and anatomic origin of explant. *Biol Reprod* 1994; **51**:222–228.
56. Henry F, Eder S, Reynaud K, Schön J, Wibbelt G, Fontbonne A, Müller K. Seminal fluid promotes in vitro sperm–oviduct binding in the domestic cat (Felis catus). *Theriogenology* 2015; **83**:1373–1380.
57. Petrunkina AM, Gehlhaar R, Drommer W, Waberski D, Töpfer-Petersen E. Selective sperm binding to pig oviductal epithelium in vitro. *Reprod Camb Engl* 2001; **121**:889–896.
58. Lloyd RE, Badia E, Fazeli A, Watson PF, Holt WV. Temporal dynamics of ram sperm binding and survival during 48-h coculture with oviducal epithelial cells. *Reprod Fertil Dev* 2008; **20**:835–845.
59. Chang H, Suarez SS. Unexpected flagellar movement patterns and epithelial binding behavior of mouse sperm in the Oviduct. *Biol Reprod* 2012; **86**:140, 1–8.
60. Ellington JE, Evenson DP, Wright RW, Jones AE, Schneider CS, Hiss GA, Brisbois RS. Higher-quality human sperm in a sample selectively attach to oviduct (fallopian tube) epithelial cells in vitro. *Fertil Steril* 1999; **71**:924–929.
61. Leemans B, Gadella BM, Sostaric E, Nelis H, Stout TAE, Hoogewijs M, Van Soom A. Oviduct binding and elevated environmental ph induce protein tyrosine phosphorylation in stallion spermatozoa. *Biol Reprod* 2014; **91**:13.
62. Petrunkina AM, Simon K, Günzel-Apel A-R, Töpfer-Petersen E. Kinetics of protein tyrosine phosphorylation in sperm selected by binding to homologous and heterologous oviductal explants: How specific is the regulation by the oviduct? *Theriogenology* 2004; **61**:1617–1634.
63. Luño V, López-Úbeda R, García-Vázquez FA, Gil L, Matás C. Boar sperm tyrosine phosphorylation patterns in the presence of oviductal epithelial cells: in vitro, ex vivo, and in vivo models. *Reproduction* 2013; **146**:315–324.
64. Gualtieri R, Talevi R. In vitro-cultured bovine Oviductal cells bind acrosome-intact sperm and retain this ability upon sperm release. *Biol Reprod* 2000; **62**:1754–1762.
65. Gimeno BF, Bariani MV, Laiz-Quiroga L, Martínez-León E, Von-Meyeren M, Rey O, Mutto AÁ, Osycka-Salut CE. Effects of in vitro interactions of oviduct epithelial cells with frozen–thawed stallion spermatozoa on their motility, viability and capacitation status. *Animals* 2021; **11**:74.
66. Hunter RH, Wilmut I. Sperm transport in the cow: Peri-ovulatory redistribution of viable cells within the oviduct. *Reprod Nutr Dev* 1984; **24**:597–608.
67. Yeste M, Lloyd RE, Badia E, Briz M, Bonet S, Holt WV. Direct contact between boar spermatozoa and porcine oviductal epithelial cell (OEC) cultures is needed for optimal sperm survival in vitro. *Anim Reprod Sci* 2009; **113**:263–278.
68. Pollard JW, Plante C, Allan King W, Hansen PJ, Betteridge KJ, Suarez SS. Fertilizing capacity of bovine sperm may be maintained by binding to oviductal epithelial cells. *Biol Reprod* 1991; **44**:102–107.
69. Morales P, Palma V, Salgado AM, Villalon M. Sperm interaction with human oviductal cells in vitro. *Hum Reprod* 1996; **11**:1504–1509.
70. Murray SC, Smith TT. Sperm interaction with fallopian tube apical membrane enhances sperm motility and delays capacitation. *Fertil Steril* 1997; **68**:351–357.
71. Coy P, García-Vázquez FA, Visconti PE, Avilés M. Roles of the oviduct in mammalian fertilization. *Reproduction* 2012; **144**:649–660.
72. Hunter RHF. Components of oviduct physiology in eutherian mammals. *Biol Rev* 2012; **87**:244–255.
73. Bureau M, Bailey JL, Sirard M-A. Influence of oviductal cells and conditioned medium on porcine gametes. *Zygote* 2000; **8**:139–144.
74. Lamy J, Corbin E, Blache M-C, Garanina AS, Uzbekov R, Mermillod P, Saint-Dizier M. Steroid hormones regulate sperm–oviduct interactions in the bovine. *Reproduction* 2017; **154**:497–508.
75. Ferraz MAMM, Henning HHW, Costa PF, Malda J, Melchels FP, Wubbolts R, Stout TAE, Vos PLAM, Gadella BM. Improved bovine

embryo production in an oviduct-on-a-chip system: Prevention of polyspermic fertilization and parthenogenic activation. *Lab Chip* 2017; **17**: 905–916.

76. Hino T, Yanagimachi R. Active peristaltic movements and fluid production of the mouse oviduct: Their roles in fluid and sperm transport and fertilization. *Biol Reprod* 2019; **101**:40–49.
77. Ishikawa Y, Usui T, Yamashita M, Kanemori Y, Baba T. Surfing and swimming of ejaculated sperm in the mouse Oviduct. *Biol Reprod* 2016; **94**:89.
78. Guidobaldi HA, Teves ME, Uñates DR, Giojalas LC. Sperm transport and retention at the fertilization site is orchestrated by a chemical guidance and oviduct movement. *Reproduction* 2012; **143**:587–596.
79. Maggi M, Baldi E, Susini T. Hormonal and local regulation of uterine activity during parturition: part I — The oxytocin system. *J Endocrinol Invest* 1994; **17**:739–739.
80. Maggi M, Baldi E, Susini T. Hormonal and local regulation of uterine activity during parturition: part II — The prostaglandin and adrenergic systems. *J Endocrinol Invest* 1994; **17**:757–770.
81. Kunz G, Beil D, Huppert P, Leyendecker G. Oxytocin–a stimulator of directed sperm transport in humans. *Reprod Biomed Online* 2007; **14**:32–39.
82. Wildt L, Kissler S, Licht P, Becker W. Sperm transport in the human female genital tract and its modulation by oxytocin as assessed by hysterosalpingoscintigraphy, hysterotonography, electrohysterography and Doppler sonography. *Hum Reprod Update* 1998; **4**: 655–666.
83. Zervomanolakis I, Ott HW, Hadziomerovic D, Mattle V, Seeber BE, Virgolini I, Heute D, Kissler S, Leyendecker G, Wildt L. Physiology of upward transport in the human female genital tract. *Ann N Y Acad Sci* 2007; **1101**:1–20.
84. Marey MA, Liu J, Kowsar R, Haneda S, Matsui M, Sasaki M, Shimizu T, Hayakawa H, Wijayagunawardane MPB, Hussein FM, Miyamoto A. Bovine oviduct epithelial cells downregulate phagocytosis of sperm by neutrophils: prostaglandin E2 as a major physiological regulator. *Reproduction* 2014; **147**:211–219.
85. Wijayagunawardane MP, Miyamoto A, Cerbito WA, Acosta TJ, Takagi M, Sato K. Local distributions of oviductal estradiol, progesterone, prostaglandins, oxytocin and endothelin-1 in the cyclic cow. *Theriogenology* 1998; **49**:607–618.
86. La Spina FA, Puga Molina LC, Romarowski A, Vitale AM, Falzone TL, Krapf D, Hirohashi N, Buffone MG. Mouse sperm begin to undergo acrosomal exocytosis in the upper isthmus of the oviduct. *Dev Biol* 2016; **411**:172–182.
87. Ded L, Hwang JY, Miki K, Shi HF, Chung J-J. 3D *in situ* imaging of female reproductive tract reveals molecular signatures of fertilizing spermatozoa in mice. *ELife* 2020; **9**:e62043.
88. Grippo AA, Way AL, Killian GJ. Effect of bovine ampullary and isthmic oviductal fluid on motility, acrosome reaction and fertility of bull spermatozoa. *J Reprod Fertil* 1995; **105**:57–64.
89. Topper EK, Killian GJ, Way A, Engel B, Woelders H. Influence of capacitation and fluids from the male and female genital tract on the zona binding ability of bull spermatozoa. *Reproduction* 1999; **115**: 175–183.
90. Way AL, Schuler AM, Killian GJ. Influence of bovine ampullary and isthmic oviductal fluid on sperm-egg binding and fertilization in vitro. *J Reprod Fertil* 1997; **109**:95–101.
91. Chang MC. Fertilizing capacity of spermatozoa deposited into the fallopian tubes. *Nature* 1951; **168**:697–698.
92. Mattner PE. Capacitation of ram spermatozoa and penetration of the ovine egg. *Nature* 1963; **199**:772–773.
93. Saint-Dizier M, Schoen J, Chen S, Banliat C, Mermillod P. Composing the early embryonic microenvironment: physiology and regulation of oviductal secretions. *Int J Mol Sci* 2020; **21**:223.
94. Boquest AC, Smith JF, Briggs RM, Duganzich DM, Summers PM. Effects of bovine oviductal proteins on bull spermatozoal function. *Theriogenology* 1999; **51**:583–595.
95. Abe H, Sendai Y, Satoh T, Hoshi H. Bovine oviduct-specific glycoprotein: a potent factor for maintenance of viability and motility of bovine spermatozoa in vitro. *Mol Reprod Dev* 1995; **42**:226–232.
96. King RS, Killian GJ. Purification of bovine Estrus-associated protein and localization of binding on Sperm. *Biol Reprod* 1994; **51**:34–42.
97. Lamy J, Nogues P, Combes-Soia L, Tsikis G, Labas V, Mermillod P, Druart X, Saint-Dizier M. Identification by proteomics of oviductal sperm-interacting proteins. *Reproduction* 2018; **155**:457–466.
98. Kumaresan A, Ansari MR, Garg A. Modulation of post-thaw sperm functions with oviductal proteins in buffaloes. *Anim Reprod Sci* 2005; **90**:73–84.
99. Rodríguez C, Killian G. Identification of ampullary and isthmic oviductal fluid proteins that associate with the bovine sperm membrane. *Anim Reprod Sci* 1998; **54**:1–12.
100. Almiñana C, Corbin E, Tsikis G, Alcântara-Neto AS, Labas V, Reynaud K, Galio L, Uzbekov R, Garanina AS, Druart X, Mermillod P. Oviduct extracellular vesicles protein content and their role during oviduct–embryo cross-talk. *Reproduction* 2017; **154**:253–268.
101. Ferraz M D AMM, Carothers A, Dahal R, Noonan MJ, Songsasen N. Oviductal extracellular vesicles interact with the spermatozoon's head and mid-piece and improves its motility and fertilizing ability in the domestic cat. *Sci Rep* 2019; **9**:9484.
102. Franchi A, Moreno-Irusta A, Domínguez EM, Adre AJ, Giojalas LC. Extracellular vesicles from oviductal isthmus and ampulla stimulate the induced acrosome reaction and signaling events associated with capacitation in bovine spermatozoa. *J Cell Biochem* 2019; **121**:2877–2888.
103. Alcântara-Neto AS, Schmaltz L, Caldas E, Blache M-C, Mermillod P, Almiñana C. Porcine oviductal extracellular vesicles interact with gametes and regulate sperm motility and survival. *Theriogenology* 2020; **155**:240–255.
104. Ramal-Sanchez M, Bernabo N, Tsikis G, Blache M-C, Labas V, Druart X, Mermillod P, Saint-Dizier M. Progesterone induces sperm release from oviductal epithelial cells by modifying sperm proteomics, lipidomics and membrane fluidity. *Mol Cell Endocrinol* 2020; **504**:110723.
105. Romero-Aguirregomezcorta J, Cronin S, Donnellan E, Fair S. Progesterone induces the release of bull spermatozoa from oviductal epithelial cells. *Reprod Fertil Dev* 2019; **31**:1463–1472.
106. Gualtieri R, Boni R, Tosti E, Zagami M, Talevi R. Intracellular calcium and protein tyrosine phosphorylation during the release of bovine sperm adhering to the fallopian tube epithelium in vitro. *Reproduction* 2005; **129**:51–60.
107. Bergqvist A-S, Rodríguez-Martínez H. Sulphated glycosaminoglycans (S-GAGs) and syndecans in the bovine oviduct. *Anim Reprod Sci* 2006; **93**:46–60.
108. Plante G, Prud'homme B, Fan J, Lafleur M, Manjunath P. Evolution and function of mammalian binder of sperm proteins. *Cell Tissue Res* 2016; **363**:105–127.
109. Ardon F, Markello RD, Hu L, Deutsch ZI, Tung C-K, Wu M, Suarez SS. Dynamics of bovine sperm interaction with epithelium differ between oviductal isthmus and ampulla. *Biol Reprod* 2016; **95**:90–90.
110. Lefebvre R, Suarez SS. Effect of capacitation on bull sperm binding to homologous oviductal epithelium. *Biol Reprod* 1996; **54**:575–582.
111. Prathalingam NS, Watson PF, Revell SG, Busby J, Holt WV. The response of bovine spermatozoa to bicarbonate and its use to assess the influence of added oviductal epithelial proteins on cryopreservation. *J Androl* 2006; **28**:407–415.
112. Dadashpour Davachi N, Zare Shahneh A, Kohram H, Zhandi M, Shamsi H, Hajiyavand AM, Saadat M. Differential influence of ampullary and isthmic derived epithelial cells on zona pellucida hardening and in vitro fertilization in ovine. *Reprod Biol* 2016; **16**:61–69.
113. Brüssow KP, Egerszegi I, Rátky J. Is the function of the porcine sperm reservoir restricted to the ovulatory period? *J Reprod Dev* 2014; **60**:395–398.
114. Ortíz ME, Gajardo G, León CG, Herrera E, Valdez E, Croxatto HB. Sperm migration through the female genital tract of the new world monkey Cebus apella. *Biol Reprod* 1995; **52**:1121–1128.

115. Smith TT, Koyanagi F, Yanagimachi R. Distribution and number of spermatozoa in the oviduct of the golden hamster after natural mating and artificial insemination. *Biol Reprod* 1987; **37**:225–234.
116. Gervasi MG, Osycka-Salut C, Sanchez T, Alonso C A I, Llados C, Castellano L, Franchi AM, Villalón M, Perez-Martinez S. Sperm release from the oviductal epithelium depends on ca(2+) influx upon activation of CB1 and TRPV1 by anandamide. *J Cell Biochem* 2016; **117**:320–333.
117. Abe H, Sendai Y, Satoh T, Hoshi H. Secretory products of bovine oviductal epithelial cells support the viability and motility of bovine spermatozoa in culture in vitro. *J Exp Zool* 1995; **272**:54–61.
118. Kumaresan A, Johannisson A, Humblot P, Bergqvist A-S. Effect of bovine oviductal fluid on motility, tyrosine phosphorylation, and acrosome reaction in cryopreserved bull spermatozoa. *Theriogenology* 2019; **124**:48–56.
119. Kumaresan A, González R, Johannisson A, Berqvist A-S. Dynamic quantification of intracellular calcium and protein tyrosine phosphorylation in cryopreserved boar spermatozoa during short-time incubation with oviductal fluid. *Theriogenology* 2014; **82**:1145–1153.
120. Küçük N, Lopes JS, Soriano-Úbeda C, Hidalgo CO, Romar R, Gadea J. Effect of oviductal fluid on bull sperm functionality and fertility under non-capacitating and capacitating incubation conditions. *Theriogenology* 2020; **158**:406–415.
121. Coy P, Canovas S, Mondejar I, Saavedra MD, Romar R, Grullon L, Matas C, Aviles M. Oviduct-specific glycoprotein and heparin modulate sperm-zona pellucida interaction during fertilization and contribute to the control of polyspermy. *Proc Natl Acad Sci* 2008; **105**:15809–15814.
122. Moros-Nicolás C, Douet C, Reigner F, Goudet G. Effect of cumulus cell removal and sperm pre-incubation with progesterone on in vitro fertilization of equine gametes in the presence of oviductal fluid or cells. *Reprod Domest Anim* 2019; **54**:1095–1103.
123. Kumaresan A, Ansari MR, Garg A, Kataria M. Effect of oviductal proteins on sperm functions and lipid peroxidation levels during cryopreservation in buffaloes. *Anim Reprod Sci* 2006; **93**:246–257.
124. Downey BR. Regulation of the estrous cycle in domestic animals — a review. *Can Vet J* 1980; **21**:301–306.
125. Einer-Jensen N, Hunter R. Counter-current transfer in reproductive biology. *Reproduction* 2005; **129**:9–18.
126. Nelis H, Bussche JV, Wojciechowicz B, Franczak A, Vanhaecke L, Leemans B, Cornillie P, Peelman L, Soom AV, Smits K. Steroids in the equine oviduct: Synthesis, local concentrations and receptor expression. *Reprod Fertil Dev* 2016; **28**:1390–1404.
127. Lamy J, Liere P, Pianos A, Aprahamian F, Mermillod P, Saint-Dizier M. Steroid hormones in bovine oviductal fluid during the estrous cycle. *Theriogenology* 2016; **86**:1409–1420.
128. De Amicis F, Santoro M, Guido C, Sisci D, Bruno R, Carpino A, Aquila S. Progesterone through progesterone receptors affects survival and metabolism of pig sperm. *Anim Reprod Sci* 2012; **135**:75–84.
129. Gimeno-Martos S, González-Arto M, Casao A, Gallego M, Cebrián-Pérez JA, Muiño-Blanco T, Pérez-Pé R. Steroid hormone receptors and direct effects of steroid hormones on ram spermatozoa. *Reproduction* 2017; **154**:469–481.
130. Rago V, Siciliano L, Aquila S, Carpino A. Detection of estrogen receptors ER-alpha and ER-beta in human ejaculated immature spermatozoa with excess residual cytoplasm. *Reprod Biol Endocrinol RBE* 2006; **4**:36.
131. Rago V, Aquila S, Panza R, Carpino A. Cytochrome P450arom, androgen and estrogen receptors in pig sperm. *Reprod Biol Endocrinol RBE* 2007; **5**:23.
132. Sebkova N, Cerna M, Ded L, Peknicova J, Dvorakova-Hortova K. The slower the better: How sperm capacitation and acrosome reaction is modified in the presence of estrogens. *Reproduction* 2012; **143**: 297–307.
133. Hunter RH, Petersen HH, Greve T. Ovarian follicular fluid, progesterone and Ca2+ ion influences on sperm release from the fallopian tube reservoir. *Mol Reprod Dev* 1999; **54**:283–291.
134. Schuetz AW, Dubin NH. Progesterone and prostaglandin secretion by ovulated rat cumulus cell-oocyte complexes. *Endocrinology* 1981; **108**:457–463.
135. Yamashita Y, Shimada M, Okazaki T, Maeda T, Terada T. Production of progesterone from de novo-synthesized cholesterol in cumulus cells and its physiological role during meiotic resumption of porcine oocytes. *Biol Reprod* 2003; **68**:1193–1198.
136. Guidobaldi HA, Teves ME, Uñates DR, Anastasía A, Giojalas LC. Progesterone from the cumulus cells is the sperm chemoattractant secreted by the rabbit oocyte cumulus complex. *PLoS One* 2008; **3**:e3040.
137. Oren-Benaroya R, Orvieto R, Gakamsky A, Pinchasov M, Eisenbach M. The sperm chemoattractant secreted from human cumulus cells is progesterone. *Hum Reprod* 2008; **23**:2339–2345.
138. Teves ME, Barbano F, Guidobaldi HA, Sanchez R, Miska W, Giojalas LC. Progesterone at the picomolar range is a chemoattractant for mammalian spermatozoa. *Fertil Steril* 2006; **86**:745–749.
139. Gatica LV, Guidobaldi HA, Montesinos MM, Teves ME, Moreno AI, Unates DR, Molina RI, Giojalas LC. Picomolar gradients of progesterone select functional human sperm even in subfertile samples. *Mol Hum Reprod* 2013; **19**:559–569.
140. Saymé N, Dite L, Krebs T, Kljajić M, Maas DHA. Positive effect of progesterone on motility and velocity of fresh, vitrified without permeable cryoprotectants and frozen with permeable cryoprotectants human spermatozoa. *Andrologia* 2018; **50**:e13133.
141. Noguchi T, Fujinoki M, Kitazawa M, Inaba N. Regulation of hyperactivation of hamster spermatozoa by progesterone: hyperactivation regulation by progesterone. *Reprod Med Biol* 2008; **7**:63–74.
142. Machado SA, Sharif M, Wang H, Bovin N, Miller DJ. Release of porcine sperm from oviduct cells is stimulated by progesterone and requires CatSper. *Sci Rep* 2019; **9**:19546.
143. Brenker C, Rehfeld A, Schiffer C, Kierzek M, Kaupp UB, Skakkebæk NE, Strünker T. Synergistic activation of CatSper Ca2+ channels in human sperm by oviductal ligands and endocrine disrupting chemicals. *Hum Reprod* 2018; **33**:1915–1923.
144. Strünker T, Goodwin N, Brenker C, Kashikar ND, Weyand I, Seifert R, Kaupp UB. The CatSper channel mediates progesterone-induced Ca 2+ influx in human sperm. *Nature* 2011; **471**:382–386.
145. Barboni B, Mattioli M, Seren E. Influence of progesterone on boar sperm capacitation. *J Endocrinol* 1995; **144**:13–18.
146. Lange-Consiglio A, Corradetti B, Perrini C, Bizzaro D, Cremonesi F. Leptin and leptin receptor are detectable in equine spermatozoa but are not involved in in vitro fertilisation. *Reprod Fertil Dev* 2016; **28**: 574.
147. Sumigama S, Mansell S, Miller M, Lishko PV, Cherr GN, Meyers SA, Tollner T. Progesterone accelerates the completion of sperm capacitation and activates CatSper Channel in spermatozoa from the rhesus Macaque. *Biol Reprod* 2015; **93**:113–117.
148. Vigil P, Toro A, Godoy A. Physiological action of oestradiol on the acrosome reaction in human spermatozoa. *Andrologia* 2008; **40**: 146–151.
149. Fujinoki M. Suppression of progesterone-enhanced hyperactivation in hamster spermatozoa by estrogen. *Reproduction* 2010; **140**:453–464.
150. Fujinoki M. Regulation and disruption of hamster sperm hyperactivation by progesterone, 17β-estradiol and diethylstilbestrol. *Reprod Med Biol* 2014; **13**:143–152.
151. Chen S, Einspanier R, Schoen J. In vitro mimicking of estrous cycle stages in porcine oviduct epithelium cells: estradiol and progesterone regulate differentiation, gene expression, and cellular Function. *Biol Reprod* 2013; **89**:54.
152. Bureau M, Bailey JL, Sirard M-A. Binding regulation of porcine spermatozoa to oviductal vesicles in vitro. *J Androl* 2002; **23**:188–192.
153. Hunter RHF, Barwise L, King R. Sperm transport, storage and release in the sheep oviduct in relation to the time of ovulation. *Br Vet J* 1982; **138**:225–232.

3.2. Modèles d'étude des interactions spermatozoïdes-oviducte

La majorité des résultats présentés dans la synthèse précédente ont été obtenus *in vitro.* Du fait des nombreux replis de la muqueuse, la lumière de l'oviducte présente une surface considérable pour les interactions cellulaires avec les gamètes puis l'embryon, mais cette lumière quasi-virtuelle n'est pas accessible à l'imagerie *in vivo,* même chez les grands herbivores. Comprendre la migration et la capacitation des spz dans l'oviducte de mammifères requiert donc de développer des modèles *in vitro*. Néanmoins, l'oviducte est un organe très complexe à mimer *in vitro*. De l'extérieur vers l'intérieur, il est doté d'un réseau de vaisseaux sanguins juxtaposé à une couche de cellules musculaires puis à une muqueuse, gorgée de replis tapissés de cellules épithéliales ciliées et non ciliées. Les modèles actuels ne reproduisent que cette dernière couche épithéliale, sans tenir compte de la morphologie tridimensionnelle de cet organe ni des autres types cellulaires. Ce dernier paragraphe fait le point sur les modèles de réservoir spermatique utilisés dans l'espèce bovine (Figure 6 page 70).

Explants d'oviducte en suspension

Les explants (appelés aussi agrégats) d'oviducte sont des fragments de muqueuse oviductale collectés par écrasement de l'oviducte et segmentation mécanique par pipetage (De Pauw *et al.*, 2002; Sostaric *et al.*, 2008). Leur activité ciliaire les maintient en suspension dans le milieu de culture. Les explants ont été utilisés pour des études d'interaction avec les spermatozoïdes après des durées très courtes (maximum 24 h) de culture dans un milieu supplémenté en sérum de veau fœtal (Walter, 1995). Pendant la culture, les cellules épithéliales ne se dédifférencient pas et maintiennent à la fois leur polarité, leurs cils ainsi que leur activité sécrétrice (Walter, 1995; Rottmayer *et al.*, 2006). Le maintien de cette morphologie épithéliale permet de reproduire les conditions de liaison avec les spermatozoïdes *in vivo* : des spermatozoïdes exclusivement liés aux cellules ciliées avec une membrane et un acrosome intact (Sostaric *et al.*, 2008). Néanmoins, ce modèle est très hétérogène avec des agrégats de formes et de tailles très variées, rendant très difficile le comptage des spermatozoïdes liés à leur surface et dans leurs replis. Seule une étude a quantifié par qRT-PCR l'expression de quelques gènes candidats dans les explants d'oviducte : l'expression des récepteurs aux estrogènes *ESR2* et à la progestérone est modifiée au bout de 24 h comparé à 30 minutes après la mise en culture (Rottmayer *et al.*, 2006).

Monocouche de cellules épithéliales sur plastique

Le modèle le plus largement utilisé depuis les années 1990 est la culture primaire de cellules épithéliales d'oviducte en monocouche sur des supports en plastique types boîte de Petri (Pollard *et al.*, 1991; Gualtieri and Talevi, 2003). Les cellules sont cultivées dans du milieu de culture supplémenté avec du sérum de veau fœtal pendant environ sept à dix jours jusqu'à confluence. Chez le bovin, ce type de culture a l'avantage d'être simple, assez rapide et les cellules survivent et se multiplient sur de longues périodes, allant jusqu'à 2-3 semaines. Le comptage des spz liés après co-incubation est simple après fixation des cellules dans des chambres de culture sur lame (type Lab-Tek) et observation au microscope. Néanmoins, les cellules épithéliales en monocouche se dédifférencient rapidement pendant la culture et perdent leur caractéristiques morphologiques et fonctionnelles. En effet, les cellules ciliées perdent leurs cils et la proportion de granules de sécrétion dans les cellules sécrétrices diminue (Walter, 1995; Sostaric *et al.*, 2008). Des modifications transcriptomiques ont été rapportées au cours de la culture avec notamment une réduction de l'expression des récepteurs à la progestérone et de l'oviductine après seulement 5 jours de culture comparée à des cellules fraîchement isolées (Schmaltz-Panneau *et al.*, 2015). Ces changements ont des effets négatifs sur l'interaction avec les spermatozoïdes : chez le bovin, la densité de liaison des spz éjaculés de taureaux est 50 à 100 fois inférieure avec des monocouches cellulaires sur plastique comparé à des explants (Sostaric *et al.*, 2008). De plus, avec ce modèle en monocouche, les spz se lient à toutes les cellules alors qu'*in vivo*, les spz se lient quasi- exclusivement aux cellules épithéliales ciliées (Sostaric *et al.*, 2008). Les modifications morphologiques et expressionnelles de cet épithélium en monocouche provoquent également un effet différentiel des facteurs impliqués dans la libération des spermatozoïdes. Chez le bovin, l'addition d'une même dose d'héparine libère 95% des spz liés à des monocouches cellulaires contre 70% liés à des explants (Ardon *et al.*, 2016; Lamy *et al.*, 2017).

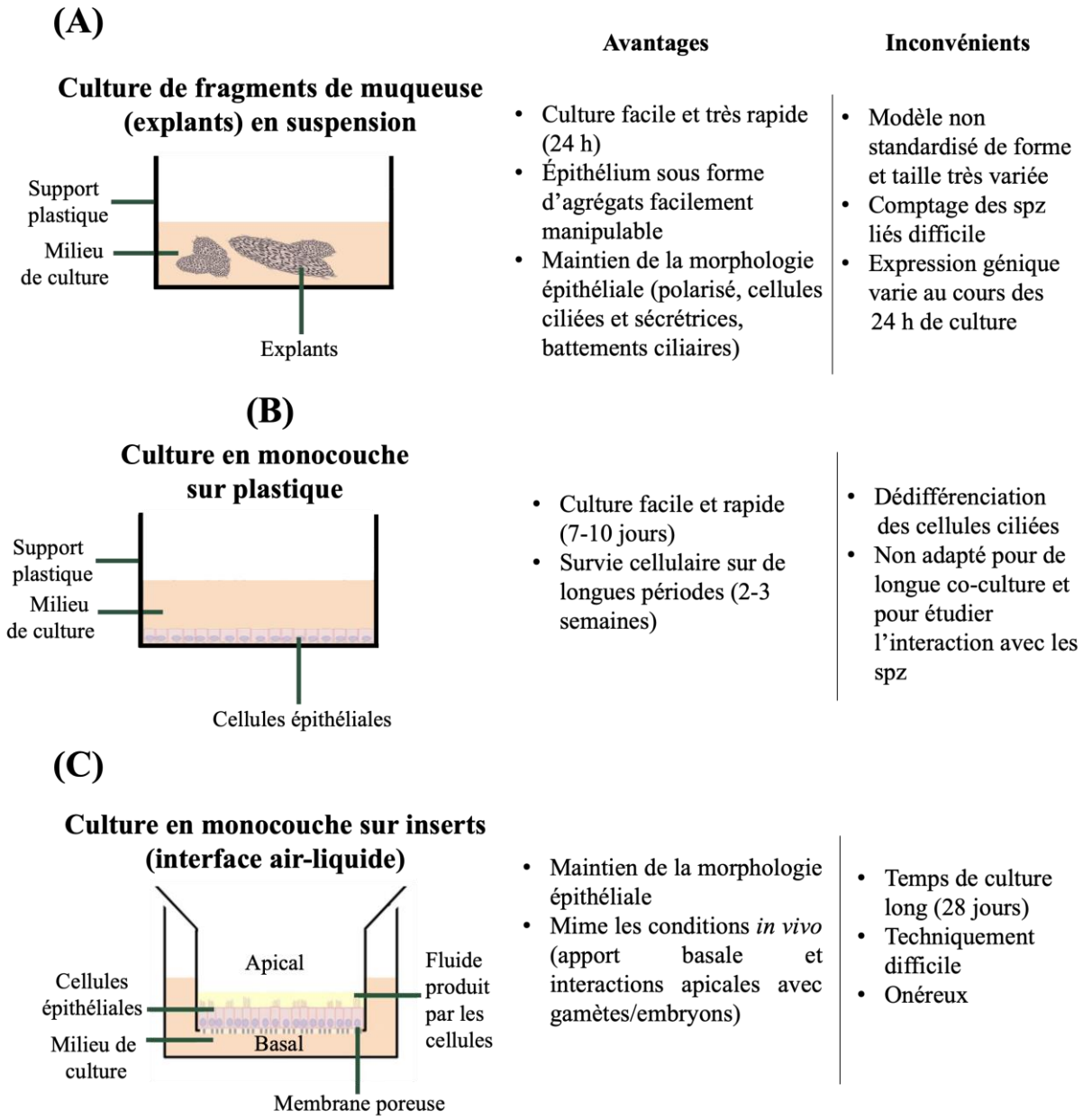

Figure 6 : Avantages et inconvénients des modèles de culture cellulaire utilisés in vitro pour étudier les interactions entre les spermatozoïdes et l'oviducte.

(**A**) Culture de fragments de muqueuse (ou explants) en suspension (Walter, 1995; De Pauw *et al.*, 2002; Rottmayer *et al.*, 2006; Sostaric *et al.*, 2008)

(**B**) Culture en monocouche sur plastique (Pollard *et al.*, 1991; Walter, 1995; Gualtieri and Talevi, 2003; Sostaric *et al.*, 2008; Schmaltz-Panneau *et al.*, 2015)

(**C**) Culture en monocouche sur insert (Chen *et al.*, 2017; Ferraz *et al.*, 2017; Chen and Schoen, 2019)

Monocouche de cellules épithéliales sur insert en interphase air-liquide

Plus récemment, des systèmes de culture de cellules épithéliales d'oviducte sur insert de collagène en interface air-liquide ont été développés dans les espèces porcine, humaine et murine (Chen and Schoen, 2019). Les cellules sont cultivées sur insert dans un premier temps avec du milieu dans les deux compartiments basal et apical (Chen and Schoen, 2019). Après une phase de prolifération cellulaire, le milieu dans le compartiment apical est supprimé afin de créer une interphase avec de l'air. Cet interphase induit la différenciation polarisée des cellules avec une activité ciliaire qui se développe après 9 à 10 jours sur environ 25% des cellules (Ferraz *et al.*, 2017; Chen and Schoen, 2019). L'analyse protéomique du fluide produit par les cellules au pôle apical a révélé que 97% des protéines étaient également présentes dans les sécrétions d'oviducte *in vivo* (Chen *et al.*, 2017). Par ailleurs, ce système de culture à l'avantage de mimer *in vitro* l'apport d'hormones, de nutriments, de métabolites via le pôle basal tout en permettant d'étudier les interactions avec les gamètes et l'embryon au pôle apical. Chez le porc, des spermatozoïdes ajoutés au pôle apical interagissait majoritairement avec les cellules ciliées, comme observée *in vivo* (Chen *et al.*, 2013). Cependant, la technicité et le coût de la culture sont élevés, et la durée de culture est longue (21 jours) avant d'obtenir des cellules différenciées utilisables pour des co-incubations avec spermatozoïde (Chen *et al.*, 2017).

En résumé de cette troisième partie, les oviductes sont inaccessibles du vivant de l'animal et les modèles *in vitro* utilisés pour étudier les interactions avec les spz sont éloignés des conditions *in vivo* ou techniquement difficiles. Les études *in vitro* ont toutefois mis en évidence que la liaison des spermatozoïdes aux cellules épithéliales de l'oviducte puis leur libération sous l'action de la progestérone conduit à la sélection d'une sous-population de spermatozoïdes montrant des signes de capacitation et à haut potentiel fécondant. Par des approches candidates, des interactions entre spermatozoïdes et protéines à la fois sécrétées dans le fluide et présentes à la surface des cellules épithéliales d'oviducte, comme les annexines A1 et A2, HSPA8 et GRP78, ont été rapportées. D'autres protéines dans le fluide oviductal se lient possiblement aux spz pendant leur migration, et une compétition de liaison s'opère probablement avec l'épithélium. De plus, les interactions successives des spz dans l'isthme, lieu de stockage, puis l'ampoule, lieu de la fécondation, n'ont pas été différenciées alors que de nombreuses données montrent des différences physiologiques importantes entre ces deux régions (chapitre 1).

Questions de recherche et démarche scientifique

Résumé de la synthèse bibliographique

Pour atteindre le lieu de la fécondation, les spermatozoïdes migrent successivement au sein de l'utérus, l'isthme puis l'ampoule de l'oviducte. Pendant leur migration, l'acquisition de la capacité fécondante des spz dépend d'interactions cellulaires et moléculaires, notamment protéiques, au sein des voies génitales femelles. Cependant, la géographie précise des protéomes traversés par les spz et leurs interactions avec l'environnement femelle restent à élucider. De plus, alors qu'*in vivo* les spz interagissent à la fois avec le fluide et les cellules bordant la lumière du tractus, la littérature rapporte des études sur les interactions entre spz et fluide, ou entre spz et cellules épithéliales de l'oviducte, mettant de côté les potentiels effets des fluides sur la liaison des spermatozoïdes aux cellules. Un autre enjeu serait donc de mieux comprendre la constitution et la régulation du réservoir spermatique par les sécrétions de l'oviducte à l'aide d'un modèle physiologique de réservoir spermatique *in vitro*.

Objectifs de la thèse et hypothèses de recherche

Les objectifs de recherche sont donc de :

(i) décrire de manière exhaustive les protéomes luminaux traversés par les spz dans les voies génitales femelles lors de leur migration et identifier leurs facteurs de variation en période péri-conceptionnelle ;

(ii) identifier avec quelles protéines interagissent les spz lors de leur migration dans l'oviducte ;

(iii) mettre au point un nouveau modèle *in vitro* de réservoir spermatique facile à cultiver, maintenant la morphologie de l'épithélium oviductal et permettant des interactions quantifiables avec les spz ;

(iv) explorer les effets des interactions avec le fluide d'oviducte sur la liaison des spz aux cellules épithéliales de l'isthme.

Différentes hypothèses sont formulées :

(1) l'abondance des protéines luminales varie dans l'utérus et l'oviducte en fonction de la région anatomique, de la proximité de l'ovaire ovulant et du stade péri-ovulatoire ;
(2) au cours de leur migration, les spermatozoïdes interagissent avec de nombreuses protéines luminales et ces interactions sont dynamiques pour répondre aux besoins de survie des spermatozoïdes en période pré-ovulatoire et de capacitation à proximité des ovocytes ;
(3) les interactions des spz avec les protéines solubles dans le fluide oviductal entrent en compétition avec leur liaison aux récepteurs membranaires des cellules épithéliales de l'isthme.

Démarche scientifique et méthodologique

L'espèce bovine est utilisée comme modèle d'étude pour des raisons biologiques, techniques et économiques. Comparée à d'autres espèces de rente comme la brebis ou la truie, la vache est une espèce mono-ovulante, intéressante pour comprendre comment cet environnement asymétrique régule la composition des fluides de l'appareil génital et la migration spermatique. L'oviducte bovin est de taille relativement importante (30 cm de long), permettant d'étudier l'effet de la région anatomique sur les interactions. De plus, la semence bovine étant bien résistante à la cryoconservation, un stock de spz issus des mêmes éjaculats des mêmes taureaux peut être utilisé pour tester l'effet de facteurs femelles sans variation liée à la qualité de la semence. Enfin, les oviductes peuvent être collectés de manière régulière en abattoir pour produire un modèle *in vitro* de réservoir spermatique à partir d'une culture primaire de cellules épithéliales.

Pour explorer les différentes hypothèses formulées, notre démarche a été la suivante (Figure 7 page 75) :

Chapitre 1 : caractérisation du protéome luminal de l'utérus d'une part, et des deux régions de l'oviducte (ampoule et isthme) d'autre part, en période péri-ovulatoire du cycle.

Pour cela, les protéines totales extraites des fluides ipsi- et controlatéraux à l'ovaire ovulant ont été analysées par spectrométrie de masse à haute résolution (nanoLC-MS/MS).

Les protéines différentiellement abondantes entre régions, stades et côtés de l'ovulation ont été mises en évidence par une analyse multivariée, et les voies de sécrétion et fonctions des protéines ont été prédites par des analyses bio-informatiques (**articles 1 et 2**).

<u>Chapitre 2 :</u> identification des protéines du fluide d'oviducte interagissant avec les spermatozoïdes pendant la période péri-ovulatoire.

Pour cela, des spermatozoïdes de taureaux ont été pré-incubés ou non avec des fluides issus d'isthme et d'ampoule en phases pré- et post-ovulatoire du cycle, puis analysés par nanoLC-MS/MS et western-blot. L'effet des fluides sur la physiologie spermatique a été analysé par CASA et cytométrie en flux. Une analyse quantitative comparant les protéomes spermatiques et luminaux a permis la mise en évidence de protéines interagissant avec les spermatozoïdes. Les fonctions de ces protéines ont été prédites par une analyse bio-informatique (**article 3 et résultats complémentaires**).

<u>Chapitre 3 :</u> développement d'un nouveau modèle *in vitro* de réservoir et étude des effets de molécules candidates du fluide d'oviducte sur la liaison des spermatozoïdes aux cellules épithéliales d'isthme.

Un modèle de sphéroides de cellules épithéliales d'isthme permettant de préserver les caractéristiques morphologiques et fonctionnelles du réservoir spermatique, et de quantifier de manière répétable la capacité de liaison des spz aux cellules a été mis au point (**chapitre d'ouvrage**). Ce modèle a été utilisé pour étudier l'effet des glycoprotéines et des glycosaminoglycanes contenus dans le fluide oviductale sur la liaison des spz aux cellules épithéliales d'isthme (**article 4 et résultats complémentaires**).

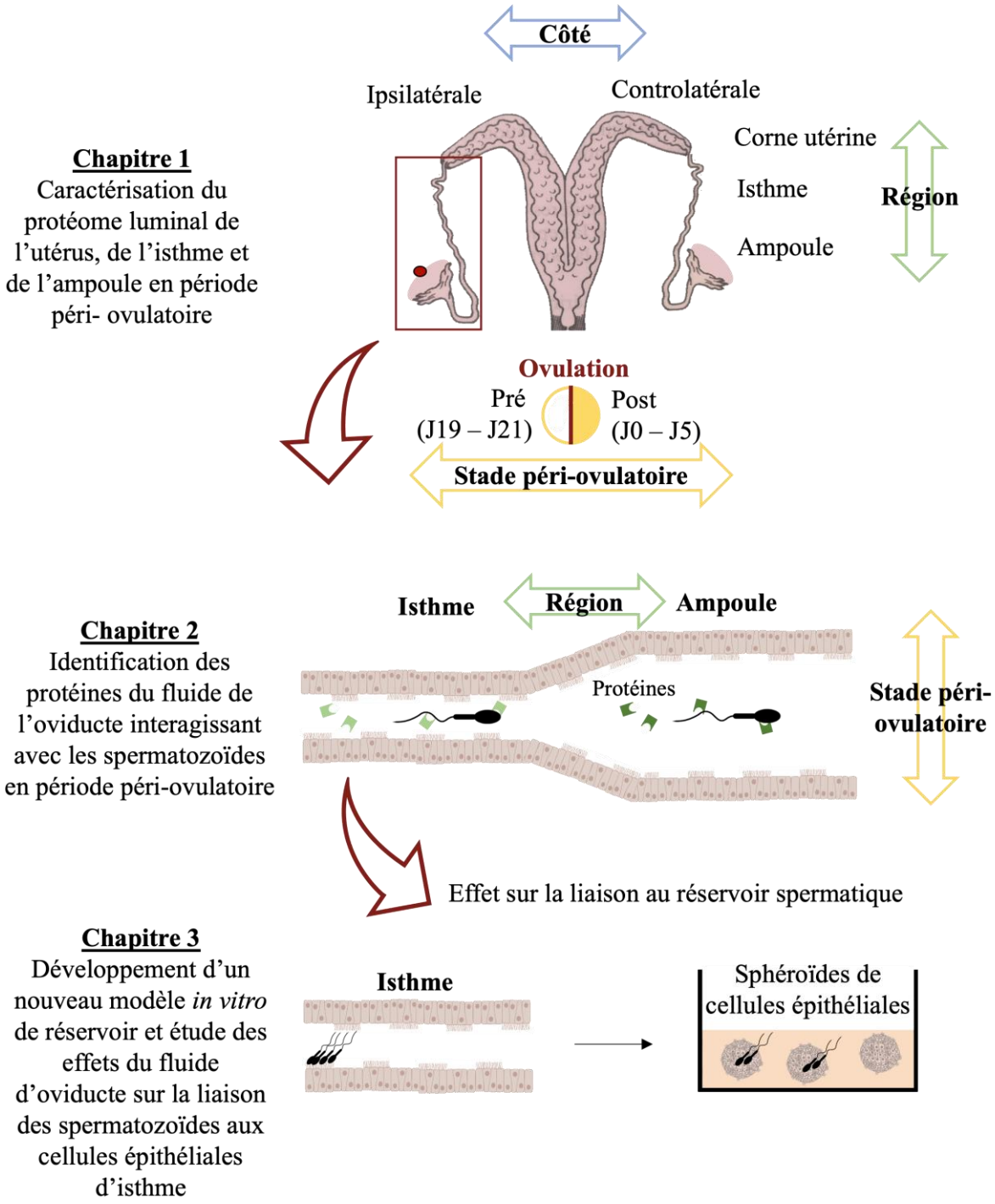

Figure 7 : Description de la démarche scientifique.

Étude expérimentale

1. Dynamique des protéomes luminaux traversés par les spermatozoïdes pendant la période péri-conceptionnelle chez le bovin

1.1. Protéome luminal de l'utérus et variations en fonction du stade péri-ovulatoire et du côté de l'ovulation

Ce travail est présenté sous la forme d'un **schéma récapitulatif** (Figure 8 page 78) et de l'**article 1** « The bovine uterine fluid proteome is more impacted by the stage of the estrous cycle than the proximity of the ovulating ovary in the periconception period » publié dans *Theriogenology* en janvier 2023.

Contexte et objectif

Les sécrétions de l'utérus en période péri-ovulatoire constituent le premier milieu femelle traversé par les spermatozoïdes, et dans lequel ils sont massivement éliminés. Au sein de ce milieu, les spz sont en contact direct avec des protéines luminales. Chez les espèces mono-ovulantes comme la vache, le protéome utérin pourrait être dissymétrique pour favoriser la migration des spz dans la corne portant l'ovaire ovulant. L'objectif de cette étude est de décrire le protéome du fluide utérin et d'évaluer les effets du stade péri-ovulatoire (pré- vs. post-ovulatoire) et de la proximité de l'ovaire ovulant (ipsi- vs. controlatérale) sur l'abondance des protéines quantifiées.

Matériel et méthodes

Les appareils génitaux de vaches adultes cyclées ont été collectés dans un abattoir proche du laboratoire et transportés sur glace pour minimiser toutes modifications post-mortem. En fonction de la morphologie des ovaires, les utérus ont été classés en deux stades du cycle estrien : stade pré-ovulatoire (approximativement 19 à 21 jours après la précédente ovulation ; n = 8 vaches) et post-ovulatoire (0 à 5 jours après l'ovulation ; n=8 vaches). Les fluides des deux cornes ipsi- et controlatérales à l'ovulation ont été collectés séparément par flush PBS (4 pools de 2 vaches par côté et stade).

Les protéines de ces fluides ont été concentrées par ultrafiltration, digérées puis analysées par nano-chromatographie liquide couplée à de la spectrométrie de masse en tandem (nanoLC-MS/MS). Les protéines ont été identifiées à l'aide de la base de données Uniprot *Bos taurus* puis quantifiées par comptage spectral. L'effet du stade péri-ovulatoire et de la proximité de l'ovaire ovulant sur l'abondance des protéines a été évalué par une analyse en composante principale et des comparaisons deux à deux via des tests de Student (logiciel R, p-value ≤ 0.05). Les voies de sécrétion des protéines ont été prédites par analyses bio-informatiques des séquences protéiques et comparaison aux protéomes publiés des vésicules extracellulaires utérines chez le bovin. Les fonctions des protéines totales et différentielles ont été prédites par analyse de type Gene ontology des gènes correspondants.

Résultats

Au total, 1214 protéines ont été identifiées dans les fluides des deux cornes utérines en période péri-ovulatoire. Parmi elles, 91% sont communes entre toutes les conditions. La prédiction des voies de sécrétion a révélé que 20% des protéines possèdent un peptide signal, 28% sont sécrétées par des voies non conventionnelles et 17% étaient précédemment identifiées dans les vésicules extracellulaires issues de fluide utérin bovin. Les protéines les plus abondantes incluent l'albumine, la myosine-9, la mucine 5B et des protéines du complément C3 et CFB. La comparaison entre les cornes ipsi- et controlatérales n'a révélé que 12 protéines différentiellement abondantes, dont 5 au stade pré-ovulatoire et 7 au stade post-ovulatoire. Entre stades, 35 protéines différentiellement abondantes ont été identifiées, dont 21 du côté ipsilatérale à l'ovaire ovulant. Les protéines identifiées ainsi que celles différentielles entre stades du côté ipsilatérale étaient impliquées dans des fonctions de liaison moléculaire, des processus métaboliques, la détoxification cellulaire et la réponse immunitaire.

Conclusion

Cette étude fournit un premier protéome utérin en période péri-ovulatoire chez le bovin. Aucun effet majeur du côté de l'ovulation sur l'abondance des protéines n'a été mis en évidence, probablement en lien avec la tonicité de l'utérus en période péri-ovulatoire. Ces résultats ne sont pas en faveur d'un environnement plus favorable aux spz dans la corne menant au site de fécondation. Ces travaux ouvrent la voie vers des études fonctionnelles sur les gamètes mâles, en particulier l'identification des protéines interagissant avec les spz et l'effet de ces interactions sur leur migration et survie avant d'atteindre l'oviducte.

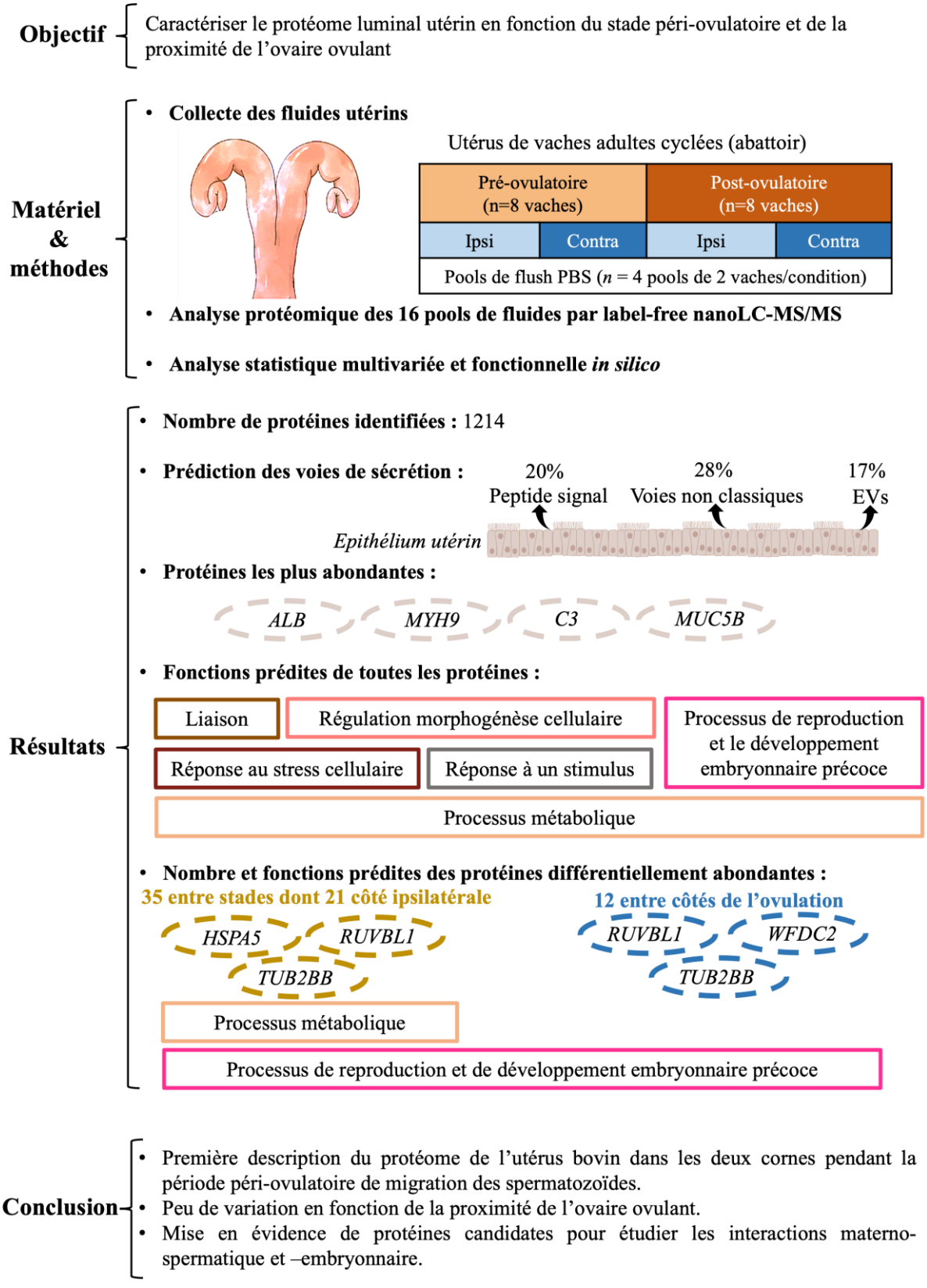

Figure 8 : Schéma récapitulatif de l'étude du protéome luminal de l'utérus en fonction du stade péri-ovulatoire et de la proximité de l'ovaire ovulant.
ALB = Albumine ; C3 = Complément C3 ; EVs = vésicules extracellulaires ; HSPA5 : protéine de choc thermique A5 ; MUC5B = Mucine 5B ; MYH9 = Myosine 9 ; RUVBL1 = RuvB-like helicase ; TUB2BB = Tubulin beta chain ; WFDC2 = WAP four-disulfide core domain 2.

Theriogenology 198 (2023) 332–343

Contents lists available at ScienceDirect

Theriogenology

journal homepage: www.theriojournal.com

The bovine uterine fluid proteome is more impacted by the stage of the estrous cycle than the proximity of the ovulating ovary in the periconception period

Coline Mahé [a, *], Paulo Marcelo [b], Guillaume Tsikis [a], Daniel Tomas [c], Valérie Labas [c], Marie Saint-Dizier [a]

[a] CNRS, IFCE, INRAE, Université de Tours, PRC, 37380, Nouzilly, France
[b] Plateforme d'Ingénierie Cellulaire & Analyses des Protéines ICAP, FR CNRS 3085 ICP, Université de Picardie Jules Verne, Amiens, France
[c] INRAE, Université de Tours, CHU de Tours, Plateforme de Phénotypage par Imagerie in/eX vivo de l'ANImal à la Molécule (PIXANIM), 37380, Nouzilly, France

ARTICLE INFO

Article history:
Received 23 November 2022
Received in revised form
4 January 2023
Accepted 5 January 2023
Available online 7 January 2023

Keywords:
Contralateral
Ipsilateral
Post-ovulatory
Pre-ovulatory
Proteomic
Uterine fluid

ABSTRACT

Uterine secretions provide a suitable environment for sperm selective migration during a couple of days preceding ovulation and for early embryo development before implantation. Our goal was to identify and quantify proteins in the bovine uterine fluid during the periovulatory period of the estrous cycle. Genital tracts with normal morphology were collected from adult cyclic *Bos taurus* females in a local slaughterhouse and classified into pre-ovulatory or post-ovulatory stages of cycle (around days 19–21 and 0–5 of cycle, respectively; n = 8 cows per stage) based on ovarian morphology. Proteins from uterine fluid collected from the utero-tubal junction to the base of each horn (four pools of two cows per condition) were analyzed by nanoLiquid Chromatography coupled with tandem Mass Spectrometry (nanoLC-MS/MS). A total of 1214 proteins were identified, of which 91% were shared between all conditions. Overall, 57% of proteins were predicted to be secreted and 17% were previously reported in uterine extracellular vesicles. Paired comparisons between uterine horns ipsilateral and contralateral to ovulation evidenced 12 differentially abundant proteins, including five at pre-ovulatory stage. Furthermore, 35 proteins differed in abundance between pre- and post-ovulatory stages, including 21 in the ipsilateral side of ovulation. Functional analysis of identified proteins demonstrated roles in binding, metabolism, cellular detoxification and the immune response. This study provides a valuable database of uterine proteins for functional studies on sperm physiology and early embryo development.

© 2023 Elsevier Inc. All rights reserved.

1. Introduction

After insemination or mating in cattle, spermatozoa interact with uterine secretions and these interactions typically occur during estrus in the pre-ovulatory period of the estrous cycle. After ovulation and fertilization, the developing embryo starts to develop in the oviduct and enters the uterine horn ipsilateral to ovulation around the morula stage, at 4–5 days after ovulation [1]. Thus, in a short period of time ranging from 2 days before to 5 days after ovulation, spermatozoa and embryo are in direct contact with the uterine fluid (UF). The UF is a complex mixture of lipids [2], metabolites [3], amino acids [4] and proteins [5–7]. *In vitro* studies in mammals evidenced various effects of the UF on mammalian sperm and early embryos [8–11]. In cattle, incubation of spermatozoa with UF from the follicular and luteal phases resulted in higher sperm viability and motility compared to controls without fluid [8]. Uterine flushes promoted sperm capacitation *in vitro* in humans [9] but decreased sperm viability, motility and acrosome integrity in pigs [10]. The addition of low concentrations of oviductal fluid and UF in culture media supported the development of *in vitro* produced bovine embryos [11]. There is evidence that proteins secreted in the female genital tract interact with spermatozoa and embryo. For instance in humans, cystatin 3 secreted in UF has been shown to interact with spermatozoa and to promote their motility without inducing premature capacitation [12]. After *in vitro* incubation with oviduct fluid, the early bovine embryo was

* Corresponding author.
E-mail address: coline.mahe@inrae.fr (C. Mahé).

https://doi.org/10.1016/j.theriogenology.2023.01.006
0093-691X/© 2023 Elsevier Inc. All rights reserved.

Abbreviations

Contra	Contralateral horn
DAPs	Differentially abundant proteins
EVs	Extracellular vesicles
GO	Gene ontology
Ipsi	Ipsilateral horn
NanoLC-MS/MS	nanoLiquid Chromatography coupled with tandem Mass Spectrometry
NWS	Normalized weighted spectra
Pre-ov	Pre-ovulatory stage
Post-ov	Post-ovulatory stage
UF	Uterine fluid

shown to internalize dozens of proteins crossing the zona pellucida as early as the 4- to 6-cell stage [13].

Spatiotemporal changes in the UF composition are expected to address the sequential requirements for sperm motility and selective migration, elimination of sperm in excess, and blastocyst differentiation during the periovulatory period. We previously demonstrated the dynamic changes in the oviduct fluid proteome occurring between the pre- and post-ovulatory stages of cycle in cattle [14]. Other studies in mares [5,15] and ewes [16] observed alterations of the UF proteome between the follicular and luteal phases of cycle. Moreover, the proximity of the ovulatory ovary may impact the proteome of the UF. In heifers, differences in the endometrial transcriptome between uterine horns ipsilateral and contralateral to the corpus luteum were evidenced on days 5–16 of cycle [17]. Although there are some proteomic reports on the UF during the luteal phase of cycle [18] and at the time of implantation [19,20] in cattle, there is currently no data in the periovulatory period. Therefore, the objective of this study was to quantitatively analyze the UF proteome in both uterine horns at pre- and post-ovulatory stages of the cycle.

2. Materials and methods

2.1. Collection of bovine uterine fluids and sample preparation

Genital tracts including the cervix, uterine horns, oviducts and ovaries from adult cyclic *Bos taurus* females were collected at a local slaughterhouse (Vendôme, France), immediately placed on ice and transported to the laboratory within 2 h after animal death. Only macroscopically normal tracts with no sign of cyst, inflammation or infection were used in this study. Tracts were classified as pre-ovulatory or post-ovulatory based on ovarian morphology. Pre-ovulatory tracts contained one pre-ovulatory follicle between 11 and 20 mm in diameter and one *corpus albicans* from the previous cycle (Pre-ov; approximately days 19–21 of cycle). Post-ovulatory tracts displayed one *corpus hemorrhagicum* less than 0.5 cm in diameter (Post-ov; approximately days 1–5 of cycle). Uterine horns ipsilateral and contralateral to the side of ovulation (pre-ovulatory follicle or early corpus luteum) were cut at their base (just before the uterine body) and flushed from the utero-tubal junction with 2 mL of cold filtered phosphate buffered saline. Each uterine horn was then opened longitudinally and examined for sign of inflammation. The uterus presenting anatomical anomaly, bleeding or signs of inflammation were excluded. Cells and cellular debris were discarded from the flushing by two successive centrifugations (2000×*g* for 10 min then 12000×*g* for 10 min at 4 °C) and UF were stored at −80 °C in 2 mL polypropylene tubes. In order to reach enough protein content, pools of two cows per side × stage condition were constituted. All UF samples were thawed on ice and pools of UF were made by mixing 400 μL of each sample. In the following, the term "sample" refers to a pool of two UF. In total, four biological replicates per condition were constituted, resulting in a total of 16 UF samples. The UF samples were concentrated 2 to 4 times by centrifugation for 1 h at 12000×*g* at 4 °C in Vivaspin units (Sartorius, Stonehouse, United Kingdom) with a molecular weight cut-off of 3-kDa. Final protein concentrations of UFs ranged between 0.7 and 2.5 mg/mL (Uptima BC Assay kit, Interchim, Montluçon, France). To assess sample quality, 5 μg of proteins per UF were migrated on 4–20% SDS-PAGE precast gels for 10 min at 80 V and 30 min at 180 V (Bio-Rad, California, United States) followed by Coomassie Blue staining (ThermoFisher, Massachusetts, United States) (see Fig. S1). Then, 50 μg of proteins per UF sample were dried in 1.5 mL polypropylene tubes using a SpeedVac system (SPD 1010-230, ThermoSavant Electronic, France) and stored at −80 °C before proteomic analysis.

2.2. Nanoliquid chromatography coupled with tandem mass spectrometry (nanoLC-MS/MS)

For proteomic analysis, 50 μg of protein were resuspended in 50 mM ammonium bicarbonate. Reduction and alkylation were performed by successive incubation at final concentration of 5 mM dithiothréitol in 50 mM ammonium bicarbonate (30 min at 56 °C) then at a final concentration of 12.5 mM iodoacetamide in 50 mM ammonium bicarbonate (30 min at room temperature in the dark). Samples were then Trypsin/Lys-C (Promega, USA) digested with 0.01% ProteaseMAX (V2072, Promega, USA) overnight at 37 °C with a ratio enzyme:substrate of 1:40. The tryptic peptide solutions were dried by vacuum centrifuge and reconstituted in 20 μL water/1% formic acid (v/v). All digested peptide mixtures were separated by on-line nanoLC and analyzed by nano-electrospray tandem mass spectrometry. The experiments were performed on an Ultimate 3000 RSLC system coupled with an Orbitrap Fusion mass spectrometer (ThermoFisher Scientific San Jose, CA, USA). The peptide mixtures were injected onto a nanotrap column (Acclaim C18, 100 μm i.d. x 2 cm length) with a flow of 5 μL min^{-1} and subsequently gradient eluted with a flow of 300 nL min^{-1} in an Easy-Spray column (Acclaim PepMap RSLC C18, 2 μm, 100 A, 75 μm × 50 cm) from 4 to 40% acetonitrile/0.1% formic acid (v/v) for 140 min. Full MS scans were acquired at high resolution (FWMH 120,000) in the Orbitrap analyzer (mass-to-charge ratio (*m/z*): 400 to 2000), while collision-induced dissociation (CID) spectra were recorded. The mass spectrometer was operated in positive and data-dependent mode to automatically switch between orbitrap-MS and linear trap MS/MS (MS2) acquisition for 3 s between master scans.

2.3. Protein identification and validation

Protein identification was performed using the Mascot search engine (version 2.7; Matrix Science, London, UK) via the Proteome Discoverer software (version 2.5, Thermo Fisher Scientific) against the Uniprot *Bos taurus* database (January 2022; 23,844 sequences). Precursor mass range of 350–5000 Da and signal-to-noise ratio of 1.5 were the criteria used for generation of peak lists. The parameters used for database searches included trypsin as enzyme, N-terminal acetylation on protein, carbamidomethylcysteine and methionine oxidation as dynamic modifications. Ion tolerance was set at 10 ppm for parent and 0.8 Da for fragment ion matches. Proteins with at least two unique peptides (False Discovery Rate (FDR) < 0.01%) were considered. Threshold probability for peptide and protein identification were set to 95.0% as specified by the Peptide Prophet algorithm [21] and the Protein Prophet algorithm [22].

2.4. Prediction of secretory pathways of identified proteins

Venn diagrams were built using the accession number on the jvenn tool online (http://jvenn.toulouse.inra.fr/app/example.html) [23]. Prediction of secretory pathways (presence of a signal peptide or unconventional secretion) was carried out using the Outcyte online tool (version 1.0; http://www.outcyte.com/) [24] and FASTA sequences as input. To confirm the presence of a signal peptide, FASTA sequences were also submitted to the SignalP online tool in Eukarya (version 6.0; http://www.cbs.dtu.dk/services/SignalP/) [25]. The gene list corresponding to identified proteins was compared to those previously reported in bovine UF-derived extracellular vesicles (EVs) [26].

2.5. Protein quantification

Proteins were quantified by a label-free approach using the spectral counting quantitative method of the Scaffold Q+ software (version 5.0.1, Proteome Software, Portland,USA, www.proteomesoftware.com). Protein abundance was then assessed in normalized weighted spectra (NWS) after normalization, as previously described [14]. Briefly, the "weighted" option is based on the assignment of each peptide to a weight according to whether they are shared or not. The normalization of spectra among the samples was realized by adjusting the sum of the selected quantitative values for all proteins within each sample to a common value, which was the average of the sums of all samples present in the experiment. This was achieved by applying a scaling factor for each sample to each protein or protein group.

2.6. Statistical analysis of data

Statistical analysis of proteins quantified with a minimum of 2.0 NWS (mean value of biological replicates) in at least one condition was performed using the Rstudio software (version 1.4.1106). Principal component analysis of all biological replicates was performed using the FactoMineR package. Protein abundance between sides in a given stage and between stages in a given side were compared by Student *t*-tests. Proteins with a *t*-test p-value $\leq$0.05 and a fold change ratio $\geq$1.5 were considered as differentially abundant proteins (DAPs).

2.7. Functional analysis of proteins

The gene symbols corresponding to all identified proteins were used for gene ontology (GO) membership analysis. The GO analysis was performed for molecular functions and biological processes containing "reproduction", "sperm", "embryo", "blastocyst" or "uterus" using the online Metascape tool and the *Homo sapiens* database [27]. Furthermore, the gene symbols of DAPs between stages in the ipsilateral horn were used to build Proteomaps online based on the Kyoto Encyclopedia of Genes and Genomes (KEGG)

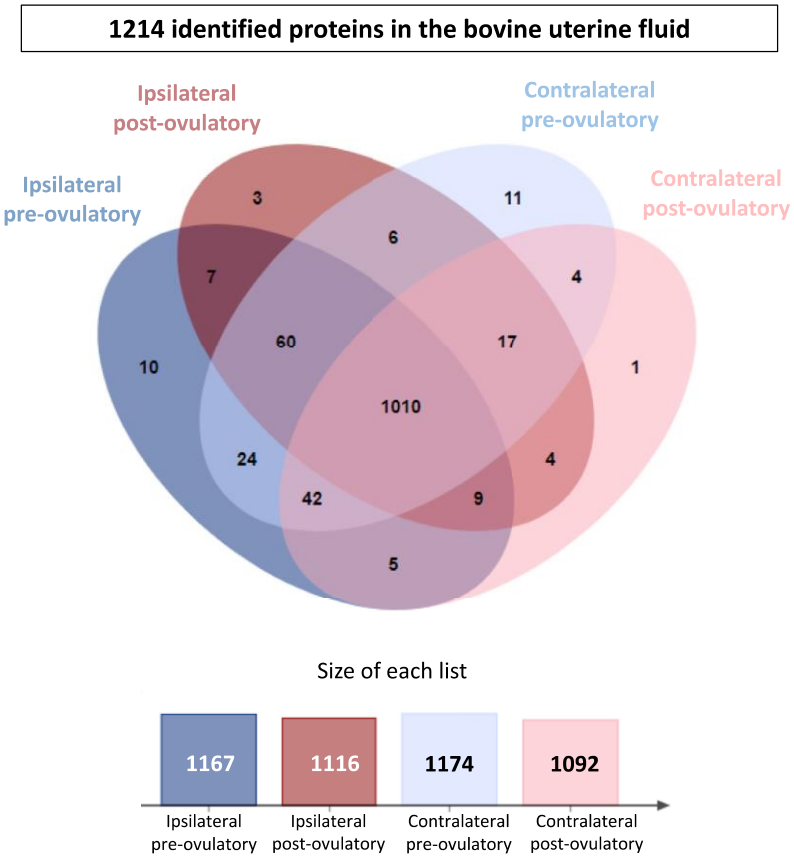

Fig. 1. Distribution of proteins identified in the bovine uterine fluid. Numbers of proteins identified in each uterine horn (ipsilateral vs. contralateral to ovulation) at each stage (pre-ovulatory vs. post-ovulatory) are indicated in the histogram.



Fig. 2. Distribution of proteins in the bovine uterine fluid according to their secretory pathways. Classical and unconventional secretion pathways were predicted using the Outcyte and SignalP online tools. Proteins previously reported in bovine UF-derived extracellular vesicles [26] are also indicated.

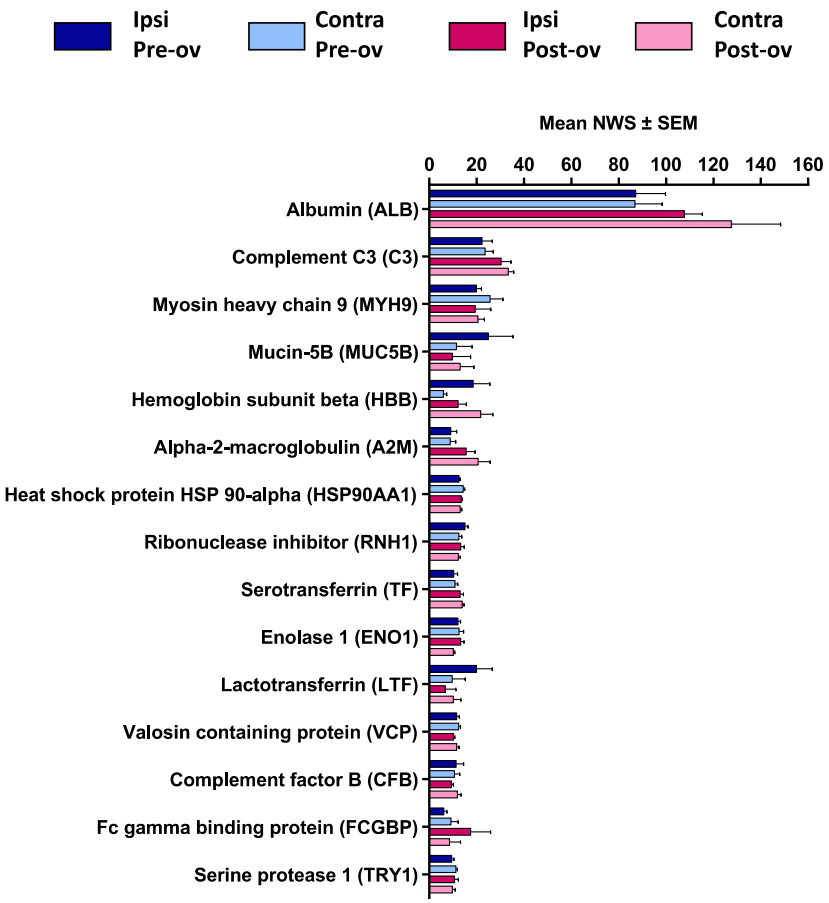

Fig. 3. Top-15 most abundant proteins quantified in the bovine uterine fluid. Data are expressed as means ± SEM of biological replicates.

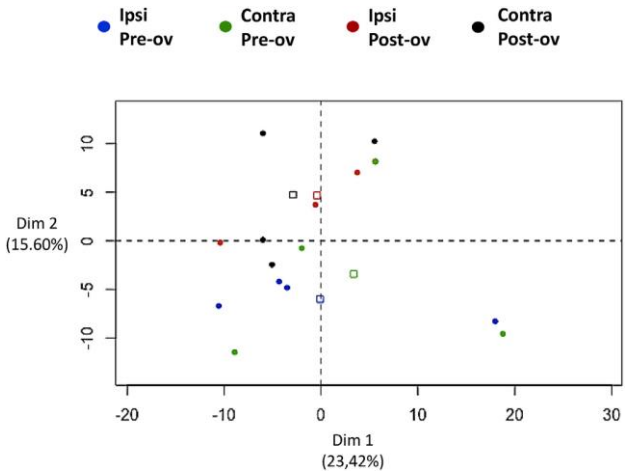

Fig. 4. Principal component analysis of quantified proteins in all samples. Each spot represents one biological replicate and the colored squares represent the means of data in a given condition.

Pathways (http://bionic-vis.biologie.uni-greifswald.de/) [28]. In the Proteomaps, functionally related proteins are arranged in polygon aeras representing the mean abundance at the pre-ovulatory stage of cycle.

3. Results

3.1. Proteins identified in the uterine fluid and secretory pathways

A total of 1214 proteins were identified in the bovine UF, of which 91% (1010/1214) were shared between all conditions (Fig. 1; see the complete list of proteins in Table S1). Proteins identified in only one condition displayed very low quantitative value (<1 NWS). Among the identified proteins, 20% (243/1214) were predicted to contain a signal peptide and to be classically secreted, while 28% (338/1214) were predicted to be secreted via unconventional pathways (Fig. 2 and Table S1). In addition, 17% of identified proteins (204/1214) were previously reported in bovine UF-derived EVs [26]. Overall, 57% (686/1214) of the identified proteins were predicted to be secreted.

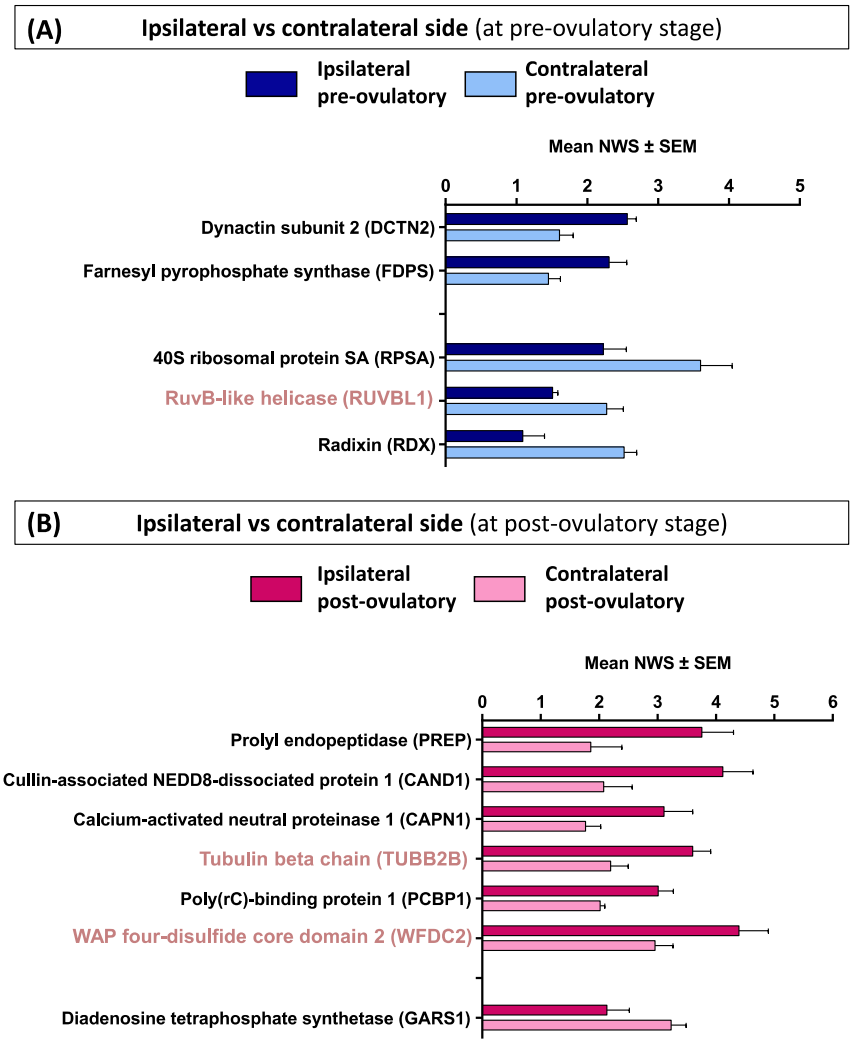

Fig. 5. Differentially abundant proteins between ipsilateral and contralateral uterine horns at pre-ovulatory (A) and post-ovulatory (B) stages of cycle. Protein names in pink were associated with the gene ontology terms containing "reproduction" (RUVBL1, WFDC2), "sperm" (RUVBL1), or "embryo" (TUBB2B). See Table S4 for the complete list of GO terms with corresponding gene symbols. (For interpretation of the references to color in this figure legend, the reader is referred to the Web version of this article.)

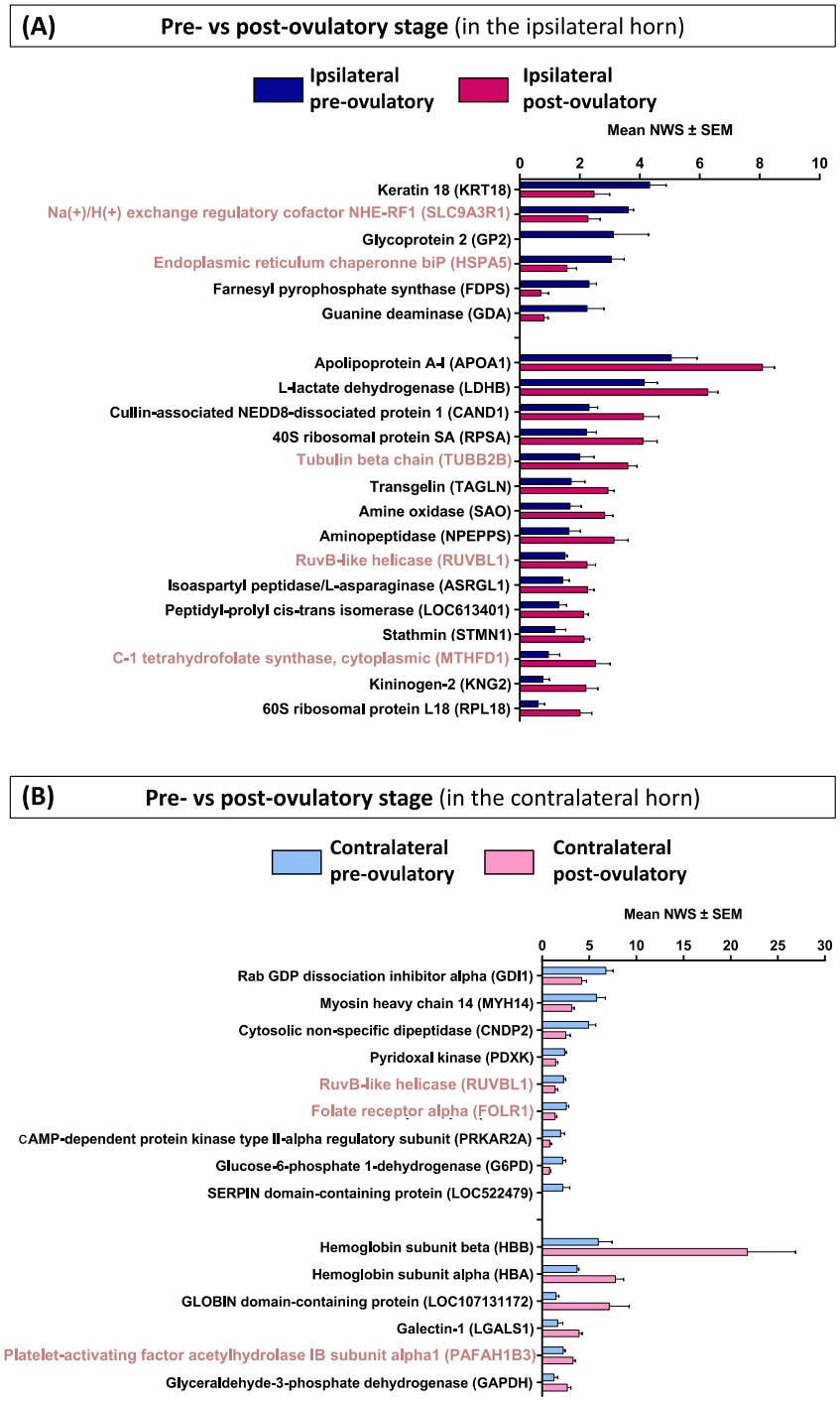

Fig. 6. Differentially abundant proteins between pre- and post-ovulatory stages of cycle in the uterine horns ipsilateral (A) and contralateral (B) to ovulation. Protein names in pink were associated with the gene ontology terms containing "reproduction" (FOLR1, HSPA5, PAFAH1B3, RUVBL1), "sperm" (FOLR1, PAFAH1B3, RUVBL1), or "embryo" (FOLR1, MTHFD1, SLC9A3R1, TUBB2B). See Table S4 for the complete list of GO terms with corresponding gene symbols. (For interpretation of the references to color in this figure legend, the reader is referred to the Web version of this article.)

(A) Gene ontology molecular functions

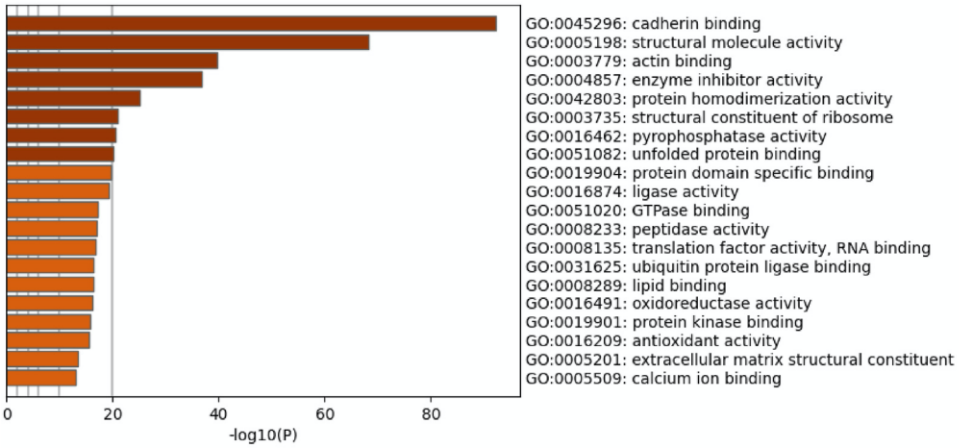

(B) Gene ontology biological processes

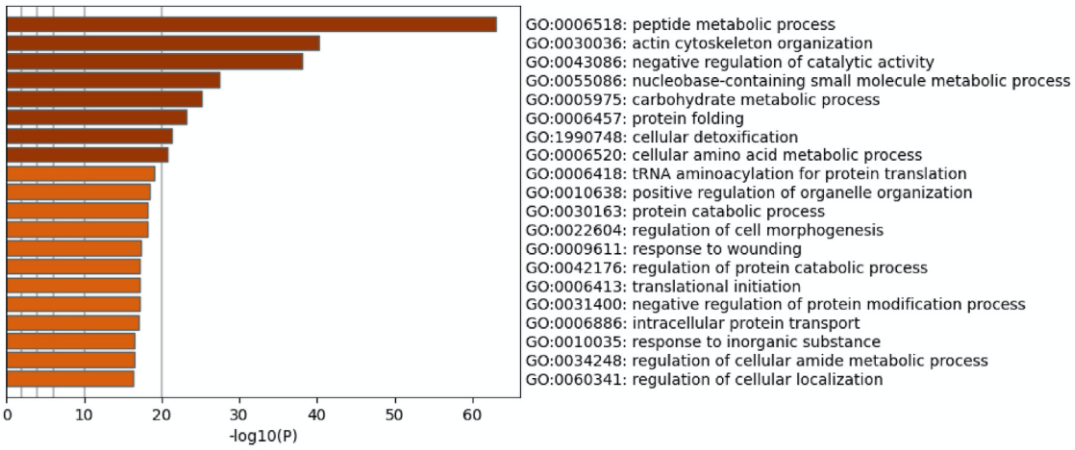

(C) Gene ontology cellular component

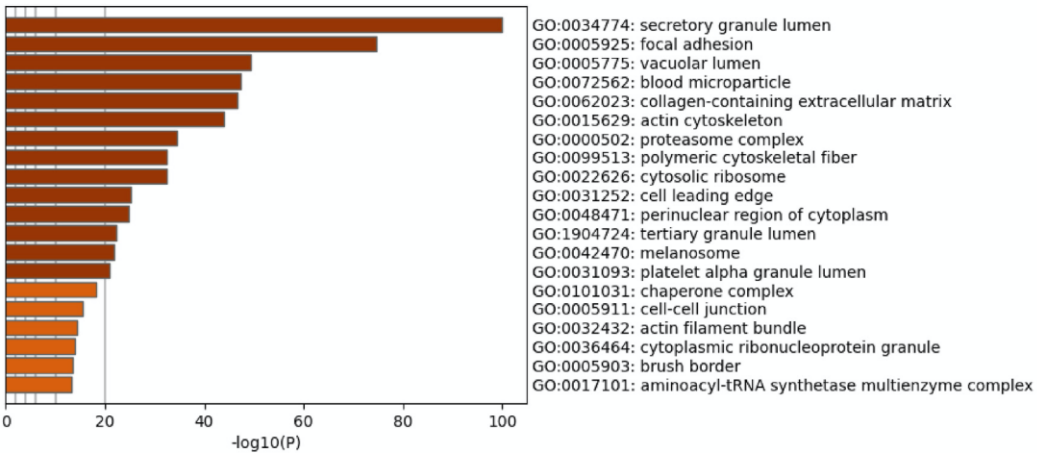

3.2. Differentially abundant proteins between horns and stages

A total of 324 proteins were retained for quantitative analysis (NWS ≥2; Table S1). The most abundant proteins included albumin (ALB), complement proteins (C3, CFB), myosin 9 (MYH9), mucin 5B, heat shock protein 90AA1 (HSP90AA1), enolase 1 (ENO1) and annexins A1 and A2 (ANXA1, 2; see the top-15 most abundant proteins in Fig. 3). Principal component analysis (Fig. 4) of quantified proteins did not show any clear discrimination between samples, although mean values of samples at pre- and post-ovulatory clustered together on the two first principal dimensions (colored squares in Fig. 4). Paired comparisons between ipsilateral and contralateral horns evidenced 12 DAPs, i.e. 4% of quantified proteins, with fold-change ratios between 1.5 and 12.1 (Fig. 5; see quantitative values and fold-change ratios in Table S2). Furthermore, 35 proteins, i.e. 11% of quantified proteins, differed in abundance between pre- and post-ovulatory stages with fold-change ratios between 1.5 and 6.9. Of those DAPs, 21 were identified in the ipsilateral side of ovulation (Fig. 6A and B; Table S2).

3.3. Functional analysis of identified and differentially abundant proteins

The Metascape GO analysis of all identified proteins showed a significant enrichment in molecular functions related to binding (cadherin binding, actin binding, unfolded protein binding and protein domain specific binding) and enzymatic activities (enzyme inhibitor activity, pyrophosphatase activity, ligase activity, peptidase activity; Fig. 7A and Table S3). Among the biological processes, UF proteins were overrepresented in several metabolic processes such as peptide metabolic process, nucleobase-containing small molecule metabolic process and carbohydrate metabolic process, among others, as well as in cellular detoxification, regulation of cell morphogenesis, protein catabolic process and response to wounding (Fig. 7B). Finally, the most enriched cellular components included secretory granules lumen, vacuolar lumen, focal adhesions and the proteasome complex (Fig. 7C).

A total of 157 proteins were associated with GO terms containing "sexual reproduction", "sperm", "embryo", "blastocyst" or "uterus" (see the lists of GO terms and proteins in Table S4). The DAPs associated with those terms are highlighted in Figs. 6 and 7. Finally, the Proteomaps in Fig. 8 shows that the DAPs between pre- and post-ovulatory stages in the horn ipsilateral to ovulation were involved in various KEGG pathways, including metabolism (SAO, LDHB, SLC9A3R1) and vesicular transport through exosomes (KRT18, CAND1).

4. Discussion

Using high-resolution mass spectrometry, this work provides a first analysis of proteins present in the bovine UF in the periovulatory period, i.e. at the time of sperm migration toward the site of fertilization and early embryo development. Overall, 91% of proteins were shared between all conditions, indicating very few specific proteins according to the proximity of the ovulatory ovary (pre-ovulatory follicle or early corpus luteum), at least during the periovulatory period. Furthermore, most proteins detected in only one condition displayed very low quantitative values, suggesting that they were probably present but not detected due to a lack of sensitivity. Overall, 324 proteins could be quantified, which represented 21% of identified proteins. Previous proteomic analyses of the bovine UF evidenced 1737 proteins, of which almost all could be quantified [6], while in another study, 699 proteins were identified but only 235 (34%) could be quantified [29]. Different quantitative approaches and sensitivity of the mass spectrometer may partly explain these discrepancies between studies.

The UF were analyzed without albumin elimination to avoid loss of proteins bound to albumin and because albumin has reported roles in sperm physiology [30–32] and participates in the bioavailability of steroid hormone in the uterus [33]. However, albumin was by far the most abundant protein, quantified three times more than all other proteins; its signal probably hindered those of other proteins. Albumin was also found in high abundance in other proteomic studies in bovine [20] and ovine [16] UF. This protein was identified as one of the main acceptors of cholesterol during bull sperm capacitation [30] and is commonly used in *in vitro* fertilization media [31]. In humans, albumin promoted H^+ efflux, one of the steps of capacitation, by interacting with its channels on sperm [32].

Overall, only 4% of proteins differed in abundance between both uterine horns. This result is in accordance with a previous proteomic study in which the proximity of the corpus luteum had no effect on uterine protein abundance on either day 7 or 15 of cycle in cows [18]. Accordingly, no difference between the ipsilateral and contralateral horns were found for metabolites [34] and amino acids [4] in the bovine UF. However, a transcriptomic study discovered 217 differentially expressed genes between ipsilateral and contralateral horns at day 5 post-estrus in synchronized heifers [17]. Taken together, these data suggest that synthesized proteins may differ in abundance inside luminal epithelial cells but not in the secretions. In cyclic cows, the contractile activity and tonicity of the uterus reaches a maximum during estrus [35], and this probably contributes to the intensive mix of proteins in the two uterine horns during this period. In the present study, the stage of the cycle had three times more effect than the side on protein abundance (11% of DAPs). In another proteomic study in cattle, 24% (40/167) of proteins differed in abundance between day 7 (early luteal phase) and day 15 (late luteal phase) of cycle [18]. In ewes, 39% of proteins were differentially abundant between estrus and the luteal phases of cycle [16]. Here, we compared stages very close in time, ranging from around 3 days before to 4–5 days after ovulation, which may explain the relatively low impact of the ovulatory stage on protein abundance.

Proteins identified in the periovulatory UF were enriched in GO terms related to the regulation of cell morphogenesis and protein catabolic process, including cathepsins (CTSB, D, F) and cysteine-rich proteins like CRIP2. This is in agreement with the fact that the endometrium is vastly remodeled during the periovulatory period and displays high rates of cell proliferation and apoptosis compared to the mid and late luteal phases [36]. CRIP2 has been identified as one secreted protein playing a role in endometrial remodeling in pigs [37]. In pigs and sheep, several cathepsins have also been reported to take part in endometrial renewal [38,39]. The identified proteins were also involved in a large panel of metabolic processes, including carbohydrate and cellular amino acid metabolism. In cattle during the early luteal phase (day 4–7 of cycle), the metabolism of amino acids is related to epithelial cell proliferation and the periovulatory remodeling of the endometrium [40]. Moreover, carbohydrates like glucose constitute a major source of energy for sperm motility and capacitation [41,42], as well as

Fig. 7. Functional enrichment analysis of proteins identified in the uterine fluid. The Metascape bar graphs represent the top 20 clusters of enriched gene ontology terms for molecular functions (A), biological processes (B), and cellular components (C). Each row represents one enriched cluster, and the darker color of the bars indicates higher significance (lower *P*-value). See Table S3 for the complete list of GO terms with corresponding gene symbols and p-values. (For interpretation of the references to color in this figure legend, the reader is referred to the Web version of this article.)

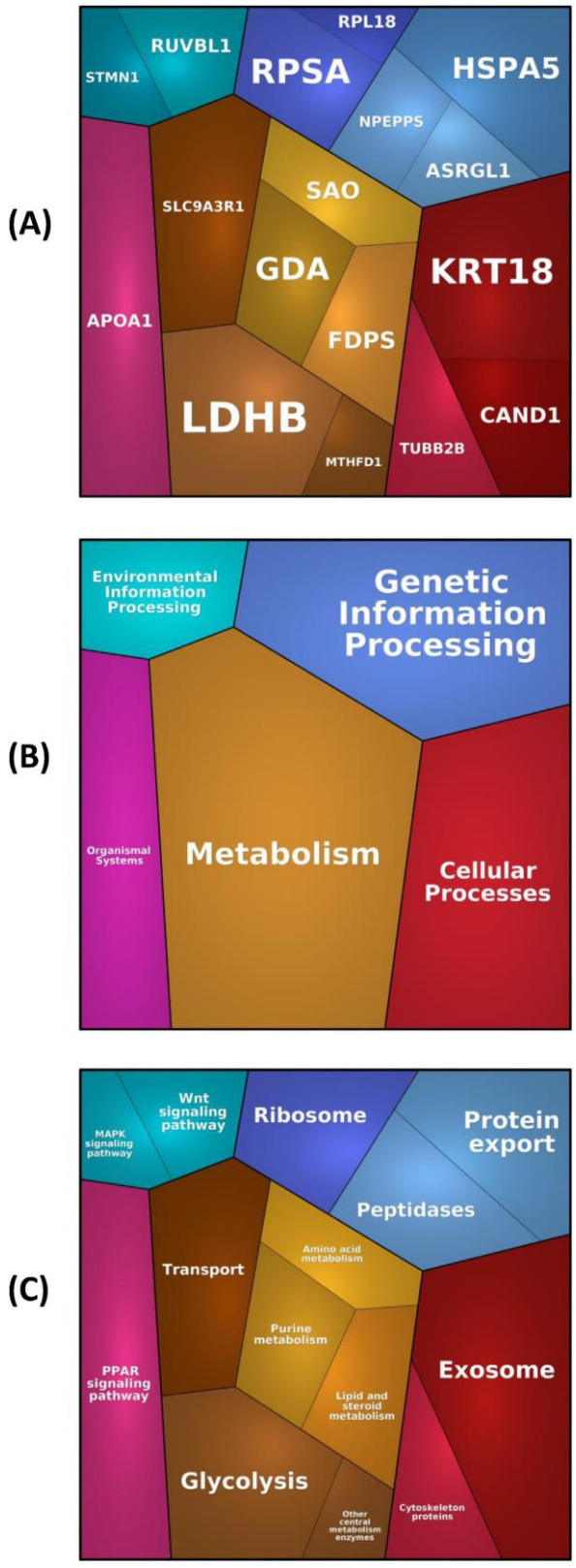

embryo development [43]. Of interest, DAPs between stages in the ipsilateral UF were also enriched in KEGG pathways related to metabolism, including the Na(+)/H(+) exchange regulatory cofactor NHE-RF1 (SLC9A3R1), which was more abundant at pre- than at post-ovulatory stages. The abundance of SLC9A3R1 in sperm has been related to male fertility in pigs [44]. In mice, SLC9A3R1 was shown to interact with sperm ion channels and was proposed as an intermediator needed for chloride influx, one of the mechanisms of capacitation [45].

Cellular detoxification was another enriched biological process and included various peroxiredoxins (PRDX 1, 2 and 6) and thioredoxins (TXN, TXNRD1, TXNDC17), all involved in the regulation of reactive oxygen species. PRDX1 and 2 were quantified at relatively high abundance (5–6 NWS on average) in all samples. The presence of those proteins in the UF suggests a role in maintaining the redox balance and controlling excessive production of reactive oxygen species in the UF. Sperm motility and embryo development depend on low levels of reactive oxygen species [46]. Peroxiredoxins 1 and 6 have been shown to protect sperm from lipid peroxidation [47] and promote sperm motility [48] in humans. Moreover, supplementation of recombinant TXN in the bovine embryo culture medium increased blastocyst rates compared to controls [49].

In addition to protection against cell oxidative stress, proteins like serpins (SERPINA10, B1, C1, D1), peroxidases (GPX, PXDN, MPO) and DAPs more abundant at Post-ov than at Pre-ov (LGALS1, RUVBL1) have reported roles in mediating the immune response [50–53]. This is in accordance with previous proteomic studies on the bovine UF, in which various proteins involved in the immune system were also identified [18,20,54]. It is well-known that a physiological immune response takes place in the uterine lumen following the first contact with sperm [55]. Neutrophils eliminate sperm through direct cell-cell interactions and neutrophil extracellular traps (NETs), which hinder sperm motility [56]. Proteins in the periovulatory UF are expected to modulate sperm elimination. SERPINB1, identified in all samples but at low abundance (<2 NWS), has been shown to restrict the formation of NETs by inhibiting the activity of neutrophil elastase *in vitro* [50,51]. Furthermore, the incubation of bull sperm with myeloperoxidase (MPO), a NET-derived protein identified below the quantitative threshold in all samples, impairs the sperm membrane, acrosome integrity and lipid peroxidation [52]. Finally, recombinant galectin-1 (LGALS1) has been shown to induce the expression of anti-inflammatory interleukin-10 and the regulatory T lymphocyte marker FOXP3 in bovine endometrium [53].

Regarding the cellular components of the identified UF proteins, the focal adhesion and proteasome complex, including numerous proteins of the 26S proteasome, were overrepresented. In accordance, in mares, uterine cytobrush sampling during estrus revealed that overexpressed genes in fertile compared to subfertile mares were involved in focal adhesions [57]. Furthermore, inhibition of proteins of the 26S proteasome reduced boar sperm tyrosine phosphorylation and Zn^{2+} efflux compared to controls [58], suggesting a role for proteasome proteins secreted in the UF in sperm capacitation.

Most proteins identified in the bovine UF were enriched in binding functions, also in accordance with previous proteomic studies in cattle [20] and horse [59]. Of interest, some of the most abundant proteins in the periovulatory UF, like annexins A1, A2 and

Fig. 8. Proteomaps of differentially abundant proteins between pre- and post-ovulatory stages of cycle in the uterine horn ipsilateral to ovulation. Each panel was built by the Proteomaps online tool. Each protein is shown by a polygon (A) and functionally related proteins are arranged in common regions based on the KEGG Pathways gene classification (B, and C). Polygon areas represent the mean abundance at the pre-ovulatory stage of cycle.

myosin-9, were previously reported to interact with sperm [60] and embryos [13] after incubation with bovine oviduct fluid *in vitro*. Although embryos interact first with the oviduct fluid, sperm interact first with the UF, then the oviduct fluid. Further studies are needed to know with which proteins sperm interact first during their uterine migration and whether those interactions compete with further interactions in the oviduct.

Proteins in the UF may be secreted via the classical reticulum endoplasmic-Golgi pathway or in EVs [61,62], and one possible mechanism of UF protein interaction with sperm and embryos is EV-mediated. In our study, 17% of proteins were reported in bovine UF-derived EVs and some DAPs more abundant at the pre-ovulatory stage (KRT18), or in the opposite, at the post-ovulatory stage (CAND1), were enriched in vesicular transport through exosomes. Interaction of spermatozoa with uterine EVs has been reported as one mechanism allowing for the delivery of SPAM1, a hyaluronidase important for the crossing of cumulus cells in mice [63]. Uterine EVs were shown to interact with human sperm head and tail after only 15 min of co-incubation and to promote tyrosine phosphorylation [64], one sign of sperm capacitation. The uptake of uterine EVs was also reported in the ovine embryo [65], suggesting important roles for further development.

Although providing valuable data on the uterine proteome, this study presents some limitations. Uterine fluids were collected from slaughterhouse tracts. Although tracts were transported on ice with less than 2 h between animal death and collection, we cannot rule out limited changes in the protein content due to post-mortem modifications. Furthermore, in order to obtain enough protein content per sample and decrease inter-individual variability, pools of two uterine flushes at the same stage of the cycle were analyzed; this precludes any evaluation of inter-individual or inter-breed variability on the UF proteome.

In conclusion, the data reported here expand our knowledge on the environment encountered by spermatozoa after insemination and the early embryo a few days after fertilization. In contrast with our previous data on the oviduct fluid proteome [14,66], no major effect of the proximity of the ovulatory ovary on protein abundance was evidenced. Further work is now needed to understand the potential role of the DAPs between stages on the adaptative response of the uterus to allow sperm migration then early embryo development in a short time window.

Data availability

The mass spectrometry proteomics data have been deposited to the ProteomeXchange Consortium [67] via the PRIDE (version 2.5.7) [68] partner repository with the dataset identifier PX038325.

CRediT authorship contribution statement

Coline Mahé: Validation, Formal analysis, Investigation, Writing – original draft, Writing – review & editing, Visualization. **Paulo Marcelo:** Formal analysis, Investigation, Resources, Writing – review & editing. **Guillaume Tsikis:** Investigation, Writing – review & editing. **Daniel Tomas:** Validation, Formal analysis, Resources, Writing – review & editing. **Valérie Labas:** Validation, Formal analysis, Resources, Writing – review & editing. **Marie Saint-Dizier:** Methodology, Investigation, Writing – original draft, Writing – review & editing, Supervision, Project administration, Funding acquisition.

Declarations of competing interest

The authors declare that they have no competing interests.

Acknowledgments

The authors warmly thank Thierry Delpuech and Albert Arnoult for collecting the tracts at the slaughterhouse. This work was funded by INRAE and Agence Nationale de la Recherche under grant number ANR-18-CE92-0049.

Appendix A. Supplementary data

Supplementary data to this article can be found online at https://doi.org/10.1016/j.theriogenology.2023.01.006.

References

[1] Hackett AJ, Durnford R, Mapletoft RJ, Marcus GJ. Location and status of embryos in the genital tract of superovulated cows 4 to 6 days after insemination. Theriogenology 1993;40:1147–53. https://doi.org/10.1016/0093-691X(93)90285-D.
[2] Simintiras CA, Sánchez JM, McDonald M, Lonergan P. Progesterone alters the bovine uterine fluid lipidome during the period of elongation. Reproduction 2019;157:399–411. https://doi.org/10.1530/REP-18-0615.
[3] Silva FACC, da Silva GF, Vieira BS, Neto AL, Rocha CC, Lo Turco EG, et al. Periestrus ovarian, uterine, and hormonal variables determine the uterine luminal fluid metabolome in beef heifers. Biol Reprod 2021;105:1140–53. https://doi.org/10.1093/biolre/ioab149.
[4] Hugentobler SA, Diskin MG, Leese HJ, Humpherson PG, Watson T, Sreenan JM, et al. Amino acids in oviduct and uterine fluid and blood plasma during the estrous cycle in the bovine. Mol Reprod Dev 2007;74:445–54. https://doi.org/10.1002/mrd.20607.
[5] Maloney S, Khan FA, Chenier TS, Diel de Amorim M, Anthony Hayes M, Scholtz EL. A comparison of the uterine proteome of mares in oestrus and dioestrus. Reprod Domest Anim 2019;54:473–9. https://doi.org/10.1111/rda.13375.
[6] Gegenfurtner K, Fröhlich T, Flenkenthaler F, Kösters M, Fritz S, Desnoës O, et al. Genetic merit for fertility alters the bovine uterine luminal fluid proteome. Biol Reprod 2020;102:730–9. https://doi.org/10.1093/biolre/ioz216.
[7] Kasvandik S, Saarma M, Kaart T, Rooda I, Velthut-Meikas A, Ehrenberg A, et al. Uterine fluid proteins for minimally invasive assessment of endometrial receptivity. J Clin Endocrinol Metab 2020;105:219–30. https://doi.org/10.1210/clinem/dgz019.
[8] Abe H, Sendai Y, Satoh T, Hoshi H. Secretory products of bovine oviductal epithelial cells support the viability and motility of bovine spermatozoa in culture in vitro. J Exp Zool 1995;272:54–61. https://doi.org/10.1002/jez.1402720107.
[9] Chirinos M, Durand M, González-González ME, Hernández-Silva G, Maldonado-Rosas I, López P, et al. Uterine flushings from women treated with levonorgestrel affect sperm functionality in vitro. Reprod Camb Engl 2017;154:607–14. https://doi.org/10.1530/REP-17-0313.
[10] Luongo C, Abril-Sánchez S, Hernández JG, García-Vázquez FA. Seminal plasma mitigates the adverse effect of uterine fluid on boar spermatozoa. Theriogenology 2019;136:28–35. https://doi.org/10.1016/j.theriogenology.2019.06.018.
[11] Hamdi M, Lopera-Vasquez R, Maillo V, Sanchez-Calabuig MJ, Núnez C, Gutierrez-Adan A, et al. Bovine oviductal and uterine fluid support in vitro embryo development. Reprod Fertil Dev 2018;30:935. https://doi.org/10.1071/RD17286.
[12] Lee RK-K, Tseng H-C, Hwu Y-M, Fan C-C, Lin M-H, Yu J-J, et al. Expression of cystatin C in the female reproductive tract and its effect on human sperm capacitation. Reprod Biol Endocrinol 2018;16:8. https://doi.org/10.1186/s12958-018-0327-0.
[13] Banliat C, Tsikis G, Labas V, Teixeira-Gomes A-P, Com E, Lavigne R, et al. Identification of 56 proteins involved in embryo–maternal interactions in the bovine oviduct. Int J Mol Sci 2020;21:466. https://doi.org/10.3390/ijms21020466.
[14] Mahé C, Lavigne R, Com E, Pineau C, Locatelli Y, Zlotkowska AM, et al. Spatiotemporal profiling of the bovine oviduct fluid proteome around the time of ovulation. Sci Rep 2022;12:4135. https://doi.org/10.1038/s41598-022-07929-3.
[15] Khan FA, Diel de Amorim M, Chenier TS. Qualitative analysis and functional classification of the uterine proteome of mares in oestrus and dioestrus. Reprod Domest Anim 2020;55:1511–9. https://doi.org/10.1111/rda.13800.
[16] Soleilhavoup C, Riou C, Tsikis G, Labas V, Harichaux G, Kohnke P, et al. Proteomes of the female genital tract during the oestrous cycle. Mol Cell Proteomics 2016;15:93–108. https://doi.org/10.1074/mcp.M115.052332.
[17] Sánchez JM, Passaro C, Forde N, Browne JA, Behura SK, Fernández-Fuertes B, et al. Do differences in the endometrial transcriptome between uterine horns ipsilateral and contralateral to the corpus luteum influence conceptus growth to day 14 in cattle? Biol Reprod 2019;100:86–100. https://doi.org/10.1093/biolre/ioy185.
[18] Faulkner S, Elia G, O'Boyle P, Dunn M, Morris D. Composition of the bovine

uterine proteome is associated with stage of cycle and concentration of systemic progesterone. Proteomics 2013;13:3333–53. https://doi.org/10.1002/pmic.201300204.
[19] Mullen MP, Elia G, Hilliard M, Parr MH, Diskin MG, Evans ACO, et al. Proteomic characterization of histotroph during the preimplantation phase of the estrous cycle in Cattle. J Proteome Res 2012;11:3004–18. https://doi.org/10.1021/pr300144q.
[20] Forde N, McGettigan PA, Mehta JP, O'Hara L, Mamo S, Bazer FW, et al. Proteomic analysis of uterine fluid during the pre-implantation period of pregnancy in cattle. Reproduction 2014;147:575–87. https://doi.org/10.1530/REP-13-0010.
[21] Keller A, Nesvizhskii AI, Kolker E, Aebersold R. Empirical statistical model to estimate the accuracy of peptide identifications made by MS/MS and database search. Anal Chem 2002;74:5383–92. https://doi.org/10.1021/ac025747h.
[22] Nesvizhskii AI, Keller A, Kolker E, Aebersold R. A statistical model for identifying proteins by tandem mass spectrometry. Anal Chem 2003;75:4646–58. https://doi.org/10.1021/ac0341261.
[23] Bardou P, Mariette J, Escudié F, Djemiel C, Klopp C. jvenn: an interactive Venn diagram viewer. BMC Bioinf 2014;15:293. https://doi.org/10.1186/1471-2105-15-293.
[24] Zhao L, Poschmann G, Waldera-Lupa D, Rafiee N, Kollmann M, Stühler K. OutCyte: a novel tool for predicting unconventional protein secretion. Sci Rep 2019;9:19448. https://doi.org/10.1038/s41598-019-55351-z.
[25] Teufel F, Almagro Armenteros JJ, Johansen AR, Gíslason MH, Pihl SI, Tsirigos KD, et al. SignalP 6.0 predicts all five types of signal peptides using protein language models. Nat Biotechnol 2022;40:1023–5. https://doi.org/10.1038/s41587-021-01156-3.
[26] Kusama K, Nakamura K, Bai R, Nagaoka K, Sakurai T, Imakawa K. Intrauterine exosomes are required for bovine conceptus implantation. Biochem Biophys Res Commun 2018;495:1370–5. https://doi.org/10.1016/j.bbrc.2017.11.176.
[27] Zhou Y, Zhou B, Pache L, Chang M, Khodabakhshi AH, Tanaseichuk O, et al. Metascape provides a biologist-oriented resource for the analysis of systems-level datasets. Nat Commun 2019;10:1523. https://doi.org/10.1038/s41467-019-09234-6.
[28] Liebermeister W, Noor E, Flamholz A, Davidi D, Bernhardt J, Milo R. Visual account of protein investment in cellular functions. Proc Natl Acad Sci USA 2014;111:8488–93. https://doi.org/10.1073/pnas.1314810111.
[29] Moraes JGN, Behura SK, Bishop JV, Hansen TR, Geary TW, Spencer TE. Analysis of the uterine lumen in fertility-classified heifers: II. Proteins and metabolites. Biol Reprod 2020;102:571–87. https://doi.org/10.1093/biolre/ioz197.
[30] Ehrenwald E, Foote RH, Parks JE. Bovine oviductal fluid components and their potential role in sperm cholesterol efflux. Mol Reprod Dev 1990;25:195–204. https://doi.org/10.1002/mrd.1080250213.
[31] Bernecic NC, Zhang M, Gadella BM, Brouwers JFHM, Jansen JWA, Arkesteijn GJA, et al. BODIPY-cholesterol can be reliably used to monitor cholesterol efflux from capacitating mammalian spermatozoa. Sci Rep 2019;9. https://doi.org/10.1038/s41598-019-45831-7.
[32] Zhao R, Dai H, Arias RJ, De Blas GA, Orta G, Pavarotti MA, et al. Direct activation of the proton channel by albumin leads to human sperm capacitation and sustained release of inflammatory mediators by neutrophils. Nat Commun 2021;12:3855. https://doi.org/10.1038/s41467-021-24145-1.
[33] Baker ME. Albumin's role in steroid hormone action and the origins of vertebrates: is albumin an essential protein? FEBS Lett 1998;439:9–12. https://doi.org/10.1016/S0014-5793(98)01346-5.
[34] Hugentobler SA, Humpherson PG, Leese HJ, Sreenan JM, Morris DG. Energy substrates in bovine oviduct and uterine fluid and blood plasma during the oestrous cycle. Mol Reprod Dev 2008;75:496–503. https://doi.org/10.1002/mrd.20760.
[35] Rodriguez-Martinez H, McKenna D, Weston PG, Whitmore HL, Gustafsson BK. Uterine motility in the cow during the estrous cycle. I. Spontaneous activity. Theriogenology 1987;27:337–48. https://doi.org/10.1016/0093-691X(87)90222-6.
[36] Arai M, Yoshioka S, Tasaki Y, Okuda K. Remodeling of bovine endometrium throughout the estrous cycle. Anim Reprod Sci 2013;142:1–9. https://doi.org/10.1016/j.anireprosci.2013.08.003.
[37] Billhaq DH, Lee S, Lee S. The potential function of endometrial-secreted factors for endometrium remodeling during the estrous cycle. Anim Sci J 2020;91. https://doi.org/10.1111/asj.13333.
[38] Song G, Bailey DW, Dunlap KA, Burghardt RC, Spencer TE, Bazer FW, et al. Cathepsin B, Cathepsin L, and Cystatin C in the Porcine Uterus and Placenta: potential roles in endometrial/placental remodeling and in fluid-phase transport of proteins secreted by uterine epithelia across placental Areolae. Biol Reprod 2010;82:854–64. https://doi.org/10.1095/biolreprod.109.080929.
[39] Song G, Spencer TE, Bazer FW. Cathepsins in the ovine uterus: regulation by pregnancy, progesterone, and interferon tau. Endocrinology 2005;146:4825–33. https://doi.org/10.1210/en.2005-0768.
[40] França MR, da Silva MIS, Pugliesi G, Van Hoeck V, Binelli M. Evidence of endometrial amino acid metabolism and transport modulation by periovulatory endocrine profiles driving uterine receptivity. J Anim Sci Biotechnol 2017;8:54. https://doi.org/10.1186/s40104-017-0185-1.
[41] Williams AC, Ford WC. The role of glucose in supporting motility and capacitation in human spermatozoa. J Androl 2001;22:680–95. https://doi.org/10.1002/j.1939-4640.2001.tb02229.x.
[42] Ferramosca A, Zara V. Bioenergetics of mammalian sperm capacitation. 2014 BioMed Res Int 2014:1–8. https://doi.org/10.1155/2014/902953.
[43] Khurana NK, Niemann H. Energy metabolism in preimplantation bovine embryos derived in vitro or in vivo. Biol Reprod 2000;62:847–56. https://doi.org/10.1095/biolreprod62.4.847.
[44] Kim K-U, Pang W-K, Kang S, Ryu D-Y, Song W-H, Rahman MS, et al. Sperm solute carrier family 9 regulator 1 is correlated with boar fertility. Theriogenology 2019;126:254–60. https://doi.org/10.1016/j.theriogenology.2018.12.023.
[45] Chávez JC, Hernández-González EO, Wertheimer E, Visconti PE, Darszon A, Treviño CL. Participation of the Cl−/HCO3− exchangers SLC26A3 and SLC26A6, the Cl− channel CFTR, and the regulatory factor SLC9A3R1 in mouse sperm capacitation. Biol Reprod 2012;86. https://doi.org/10.1095/biolreprod.111.094037.
[46] Ribeiro JC, Braga PC, Martins AD, Silva BM, Alves MG, Oliveira PF. Antioxidants present in reproductive tract fluids and their relevance for fertility. Antioxidants 2021;10:1441. https://doi.org/10.3390/antiox10091441.
[47] Lee D, Moawad AR, Morielli T, Fernandez MC, O'Flaherty C. Peroxiredoxins prevent oxidative stress during human sperm capacitation. Mol Hum Reprod 2016;23:106–15. https://doi.org/10.1093/molehr/gaw081.
[48] Gong S, Gabriel MCS, Zini A, Chan P, O'Flaherty C. Low amounts and high thiol oxidation of peroxiredoxins in spermatozoa from infertile men. J Androl 2012;33:1342–51. https://doi.org/10.2164/jandrol.111.016162.
[49] Bing YZ, Hirao Y, Takenouchi N, Che LM, Nakamura H, Yodoi J, et al. Effects of thioredoxin on the preimplantation development of bovine embryos. Theriogenology 2003;59:863–73. https://doi.org/10.1016/S0093-691X(02)01158-5.
[50] Majewski P, Majchrzak-Gorecka M, Grygier B, Skrzeczynska-Moncznik J, Osiecka O, Cichy J. Inhibitors of serine proteases in regulating the production and function of neutrophil extracellular traps. Front Immunol 2016;7. https://doi.org/10.3389/fimmu.2016.00261.
[51] Farley K, Stolley JM, Zhao P, Cooley J, Remold-O'Donnell E. A serpinB1 regulatory mechanism is essential for restricting neutrophil extracellular trap generation. 1950 J Immunol Baltim Md 2012;189:4574–81. https://doi.org/10.4049/jimmunol.1201167.
[52] Moya C, Rivera-Concha R, Pezo F, Uribe P, Schulz M, Sánchez R, et al. Adverse effects of single neutrophil extracellular trap-derived components on bovine sperm function. Animals 2022;12:1308. https://doi.org/10.3390/ani12101308.
[53] Chaney HL, Grose LF, LaBarbara JM, Sirk AW, Blancke AM, Sánchez JM, et al. Galectin-1 induces gene and protein expression related to maternal-conceptus immune tolerance in bovine endometrium. Biol Reprod 2022;106:487–502. https://doi.org/10.1093/biolre/ioab215.
[54] Faulkner S, Elia G, Mullen MP, O'Boyle P, Dunn MJ, Morris D. A comparison of the bovine uterine and plasma proteome using iTRAQ proteomics. Proteomics 2012;12:2014–23. https://doi.org/10.1002/pmic.201100609.
[55] Fair T. The contribution of the maternal immune system to the establishment of pregnancy in cattle. Front Immunol 2015;6. https://doi.org/10.3389/fimmu.2015.00007.
[56] Wrenzycki C. Interaction of sperm cells with the female reproductive tract in cattle: focus on neutrophil extracellular trap formation. Anim Reprod Sci 2022:107056. https://doi.org/10.1016/j.anireprosci.2022.107056.
[57] Weber KS, Wagener K, Blanco M, Bauersachs S, Bollwein H. A comparative analysis of the intrauterine transcriptome in fertile and subfertile mares using cytobrush sampling. BMC Genom 2021;22:377. https://doi.org/10.1186/s12864-021-07701-3.
[58] Qu X, Han Y, Chen X, Lv Y, Zhang Y, Cao L, et al. Inhibition of 26 S proteasome enhances AKAP3-mediated cAMP-PKA signaling during boar sperm capacitation. Anim Reprod Sci 2022:107079. https://doi.org/10.1016/j.anireprosci.2022.107079.
[59] Smits K, Willems S, Van Steendam K, Van De Velde M, De Lange V, Ververs C, et al. Proteins involved in embryo-maternal interaction around the signalling of maternal recognition of pregnancy in the horse. Sci Rep 2018;8:5249. https://doi.org/10.1038/s41598-018-23537-6.
[60] Lamy J, Nogues P, Combes-Soia L, Tsikis G, Labas V, Mermillod P, et al. Identification by proteomics of oviductal sperm-interacting proteins. Reproduction 2018;155:457–66. https://doi.org/10.1530/REP-17-0712.
[61] Almiñana C, Rudolf Vegas A, Tekin M, Hassan M, Uzbekov R, Fröhlich T, et al. Isolation and characterization of equine uterine extracellular vesicles: a comparative methodological study. Int J Mol Sci 2021;22:979. https://doi.org/10.3390/ijms22020979.
[62] Hamdi M, Cañon-Beltrán K, Mazzarella R, Cajas YN, Leal CLV, Gutierrez-Adan A, et al. Characterization and profiling analysis of bovine oviduct and uterine extracellular vesicles and their miRNA cargo through the estrous cycle. Faseb J 2021;35:e22000. https://doi.org/10.1096/fj.202101023R.
[63] Griffiths GS, Galileo DS, Reese K, Martin-DeLeon PA. Investigating the role of murine epididymosomes and uterosomes in GPI-linked protein transfer to sperm using SPAM1 as a model. Mol Reprod Dev 2008;75:1627–36. https://

doi.org/10.1002/mrd.20907.
[64] Franchi A, Cubilla M, Guidobaldi HA, Bravo AA, Giojalas LC. Uterosome-like vesicles prompt human sperm fertilizing capability. Mol Hum Reprod 2016. https://doi.org/10.1093/molehr/gaw066. molehr;gaw066v2.
[65] Burns GW, Brooks KE, Spencer TE. Extracellular vesicles originate from the conceptus and uterus during early pregnancy in sheep. Biol Reprod 2016;94. https://doi.org/10.1095/biolreprod.115.134973.
[66] Lamy J, Labas V, Harichaux G, Tsikis G, Mermillod P, Saint-Dizier M. Regulation of the bovine oviductal fluid proteome. Reproduction 2016;152:629–44. https://doi.org/10.1530/REP-16-0397.
[67] Deutsch EW, Bandeira N, Sharma V, Perez-Riverol Y, Carver JJ, Kundu DJ, et al. The ProteomeXchange consortium in 2020: enabling 'big data' approaches in proteomics. Nucleic Acids Res 2019:gkz984. https://doi.org/10.1093/nar/gkz984.
[68] Perez-Riverol Y, Csordas A, Bai J, Bernal-Llinares M, Hewapathirana S, Kundu DJ, et al. The PRIDE database and related tools and resources in 2019: improving support for quantification data. Nucleic Acids Res 2019;47:D442–50. https://doi.org/10.1093/nar/gky1106.

1.2. Protéome luminal de l'oviducte et variations en fonction de la région anatomique, du stade péri-ovulatoire et du côté de l'ovulation

Ce travail est présenté sous la forme d'un **schéma récapitulatif** (Figure 9 page 93) et de l'**article 2** « Spatiotemporal profiling of the bovine oviduct fluid proteome around the time of ovulation » publié dans *Scientific Reports* en mars 2022.

Contexte et objectif

Pendant la période péri-ovulatoire, les sécrétions de l'oviducte offrent des conditions optimales pour la survie des spermatozoïdes dans l'isthme (où se situe le réservoir spermatique) puis la fécondation dans l'ampoule. Dans les 4-5 jours suivant l'ovulation, l'isthme est également le lieu du développement embryonnaire précoce. La littérature rapporte un rôle important des protéines dans les interactions entre gamètes/embryon et environnement maternel au sein de l'oviducte. Afin de mieux comprendre la régulation de cet environnement, l'objectif de cette étude est d'évaluer l'effet de la région de l'oviducte (isthme vs ampoule), du stade relatif à l'ovulation (pré- vs. post-ovulatoire) et de la proximité de l'ovaire ovulant (ipsi- vs controlatérale) sur la composition protéique du fluide d'oviducte.

Matériel et méthodes

Les oviductes et ovaires de vaches adultes cyclées ont été collectés dans un abattoir proche du laboratoire et transportés sur glace. En fonction de la morphologie des ovaires, les oviductes ont été classés au stade pré- ou post-ovulatoire (n=16 vaches par stade) du cycle estrien. Les fluides d'isthme et d'ampoule des deux côtés de l'ovulation et aux deux stades du cycle ont été collectés séparément par flush PBS. Pour l'analyse protéomique, 4 pools de 4 vaches ont été constitués pour les 8 conditions (2 régions × 2 stades × 2 côtés). Les protéines des 32 échantillons ont été digérées puis analysées par nanoLC-MS/MS. Les protéines ont été identifiées dans la base de données Unitprot *Bos taurus* puis quantifiées par comptage spectral.

Les effets globaux de la région anatomique, du stade péri-ovulatoire et de la proximité de l'ovaire ovulant sur les abondances protéiques ont été analysés par analyse en composante principale et clustering hiérarchique. Les protéines différentiellement abondantes en fonction des trois facteurs ont été identifiées par des comparaisons deux à deux via des tests de Student (logiciel R, p-value ≤ 0.05).

Les voies de sécrétion des protéines ont été prédites par analyses bio-informatiques des séquences protéiques et comparaison aux protéomes publiés des vésicules extracellulaires du fluide oviductal bovin. Les fonctions des protéines différentielles ont été prédites par analyse de type Gene ontology des gènes correspondants.

Résultats

Au total, 3760 protéines ont été identifiées dans le fluide oviductal. Sur l'ensemble de ces protéines, 10% sont prédites comme étant sécrétées via un peptide signal, 27% de manière non conventionnelle et 41% précédemment identifiées dans les vésicules extracellulaires de fluide. Les protéines les plus abondantes incluent l'albumine, plusieurs protéines de chocs thermiques (HSPAA1, A5, A8, B1), la molécule CD109, l'oviductine et la myosine-9. L'analyse en composante principale a montré que la région anatomique était la plus grande source de variation entre échantillons, suivie de la proximité de l'ovaire ovulant et du stade péri-ovulatoire. En accord, 8 à 12% des protéines varient en abondance selon la région, 3-8% selon la proximité de l'ovaire ovulant et 2% selon le stade péri-ovulatoire. L'analyse fonctionnelle des protéines différentiellement abondantes a révélé un large panel de fonctions biologiques parmi lesquelles la réponse au stress, la régulation de la prolifération et l'adhésion cellulaire, et des fonctions associées à la maturation des gamètes, la fécondation et le développement embryonnaire.

Conclusion

Cette étude présente une analyse exhaustive et dynamique du paysage protéique de la lumière de l'oviducte en période péri-conceptionnelle. Ces résultats montrent pour la première fois que l'ampoule et l'isthme, pourtant très proches anatomiquement, hébergent des micro-environnements spécifiques. Cette régulation spatio-temporelle de l'oviducte permet probablement de répondre aux besoins de survie puis de capacitation des spz avant la fécondation. Ces travaux fournissent également de nombreuses protéines candidates pour l'étude des interactions entre les gamètes, l'embryon et l'environnement maternel.

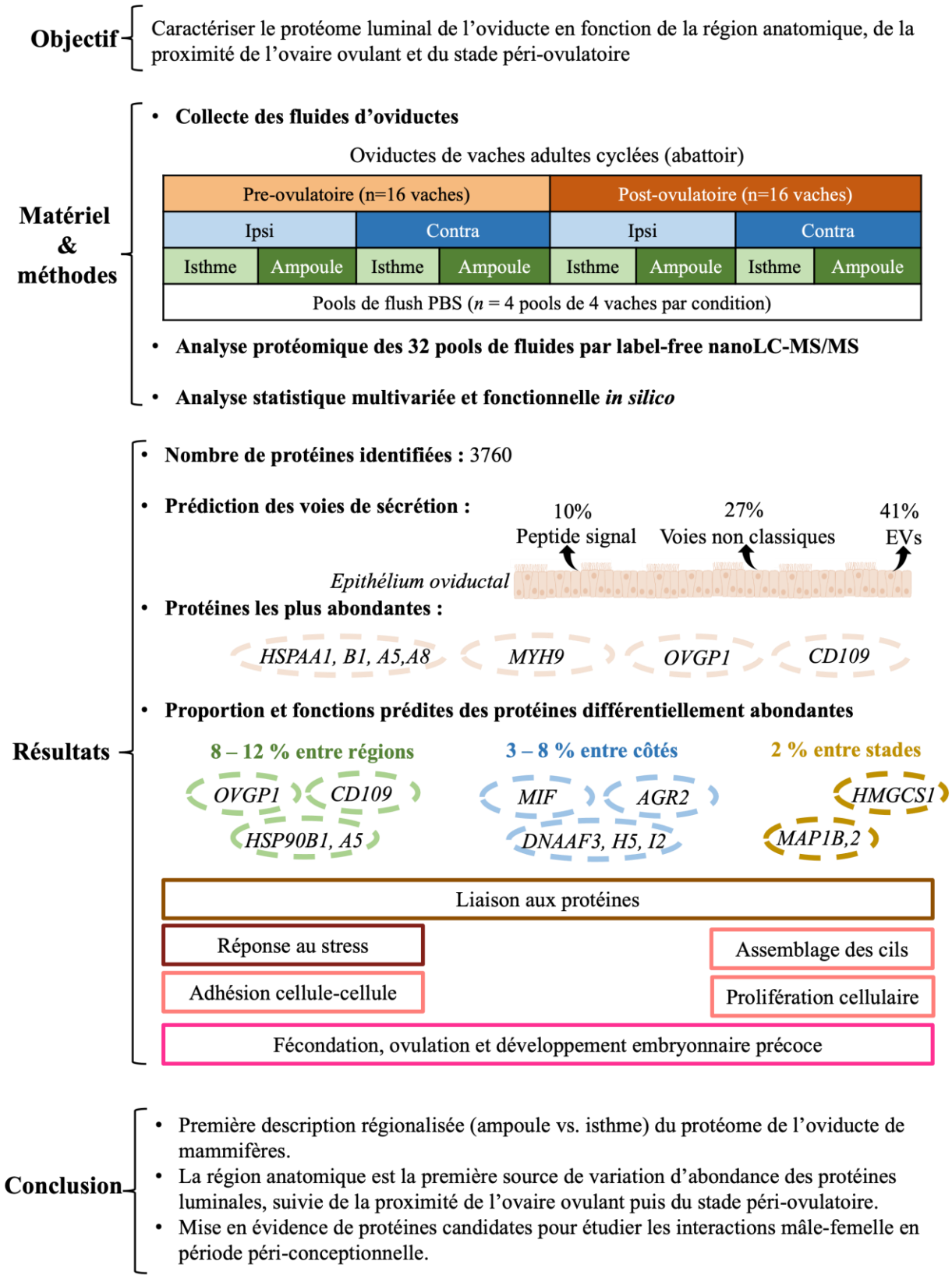

Figure 9 : Schéma récapitulatif de l'étude du protéome luminal de l'oviducte en fonction de la région, du stade péri-ovulatoire et de la proximité de l'ovaire ovulant.
AGR2 = protéine disulphide isomérase ; DNA = protéine axonémale dynéine ; HMGCS1 = 3-hydroxy-3-methylglutaryl coenzyme A synthase ; EVs = vésicules extracellulaires ; HSP = protéine de choc thermique ; MAP = protéines des microtubules ; MIF = Facteur inhibiteur de la migration des macrophages ; MYH = Myosine ; OVGP1 = oviductine

www.nature.com/scientificreports

scientific reports

Check for updates

OPEN

Spatiotemporal profiling of the bovine oviduct fluid proteome around the time of ovulation

Coline Mahé[1]✉, Régis Lavigne[2,3], Emmanuelle Com[2,3], Charles Pineau[2,3], Yann Locatelli[1,4], Aleksandra Maria Zlotkowska[5,8], Carmen Almiñana[1,6], Guillaume Tsikis[1], Pascal Mermillod[1], Jennifer Schoen[5,8] & Marie Saint-Dizier[1,7]

Understanding the composition of the oviduct fluid (OF) is crucial to better comprehend the microenvironment in which sperm capacitation, fertilization and early embryo development take place. Therefore, our aim was to determine the spatiotemporal changes in the OF proteome according to the anatomical region of the oviduct (ampulla *vs.* isthmus), the proximity of the ovulating ovary (ipsilateral *vs.* contralateral side) and the peri-ovulatory stage (pre-ovulatory or Pre-ov *vs.* post-ovulatory or Post-ov). Oviducts from adult cyclic cows were collected at a local slaughterhouse and pools of OF were analyzed by nanoLC-MS/MS and label-free protein quantification (n = 32 OF pools for all region × stage × side conditions). A total of 3760 proteins were identified in the OF, of which 65% were predicted to be potentially secreted. The oviduct region was the major source of variation in protein abundance, followed by the proximity of the ovulating ovary and finally the peri-ovulatory stage. Differentially abundant proteins between regions, stages and sides were involved in a broad variety of biological functions, including protein binding, response to stress, cell-to-cell adhesion, calcium homeostasis and the immune system. This work highlights the dynamic regulation of oviduct secretions and provides new protein candidates for interactions between the maternal environment, the gametes and the early embryo.

In vivo, pregnancy establishment requires a sequence of events in the different segments of the oviduct around the time of ovulation. After migration through the uterus, sperm reach the isthmus (i.e., the caudal part of the oviduct) and bind to oviduct epithelial cells (OECs) to form a sperm reservoir until ovulation time when they are gradually released toward the ampulla[1,2]. From the isthmus to the ampulla, spermatozoa are progressively capacitated and acquire the ability to fertilize oocytes[3]. In the immediate post-ovulatory period, the oocyte and surrounding cumulus cells go through the ampulla where fertilization takes place[4]. In the 3–5 days following ovulation, cell divisions of the zygote start in the isthmus and the early embryo finally enters the uterus[5].

Under physiological conditions, the oviduct fluid (OF) offers an optimal environment for these early reproductive events. The OF is a complex mixture of small metabolites, lipids, glycans and proteins originating from secretions of the luminal epithelium, selective ultrafiltrate from the circulating plasma and putative inputs from the follicular fluid[6]. Previous work from our group showed that the steroidomic[7], metabolomic[8] and proteomic[9] composition of the bovine OF varied throughout the estrous cycle and according to the proximity of the Pre-ov follicle (POF) or corpus luteum (CL). Furthermore, variations in gene expression have been reported between ampulla and isthmus[10–13]. However, whether these variations in gene expression are translated into variations in OF protein abundance between ampulla and isthmus is currently not known. Recently, a small set of OF

[1]CNRS, IFCE, INRAE, Université de Tours, PRC, 37380 Nouzilly, France. [2]Inserm, EHESP, Irset (Institut de Recherche en santé, environnement et travail) – UMR-S 1085, Univ Rennes, 35000 Rennes, France. [3]Protim, Biosit – UMS 3480 CNRS, US 018 Inserm, Univ Rennes, 35000 Rennes, France. [4]Laboratoire de la Réserve Zoologique de la Haute Touche, MNHN, Obterre, France. [5]Institute of Reproductive Biology, Leibniz Institute for Farm Animal Biology, FBN, Dummerstorf, Germany. [6]Functional Genomics Group, Institute of Veterinary Anatomy, Vetsuisse Faculty Zurich, University of Zurich, 8315 Lindau, Switzerland. [7]Tours University, Faculty of Sciences and Techniques, Tours, France. [8]Present address: Department of Reproduction Biology, Leibniz Institute for Zoo and Wildlife Research (IZW), Berlin, Germany. ✉email: coline.mahe@inrae.fr

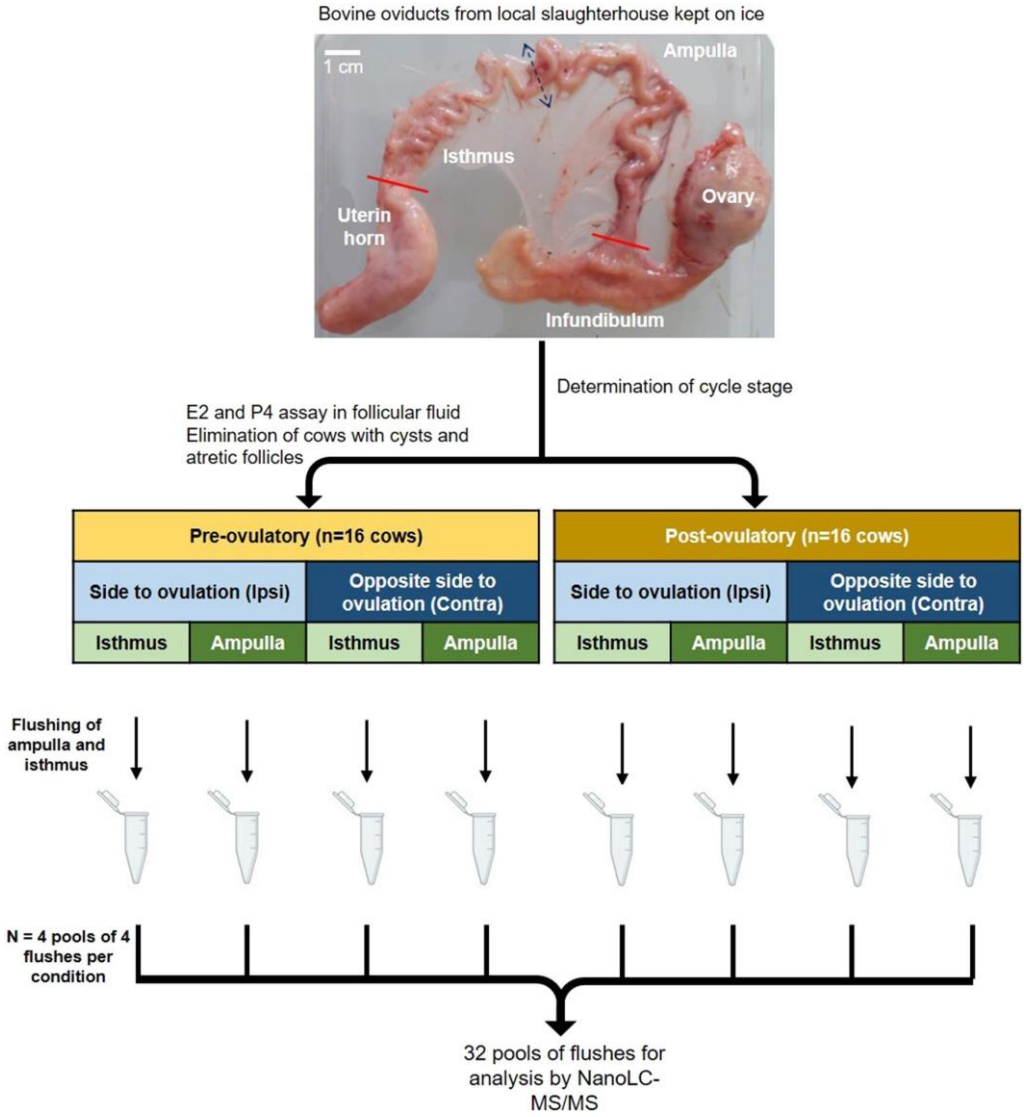

Figure 1. Experimental design of bovine oviduct fluid collection. E2: 17β-estradiol; P4: progesterone. See "Methods" section for further details.

proteins were reported to vary in abundance between cyclic and pregnant cows on day 3 post-estrus, with slight differences between the ampulla and isthmus[14]. Region-related differences in oviductal secretions were reported in vitro: effects of OF-derived extracellular vesicles (EVs)[15] and OF proteins[16] on sperm viability and capacitation differed between ampulla and isthmus. Moreover, the quality of embryos developed in vitro with bovine OF-derived EVs[17] or ovine OECs[18] differed depending on the ampullary or isthmic origin of the EVs or OECs.

The spatiotemporal variation in OF proteome remains unclear. We hypothesize that the OF proteome is monitored by a complex set of factors: the anatomical region of the oviduct, the proximity of POF/CL and the stage of cycle. A dynamic variation between the ampulla and isthmus in the oviduct ipsilateral to ovulation, but also between the Pre-ov and Post-ov stages are expected, in response to the specific requirements of gametes and embryos. Therefore, the objective of this study was to determine the effect on the OF proteome of (1) the region (isthmus *vs*. ampulla), (2) the proximity of the ovulating ovary (ipsilateral *vs*. contralateral side) and (3) the peri-ovulatory stage (Pre-ov *vs*. Post-ov) using nanoLC-MS/MS analysis.

Results

Proteins identified in the bovine OF and predicted secretory pathways. Thirty pools of OF were made (4 cows per pool, 8 region × stage × side conditions) and analyzed by nanoLC-MS/MS (see Fig. 1). A total of 3760 proteins were identified in the bovine OF (Supplementary Data S1). To determine if some proteins were

specific to one region, stage or side, the overlap between conditions was evaluated. Overall, 77% (2894/3760) of proteins were shared between conditions. Of the remaining 23%, only 34 proteins were quantified with more than 5 normalized weighted spectra (NWS, mean values) in one specific region, side or stage (see Supplementary Data S1).

To determine the potential pathways by which proteins were exported into the OF, peptide signal sequences were identified and unconventional secretion pathways were predicted using the Outcyte 1.0 and SignalP 5.0 server on the list of protein gene names. Overall, 37% (1373/3738) of the proteins identified were shown as potentially secreted proteins. Of those, 10% (360/3738) contained a signal peptide and were predicted to be classically secreted while 27% (1013/3738) were predicted to be potentially secreted via unconventional pathways (see the prediction scores and cleavage site positions in Supplementary Data S1). In addition, 41% (1551/3738) of the proteins identified in the bovine OF were previously reported in EVs derived from oviduct epithelial cells (see the list of proteins and origin in Supplementary Data S1)[19–21]. Of the 1551 proteins potentially originated in oEVs, 498 (13%) were previously predicted as potentially secreted by the Outcyte and SignalP tools. By merging the three lists, a total of 2426 proteins (65%) were predicted to be secreted by classical or non-classical (including EVs) pathways.

Spatiotemporal profiling of the OF proteome and functional analysis. To obtain an overview of proteomic data, a principal component analysis (PCA) of proteins quantified with min 2 normalized weighted spectra (NWS) in at least one condition was carried out (3009 proteins). PCA showed a clear separation between the ampullary and isthmic samples (Fig. 2a). Two samples in the Pre-ov ipsilateral isthmus group had to be discarded from further analysis because they had a low MS signal resulting in 50% less proteins identified than in all other samples.

To evaluate more specifically which factors among the region, the peri-ovulatory stage and the proximity of the ovulating ovary most affected the OF proteome, a hierarchical clustering of differentially abundant proteins (DAPs, ANOVA p-value ≤ 0.05) was performed. The heatmap representation of this analysis confirmed that the main differences in protein abundance were between the anatomical regions (ampulla *vs*. isthmus), followed by the proximity of the ovulating ovary (ipsilateral *vs*. contralateral) and finally the stage around ovulation time (Pre-ov *vs*. Post-ov) (Fig. 2b). Based on these findings, statistical analyses comparing ampulla *vs*. isthmus, ipsilateral *vs*. contralateral and Pre-ov *vs*. Post-ov datasets were performed. Overall, pair-wise comparisons (t-test p-value ≤ 0.05) considering a fold-change ratio ≥ 2 evidenced highest numbers of DAPs when comparing ampulla and isthmus (236–354 DAPs, *i.e.,* 8–12% of quantified proteins), followed by those between ipsi- and contralateral sides (83–248 DAPs, i.e. 3–8% of quantified proteins) and finally between the Pre-ov and Post-ov stages (50–67 DAPs, i.e. 2% of quantified proteins; see Fig. 3). Interestingly, the post-ovulatory isthmus, *i.e.,* the place and time of early embryo development, displayed the highest number of DAPs when comparing the ipsilateral with contralateral oviducts. Top-20 DAPs between regions, sides of ovulation and stages are shown in Figs. 4, 5 and 6 respectively (see Supplementary Datas S2–4 for all DAPs with accession numbers, molecular weight, p-value and fold-changes).

To evaluate the functions underlying those variations, an enrichment analysis of genes corresponding to DAPs was undertaken in the Database for Annotation, Visualization and Integrated Discovery (DAVID). This analysis for the effect of the region and stage was performed only on samples from the ipsilateral side. Analysis of the gene ontology (GO) terms associated with DAPs between regions of the oviduct indicated that 67 and 68 biological processes (BP) and molecular functions (MF) were overrepresented (p-value ≤ 0.05) at Pre-ov and Post-ov stages, respectively (Supplementary Data S2). Of those, 21 were shared between stages, including protein binding, cell–cell adhesion, protein folding, calcium ion binding and carbohydrate metabolic process as the most significant at both Pre- and Post-ov (in yellow in Supplementary Data S2). BP/MF overrepresented only at Pre-ov included protein disulfide isomerase activity, response to endoplasmic reticulum stress, redox homeostasis, negative regulation of apoptotic process, and microtubule motor activity (in green in Supplementary Data S2). BP/MF overrepresented only at Post-ov included calcium-dependent protein binding, calmodulin binding and cellular response to catecholamine stimulus (in blue in Supplementary Data S2). To further decipher the role of DAPs, Proteomaps were carried out on overabundant proteins in each region of the ipsilateral oviduct. At Pre-ov, proteins overabundant in the isthmus were mainly involved in protein processing in endoplasmic reticulum and protein export, while proteins overabundant in the ampulla were more specifically involved in the immune and endocrine systems in addition to the isthmic pathways (Fig. 7). Proteomaps generated at post-ovulatory stages displayed globally the same pathways (Supplementary Fig. S2). To point out proteins potentially involved in the reproductive events taking place in the oviduct, proteins overabundant in the ipsilateral isthmus or ampulla were further analyzed through the Metascape[22] membership tool. Proteins associated with the membership terms 'sperm', 'oocyte/ovulation', 'fertilization' and 'embryo' are shown in Fig. 8 (see the exhaustive list of GO terms in Membership analysis Metascape Supplementary Data S2).

Regarding the DAPs between ipsilateral and contralateral oviducts, analysis of the GO terms associated with DAPs between ipsilateral and contralateral oviducts evidenced protein binding as the only enriched MF shared between conditions (Supplementary Data S3). In the ampulla, overrepresented BP/MF included protein binding, endosomal transport, protein transport and multivesicular body assembly among the most significant GO terms at both stages. In the isthmus, the highest number (61) of specifically enriched GO terms was evidenced at Post-ov including mucus secretion, epidermal growth factor (EGF) receptor signaling pathway, ERBB2 signaling pathway and 1-phosphatidylinositol (PI)-3-kinase activity as the most significant ones. In addition, a number of DAPs between sides were associated with the membership terms related to early reproductive events (Fig. 8b and Supplementary Data S3).

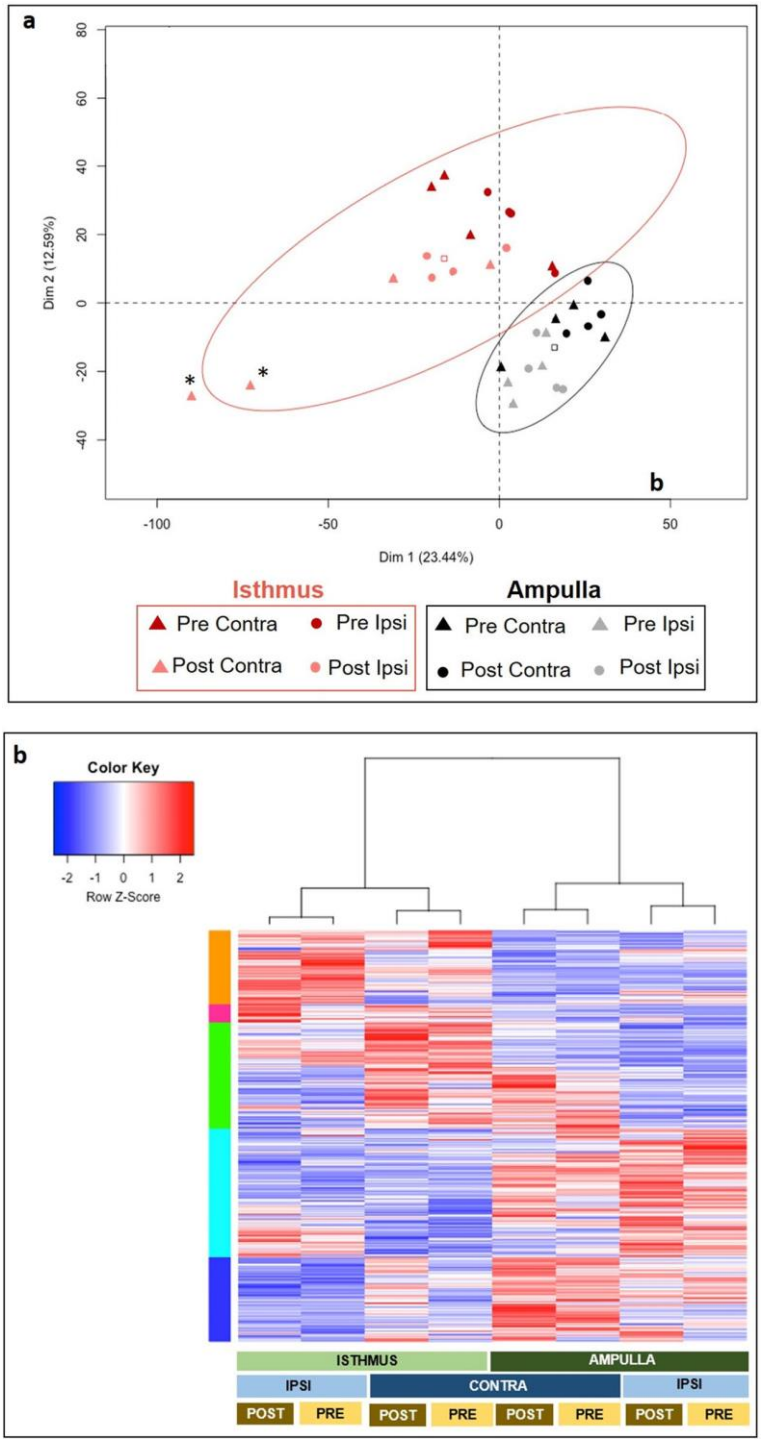

Figure 2. Principal component analysis of all samples (**a**) and heatmap of the 1491 differentially abundant proteins (**b**). (**a**) Principal component analysis of the 32 OF samples showing a separation between regions of the oviduct (red, isthmus; black, ampulla). Each spot represents one biological sample in a given region × stage × side condition (see legends for corresponding form and color). Each ellipse encloses 93–100% of samples for each region. The square in each ellipse represents the mean of data for a given region. Two outsiders in the Pre-ov ipsilateral isthmus group (asterisks) were discarded. (**b**) Heatmap and hierarchical clustering of the 1491 differentially abundant proteins (DAPs; ANOVA p-value ≤ 0.05) identified across regions, stages and sides. Each line corresponds to one protein. For a given protein, blue lines represent higher abundance while red lines represent lower abundance compared to other conditions. White lines represent the median abundance values. Five clusters of proteins were identified by unsupervised hierarchical clustering (vertical multicolored bars on the left). Light and dark blue bars indicate clusters with higher abundance in the isthmus than in the ampulla while orange bar indicates one cluster displaying higher abundance in the ampulla than in the isthmus. The proximity between regions, stages and side of ovulation are shown by the hierarchical tree on top.

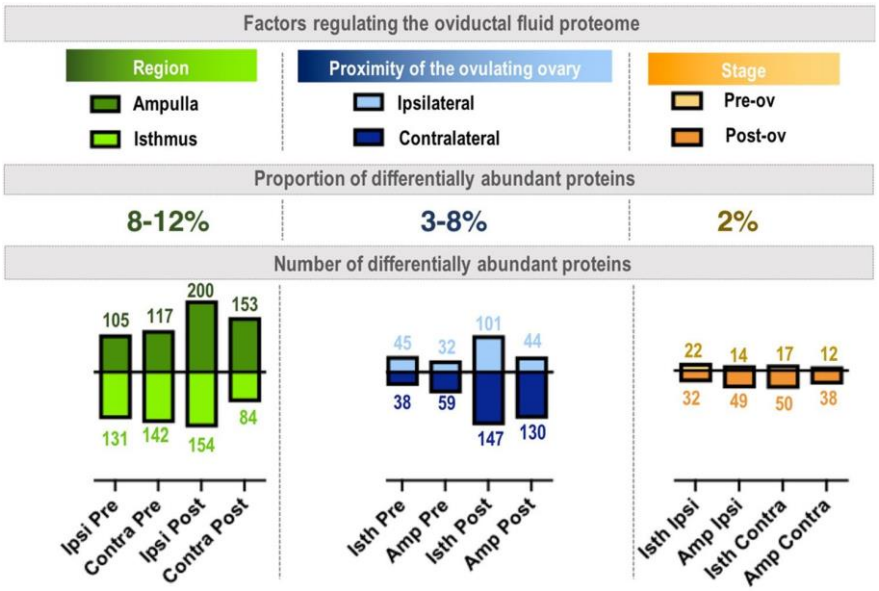

Figure 3. Numbers and proportions of differentially abundant proteins according to the region, proximity of ovulating ovary and peri-ovulatory stage. Proteins were considered as differentially abundant with a t-test p-value ≤ 0.05 and a fold-change ratio ≥ 2 or ≤ 0.5. Each bar represents the number of overabundant proteins (with a min mean value of 2 NWS) in each region × stage × side conditions.

Regarding the DAPs between Pre-ov and Post-ov stages in the ipsilateral oviduct, analysis of the GO terms associated with DAPs between Pre-ov and Post-ov samples in the ipsilateral oviduct evidenced 6 and 5 over-represented BP/MF in the ampulla and isthmus, respectively, of which only protein binding was shared (Supplementary Data S4). BP overrepresented exclusively in the ampulla included regulation of cilium assembly, intraciliary transport and negative regulation of cell proliferation while artery smooth muscle contraction and vasodilatation were overrepresented only in the isthmus (see Supplementary Data S4). The DAPs associated with membership terms related to oviduct events are shown in Supplementary Data S4.

Discussion

The present study provides an extensive analysis of the bovine OF proteome considering three factors of variation, i.e., the anatomical oviduct region, the peri-ovulatory stage and the proximity of the ovulating ovary. The main findings of this study are that (i) 8 to 12% of the proteins quantified varied in abundance between ampulla and isthmus, in accordance with our hypothesis that each segment of the oviduct may respond to specific requirements for the gametes and embryos in case of pregnancy; (ii) the region of the oviduct was more determining than the proximity of the ovulating ovary and the peri-ovulatory stage on protein abundance; (iii) OF proteins varying in abundance are involved in a broad variety of biological functions, including protein binding, response to stress, calcium homeostasis, and lipid and carbohydrate metabolism, which may play key roles in gamete/embryo-oviduct interactions.

Transport of oviducts were carried out on ice, bringing contractions and any chemical reactions to a halt and with limited time after animal death. The process of OF collection was conducted at 4 °C and the quality and homogeneity of protein samples were checked by electrophoresis on SDS-PAGE, however, we cannot exclude minor protein modifications due to post-mortem collection. Leese et al. in 2008 recommended that 1–2 min post-mortem was the optimal time for sample collection in laboratory animals but quite difficult with large animals such as cattle[23]. Various methods of collection of the oviduct fluid were used over the past 50 years[23]. In the late 70s, micro-volume of OF were collected by aspiration under general anesthesia in mice[24,25]. To retrieve larger volume of fluid, the OF was later collected by oviduct cannulation through the infundibulum for several weeks in cattle[26,27]. However, alterations of fluid composition by inflammation and flow disruption have pushed towards a faster OF collection within hours under general anesthesia[28]. In the 90s, OF were also collected ex vivo during blood perfusion of the genital tract after hysterectomy in women[29] and in small laboratory animals like rabbits[30]. However, due to ethical, technical and economic barriers in large animals such as cattle, the post-mortem recovery of oviducts at the slaughterhouse with time periods of 1 to 4 h between animal death and OF collection is preferably used[9,13,14,31,32]. One benefit of post-mortem collection is the absence of contamination with inflammatory products and less hemoglobin than observed after oviduct cannulation[33].

More than 3700 proteins were identified in the bovine OF, which is the most comprehensive OF proteome published so far in mammals[9,33–36]. From the total of protein identified in our study, 37% were predicted as potentially secreted and 10% contained a signal peptide. These proportions of secreted proteins are comparable to those

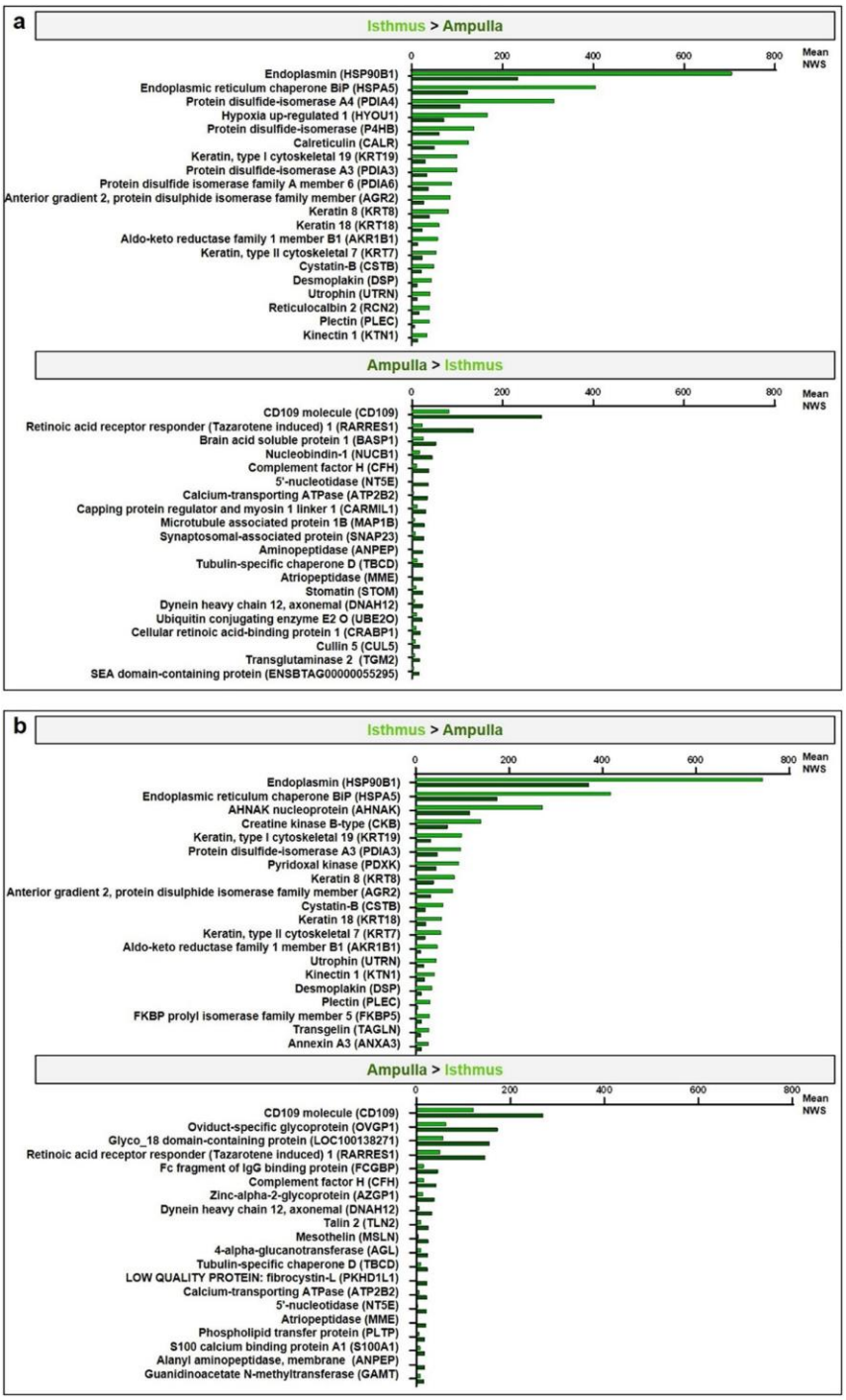

Figure 4. Mean quantitative values of the top-20 differentially abundant proteins between regions in the ipsilateral oviduct at pre-ovulatory (**a**) and post-ovulatory (**b**) stages.

previously reported in the OF in cattle[34,35] and sheep[37]. It is unclear how intracellular proteins could be exported in high proportions to the oviductal lumen. Considering the very low volume of OF in both ampulla (< 50 µL) and isthmus (< 10 µL) and to avoid cell damage, the samples were collected by gentle flushing. Centrifugations

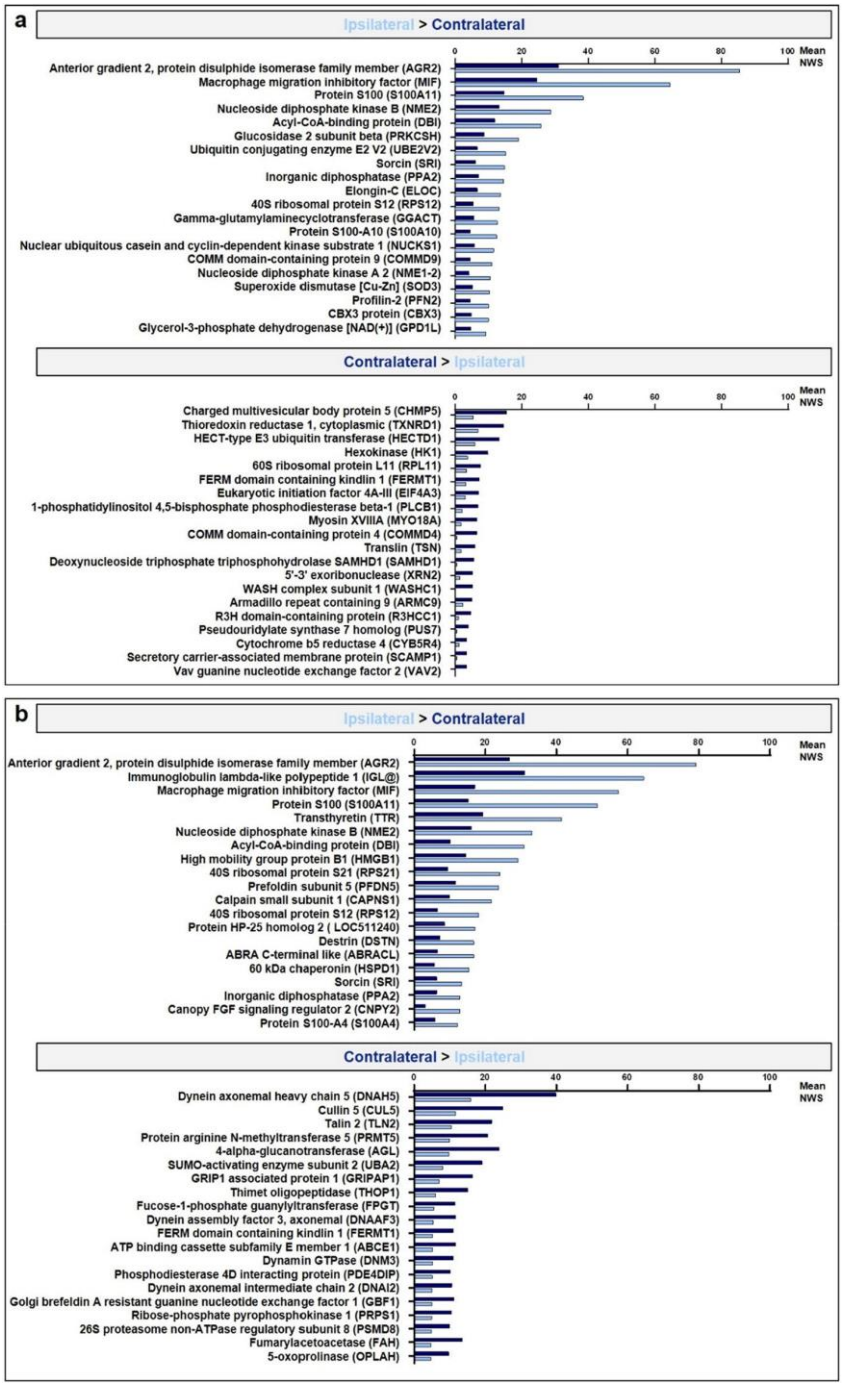

Figure 5. Mean quantitative values of the top-20 differentially abundant proteins according to the proximity of the ovulating ovary in the isthmus at pre-ovulatory (**a**) and at post-ovulatory (**b**) stages.

were then carried out to eliminate cell debris. The high rate of renewal of the oviduct epithelium during estrus[38,39] may lead to intracellular release of proteins into the OF. Moreover, and in the light of our results, it is very likely that intracellular proteins could be derived from apocrine or non-canonical secretory pathways, as it has been

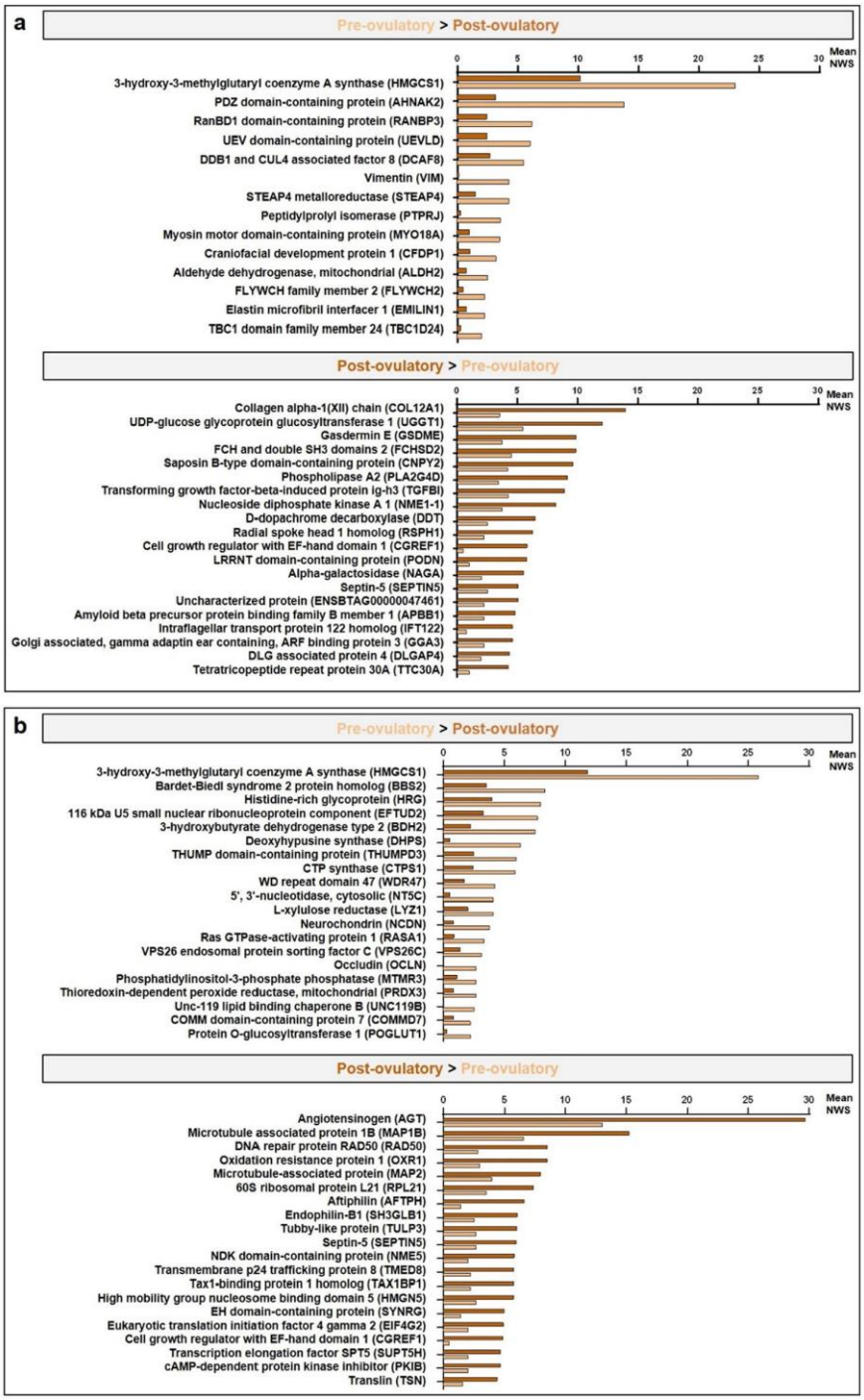

Figure 6. Mean quantitative values of top-20 differentially abundant proteins between stages in the ipsilateral ampulla (**a**) and isthmus (**b**).

shown for annexins (ANXAs)[19,40]. The number of proteins previously identified in OF-derived EVs were higher in cats and pigs (1149 and 1704 proteins) than in cattle (316 proteins) so all three species were considered for

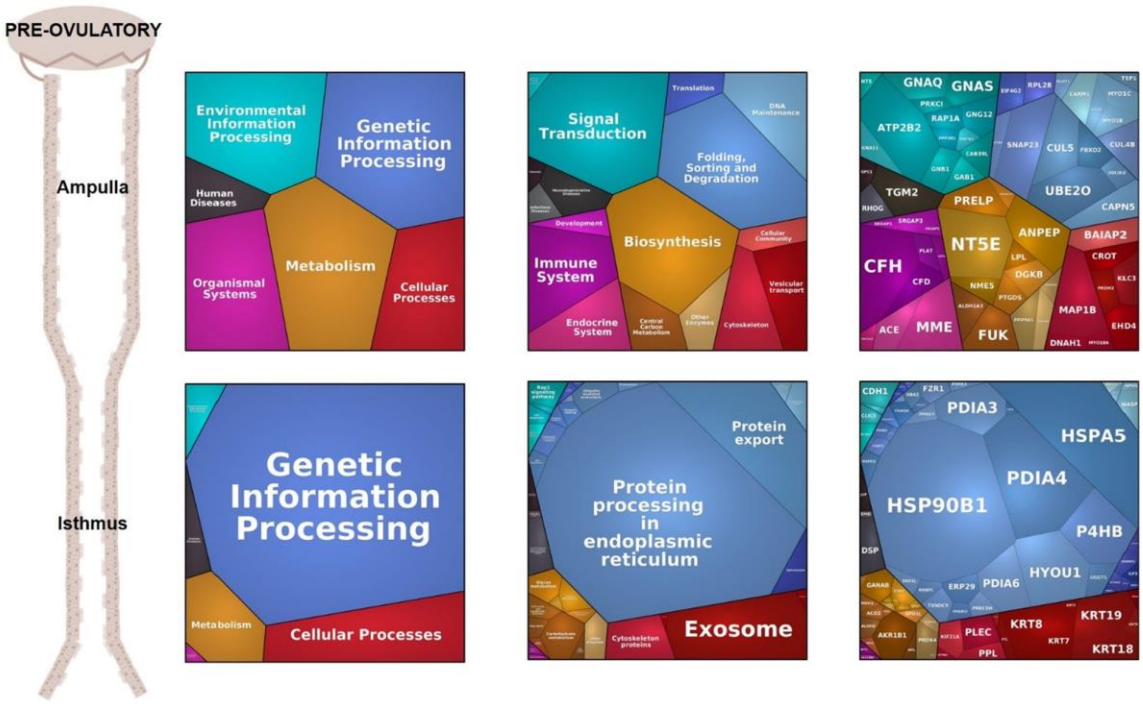

Figure 7. Proteomaps of overabundant proteins in the ipsilateral ampulla and isthmus at Pre-ov stage. Proteomaps were generated using the KEGG (Kyoto Encyclopedia of Genes and Genomes) Pathway gene classification. Functional categories (left and middle panels) and proteins (right panels) are shown by polygons. Areas of polygons illustrate protein normalized abundance in each region. Functions and proteins linked are organized in common regions and coded using similar colors.

the analysis and in accordance, a high proportion of intracellular proteins were previously identified in EVs derived from OF[19–21].

The most abundant proteins quantified in the OF included several HSPs (HSP90B1, HSP90AA1, HSP90AB1, HSPA8, HSPA5 also known as GRP78), CD109 molecule, complement C3, myosins (MYH9, MYH14) and the oviduct-specific glycoprotein or oviductin (OVGP1), as previously reported[9,33,35]. The majority (77%) of proteins quantified were detected in all conditions. The remaining 23% had on average low levels of detection (NWS < 5), suggesting that these proteins could have been detected with a higher sensitivity. Although, little attention has been paid to this small set of proteins, we should not rule out that they may have an important role in the oviduct. The use of mass spectrometer with higher sensitivity could determine whether these proteins were only present in a specific segment of the oviduct or stage, although in small amounts.

The region-related changes in the OF proteome are presented for the first time, providing valuable information on the specific requirements of gametes and embryos. Furthermore, the region was the greatest source of variation in the oviduct proteome. These results are in agreement with previous transcriptomic data evidencing differentially expressed genes between the ampulla and isthmus in cattle[10–13]. Also in accordance, the abundance of specific proteins was differently regulated in each region after insemination in rabbits[41] and between pregnant and cyclic cows[14]. Differences in the vascularization[42] and in the proportion of ciliated cells[39] between isthmus and ampulla could explain this variation in OF proteome. It is well known that sex steroid hormones are major regulators of oviduct physiology and secretory activity[6]. To our knowledge, the region-specific concentrations of progesterone and estradiol in the oviduct have not been reported to date. However, the expression of progesterone receptors was reported to vary according to the oviduct region: transcripts for nuclear receptors (PGR) were more abundant in the isthmus while those for progesterone membrane component 2 (PGRMC2) were higher in the ampulla in cattle[10]. Furthermore, it was shown in gilts that each oviductal region responded differently to estradiol, leading to different regional patterns of secretion[43]. Taken together, the observed region-specific profiling of the OF proteome could result from differences in blood flow, proportion of secretory cells, gene expression and steroid hormone receptivity between ampulla and isthmus.

After mating or insemination, sperm cross the uterus and reach the isthmus where they interact with both OECs and oviduct secretions; these interactions are believed to create an optimal environment for sperm storage until ovulation[2,44]. Of the BP/MF overrepresented exclusively at Pre-ov, proteins involved in cell redox homeostasis (including PRDX3, PRDX4, PDIA3, PDIA6 among others), negative regulation of apoptotic process (incl. HSPA5, HSP90B1, RGN) and microtubule motor activity (incl. DNAH1, KLC3, KIF21A) may be considered as possible candidates to provide an optimal environment for sperm survival and motility until fertilization. Of

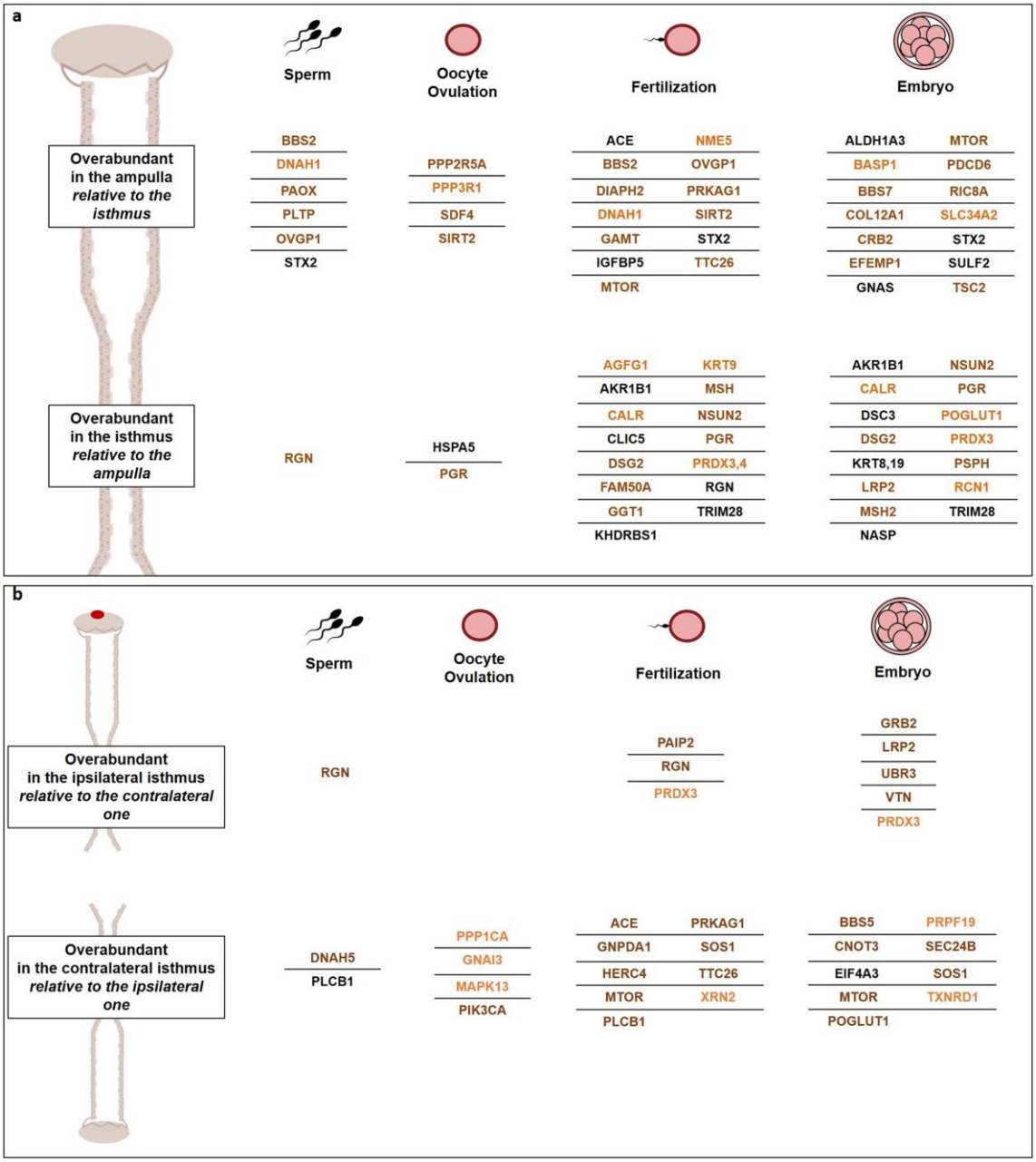

Figure 8. Potential reproductive targets of OF proteins differentially abundant according to the (**a**) ipsilateral regions and (**b**) proximity of the ovulating ovary in the ipsilateral isthmus at both peri-ovulatory stages. Colors indicate the stage at which the protein is overabundant. Orange, overabundant at pre-ovulatory; brown, overabundant at post-ovulatory; black, overabundant at both stages.

those protein candidates, HSP90B1, HSPA5 and PDIA3 were among the most abundant proteins in the isthmus (NWS ≥ 100) and were also 2 to 3 times more abundant than in the ampulla at Pre-ov. HSP90B1, PDIA3 and HSPA5 were previously identified as sperm-binding proteins in the OF in cattle[45]. In humans, the inhibition of PDIA3 by specific antibodies reduced sperm ability to bind to the zona pellucida[46]. In addition, both HSP90B1 and HSPA5 promoted sperm-zona binding in human[47] and pigs[48]. Recombinant HSPA5 enhanced human sperm calcium influx, one step of sperm capacitation[49]. Calreticulin (CALR) was another protein found 2.5 times more abundant in the isthmus compared to the ampulla at Pre-ov. Calreticulin is a calcium-binding protein required for cumulus oocyte complex development[50]. Moreover, addition of recombinant CALR in the fertilization medium blocked polyspermy in pigs[51].

After ovulation, sperm undergo capacitation and migrate gradually toward the ampulla where fertilization takes place, then embryo development starts in the isthmus. Hence, we focused on identified proteins that could play a key role in supporting fertilization, embryo transport and development. Numerous DAPs between regions (incl. HSPA5, HSP90B1, ANXA3, ANXA6, MYO1D, MYO1B, PHKB) were involved in calcium homeostasis, including calcium ion binding and calcium-dependent protein binding. Calcium is well known to play major roles in sperm functions such as motility, capacitation and acrosome reaction[52]. In addition, several proteins (GNAS, GNG2, GNB1) were involved in cell response to catecholamines. Catecholamines have been implicated in the spontaneous contractions of the bovine oviduct[53] and may help embryo transport towards the isthmus. Among the overabundant proteins in the ampulla at Post-ov, oviductin (OVGP1) was among the most abundant proteins (NWS > 150) and 2.7 times more abundant than in the isthmus. Similarly, OVGP1 transcripts were more abundant in the ampulla than in the isthmus at day 4 post-ovulation in cows[12]. OVGP1 is an oviduct-specific glycoprotein secreted around the time of ovulation that plays major roles in zona pellucida hardening and control of polyspermy in mammals[54,55]. Addition of recombinant OVGP1 in a fertilization medium improved sperm-zona pellucida binding in hamster[56] and humans[57]. Moreover, purified or recombinant OVGP1 positively influenced sperm viability, motility and capacitation in buffaloes[58] and humans[57]. Furthermore, numerous proteins over-abundant in the ampulla were involved in the immune system (incl. CFH, CFD, PLAT, PLTP). Complement factor H (CFH) acts as a soluble inhibitor of complement and plays as such an essential role in maintaining a well-balanced immune response. CFH was reported in boar seminal plasma and it was shown that sperm possessing CFH in their outer acrosomal region evaded complement attack in the female tract[59]. The mRNAs for phospholipid transfer protein (PLTP) were reported in the oviduct epithelium of mice and increased in abundance in the presence of embryos but not in pseudo-pregnant mice, suggesting important roles during early development[60].

Beyond the oviduct region, the proximity of the ovulating ovary was another factor correlated with OF protein abundance. The regulatory effect of the POF/CL on OF proteome around the time of ovulation was previously described in cattle[9] and horse[61]. Differentially expressed genes between sides were also identified in the ampulla and isthmus on day 3 post-estrus in cattle[62]. The proportion of secretory cells was reported to be equivalent between ipsilateral and contralateral oviducts[63]. However, highly asymmetrical concentrations of sex steroid hormones were reported in the bovine oviduct, with up to 3.5 times more estradiol before ovulation[64] and up to 16 times more progesterone after ovulation[7] in the ipsilateral oviduct than in the contralateral one. An asymmetry in the local vascularization and anatomy of the oviduct were also reported, with a thicker, more edematous and more transparent wall in the ipsilateral side[65]. Overall, those differences in monovular species could probably be involved in the asymmetrical regulation of oviduct secretions.

The POF/CL effect was expected to be an important regulatory factor, preparing the suitable environment for early embryo development. In accordance, the Post-ov isthmus was the most affected by the proximity of the POF/CL, with 248 DAPs compared with 83–177 DAPs in other pair-wise comparisons between sides of ovulation. In line with the present data, transcriptomic analysis of bovine OECs identified 13 times more differentially expressed genes between sides of ovulation in the isthmus than in the ampulla on Day 3 post-estrus[62]. In a previous proteomic study in cattle, the proportion of DAPs in the entire oviduct was also higher at Post-ov than at Pre-ov[9]. The signaling pathways most significantly altered by the proximity of ovulating ovary included the EGFR, ERBB2 and PI3-kinase (PI3K) pathways after ovulation. Recent results in dogs show that exosomes secreted by oviduct cells mediate the EGFR/mitogen-activated protein kinase (MAPK) signaling pathway, which is one of the prerequisite pathways for further development, in cumulus cells[66]. The PI3K pathway plays also pivotal roles in numerous reproductive processes[67]. The PI3K-Akt pathway was one of the most affected pathways in the oviduct after mating, as shown in a transcriptomic study in pigs[68].

Studies on the factors correlated with differential protein abundance close to the ovulation time are still scarce because most studies compared the estrus/follicular phase to the luteal phase, with a time interval of around 5–12 days between conditions[11,37,69]. The time relative to ovulation (Pre-ov vs. Post-ov) was the factor with least variation between samples with only 2% of DAPs identified in the ampulla and isthmus. Higher rates of DAPs (13–17%) were previously evidenced in the bovine OF between stages but with no region separation[9]. Recently, differences before and after ovulation were reported in the equine OF proteome[36]. These authors reported 15 proteins downregulated in post-ovulatory OF compared to the pre-ovulatory counterpart, while 156 upregulated in post-ovulatory OF compared to pre-ovulatory OF. It is to note that the Pre-ov and Post-ov stages covered approximately 3–4 days around ovulation time and represented a limited time window relative to the 21 to 25-day length of the estrous cycle, which may explain the limited number of DAPs. Functions such as regulation of cilium assembly, intraciliary transport and negative regulation of cell proliferation were affected by the peri-ovulatory stage in the ampulla. The proportions of ciliated cells and of proliferative cells in the oviduct epithelium was reported to change during the estrous cycle in cows[39] with an increase during the follicular phase and a decrease in the luteal phase, which may account for this stage-specific enrichment.

One limitation of the present study is the lack of information on cows' breed, age and metabolic status at the time of OF collection since the samples were collected at a slaughterhouse. The OF proteome was obtained from a total of 32 animals, providing data representative for this species, yet, the samples were analyzed in pools of 4 animals, precluding any evaluation of individual variations.

In conclusion, this study provides a comprehensive characterization of the bovine OF proteome, revealing a fine-tune regulation of the OF according to the anatomical region of the oviduct, the proximity to the ovary and the stage of the cycle. The strong modulatory effect of the oviduct regions points out the anatomical region as the major regulator of OF proteome for the first time. Moreover, the in deep detail of the spatiotemporal proteomic changes of the OF around the ovulation window, enhance our understanding of the oviductal milieu supporting the early reproductive events. The proteins identified here paved the way for future functional experiments towards improving sperm and embryo biotechnologies.

Methods

Collection of bovine oviductal fluid (OF). Both oviducts from adult cyclic cows were collected at a local slaughterhouse (40 min from the lab), placed immediately on ice and transported to the laboratory within max 2 h after animal death. The oviducts were classified into pre-ovulatory (Pre-ov; presence of a *corpus albicans* and one pre-ovulatory follicle of 11–20 mm in diameter, corresponding to approximately days 19–21 of cycle) or post-ovulatory (Post-ov; presence of an early *corpus luteum* made with red loosely organized tissue less than 1 cm in diameter, corresponding to approximately day 1–4 of cycle), as previously described[70]. Oviducts ipsilateral and contralateral to ovulation side were trimmed free of surrounding tissue and vessels and linearized. After removal of the infundibulum and utero-tubal junction, both oviducts were divided into two parts at the ampullary-isthmic junction. The ampulla and isthmus were individually flushed with 200 µL of cold sterile protein-free phosphate buffered saline (PBS) and kept on ice. Cellular debris and cells were eliminated from the OF by two centrifugations (2000*g* for 10 min then 12000*g* for 10 min) at 4 °C. Samples were stored at − 80 °C until proteomic analysis. A total of 18 Pre-ov and 16 Post-ov cows were collected. In the Pre-ov group, in order to exclude animals with ovarian cyst or atretic follicle, the follicular fluid of the Pre-ov follicle was collected and stored at − 80 °C for steroid hormone analysis, as previously described[71]. Concentrations of P4 were measured by a competitive enzyme-linked immunosorbent assay according to a method previously described[72] whereas E2 concentrations were measured using the BioSource E2-EASIA kit (BioSource Europe S.A., Louvain-la-Neuve, Belgium). Assays were performed in duplicate. Two cows were excluded from the Pre-ov group based on intra-follicular P4 concentrations higher than 160 ng/mL, as previously described[7]. In the resulting Pre-ov group (n = 16), the ranges of P4 and E2 intra-follicular concentrations were 19.4–134.2 ng/mL and 103 to > 2000 ng/mL, respectively.

Preparation of OF samples for proteomic analyses. The OF samples were thawed on ice and pools of 100 µL of OF were made by mixing 25 µL of individual samples. Four pools of 4 cows per side × region × stage condition were constituted, leading to 32 OF samples distributed in 8 conditions (Pre-ov ipsilateral ampulla; Pre-ov ipsilateral isthmus; Pre-ov contralateral ampulla; Pre-ov contralateral isthmus; Post-ov ipsilateral ampulla; Post-ov ipsilateral isthmus; Post-ov contralateral ampulla and Post-ov contralateral isthmus). In the following, the term "sample" refers to these pools of OF. Protein concentration of OF samples was assessed using the Uptima BC Assay kit (Interchim, Montluçon, France) according to manufacturer's instructions and using bovine serum albumin as a standard. The homogeneity and quality of samples was checked after migration of the OF pools (5 µg proteins per lane) on a 4–20% SDS-PAGE (80 V, 10 min and 180 V 30 min) and staining with Coomassie blue (see Supplementary Fig. S3).

Nanoliquid chromatography coupled with tandem mass spectrometry (NanoLC-MS/MS). For proteomic analysis, 10 µg of proteins per sample were prepared using the PreOmics iST-BCT kit (PreOmics GmbH, Martinsried, Germany) following the manufacturer's instructions. Briefly, proteins were lysed, denatured, reduced and alkylated for 10 min at 95° then Trypsin/LysC digested for 60 min at 37 °C. Purification and elution of peptides were then carried out for 1 h at room temperature. Samples were then purified from salts, contaminants and other detergents, using reversed phase SDBS spin cartridge (PreOmics GmbH, Martinsried, Germany). Peptide injection and analysis were performed as previously described[32]. The resulting peptide mixtures were loaded on a 75 µm × 250 mm IonOpticks Aurora 2 C18 column (Ion Opticks Pty Ltd., Bundoora, Australia). A gradient of basic reversed-phase buffers (Buffer A: 0.1% formic acid, 98% H_2O MilliQ, 2% acetonitrile; Buffer B: 0.1% formic acid, 100% acetonitrile) was run on a NanoElute HPLC System (Bruker Daltonik GmbH, Bremen, Germany) at a flow rate of 400 nL/min at 50 °C. The liquid chromatography (LC) run lasted for 120 min (2% to 15% of buffer B during 60 min; up to 25% at 90 min; up to 37% at 100 min; up to 95% at 110 min and finally 95% for 10 min to wash the column). The column was coupled online to a TIMS TOF Pro (Bruker Daltonik GmbH, Bremen, Germany) with a CaptiveSpray ion source (Bruker Daltonik). The temperature of the ion transfer capillary was set at 180 °C. Ions were accumulated for 114 ms, and mobility separation was achieved by ramping the entrance potential from − 160 to − 20 V within 114 ms. The acquisition of the MS and MS/MS mass spectra was done with average resolutions of 60,000 and 50,000 full width at half maximum (mass range 100–1700 m/z), respectively. To enable the PASEF method, precursor m/z and mobility information was first derived from full scan TIMS-MS experiments (with a mass range of m/z 100–1700). The quadrupole isolation width was set to 2 and 3 Th and, for fragmentation, the collision energies varied between 31 and 52 eV depending on the precursor mass and charge. TIMS, MS operation and PASEF were controlled and synchronized using the control instrument software OtofControl 6.2 (Bruker Daltonik). LC–MS/MS data were acquired using the PASEF method with a total cycle time of 1.31 s, including 1 TIMS MS scan and 10 PASEF MS/MS scans. The 10 PASEF scans (100 ms each) containing, on average, 12 MS/MS scans per PASEF scan. Ion mobility-resolved mass spectra, nested ion mobility vs. m/z distributions, as well as summed fragment ion intensities were extracted from the raw data file with DataAnalysis 5.3 (Bruker Daltonik GmbH, Bremen, Germany). Signal-to-noise (S/N) ratio were increased by summations of individual TIMS scans. Mobility peak positions and peak half-widths were determined based on extracted ion mobilograms (± 0.05 Da) using the peak detection algorithm implemented in the DataAnalysis software. Features detection were also performed using DataAnalysis 5.3 software and exported in .mgf format.

Protein identification and data validation. Peptides were identified using the MASCOT software (version 2.5.1; Matrix Science, London, UK) against the Uniprot *Bos taurus* database (May 2019, 23,523 sequences) using its automatic decoy database search to calculate a false discovery rate (FDR). The parameters used for database searches included trypsin as enzyme (one missed cleavage allowed), carbamidomethylcysteine as fixed

modification, oxidation of methionine and N-terminal protein acetylation as variable modifications. Monoisotopic mass was considered and mass tolerance was set at 15 ppm for MS ions and 0.05 Da for MS/MS ions. Mascot results from the target and decoy databases were incorporated to Scaffold Q + software (version 5.0.1, Proteome Software, Portland, USA, http://www.proteomesoftware.com). Threshold for peptide and protein identification were set to 95.0% as specified by the Peptide Prophet algorithm[73] and the Protein Prophet algorithm[74].

Label-free protein quantification and statistical analysis. All proteins containing at least two unique peptides (False discovery rate (FDR) < 0.01%) were considered for protein quantification. The abundance of proteins was assessed using the Spectrum Count quantitative method and the "weighted spectra" option of the Scaffold software, as previously described[32]. The weighted spectra option of Scaffold is based on the assignment of each peptide to a weight according to whether they are shared or not between identified proteins. The normalization of data was achieved by multiplying each spectrum count in each sample by the average count over the sample's total spectrum count.

Statistical analysis was assessed on proteins with on average 2 normalized weighted spectra (NWS) or more in at least one condition. To obtain an overview of proteomic data, principal component analysis (PCA) of all samples was carried out using the FactoMineR and ggplot2 packages of RStudio software (version 1.4.1106). Analysis of variance on biological replicates and a heatmap representation of differentially abundant proteins (DAPs; p-value ≤ 0.05) were carried out using the FactoMineR and gplot packages of RStudio. Pair-wise comparison between stage × region × side conditions were evaluated by Student *t*-tests using the Scaffold software. Proteins were considered as differentially abundant with a t-test p-value ≤ 0.05 and a min fold-change ratio of 2. Lists of top-20 differentially abundant proteins are the quantitatively major proteins (based on NWS) at one given stage, side or region.

Prediction of secretory pathways and functional enrichment analysis. Identification of signal peptide-containing proteins and prediction of unconventional protein secretion (UPS) was first carried out using the Outcyte 1.0 online tool (http://www.outcyte.com/). The list of gene names was used as input and the default score threshold of 0.5 was considered for UPS prediction. Proteins having a transmembrane domain and predicted to be intracellular were also predicted by this software. The identification of signal peptide sequences was then checked on all proteins using the SignalP online tool (version 5.0; http://www.cbs.dtu.dk/services/SignalP/). Proteins identified were also compared to those previously reported in OF-derived EVs in cattle[19], cats[20] and to OEC-derived EVs in pigs[21]. The gene enrichment analysis was performed separately for each pairwise comparison except for region and stage effects for which the analysis was restricted to the ipsilateral side of ovulation. The gene lists of DAPs were first imported in the Database for Annotation, Visualization and Integrated Discovery (DAVID version 6.8) for gene ontology (GO) analysis. Overrepresented molecular functions (MF) and biological processes (BP) GO terms with a p-value < 0.05 were considered as significant. The KEGG pathways associated with DAPs were further analyzed using the Proteomaps software (http://bionic-vis.biologie.uni-greifswald.de/). Proteomaps graphics were generated from NWS values of overabundant DAPs in each pair-wise comparison. To evaluate the potential roles of DAPs in oviductal events, the Metascape Membership analysis tool was used (https://metascape.org/)[22]. Enrichment analysis of DAPs matching the membership terms "sperm", "oocyte", "ovulation", "fertilization" and "embryo" were retained. The *Homo sapiens* genome was used as background dataset for all analyses as it is better annotated than the *Bos taurus* genome.

Data availability

The mass spectrometry data have been deposited to the ProteomeXchange Consortium via PRIDE (https://www.ebi.ac.uk) with the dataset identifier PXD030915 and 10.6019/PXD030915

Received: 15 October 2021; Accepted: 24 February 2022
Published online: 09 March 2022

References

1. Suarez, S. S. Mammalian sperm interactions with the female reproductive tract. *Cell Tissue Res* **363**, 185–194 (2016).
2. Mahé, C. *et al.* Sperm migration, selection, survival, and fertilizing ability in the mammalian oviduct. *Biol. Reprod.* **105**, 317–331 (2021).
3. Ded, L., Hwang, J. Y., Miki, K., Shi, H. F. & Chung, J.-J. 3D in situ imaging of the female reproductive tract reveals molecular signatures of fertilizing spermatozoa in mice. *Elife* **9**, e62043 (2020).
4. Coy, P., García-Vázquez, F. A., Visconti, P. E. & Avilés, M. Roles of the oviduct in mammalian fertilization. *Reproduction* **144**, 649–660 (2012).
5. Li, S. & Winuthayanon, W. Oviduct: Roles in fertilization and early embryo development. *J. Endocrinol.* **232**, R1–R26 (2017).
6. Saint-Dizier, M., Schoen, J., Chen, S., Banliat, C. & Mermillod, P. Composing the early embryonic microenvironment: Physiology and regulation of oviductal secretions. *Int. J. Mol. Sci.* **21**, 223 (2020).
7. Lamy, J. *et al.* Steroid hormones in bovine oviductal fluid during the estrous cycle. *Theriogenology* **86**, 1409–1420 (2016).
8. Lamy, J. *et al.* Metabolomic profiling of bovine oviductal fluid across the oestrous cycle using proton nuclear magnetic resonance spectroscopy. *Reprod. Fertil. Dev.* **30**, 1021 (2018).
9. Lamy, J. *et al.* Regulation of the bovine oviductal fluid proteome. *Reproduction* **152**, 629–644 (2016).
10. Saint-Dizier, M., Sandra, O., Ployart, S., Chebrout, M. & Constant, F. Expression of nuclear progesterone receptor and progesterone receptor membrane components 1 and 2 in the oviduct of cyclic and pregnant cows during the post-ovulation period. *Reprod. Biol. Endocrinol.* **10**, 76 (2012).
11. Cerny, K. L., Garrett, E., Walton, A. J., Anderson, L. H. & Bridges, P. J. A transcriptomal analysis of bovine oviductal epithelial cells collected during the follicular phase versus the luteal phase of the estrous cycle. *Reprod. Biol. Endocrinol.* **13**, 84 (2015).
12. Gonella-Diaza, A. M. *et al.* Size of the ovulatory follicle dictates spatial differences in the oviductal transcriptome in cattle. *PLoS ONE* **10**, e0145321 (2015).

13. Maillo, V. *et al.* Spatial differences in gene expression in the bovine oviduct. *Reproduction* **152**, 37–46 (2016).
14. Rodríguez-Alonso, B. *et al.* Spatial and pregnancy-related changes in the protein, amino acid, and carbohydrate composition of bovine oviduct fluid. *IJMS* **21**, 1681 (2020).
15. Franchi, A., Moreno-Irusta, A., Domínguez, E. M., Adre, A. J. & Giojalas, L. C. Extracellular vesicles from oviductal isthmus and ampulla stimulate the induced acrosome reaction and signaling events associated with capacitation in bovine spermatozoa. *J. Cell Biochem.* **121**, 2877–2888 (2020).
16. Kumaresan, A., Ansari, M. R. & Garg, A. Modulation of post-thaw sperm functions with oviductal proteins in buffaloes. *Anim. Reprod. Sci.* **90**, 73–84 (2005).
17. Lopera-Vasquez, R. *et al.* Effect of bovine oviductal fluid on development and quality of bovine embryos produced in vitro. *Reprod. Fertil. Dev.* **29**, 621 (2017).
18. Dashti, S., Zare Shahneh, A., Kohram, H., Zhandi, M. & Dadashpour Davachi, N. Differential influence of ovine oviduct ampullary and isthmic derived epithelial cells on in vitro early embryo development and kinetic. *Small Ruminant Res.* **136**, 197–201 (2016).
19. Almiñana, C. *et al.* Oviduct extracellular vesicles protein content and their role during oviduct–embryo cross-talk. *Reproduction* **154**, 253–268 (2017).
20. Ferraz, M. D. A. M. M., Carothers, A., Dahal, R., Noonan, M. J. & Songsasen, N. Oviductal extracellular vesicles interact with the spermatozoon's head and mid-piece and improves its motility and fertilizing ability in the domestic cat. *Sci. Rep.* **9**, 9484 (2019).
21. Laezer, I. *et al.* Dynamic profile of EVs in porcine oviductal fluid during the periovulatory period. *Reproduction* **159**, 371–382 (2020).
22. Zhou, Y. *et al.* Metascape provides a biologist-oriented resource for the analysis of systems-level datasets. *Nat. Commun.* **10**, 1523 (2019).
23. Leese, H. J. *et al.* Female reproductive tract fluids: Composition, mechanism of formation and potential role in the developmental origins of health and disease. *Reprod. Fertil. Dev.* **20**, 1 (2008).
24. Roblero, L., Biggers, J. D. & Lechene, C. P. Electron probe analysis of the elemental microenvironment of oviducal mouse embryos. *Reproduction* **46**, 431–434 (1976).
25. Borland, R. M., Hazra, S., Biggers, J. D. & Lechene, C. P. The elemental composition of the environments of the gametes and preimplantation embryo during the initiation of pregnancy. *Biol. Reprod.* **16**, 147–157 (1977).
26. Kavanaugh, J. F. & Killian, G. J. Bovine oviductal cannulations. *J. Investig. Surg.* **1**, 201–208 (1988).
27. Gerena, R. L. & Killian, G. J. Electrophoretic characterization of proteins in oviduct fluid of cows during the estrous cycle. *J. Exp. Zool.* **256**, 113**–**120 (1990).
28. Hugentobler, S. A. *et al.* Amino acids in oviduct and uterine fluid and blood plasma during the estrous cycle in the bovine. *Mol. Reprod. Dev.* **74**, 445–454 (2007).
29. Tay, J. I. *et al.* Human tubal fluid: production, nutrient composition and response to adrenergic agents. *Hum. Reprod.* **12**, 2451–2456 (1997).
30. Leese, H. J. & Gray, S. M. Vascular perfusion: A novel means of studying oviduct function. *Am. J. Physiol. Endocrinol. Metab.* **248**, E624–E632 (1985).
31. Elhassan, Y. M. *et al.* Amino acid concentrations in fluids from the bovine oviduct and uterus and in ksom-based culture media. *Theriogenology* **55**, 1907–1918 (2001).
32. Banliat, C. *et al.* Identification of 56 proteins involved in embryo-maternal interactions in the bovine oviduct. *Int. J. Mol. Sci.* **21**, 466 (2020).
33. Papp, S. M. *et al.* A novel approach to study the bovine oviductal fluid proteome using transvaginal endoscopy. *Theriogenology* **132**, 53–61 (2019).
34. Pillai, V. V., Weber, D. M., Phinney, B. S. & Selvaraj, V. Profiling of proteins secreted in the bovine oviduct reveals diverse functions of this luminal microenvironment. *PLoS ONE* **12**, e0188105 (2017).
35. Gegenfurtner, K. *et al.* Influence of metabolic status and genetic merit for fertility on proteomic composition of bovine oviduct fluid. *Biol. Reprod.* **101**, 893–905 (2019).
36. Fernández-Hernández, P. *et al.* The proteome of equine oviductal fluid varies before and after ovulation: A comparative study. *Front. Vet. Sci.* **8**, 694247 (2021).
37. Soleilhavoup, C. *et al.* Proteomes of the female genital tract during the oestrous cycle. *Mol. Cell Proteomics* **15**, 93–108 (2016).
38. Ghosh, A., Syed, S. M. & Tanwar, P. S. In vivo genetic cell lineage tracing reveals that oviductal secretory cells self-renew and give rise to ciliated cells. *Development* **144**, 3031–3041 (2017).
39. Ito, S., Kobayashi, Y., Yamamoto, Y., Kimura, K. & Okuda, K. Remodeling of bovine oviductal epithelium by mitosis of secretory cells. *Cell Tissue Res.* **366**, 403–410 (2016).
40. Popa, S. J., Stewart, S. E. & Moreau, K. Unconventional secretion of annexins and galectins. *Semin. Cell Dev. Biol.* **83**, 42–50 (2018).
41. Yu, H. *et al.* Identification of rabbit oviductal fluid proteins involved in pre-fertilization processes by quantitative proteomics. *Proteomics* **19**, 1800319 (2019).
42. Gutiérrez, H. A., Latorre, R., MartÍnez BagÁn, E., Sánchez Margallo, F. M. & López Albors, O. Quantitative evaluation of the vasculature supplying the oviduct in pre-pubertal and sexually mature sows: Quantitative evaluation of the vasculature. *Anat. Rec.* **298**, 1978–1983 (2015).
43. Buhi, W. C., Ashworth, C. J., Bazer, F. W. & Alvarez, I. M. In vitro synthesis of oviductal secretory proteins by estrogen-treated ovariectomized gilts. *J. Exp. Zool.* **262**, 426–435 (1992).
44. Holt, W. V. & Fazeli, A. Sperm storage in the female reproductive tract. *Annu. Rev. Anim. Biosci.* **4**, 291–310 (2016).
45. Lamy, J. *et al.* Identification by proteomics of oviductal sperm-interacting proteins. *Reproduction* **155**, 457–466 (2018).
46. Wong, C.-W. *et al.* The roles of protein disulphide isomerase family A, member 3 (ERp57) and surface thiol/disulphide exchange in human spermatozoa–zona pellucida binding. *Hum. Reprod.* **32**, 733–742 (2017).
47. Marín-Briggiler, C. I. *et al.* Glucose-regulated protein 78 (Grp78/BiP) is secreted by human oviduct epithelial cells and the recombinant protein modulates sperm–zona pellucida binding. *Fertil. Steril.* **93**, 1574–1584 (2010).
48. Mondéjar, I., Martínez-Martínez, I., Avilés, M. & Coy, P. Identification of potential oviductal factors responsible for zona pellucida hardening and monospermy during fertilization in mammals. *Biol. Reprod.* **89**, 67–1 (2013).
49. Lachance, C., Bailey, J. L. & Leclerc, P. Expression of Hsp60 and Grp78 in the human endometrium and oviduct, and their effect on sperm functions. *Hum. Reprod.* **22**, 2606–2614 (2007).
50. Tokuhiro, K. *et al.* Calreticulin is required for development of the cumulus oocyte complex and female fertility. *Sci. Rep.* **5**, 14254 (2015).
51. Saavedra, M. D. *et al.* Calreticulin from suboolemmal vesicles affects membrane regulation of polyspermy. *Reproduction* **147**, 369–378 (2014).
52. Bernecic, N. C., Gadella, B. M., Leahy, T. & de Graaf, S. P. Novel methods to detect capacitation-related changes in spermatozoa. *Theriogenology* **137**, 56–66 (2019).
53. Kotwica, G. *et al.* The concentrations of catecholamines and oxytocin receptors in the oviduct and its contractile activity in cows during the estrous cycle. *Theriogenology* **60**, 953–964 (2003).
54. Coy, P. *et al.* Hardening of the zona pellucida of unfertilized eggs can reduce polyspermic fertilization in the pig and cow. *Reproduction* **135**, 19–27 (2008).

55. Algarra, B. *et al.* The C-terminal region of OVGP1 remodels the zona pellucida and modifies fertility parameters. *Sci. Rep.* **6**, 1–12 (2016).
56. Yang, X., Zhao, Y., Yang, X. & Kan, F. W. K. Recombinant hamster oviductin is biologically active and exerts positive effects on sperm functions and sperm-oocyte binding. *PLoS ONE* **10**, e0123003 (2015).
57. Zhao, Y. & Kan, F. W. K. Human OVGP1 enhances tyrosine phosphorylation of proteins in the fibrous sheath involving AKAP3 and increases sperm-zona binding. *J. Assist. Reprod. Genet.* **36**, 1363–1377 (2019).
58. Choudhary, S. *et al.* Effect of recombinant and native buffalo OVGP1 on sperm functions and in vitro embryo development: A comparative study. *J. Anim. Sci. Biotechnol.* **8**, 1–12 (2017).
59. Sakaue, T. *et al.* Factor H in porcine seminal plasma protects sperm against complement attack in genital tracts. *J. Biol. Chem.* **285**, 2184–2192 (2010).
60. Lee, K.-F. *et al.* Phospholipid transfer protein (PLTP) mRNA expression is stimulated by developing embryos in the oviduct. *J. Cell. Biochem.* **95**, 740–749 (2005).
61. Smits, K. *et al.* Proteome of equine oviducal fluid: effects of ovulation and pregnancy. *Reprod. Fertil. Dev.* **29**, 1085 (2017).
62. Locatelli, Y. *et al.* Relative effects of location relative to the corpus luteum and lactation on the transcriptome of the bovine oviduct epithelium. *BMC Genomics* **20**, 233 (2019).
63. Sostaric, E. *et al.* Sperm binding properties and secretory activity of the bovine oviduct immediately before and after ovulation. *Mol. Reprod. Dev.* **75**, 60–74 (2008).
64. Wijayagunawardane, M. P. *et al.* Local distributions of oviductal estradiol, progesterone, prostaglandins, oxytocin and endothelin-1 in the cyclic cow. *Theriogenology* **49**, 607–618 (1998).
65. Kölle, S. *et al.* Ciliary transport, gamete interaction, and effects of the early embryo in the oviduct: Ex vivo analyses using a new digital videomicroscopic system in the cow. *Biol. Reprod.* **81**, 267–274 (2009).
66. Lee, S. H., Oh, H. J., Kim, M. J. & Lee, B. C. Exosomes derived from oviduct cells mediate the EGFR/MAPK signaling pathway in cumulus cells. *J. Cell Physiol.* **235**, 1386–1404 (2020).
67. Acosta-Martínez, M. PI3K: An attractive candidate for the central integration of metabolism and reproduction. *Front. Endocrinol.* **2**, 110 (2012).
68. Álvarez-Rodríguez, M., Martinez, C. A., Wright, D. & Rodríguez-Martinez, H. The role of semen and seminal plasma in inducing large-scale genomic changes in the female porcine peri-ovulatory tract. *Sci. Rep.* **10**, 5061 (2020).
69. Bauersachs, S. *et al.* Monitoring gene expression changes in bovine oviduct epithelial cells during the oestrous cycle. *J. Mol. Endocrinol.* **32**, 449–466 (2004).
70. Ireland, J. J., Murphee, R. L. & Coulson, P. B. Accuracy of predicting stages of bovine estrous cycle by gross appearance of the corpus luteum. *J. Dairy Sci.* **63**, 155–160 (1980).
71. Adib, A. *et al.* Progesterone improves the maturation of male-induced preovulatory follicles in anoestrous ewes. *Reproduction* **148**, 403–416 (2014).
72. Rico, C. *et al.* Regulation of anti-müllerian hormone production in the cow: A multiscale study at endocrine, ovarian, follicular, and granulosa cell levels1. *Biol. Reprod.* **84**, 560–571 (2011).
73. Keller, A., Nesvizhskii, A. I., Kolker, E. & Aebersold, R. Empirical statistical model to estimate the accuracy of peptide identifications made by MS/MS and database search. *Anal. Chem.* **74**, 5383–5392 (2002).
74. Nesvizhskii, A. I., Keller, A., Kolker, E. & Aebersold, R. A statistical model for identifying proteins by tandem mass spectrometry. *Anal. Chem.* **75**, 4646–4658 (2003).

Acknowledgements
We are grateful to Marc Chodkiewicz for the critical reading of this paper. The authors thank Thierry Delpuech and Albert Arnoult for collecting the oviducts at the slaughterhouse. The authors thank the laboratory of hormonal assay (PRC, INRAE, Nouzilly) for the assessment of P4 concentration in OF and pre-ovulatory follicular fluid.

Author contributions
M.S.D., P.M. and J.S. designed the study; C.M. and M.S.D. wrote the manuscript; M.S.D. and G.T. collected and prepared the OF; Y.L. did the hormonal assays; R.L. and E.C. did the MS analyses; C.M. analyzed the proteomic data; C.A. and A.M.Z. made complementary data analysis; C.P. supervised the MS analyses; all authors corrected the manuscript; M.S.D. administrated and supervised the study.

Funding
This work was funded by INRAe and Agence Nationale de la Recherche under the grant number ANR-18-CE92-0049. This work was also supported by grants from Biogenouest, Infrastructures en Biologie Santé et Agronomie (IBiSA) and Conseil Régional de Bretagne awarded to Protim proteomics core facility.

Competing interests
The authors declare no competing interests.

Additional information
Supplementary Information The online version contains supplementary material available at https://doi.org/10.1038/s41598-022-07929-3.

Correspondence and requests for materials should be addressed to C.M.

Reprints and permissions information is available at www.nature.com/reprints.

Publisher's note Springer Nature remains neutral with regard to jurisdictional claims in published maps and institutional affiliations.

2. Protéome d'interaction des spermatozoïdes pendant leur migration dans l'oviducte en période péri-conceptionnelle chez le bovin

Ce travail est présenté sous la forme d'un **schéma récapitulatif** (Figure 10 page 112) et de l'**article 3** « The sperm-interacting proteome in the bovine ampulla and isthmus during the periovulatory period » publié dans *Journal of Animal Science and Biotechnology* en Février 2023. Des **résultats complémentaires** portant sur les effets des fluides d'isthme et d'ampoule sur la physiologie des spermatozoïdes sont présentés Figure 11 et 12 pages 135 - 136.

Contexte et objectif

Dans l'oviducte, les spz interagissent avec des protéines solubles dans le fluide, certaines jouant des rôles dans leur survie (HSPA8) et leur capacitation (albumine, OVGP1). Cependant chez les mammifères, seules quelques protéines interagissant avec les spz (SIP) dans l'oviducte ont été identifiées, et ce, essentiellement par des approches candidates (western-blot, immunohistochimie). Les SIP, pendant la migration spermatique depuis l'isthme, où les spz sont stockés, jusqu'à l'ampoule, où la fécondation a lieu, restent à découvrir. Nos objectifs étaient d'identifier et quantifier de nouvelles SIP dans le fluide d'oviducte, et de déterminer l'effet du stade péri-ovulatoire et de la région anatomique sur l'abondance des SIP sur les spz. L'effet des FO sur les paramètres de mobilité et de capacitation des spz a été mesuré en parallèle.

Matériel et Méthodes

Les oviductes de 16 vaches adultes cyclées aux stades pré- et post-ovulatoire (8 vaches par stade) ont été collectés dans un abattoir proche du laboratoire. Les fluides d'isthme et d'ampoule ipsilatéraux à l'ovulation ont été collectés séparément par des flush PBS pour constituer un total de 4 pools de fluide par condition : isthme pré-ovulatoire, ampoule pré-ovulatoire, isthme post-ovulatoire et ampoule post-ovulatoire. Un pool de spermatozoïdes bovins préalablement congelés dans un milieu dépourvu en protéines et lavés sur Percoll a été incubé avec du PBS (spz-PBS ou témoins) ou avec des FO de chaque condition (spz-FO) à 38,5°C pendant 1 h. La concentration finale en protéines dans les FO a été ajustée à 3 mg/mL.

Après incubation, les spz et les FO de chaque condition ont été séparés par centrifugation et analysés par nanoLC-MS/MS après extraction protéique. Les SIP ont été définies selon les critères suivants : (i) détection dans les FO **et** (ii) détection spécifique dans les spz-FO (aucune détection dans les spz témoins) **ou** détection significativement plus élevée dans les spz-FO que les spz-PBS (t-test avec $p \leq 0,05$) avec un ratio minimum de 3. Certaines SIP ont été validées par western-blot. Les fonctions des SIP ont été prédites par analyse de type Gene ontology des gènes correspondants. Les SIP différentiellement abondantes entre stades et régions ont été identifiées par des tests de Student (logiciel R ; $p \leq 0.05$).

En parallèle de cette analyse protéomique, différents paramètres physiologiques des spz ont été évalués au début et après 1, 3 et 6 h d'incubation dans chaque condition. La mobilité des spz a été mesurée au CASA, et la fluidité membranaire (marquage Merocyanine 540), l'intégrité de la membrane (marquage iodure de propidium ou DRAQ7) et la réaction acrosomique spontaneée et induite par l'ionophore calcique (marquage PNA) des spz ont été mesurés par cytométrie en flux. Pour ces analyses, les fluides d'oviducte ont été récupérés par flush avec un milieu non-capacitant à pH 7.4 (Tyrode-HEPES supplémenté avec du pyruvate, lactate et de l'alcool polyvinylique). L'effet du traitement sur les paramètres spermatiques a été analysé par une analyse de variance à chaque temps d'incubation ($p \leq 0.05$).

Résultats

L'analyse comparative entre les protéines quantifiées dans les spz d'une part (2333 protéines) et les FO d'autre part (2471 protéines) a permis l'identification de 245 SIP, toutes conditions confondues. Au total, 83% de ces protéines ont été prédites comme sécrétées : 10% via un peptide signal, 21% par des voies non conventionnelles et 78% précédemment identifiées dans les vésicules extracellulaires de FO bovin. Les SIP les plus abondantes incluent les myosines MYH9, MYH10, et MYH14, l'oviductine (OVGP1), les protéines de choc thermique HSPA5 HSPA8 et HSPB1, et les annexines A1 et A2. Le plus petit nombre de SIP (113) a été mis en évidence dans l'ampoule post-ovulatoire, lieu et moment de la fécondation, et le plus grand nombre (187 SIP) dans l'isthme pré-ovulatoire, lieu et moment du réservoir spermatique. Au total, 41 SIP (17%) étaient différentiellement abondantes entre les stades pré- et post-ovulatoire dans une région donnée ou entre les régions à un stade donné ($p \leq 0,05$). De plus, 76 SIP (31%) ont été identifiées dans une seule et unique condition. Les SIP ont divers rôles prédits, notamment dans la liaison, la réponse cellulaire au stress, la régulation de la motilité cellulaire, la fécondation et le développement embryonnaire précoce.

Conclusion

Cette étude propose une nouvelle méthode d'identification des protéines d'interaction par la spectrométrie de masse, qui pourrait être appliquée à d'autres cellules en interaction avec des fluides biologiques. Ces résultats fournissent pour la première fois une liste exhaustive de protéines interagissant avec les spz dans l'oviducte et mettent en évidence des changements dynamiques d'interactions au cours de leur migration. La localisation des interactions sur les spermatozoïdes et leurs rôles restent à déterminer, mais les protéines identifiées sont de bonnes candidates pour améliorer des milieux de conservation des spermatozoïdes et des milieux de fécondation *in vitro*.

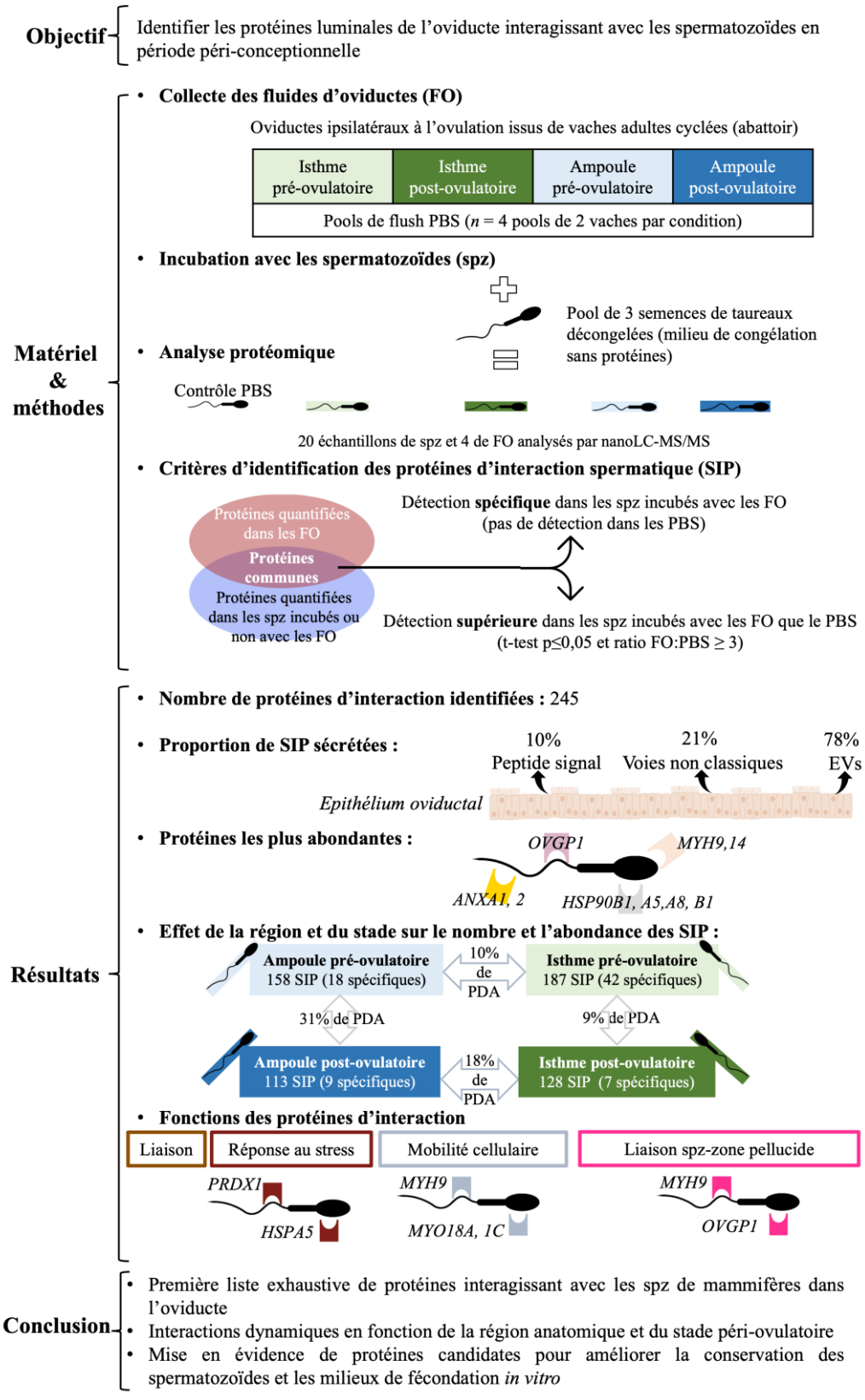

Figure 10 : Schéma récapitulatif de l'étude des protéines interagissant avec les spermatozoïdes dans l'oviducte en période péri-conceptionnelle.
ANX = Annexine ; EVs = vésicules extracellulaires ; FO = Fluide d'oviducte ; HSP = protéine de choc thermique ; MYO/H = myosine ; OVGP1 = oviductine ; SIP = protéines d'interaction ; PDA = protéines différentiellement abondante ; PRDX = péroxiredoxine ; spz = spermatozoïde

Mahé *et al.*
Journal of Animal Science and Biotechnology (2023) 14:30
https://doi.org/10.1186/s40104-022-00811-2

Journal of Animal Science and Biotechnology

RESEARCH

Open Access

The sperm-interacting proteome in the bovine isthmus and ampulla during the periovulatory period

Coline Mahé[1*], Régis Lavigne[2,3], Emmanuelle Com[2,3], Charles Pineau[2,3], Aleksandra Maria Zlotkowska[4,5], Guillaume Tsikis[1], Pascal Mermillod[1], Jennifer Schoen[4,5] and Marie Saint-Dizier[1]

Abstract

Background Spermatozoa interact with oviduct secretions before fertilization in vivo but the molecular players of this dialog and underlying dynamics remain largely unknown. Our objectives were to identify an exhaustive list of sperm-interacting proteins (SIPs) in the bovine oviduct fluid and to evaluate the impact of the oviduct anatomical region (isthmus vs. ampulla) and time relative to ovulation (pre-ovulatory vs. post-ovulatory) on SIPs number and abundance.

Methods Pools of oviduct fluid (OF) from the pre-ovulatory ampulla, pre-ovulatory isthmus, post-ovulatory ampulla, and post-ovulatory isthmus in the side of ovulation were collected from the slaughterhouse. Frozen-thawed bull sperm were incubated with OF or phosphate-buffered saline (control) for 60 min at 38.5 °C. After protein extraction and digestion, sperm and OF samples were analyzed by nanoLC-MS/MS and label-free protein quantification.

Results A quantitative comparison between proteins identified in sperm and OF samples (2333 and 2471 proteins, respectively) allowed for the identification of 245 SIPs. The highest number (187) were found in the pre-ovulatory isthmus, i.e., time and place of the sperm reservoir. In total, 41 SIPs (17%) were differentially abundant between stages in a given region or between regions at a given stage and 76 SIPs (31%) were identified in only one region × stage condition. Functional analysis of SIPs predicted roles in cell response to stress, regulation of cell motility, fertilization, and early embryo development.

Conclusion This study provides a comprehensive list of SIPs in the bovine oviduct and evidences dynamic spatio-temporal changes in sperm-oviduct interactions around ovulation time. Moreover, these data provide protein candidates to improve sperm conservation and in vitro fertilization media.

Keywords Ampulla, Fallopian tube, Interactome, Isthmus, Oviduct, Ovulation, Post-ovulatory, Pre-ovulatory, Proteomics, Spermatozoa

*Correspondence:
Coline Mahé
coline.mahe@inrae.fr
[1] CNRS, IFCE, INRAE, Université de Tours, PRC, 37380 Nouzilly, France
[2] Univ Rennes, Inserm, EHESP, Irset (Institut de Recherche en Santé, Environnement Et Travail) - UMR-S 1085, F-35000 Rennes, France
[3] Univ Rennes, CNRS, Inserm, Biosit UAR 3480 US_S 018, Protim Core Facility, 35000 Rennes, France
[4] Institute of Reproductive Biology, Leibniz Institute for Farm Animal Biology, FBN, Dummerstorf, Germany
[5] Present Address: Department of Reproduction Biology, Leibniz Institute for Zoo and Wildlife Research (IZW), Berlin, Germany

© The Author(s) 2023. **Open Access** This article is licensed under a Creative Commons Attribution 4.0 International License, which permits use, sharing, adaptation, distribution and reproduction in any medium or format, as long as you give appropriate credit to the original author(s) and the source, provide a link to the Creative Commons licence, and indicate if changes were made. The images or other third party material in this article are included in the article's Creative Commons licence, unless indicated otherwise in a credit line to the material. If material is not included in the article's Creative Commons licence and your intended use is not permitted by statutory regulation or exceeds the permitted use, you will need to obtain permission directly from the copyright holder. To view a copy of this licence, visit http://creativecommons.org/licenses/by/4.0/. The Creative Commons Public Domain Dedication waiver (http://creativecommons.org/publicdomain/zero/1.0/) applies to the data made available in this article, unless otherwise stated in a credit line to the data.

Background

Upon the end of their migration through the female genital tract, mammalian spermatozoa encounter secretions from the oviduct, where the final steps of sperm capacitation and fertilization take place [1]. Before ovulation, a subpopulation of sperm binds to oviduct epithelial cells in the isthmus, the caudal part of the oviduct, and builds the so-called functional sperm reservoir [2, 3]. Around the time of ovulation, spermatozoa are progressively released towards the ampulla, the distal part of the oviduct, where they meet the oocyte [1]. Numerous in vitro studies have demonstrated that oviduct fluid (OF) proteins modulate sperm viability and mobility in cattle [4–7] and humans [8]. Furthermore, the effect of OF proteins on sperm varies according to the estrous cycle stage and the oviduct region from which the OF originates [5, 6]. In particular, OF proteins from the peri-ovulatory (non-luteal) phase better favored post-thawed sperm viability, acrosome integrity, and motility compared to OF proteins from the luteal phase in cattle [6]. In addition, proteins from the isthmus preserved post-thawed sperm motility and acrosome integrity compared to proteins from the ampulla [5]. Therefore, the synchronization of events leading to the acquisition of sperm fertilizing ability may be monitored by spatiotemporal regulation of sperm interactions with OF proteins.

Proteins in the OF have different origins. The epithelium lining the oviductal lumen actively produces proteins secreted or released as cargo of oviduct extracellular vesicles (oEVs) [9–11]. Furthermore, OF proteins can originate from epithelial cell death (apoptosis and necrosis). Proteins originating from sub-epithelial structures reach the lumen via diffusion or other transport mechanisms [12]. The bovine OF proteome is highly regulated according to the estrous cycle stage [9, 13]. In addition, recent work from our laboratory showed that the oviduct anatomical region (isthmus vs. ampulla) also has a significant impact on the OF proteome [14].

However, the molecular mechanisms underlying the dynamic and close-up dialog between spermatozoa and OF proteins around ovulation time are still poorly understood.

The membrane of bull sperm is a complex mixture of phospholipids, glycans, and proteins originating from the seminal plasma [15, 16]. These are all potential binding partners for proteins in the OF. Blots of bull sperm membranes incubated with labeled OF showed sperm-interacting proteins (SIPs) ranging from around 20 to 140 kDa [17–19]. Immunodetection identified some SIPs including oviductin (OVGP1) [18], heat shock proteins (HSP) A5 (also known as glucose-regulated protein 78, GRP78), and HSPA8 [20, 21]. Recently, quantitative proteomic approaches have emerged as methods to explore SIPs more in-depth [22–24]. In our previous study using quantitative proteomics, the whole oviduct was used for OF collection, precluding any evaluation of the spatial regulation of SIPs. We hypothesize that the sperm-OF protein interaction varies in number and abundance between the ampulla and isthmus and also during ovulation, which would allow us to identify candidates involved in the formation of the sperm reservoir (pre-ovulatory isthmus). Thus, the objectives of this study were to identify an exhaustive list of SIPs in the bovine OF and to evaluate the impact of the oviduct anatomical region (isthmus vs. ampulla) and time relative to ovulation (pre-ovulatory (Pre-ov) vs. post-ovulatory (Post-ov)) on SIPs numbers and abundance using nanoLC-MS/MS analysis.

Methods

Collection of bovine oviduct fluid from the ampulla and isthmus

Bovine OF were collected from adult cyclic cows at a local slaughterhouse (40 min from the lab). Pairs of oviducts and ovaries were immediately placed on ice to stop muscular contractions and post-mortem modifications, transported to the laboratory, and classified according to ovarian morphology as previously described [25]. Only oviducts ipsilateral to ovulation at either pre-ovulatory or post-ovulatory stage of cycle were used. Pre-ovulatory ovaries contained one corpus albicans and one follicle of 11–20 mm in diameter (approximately days 19–21 of cycle). Post-ovulatory ovaries contained one early corpus luteum consisting of red, loosely organized tissue less than 1 cm in diameter (approximately days 1–4 of cycle). After removing the ovaries and surrounding tissues, the oviducts were cut at the ampulla-isthmus junction. Preliminary experiments by immunoblotting showed that a minimal concentration of 3 mg/mL of proteins in OF was needed to observe a sperm signal for myosin 9 (MYH9), a protein known to interact with bull sperm [22, 26], after incubation with OF. In addition, preliminary experiments showed that at least two isthmus samples, the narrowest part of the oviduct, were needed to reach a minimum of 3.5 mg/mL of proteins after flushing with 200 µL of phosphate-buffered saline (PBS). Therefore, on collection day, pools of isthmus and ampulla samples from 2 cows at the Pre-ov or Post-ov stage were formed and serially flushed with 200 µL of sterile protein-free PBS at 4 °C: one oviduct region was flushed with 200 µL of PBS and this fluid was re-used to flush the second oviduct region from the second cow. In the following, the term "OF" refers to one pool of OF flushes. All OF were kept on ice before two successive centrifugations (2000 × *g* then 12,000 × *g*, 4 °C, 10 min each) to eliminate cells and cellular debris. One aliquot was used for protein concentration measurement

using the Uptima BC Assay kit (Interchim, Montluçon, France). Bovine serum albumin was used as a standard. Aliquots of flushes were stored at − 80 °C until used for sperm incubation and proteomic analysis. In total, four OF were collected per region × stage condition resulting in 16 OF (2 cows per OF). On the day of incubation, one OF per region × stage condition (Pre-ov isthmus, Pre-ov ampulla, Post-ov isthmus and Post-ov ampulla) was thawed on ice and the OF at 3.5 mg/mL was divided into two aliquots of 100 µL to assess (1) sperm-interacting proteins by proteomics and (2) sperm motility, membrane fluididity and integrity (see below).

Assessment of sperm motility, membrane fluidity, acrosome reaction and viability

Bull semen was stored in a protein-free preservation medium (OptiXcell, IMV Technologies, L'Aigle, France) in liquid nitrogen. Assessment of sperm parameters was achieved at the start of incubation (T0) and after 1 and 3 h of incubation with OF. Sperm motility, progressive motility, amplitude of lateral head (ALH), linearity (LIN), average path velocity (VAP), curvilinear velocity (VCL) and straight line velocity (VSL) were evaluated on a Mackler chamber by computer-assisted sperm analysis (IVOS II, Animal Breeder software, version 1.8, Hamilton Thorne, Massachusetts, United States). To avoid sperm binding to the slide, 1% of bovine serum albumin was added to the PBS control samples. In parallell, aliquots of sperm were incubated 10 min at room temperature in 200 µL PBS with either (i) 7.5 µmol/L propidium iodide (PI, 81845, Sigma, Missouri, United States) and 1 µmol/L peanut agglutinin fluorescein (PNA, FL-1071, Vector laboratories, New Jersey, United States) to assess sperm membrane integrity and acrosome reaction, or (ii) 1.5 µmol/L DRAQ7 (D15106, Invitrogen, Massachussetts, United States) and 2.7 µmol/L Merocyanine 540 (323756, Sigma, Missouri, United States) to assess sperm membrane fluidity (lipid disorder). Sperm were next analyzed by flow cytometry (MACSQuant Analyzer 10, Miltenyi Biotec, Bergisch Gladbach, Germany). Propidium iodure (filter 1) and DRAQ7 (filter 2) fluorescence was collected through a 655–730 nm filter, PNA fluorescence through a 500–550 filter (filter 3) and merocyanine 540 fluorescence through a 565–605 filter (filter 4). Voltage settings were 410 V for forward scatter, 446 V for side scatter, 470 V for filter 1, 350 V for filter 2, 420 V for filter 3 and 400 V for filter 4. Data analysis was performed on at least 20,000 events with Flowjo software (version 10.4). Four replicates were carried out.

Sperm incubation with ampullary and isthmic fluid and preparation of protein samples

The experimental design of the study is shown in Fig. 1. In order to test the impact of female factors (oviduct region and ovulatory stage) on sperm-interacting proteins, the semen from the same pool of three Holstein bulls were used for all proteomic experiments. Sperm incubation with OF was undertaken as previously described [22] with slight modifications. A pool of 21 straws (7 straws per bull; approximately 20×10^6 sperm per straw) were thawed in a water bath (37 °C, 3 min). The semen was washed on 45%–90% Percoll gradients (2.5 mL of Percoll 45 and 2.5 mL of Percoll 90; 700 g, 20 min, 25 °C; 1 mL of semen per gradient). The pooled sperm pellet was then washed with 2 mL of PBS (300 × *g*, 10 min, 25 °C) and sperm concentration in the pellet with some residual PBS was assessed in a Thoma cell counting chamber. For incubation with OF, 4.8 million of sperm in 20 µL PBS were added to 100 µL of PBS (control) or 100 µL OF containing 3.6 mg/mL protenis, resulting in a final sperm concentration of 40×10^6/mL and OF concentration of 3 mg/mL proteins. Incubations were achieved in 1.5 mL polypropylene tubes for 60 min in a water bath at 38.5 °C. Preliminary data showed that this 60-min incubation time was enough to allow sperm-protein interactions without inducing capacitation, i.e., alteration of the sperm membrane [27]. After incubation, OF were recovered by centrifugation (4000 × *g*, 10 min, 4 °C), and sperm were washed twice in 1 mL of cold PBS (4000 × *g*, 10 min, 4 °C). Four replicates with four different pools of OF were done, resulting in 20 sperm samples.

Sperm pellets were resuspended in 25 µL of Tris–HCl at 10 mmol/L pH 6.8 containing 2% (w/v) of sodium dodecyl sulfate (SDS) and 0.05% (v/v) of a protease inhibitor cocktail (P2714, Sigma, Missouri, United States) then sonicated for 10 s at ambient temperature, and finally centrifuged for 10 min at 15,000 × *g* at 4 °C. The OF used for sperm incubation were pooled per region × stage condition, resulting in four pools of OF (Pre-ov isthmus, Pre-ov ampulla, Post-ov isthmus, and Post-ov ampulla). Samples of sperm and OF were assayed for protein concentration (Uptima BC Assay kit) and then stored at − 20 °C until proteomic analysis.

Nanoliquid chromatography coupled with tandem mass spectrometry (NanoLC-MS/MS)

For proteomic analysis, sperm and OF pools (7 µg and 10 µg of proteins per sample, respectively) were prepared using the PreOmics iST-BCT kit (PreOmics GmbH, Planegg, Germany) following the manufacturer's instructions. Briefly, proteins were lysed, denatured, reduced, and alkylated for 10 min at 95 °C, and then Trypsin/LysC digested for 60 min at 37 °C. Samples were then purified from salts, contaminants, and other detergents, using the provided spin cartridge (PreOmics GmbH). The resulting peptide mixtures were loaded on a 75 µm × 250 mm IonOpticks Aurora 2 C18 column (Ion Opticks Pty Ltd.,

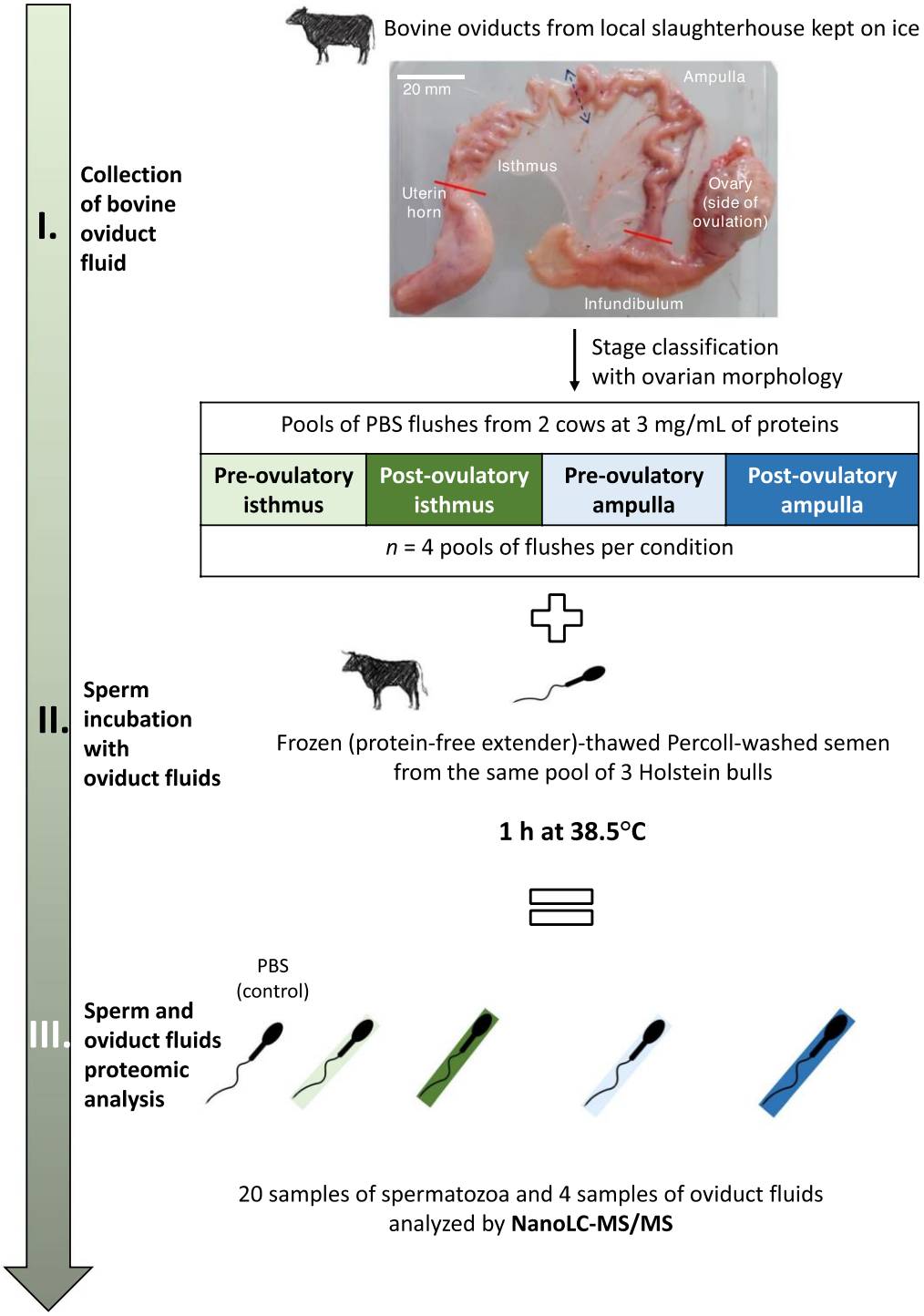

Fig. 1 Experimental design for the identification of sperm-interacting proteome in the bovine oviduct fluid. PBS flushes from the pre-ovulatory isthmus, pre-ovulatory ampulla, post-ovulatory isthmus and post-ovulatory ampulla from two cows were pooled. Four pools of flushes per condition were constituted and incubated with the same pool of sperm for 1 h at 38.5 °C. Sperm and oviduct fluid were then analyzed by NanoLC-MS/MS

Bundoora, Australia). A gradient of basic reversed-phase buffers (Buffer A: 0.1% formic acid, 98% H_2O MilliQ, 2% acetonitrile; Buffer B: 0.1% formic acid, 100% acetonitrile) was run on a NanoElute HPLC System (Bruker Daltonik GmbH, Bremen, Germany) at a flow rate of 400 nL/min at 50 °C. The liquid chromatography (LC) run lasted for 120 min (2% to 15% of buffer B during 60 min; up to 25% at 90 min; up to 37% at 100 min; up to 95% at 110 min and finally 95% for 10 min to wash the column). The column was coupled online to a TIMS TOF Pro (Bruker Daltonik GmbH, Bremen, Germany) with a CaptiveSpray ion source (Bruker Daltonik). The temperature of the ion transfer capillary was set at 180 °C. Ions were accumulated for 114 ms, and mobility separation was achieved by ramping the entrance potential from − 160 V to − 20 V within 114 ms. The MS and MS/MS mass spectra were acquired with average resolutions of 60,000 and 50,000 full widths at half maximum (mass range 100–1700 *m/z*), respectively. To enable the PASEF method, precursor *m/z* and mobility information was first derived from full scan TIMS-MS experiments (with a mass range of *m/z* 100–1700). The quadrupole isolation width was set to 2 and 3 Th, and for fragmentation, the collision energies varied between 31 and 52 eV depending on the precursor mass and charge. TIMS, MS operation, and PASEF were controlled and synchronized using the control instrument software OtofControl 6.2 (Bruker Daltonik). LC–MS/MS data were acquired using the PASEF method with a total cycle time of 1.31 s, including 1 TIMS MS scan and 10 PASEF MS/MS scans. The 10 PASEF scans (100 ms each) contained, on average, 12 MS/MS scans per PASEF scan. Ion mobility-resolved mass spectra, nested ion mobility vs. *m/z* distributions, as well as summed fragment ion intensities were extracted from the raw data file with DataAnalysis 5.3 (Bruker Daltonik GmbH, Bremen, Germany). Signal-to-noise (S/N) ratios were increased by summations of individual TIMS scans. Mobility peak positions and peak half-widths were determined based on extracted ion mobilograms (± 0.05 Da) using the peak detection algorithm implemented in the DataAnalysis software. Feature detections were also performed using DataAnalysis 5.3 software and exported in .mgf format.

Quantification and validation of proteins identified by mass spectrometry

Peptides were identified using the *Bos taurus* UniprotKB database (May 2021; 37,514 sequences) and the MASCOT software (version 2.5.1; Matrix Science, London, UK) using its automatic decoy database search to calculate a false discovery rate (FDR). The parameters used for database searches included trypsin as the enzyme (one missed cleavage allowed), carbamidomethylcysteine as a fixed modification, oxidation of methionine, and N-terminal protein acetylation as variable modifications. Monoisotopic mass was considered, and mass tolerance was set at 15 ppm for MS ions and 0.05 Da for MS/MS ions. Mascot results from the target and decoy databases were then incorporated into Scaffold Q + software (version 5.0.1, Proteome Software, Portland, USA). The peptide and protein identification thresholds were set to 95.0% as specified by the Peptide Prophet algorithm [28] and the Protein Prophet algorithm [29]. All proteins containing at least two unique peptides with an FDR < 0.01% were considered for protein quantification. Protein abundance was assessed using the Spectrum Count quantitative method and the "weighted spectra" option of the Scaffold software, as previously described [14]. The weighted spectra option of Scaffold is based on the assignment of each peptide to a weight according to whether they are shared or not between identified proteins. The normalization of data was achieved by multiplying each spectrum count in each sample by the average count over the sample's total spectrum count.

Identification of sperm-interacting proteins

Proteins were considered as SIPs originating from the OF if they met the following criteria: (i) detection by nanoLC-MS/MS in the OF with a minimum level of 5.0 NWS and (ii) detected exclusively in sperm treated with OF (i.e., no detection in control sperm incubated with PBS) with ≥ 5.0 NWS on average in at least one stage × region condition or (iii) detected in significantly higher abundance in OF-treated sperm than in controls (*t*-test with a *P*-value ≤ 0.05) with at least 5.0 NWS and a mean treated:control fold-change ratio ≥ 3.0 in OF-treated condition.

Immunodetection of HSPA5, MYH9, and PRDX6 in protein samples from oviduct fluid and spermatozoa

The SIPs HSPA5, previously known to interact with bull sperm [20, 21], MYH9, and PRDX6 were validated by immunoblotting. The semen from three Holstein bulls different than those used for proteomics and stored under the same conditions (OptiXcell preservation medium, liquid nitrogen) were incubated with OF from ampulla or isthmus at Pre-ov and Post-ov as described earlier. PBS was used as control. After sperm protein extraction, 5 µg of OF and 20 µg of sperm proteins were migrated on a 4%–20% SDS-PAGE gel (Bio-Rad, Hercules, CA, USA). Semi-liquid transfers on a nitrocellulose membrane were performed using the Trans-blot Turbo Transfer System (Bio-Rad) and the "Mixed molecular weight" program. Membranes were stained for 5 min with Ponceau red to check the homogeneity between lanes and for data normalization [30]. Proteins were then blocked for 2 h with Tris-buffered saline supplemented with 0.5%

Tween 20 supplemented with 5% of lyophilized low-fat milk (TBST–milk). Membranes were then incubated with primary antibodies (see the list of primary antibodies in Additional file 1: Table S1), diluted in TBST-milk overnight at 4 °C, and washed (× 4, 10 min) with TBST. Membranes were incubated for 1 h at 37 °C with secondary antibodies conjugated to horseradish peroxidase diluted in 1:2500 in TBST-milk (Sigma, Missouri, United States) (see the list of secondary antibodies in Additional file 1: Table S1). The peroxidase was revealed with chemiluminescent substrates (ECL Clarity Max, Bio-Rad) and the images were digitized with a cooled CCD Camera (ImageMaster VDS-CL, Amersham Biosciences). Signal quantification was assessed by densitometry using an Image Scanner (Amersham Biosciences, GE Healthcare Life Sciences) and the TotalLab Quant software (version 11.4, TotalLab, Newcastle upon Tyne, UK). Three replicates with different OF were performed for each protein.

Statistical analysis of data

Data were analyzed using the Rstudio software (version 1.4.1106). CASA and flow cytometry data were analyzed by analysis of variance (ANOVA) and Tuckey post test at each time (P-value ≤ 0.05). Pairwise comparisons of SIPs between regions at a given stage and between stages at a given region were analyzed by t-tests. Proteins were considered differentially abundant with a P-value ≤ 0.050. The distribution of SIPs between conditions was analyzed by Venn diagrams using jvenn tool online [31].

Prediction of secretory pathways and functional enrichment analysis

In order to detect a signal peptide or to predict unconventional secretion pathways, FASTA sequences of SIPs were used as input into the Outcyte online tool (version 1.0) [32]. The presence of signal peptides was further confirmed by SignalP 6.0 in Eukarya organism [33]. In order to predict a secretion via extracellular vesicles (EVs), the gene list of SIPs was compared with gene lists previously reported in bovine [9], feline [34], and porcine [35] oviduct EVs. Functional classification terms for gene ontology (GO), molecular function (MF), and biological processes (BP) were obtained using the Protein Analysis Through Evolutionary Relationships (PANTHER version 17.0) with the gene list as input and *Bos taurus* as background. Enrichment analysis for GO, MF, and BP were carried out using the SIP gene lists as input in Metascape and the *Homo Sapiens* database as background [36]. To go further into the potential functions of SIPs, membership annotations (in GO, MF, and BP name or description) for "cell motility," "sperm," "fertilization," and "oviduct" were also analyzed with Metascape.

Protein–protein interaction networks and KEGG pathway enrichment analysis (P-value < 0.01) of SIPs were carried out using the corresponding list of gene names in STRING (Search Tool for the Retrieval of Interacting Genes/proteins; version 11.5) and *Bos taurus* as background [37]. For the construction of the interaction network, a minimum interaction score of 0.4 and the following interaction sources (text mining, experiments, databases, and co-expression) were selected in the settings. Line thickness between proteins represents the degree of confidence of interaction predictions. The disconnected nodes in the network were discarded. The networks were then imported into Cytoscape for color adjustments (version 3.9.0) [38].

Results

Sperm parameters during incubation with oviduct fluid

After 1 h of incubation with OF, no difference between conditions were found for sperm motility parameters, membrane fluidity and acrosome reaction (Fig. 2 and Additional File 7: Fig. S1). After 3 h, the OF from post-ovulatory ampulla increased sperm membrane fluidity compared to that from isthmus ($P < 0.05$). Furthermore, the OF from post-ovulatory isthmus maintained higher sperm viability compared to that from pre-ovulatory ampulla ($P < 0.05$).

Classification and secretory pathways of identified sperm-interacting proteins

The sperm-interacting proteome was assessed after 1 h of incubation with OF in all conditions.

A total of 2333 proteins were identified in sperm treated with OF, of which 245 (11%) were defined as SIPs originating from the OF. The 245 SIPs represented 10% of the 2471 proteins quantified with more than 5.0 normalized weighted spectra (NWS) in the different pools of OF and 18.9% of the 1294 proteins shared by sperm and OF (Fig. 3A). Table 1 shows the top 25 SIPs when considering the four stage × region conditions (see all proteins identified in Additional file 2: Table S2 and all SIPs with quantitative data in Additional file 3: Table S3). Myosin heavy chain 9 (MYH9) was the most abundant SIP in all conditions.

Overall, 155 SIPs (63%), including MYH10 and tropomyosin alpha-3 chain (TPM3), were detected exclusively in at least one OF-treated sperm condition (with no detection in control samples). Furthermore, 90 SIPs (37%), including OVGP1, MYH9, HSPA5, and peroxiredoxin-6 (PRDX6), were detected at significantly higher abundances in at least one OF-treated sperm condition compared to the controls (P-value ≤ 0.05 and fold-change ratio ≥ 3.0; Table 1). Immunoblotting of sperm protein extracts showed higher signals in OF-treated than control sperm for HSPA5, and signals exclusively in OF-treated samples for MYH9 and PRDX6 (Additional file 8: Fig. S2).

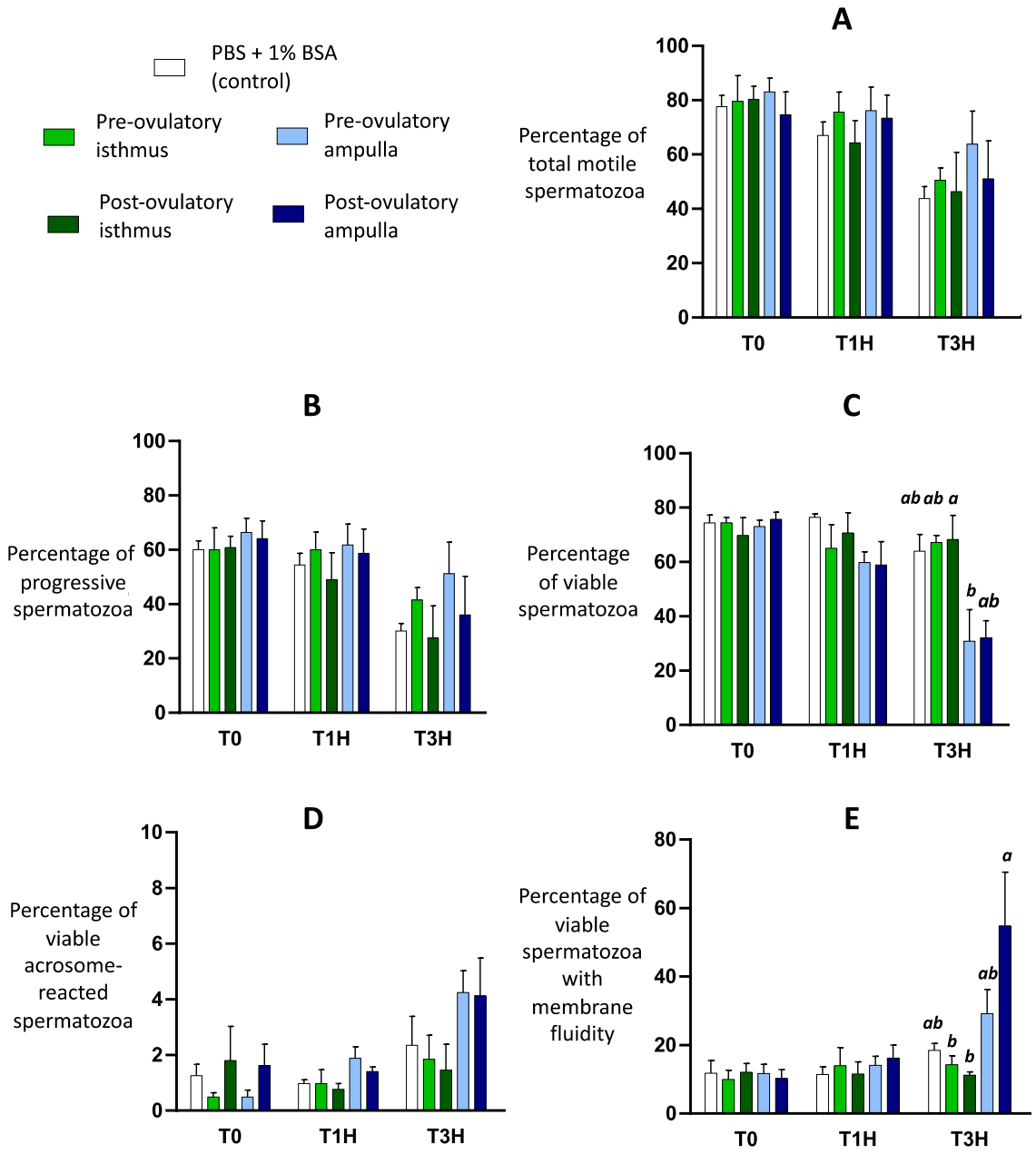

Fig. 2 Sperm parameters during incubation with oviduct fluid (treated groups) or PBS (controls). Sperm motility (**A**, **B**) was assessed by computer assisted sperm analysis (CASA). Sperm viability (**C**), acrosome reaction (**D**) and membrane lipid disorder (**E**) were assessed by flow cytometry. Data are means ± SEM of 4 replicates

The GO classification of SIPs using PANTHER indicated that 52% were binding proteins, 23% catalytic proteins, and 10% structural proteins (Fig. 3B). The prediction of protein secretory pathways indicated that 5% (13/245) of SIPs possessed a peptide signal and were predicted to be classically secreted, while 21% (52/245) were secreted via unconventional pathways. In addition, 78% (190/245) of SIPs were previously

Table 1 Top 25 most abundant sperm-interacting proteins (SIPs) identified in the oviduct fluid (OF) derived from the ampulla and isthmus just before (Pre-ov) and after (Post-ov) ovulation

Protein name	Gene symbol	Mean NWS in OF-treated sperm	OF:control sperm ratio in				Predicted secretion pathways	Reported role in sperm physiology and fertilization
			Pre-ov isthmus	Pre-ov ampulla	Post-ov isthmus	Post-ov ampulla		
Myosin heavy chain 9	*MYH9*	284.4	45.9	66.4	54.3	119.4	EVs	OVGP1 partner on human sperm [26]
Myosin heavy chain 14	*MYH14*	184.0	66.4	75.3	86.2	140.7	EVs	-
AHNAK nucleoprotein	*AHNAK*	101.4	512.7	341.1	509.2	287.5	EVs	-
Endoplasmic reticulum chaperone BiP	*HSPA5*	83.8	3.3	3.0	3.5	4.5	EVs and classical	Human sperm capacitation [39] and binding to zona pellucida [40]
Tubulin polymerization-promoting protein family member 3	*TPPP3*	81.6	17.8	17.4	17.9	7.2	EVs	-
Myosin-10	*MYH10*	70.3	*No detection in control*				EVs	-
Heat shock protein beta-1	*HSPB1*	59.9	134.9	284.1	199.6	179.0	EVs	-
Myosin light polypeptide 6	*MYL6*	58.1	22.3	31.5	33.9	34.0	EVs and unconv	-
Oviduct-specific glycoprotein	*OVGP1*	52.5	28.7	24.5	21.3	22.1	EVs	Bovine sperm capacitation [41], binding to zona pellucida and monospermy [42]
Heat shock cognate 71 kDa protein	*HSPA8*	38.6	3.0	3.3	2.7	2.5	EVs	Bovine sperm survival, membrane fluidity and monospermy [21]
Tropomodulin 3	*TMOD3*	36.0	23.9	50.2	44.0	34.7	Unconv	-
Protein disulfide-isomerase	*PDIA3*	33.7	4.7	4.2	5.3	3.4	EVs and classical	Human sperm binding to zona pellucida [43]
Keratin, type II cytoskeletal 8	*KRT8*	32.7	332.5	129.3	338.4	66.3	EVs	-
Actin, cytoplasmic 1	*ACTB*	31.7	2.9	4.7	3.9	4.1	EVs	-
Actin, cytoplasmic 2	*ACTG1*	31.5	2.9	4.5	3.7	3.9	EVs	-
Endoplasmin	*HSP90B1*	28.9	4.2	4.1	3.4	5.3	EVs and classical	KO mouse unable to fertilize oocytes [44] Binding partner of PDIA4 for monospermy in pigs [45]
Hypoxia up-regulated 1	*HYOU1*	27.5	5.6	3.2	5.3	4.7	EVs	-

Table 1 (continued)

Protein name	Gene symbol	Mean NWS in OF-treated sperm	OF:control sperm ratio in				Predicted secretion pathways	Reported role in sperm physiology and fertilization
			Pre-ov isthmus	Pre-ov ampulla	Post-ov isthmus	Post-ov ampulla		
Elongation factor 1-alpha 1	*EEF1A1*	23.4	6.9	13.4	11.5	8.1	EVs and unconv	-
Tropomyosin alpha-3 chain	*TPM3*	23.3	*No detection in control*				EVs and unconv	-
Brain acid soluble protein 1	*BASP1*	22.9	5.1	8.9	4.1	4.5	EVs	-
Annexin A1	*ANXA1*	22.8	2.1	3.0	1.8	2.8	EVs and unconv	Bovine sperm binding to oviduct epithelial cells [46]
Na(+)/H(+) exchange regulatory cofactor NHE-RF1	*SLC9A3R1*	21.6	*No detection in control*				EVs	-
Protein disulfide-isomerase A4	*PDIA4*	20.7	26.8	26.8	27.3	31.7	EVs and classical	Penetration rate and monospermy in pigs [47] Binding partner of HSP90B1 for monospermy in pigs [45]
Annexin A2	*ANXA2*	20.6	69.6	118.3	69.2	78.9	EVs and unconv	Bovine sperm binding to oviduct epithelial cells [46]
40S ribosomal protein S3a	*RPS3A*	19.8	74.4	77.3	70.2	29.7	EVs and unconv	-

Proteins are classified in decreasing order of quantified level in OF-treated spermatozoa (mean ± SEM of 4 conditions; $n = 4$ replicates per condition). Fold-change ratios between OF-treated and control sperm groups are indicated for each condition (a value in italics means exclusive detection in OF-treated spermatozoa). The secretion pathway was predicted using Outcyte and SignalP and by comparison with reported lists of proteins in OF-derived EVs. 'Classical' means secretion via a signal peptide; 'Unconv' means via unconventional pathways (including paracrine and EV-secretion pathways); 'EVs' means previously reported in OF-derived EVs. The main roles reported in sperm physiology and/or fertilization in mammals are indicated (a dash means no report found).

NWS: normalized weighted spectra

reported in oviduct extracellular vesicles in mammals [9, 34, 35] with overlaps with the two previous categories of secretion (Fig. 3C and Additional file 3: Table S3). Overall, 83% (203/245) of SIPs were predicted to be secreted by conventional or unconventional pathways.

Impact of the oviduct anatomical region and peri-ovulatory stage on numbers and abundance of sperm-interacting proteins

Figure 4A and B show counts and the top 20 most abundant SIPs in both oviduct regions at Pre-ov and Post-ov, respectively (see Additional file 4: Table S4 for quantitative values).

The highest number of SIPs (187/245) was identified in the Pre-ov isthmus, i.e., time and place of oviduct reservoir. In contrast, the lowest (113/245) was identified in the Post-ov ampulla, i.e., time and place of fertilization. This difference in numbers of SIPs could not be explained by differences in protein numbers in the OF (Additional file 2: Table S2). Furthermore, 76 SIPs (31%) were identified in only one region × stage condition: 42 (17%) in the Pre-ov isthmus, 18 (7%) in the Pre-ov ampulla, 9 (4%) in the Post-ov ampulla, and 7 (3%) in the Post-ov isthmus (Fig. 5).

In total, the abundance of 41 SIPs (17%) was impacted by the peri-ovulatory stage or anatomical region (Fig. 6). Considering the SIPs common to both stages in a given region, 9% (9/105) and 31% (26/85) were differentially abundant between Pre-ov and Post-ov in the isthmus and ampulla, respectively (Fig. 6A). Considering the SIPs common to both regions at a given stage, 10% (12/117)

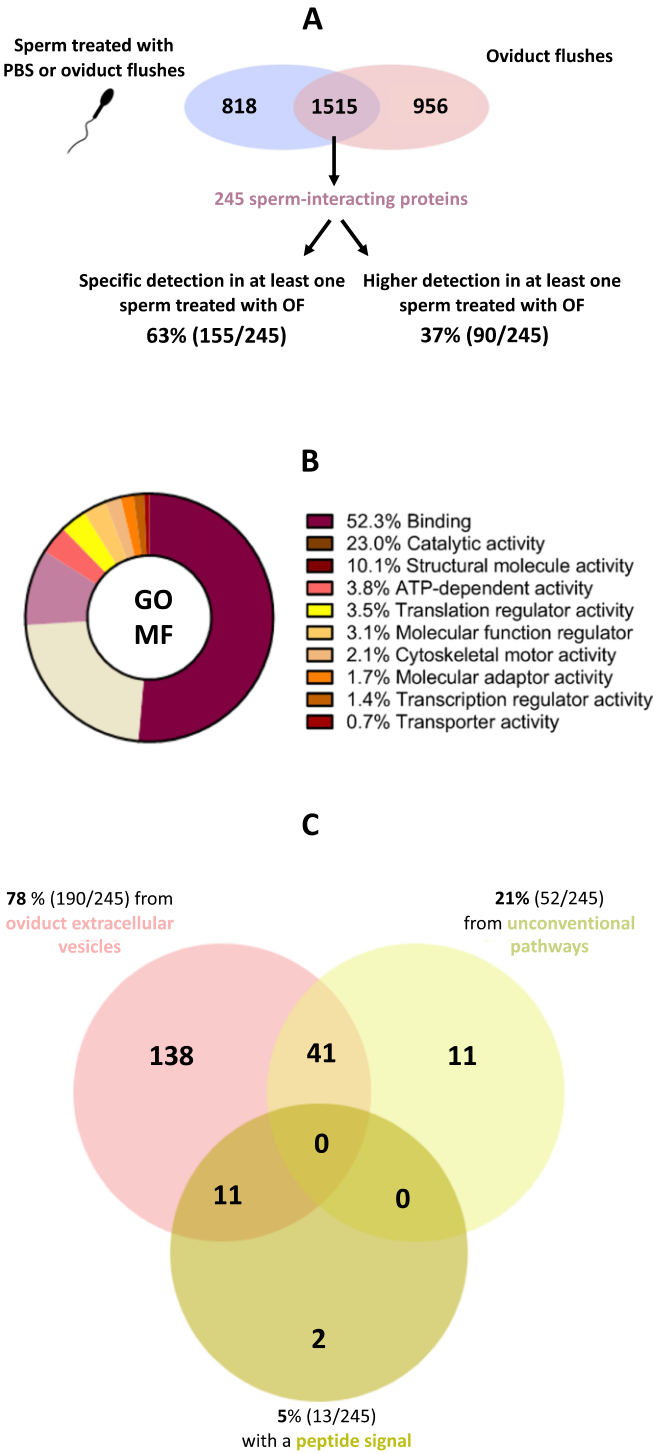

Fig. 3 Classification of sperm-interacting proteins according to their (**A**) criteria of identification, (**B**) gene ontology (GO) molecular functions (MF) from PANTHER, and (**C**) predicted secretory pathways. Prediction of secretion by unconventional pathways and with a peptide signal were carried out using Outcyte and SignalP 6.0 tools online. The proportion of SIPs potentially secreted by oviduct extracellular vesicles were previously reported in cattle [9], cats [34], and pigs [35]

and 18% (13/73) were differentially abundant between isthmus and ampulla at Pre-ov and Post-ov, respectively (Fig. 6B). Furthermore, there was no correlation between the initial abundance of SIPs in the OF and their abundance in OF-treated spermatozoa (see scatter plots in Additional file 9: Fig. S3).

Functional analysis of SIPs and protein–protein interaction networks

The top 20 GO terms of the Metascape enrichment analysis for molecular functions (GO MF) and biological processes (GO BP) of SIPs are presented in Fig. 7A and B, respectively (see all GO terms and *P*-values in Additional file 5: Table S5). A significant overrepresentation of SIPs in functions such as cadherin binding, structural molecule activity, actin binding, cytoskeletal motor activity, and ATP-dependent activity was seen. Furthermore, SIPs were enriched in processes like cytoskeleton organization, microtubule-based processes, actomyosin structure organization, and regulation of cellular responses to stress.

The possible roles of SIPs in periconception events in the oviduct were further studied using the Metascape membership tool [36]. Proteins associated with the membership terms 'cell motility,' 'sperm,' 'fertilization,' and 'oviduct' are presented in Fig. 8. In total, 46 SIPs were retrieved with these particular terms, including 32 in cell motility, 11 in fertilization, and 7 in oviduct functions. Reported roles in sperm physiology and fertilization are also indicated in Table 1.

To analyze the possible interactions between SIPs, protein–protein interaction networks were built separately in each condition using STRING. Figure 9A shows the network obtained in the Pre-ov isthmus for all SIPs. Numerous interactions were described between SIPs, some of them being involved in pathways related to RNA and protein processing, tight junction and estrogen signaling. As MYH9 was the most abundant SIP, a focus on this protein is shown in Fig. 9B (see Additional file 10: Fig. S4 for other conditions and Additional file 6: Table S6 for network details). In this network, MYH9 was in a node core interacting with 19 other SIPs, including OVGP1, MYH10, HSP90B1, and HSPA8. MYH9 and other myosins (MYH10, MYH11) were involved in pathways related to regulation of actin cytoskeleton, tight junction and vascular smooth muscle contraction.

Discussion

Using an MS-based quantitative approach, this study provides a comprehensive list of SIPs in the bovine OF, including proteins already well known to interact with bull spermatozoa. These data show changes induced by the oviduct anatomical region and ovulation time on the number and abundance of SIPs, which correlates with the hypothesis that synchronization of events leading to fertilization is monitored by dynamic interactions between sperm and oviduct secretions.

Identification of sperm-interacting proteins by quantitative proteomics

Overall, 11% of proteins detected in sperm treated with OF were considered to be SIPs. In a previous proteomic study in pigs, 63% (64/102) of sperm proteins were considered as SIPs after incubation with OF [24]. However, in that study, all proteins shared between OF-treated sperm and OF were classified as potential SIPs without comparison with a sperm control group and quantitative criteria [24]. Here we used quantitative proteomics and comparison between normalized levels of proteins in the OF and spermatozoa incubated with or without OF for identifying SIPs. Two criteria were required to define a SIP: significant detection in the OF used for sperm incubation and exclusive or significantly higher abundance in OF-treated sperm with a fold-change ratio of at least 3.0 compared to controls. Of note, the proteins well known to interact with bull sperm, including HSPA8 [21], HSPA5 (GRP78) [20], and OVGP1 [18], were all quantified with a higher abundance in OF-treated than control sperm, confirming the interest of using quantitative proteomic approaches to indentify sperm-interacting proteins. In our previous proteomic study, HSPA8, HSPA5 and OVGP1 were detected in OF-treated sperm but not in control sperm [22]. This difference is likely due to higher peptide separation by chromatography and greater sensitivity of the MS instrument used, which led to more proteins identified in all groups of spermatozoa (around 2300 vs. 500 proteins in our previous study). Furthermore, MYH9 and PRDX6 were detected higher in OF-treated sperm than in PBS by proteomics whereas they were exclusively detected in OF-treated sperm by immunoblotting, which may be explained by the different sensitivities of the methods.

Origin and possible binding mechanisms of sperm-interacting proteins

As expected, a majority (52%) of SIPs were classified by PANTHER as binding proteins. Note that OF were collected by gentle pressure to avoid cell lysis, then two successive centrifugations were carried out to eliminate cells and cellular debris. Thus, the SIPs were present in the oviduct lumen exclusively. The SIPs overrepresented in actin cytoskeleton organization processes included several myosins (MYH9, MYH10, MYH14,

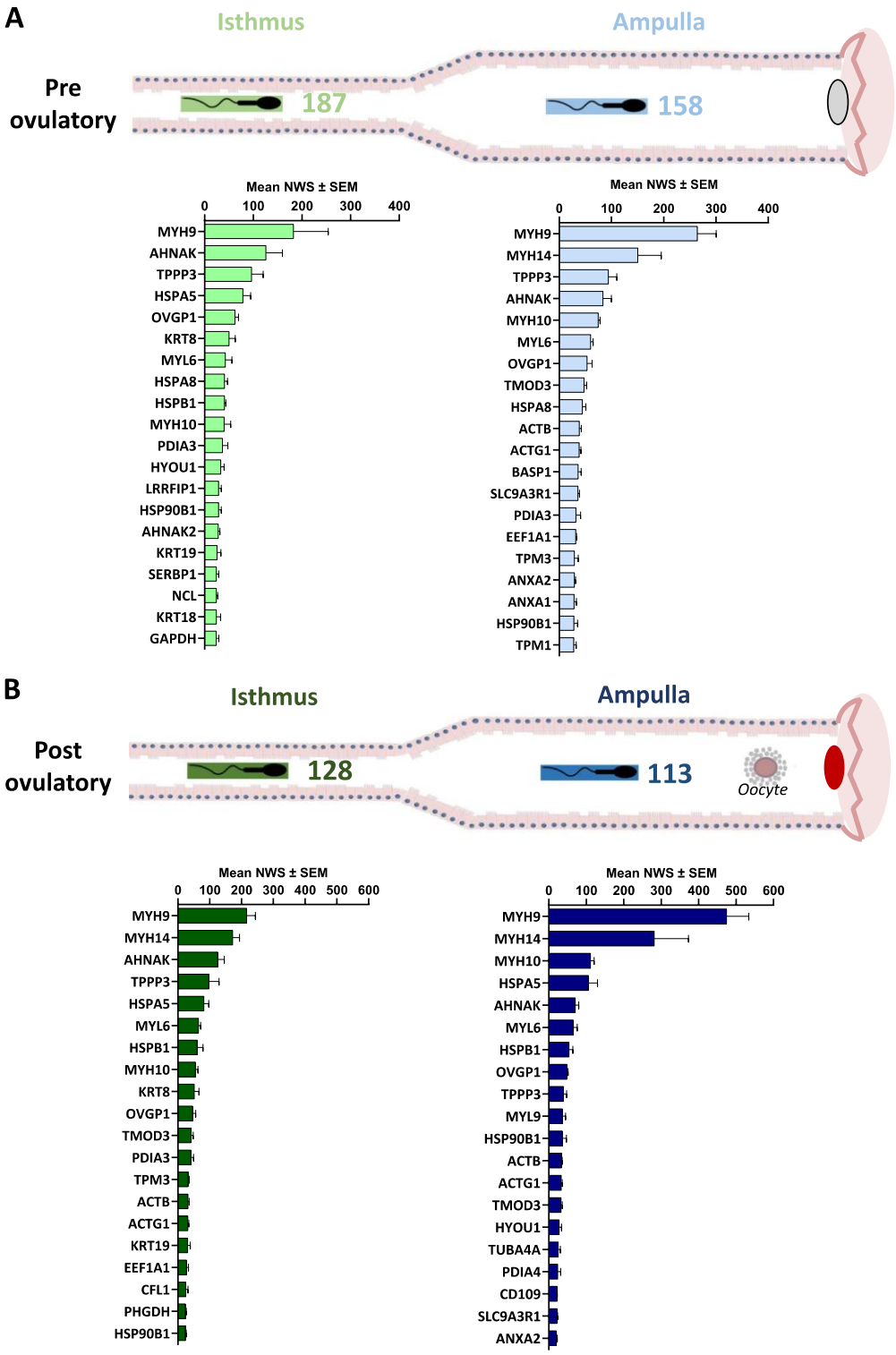

Fig. 4 Numbers and mean normalized quantitative values (± SEM) of top 20 sperm-interacting proteins in the isthmus and ampulla at (**A**) pre-ovulatory and (**B**) post-ovulatory cycle stages

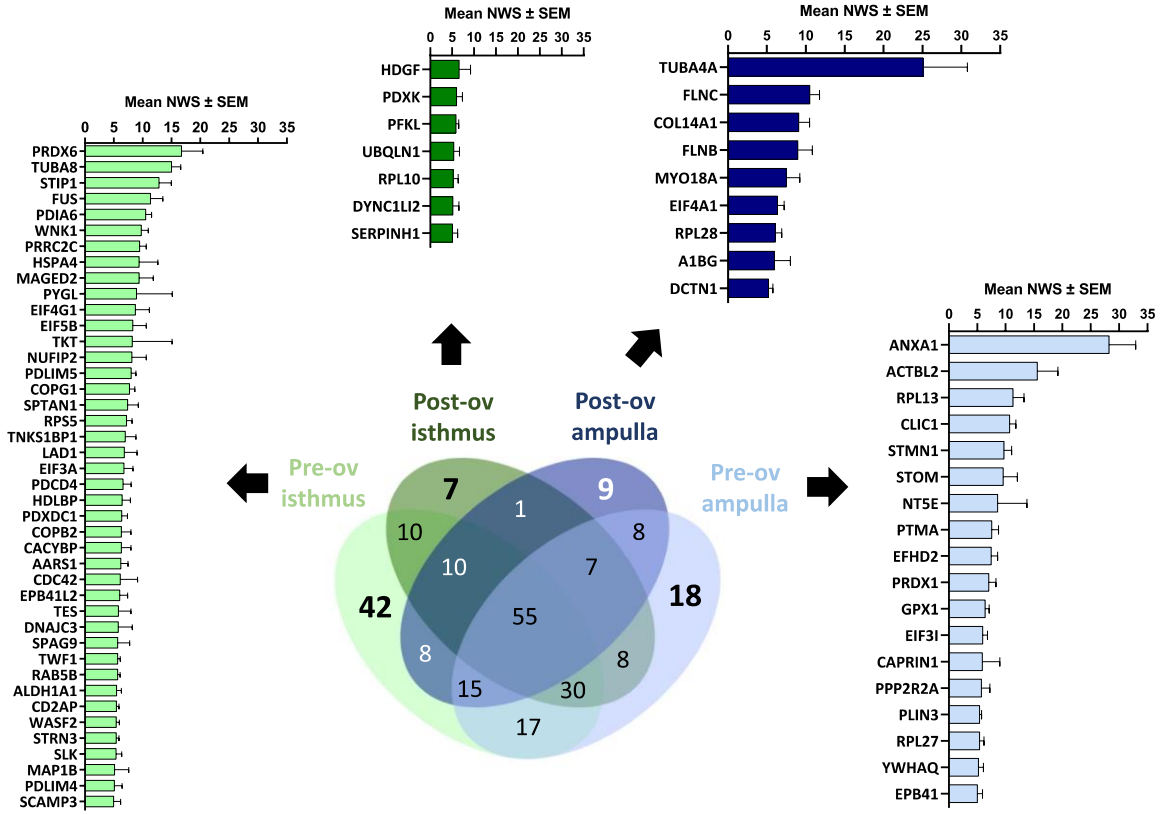

Fig. 5 Distribution and mean normalized quantitative values (± SEM) of sperm-interacting proteins identified in only one oviduct region (isthmus versus ampulla) at pre-ovulatory and post-ovulatory cycle stages

and MYL6), tropomyosin 3 (TPM3), and some heat shock proteins (HSP90B1, HSPA8, HSPA5). Consistent with our data, a previous study that used proteomics to identify a subset of 70 kDa oviductal surface proteins that bound to bull spermatozoa reported HSPA8, HSP90B1, HSPA5, and TPM3 as potential SIPs [21].

To our knowledge, receptors for the above proteins on sperm membranes are not known. However, SIPs may anchor to the sperm membrane through lipid interactions. MYH9, MYH10, and MYH14 belong to the class II of mammalian non-muscle myosins, consisting of two heavy chains, two essential light chains, and a pair of regulatory light chains [48]. MYH9, MYH10, and MYH14 (also known as non-muscle myosins II-A, II-B, and II-C) were reported to bind to liposomes made with various phospholipids with concomitant dissociation of their regulatory chain [49].

The SIPs may also interact through binding to sperm surface proteins. MYH9 has been previously identified as a binding partner of OVGP1 on the surface of human spermatozoa [26].

In addition, SIPs may interact with sperm through rapid fusion or binding with oviduct EVs. Extracellular vesicles are important mediators of cell–cell communications as they transfer not only proteins but also small RNAs, phospholipids, and metabolites [50]. Of the 245 SIPs, 78% were previously reported in oviductal EVs, including exosomes and microvesicles. This proportion was much higher than those reported for proteins identified in the whole bovine OF [14], indicating an enrichment in EV-secreted proteins among SIPs. Interactions between spermatozoa and oviduct EVs have already been described in cats [34], cattle [10], pigs [51], and mice [52]. In mice, it was shown that the plasma membrane calcium/calmodulin-dependent calcium ATPases 4, which has an essential function in sperm motility, was delivered to sperm through membrane fusion with oviduct EVs via integrins and CD9 tetraspanin [52]. In cattle, spermatozoa have been shown to uptake EVs derived from bovine OF after only 15 min of co-incubation. Those interactions regulated protein tyrosine phosphorylation and intracellular calcium levels, two processes

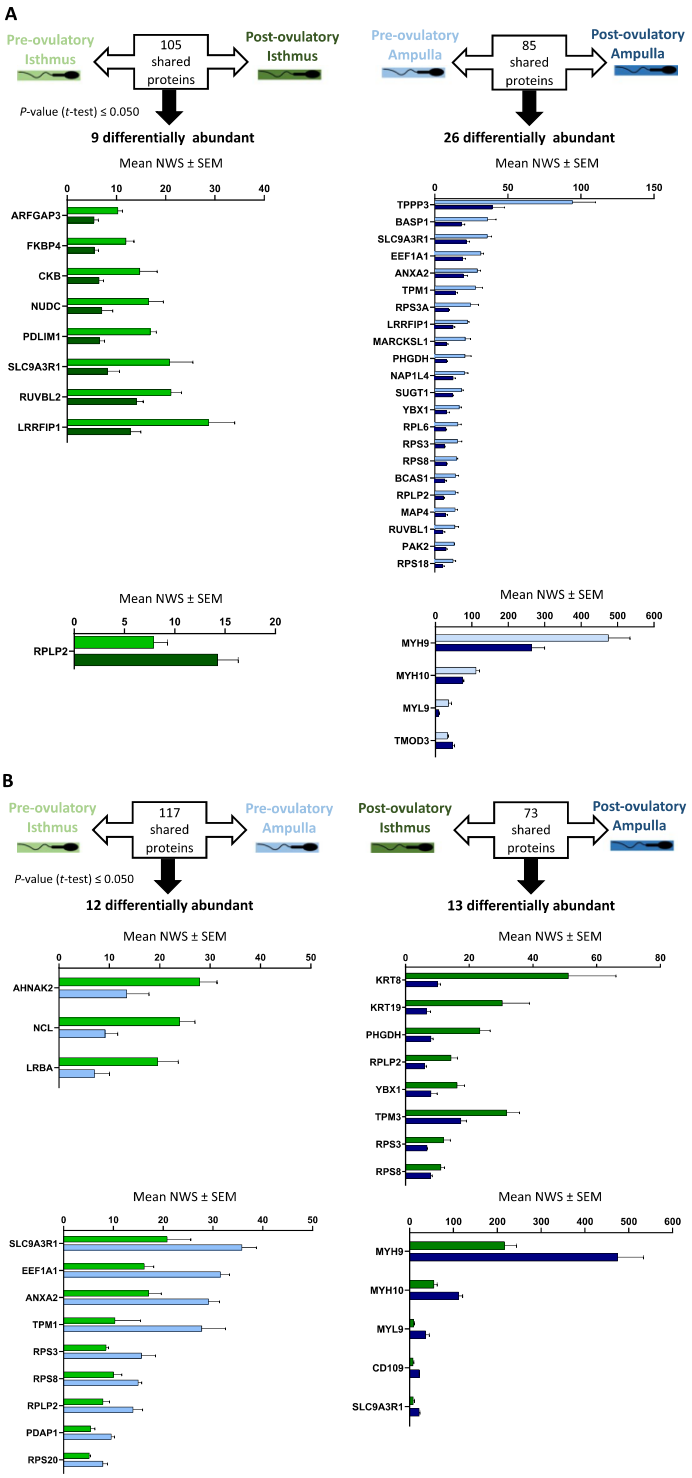

Fig. 6 Numbers and mean normalized quantitative values (± SEM) of differentially abundant sperm-interacting proteins (**A**) between pre-ovulatory and post-ovulatory cycle stages in the isthmus and ampulla and (**B**) between ampulla and isthmus at pre-ovulatory and post-ovulatory stages. SIPs shared between either stages or regions were considered as differentially abundant with a *P*-value ≤ 0.050 after the Student's *t*-test

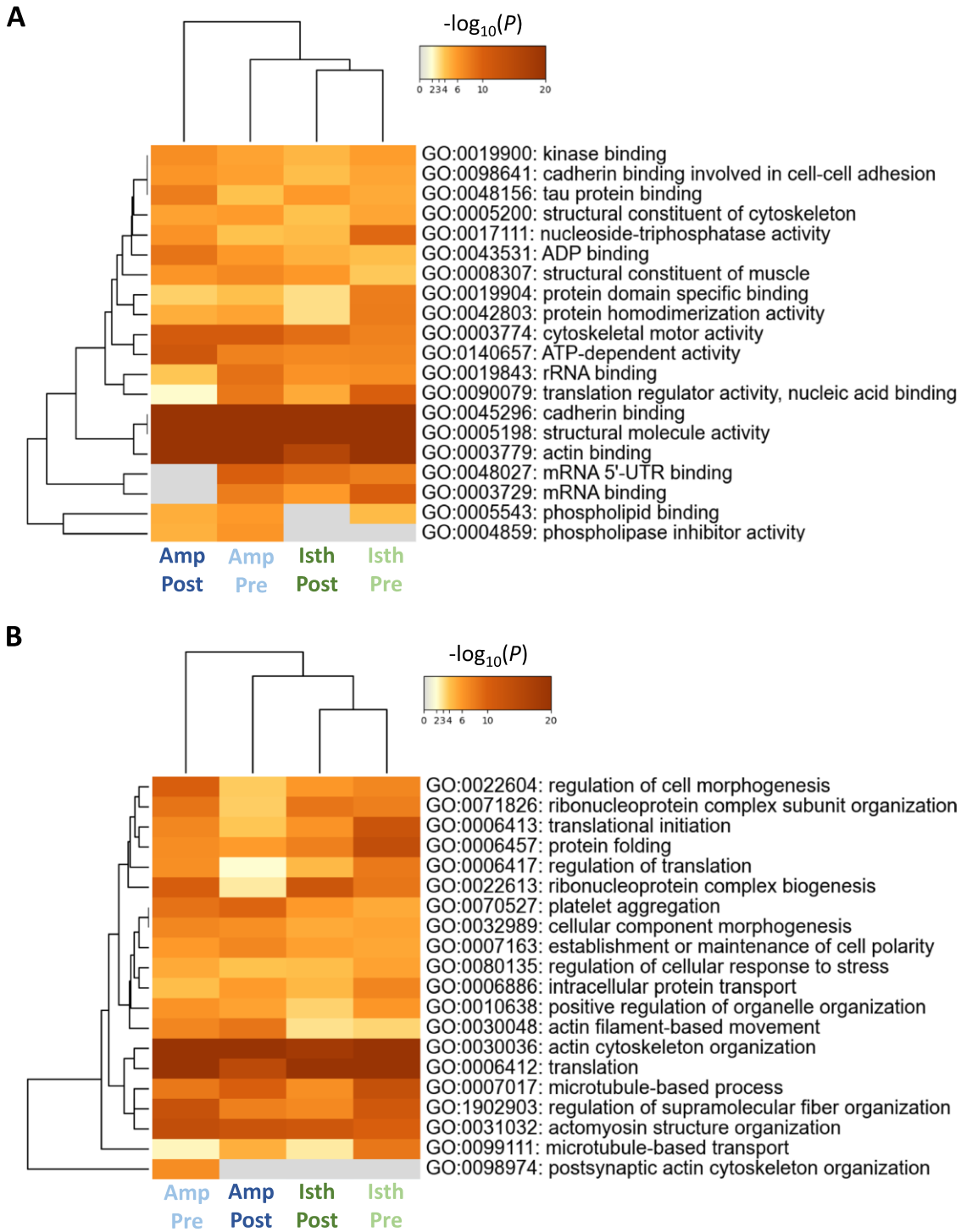

Fig. 7 Functional enrichment analysis of sperm-interacting proteins for Gene ontology (**A**) Molecular Functions and (**B**) Biological Processes in the ampulla and isthmus pre-ovulatory and post-ovulatory stages. The analysis was made using Metascape**.** Amp Post: post-ovulatory ampulla; Amp Pre: pre-ovulatory ampulla; Isth Post: post-ovulatory isthmus; Isth Pre: pre-ovulatory isthmus

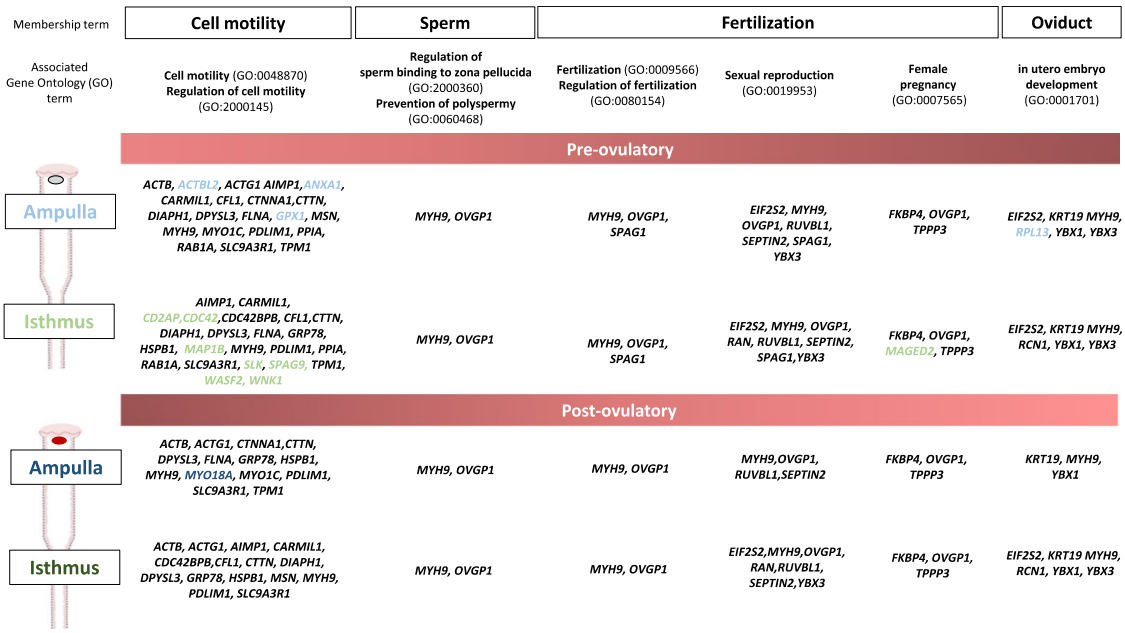

Fig. 8 Sperm-interacting proteins associated with terms related to cell motility, sperm, fertilization, and oviduct. Membership analysis was carried out with the online Metascape tool and the *Homo Sapiens* database. For each membership term, the gene ontology (GO) terms associated with SIPs are indicated below. The colored gene symbols indicate SIPs identified in only one region × stage

related to sperm capacitation [10]. In addition, EVs derived from follicular fluid were reported to modulate bull sperm viability, capacitation, and acrosome reaction [53]. Taken together, these data reinforce the idea that oviduct EVs may be key players of protein cargo delivery for the acquisition of sperm fertilizing ability in vivo.

Spatiotemporal regulation of sperm-interacting proteins

Up to 31% of SIPs changed in numbers and abundance between oviduct anatomical regions and peri-ovulatory stages. This is in line with our previous report showing 9 differentially abundant SIPs over the 14 identified in luteal, pre-ovulatory, and post-ovulatory OF [22]. Also consistent with our results, the effects of OF and OF-derived EVs on bull sperm, as reported by several in vitro studies, change according to the anatomical region [10, 54] and cycle stage [27].

There was no relationship between the initial abundance of SIPs in the OF and their abundance in OF-treated spermatozoa. This indicates highly specific sperm-protein interactions.

In order to avoid a bull effect in this study, the same pool of semen from three bulls was used for all incubations with OF. Therefore, the changes observed in sperm proteomics are expected to be due to differences in OF protein composition. It has been reported that up to 12% of proteins in the OF change in abundance according to the anatomical region and peri-ovulatory stage [14]. As shown by the protein–protein interaction network built by STRING, most SIPs may interact with each other. Therefore, some SIPs may anchor rapidly to the sperm membrane and lead to other protein interactions over time and depending on the OF protein composition. Our data suggest dynamic sperm-OF interactions as the sperm progresses toward the oocyte. The beneficial role of sequential interactions on sperm fertilizing ability remains to be tested.

Sperm-interacting proteins in the pre-ovulatory isthmus and possible impact on sperm binding to the sperm reservoir

The pre-ovulatory isthmus is the expected place of sperm storage in mammals [3, 55, 56]. A total of 42 SIPs were identified exclusively in the isthmus just before ovulation, including peroxiredoxin-6 (PRDX6). PRDX6 is well known to play roles in protecting cells from oxidative stress [57–59] and was reported to protect human and mouse spermatozoa from oxidation [60]. In particular, PRDX6 has both peroxidase and calcium-independent phospholipase activites. Inhibition of PRDX6 increased

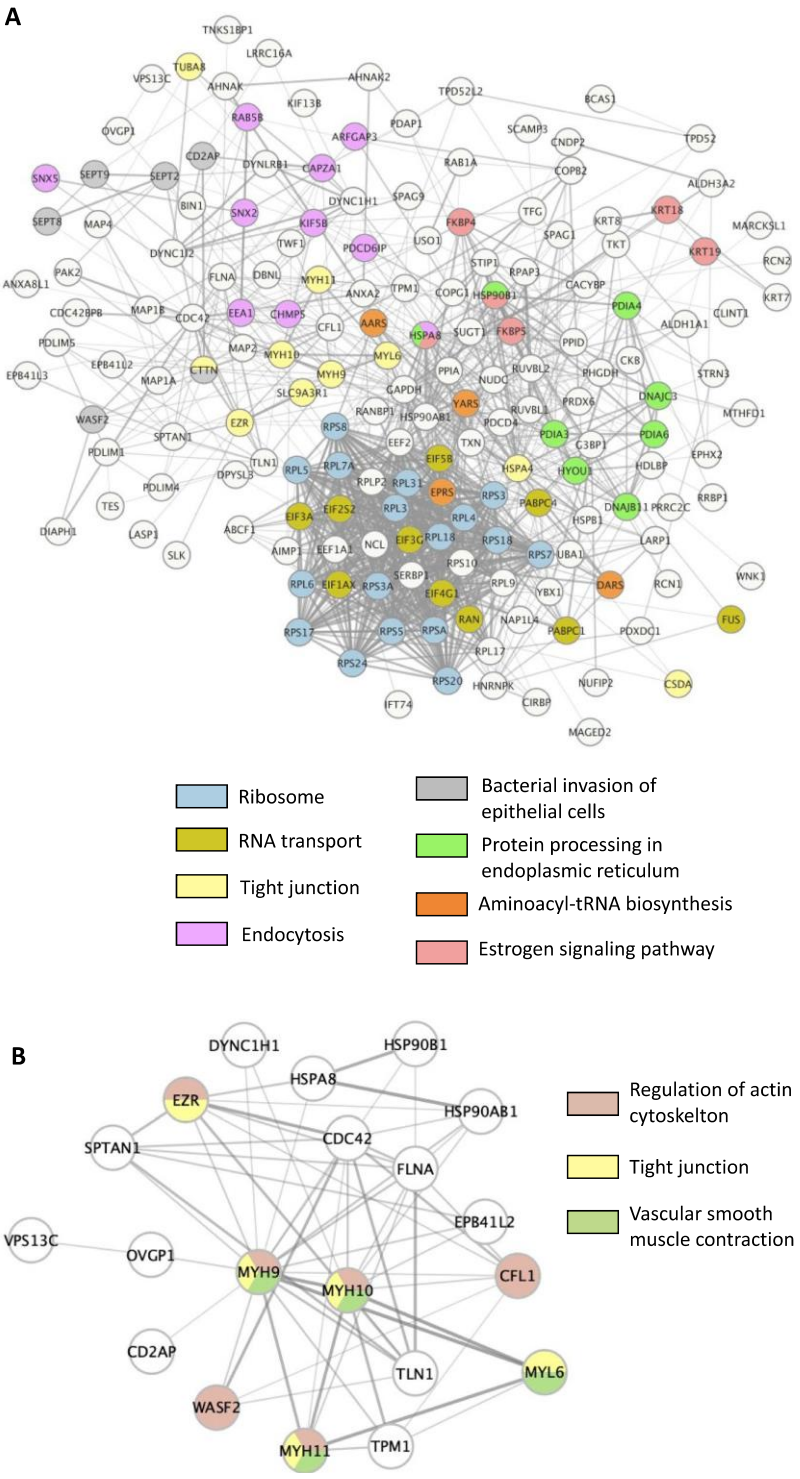

Fig. 9 Predicted protein–protein interaction networks and KEGG pathway enrichment analysis of (**A**) all sperm-interacting proteins in the pre-ovulatory isthmus or (**B**) MYH9 and OVGP1. Networks were built using STRING and Cytoscape with a minimum interaction score of 0.4. Line thickness between proteins represents the degree of confidence prediction of the interaction

sperm DNA damage [58] and the production of reactive oxygen species during capacitation [59].

Sperm binding to oviduct epithelial cells is mediated by membrane glycoproteins, including annexins A1, A2, A4, and A5 [46], HSPA5 [20], and HSPA8 [21]. ANXA2, HSPA5, and HSPA8 were among the most abundant SIPs in the Pre-ov isthmus. Furthermore, HSPA5, ANXA1, and ANXA2 were among the top 20 most abundant SIPs in the Pre-ov ampulla, while ANXA4 and ANXA5 were identified as SIPs in the Pre-ov and Post-ov ampullas. Therefore, a binding competition between the OF and sperm receptors on luminal oviduct cells is expected, which may lead to a decrease in sperm binding to the sperm reservoir. Further studies are needed to clarify the impact of SIPs on sperm binding to oviduct epithelial cells.

Potential roles of SIPs on sperm capacitation and focus on OVGP1 and MYH9

The reported roles of the most abundant SIPs in sperm physiology and fertilization are indicated in Table 1. Sperm capacitation is a timed process starting with an elevation of intracellular calcium and includes phospholipid remodeling, protein tyrosine phosphorylation, and hyperactivated motility, allowing sperm to cross the cumulus cells and the zona pellucida and eventually fuse with the oocyte [61]. After 3 h of co-incubation, OF from the ampulla increased sperm membrane fluidity compared to OF from the isthmus. In accordance, proteins [5] and oEVs [10] purified from the ampullary OF induced the capacitation of bull sperm in vitro. Though the contribution of SIPs to the acquisition of hyperactivated motility remains to be explored, the enrichment analysis of SIPs highlighted functions such as cytoskeletal motor activity and microtubule motor activity, which are all needed for flagellar movements [62]. Additionally, some SIPs were associated with the GO terms "sperm binding to zona pellucida," "prevention of polyspermy," and "fertilization," for which OVGP1 and MYH9 were most frequently cited. MYH9 was the most abundant SIP, and OVGP1 was among the top 10 in all conditions. OVGP1 has been shown to interact with spermatozoa in bovine [18], humans [63], and hamsters [64]. It has been previously identified as a promoter of sperm viability, motility, and capacitation in buffaloes [41]. Moreover, incubation of human spermatozoa with recombinant OVGP1 enhanced sperm capacitation [65] and binding to the oocyte [66].

Moreover, non-muscle myosins have well-documented roles in cell migration, adhesion, and movement [67–70]. In particular, MYH9 was shown to interact with the calcium-dependent S100 family member S100A4 to promote the motility of human cancer cells [67]. Of note, several S100 proteins (S100A11, S100A2, S100A14, S100B) were found in the proteome of bull sperm in the present study. A recent study reported cytoskeletal abnormalities of Sertoli cells and infertility in male mice with mutations in MYH9 [68]. Moreover, MYH9 has well-documented roles in cell exocytosis [71, 72], a process essential for sperm acrosome reaction and fertilization [73]. The numerous myosins identified as SIPs in this study (MYH9, MYH10, MYH14, MYH11, MYL6, MYL9, MYO6, MYO18A, MYO1C) open up new exciting research perspectives on sperm capacitation.

Limitations of the study

Post-mortem collection of OF was chosen to avoid contamination by inflammatory cells and hemoglobin and for ethical and economic reasons. Though oviducts were immediately placed on ice after collection, some minor modifications in OF protein content cannot be excluded.

OF protein concentration was set at 3 mg/mL to detect sperm-interacting proteins according to preliminary data on MYH9, a known SIP, using immunoblotting. However, this concentration may not be adequate for the identification of all potential SIPs, which have various initial abundance in the OF and may have different binding affinity on sperm.

The same pool of semen from three bulls was used in this study in order to focus of female factors regulating SIPs. However, sperm-OF interactions may vary from one bull to another. Furthermore, frozen-thawed spermatozoa were used in this study for practical reasons and because artificial insemination is typically made with frozen semen in cattle. However, the cryopreservation procedure induces sperm surface modifications [74] which may modify protein interactions. Furthermore, a short incubation time (60 min) was chosen because it was sufficient to allow sperm protein interactions without affecting sperm membrane integrity and motility. However, in vivo, mammalian spermatozoa may stay up to several days in the oviduct until fertilization [75]. Longer incubation times would probably enable more and/or different OF proteins to interact with spermatozoa.

Conclusion

To conclude, this study provides new information on OF proteins interacting with bull spermatozoa around the time of ovulation. Some of these proteins fluctuated in number and abundance, suggesting rapid changes in in vivo sperm protein surfaces, possibly to promote sperm capacitation and fertilization in the oviduct. Further work is now needed to assess the effect of recombinant SIPs on sperm, with potential applications in media used for sperm conservation, insemination, and in vitro fertilization.

Supplementary Information

The online version contains supplementary material available at https://doi.org/10.1186/s40104-022-00811-2.

Additional file 1: Table S1. List of antibodies used for immunoblotting.

Additional file 2: Table S2. List of proteins identified and quantified in oviduct fluid (OF) from ampulla and isthmus at pre-ovulatory (Pre-ov) and post-ovulatory (Post-ov) stages and in OF-treated and control bull spermatozoa.

Additional file 3: Table S3. List of all sperm-interacting proteins and prediction of conventional and unconventional secretion pathways by Outcyte and SignalP and previous reports in oviduct extracellular vesicles.

Additional file 4: Table S4. List of sperm-interacting proteins quantified in the pre-ovulatory and post-ovulatoryampulla and isthmus with normalized quantitative values and fold-change ratios betweentreated and control sperm.

Additional file 5: Table S5. Functional enrichment analysis of sperm-interacting proteins for Gene Ontology (GO) Molecular Functions (MF) and Biological Processes (BP) from Metascape.

Additional file 6: Table S6. Protein-protein interaction network from STRING of all sperm-interacting proteins in each region × stage condition.

Additional file 7: Fig. S1. Sperm amplitude of lateral head (ALH), linearity (LIN), average path velocity (VAP), curvilinear velocity (VCL) and straight linevelocity (VSL) during the 60-min incubation with oviduct fluid (treated groups) or PBS (controls). Data are means ± SEM of 4 replicates.

Additional file 8: Fig. S2. Immunoblotting of HSPA5, MYH9 and PRDX6 in oviduct fluid used for sperm incubation and in sperm samples. The histograms indicate the mean levels of signals from three replicates. Letters indicated the significant level after ANOVA and Tuckey post-test between PBS (control) and OF-treated spz : b: *P*-value < 0.05;c: *P*-value < 0.01; d: *P*-value < 0.001.

Additional file 9: Fig. S3. Scatter plots of the abundance of sperm-interacting proteins (SIPs) intreated spermatozoa according to the initial abundance in oviduct fluid.

Additional file 10: Fig. S4. Protein-proteininteraction network of sperm-interacting proteins identified in the (A) post-ovulatoryisthmus, (B) pre-ovulatory ampulla, and (C) post-ovulatory ampulla.

Acknowledgements

The authors thank Benoit Guyonnet and Olfa Ghazouhani (Union Evolution, France) for providing bull semen. The authors thank Valérie Labas and PIXANIM (INRAE, Nouzilly, France) for using the proteomic software Scaffold. The authors warmly thank Thierry Delpuech and Albert Arnoult for collecting the oviducts at the slaughterhouse.

Author contributions

MSD, PM, and JS designed the study; CM and MSD wrote the manuscript; MSD and CM collected and prepared the OF; RL and EC did the MS analyses; CM analyzed the proteomic data; AMZ participated in the analysis and interpretation of data: CM and GT performed and analyzed the data from CASA and flow cytometry; CP supervised the MS analyses; all authors corrected the manuscript; MSD administrated and supervised the study. All authors read and approved the final manuscript.

Funding

This work was funded by INRAE and Agence Nationale de la Recherche under the grant number ANR-18-CE92-0049. This work was also supported by grants from Biogenouest, Infrastructures en Biologie Santé et Agronomie (IBiSA) and Conseil Régional de Bretagne awarded to Protim proteomics core facility.

Availability of data and materials

The datasets supporting the conclusions of this article are available in the ProteomeXchange Consortium via the PRIDE (Perez-Riverol et al., 2022) repository (www.ebi.ac.uk/pride/archive/login). Username: reviewer_pxd035271@ebi.ac.uk; Password: oFb3r6W5.

Declarations

Ethics approval and consent to participate

Not applicable.

Consent for publication

Not applicable.

Competing interests

The authors declare that they have no competing interests.

Received: 15 July 2022 Accepted: 24 November 2022
Published online: 17 February 2023

References

1. Coy P, García-Vázquez FA, Visconti PE, Avilés M. Roles of the oviduct in mammalian fertilization. Reproduction. 2012;144:649–60.
2. Hunter RH, Wilmut I. Sperm transport in the cow: peri-ovulatory redistribution of viable cells within the oviduct. Reprod Nutr Dev. 1984;24:597–608.
3. Lefebvre R, Chenoweth PJ, Drost M, LeClear CT, MacCubbin M, Dutton JT, et al. Characterization of the oviductal sperm reservoir in cattle. Biol Reprod. 1995;53:1066–74.
4. Boquest AC, Smith JF, Briggs RM, Duganzich DM, Summers PM. Effects of bovine oviductal proteins on bull spermatozoal function. Theriogenology. 1999;51:583–95.
5. Kumaresan A, Ansari MR, Garg A. Modulation of post-thaw sperm functions with oviductal proteins in buffaloes. Anim Reprod Sci. 2005;90:73–84.
6. Kumaresan A, Ansari MR, Garg A, Kataria M. Effect of oviductal proteins on sperm functions and lipid peroxidation levels during cryopreservation in buffaloes. Anim Reprod Sci. 2006;93:246–57.
7. Imam S, Ansari M, Kumar A, Singh C, Bharti V, Kumaresan A. Effect of oviductal proteins on structural and functional characteristics of cryopreserved sperm in murrah buffaloes. Reprod Domest Anim. 2010;45:302–6.
8. Zumoffen CM, Caille AM, Munuce MJ, Cabada MO, Ghersevich SA. Proteins from human oviductal tissue-conditioned medium modulate sperm capacitation. Hum Reprod. 2010;25:1504–12.
9. Almiñana C, Corbin E, Tsikis G, Alcântara-Neto AS, Labas V, Reynaud K, et al. Oviduct extracellular vesicles protein content and their role during oviduct–embryo cross-talk. Reproduction. 2017;154:253–68.
10. Franchi A, Moreno-Irusta A, Domínguez EM, Adre AJ, Giojalas LC. Extracellular vesicles from oviductal isthmus and ampulla stimulate the induced acrosome reaction and signaling events associated with capacitation in bovine spermatozoa. J Cell Biochem. 2019;121:2877–88.
11. Hamdi M, Cañon-Beltrán K, Mazzarella R, Cajas YN, Leal CLV, Gutierrez-Adan A, et al. Characterization and profiling analysis of bovine oviduct and uterine extracellular vesicles and their miRNA cargo through the estrous cycle. FASEB J. 2021;35:e22000.
12. Saint-Dizier M, Schoen J, Chen S, Banliat C, Mermillod P. Composing the early embryonic microenvironment: physiology and regulation of oviductal Secretions. Int J Mol Sci. 2020;21:223.
13. Lamy J, Labas V, Harichaux G, Tsikis G, Mermillod P, Saint-Dizier M. Regulation of the bovine oviductal fluid proteome. Reproduction. 2016;152:629–44.
14. Mahé C, Lavigne R, Com E, Pineau C, Locatelli Y, Zlotkowska AM, et al. Spatiotemporal profiling of the bovine oviduct fluid proteome around the time of ovulation. Sci Rep. 2022;12:4135.
15. Tecle E, Gagneux P. Sugar-coated sperm: unraveling the functions of the mammalian sperm glycocalyx. Mol Reprod Dev. 2015;82:635–50.
16. Plante G, Prud'homme B, Fan J, Lafleur M, Manjunath P. Evolution and function of mammalian binder of sperm proteins. Cell Tissue Res. 2016;363(105):27.
17. McNutt T, Rogowski L, Vasilatos-Younken R, Killian G. Adsorption of oviductal fluid proteins by the bovine sperm membrane during in vitro capacitation. Mol Reprod Dev. 1992;33:313–23.

18. King RS, Killian GJ. Purification of bovine estrus-associated protein and localization of binding on sperm. Biol Reprod. 1994;51:34–42.
19. Rodríguez C, Killian G. Identification of ampullary and isthmic oviductal fluid proteins that associate with the bovine sperm membrane. Anim Reprod Sci. 1998;54:1–12.
20. Boilard M, Reyes-Moreno C, Lachance C, Massicotte L, Bailey JL, Sirard M-A, et al. Localization of the chaperone proteins GRP78 and HSP60 on the luminal surface of bovine oviduct epithelial cells and their association with spermatozoa. Biol Reprod. 2004;71:1879–89.
21. Elliott RMA, Lloyd RE, Fazeli A, Sostaric E, Georgiou AS, Satake N, et al. Effects of HSPA8, an evolutionarily conserved oviductal protein, on boar and bull spermatozoa. Reproduction. 2009;137:191–203.
22. Lamy J, Nogues P, Combes-Soia L, Tsikis G, Labas V, Mermillod P, et al. Identification by proteomics of oviductal sperm-interacting proteins. Reproduction. 2018;155:457–66.
23. Itze-Mayrhofer C, Brem G. Quantitative proteomic strategies to study reproduction in farm animals: female reproductive fluids. J Proteomics. 2020;225:103884.
24. Luongo C, González-Brusi L, Cots-Rodríguez P, Izquierdo-Rico MJ, Avilés M, García-Vázquez FA. Sperm proteome after interaction with reproductive fluids in porcine: from the ejaculation to the fertilization site. Int J Mol Sci. 2020;21:6060.
25. Ireland JJ, Murphee RL, Coulson PB. Accuracy of predicting stages of bovine estrous cycle by gross appearance of the corpus luteum. J Dairy Sci. 1980;63:155–60.
26. Kadam KM, D'Souza SJ, Bandivdekar AH, Natraj U. Identification and characterization of oviductal glycoprotein-binding protein partner on gametes: epitopic similarity to non-muscle myosin IIA, MYH 9. Mol Hum Reprod. 2006;12:275–82.
27. Kumaresan A, Johannisson A, Humblot P, Bergqvist A-S. Effect of bovine oviductal fluid on motility, tyrosine phosphorylation, and acrosome reaction in cryopreserved bull spermatozoa. Theriogenology. 2019;124:48–56.
28. Keller A, Nesvizhskii AI, Kolker E, Aebersold R. Empirical statistical model to estimate the accuracy of peptide identifications made by MS/MS and database search. Anal Chem. 2002;74:5383–92.
29. Nesvizhskii AI, Keller A, Kolker E, Aebersold R. A statistical model for identifying proteins by tandem mass spectrometry. Anal Chem. 2003;75:4646–58.
30. Romero-Calvo I, Ocón B, Martínez-Moya P, Suárez MD, Zarzuelo A, Martínez-Augustin O, et al. Reversible ponceau staining as a loading control alternative to actin in western blots. Anal Biochem. 2010;401:318–20.
31. Bardou P, Mariette J, Escudié F, Djemiel C, Klopp C. jvenn: an interactive Venn diagram viewer. BMC Bioinform. 2014;15:293.
32. Zhao L, Poschmann G, Waldera-Lupa D, Rafiee N, Kollmann M, Stühler K. OutCyte: a novel tool for predicting unconventional protein secretion. Sci Rep. 2019;9:19448.
33. Teufel F, Almagro Armenteros JJ, Johansen AR, Gíslason MH, Pihl SI, Tsirigos KD, et al. SignalP 6.0 predicts all five types of signal peptides using protein language models. Nat Biotechnol. 2022;40:1023–5.
34. Ferraz MdAMM, Carothers A, Dahal R, Noonan MJ, Songsasen N. Oviductal extracellular vesicles interact with the spermatozoon's head and mid-piece and improves its motility and fertilizing ability in the domestic cat. Sci Rep. 2019;9:9484.
35. Laezer I, Palma-Vera SE, Liu F, Frank M, Trakooljul N, Vernunft A, et al. Dynamic profile of EVs in porcine oviductal fluid during the periovulatory period. Reproduction. 2020;159:371–82.
36. Zhou Y, Zhou B, Pache L, Chang M, Khodabakhshi AH, Tanaseichuk O, et al. Metascape provides a biologist-oriented resource for the analysis of systems-level datasets. Nat Commun. 2019;10:1523.
37. Szklarczyk D, Franceschini A, Wyder S, Forslund K, Heller D, Huerta-Cepas J, et al. STRING v10: protein–protein interaction networks, integrated over the tree of life. Nucleic Acids Res. 2015;43:D447–52.
38. Shannon P, Markiel A, Ozier O, Baliga NS, Wang JT, Ramage D, et al. Cytoscape: a software environment for integrated models of biomolecular interaction networks. Genome Res. 2003;13:2498–504.
39. Lachance C, Bailey JL, Leclerc P. Expression of HSP60 and GRP78 in the human endometrium and oviduct, and their effect on sperm functions. Hum Reprod. 2007;22:2606–14.
40. Marín-Briggiler CI, González-Echeverría MF, Munuce MJ, Ghersevich S, Caille AM, Hellman U, et al. Glucose-regulated protein 78 (GRP78/BiP) is secreted by human oviduct epithelial cells and the recombinant protein modulates sperm–zona pellucida binding. Fertil Steril. 2010;93:1574–84.
41. Choudhary S, Kumaresan A, Kumar M, Chhillar S, Malik H, Kumar S, et al. Effect of recombinant and native buffalo OVGP1 on sperm functions and in vitro embryo development: a comparative study. J Animal Sci Biotechnol. 2017;8:69.
42. Coy P, Canovas S, Mondejar I, Saavedra MD, Romar R, Grullon L, et al. Oviduct-specific glycoprotein and heparin modulate sperm-zona pellucida interaction during fertilization and contribute to the control of polyspermy. PNAS. 2008;105:15809–14.
43. Wong C-W, Lam KKW, Lee C-L, Yeung WSB, Zhao WE, Ho P-C, et al. The roles of protein disulphide isomerase family A, member 3 (ERP57) and surface thiol/disulphide exchange in human spermatozoa–zona pellucida binding. Hum Reprod. 2017;32:733–42.
44. Audouard C, Christians E. HSP90B1 knockout targeted to male germline: a mouse model for globozoospermia. Fertil Steril. 2011;95:1475–7.e4.
45. Mondéjar I, Martínez-Martínez I, Avilés M, Coy P. Identification of potential oviductal factors responsible for zona pellucida hardening and monospermy during fertilization in mammals. Biol Reprod. 2013;89(3):671–8.
46. Ignotz GG, Cho MY, Suarez SS. Annexins are candidate oviductal receptors for bovine sperm surface proteins and thus may serve to hold bovine sperm in the oviductal reservoir. Biol Reprod. 2007;77:906–13.
47. García-Martínez S, Gadea J, Coy P, Romar R. Addition of exogenous proteins detected in oviductal secretions to in vitro culture medium does not improve the efficiency of in vitro fertilization in pigs. Theriogenology. 2020;157:490–7.
48. Asensio-Juárez G, Llorente-González C, Vicente-Manzanares M. Linking the landscape of MYH9-related diseases to the molecular mechanisms that control non-muscle myosin II-A function in cells. Cells. 2020;9:1458.
49. Liu X, Shu S, Billington N, Williamson CD, Yu S, Brzeska H, et al. Mammalian nonmuscle myosin II binds to anionic phospholipids with concomitant dissociation of the regulatory light chain. J Biol Chem. 2016;291:24828–37.
50. Almiñana C, Bauersachs S. Extracellular vesicles: multi-signal messengers in the gametes/embryo-oviduct cross-talk. Theriogenology. 2020;150:59–69.
51. Alcântara-Neto AS, Schmaltz L, Caldas E, Blache M-C, Mermillod P, Almiñana C. Porcine oviductal extracellular vesicles interact with gametes and regulate sperm motility and survival. Theriogenology. 2020;155:240–55.
52. Al-Dossary AA, Bathala P, Caplan JL, Martin-DeLeon PA. Oviductosome-sperm membrane interaction in cargo delivery. J Biol Chem. 2015;290:17710–23.
53. Hasan MM, Reshi QUA, Lättekivi F, Viil J, Godakumara K, Dissanayake K, et al. Bovine follicular fluid derived extracellular vesicles modulate the viability, capacitation and acrosome reaction of bull spermatozoa. Biology. 2021;10:1154.
54. Grippo AA, Way AL, Killian GJ. Effect of bovine ampullary and isthmic oviductal fluid on motility, acrosome reaction and fertility of bull spermatozoa. J Reprod Fertil. 1995;105:57–64.
55. Hunter RHF, Nichol R. Transport of spermatozoa in the sheep oviduct: preovulatory sequestering of cells in the caudal isthmus. J Exp Zool. 1983;228:121–8.
56. Suarez S, Redfern K, Raynor P, Martin F, Phillips D. Attachment of boar sperm to mucosal explants of oviduct in vitro: possible role in formation of a sperm reservoir. Biol Reprod. 1991;44:998–1004.
57. Salovska B, Kondelova A, Pimkova K, Liblova Z, Pribyl M, Fabrik I, et al. Peroxiredoxin 6 protects irradiated cells from oxidative stress and shapes their senescence-associated cytokine landscape. Redox Biol. 2022;49:102212.
58. Fernandez MC, O'Flaherty C. Peroxiredoxin 6 is the primary antioxidant enzyme for the maintenance of viability and DNA integrity in human spermatozoa. Hum Reprod. 2018;33:1394–407. https://doi.org/10.1093/humrep/dey221.
59. Lee D, Moawad AR, Morielli T, Fernandez MC, O'Flaherty C. Peroxiredoxins prevent oxidative stress during human sperm capacitation. Mol Hum Reprod. 2016;23:106–15. https://doi.org/10.1093/molehr/gaw081.
60. O'Flaherty C. Peroxiredoxin 6: the protector of male fertility. Antioxidants. 2018;7:173.
61. Mostek A, Janta A, Majewska A, Ciereszko A. Bull sperm capacitation is accompanied by redox modifications of proteins. IJMS. 2021;22:7903.
62. Inaba K. Sperm flagella: comparative and phylogenetic perspectives of protein components. Mol Hum Reprod. 2011;17:524–38.

63. Zhao Y, Yang X, Jia Z, Reid RL, Leclerc P, Kan FWK. Recombinant human oviductin regulates protein tyrosine phosphorylation and acrosome reaction. Reproduction. 2016;152:561–73.
64. Yang X, Zhao Y, Yang X, Kan FWK. Recombinant hamster oviductin is biologically active and exerts positive effects on sperm functions and sperm-oocyte binding. Travis AJ, editor. PLOS ONE. 2015;10:e0123003.
65. Vanderkooi SC, Zhao Y, Lima PDA, Kan FWK. Recombinant human OVGP1 increases intracellular calcium and further potentiates the effects of progesterone on human sperm. J Assist Reprod Genet. 2022. https://doi.org/10.1007/s10815-022-02591-0.
66. Zhao Y, Kan FWK. Human OVGP1 enhances tyrosine phosphorylation of proteins in the fibrous sheath involving AKAP3 and increases sperm-zona binding. J Assist Reprod Genet. 2019;36:1363–77.
67. Li Z-H, Bresnick AR. The S100A4 metastasis factor regulates cellular motility via a direct interaction with myosin-IIA. Cancer Res. 2006;66:5173–80.
68. Sung DC, Ahmad M, Lerma Cervantes CB, Zhang Y, Adelstein RS, Ma X. Mutations in non-muscle myosin 2A disrupt the actomyosin cytoskeleton in Sertoli cells and cause male infertility. Dev Biol. 2021;470:49–61.
69. Conti MA, Adelstein RS. Nonmuscle myosin II moves in new directions. J Cell Sci. 2008;121:11–8.
70. Vicente-Manzanares M, Ma X, Adelstein RS, Horwitz AR. Non-muscle myosin II takes centre stage in cell adhesion and migration. Nat Rev Mol Cell Biol. 2009;10:778–90.
71. Togo T, Steinhardt RA. Nonmuscle myosin IIA and IIB have distinct functions in the exocytosis-dependent process of cell membrane repair. MBoC. 2004;15:688–95. https://doi.org/10.1091/mbc.E03-06-0430.
72. Andzelm MM, Chen X, Krzewski K, Orange JS, Strominger JL. Myosin IIA is required for cytolytic granule exocytosis in human NK cells. J Exp Med. 2007;204:2285–91.
73. Wassarman PM. Mammalian fertilization. Cell. 1999;96:175–83.
74. Pons-Rejraji H, Bailey JL, Leclerc P. Cryopreservation affects bovine sperm intracellular parameters associated with capacitation and acrosome exocytosis. Reprod Fertil Dev. 2009;21:525.
75. Holt WV, Fazeli A. Sperm storage in the female reproductive tract. Annu Rev Anim Biosci. 2016;4:291–310.

Ready to submit your research? Choose BMC and benefit from:

- fast, convenient online submission
- thorough peer review by experienced researchers in your field
- rapid publication on acceptance
- support for research data, including large and complex data types
- gold Open Access which fosters wider collaboration and increased citations
- maximum visibility for your research: over 100M website views per year

At BMC, research is always in progress.

Learn more biomedcentral.com/submissions

BMC

Résultats complémentaires : effets des fluides d'isthme et d'ampoule péri-ovulatoires sur la physiologie des spermatozoïdes

Les effets sur la mobilité spermatique sont tous détectés en début d'incubation, au temps T0, qui correspond à environ 5 à 10 minutes après la mise en contact des spz avec les fluides, avec un effet globalement positif des fluides d'ampoule par rapport à ceux d'isthme (Figure 11 page 135). A T0, les proportions de spz mobiles et progressifs sont plus élevés dans l'ampoule pré-ovulatoire que dans l'isthme post-ovulatoire ; l'ampoule post-ovulatoire est également plus favorable à la mobilité progressive (Figure 11A et 11B). Cette tendance reste la même pendant toute l'incubation sans être significative. De plus, à T0, la fréquence des battements flagellaires (BCF) est plus élevée dans l'ampoule post-ovulatoire que dans l'isthme pré-ovulatoire et le témoin (milieu non capacitant) (Figure 11F).

A l'opposé, les effets des fluides sur la viabilité spermatique ne sont visibles qu'après 6 h d'incubation : le pourcentage de spermatozoïdes viables est en moyenne 20% plus faible dans les FO d'isthme post-ovulatoire que dans le milieu témoin non capacitant (Figure 12A page 136). Les FO n'ont pas d'effet significatif sur la déstabilisation membranaire et la réaction acrosomique spontanée (Figure 12B et 12C). En revanche, à partir de 3 h d'incubation, les fluides d'isthme post-ovulatoire augmentent fortement le pourcentage de spermatozoïdes ayant réalisé leur réaction acrosomique induite par l'ionophore calcique par rapport au milieu témoin (Figure 12D).

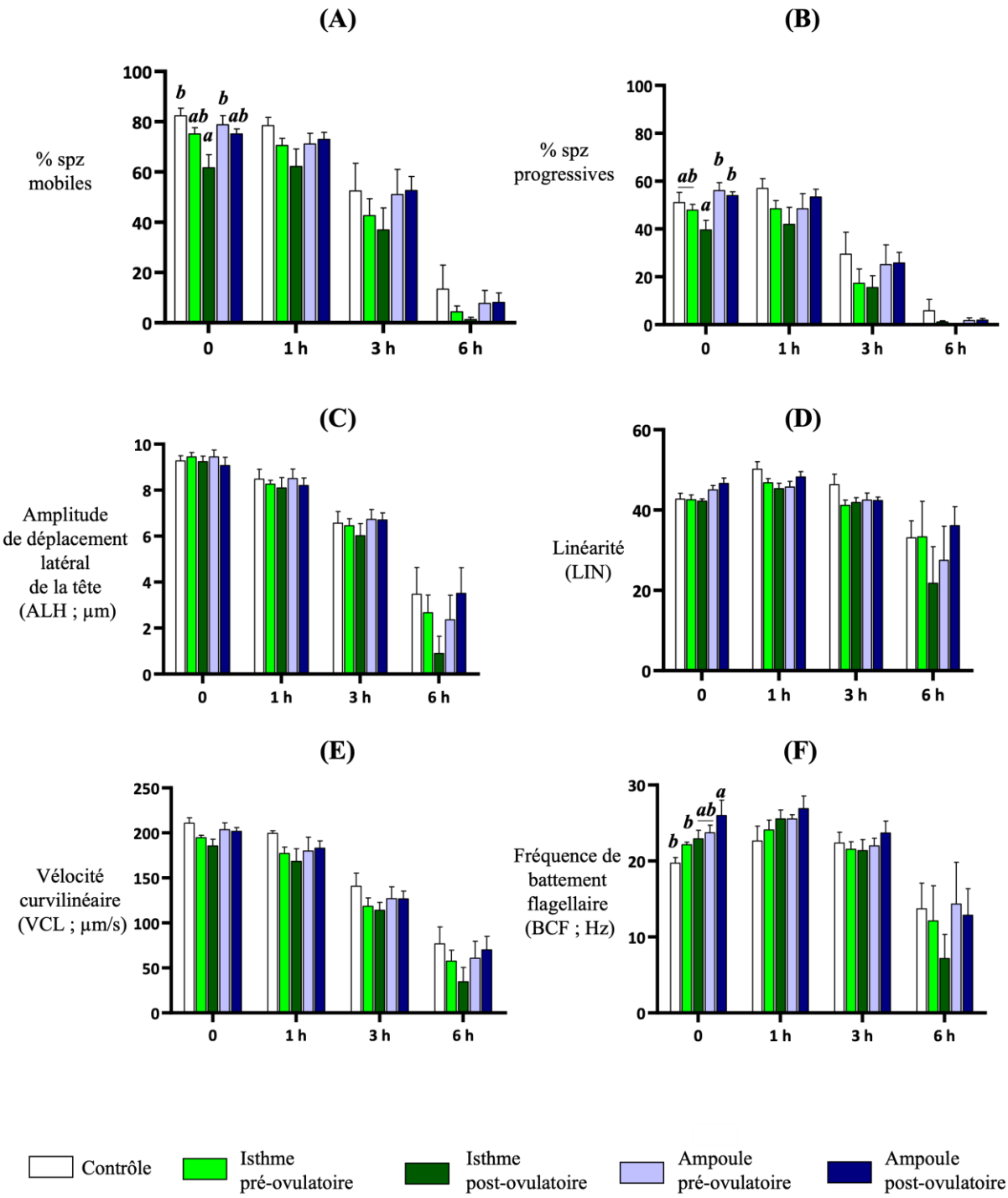

Figure 11 : Effets des fluides d'isthme et d'ampoule péri-ovulatoires sur la mobilité des spermatozoïdes.

Les données sont présentées sous forme de moyenne ± SEM (n=5 répliques biologiques) et des lettres différentes signifient une différence significative avec un $p \leq 0,05$

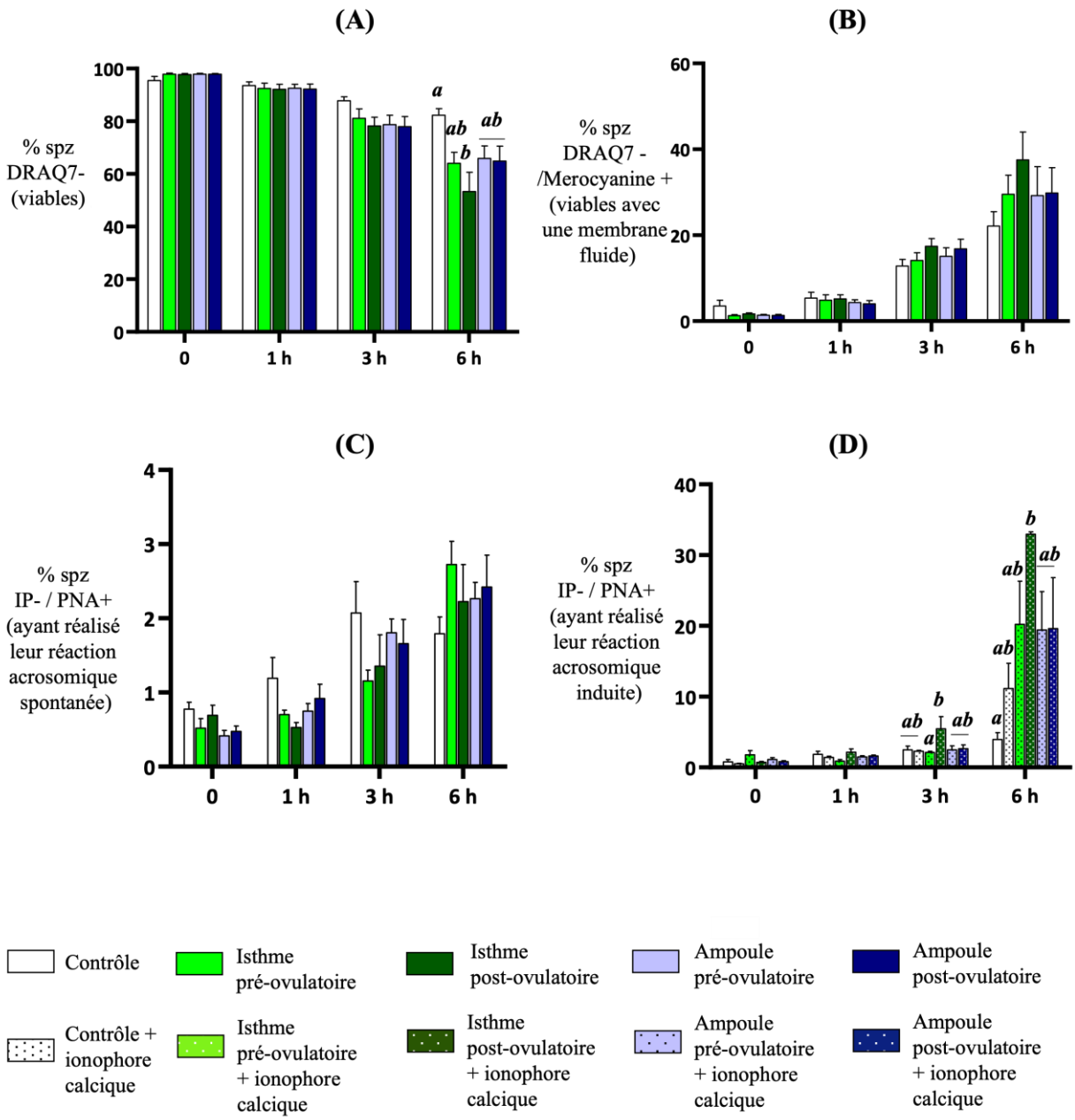

Figure 12 : Effets des fluides d'isthme et d'ampoule péri-ovulatoires sur la viabilité, la fluidité membranaire et la réaction acrosomique des spermatozoïdes.

Les données sont présentées sous forme de moyenne ± SEM (n=5 répliques biologiques) et des lettres différentes signifient une différence significative avec un $p \leq 0,05$

3. Effets des interactions avec le fluide d'oviducte sur la liaison des spermatozoïdes au réservoir

Ce travail est présenté sous la forme d'un schéma récapitulatif (Figure 13 page 141) et de l'**article 4** « Sperm-fluid-cell interplays in the bovine oviduct: glycoprotein N-glycans and glycosaminoglycans modulate sperm binding to the reservoir » en préparation. Des **résultats complémentaires** portant sur les effets de l'albumine, l'annexine A1 et la progestérone sur la liaison des spz aux sphéroïdes, et sur l'effet libérateur du FO, sont présentés Figure 14 page 179. La méthode de préparation des sphéroïdes, nouveau modèle de réservoir *in vitro* mis au point pendant la thèse, est aussi présentée sous la forme d'un **chapitre d'ouvrage** intitulé « Assessment of sperm binding capacity in the oviduct reservoir using an *in vitro* model of epithelial spheroids in cattle » soumis en janvier 2023 sur invitation dans *Spermatology : Methods and Protocols*, ouvrage qui sera édité dans la série *Methods in Molecular Biology* (Annexe 1).

Contexte et objectif

Lors de leur entrée dans l'isthme, les spermatozoïdes interagissent d'abord avec le fluide luminal puis, pour certains d'entre eux (dont la proportion n'est pas connue), avec les cellules épithéliales bordant la lumière pour former un « réservoir spermatique fonctionnel ». Les mécanismes sous-jacents ont surtout été étudiés *in vitro* avec des monocouches cellulaires, perdant rapidement (en 5-7 jours) leurs caractéristiques morphologiques et fonctionnelles. De plus, certains laboratoires ont étudié les interactions spz-fluide, mais sans cellules en co-culture, tandis que d'autres se sont penchés sur les interactions spz-cellules, mais sans ajout de fluide. Les objectifs étaient donc de développer un nouveau modèle de réservoir spermatique facile à utiliser et avec des cellules épithéliales différenciées pour étudier *in vitro* les effets du FO et de ses composants sur la liaison des spermatozoïdes au réservoir. Nos hypothèses étaient que (i) les SIP identifiées dans le FO entrent en compétition avec les récepteurs spermatiques à la surface des cellules épithéliales de l'isthme, diminuant le nombre de spz pouvant se lier aux cellules ; (ii) les glycosaminoglycanes du FO interagissent aussi avec les spz bovins, notamment leurs BSPs de surface, et ces interactions peuvent modifier la capacité de liaison au réservoir.

Matériel et méthodes

À partir d'isthmes pré-ovulatoires d'abattoir, des fragments de muqueuse oviductale sont mis en culture dans un milieu TCM199 supplémenté avec 10% de sérum de veau fœtal à 38,8°C et 5% de CO_2. Après 4 jours de culture, ces fragments forment spontanément des sphéroïdes, avec une cavité centrale et le pôle apical des cellules orienté vers l'extérieur. Les sphéroïdes sont triés afin d'obtenir une population uniforme sans replis de 100 µm de diamètre et avec des battements ciliaires vigoureux. Des groupes de 20 sphéroïdes ont été incubés dans 65 µL de milieu avec un pool de spz (issus de 3 taureaux en proportions équivalentes) décongelés et lavés sur Percoll, à une concentration finale de 1.10^6/mL pendant 1 h à 38.8°C. Différents FO intacts ou modifiés ont été testés (voir plus bas). Après incubation, les complexes spz-sphéroïdes ont été lavés pour éliminer les spz peu ou non liés puis fixés. La densité des spermatozoïdes liés à la surface des sphéroïdes a été déterminée après marquage au Hoechst et observation en microscopie confocale.

Afin de vérifier l'origine épithéliale des sphéroïdes et déterminer leur proportion de cellules ciliées, 20 sphéroïdes issus de 5 répliques biologiques ont été immunomarqués avec des anticorps dirigés contre la pan-cytokératine, la vimentine et l'alpha-tubuline acétylée, puis observés en microscopie confocale. Afin de mieux caractériser les interactions avec les spz, les complexes spz-sphéroïdes ont également été observés par microscopie électronique à balayage en partenariat avec la plateforme MIMA2 de l'INRAE de Jouy-en-Josas.

Différents milieux de co-incubation des spz avec les sphéroïdes ont été testés : (i) des fluides d'oviducte entier pré-ovulatoire, d'ampoule ou d'isthme aux stades pré- et post-ovulatoires et à des concentrations finales de 0,06 à 4 mg/mL de protéines ; (ii) des fractions ultrafiltrées de FO avec un cut-off de 3 kDa ; (iii) du FO dont les protéines ont été dénaturées par chauffage (10 min à 100°C), digérées (traitement par la protéinase K puis ultrafiltration avec un cut-off de 50 kDa) ou N-déglycosylées (traitement par la PNGase F puis ultrafiltration avec un cut-off de 5 kDa) ; (iv) de l'acide hyaluronique purifiée à des concentrations finales de 10 à 1000 µg/mL ; (v) du sulfate d'héparane purifié à des concentrations finales de 10 à 1000 µg/mL et du FO pré-traité par les héparinases I, II et III. Un milieu témoin non capacitant (Tyrode-HEPES + pyruvate, lactate, alcool polyvinylique à pH 7.4 ; milieu TLP) a été utilisé dans toutes les expériences. Tous les fluides d'oviducte ont été collectés par flush et dilués avec ce milieu. Pour chacun des traitements testés, la mobilité des spermatozoïdes a été analysée en parallèle par CASA pendant la durée de l'incubation.

Toutes les expériences sont répétées au moins 3 fois. Entre répliques biologiques, seul le pool de spz reste le même : différents pools de fluides et de nouveaux sphéroïdes sont utilisés. L'effet des traitements sur la densité relative de spz liés aux sphéroïdes et sur les paramètres spermatiques a été analysé par une analyse de variance suivi d'un post-test de Tuckey ($p \leq 0,05$).

Résultats

Les sphéroïdes contiennent des cellules épithéliales polarisées et bien différenciées avec en moyenne 25 % (± 2%) de cellules ciliées. La liaison des spz se fait par leur tête avec une membrane acrosomique intacte et en moyenne 85 % (± 3%) des spz sont liés aux cils des cellules ciliées. Dans le milieu témoin, les spz se lient aux sphéroïdes dès 5 min de co-incubation et la densité des spz liés augmente jusqu'à 60 min : elle est en moyenne de 1421 ± 90 spz/mm^2 après 60 min et ne varie pas significativement entre répliques biologiques.

Comparé au milieu témoin, le FO à 1 mg/mL de protéines diminue significativement de 80 à 90% la densité de spz liés aux sphéroïdes après 1 h d'incubation, et ce, quels que soient la région anatomique et le stade du cycle d'où provient le FO. Le FO n'affecte ni la mobilité ni la viabilité des spz et l'inhibition de liaison est visible dès les 5 premières minutes de co-incubation, ce qui suggère une compétition de liaison pour les spz entre composants du FO et cellules ciliées. La suite des expériences vise à identifier quels composants du FO sont responsables de cet effet.

La fraction du FO supérieure à 3 kDa, mais pas celle inférieure à 3 kDa, reproduit l'effet du FO sur la densité spermatique, ce qui oriente vers un rôle des macromolécules solubles (protéines, glycoprotéines et GAG). Cet effet augmente avec la concentration protéique du FO. Cependant, le FO dans lequel les protéines ont été dénaturées ou digérées reproduisent à l'identique l'effet du FO natif, ce qui exclut les protéines et chaines protéiques des glycoprotéines et protéoglycanes. En revanche, après N-déglycosylation des glycoprotéines du FO, les N-glycanes isolées (< 5 kDa) reproduisent l'effet du FO, mettant en évidence un rôle de ces chaines glycosylées dans la compétition de liaison aux cellules. Concernant l'effet possible des GAG, le FO dans lequel le sulfate d'héparane (GAG sulfaté le plus abondant du FO) a été digéré diminue la densité spermatique mais moins que le FO natif (60% vs. 80%). De plus, le sulfate d'héparane purifié diminue la densité spermatique de manière dose-dépendante, ce qui oriente vers un rôle de ce GAG sulfaté dans la compétition de liaison aux cellules.

Au contraire, l'acide hyaluronique, un GAG non sulfaté du FO, tend à augmenter la liaison des spz aux sphéroïdes. Les différents traitements ci-dessus n'ont pas eu d'effet sur les proportions de spz mobiles et progressifs, exceptés la dénaturation du FO et le sulfate d'héparane à partir de 100 µg/mL, qui ont diminué d'en moyenne 30% la proportion de spz mobiles.

Conclusion

Les sphéroïdes constituent un nouveau modèle *in vitro* d'épithélium oviductal conservant les caractéristiques morphologiques et fonctionnelles des cellules d'origine, et permettant d'étudier les interactions spz-oviducte. En utilisant ce modèle, nous avons montré que des macromolécules du FO, dont des glycoprotéines N-glycosylées, le sulfate d'héparane et l'acide hyaluronique, modulent la capacité de liaison des spz aux cellules ciliées. Il reste à étudier les effets de cette liaison aux cellules sur la capacité fécondante des spz. Ces travaux améliorent notre compréhension de la constitution du réservoir spermatique dans l'oviducte et ouvrent de nouvelles perspectives pour améliorer la sélection des spz en insémination animale et pour la fécondation *in vitro*.

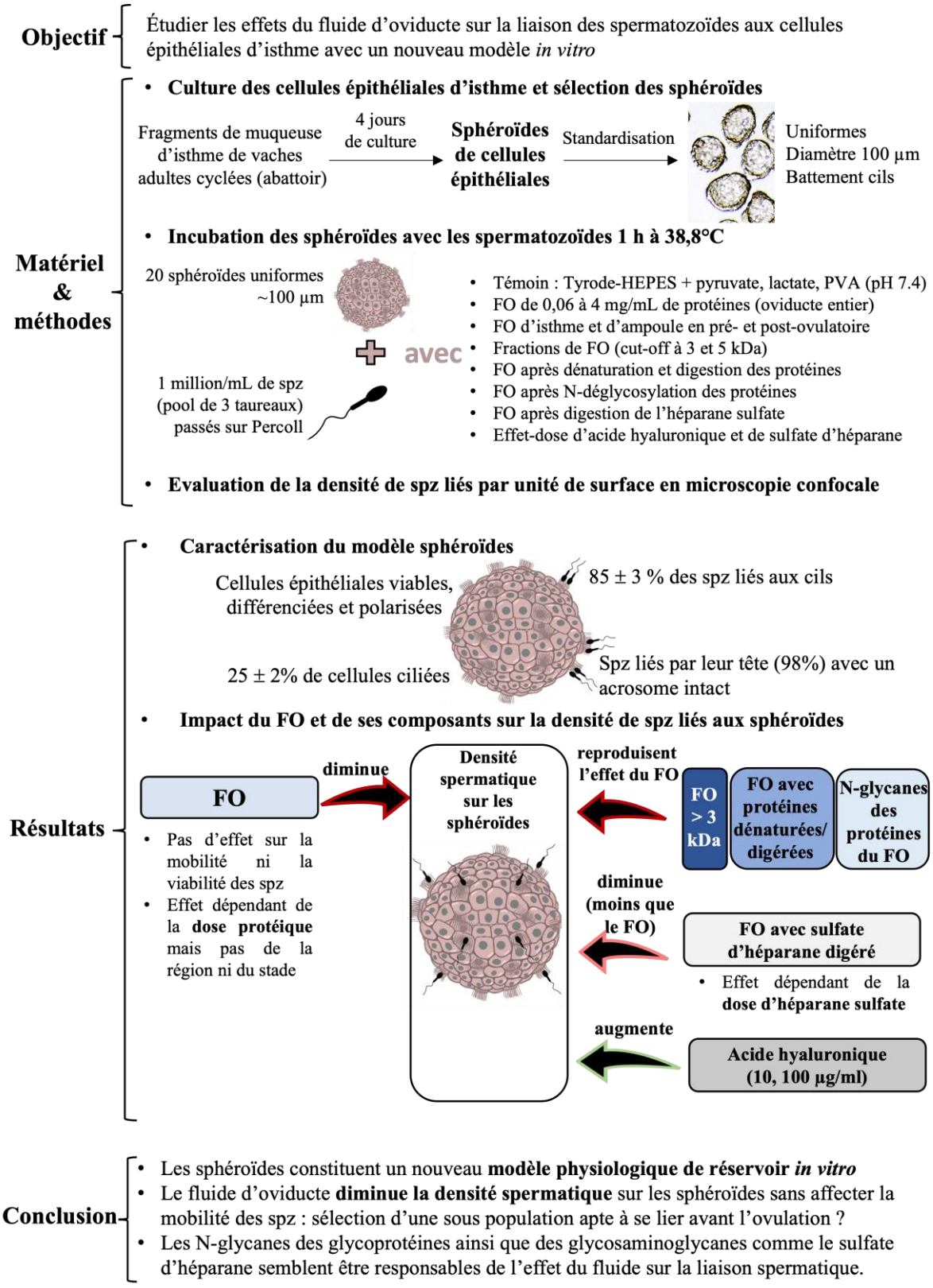

Figure 13 : Schéma récapitulatif de l'étude de l'effet du fluide d'oviducte et de ses composants sur la liaison des spermatozoïdes au réservoir modélisé in vitro par des sphéroïdes de cellules épithéliales d'isthme.

Sperm-fluid-cell interplays in the bovine oviduct: glycoprotein N-glycans and glycosaminoglycans modulate sperm binding to the reservoir

Coline Mahé[1,*], Thanya Pranomphon[1,2], Karine Reynaud[1], Ludivine Laffont[1], Thierry Meylheuc[3], Jennifer Schoen[4,], Pascal Mermillod[1], Marie Saint-Dizier[1,5,*]

[1] CNRS, IFCE, INRAE, Université de Tours, PRC, 37380, Nouzilly, France

[2] Embryo Technology and Stem Cell Research Center, School of Biotechnology, Suranaree University of Technology, Nakhon Ratchasima, Thailand

[3] INRAE, Pathologie Végétale, F-84143 Avignon, France

[4] Department of Reproduction Biology, Leibniz Institute for Zoo and Wildlife Research (IZW), Berlin, Germany

[5] Tours University, Faculty of Sciences and Techniques, Tours, France

*Corresponding author**:** coline.mahe@inrae.fr or marie.saint-dizier@univ-tours.fr

Abstract

Entering the oviduct for fertilization, spermatozoa are in contact with the oviduct fluid (OF) and can bind to luminal epithelial cells in the isthmus to form a sperm reservoir. The objective of this study was to examine how the OF modulates sperm adhesion to the oviduct reservoir using an *in vitro* model of oviduct epithelial spheroids (OES). Bovine oviducts from a local slaughterhouse were used to collect OF and isthmic fragments for *in vitro* culture of OES. Compared to a non-capacitating control medium, the pre-ovulatory OF significantly decreased by 80-90% the density of spermatozoa bound to OES without affecting sperm motility, membrane integrity and sperm-cilia interactions. This effect on sperm binding was reproduced with (i) OF from different cycle stages and oviduct anatomical regions; (ii) OF fractions more than 3-5 kDa; (iii) modified OF in which proteins were denatured or digested; (iv) OF fractions less than 5 kDa enriched with glycoprotein N-glycans; and (v) heparane sulfate but not hyaluronic acid, two glycosaminoglycans present in the OF. In conclusion, the OF prevents a sperm subpopulation to bind to oviduct epithelial cells without affecting sperm motility and this effect was due to macromolecules, including N-glycosylated proteins and heparane sulfate.

Keywords: oviduct, glycoproteins, glycosaminoglycans, heparan sulfate, hyaluronic acid, isthmus, tubal fluid, N-glycans, reservoir, sperm.

Introduction

Successful fertilization in mammals relies on the well-timed meeting of spermatozoa and oocyte in the oviduct. Entering the oviduct, spermatozoa are in contact with the oviduct fluid (OF) while a subpopulation firmly binds to oviduct epithelial cells in the first part of the oviduct, called the isthmus, to form a sperm reservoir[1,2].

Sperm binding to the oviduct reservoir is believed to lengthen sperm life time in case of desynchrony between mating and ovulation, and to promote fertilizing ability after sperm release[3–5]. Direct observation in the mice oviduct suggests that spermatozoa not only bind to isthmic epithelial cells but detach and reattach several times as they ascend toward the oocyte, displaying dynamic sperm-fluid-cell interplays before conception[6]. However, the way the OF components regulate sperm binding to the oviduct epithelium is unclear.

The OF is a complex biological fluid containing proteins, glycosaminoglycans, metabolites, hormones and lipids that are highly regulated across cycle in the bovine[7]. Previous data from our lab identified 245 proteins in the bovine OF that interact with spermatozoa[8] including those previously proposed as sperm receptors in the isthmic reservoir, i.e. annexins A1, A2, A4, A5 and heat shock proteins 60 and A5, among others[4,9,10]. Furthermore, bull spermatozoa were shown to bind with high affinity to Lewis A sugar motifs[11] that were found among the N- and O-glycans linked to glycoproteins extracted from bovine isthmic epithelial cells [12,13]. Therefore, it is expected that proteins and glycans linked to those proteins in the OF compete with the same (glyco)proteins located on the oviduct epithelium and decrease sperm binding to epithelial cells. Additionally, hyaluronic acid (HA) is a high molecular weight non-sulfated glycosaminoglycan highly present in the OF[14,15]. HA-binding proteins were evidenced at the surface of bovine oviduct epithelial cells[14] and on bull spermatozoa[16]. There is evidence that motile bull spermatozoa are able to selectively bind to HA *in vitro*[17,18]. HA is therefore a good candidate to regulate sperm binding to the reservoir in cattle. Moreover, the sulfated glycosaminoglycan heparan sulfate (HS), also abundant in the bovine OF[15], was shown to bind with high affinity to binder of sperm proteins (BSPs), a group of sperm surface proteins involved in sperm binding to the oviduct reservoir[19]. Heparin, which is chemically close to heparan sulfate, was found to inhibit bull sperm binding to oviduct epithelial cell monolayers[19] and to induce the release of bound spermatozoa from cells within minutes *in vitro*[5,20].

Therefore, we hypothesized that glycosaminoglycans and glycoproteins in the OF may interact with spermatozoa and decrease their ability to bind to the oviduct epithelium.

Numerous *in vitro* studies assessed sperm interactions with oviduct epithelial cells in chemically defined culture media[21–24] and some others focused on the effect of OF on sperm physiology[25,26], but data on the effect of OF on sperm-epithelial cell interactions are currently lacking. Moreover, most studies on sperm-cell interactions used oviduct epithelial explants presenting great heterogeneity in surface binding[21,22,27], or epithelial cell monolayers losing rapidly their cilia[23,24,28]. The objective of this study was to evaluate the impact of OF and its components on sperm binding to the oviduct reservoir using a new well-standardized and differentiated *in vitro* model of isthmic epithelial cell spheroids.

Results

Characterization of oviduct epithelial spheroids as a model to study sperm-oviduct interactions

Epithelial cell spheroids naturally formed after 2-4 days of culture of isthmic mucosa fragments collected from post-pubertal cows at the pre-ovulatory stage of cycle. At day 4, the floating spheroids selected for sperm co-incubation were homogeneous in shape and size (100 µm in diameter) and displayed a columnar epithelium with outward ciliary beating (Fig. 1a). Immunostaining of OES showed a positive signal for the epithelial marker cytokeratin and a negative signal for the mesenchymal marker vimentin (Fig. 1 b-c). On average, 25 ± 2 % of cells composing the spheroids were ciliated (n= 100 OES from 5 replicates; Fig. 1d).

After incubation with spermatozoa, 85 ± 3 % were found to bind to cilia while others bound to non-ciliated cells (n=100 sperm-OES complexes from 5 replicates; Fig. 1d-e). Scanning electron microscopy revealed that 93% of bound sperm were morphologically normal. Among bound sperm, 93% were attached exclusively with their head and 7% with both head and midpiece or flagella (n= 80 spermatozoa from one replicate; Fig. 1e).

Quantitative analysis of sperm binding to OES in the control TLP medium showed that the density of bound spermatozoa increased significantly from 5 to 60 min (Fig. 2). The bound sperm density was repeatable between replicates with different pools of OES (CV of 14%) and reached on average 1416 ± 149 spermatozoa/mm² after 60 min (n = 600 sperm-OES complexes from 30 replicates). Following experiments aimed at studying the effect of the OF on sperm binding to OES. The experimental design is summarized in Supplementary Figure S1.

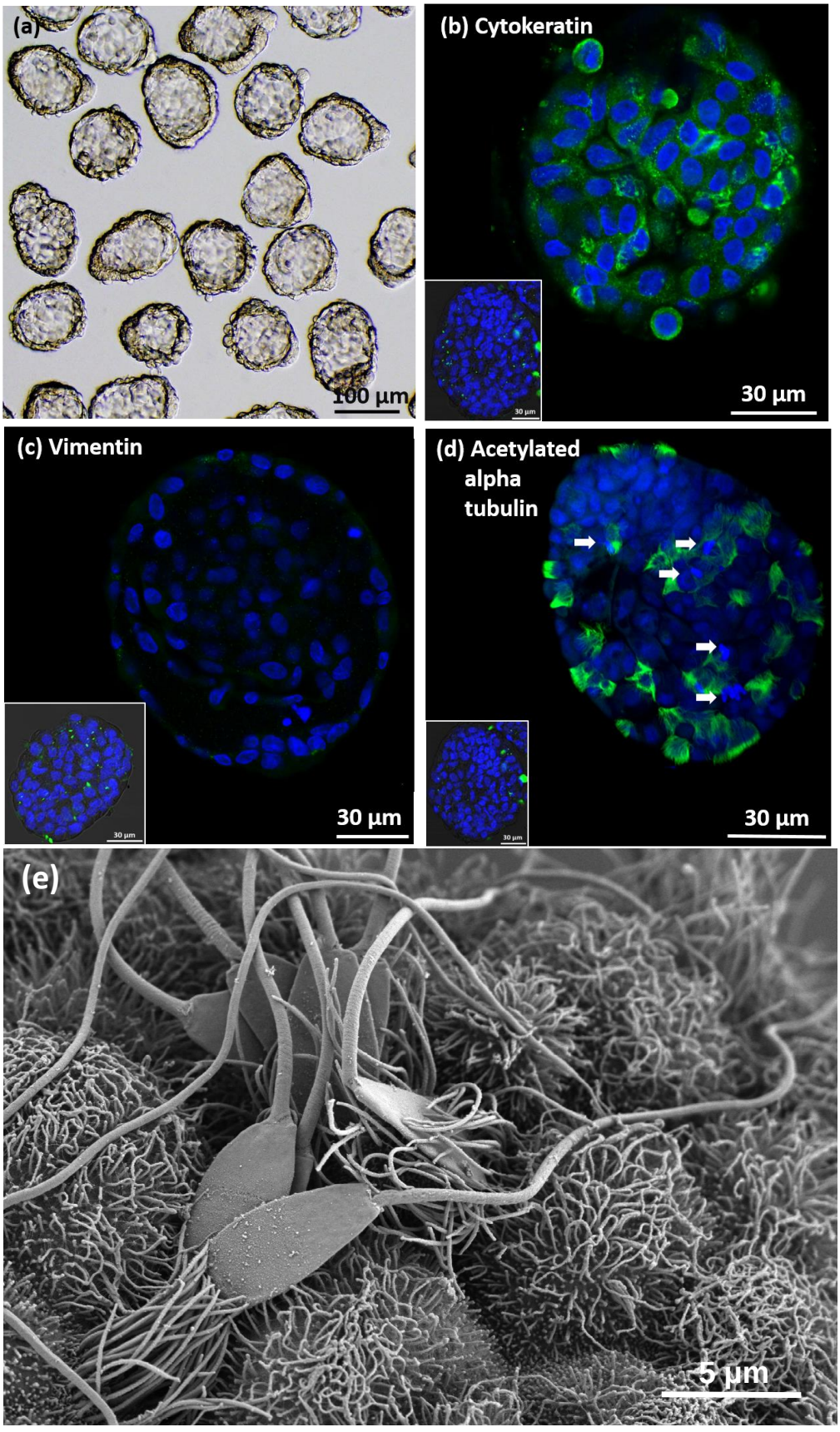
(a)
100 µm
(b) Cytokeratin
30 µm
(c) Vimentin
30 µm
(d) Acetylated alpha tubulin
30 µm
(e)
5 µm

Figure 1. Characterization of bovine isthmic epithelial spheroids as an *in vitro* model to study sperm-oviduct interactions. Spheroids uniform in shape and size were selected for sperm co-incubation (a). Spheroid epithelial cells stained positively for anti-cytokeratin (b, green signal) and negatively for anti-vimentin (c) antibodies (nuclei are stained in blue). Sperm-spheroid complex immunostained for acetylated alpha-tubulin (in green) and stained with Hoechst (in blue) showed sperm heads bound to cilia (d, arrows). Sperm-spheroid complex observed under scanning electron microscopy showing sperm heads with intact acrosome firmly attached to cilia (e). Inserts in (b-d) show negative controls incubated with the immunoglobulin isotype of primary antibody.

Impact of the oviduct fluid on sperm binding to oviduct epithelial spheroids

Experiment 1 showed that OF collected at the pre-ovulatory stage of cycle, *i.e.* the time at which cows are usually inseminated, significantly decreased sperm binding to OES compared to the control non-capacitating medium ($p < 0.05$; Fig. 2). In the presence of OF, the density of bound sperm on OES was 87-% lower than in the control as soon as 5 min after sperm addition ($p < 0.001$) and remained significant during the 60-min incubation (Fig. 2). The OF at the same protein concentration did not affect any sperm motility parameters nor membrane or acrosome integrity (data on sperm are summarized in Supplementary Data S1). Scanning electron microscopy did not evidence any differences between OF-treated and control groups in the proportions of spermatozoa bound to cilia (80% *vs*. 87%), morphologically normal bound spermatozoa (97% *vs*. 93%), those bound exclusively with their head (90% *vs*. 93%) or with head and midpiece or flagella (10% *vs*. 7%) after 60-min incubation (n= 60 and 80 spermatozoa in OF-treated and control groups, respectively).

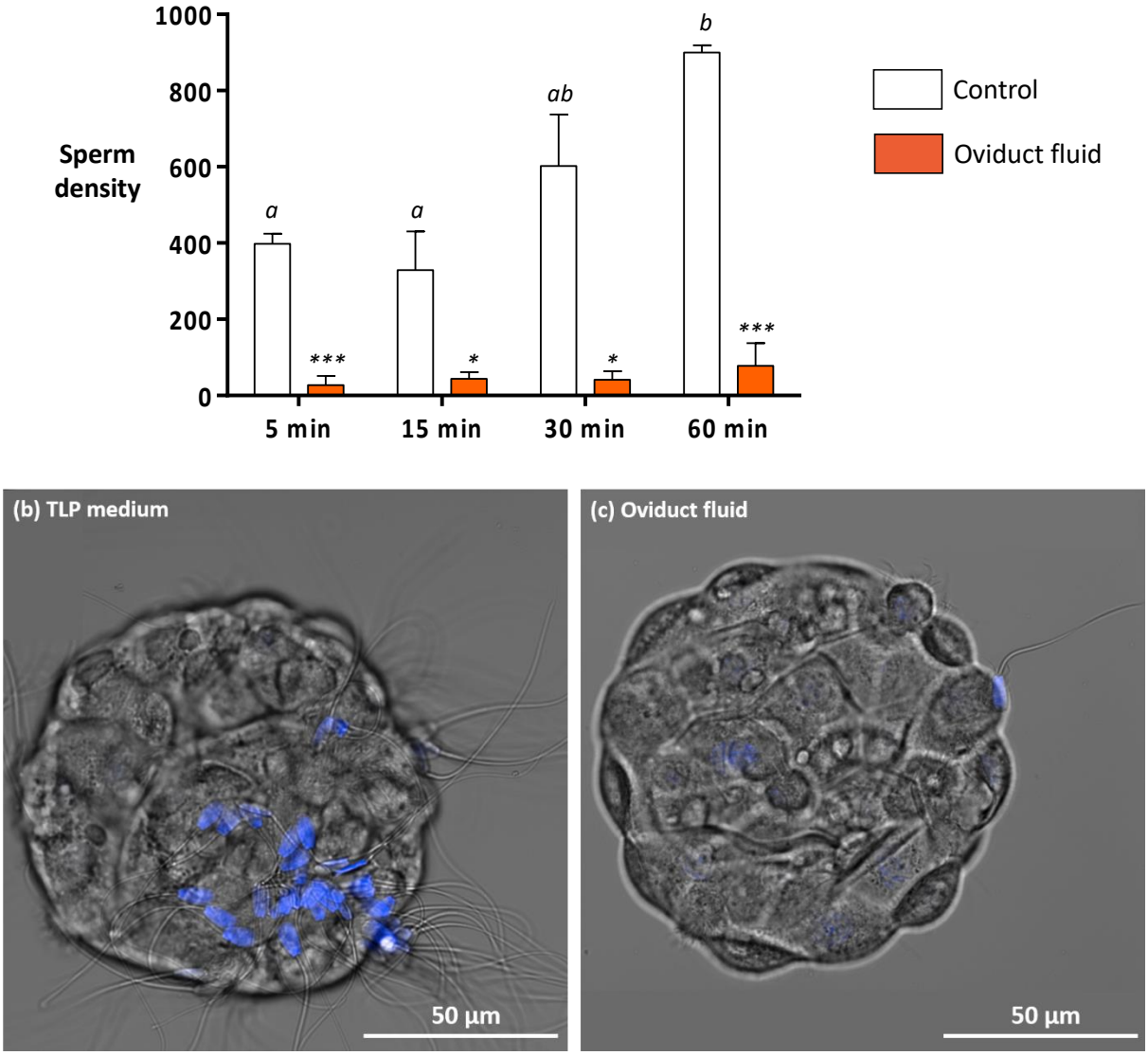

Figure 2. Kinetics of sperm binding to oviduct epithelial spheroids in the non-capacitating control medium and in the pre-ovulatory oviduct fluid (Experiment 1).

(a) Spermatozoa and spheroids were incubated in the control TLP medium (white bars) or pre-ovulatory OF at a final protein concentration of 1 mg/mL (orange bars) for 5, 15, 30 and 60 min. Data are mean ± SEM of bound sperm per mm² (n = 3 replicates). Different letters indicate differences between time points in the control group (p-value < 0.05). Asterisks indicate differences between control and OF groups at each time point. **P-value* < 0.05**; ****P-value* < 0.001. (b,c) Confocal microscopy pictures of sperm-spheroid complexes after incubation for 60 min in TLP medium (left) or pre-ovulatory oviduct fluid at 1 mg/mL of proteins (right). Sperm nuclei appear in blue.

Experiment 2 showed that the OF had similar effects on sperm binding to OES regardless of the stage of cycle (pre-ovulatory *vs*. luteal phase; Fig. 3a) or oviduct anatomical region (isthmus *vs*. ampulla; Fig. 3b) from which the fluid originated. Following experiments aimed at identifying which molecules were involved in the effect of OF on sperm binding. In the following, the term OF refers to fluid collected from whole oviducts at the pre-ovulatory stage of cycle.

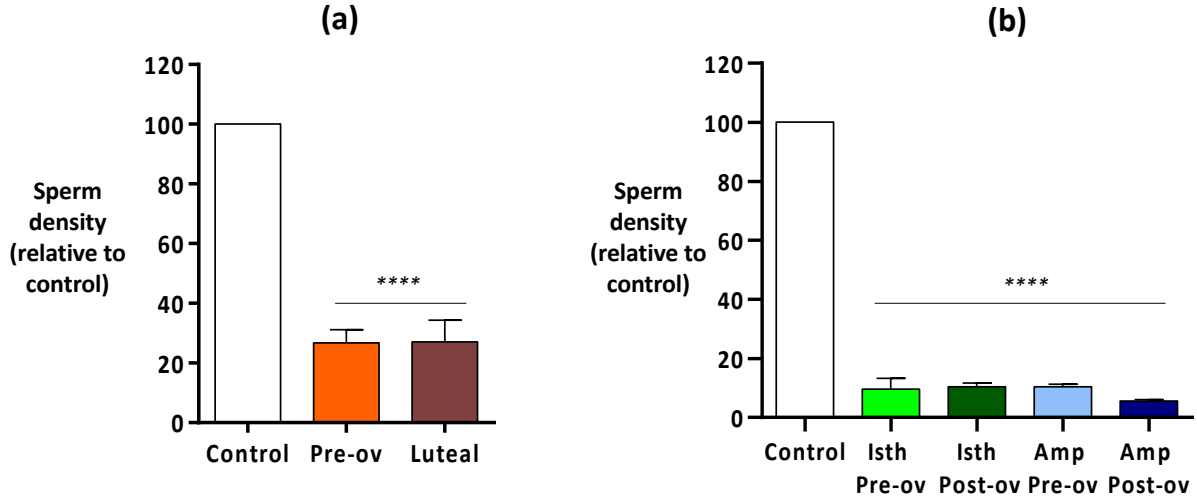

Figure 3. Effect of the stage of cycle (a) and anatomical region (b) from which the oviduct fluid originated on sperm binding to oviduct epithelial spheroids (Experiment 2).

Spermatozoa and spheroids were incubated for 60 min in the TLP medium (control) or in the OF collected from whole oviducts at the pre-ovulatory (Pre-ov) or luteal (Luteal) phases of cycle (a), or from the isthmus (Isth) or ampulla (Amp) at pre-ovulatory Pre-ov) or post-ovulatory (Post-ov) phases of cycle. All OF samples were used at a final protein concentration of 1 mg/mL. Data are mean ± SEM of bound sperm per mm² relative to control (n= 3 replicates). ****P- value < 0.0001 as compared to the control group.

Impact of secreted proteins and glycoprotein N-glycans on sperm binding to oviduct epithelial spheroids

Experiment 3 showed that the OF fraction above 3 kDa, but not that below 3 kDa, reproduced the effect of OF on sperm binding, suggesting an involvement of macromolecules (Fig. 4).

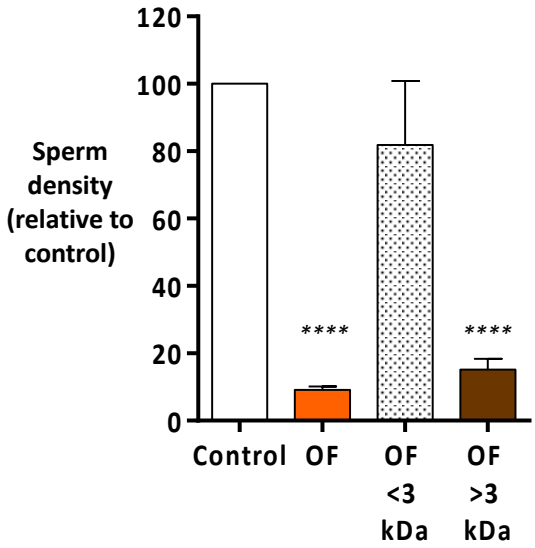

Figure 4. Effect of ultra-filtrated fractions of pre-ovulatory oviduct fluid on sperm binding to oviduct epithelial spheroids (Experiment 3).

Spermatozoa and spheroids were incubated for 60 min with pre-ovulatory OF after ultrafiltration with a cut-off of 3 kDa. Native OF at a final protein concentration of 1 mg/mL was included (OF). TLP medium was used as control. Data are mean ± SEM of bound sperm per mm² relative to control (n=4 replicates). ****P-$value$ < 0.0001 as compared to the control group.

In accordance, Experiment 4 showed that the OF decreased the density of bound sperm on OES in a protein dose-dependent manner (Fig. 5a). However, the OF in which proteins were denatured by heating (10 min at 100°C) or enzymatically digested (proteinase K treatment) decreased bound sperm density similarly to the native OF (Fig. 5b).

Sperm motility was negatively affected by OF denaturation but not digestion treatment (33,5 and 58,7% of motile spermatozoa, respectively, compared to 65,9% in the control group after 60 min, $p<0.05$ for denaturation only; Supplementary Data S1). Results of Experiment 4 indicated that the amino acid chains of soluble glycoproteins and non-glycosylated proteins were not involved in the effect of OF on sperm binding to OES.

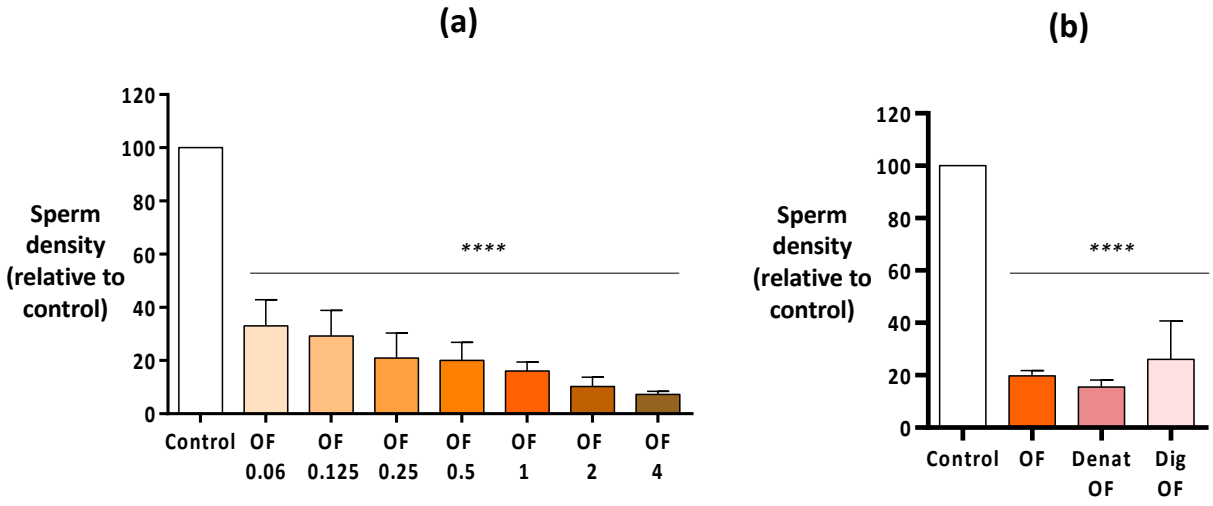

Figure 5. Effect of proteins in the oviduct fluid on sperm binding to oviduct epithelial spheroids (Experiment 4).

Spermatozoa and spheroids were incubated for 60 min in the pre-ovulatory OF at final protein concentrations of 0.06, 0.125, 0.25, 0.5, 1, 2 or 4 mg/mL (a), or in the OF at final concentration of 1 mg/mL of proteins (OF) and after protein denaturation by heating (Denat OF) or protein digestion by proteinase K treatment (Dig OF). TLP medium was used as control (a,b). Data are mean ± SEM of bound sperm per mm² relative to control (n=4 replicates for each experiment). ****P-*value* < 0.0001 as compared to the control group.

In order to explore the role of glycoprotein N-glycans on sperm binding, OF fractions enriched in free N-glycans after enzymatic removal of N-linked oligosaccharides (fraction < 5-kDa after treatment with Remove-iT® PNGase F) and remaining macromolecules (fraction > 5-kDa) were prepared (Experiment 5).

Those treatments did not have any adverse effect on sperm motility (Supplementary Data S1). The OF fractions < and > 5 kDa after N-glycan removal induced a significant decrease in the density of bound sperm to OES compared to control ($p<0.001$), similarly to the native OF and native OF fraction > 5 kDa (Fig. 6). On the contrary, the native OF fraction < 5 kDa did not have any significant effect on bound sperm density compared to control, similarly to the OF fraction < 3 kDa in Fig. 4.

These results suggest that glycoproteins bearing N-glycans as well as other macromolecules > 5 kDa in the OF were involved in the effect of OF on sperm binding to OES.

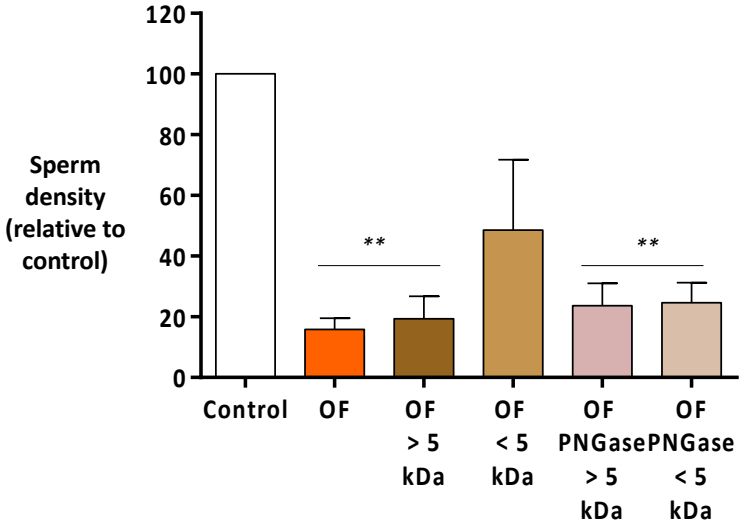

Figure 6. Effect of N-glycans linked to glycoproteins in the oviduct fluid on sperm binding to oviduct epithelial spheroids (Experiment 5).

Spermatozoa and spheroids were incubated for 60 min with 5-kDa cut-off fractions of the OF pre-treated with the Remove-iT® PNGase F (OF PNGase > and < 5 kDa). The OF PNGase < 5 kDa fraction was enriched in free N-glycans. The OF 5-kDa cut-off fractions without any pre-treatment (OF > and < 5 kDa) and native OF (OF) were also included.

The TLP medium was used as control. Data are mean ± SEM of bound sperm per mm² relative to control (n=3 replicates). **P-value < 0.01 as compared to the control group.

Impact of secreted glycosaminoglycans on sperm binding to spheroids

As Experiments 3 and 5 evidenced a role of macromolecules in the effect of OF, hyaluronic acid (HA, 4-8000 kDa) and heparan sulfate (HS, 10-70 kDa)[29], two glycosaminoglycans naturally present in the OF[15], were tested on sperm binding to OES (Experiment 6). HA between 10 and 1000 µg/mL did not have any effect on sperm motility, except a moderate decrease in curvilinear velocity (VCL) and amplitude lateral head displacement (ALH) at T0.

After 60 min, HS at highest dose (1000 µg/mL) decreased the proportions of motile and progressive sperm (40.2% and 25.3%, respectively) compared to the control medium (66.0% and 45.8%, respectively, $p<0.05$) while HS at 100 µg/mL slightly decreased the proportion of progressive sperm without affecting total motility (see Supplementary Data S1). HA at 10 and 100 µg/mL tended to increase bound sperm densities on OES compared to control, although this effect was not significant (Fig. 7a). On the contrary, HS decreased sperm binding on OES in a dose-dependent manner: sperm density on OES was decreased by 36% at 100 µg/mL HS and by 75% at 1000 µg/mL HS compared to control (p-values = 0.1 and < 0.001, respectively; Fig. 7b). In accordance, the OF in which HS was removed by heparinases (OF-HS) had lower effect on sperm binding than the native OF: compared to control, sperm density on OES was decreased by 60% with the OF-HS *vs*. by 80% with the native OF (p-values < 0.001 and < 0.0001, respectively; Fig. 7b). These results suggest that HS but not HA was involved in the effect of OF on sperm binding.

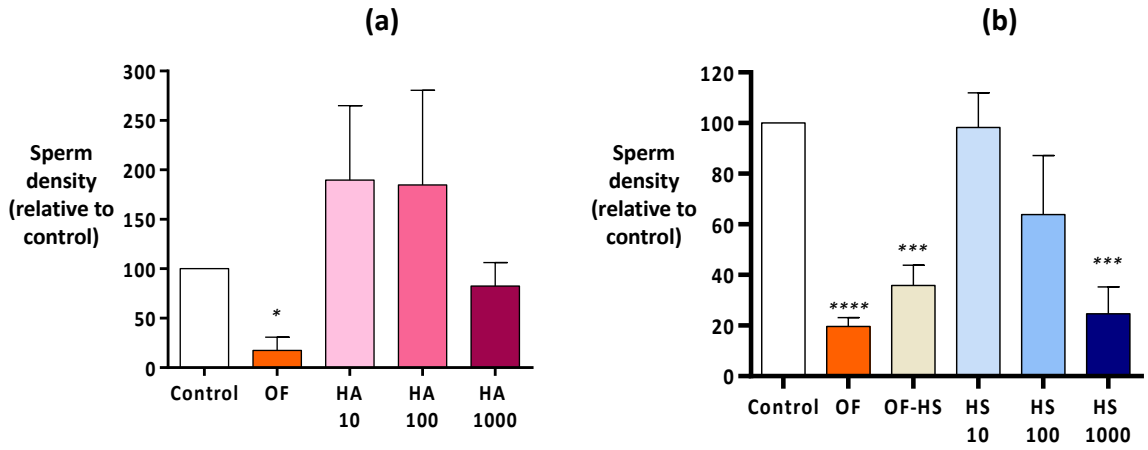

Figure 7. Effect of hyaluronic acid and heparan sulfate on sperm density on bovine oviduct epithelial spheroids (Experiment 6).

Spermatozoa and spheroids were incubated for 60 min with hyaluronic acid (HA) at 10, 100 and 1000 µg/mL (a), or with heparan sulfate (HS) at 10, 100 and 1000 µg/mL and OF in which heparan sulfate was digested with heparinases (OF-HS, b). Native OF at final protein concentration of 1 mg/mL was included (OF) and TLP medium was used as control in each experiment. Data are mean ± SEM of bound sperm per mm² relative to control (n = 4 replicates for each experiment). *P-value < 0.05; ***P-value < 0.001; ****P-value < 0.0001 as compared to the control group.

Discussion

Spermatozoa interact with the OF before they bind to the isthmus luminal cells in the so-called sperm reservoir. The present study examined the effect of OF on sperm-oviduct interactions using a newly characterized *in vitro* model of isthmic epithelial spheroids. The main findings of this study are that: (i) the OF prevents a sperm subpopulation to bind to OES without affecting sperm motility, membrane integrity and sperm-cilia interactions; (ii) the effect of OF on sperm binding was massive and did not vary according to the cycle stage and oviduct anatomical region the OF originated from; (iii) macromolecules larger than 3-5 kDa, among which N-glycosylated glycoproteins and heparane sulfate, were involved in the effect of OF on sperm binding; (iv) hyaluronic acid tended to increase sperm binding to OES.

Exploring periconception events in mammals requires the use of *in vitro* models to overcome the difficulties to access oviducts by surgery and avoid sacrifice of females. Based on *in vivo* observations, spermatozoa bind mostly to ciliated cells in the isthmus[21], pointing out the importance of keeping epithelial differentiation *in vitro*. Up to now, most studies on sperm-oviduct interactions used OEC aggregates or explants a few hours after collection[2,21,22] or OEC monolayers reaching confluence after 5-7 days of culture[23,24,28]. One study in pigs mentioned vesicles formed from OEC in primary culture but without any characterization of the model[30]. The main limitation of aggregates or explants is the lack of standardization of the outward surface and difficulty to assess bound sperm density due to numerous folds, whereas the main limitation of OEC monolayers grown on plastic dish is that cells rapidly loose epithelial differentiation and cilia[31]. Here, we used oviduct epithelial spheroids containing well-differentiated epithelial cells and a repeatable proportion of 25% ciliated cells after 4 days of culture. This proportion of ciliated cells was similar (20-40%) to those previously assessed in sections of isthmus from post-pubertal cows[32].

Furthermore**,** the spheroids offer the possibility to be selected according to their size (here 100 µm in diameter) and shape (round without folds), providing a standardized model to study sperm-oviduct interactions.

In accordance with our initial hypothesis, the OF decreased sperm binding to OES compared to the control medium. This effect was very repeatable over more than 30 replicates, decreasing by 80 to 90% the sperm density per surface unit as compared to control. Surprisingly, this effect was not restricted to the pre-ovulatory period and evidenced whatever the stage of cycle or anatomical region the OF originated. The OF-induced decrease in sperm binding was not due to a decrease in sperm motility or membrane damage during the 60-min incubation. This effect was either not due to a difference in binding surface on OES as spheroids were homogeneous in size and contained similar proportions of ciliated cells (25%). Furthermore, the OF did not have any adverse effect on spheroid cell viability, as evidenced by ethidium homodimer staining (data not shown). Although less spermatozoa bound to spheroids in the presence of OF, cilia morphology and sperm-cilia interactions were very similar in both OF-treated and control groups. Observation of sperm-OES complexes by scanning electron microscopy evidenced close sperm-cilia interactions, more than 90% of spermatozoa being bound exclusively by their head or by head and midpiece or flagella. Similar patterns of sperm-cilia interactions were observed after insemination in cattle[33] but with no quantitative data. Spermatozoa with intact acrosome and no morphological abnormalities (for more than 93%) bound to OES, similarly to previous observations in the bovine oviduct epithelium *in vivo*[21]. In the present study, spermatozoa were used after Percoll gradient centrifugation to remove the commercial extender and obtain homogeneous sperm populations, which probably contributed to the high proportion of spermatozoa with no abnormalities that were observed.

The effect of the OF was rapid, the kinetics showing much lower bound sperm density than in the control group as soon as 5 min after sperm addition By contrast, sperm binding increased progressively from 5 to 60 min after sperm addition in the control group. Given that both OES and sperm were in contact with the OF, we cannot exclude a combined action of the OF on both the sperm membrane and sperm binding sites at the surface of spheroids. Based on our recent proteomic data which identified 245 proteins interacting with bull sperm in the OF, including those previously identified as sperm receptors on oviduct epithelial cells[8], our hypothesis was that sperm rapidly interact with soluble proteins in the OF, preventing further attachment at the surface of OES by a process of binding competition. The hypothesis of sperm binding competition against OF proteins was supported by the fact that fluid fractions above 3 or 5 kDa, but not those below these thresholds, reduced bound sperm density on OES by 90%, similarly to the native OF as compared to control medium. This result let us to exclude small molecules like fucose (180 Da), previously identified as competing with bull sperm binding to oviduct explants *in vitro*[34]. This also let us to exclude progesterone (314 Da), previously identified as a sperm releasing factor after binding to OEC *in vitro*[5,35]. However, when proteins in the OF were digested by proteinase K, the effect on sperm binding was similar to that of the native OF, orienting us toward a mechanism independent of the amino acid part of glycoproteins and non-glycosylated proteins. In accordance, the density of sperm bound to OES was not altered by 1 mg/mL of albumin, a non-glycosylated protein among the five most abundant in the bovine OF[36] (Supplementary Figure S2). Proteinase K treatment cut the amino acid chains of proteins but has no effect on glycan chains linked to these amino acid chains: it was hypothesized that the glycans released in the OF by enzymatic digestion could be responsible for the sperm binding competition.

A recent mass spectroscopy analysis of glycans extracted from isthmic epithelial cells in cattle revealed that many N-linked glycans carry the trisaccharide Lewis A motif, to which bull sperm bind with high affinity[13], orienting us toward the potential role of N-glycans in the OF. The PNGase F is the most effective method to remove specifically all N-linked oligosaccharides from glycoproteins but the enzyme remains active for 24-72 hours. As a wide range of glycans are also present at the surface of spermatozoa[37] and OEC[13], the removal of the PNGase F from the OF under native conditions was possible thanks to the use of Remove-iT PNGase F. Our results show that the OF fraction below 5 kDa and enriched with glycoprotein N-glycans (after PNGase digestion and removal), but not the native OF fraction below 5 kDa, reproduced the inhibitory effect of the native OF on sperm binding, indicating that glycoprotein N-glycans were involved, at least partially, in the OF effect. It is thus likely that spermatozoa bound to the Lewis A motifs on released N-glycans in the OF, preventing them to bind to OES. It is however to note that the OF fraction more than 5 kDa after PNGase digestion was still effective to inhibit sperm binding on OES, suggesting a role for other macromolecules on sperm binding competition.

Beyond the role of glycans linked to glycoproteins, sperm-oviduct interactions may be modulated by GAG and proteoglycans, which are proteins linked to sulphated GAG chains. Although data are scarce and rather old, the non-sulfated HA and HS were reported as the two most abundant GAGs in the OF of post-pubertal cows, accounting for 39% and 26% of the total amount of GAG, respectively[15]. To our knowledge, there is currently no data on the amount of HS in the bovine OF.

The total amount of HA measured in the OF of dairy cows ranged from 0 to 18.7 µg per day with great variations between individual samples across the cycle and between animals[14].

In this study, the densities of bound sperm to OES in the presence of HA at 10 and 100 µg/mL tended to be higher than in the control group, without changing sperm motility. The lack of significance was due to a high heterogeneity between replicates. There is evidence from *in vitro* studies that bull and human sperm bind to HA[17,18,38]. Furthermore, HA was shown to increase the motility, intracellular concentration of calcium in human sperm[39] and tyrosine phosphorylation in bull sperm[40] *in vitro*. We hypothesize that HA may increase bull sperm motility and their probability to bind to OES during the 60-min incubation. However, this hypothesis was not supported by our motility data. Nevertheless, HA was excluded from the lists of OF components responsible for the inhibitory effect of the OF on sperm binding.

On the contrary, HS, a heavily sulphated GAG, decreased sperm binding to OES in a dose-dependent manner. Furthermore, the OF deprived of HS was 20% less effective than the native OF for inhibiting sperm binding compared to control, suggesting that HS interacts with sperm and prevents them to bind to OES. In line with our results, HS but not HA was shown to bind with high affinity to purified binder of sperm proteins (BSPs)[19]. Binder of Sperm Protein 1 (BSP-1, also called PDC-109 or BSP-A1/A2), BSP-3 (or BSP-A3), and BSP-5 (or BSP-30KDa) are seminal plasma-derived proteins coating bull sperm surface at ejaculation and playing a key role in sperm binding to OEC[41,42]. The proteins of the BSP family have several interaction partners, including sulfated GAG and annexins, which may explain their role in regulating sperm binding to the oviduct reservoir[43]. It has been hypothesized that GAG close to heparin are released from the follicular fluid into the oviduct at the time of ovulation, allowing sperm detachment from the reservoir through interactions with both BSPs and annexins for subsequent fertilization[43]. From our results, this scenario is unlikely: HS in the OF collected before ovulation had already an inhibitory effect on sperm binding, and the effect of the OF did not differ according to the cycle stage.

Therefore, it is likely that instead of triggering sperm detachment, HS in the oviduct lumen restrains sperm adhesion to the reservoir during the whole peri-ovulatory period. Other sulfated GAGs previously shown to interact with purified BSPs *in vitro*, like dermatan sulfate (also known as chondroitin sulfate B)[19], may be involved in the regulation of sperm binding to the oviduct epithelium.

One limitation of this study is the lack of information on animals used for OF and cell collection since the samples were collected at a slaughterhouse. However, the OF effect on sperm binding was very repeatable over 3 years of experiments, regardless of collection date and animal breed, suggesting a very conserved effect of OF on sperm binding. In addition, the same pool of semen was used in all experiments in order to focus on female factors regulating sperm-oviduct interactions, but the effect of OF may vary from one bull to another. Another limitation is that, due to the collection process by flushing, the OF was diluted, leading to much lower protein concentrations than those evaluated in the native OF (1-5 *vs*. 50-60 mg/mL proteins). It could be hypothesized that the inhibitory effect of the OF on sperm binding is even stronger *in vivo* and may contribute to the selection of a sperm subpopulation able to bind to the oviduct reservoir before ovulation.

In conclusion, this study proposed a new *in vitro* model of oviduct sperm reservoir, the isthmic epithelial spheroids containing 25% ciliated cells. The model is easily reproducible and standardizable for further studies on sperm-oviduct interactions in different fluidic environments. The present study evidenced for the first time that macromolecules present in the OF rapidly prevents a sperm subpopulation to bind to isthmic epithelial cells. The effect probably implied a sperm binding competition between soluble glycoproteins in the OF and binding sites at the surface of OES.

Our results also suggest that heparan sulfate restrains sperm binding to the oviduct epithelium. Further work is required to explore the roles of O-glycans and other OF macromolecules on sperm-oviduct interactions and functional roles of sperm selective binding in the isthmus on subsequent fertilization.

Methods

Media and reagents

Chemicals for media were obtained from Sigma-Merck (Missouri, United States) and ThermoFisher Scientific (Massachusetts, USA). Hepes-buffered Tyrode's lactate pyruvate medium (TLP medium) contained 100 mM NaCl, 3.1 mM KCl, 0.3 mM NaH_2PO_4, 2.1 mM $CaCl_2$, 0.4 mM $MgCl_2$, 1 mM sodium pyruvate, 27.4 mM sodium lactate, 10 mM Hepes and 1 mg/mL polyvinyl alcohol (PVA)[25,44]. PVA was used instead of albumin to avoid sperm capacitation[45] . The pH of TLP medium was adjusted to 7.4 with NaOH 1 M and the osmolarity to 300 mOsm with NaCl. TLP medium was stored at 4°C for maximum two weeks. M199 culture medium (Medium 199, Earle's salts; 31150-022) was supplemented with 2.5% Hepes (15630-080, ThermoFisher Scientific, Massachusetts, United States), 0.5% of gentamycin (G1272, Sigma, Missouri, United States) and 10% heat-treated fetal calf serum (A5256701, ThermoFisher Scientific, Massachusetts, United States). Media were passed through sterile 0.22-µm filters (SLGV013SL) before use. The TLP medium was placed minimum 1 h at 38.8°C before use for sperm incubation or at 4°C before use for oviduct flushing. The M199 medium was placed at 38.8°C under humidified atmosphere containing 20% O_2 and 5% CO_2 minimum 1 h before use for cell culture. Although otherwise specified, reagents were obtained from Sigma-Merck.

Culture of isthmic mucosa fragments and selection of oviduct epithelial spheroids (OES)

Bovine oviducts and ovaries were collected at a local slaughterhouse (Vendôme, 45 min from the laboratory) and transported on ice to avoid post-mortem modifications. Pairs of oviducts from two cows at pre-ovulatory stage of cycle (one follicle of 11 – 20 mm in diameter and a *corpus albicans, i.e.* corresponding to approximately days 19 to 21 of estrous cycle) were isolated from surrounding vessels and tissues and cut at the utero-tubal and ampullary junctions to isolate the isthmus (around 5-cm long)[46]. Isthmic sections were rapidly washed in 70% ethanol, rinsed in NaCl 0.9%, then both extremities (around 5 mm) were cut with a sterile scalpel to avoid any contamination. The isthmus mucosa was then expelled with forceps in 10 mL of M199 culture medium, vortexed for 1 min then incubated at 38.8°C for 10 min for cell sedimentation. After elimination of supernatant, the pellet was resuspended in 10 mL of culture medium and the vortex-sedimentation process was repeated. Finally, the pellet was diluted 10 times in the culture medium and 50 µL of resulting mixture was added to 450 µL of M199 medium. Isthmic mucosa fragments were cultured for 4 days in four-well culture plates (176740, ThermoFisher Scientific, Massachusetts, USA) at 38.8°C in a humidified atmosphere containing 20% O_2 and 5% CO_2. At day 4, a cavity was formed within mucosa fragments, forming spheroids of various size and shape and with the apical side of epithelial cells oriented outside. Spheroids of approximately 100 µm in diameter, homogeneous in form, with vigorous cilia beating and no surface folding were selected for sperm binding studies (Fig. 1a).

Cell viability and immunostaining of oviduct epithelial spheroids (OES)

The cell viability of the OES was assessed after 4 days in M199 medium and up to 4 h in the TLP and OF media at 0,06 and 4 mg/mL of proteins (in which incubation with spermatozoa were achieved) after immunostaining with ethidium homodimer-1 (L3224, Invitrogen, Massachusetts, USA).

OES were incubated in 500 µL of culture medium and 1 µL of ethidium homodimer-1 and Hoechst (B2261) for 45 min at 38.8°C in a humidified atmosphere containing 20% O_2 and 5% CO_2 and directly observed under confocal microscopy (Zeiss LSM 700, Carl Zeiss, Oberkochen, Germany).

To further characterize the OES, immunostaining for pan-cytokeratin (epithelial cell marker), vimentin (stromal cell marker) and acetylated alpha-tubulin (marker of ciliated cells) was performed as previously described[47,48]. Briefly, OES were fixed (4% paraformaldehyde in PBS supplemented with 1 % of bovine serum albumin (PBS-BSA), 1 h at 37°C), washed three times in PBS BSA then incubated in a blocking solution (10% goat serum in PBS-BSA, 30 min, room temperature) then incubated overnight at room temperature with the primary antibody (anti-cytokeratin, C2931; anti-vimentin, V6630; anti-acetylated tubulin, T7451; final concentrations at 30, 100 and 2 µg/mL, respectively). To assess the proportions of sperm bound to ciliated cells, immunostaining for acetylated alpha-tubulin (T7451; final concentration of 2 µg/mL) was performed on sperm-OES complexes. Control OES were incubated with IgG1 (M9269) at the same concentration than primary antibody. After washing in PBS-BSA, OES were then incubated with the secondary antibody coupled with Alexa Fluor 488 (A11001, Invitrogen, Massachusetts, USA; final concentration at 2 µg/mL) for 1 h at room temperature under agitation. After washing in PBS-BSA, OES or sperm-OES complexes were stained with Hoechst (B2261, 10 µg/mL) and observed under confocal microscopy. For each antibody, a total of 100 OES from five different replicates were evaluated.

Preparation of spermatozoa, assessment of sperm motility and membrane integrity

A pool of semen from the same ejaculates of two Normande and one Holstein bulls (Union Evolution, Noyal-sur-Vilaine, France) and previously frozen in Optidyl extender (IMV technologies, L'Aigle, France) were used for all experiments.

Semens were thawed 3 min in a water bath at 37°C then washed on a 45%-90% Percoll gradient by centrifugation (700×*g*, 20 min, 25°C). An aliquot of the sperm pellet was used to assess sperm concentration in a Thoma cell counting chamber. Sperm were then washed in 1 mL of TLP medium for 10 min at 300×*g* at 25°C before incubation with spheroids. Just before and at the end of each incubation, sperm motility was assessed using computer-assisted sperm analysis (CASA, IVOS II, IMV technologies). Proportions of motile spermatozoa before and after incubation were typically more than 70 and 60%, respectively (Supplementary Data S1). In some experiments, aliquots of spermatozoa were analyzed by flow cytometry (MACSQuant Analyzer 10, Miltenyi Biotec, Germany) after incubation for 10 min at room temperature in 200 µL TLP with 7.5 µM propidium iodide (PI, Sigma 81845) and 1 µM peanut agglutinin fluorescein (PNA, Vector FL-1071) to assess sperm membrane integrity and acrosome reaction, respectively.

Sperm addition to spheroids and quantification of bound sperm density

Two hours before sperm cell addition, OES were rapidly washed in M199 medium then transferred in 500 µL of TLP medium at 38.8°C (with no CO_2 to avoid the formation of bicarbonate). Just before sperm addition, groups of 20 OES in 10 µL of TLP medium were transferred in 50 µL of medium (TLP or treatment) in a sterile 96-well culture plate at 38.8°C. Sperm were added in 5 µL of TLP so that the final volume of sperm-OES incubation was 65 µL. Preliminary data using increasing concentrations of spermatozoa added to 20 OES in the TLP medium showed that the density of bound sperm reached a plateau at 1 million of spermatozoa per mL. Therefore, the final sperm concentration added to a group of 20 OES was 1 million of spermatozoa per mL in a final volume of 65 µL.

After incubation, sperm-OES complexes were gently washed three times in 500 µL of TLP medium at 38.8°C using a glass pipette (400-µm in diameter) in order to eliminate slightly attached spermatozoa, then immediately fixed in 2,5% glutaraldehyde diluted in 0.1 M sodium cacodylate (27746.180, Prolabo, France) for 1 h at 37°C. After three washing in PBS-BSA, sperm-OES complexes were kept at 4°C overnight until further analysis. Preliminary experiments showed that this procedure did not induce sperm detachment from OES. Nuclei of both sperm and OES were stained with Hoechst (B2261; 10 µg/mL) for 30 min under gentle agitation at room temperature. After two washes in PBS-BSA, OES were placed on Superfrost slide (J1800AMNZ, Epredia, Breda, Netherlands), mounted under coverslip and analyzed by confocal microscopy (Zeiss LSM 700, Oberkochen, Germany). In order to visualize all sperm heads, both sides of the OES was observed under 405 excitation wavelength and pictures were saved. The total number of bound spermatozoa per OES and areas of OES were quantified using the ImageJ software (version 1.53t). Bound sperm density was calculated as the total number of bound sperm on the two sides of spheroids divided by the total area of spheroids.

Collection and preparation of oviduct fluid samples

Bovine oviduct fluids were collected from adult cyclic cows at a local slaughterhouse. Pairs of oviducts and ovaries were immediately placed on ice, transported to the laboratory, and classified according to ovarian morphology as previously described[46]. Oviducts ipsilateral and contralateral to ovulation at either the pre-ovulatory, post-ovulatory (presence of an early corpus luteum consisting of red, loosely organized tissue less than 1 cm in diameter, approximately days 1 to 4 of cycle) or luteal stage of cycle (presence of a well-formed brown or orange *corpus luteum* more than 1 cm in diameter) were used. The ovaries, surrounding tissues and infundibulum were removed before flushing with TLP medium at 4°C. For most experiments, the whole oviducts were flushed with 500 µL of TLP.

In some case, the oviducts were cut at the ampullary-isthmus junction and each section (isthmus and ampulla) was flushed separately with 200 µL of TLP. Cells and cellular debris were discarded through two successive centrifugations (2000×*g* for 10 min at 4°C then 12,000×*g* for 10 min at 4°C). An OF aliquot was used for protein concentration using the Uptima BC Assay kit (Interchim, Montluçon, France). The protein concentrations of OF at collection time ranged from 1 to 4 mg/mL. The OF samples used for incubation with OES and sperm were pools of OF collected from ipsi- and contralateral oviducts from two cows at the same stage of cycle and stored at -80°C until use (one freezing-thawing cycle before use). The final protein concentration was adjusted at the time of thawing.

To obtain OF filtration fractions, 500 µL of pre-ovulatory OF at a final protein concentration of 1 mg/mL were centrifuged on a Vivaspin® ultrafiltration unit (3-kDa cut-off; VS0191, Sartorius, Göttingen, Germany) at 12,000×*g* for 1 h at 4°C. The fractions at the top (above 3 kDa) and at bottom (below 3kDa) of the unit were collected, assayed for protein concentration and stored at -20°C until use. SDS PAGE electrophoresis were achieved to check the efficiency of ultrafiltration.

For protein denaturation, pre-ovulatory OF at 1 mg/mL of proteins was treated for 10 min at 100°C then keep at room temperature for 20 min before use. For protein digestion, pre-ovulatory OF at 1 mg/mL of proteins was incubated in TLP medium supplemented with 200 µg/mL of proteinase K (A3830, AppliChem, Germany) overnight at 56°C. The proteinase K was discarded from the OF via ultrafiltration (Vivaspin® 50 kDa cut-off, VS0132, Sartorius, Göttingen, Germany) for 10 min at 12,000×*g*. Bradford protein assay (Interchim, Montluçon, France) and SDS-PAGE electrophoresis were achieved to assess the efficiency of digestion and elimination of proteinase K. The proteinase K-free digested OF fraction below the 50-kDa cut-off was stored at -20°C before use.

To remove N-glycans from OF glycoproteins, pre-ovulatory OF was treated with Remove iT® PNGase F, a PNGase F tagged with chitin binding domain to facilitate its removal from the reaction (P0706S, NewEngland BioLabs, Massachusetts, United States), according to the manufacturer instructions. Briefly, 9 µL of pre-ovulatory OF at 2.2 mg/mL proteins were incubated with 2 µL of Remove iT® PNGase F, 2 µL of Glycobuffer and 7 µL of demineralized water for 1 h at 37°C. PNGase F was then removed from the OF using chitin magnetic beads and a magnetic separation rack (E8036S and S1506S, NewEngland BioLabs, Massachusetts, United States). The PNGase-treated OF was added to 50 µL of beads previously washed with TLP and incubated for 10 min at 4°C under shaking. The tube was then placed 30 s on the magnetic rack to attract beads and eliminate the PNGaseF. Then the OF supernatant was recovered and stored at -20°C before use. In order to isolate released N-glycans, samples were then centrifuged on a Vivaspin® unit with a 5-kDa cut-off for 2 h at 4°C at 12,000×*g*, resulting in fractions enriched in N-glycans (OF PNGase < 5 kDa) and remaining macromolecules (OF PNGase > 5 kDa). Both fractions were stored at -20°C before use. The release of N-glycans was checked by SDS PAGE electrophoresis of native and PNGase-treated OF on a 4-20% precast gel (Bio Rad, California, USA).

In order to eliminate HS from the OF, pre-ovulatory OF at 1 mg/mL of proteins was incubated in TLP medium supplemented with a mixture of heparinases I, II and III (H3917, H6512, v/v) at a final concentration of 0.1 UI/mL for 5 h at 37°C. The heparinases were discarded from the OF via ultrafiltration (Vivaspin® 50 kDa cut-off, VS0132, Sartorius, Göttingen, Germany) for 10 min at 12,000×*g* at 4°C. SDS-PAGE electrophoresis was achieved to assess the elimination of heparinases from the OF. Treated samples were stored at -20°C before use.

Observation of sperm-cilia interactions by scanning electron microscopy

Sperm-OES complexes were immersed in a fixative solution (2,5% glutaraldehyde in 0.2 M sodium cacodylate buffer, pH 7.4) and stored at 4°C until processing. The fixative was removed, and samples were rinsed in the sodium cacodylate solution (pH 7.4). They were deposited on sterile cover-glasses discs (Marienfeld, VWR, France). The samples underwent progressive dehydration by soaking in a graded series of ethanol (50 to 100%) before critical-point drying under CO2. Samples were mounted on aluminum SEM sample stubs (15 mm diameter x 6 mm M4, Micro to Nano, Haarlem, Netherlands) with carbon adhesive discs (Agar Scientific, Oxford Instruments SAS, Gometz-la-Ville, France) and sputter coated with Gold-Palladium (Polaron SC7640, Milexia, Verrières-le-buisson, France) for 220 s at 10 mA. Samples were visualized by field emission gun scanning electron microscopy (SEM FEG). They were viewed as secondary electron (2 kV) with a Hitachi S4500 instrument (Milexia, Verrières-le-buisson, France). Samples preparation and scanning Electron Microscopy analyses were performed at the Microscopy Platform of the INRAE PACA center, Avignon, France.

Experimental design

The general design of experiments is presented in Supplementary Figure S1. For all experiments, sperm motility was assessed by CASA at 0 and 60 min of incubation with native OF and TLP medium as controls.

Experiment 1 evaluated the kinetics of sperm binding to OES in control conditions and with OF. Sperm and OES were incubated for 5, 15, 30 and 60 min in the TLP medium or in the presence of pre-ovulatory OF at a final protein concentration of 1 mg/mL.

Experiment 2 evaluated the effect of the stage of cycle (pre-ovulatory *vs*. luteal phase of cycle) and oviduct anatomical region (ampulla *vs*. isthmus) from which the OF originated on sperm binding.

For each experiment, sperm and OES were incubated for 60 min in the presence of OF at a final protein concentration of 1 mg/mL. Preliminary experiments showed that more than 99% cells in OES were viable (showed negative signal for ethidium homodimer) after 60 min in TLP and OF. TLP medium was used as control.

Experiment 3 evaluated the effect of OF ultra-filtrated fractions on sperm binding. Sperm and OES were incubated for 60 min in fractions > and < 3 kDa of pre-ovulatory OF. TLP medium was used as control.

Experiment 4 evaluated the effect of OF proteins on sperm binding. Sperm and spheroids were incubated for 60 min with pre-ovulatory OF at 0.06, 0.125, 0.25, 0.5, 1, 2 or 4 mg/mL of proteins. Sperm and OES were incubated for 60 min in pre-ovulatory OF in which proteins were denatured by heating or digested by proteinase K. TLP medium and native OF were used as controls. In addition, sperm and OES were incubated with 1 mg/mL of fatty acid-free albumin (A3803).

Experience 5 evaluated the effect of N-glycans released from OF glycoproteins on sperm binding. Sperm and OES were incubated for 60 min with 5-kDa cut-off fractions of the OF treated with Remove-iT® PNGase F. TLP medium and native OF were used as controls.

Experience 6 evaluated the effect of HA and HS on sperm binding. Sperm and OES were incubated for 60 min in pre-ovulatory OF treated with heparinases I, II & III (OF-HS). In addition, purified heparan sulfate (H7640) and hyaluronic acid (53747) diluted at 10, 100 and 1000 µg/mL in TLP medium were tested on sperm binding. TLP medium and native OF were used as controls.

Each experiment was repeated three to five times with OES and OF samples from different cows.

Statistical analysis

Unless specified, data are presented as mean ± SEM of bound sperm density per mm^2 relative to the control group in the TLP medium. Statistical analysis was performed using GraphPad Prism software (version 8.1.1). Bound sperm densities and motility parameters were compared between conditions using ANOVA and Tuckey's post-tests for pair-wise comparisons. Proportions of spermatozoa observed by SEM were compared by Chi-square tests. A *P*-value < 0.05 was considered as significant.

References

1. Hunter, R. H. F. & Nichol, R. Transport of spermatozoa in the sheep oviduct: preovulatory sequestering of cells in the caudal isthmus. *J. Exp. Zool.* **228**, 121–128 (1983).

2. Lefebvre, R. *et al.* Characterization of the oviductal sperm reservoir in cattle. *Biol Reprod* **53**, 1066–1074 (1995).

3. Boilard, M., Bailey, J., Collin, S., Dufour, M. & Sirard, M.-A. Effect of bovine oviduct epithelial cell apical plasma membranes on sperm function assessed by a novel flow cytometric approach. *Biology of Reproduction* **67**, 1125–1132 (2002).

4. Boilard, M. *et al.* Localization of the chaperone proteins GRP78 and HSP60 on the luminal surface of bovine oviduct epithelial cells and their association with spermatozoa. *Biol Reprod* **71**, 1879–1889 (2004).

5. Lamy, J. *et al.* Steroid hormones regulate sperm–oviduct interactions in the bovine. *Reproduction* **154**, 497–508 (2017).

6. Chang, H. & Suarez, S. S. Unexpected flagellar movement patterns and epithelial binding behavior of mouse sperm in the oviduct. *Biology of Reproduction* **86**, (2012).

7. Saint-Dizier, M., Schoen, J., Chen, S., Banliat, C. & Mermillod, P. Composing the early embryonic microenvironment: physiology and regulation of oviductal secretions. *Int J Mol Sci* **21**, 223 (2020).

8. Mahé, C. *et al.* The sperm-interacting proteome in the bovine isthmus and ampulla during the periovulatory period. *Under review in Journal of Animal Science and Biotechnology* (2023).

9. Ignotz, G. G., Cho, M. Y. & Suarez, S. S. Annexins are candidate oviductal receptors for bovine sperm surface proteins and thus may serve to hold bovine sperm in the oviductal reservoir. *Biol Reprod* **77**, 906–913 (2007).

10. Elliott, R. M. A. *et al.* Effects of HSPA8, an evolutionarily conserved oviductal protein, on boar and bull spermatozoa. *Reproduction* **137**, 191–203 (2009).

11. Suarez, S. S., Revah, I., Lo, M. & Kölle, S. Bull sperm binding to oviductal epithelium is mediated by a Ca2+-dependent lectin on sperm that recognizes Lewis-a trisaccharide. *Biology of Reproduction* **59**, 39–44 (1998).

12. Miller, D. J. Review: The epic journey of sperm through the female reproductive tract. *Animal* **12**, s110–s120 (2018).

13. Dutta, S. *et al.* Sulfated Lewis A trisaccharide on oviduct membrane glycoproteins binds bovine sperm and lengthens sperm lifespan. *Journal of Biological Chemistry* **294**, 13445–13463 (2019).

14. Bergqvist, A.-S. *et al.* Hyaluronan and its binding proteins in the epithelium and intraluminal fluid of the bovine oviduct. *Zygote* **13**, 207–218 (2005).

15. Lee, C. N. & Ax, R. L. Concentrations and composition of glycosaminoglycans in the female bovine reproductive tract. *Journal of Dairy Science* **67**, 2006–2009 (1984).

16. Ranganathan, S., Ganguly, A. K. & Datta, K. Evidence for presence of hyaluronan binding protein on spermatozoa and its possible involvement in sperm function. *Mol. Reprod. Dev.* **38**, 69–76 (1994).

17. Liaudat, A. C. *et al.* Bull sperm selection by attachment to hyaluronic acid semi-interpenetrated hydrogels. *Reprod Domestic Animals* **57**, 228–232 (2022).

18. Blois, D. A. *et al.* Interaction between hyaluronic acid semi-interpenetrated hydrogel with bull spermatozoa: studies of sperm attachment–release and sperm quality. *Adv. Mater. Interfaces* **8**, 2101155 (2021).

19. Thérien, I., Bergeron, A., Bousquet, D. & Manjunath, P. Isolation and characterization of glycosaminoglycans from bovine follicular fluid and their effect on sperm capacitation. *Mol Reprod Dev* **71**, 97–106 (2005).

20. Talevi, R. & Gualtieri, R. Sulfated glycoconjugates are powerful modulators of bovine sperm adhesion and release from the oviductal epithelium in vitro. *Biol Reprod* **64**, 491–498 (2001).

21. Sostaric, E. *et al.* Sperm binding properties and secretory activity of the bovine oviduct immediately before and after ovulation. *Mol. Reprod. Dev.* **75**, 60–74 (2008).

22. De Pauw, I. M. C., Van Soom, A., Laevens, H., Verberckmoes, S. & de Kruif, A. Sperm binding to epithelial oviduct explants in bulls with different nonreturn rates investigated with a new in vitro model. *Biol Reprod* **67**, 1073–1079 (2002).

23. Gualtieri, R. & Talevi, R. In vitro-cultured bovine oviductal cells bind acrosome-intact sperm and retain this ability upon sperm release. *Biol Reprod* **62**, 1754–1762 (2000).

24. Lamy, J. *et al.* Steroid hormones regulate sperm–oviduct interactions in the bovine. *Reproduction* **154**, 497–508 (2017).

25. Kumaresan, A., Johannisson, A., Humblot, P. & Bergqvist, A.-S. Effect of bovine oviductal fluid on motility, tyrosine phosphorylation, and acrosome reaction in cryopreserved bull spermatozoa. *Theriogenology* **124**, 48–56 (2019).

26. Kumaresan, A., González, R., Johannisson, A. & Berqvist, A.-S. Dynamic quantification of intracellular calcium and protein tyrosine phosphorylation in cryopreserved boar spermatozoa during short-time incubation with oviductal fluid. *Theriogenology* **82**, 1145–1153 (2014).

27. Ardon, F. *et al.* Dynamics of bovine sperm interaction with epithelium differ between oviductal isthmus and ampulla. *Biology of Reproduction* **95**, 90–90 (2016).

28. Ellington, J. E., Padilla, A. W., Vredenburgh, W. L., Dougherty, E. P. & Foote, R. H. Behavior of bull spermatozoa in bovine uterine tube epithelial cell co-culture: an in vitro model for studying the cell interactions of reproduction. *Theriogenology* **35**, 977–989 (1991).

29. Gandhi, N. S. & Mancera, R. L. The structure of glycosaminoglycans and their interactions with proteins. *Chemical Biology & Drug Design* **72**, 455–482 (2008).

30. Bureau, M., Bailey, J. L. & Sirard, M.-A. Binding regulation of porcine spermatozoa to oviductal vesicles In vitro. *Journal of Andrology* **23**, 188–192 (2002).

31. Walter, I. Culture of bovine oviduct epithelial cells (BOEC). *Anat. Rec.* **243**, 347–356 (1995).

32. Ito, S., Kobayashi, Y., Yamamoto, Y., Kimura, K. & Okuda, K. Remodeling of bovine oviductal epithelium by mitosis of secretory cells. *Cell Tissue Res* **366**, 403–410 (2016).

33. Hunter, R. H., Fléchon, B. & Fléchon, J. E. Distribution, morphology and epithelial interactions of bovine spermatozoa in the oviduct before and after ovulation: a scanning electron microscope study. *Tissue Cell* **23**, 641–656 (1991).

34. Lefebvre, R., Lo, M. C. & Suarez, S. S. Bovine sperm binding to oviductal epithelium involves fucose recognition. *Biol Reprod* **56**, 1198–1204 (1997).

35. Romero-Aguirregomezcorta, J., Cronin, S., Donnellan, E. & Fair, S. Progesterone induces the release of bull spermatozoa from oviductal epithelial cells. *Reprod. Fertil. Dev.* **31**, 1463–1472 (2019).

36. Mahé, C. *et al.* Spatiotemporal profiling of the bovine oviduct fluid proteome around the time of ovulation. *Sci Rep* **12**, 4135 (2022).

37. Xin, A.-J. *et al.* Comprehensive profiling of accessible surface glycans of mammalian sperm using a lectin microarray. *Clin Proteom* **11**, 10 (2014).

38. West, R. *et al.* Sperm selection with hyaluronic acid improved live birth outcomes among older couples and was connected to sperm DNA quality, potentially affecting all treatment outcomes. *Human Reproduction* **37**, 1106–1125 (2022).

39. Bains, R., Miles, D. M., Carson, R. J. & Adeghe, J. Hyaluronic acid increases motility/intracellular CA2+ concentration in human sperm in vitro. *Arch Androl* **47**, 119–125 (2001).

40. Fernández, S. & Córdoba, M. Hyaluronic acid-induced capacitation involves protein kinase C and tyrosine kinase activity modulation with a lower oxidative metabolism in cryopreserved bull sperm. *Theriogenology* **122**, 68–73 (2018).

41. Gwathmey, T. M., Ignotz, G. G. & Suarez, S. S. PDC-109 (BSP-A1/A2) promotes bull sperm binding to oviductal epithelium in vitro and may be involved in forming the oviductal sperm reservoir. *Biol. Reprod.* **69**, 809–815 (2003).

42. Gwathmey, T. M., Ignotz, G. G., Mueller, J. L., Manjunath, P. & Suarez, S. S. Bovine seminal plasma proteins PDC-109, BSP-A3, and BSP-30-kDa share functional roles in storing sperm in the oviduct. *Biol. Reprod.* **75**, 501–507 (2006).

43. Plante, G., Prud'homme, B., Fan, J., Lafleur, M. & Manjunath, P. Evolution and function of mammalian binder of sperm proteins. *Cell Tissue Res* **363**, 105–127 (2016).

44. Parrish, J. J., Susko-Parrish, J., Winer, M. A. & First, N. L. Capacitation of bovine sperm by heparin. *Biol Reprod* **38**, 1171–1180 (1988).

45. Visconti, P. E. *et al.* Cholesterol efflux-mediated signal transduction in mammalian sperm. *Journal of Biological Chemistry* **274**, 3235–3242 (1999).

46. Ireland, J. J., Murphee, R. L. & Coulson, P. B. Accuracy of predicting stages of bovine estrous cycle by gross appearance of the corpus luteum. *J Dairy Sci* **63**, 155–160 (1980).

47. Lopera-Vásquez, R. *et al*. Extracellular vesicles from BOEC in in vitro embryo development and quality. *PLoS ONE* **11**, e0148083 (2016).

48. Ito, S., Yamamoto, Y. & Kimura, K. Analysis of ciliogenesis process in the bovine oviduct based on immunohistochemical classification. *Mol Biol Rep* **47**, 1003–1012 (2020).

Acknowledgements

The authors warmly thank Benoît Marteau, Thierry Delpuech and Albert Arnould for collecting the oviducts at slaughterhouse. The authors thank the PIC platform in the PRC Unit for their valuable help in confocal microscopy, and Union Evolution, France, for providing bull semen required for this study.

Author contributions

M.S.D., P.M. and C.M. designed the study; C.M. did the experiments with the help of L.L., T.P. and K.R.; K.R. and T.M. did the SEM analysis; C.M. did the image and statistical analyses; C.M. and M.S.D. wrote the manuscript; M.S.D. and J.S. administrated the study; M.S.D. supervised the study; all authors corrected the manuscript.

Funding

This work was funded by INRAE and Agence Nationale de la Recherche under the grant number ANR-18-CE92-0049.

Competing interests

The authors declare no competing interests.

Supplementary information

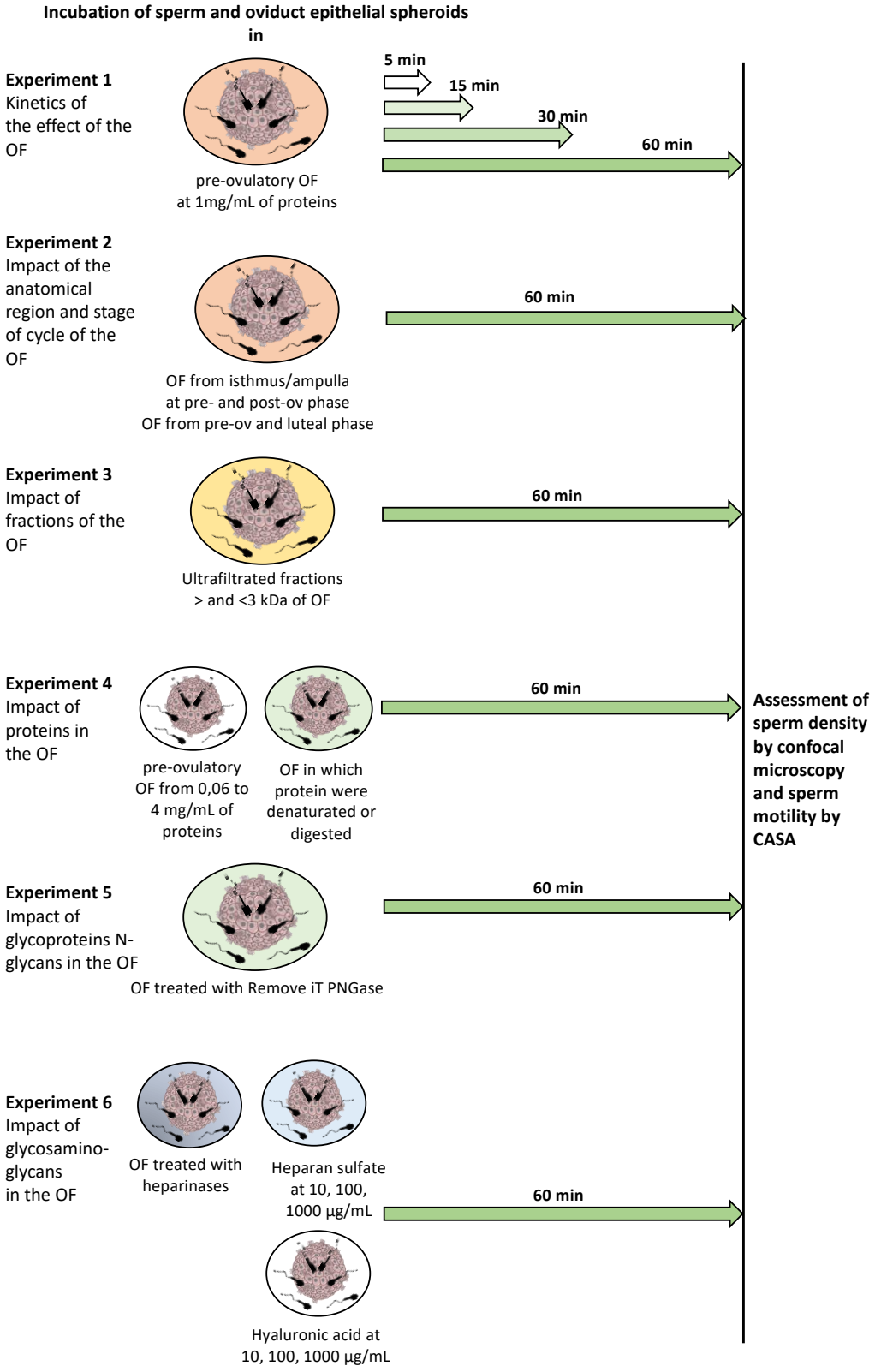

Supplementary Figure 1. Experimental design for sperm-oviduct epithelial spheroids incubation

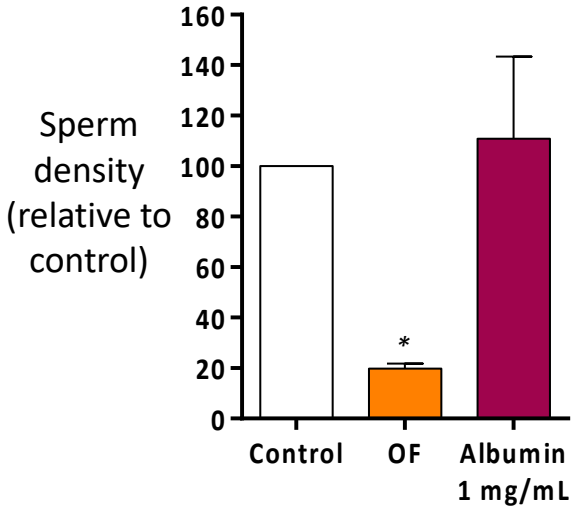

Supplementary Figure 2. Effect of bovine serum albumin on sperm binding to oviduct epithelial spheroids

Résultats complémentaires : effet de l'annexine A1, de l'albumine, de la progestérone et effet libérateur du fluide d'oviducte sur la liaison des spermatozoïdes aux sphéroïdes

En complément des résultats précédents, trois molécules candidates ont été testées sur la liaison des spz sur les sphéroïdes (Figure 14 page 179) :

- l'annexine A1, une protéine abondante dans le FO bovin (dans le top 20, chapitre 1), identifiée parmi les protéines d'interaction (chapitre 2) et préalablement proposée comme récepteur des spz de taureaux à la surface des cellules épithéliales d'oviducte (Ignotz *et al.*, 2007). La protéine utilisée est l'annexine A1 recombinante humaine produite en système procaryote (don du Professeur Chris Reutelingsperger, Faculty of Health, Medicine and Life Sciences, University of Maastricht, Pays-bas) et dont la bioactivité avait été validée *in vivo* chez la souris (Kusters *et al.*, 2015), testée ici entre 10 et 1000 µg/mL ;

- l'albumine, protéine non glycosylée très abondante dans le FO bovin (dans le top 3, chapitre 1), non identifiée parmi les SIP (chapitre 2) mais connue pour son rôle capacitant sur les spz de taureaux (Ehrenwald *et al.*, 1990; Bernecic *et al.*, 2019) ;

- la progestérone, hormone dosée dans le FO bovin autour de 6 ng/mL en période pré-ovulatoire (Lamy *et al.*, 2016a) et libérant *in vitro* les spz liés aux cellules épithéliales d'oviducte par une action calcium-dépendante (Lamy *et al.*, 2017; Romero-Aguirregomezcorta *et al.*, 2019). La dose utilisée (1 ng/mL de progestérone) est proche des concentrations moyennes mesurées dans le FO actif à 1 mg/mL de protéines (0,8 ± 0,13 ng/mL) et sa fraction ultrafiltrée supérieure à 3 kDa (1,2 ± 0,0 ng/mL). La teneur en progestérone de la fraction ultrafiltrée inférieure à 3 kDa était inférieure à la limite de détection.

Les résultats montrent que ni l'annexine A1 ni l'albumine n'ont d'effet sur la liaison des spz aux sphéroïdes (Figure 14A et B). En revanche, la progestérone à 1 ng/mL augmente la densité des spz liés aux sphéroides par rapport au milieu témoin ($p = 0,07$) (Figure 14C).

Afin d'évaluer l'effet libérateur du FO pré-ovulatoire sur les spz liés, les spermatozoïdes et les sphéroïdes ont été incubés pendant 30 minutes dans le milieu contrôle puis les complexes spermatozoïdes-sphéroïdes ont été transférés après un lavage doux dans du FO pré-ovulatoire à 1 mg/mL de protéines pendant 30 minutes (Témoin 30 + FO 30). Trois groupes contrôle ont été inclus : un avec des spermatozoïdes et des sphéroïdes incubés pendant 60 minutes dans le milieu contrôle (Témoin 60), un avec des spermatozoïdes et des sphéroïdes incubés pendant 60 minutes dans du FO pré-ovulatoire (FO 60), et un avec des spermatozoïdes et des sphéroïdes incubés pendant 30 minutes dans le milieu témoin, puis les complexes spz-sphéroïdes ont été transférés après un lavage doux dans le même milieu témoin pendant 30 minutes supplémentaires afin d'évaluer l'effet de la manipulation sur la densité des spermatozoïdes (Témoin 30+30). Après transfert des complexes spz-sphéroïdes dans le FO, la densité de spz liés diminue d'en moyenne 60% par rapport au témoin manipulé (Témoin 30 + FO 30 vs. Témoin 30+30), montrant que le FO induit la libération d'une majorité de spermatozoïdes liés aux sphéroïdes (Figure 14D page 179).

En conclusion, l'annexine A1 en solution ne diminue pas la capacité de liaison des spz aux sphéroides quelle que soit la dose, ce qui suggère que les spz ne se lient pas à l'annexine A1 recombinante et/ou que l'annexine A1 n'est pas impliquée dans la liaison des spz aux cellules. L'albumine ne modifie pas non plus la capacité de liaison des spz, au moins pendant les 60 min d'incubation. L'albumine pourrait cependant jouer un rôle important de liaison à la progestérone, et moduler ainsi la biodisponibilité de cette hormone dans l'oviducte. Enfin, le FO induit en 30 min la libération d'une majorité de spz liés aux sphéroïdes : cet effet pourrait s'expliquer par la liaison des spz aux N-glycanes et glycosaminoglycanes du fluide. La capacitation de ces spz libérés reste à évaluer.

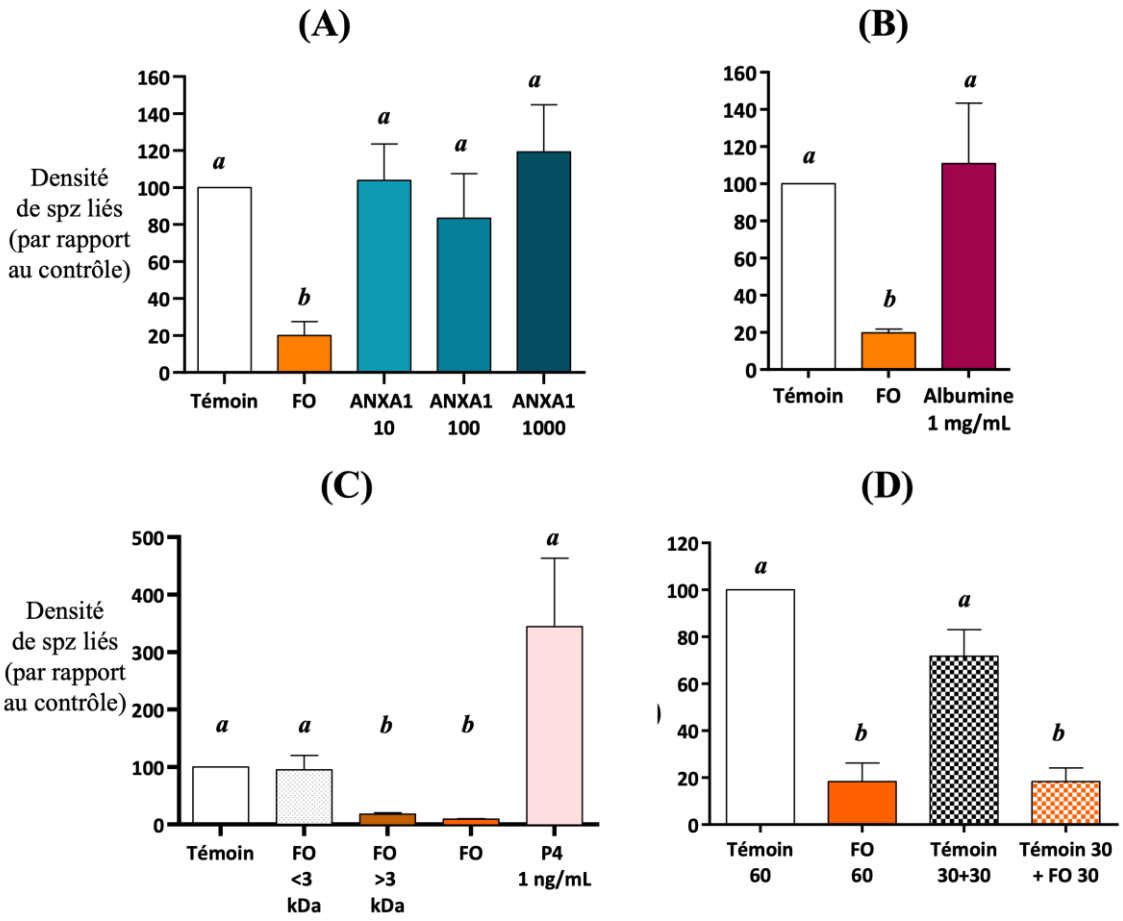

Figure 14 : Effets de l'annexine A1, de l'albumine, de la progestérone et effet libérateur du fluide d'oviducte sur la liaison des spermatozoïdes aux sphéroïdes.

Les données sont présentées sous forme de moyenne ± SEM (n=4 répliques biologiques) de densité de spz. Des lettres différentes signifient une différence significative avec un $p \leq 0,05$. FO = Fluide d'oviducte natif ; (C) P4 = progestérone ; (D) Témoin 60 = spz et sphéroïdes incubés pendant 60 minutes dans le milieu contrôle ; FO 60 = spz et sphéroïdes incubés pendant 60 minutes dans le fluide d'oviducte ; Témoin 30 + 30 = spz et sphéroïdes incubés pendant 30 minutes dans le milieu contrôle puis 30 min dans le milieu contrôle ; Témoin 30 + FO 30 = spz et sphéroïdes incubés pendant 30 minutes dans le milieu contrôle puis 30 min dans le fluide d'oviducte.

Discussion et perspectives

L'environnement femelle offre aux spermatozoïdes des conditions très discriminantes, aboutissant à une sous-population « élite » de spermatozoïdes autour de l'ovocyte au moment opportun. Afin de mieux comprendre cet environnement, le premier chapitre de cette thèse est consacré à la description du paysage protéique traversé par les spz depuis l'utérus, où les spz entament leur migration, jusqu'à l'oviducte, centre de la capacitation et la fécondation. Ces études ont fourni, grâce à la spectrométrie de masse à haute résolution, un portrait exhaustif des protéomes des voies génitales femelles.

Afin d'étudier les interactions entre l'environnement maternel et les gamètes aux portes de la fécondation, le deuxième chapitre s'est focalisé sur les interactions entre les protéines luminales de l'oviducte et les spermatozoïdes en période péri-conceptionnelle. Cette étude met en évidence 245 protéines s'associant potentiellement aux spermatozoïdes tout au long de leur migration dans l'oviducte. Une analyse complémentaire a confirmé que le fluide d'oviducte pouvait modifier la viabilité, la mobilité et la réaction acrosomique des spermatozoïdes en fonction de la région anatomique et du stade péri-ovulatoire.

Enfin, le troisième chapitre s'est penché sur les effets de ces interactions sur la constitution du réservoir spermatique. Cette étude a permis de caractériser un nouveau modèle de réservoir *in vitro* appelé sphéroïde, reproduisant la morphologie de l'épithélium et les interactions avec les spermatozoïdes. Grâce à ce modèle, un effet inhibiteur des sécrétions de l'oviducte sur la liaison des spermatozoïdes aux cellules a été mis en évidence, impliquant le. sulfate d'héparane ainsi que des N-glycanes liés aux protéines sécrétées.

1. Les spermatozoïdes traversent un environnement protéique changeant au cours de leur migration jusqu'au site de fécondation

1.1. De l'utérus à l'oviducte : les protéines luminales varient en fonction du stade péri-ovulatoire et de la proximité de l'ovaire ovulant

Différentes voies de sécrétion aboutissent à la formation des protéomes luminaux de l'utérus et l'oviducte

Le chapitre 1 offre une première description exhaustive des protéines présentes dans les deux cornes utérines et les deux oviductes avec une segmentation isthme-ampoule en période péri-ovulatoire chez la vache. Les études antérieures sur les sécrétions utérines s'étaient focalisées sur la phase péri-implantatoire des vaches gestantes et la phase lutéale des femelles cyclées (Mullen *et al.*, 2012; Faulkner *et al.*, 2013; Forde *et al.*, 2014). Comparé à l'utérus, un intérêt particulier avait été accordé aux protéines de l'oviducte, sans pour autant distinguer les sécrétions de l'isthme et de l'ampoule (Lamy *et al.*, 2016b; Pillai *et al.*, 2017; Papp *et al.*, 2019), deux régions de morphologie différente et assurant des fonctions bien distinctes autour du moment de la fécondation (cf. synthèse bibliographique). À notre connaissance, une seule étude chez la brebis avait caractérisé le protéome des sécrétions luminales dans l'utérus et l'entièreté de l'oviducte (Soleilhavoup *et al.*, 2016). Cette thèse permet donc de caractériser pour la première fois dans une seule étude un répertoire de protéines luminales des voies génitales femelles de mammifère.

Dans l'utérus et l'oviducte, l'analyse prédictive des voies de sécrétion a montré que seulement 10 à 20% des protéines luminales étaient sécrétées classiquement via un peptide signal et 28% par d'autres voies. De plus, 17 et 41% des protéines avaient respectivement été identifiées dans les vésicules extracellulaires de fluides utérin et d'oviducte bovins. Au total, 57% des protéines dans la lumière utérine et 65% dans la lumière oviductale étaient prédites comme sécrétées. La proportion restante (35 à 43%) sont donc des protéines intracellulaires non attendues dans la lumière, parmi lesquelles on trouve majoritairement des protéines structurales (tubulines, dynéines) et intraorganelles (protéines ribosomales, protéines impliquées dans la transcription et la traduction). Des études antérieures sur le fluide utérin et oviductal bovin ont décrits 74% et 89% respectivement de protéines sans voies prédites, sans considérer la sécrétion par les vésicules extracellulaires (Pillai *et al.*, 2017; Aranciaga *et al.*, 2021).

Les épithéliums utérin et d'oviducte subissent un remodelage important au cours de chaque cycle (Arai *et al.*, 2013; Ito *et al.*, 2016), conduisant au relarguage physiologique de débris cellulaires dans la lumière. La méthode de collecte des fluides par flushing pourrait aussi être à l'origine d'une lyse cellulaire, augmentant artificiellement ce taux de protéines intracellulaires.

L'analyse protéomique de la lumière de l'oviducte a été plus exhaustive que celle de l'utérus, avec 3760 protéines identifiées par deux peptides uniques. Cette disparité dans le nombre de protéines identifiées pourrait provenir de différences au niveau de la méthode de séparation des peptides ionisés (étape supplémentaire de séparation en fonction de leur mobilité pour les fluides d'oviducte). De plus, les protéines fortement abondantes dans les fluides analysés ont probablement masqué le signal d'autres protéines luminales utérines. L'albumine a été quantifiée à des abondances deux à trois fois plus élevées que les autres protéines les plus abondantes dans les sécrétions utérines tandis que, dans l'oviducte, elle est la 5e protéine la plus abondamment quantifiée. Les fluides n'ont pas été déplétées en albumine car cette protéine se lie potentiellement à de nombreuses autres protéines (Menezo and Khatchadourian, 1986) qui auraient également été éliminées et car l'albumine joue un rôle dans la capacitation des spermatozoïdes de taureaux et dans la biodisponibilité de la progestérone (Ehrenwald *et al.*, 1990; Baker, 1998; Bernecic *et al.*, 2019). Il ressort donc de ces résultats que les spermatozoïdes traversent des milieux très riches en albumine dès leur entrée dans l'utérus. De plus, 84% des protéines identifiées dans l'utérus ont été également identifiées dans l'oviducte à des abondances élevées. Les spermatozoïdes traversent donc des milieux contenant globalement les mêmes protéines mais probablement à des abondances différentes.

L'ovulation est une étape clé modifiant la composition des protéomes luminaux

Dans l'utérus, comparé à la proximité de l'ovaire ovulant, le stade du cycle était le facteur impactant le plus l'abondance des protéines, avec 11% de protéines différentielles entre les stades pré- et post-ovulatoires. Dans l'oviducte, 2% de protéines différentiellement abondantes ont été identifiées entre ces deux stades. L'ovulation est donc un facteur de variation de l'abondance des protéines luminales utérines et oviductales. Les précédentes études s'étaient davantage focalisées sur les différences entre la phase folliculaire/estrus et la phase lutéale dans l'utérus et l'oviducte de brebis (Soleilhavoup *et al.*, 2016) et de jument (Maloney *et al.*, 2019) et au cours de la phase lutéale dans l'utérus de vache (Faulkner *et al.*, 2013).

À notre connaissance, seules deux études avaient étudié le protéome en fonction du stade péri-ovulatoire, une chez la vache et l'autre chez la jument, uniquement dans l'oviducte et avaient identifié jusqu'à 17% de protéines différentielles (Lamy *et al.*, 2016b; Fernández-Hernández *et al.*, 2021).

Dans l'utérus, parmi les 35 protéines différentielles entre stades, 21 ont été identifiées au niveau de la corne ipsilatérale, la plus proche de l'ovaire ovulant. Ces changements rapides d'abondance protéique en période péri-ovulatoire pourraient répondre aux besoins des spermatozoïdes pendant leur migration avant l'ovulation, puis de l'embryon après l'ovulation. Par exemple, des protéines comme HSPA5 ou l'échangeur Na+/H+ SLC9A3R1 étaient plus abondantes au stade pré-ovulatoire que juste après l'ovulation. Chez le porcin, des spermatozoïdes incubés avec un antagoniste d'HSPA5 voyaient leur mobilité diminuée comparé à la condition témoin (Lee *et al.*, 2022). À l'inverse, des protéines comme la C-1-tétrahydrofolate synthase, cytoplasmique (MTHFD1) et la tubuline beta TUBB2B étaient plus abondantes en post- qu'en pré-ovulatoire. Chez des souris KO pour le gène MTHFD1, une forte mortalité embryonnaire a été observée (MacFarlane *et al.*, 2009). En revanche, les quelques protéines variant en abondance entre stades dans l'oviducte semblent majoritairement jouer un rôle dans les variations histologiques de l'oviducte au cours du cycle. En effet, dans l'isthme, ces protéines étaient particulièrement impliquées dans la vasomotricité (angiotensinogène AGT) et, dans l'ampoule, dans la régulation de l'assemblage ciliaire et la régulation négative de la prolifération cellulaire (protéines de transport intraflagellaire IFT ou l'inhibiteur de métalloprotéinase TIMP2).

Les protéomes luminaux des cornes utérines et des oviductes ne sont pas symétriques

Les protéines luminales varient également en abondance en fonction de la proximité de l'ovaire ovulant dans l'utérus et l'oviducte : 4 % des protéines quantifiées différaient en abondance entre les deux cornes utérines et 3 à 8 % entre les deux oviductes. Des études transcriptomiques antérieures ont mis en évidence plusieurs centaines de gènes différentiellement exprimés entre les côtés ipsi- et controlatérales dans l'utérus et l'oviducte quelques jours après l'estrus chez le bovin (Locatelli *et al.*, 2019; Sánchez *et al.*, 2019). Ces résultats suggèrent que les protéines varient davantage en abondance dans les cellules épithéliales que dans la lumière.

Chez des vaches cycliques, l'activité contractile et la tonicité de l'utérus et de l'oviducte atteignent un maximum pendant la phase péri-ovulatoire, contribuant probablement à un mélange de protéines pendant cette période (Rodriguez-Martinez *et al.*, 1987; Bennett *et al.*, 1988).

Les protéines de l'oviducte varient particulièrement entre côtés de l'ovulation en période post-ovulatoire dans l'isthme (8% de protéines différentielles). En accord, 13 fois plus de gènes différentiellement exprimés entre côtés avaient été identifiés dans les cellules épithéliales de l'isthme comparé à l'ampoule, 3 jours après l'estrus chez la vache laitière (Locatelli *et al.*, 2019). Dans la même étude, le récepteur à la progestérone était différentiellement exprimé entre côtés mais uniquement dans l'isthme, suggérant que cette région serait plus sensible et réactive à la progestérone. Par ailleurs, les protéines différentiellement abondantes entre côtés dans l'isthme post-ovulatoire pourraient avoir des fonctions importantes dans le développement embryonnaire précoce. Leur implication prédite par l'analyse fonctionnelle dans la voie des PI3-kinases est en faveur de cette hypothèse. Chez l'humain, le bovin et la souris, un inhibiteur spécifique de protéines impliquées dans la voie des PI3-kinases diminuait la proportion de spermatozoïdes ayant réalisé leur réaction acrosomique induite par de l'AMP cyclique ou du ionophore calcique (Breitbart *et al.*, 2010). De même chez la souris, une inhibition pharmacologique des PI3 kinases dans le milieu de culture diminuait le nombre d'embryons atteignant le stade morula (Lu *et al.*, 2004).

Avantages et inconvénients de la collecte en abattoir

Une limite commune à ces études protéomiques est l'origine du matériel biologique utilisé, collecté en abattoir sur des femelles dont on ne connait ni l'historique, ni le statut métabolique et ni l'origine génétique. Néanmoins, l'abattoir a permis d'inclure un nombre important d'animaux dans les analyses (32 pour l'oviducte, 16 pour l'utérus). Techniquement, il n'aurait pas été possible de séparer le fluide d'ampoule de celui d'isthme par des collectes *in vivo* après cannulation de l'oviducte sous anesthésie. Pour limiter les modifications post-mortem, les utérus et oviductes ont été immédiatement placés sur glace et ce, pendant toute la durée du transport entre l'abattoir et le laboratoire, mais il n'est pas exclu que les protéines aient subit des modifications mineures. Un gros avantage de la méthode de collecte post-mortem est l'absence de contamination par des cellules sanguines ou inflammatoires, mesurées à des niveaux supérieurs dans des fluides collectés après cannulation des oviductes sous anesthésie que ceux collectés après abattage de l'animal (Pillai *et al.*, 2017; Papp *et al.*, 2019).

La détermination des stades du cycle à partir de la morphologie des ovaires est également une méthode fiable, validée dans le laboratoire par des analyses antérieures d'hormones stéroïdiennes (Lamy *et al.,* 2016a) et l'abattage de vaches à différents stades après synchronisation des chaleurs (Banliat *et al.*, 2022).

1.2. De l'isthme à l'ampoule : les protéines interagissant avec les spermatozoïdes varient en fonction de la région anatomique et du stade péri-ovulatoire

La composition initiale du fluide d'oviducte détermine les interactions avec la surface du spermatozoïde

Étant donné l'impossibilité d'accéder à la lumière de l'oviducte *in vivo,* nous avons co-incubé des spz avec des fluides d'oviducte de différentes origines *in vitro* pour évaluer l'effet de la région anatomique et du stade péri-ovulatoire sur les interactions spz-protéines. Il a été envisagé d'injecter des spz dans des sections d'oviducte *ex vivo* mais les modifications post-mortem rapides de l'épithélium et la nécessité d'obtenir au moins 7 µg de protéines pour les analyses protéomiques nous ont fait préférer la méthode de co-incubation *in vitro*. L'objectif étant d'évaluer les effets femelles sur les interactions, le même pool de semences pour toutes les analyses a été utilisé.

Les proportions de protéines différentielles entre régions et entre stades, analysées avec les mêmes méthodes, étaient plus importantes sur les spermatozoïdes qu'au sein des fluides d'oviducte. Sur les spermatozoïdes, de 9 à 31% des protéines étaient différentiellement abondantes entre stades contre seulement 2% dans les fluides. De même, 10 à 18% des protéines d'interaction étaient différentiellement abondantes entre régions contre 8 à 12% dans le fluide. Ces résultats montrent que des changements mineurs de la composition des fluides induisent des changements importants des interactions spz-protéines au sein de ces fluides. Par ailleurs, pour le protéome du fluide, l'analyse en composante principale et les comparaisons deux à deux ont révélé que la région était la plus grande source de variation de l'abondance protéique devant la proximité de l'ovaire ovulant et le stade péri-ovulatoire. Sur les spermatozoïdes, le stade du cycle semble être le facteur jouant le plus sur le protéome d'interaction, en particulier dans l'ampoule (31% de protéines différentielles).

La régulation fine des protéines d'interaction pourrait être un moyen de répondre aux besoins spécifiques des spermatozoïdes au cours de leur migration dans l'oviducte : leur survie dans l'isthme pré-ovulatoire, leur capacitation dans l'ampoule pré-ovulatoire et la fécondation dans l'ampoule post-ovulatoire. Par exemple, la myosine-9 était l'une des protéines les plus abondantes dans le fluide et la plus abondante sur les spermatozoïdes. Avec d'autres myosines (MYH10, MYL9), elle était également différentiellement régulée sur les spermatozoïdes entre stades dans l'ampoule et entre régions au stade post-ovulatoire. Ces myosines non-musculaires de classe II ont été décrites pour être particulièrement impliquées dans la migration, l'adhésion et le mouvement cellulaire (Li and Bresnick, 2006; Sung *et al.*, 2021). En particulier, il a été montré que MYH9 interagissait avec une autre protéine, S100A4, pour favoriser la mobilité des cellules cancéreuses humaines (Li and Bresnick, 2006). Cependant, le rôle direct de la myosine-9 sur la mobilité et la capacitation des spermatozoïdes n'a pas encore été étudié à ce jour. La littérature lui a en revanche attribué des rôles dans l'exocytose cellulaire (Wassarman, 1999; Pons-Rejraji *et al.*, 2009), un processus essentiel pour la réaction acrosomique. À l'inverse, d'autres protéines avec des abondances différentielles entre régions dans le fluide d'oviducte interagissaient à des niveaux similaires avec les spermatozoïdes tout au long de l'oviducte. Par exemple, les protéines de chocs thermiques HSP90B1 et HSPA5 étaient plus abondantes dans l'isthme que l'ampoule mais quantifiées à des valeurs similaires dans le protéome d'interaction spermatique de ces deux régions. Ces protéines ont des rôles connus sur la physiologie spermatique : HSPA5 accroît l'influx calcique pendant la capacitation des spermatozoïdes humains (Lachance *et al.*, 2007). Chez le porcin et l'humain, l'addition de HSP90B1 et HSPA5 purifiées au milieu de culture favorise la liaison des spermatozoïdes à la zone pellucide de l'ovocyte (Marín-Briggiler *et al.*, 2010; Mondéjar *et al.*, 2013). Un autre exemple concerne l'oviductine qui était plus abondante dans l'ampoule que dans l'isthme au stade post-ovulatoire mais quantifiée à des niveaux relativement constants sur les spz. Cette protéine joue vraisemblablement des rôles importants à la fois dans l'isthme et l'ampoule. L'oviductine, qu'elle soit purifiée ou recombinante, influence positivement la viabilité, la motilité et la capacitation des spermatozoïdes chez le buffle et l'humain (Zhao *et al.*, 2016; Choudhary *et al.*, 2017). De plus, l'ajout d'oviductine recombinante dans du milieu de fécondation améliore la liaison entre les spz et la zone pellucide chez le hamster et l'homme (Yang *et al.*, 2015; Zhao *et al.*, 2016).

Les spermatozoïdes interagissent de manière sélective avec des protéines solubles et intra-vésiculaires sécrétées dans la lumière de l'oviducte

Les 245 protéines d'interaction identifiées correspondent à seulement 10 % de toutes les protéines quantifiées dans les fluides. De plus, l'analyse prédictive des voies de sécrétion a révélé que 83% des protéines d'interaction étaient sécrétées dans le fluide oviductal, contre 65% pour toutes les protéines luminales, suggérant que les spermatozoïdes sélectionnent des protéines sécrétées. Par ailleurs, 78% des protéines d'interaction ont été précédemment identifiées dans les vésicules extracellulaires de vache, contre 41% pour toutes les protéines du fluide d'oviducte (Almiñana *et al.*, 2017; Ferraz *et al.*, 2019; Laezer *et al.*, 2020). Ces résultats suggèrent que les spz interagissent avec les vésicules extracellulaires des fluides (centrifugés à 12 000 *g* donc non déplétés en exosomes) pendant les 60 minutes d'incubation. Les interactions spz-EV ont été mises en évidence récemment chez le bovin, le chat et le porc, rapportant une interaction rapide (en 15 minutes) ayant des effets positifs sur la mobilité, l'intégrité de l'acrosome, l'influx calcique lors de la capacitation et la monospermie (Ferraz *et al.*, 2019; Franchi *et al.*, 2019; Alcântara-Neto *et al.*, 2020).

L'abondance des protéines sur les spermatozoïdes n'était pas corrélée à leur abondance initiale dans les fluides, suggérant une interaction spécifique avec les protéines identifiées, confirmée pour certaines par western-blot. Pour localiser ces interactions sur les spz et en évaluer les rôles, des immunocytochimies contre plusieurs protéines d'interaction (annexine A1, myosine 9, oviductine, tubuline alpha 8) ont été réalisées. Cependant, le signal obtenu était soit non-spécifique (signal positif avec l'immunoglobuline correspondant à l'anticorps primaire), soit similaire entre les spermatozoïdes témoins (pré-incubés dans le PBS) et ceux pré-incubés dans le fluide. Ces résultats mettent en lumière la difficulté d'obtenir des anticorps spécifiques et adaptés à l'immunocytochimie du spermatozoïde, cellule recouverte de spermadhésines (BSPs) avec une forte affinité de liaison pour une grande diversité de glycoprotéines y compris visiblement des immunoglobulines (Plante *et al.*, 2016). Ces résultats posent également question sur la spécificité des interactions identifiées dans nos conditions expérimentales *in vitro* (fluide fortement dilué, incubation courte d'1h), conditions assez éloignées des conditions physiologiques.

En résumé, le protéome luminal est régulé de manière différentielle en fonction du stade péri-ovulatoire et de la proximité de l'ovaire ovulant dans l'utérus et l'oviducte, probablement pour orchestrer dans le premier l'élimination des spermatozoïdes anormaux et dans le second leur survie et capacitation. Au sein de l'oviducte, les protéines interagissant avec les spz sont affectées à la fois par le stade péri-ovulatoire et la région traversée, ce qui permettrait de cibler et répondre rapidement aux besoins contrastés des spermatozoïdes au cours de leur migration avant (maintien de la viabilité) et après (capacitation) l'ovulation (figure 15 page 194).

2. L'interaction des spermatozoïdes avec le fluide d'oviducte modifie leur physiologie et leur capacité à se lier au réservoir spermatique

2.1. L'isthme et l'ampoule modulent différemment la physiologie des spermatozoïdes mais ces différences sont discrètes

Dans nos conditions, les effets du fluide d'oviducte sur la mobilité ne sont visibles qu'en tout début d'incubation (5 à 10 min) : la proportion de spz mobiles et progressifs était plus élevée dans l'ampoule pré-ovulatoire que dans l'isthme post-ovulatoire. L'ampoule post-ovulatoire avait aussi un effet positif sur la mobilité progressive et les battements flagellaires par rapport aux fluides d'isthme. Pendant la phase folliculaire, une étude antérieure chez le bovin mettait aussi en évidence une proportion de spz mobiles deux fois plus importante dans des flushs d'ampoule que dans des flushs d'isthme après 1 h d'incubation (Abe *et al.*, 1995a). En accord avec nos résultats, des vésicules extracellulaires extraites de fluides d'ampoule interagissaient avec les spz et induisaient en l'espace de 5 min un influx calcique plus important que celui des fluides d'isthmes bovins (Franchi *et al.*, 2019). Parmi les protéines d'interaction spermatique identifiées après 1 h d'incubation, une grande proportion différait en abondance entre ampoule et isthme (10-18%), dont des myosines (MYH9,10, MYL9, TPM3), ce qui pourrait participer aux mécanismes menant à ces différences de mobilité visibles en début d'incubation

Hormis la région, un effet du stade péri-ovulatoire sur la réaction acrosomique a également été identifié dans l'isthme, mais seulement après 3 heures d'incubation. Les spermatozoïdes incubés dans le fluide d'isthme post-ovulatoire étaient significativement plus nombreux à faire leur réaction acrosomique induite par l'ionophore calcique comparés à l'isthme pré-ovulatoire après 3 h et à la condition témoin après 6 h. Ces résultats vont de pair avec l'augmentation de la fluidité membranaire (coloration par la mérocyanine) observée dans l'isthme post-ovulatoire après 6 h d'incubation. En parallèle de ces effets différentiels sur la réaction acrosomique dans l'isthme, une variation importante des protéines d'interaction dans cette région a été observée. En effet, entre fluides d'isthme pré-ovulatoire et post-ovulatoire, le nombre de protéines d'interaction change (de 187 à 128) et 9 % des protéines diffèrent en abondance. Ces protéines pourraient être des acteurs majeurs dans les changements membranaires et acrosomales des spermatozoïdes dans l'isthme avant et après l'ovulation.

2.2. Les sécrétions de l'oviducte ont un effet majeur sur la liaison des spermatozoïdes au réservoir

Les sphéroïdes : un nouveau modèle pour étudier les interactions dans l'oviducte

Après quelques jours de culture, les fragments de muqueuse d'oviducte forment une cavité centrale, le côté apical des cellules orienté à l'extérieur. Cette disposition spontanée des cellules facilite l'étude des interactions avec les spermatozoïdes, mais aussi les embryons. Comparé aux autres modèles *in vitro* évoqués dans l'étude bibliographique, les sphéroïdes offrent plusieurs avantages. D'une part, les sphéroïdes sont rapidement formés, après seulement 2 à 3 jours de culture, avec des cellules d'origine épithéliale bien différenciées et de vigoureux battements ciliaires. Au contraire, le modèle de cellules en monocouche sur plastique nécessitait 7 à 10 jours de culture pour obtenir des cellules à confluence mais partiellement dédifférenciées (Schmaltz-Panneau *et al.*, 2015). Facilement manipulables, les sphéroïdes peuvent être sélectionnés afin de constituer une population homogène en taille et en forme, offrant ainsi entre conditions expérimentales la même surface de liaison aux spermatozoïdes. Les explants ou fragments d'oviducte en suspension utilisés quelques heures après la mise en culture, sont également un modèle physiologique d'épithélium facilement manipulable mais avec des agrégats de cellules de formes et tailles très hétérogènes (De Pauw *et al.*, 2002).

D'autre part, les sphéroïdes sont arrondis et comptent en moyenne 25% de cellules ciliées, les battements ciliaires créant des microflux de fluide, à l'image de l'environnement traversé par les spermatozoïdes dans l'oviducte *in vivo*. Tel qu'i*n vivo*, 85% des spermatozoïdes se lient aux cellules ciliées via leur tête avec un acrosome et une membrane intacte (Sostaric *et al.*, 2008; Ito *et al.*, 2016). Néanmoins, les sphéroïdes reproduisent seulement la couche épithéliale de l'oviducte, sans considérer la morphologie tridimensionnelle complexe de cet organe (nombreux replis muqueux) ni ses couches cellulaires sous-jacentes (fibroblastes, endothélium et apport d'hormones par les vaisseaux sanguins), qui ont nécessairement un impact sur les interactions avec les spz.

Particularités des interactions spermatiques dans l'isthme pré-ovulatoire

Le nombre maximum de protéines interagissant avec les spz (187/245) a été identifiée dans l'isthme pré-ovulatoire, lieu et moment supposé du réservoir. Ces résultats soulignent la particularité de cet environnement pour les gamètes mâles. Chez le bovin, ce stockage est médié par la liaison des spz aux cellules épithéliales de l'oviducte via des glycoprotéines membranaires, notamment les annexines A1, A2, A4 et A5, et les protéines de chocs thermiques HSPA5 et A8 (Boilard *et al.*, 2004; Ignotz *et al.*, 2007; Elliott *et al.*, 2009). Ces protéines figuraient parmi les protéines d'interaction les plus abondantes dans l'isthme au stade pré-ovulatoire. Dès leur entrée dans l'oviducte, les spermatozoïdes interagissent d'abord avec le fluide, puis probablement, pour une partie d'entre eux seulement, avec les cellules luminales ciliées. Les rares images *in vivo* chez la souris montrent qu'au cours de leur migration, les spz peuvent se lier et se détacher de ces cellules puis répéter cette action jusqu'à leur arrivée au niveau de l'ovocyte (Chang and Suarez, 2012). Néanmoins, la proportion de spz qui se lient aux cellules, la séquence exacte des interactions avec les cellules, et les fonctions de ces interactions restent pour le moment des énigmes.

Par ailleurs, le rôle des protéines d'interaction peut différer en fonction de leur localisation sur le spz. D'après des études antérieures, des protéines comme l'oviductine et HSPA8 peuvent se lier à la tête mais également à la pièce intermédiaire et au flagelle (Abe *et al.*, 1995b; Elliott *et al.*, 2009). Or, les spz se lient quasiment exclusivement par leur tête aux cellules ciliées. Les protéines interagissant au niveau de la tête pourraient donc interférer avec la liaison aux cils tandis que celles de la pièce intermédiaire et du flagelle pourraient jouer un rôle sur d'autres paramètres comme la mobilité.

Les protéines d'interaction pourraient aussi participer au maintien de la viabilité spermatique (Boilard *et al.*, 2004). Parmi elles, la peroxiredoxine-6 (PRDX6) était la plus abondante parmi celles spécifiquement identifiées dans l'isthme pré-ovulatoire. Chez l'humain, une incubation avec un inhibiteur de PRDX6 augmente la proportion de spermatozoïdes avec des dommages à l'ADN et une oxydation lipidique (Fernandez and O'Flaherty, 2018). Cette protéine pourrait donc participer au maintien de la viabilité des spz lors de leur stockage dans l'isthme en période pré-ovulatoire.

Les macromolécules sécrétées dans la lumière de l'oviducte inhibent la liaison des spermatozoïdes aux cellules épithéliales

La co-incubation simultanée entre spermatozoïdes, sphéroïdes et fluide d'oviducte a montré que le fluide empêche, dès les 5 premières minutes, la liaison d'une sous-population de spz aux cellules épithéliales sans altérer ni leur mobilité ni l'intégrité de leur membrane. Ce résultat suggère que le fluide sélectionne rapidement une sous-population de spz capables de se lier au réservoir. Chez le porcin, l'humain et le bovin, seuls des spz mobiles, non capacités, avec une membrane et un acrosome intact sont capables de se lier à des cellules épithéliales d'oviducte dans un milieu non capacitant *in vitro* (Lefebvre and Suarez, 1996; Ellington *et al.*, 1999; Gualtieri and Talevi, 2000; Petrunkina *et al.*, 2004). Le fluide exercerait donc une sélection encore plus stricte sur la qualité des spz pour la liaison au réservoir avant l'ovulation.

Sachant que les protéines préalablement identifiées comme récepteurs spermatiques sur les cellules ont aussi été identifiées dans cette thèse comme protéine d'interaction dans le fluide, notre hypothèse était qu'une compétition de liaison vis-à-vis de ces protéines entre les deux compartiments (fluide vs. membrane) menait à la diminution de nombre de spz pouvant se lier. Nous avons mis en évidence que les chaines protéiques des glycoprotéines solubles et les protéines non glycosylées du fluide n'étaient pas impliquées dans l'effet inhibiteur sur la liaison spermatique. De plus, l'annexine A1, identifiée comme récepteur spermatique à la surface des cellules (Ignotz *et al.*, 2007) et comme protéine d'interaction dans notre étude, n'avait aucun effet sur la liaison des spermatozoïdes aux sphéroïdes. En revanche, les N-glycanes liés à ces protéines semblent jouer un rôle dans l'effet du fluide. Donc notre hypothèse de travail n'est pas invalidée : il y aurait bien une compétition de liaison entre les chaines sucrées des glycoprotéines du fluide et celles exprimées à la surface des cellule épithéliales. Pour l'instant, la proportion de protéines N-glycosylées parmi les protéines d'interaction dans le fluide, mais aussi à la surface des cellules d'oviducte, est inconnue.

D'autres sucres à haut poids moléculaire, libres ou liées à des protéines dans le fluide, semblent également impliqués dans l'effet du fluide sur la liaison. C'est le cas du sulfate d'héparane, le plus abondant glycosaminoglycane sulfaté du fluide d'oviducte (Lee and Ax, 1984). En effet, le fluide traité aux héparinases diminuent la liaison des spermatozoïdes aux cellules mais dans une moindre mesure comparé au fluide natif (60 vs 80%). Son homologue, l'héparine, est classiquement utilisé pour la capacitation des spz de taureau *in vitro* mais aussi comme agent libérateur des spz des cellules épithéliales d'oviducte (Parrish *et al.*, 1989; Ardon *et al.*, 2016). La progestérone a également été proposée comme agent libérateur du réservoir chez le bovin et le porcin (Lamy *et al.*, 2017; Machado *et al.*, 2019). À doses physiologiques chez la vache et la truie (autour de 5 ng/mL en période pré-ovulatoire et 50 ng/mL après l'ovulation), cette hormone libère 30 à 50 % des spermatozoïdes liés à des cellules épithéliales d'oviducte *in vitro* (Ballester *et al.*, 2014; Lamy *et al.*, 2016b, 2017; Machado *et al.*, 2019). Cette libération par la progestérone améliore les taux de fécondation et d'embryons au stade blastocyste comparé à une libération spontanée de spz à des monocouches cellulaires chez le bovin (Lamy *et al.*, 2017). De manière inattendue, nous avons observé que la progestérone seule à 1 ng/mL augmentait la densité de spz liés aux sphéroïdes comparés au milieu témoin, et ne participait donc pas à l'effet du fluide. La progestérone mesurée à 1 ng/mL dans le fluide d'oviducte pré-ovulatoire ne semble donc pas bioactive dans nos conditions *in vitro*. Comme dans le plasma circulant, la progestérone peut être liée temporairement à des protéines comme l'albumine, un médiateur connu du transport de cette hormone dans le sang et l'une des protéines les plus abondantes dans le fluide d'oviducte (Watanabe *et al.*, 1991; Mahé *et al.*, 2022). Nos résultats posent la question de la bioactivité et du véritable rôle de la progestérone dans la régulation du réservoir spermatique chez les mammifères.

Enfin, le fluide ajouté aux complexes sphéroïdes-spz déjà formés libère 80% des spz liés aux cellules. Nos hypothèses sont donc que les glycoprotéines et GAG sulfatés du fluide, par des mécanismes de compétition et de masquage des sites de liaison des BSPs, sélectionnent une sous-population de spz capables de se lier au réservoir et participent à leur libération en période péri-ovulatoire. Cette liaison - libération participerait à la sélection de spermatozoïdes à haut potentiel fécondant.

En résumé, dans l'oviducte, les protéines luminales interagissent avec les spz de manière différentielle entre régions de l'oviducte, probablement pour moduler leur attachement aux cellules épithéliales et leur capacitation en période péri-conceptionnelle. Au niveau de l'isthme, le fluide sélectionne une sous population de spermatozoïdes pour la liaison aux cellules. Il a probablement aussi un effet libérateur sur ces spz après l'ovulation (figure 15 page 194).

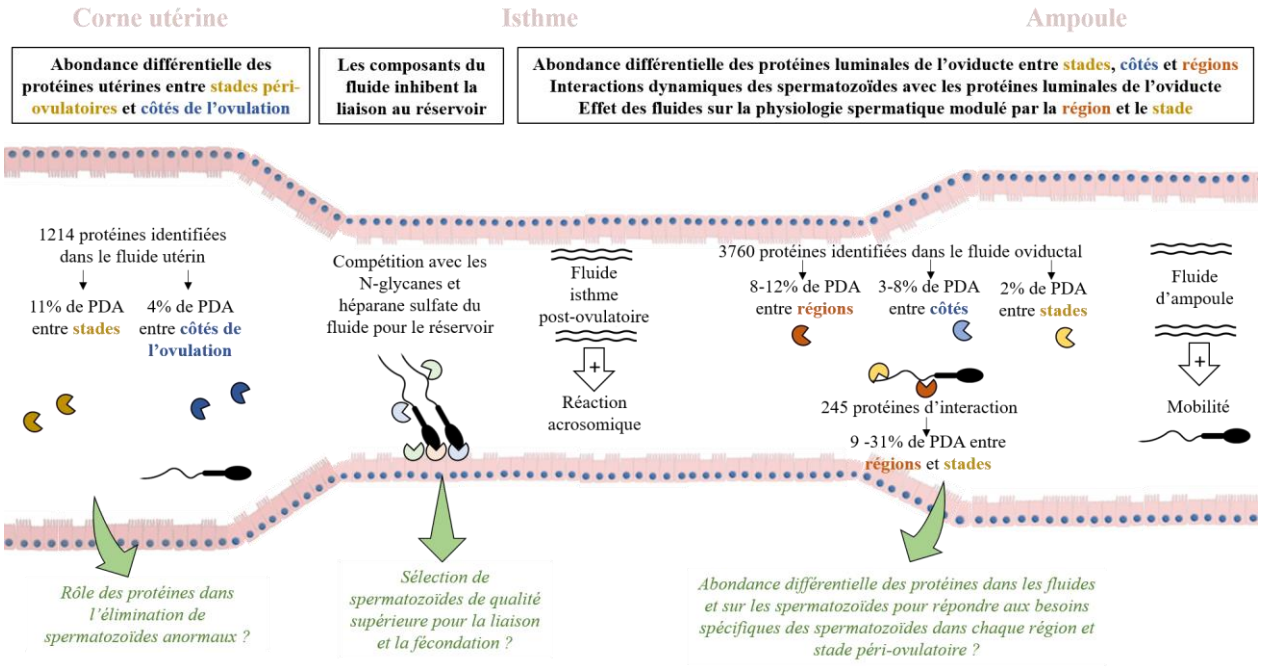

Figure 15 : Illustration des résultats et hypothèses sur les interactions fonctionnelles entre les spermatozoïdes et l'environnement maternel en période péri-conceptionnelle.

PDA = protéines différentiellement abondantes ; spz = spermatozoïdes

3. Perspectives

3.1. Raffiner le modèle de réservoir *in vitro*

Une perspective de ce travail serait de mettre en place un modèle d'oviducte *in vitro* reproduisant les microflux et l'anatomie complexe de la lumière de cet organe, permettant une étude plus physiologique des interactions avec les gamètes et l'embryon. Le but du modèle serait de reproduire le flux à contre-courant de migration des spermatozoïdes *in vivo* grâce notamment au système micro-fluidique (Ferraz *et al.*, 2017). Le principe serait de faire séquentiellement migrer les spermatozoïdes dans des fluides et/ou des protéines produits *in vitro* issu(e)s de l'utérus pré-ovulatoire, de l'isthme pré-ovulatoire en présence de sphéroïdes puis de l'ampoule post-ovulatoire en présence d'ovocytes maturés *in vitro*. Afin d'éviter d'utiliser du matériel provenant d'abattoir, un objectif serait de créer des milieux synthétiques proches de l'environnement protéique *in vivo*. Ces travaux ont permis de mettre en lumière des protéines candidates pouvant être utiliser pour générer, à l'aide de protéines recombinantes, ces milieux se rapprochant de ceux rencontrés par les spermatozoïdes *in vivo* dans l'utérus et l'oviducte. De plus, le répertoire protéique décrit dans ces études permet également d'avoir une référence pour des milieux synthétisés par les sphéroïdes en culture.

3.2. Comprendre les mécanismes d'interaction avec les protéines luminales du tractus femelle

Une première perspective serait d'étudier la spécificité des interactions protéiques identifiées, en utilisant soit des fluides biologiques non habituellement rencontrés par les spermatozoïdes (fluide hors tractus femelle) ou en incubant des fluides bovins avec des spermatozoïdes issus d'autres espèces animales. Cette spécificité pourrait également être évaluée en identifiant les protéines oviductales interagissant avec d'autres types cellulaires comme des fibroblastes ou des globules rouges.

Une autre perspective concerne l'origine de ces protéines d'interaction et le rôle des vésicules extracellulaires dans les interactions. De précédentes études chez le bovin ont montré que les vésicules extracellulaires d'isthme et d'ampoule interagissaient principalement avec la tête du spermatozoïdes et avaient des effets différentiels sur l'influx calcique, étape clé de la capacitation (Franchi *et al.*, 2019). Néanmoins, les potentielles différences d'interaction pendant la période péri-ovulatoire dans l'ampoule et l'isthme n'ont pas encore été étudié. Pour répondre à cette question, les spermatozoïdes seront incubés avec des vésicules extracellulaires d'isthme et d'ampoule au stade pré- et post-ovulatoire afin de déterminer la localisation, les mécanismes d'interaction ainsi que leurs effets sur la physiologie spermatique. Il sera intéressant de suivre si certaines protéines intra-exosomales s'internalisent dans les spz par immunogold et microscopie électronique.

Enfin, une autre perspective serait de comprendre l'effet de facteurs mâles sur les interactions avec les protéines du fluide. L'état physiologique des spermatozoïdes évolue au cours de leur migration : est-ce que les protéines interagissent de la même façon avec des spermatozoïdes capacités, en hyperactivation, ayant fait leur réaction acrosomique ? Pour répondre à ces questions, des fluides pourraient être incubés avec des semences issues de taureaux à proportions contrastées de spz anormaux ou préalablement triés en cytométrie de flux pour différents paramètres (taux de survie, d'acrosome intact). Il serait aussi intéressant de tester des semences issues de taureaux à fertilité contrastée *in vivo*.

3.3. Mieux comprendre les mécanismes d'inhibition de la liaison aux cellules par le fluide d'oviducte

La principale perspective est de préciser les mécanismes mis en jeu dans l'effet du fluide sur la liaison des spermatozoïdes aux sphéroïdes. D'abord, est-ce que cet effet passe par les spermatozoïdes, les sphéroïdes, ou les deux ? Des pré-incubations avec le fluide soit des sphéroïdes soit des spz permettrait de répondre à cette question. Ensuite, d'autres composés que les N-glycanes et l'héparane sulfate sont impliqués puisque l'élimination de ces molécules n'annule pas complètement les effets inhibiteurs du fluide (le fluide pré-digéré par les héparinases et la fraction > 5 kDa sans N-glycanes continuent à inhiber la liaison des spz aux sphéroïdes).

Il nous reste à tester l'élimination des O-glycanes liés aux protéines solubles et l'effet d'autres glycosaminoglycanes sulfatés sur la liaison. L'élimination de la O-glycosidase du fluide après réaction enzymatique est un problème à résoudre (pas d'enzyme commerciale taggée comme la PNGase F).

Ensuite, l'effet de la séquence liaison-libération des spermatozoïdes aux sphéroïdes sur la capacité fécondante des spz est également une piste à explorer. Le système micro-fluidique permettrait notamment de mettre en contact les spermatozoïdes dans une première chambre avec des sphéroïdes et du fluide, puis dans une seconde chambre avec des complexe ovocyte-cumulus. Il serait également intéressant de comparer en termes de physiologie et capacité fécondante les sous-populations de spermatozoïdes liés aux sphéroïdes et libres dans le milieu en présence du fluide d'oviducte et dans le milieu témoin.

Conclusion générale

Comprendre comment la femelle régule la physiologie et la migration des spermatozoïdes au cours de leur migration était le fil conducteur de cette thèse. Ce travail a permis de mettre en évidence une régulation complexe et spécifique des protéines luminales de l'utérus et des différentes régions de l'oviducte. Ce travail a également mis à jour plusieurs dizaines de protéines interagissant différentiellement avec les spz selon la composition initiale des sécrétions femelles. Cette régulation dynamique et fine des interactions mâle-femelle contribue probablement à l'acquisition de la fécondance des spermatozoïdes dans l'ampoule post-ovulatoire, c'est-à-dire au bon endroit et au bon moment pour la fécondation. Ces données mettent donc en lumière des protéines pouvant être potentiellement utilisées dans les milieux de conservation des spermatozoïdes pour l'insémination artificielle, la fécondation *in vitro* et la conservation de la biodiversité animale. Enfin, le développement d'un nouveau modèle de réservoir *in vitro* a permis de mettre en évidence un effet sélectif du fluide d'oviducte pour la liaison aux cellules épithéliales de l'isthme, participant probablement à la sélection des meilleurs pour la fécondation. Mimer *in vitro* l'environnement rencontré *in vivo* par les spermatozoïdes dans l'oviducte permettrait de mieux comprendre cette sélection et de l'utiliser pour trouver de nouveaux marqueurs de fertilité et améliorer l'aptitude au développement des embryons produits *in vitro*.

Bibliographie

Abe H and Oikawa T (1993) Observations by scanning electron microscopy of oviductal epithelial cells from cows at follicular and luteal phases. *The Anatomical Record* **235** 399–410.

Abe H, Sendai Y, Satoh T and Hoshi H (1995a) Secretory products of bovine oviductal epithelial cells support the viability and motility of bovine spermatozoa in culture in vitro. *The Journal of Experimental Zoology* **272** 54–61.

Abe H, Sendai Y, Satoh T and Hoshi H (1995b) Bovine oviduct-specific glycoprotein: A potent factor for maintenance of viability and motility of bovine spermatozoa in vitro. *Molecular Reproduction and Development* **42** 226–232.

Alcântara-Neto AS, Schmaltz L, Caldas E, Blache M-C, Mermillod P and Almiñana C (2020) Porcine oviductal extracellular vesicles interact with gametes and regulate sperm motility and survival. *Theriogenology* **155** 240–255.

Akthar I, Suarez SS, Morillo VA, Sasaki M, Ezz MA, Takahashi K, Shimada M, Marey MA and Miyamoto A (2020) Sperm enter glands of preovulatory bovine endometrial explants and initiate inflammation. *Reproduction* **159** 181–192.

Alavi-Shoushtari SM, Asri-Rezai S and Abshenas J (2006) A study of the uterine protein variations during the estrus cycle in the cow: A comparison with the serum proteins. *Animal Reproduction Science* **96** 10–20.

Almiñana C, Corbin E, Tsikis G, Alcântara-Neto AS, Labas V, Reynaud K, Galio L, Uzbekov R, Garanina AS, Druart X *et al.* (2017) Oviduct extracellular vesicles protein content and their role during oviduct–embryo cross-talk. *Reproduction* **154** 253–268.

Almiñana C, Tsikis G, Labas V, Uzbekov R, da Silveira JC, Bauersachs S and Mermillod P (2018) Deciphering the oviductal extracellular vesicles content across the estrous cycle: implications for the gametes-oviduct interactions and the environment of the potential embryo. *BMC Genomics* **19** 622.

Almiñana C, Rudolf Vegas A, Tekin M, Hassan M, Uzbekov R, Fröhlich T, Bollwein H and Bauersachs S (2021) Isolation and characterization of equine uterine extracellular vesicles: a comparative methodological study. *International Journal of Molecular Sciences* **22** 979.

Arai M, Yoshioka S, Tasaki Y and Okuda K (2013) Remodeling of bovine endometrium throughout the estrous cycle. *Animal Reproduction Science* **142** 1–9.

Aranciaga N, Morton JD, Maes E, Gathercole JL and Berg DK (2021) Proteomic determinants of uterine receptivity for pregnancy in early and mid-postpartum dairy cows. *Biology of Reproduction* **105** 1458–1473.

Ardon F, Markello RD, Hu L, Deutsch ZI, Tung C-K, Wu M and Suarez SS (2016) Dynamics of bovine sperm interaction with epithelium differ between oviductal isthmus and ampulla. *Biology of Reproduction* **95** 90–90.

Austin CR (1951) Observations on the penetration of the sperm into the mammalian egg. *Australian Journal of Biological Sciences* **4** 581–596.

Avilés M, Gutiérrez-Adán A and Coy P (2010) Oviductal secretions: will they be key factors for the future ARTs? *MHR: Basic Science of Reproductive Medicine* **16** 896–906.

Baker RD and Degen AA (1972) Transport of live and dead boar spermatozoa within the reproductive tract of gilts. *Reproduction* **28** 369–377.

Baker ME (1998) Albumin's role in steroid hormone action and the origins of vertebrates: is albumin an essential protein? *FEBS Letters* **439** 9–12.

Ballester L, Romero-Aguirregomezcorta J, Soriano-Úbeda C, Matás C, Romar R and Coy P (2014) Timing of oviductal fluid collection, steroid concentrations, and sperm preservation method affect porcine in vitro fertilization efficiency. *Fertility and Sterility* **102** 1762-1768.e1.

Banliat C, Tomas D, Teixeira-Gomes A-P, Uzbekova S, Guyonnet B, Labas V and Saint-Dizier M (2019) Stage-dependent changes in oviductal phospholipid profiles throughout the estrous cycle in cattle. *Theriogenology* **135** 65–72.

Banliat C, Mahé C, Lavigne R, Com E, Pineau C, Labas V, Guyonnet B, Mermillod P and Saint-Dizier M (2022) Dynamic changes in the proteome of early bovine embryos developed in vivo. *Frontiers in Cell and Developmental Biology* **10** 863700.

Barone R (2001) Splanchnologie II. *Anatomie comparée des mammifères domestiques*. **4**

Barrios B (2005) Immunocytochemical localization and biochemical characterization of two seminal plasma proteins that protect ram spermatozoa against cold shock. *Journal of Andrology* **26** 539–549.

Bathala P, Fereshteh Z, Li K, Al-Dossary AA, Galileo DS and Martin-DeLeon PA (2018) Oviductal extracellular vesicles (oviductosomes, OVS) are conserved in humans: murine OVS play a pivotal role in sperm capacitation and fertility. *MHR: Basic Science of Reproductive Medicine*.

Battistelli M and Falcieri E (2020) Apoptotic bodies: particular extracellular vesicles involved in intercellular communication. *Biology* **9** 21.

Bedford JM and Yanagimachi R (1992) Initiation of sperm motility after mating in the rat and hamster. *Journal of Andrology* **13** 444–449.

Bennett WA, Watts TL, Blair WD, Waldhalm SJ and Fuquay JW (1988) Patterns of oviducal motility in the cow during the oestrous cycle. *Journal of Reproduction and Fertility* **83** 537–543.

Bergqvist A-S and Rodríguez-Martínez H (2006) Sulphated glycosaminoglycans (S-GAGs) and syndecans in the bovine oviduct. *Animal Reproduction Science* **93** 46–60.

Bergqvist A-S, Yokoo M, Heldin P, Frendin J, Sato E and Rodríguez-Martínez H (2005) Hyaluronan and its binding proteins in the epithelium and intraluminal fluid of the bovine oviduct. *Zygote* **13** 207–218.

Bernecic NC, Gadella BM, de Graaf SP and Leahy T (2020) Synergism between albumin, bicarbonate and cAMP upregulation for cholesterol efflux from ram sperm. *Reproduction* **160** 269–280.

Boilard M, Reyes-Moreno C, Lachance C, Massicotte L, Bailey JL, Sirard M-A and Leclerc P (2004) Localization of the chaperone proteins GRP78 and HSP60 on the luminal surface of bovine oviduct epithelial cells and their association with spermatozoa. *Biology of Reproduction* **71** 1879–1889.

Breitbart H, Rotman T, Rubinstein S and Etkovitz N (2010) Role and regulation of PI3K in sperm capacitation and the acrosome reaction. *Molecular and Cellular Endocrinology* **314** 234–238.

Caetano LC, Verruma CG, Pinaffi FLV, Jardim IB, Furtado GP, Silva LA, Furtado CLM and Rosa-e-Silva ACJ de S (2022) *In vivo* and *in vitro* matured bovine oocytes present a distinct pattern of single-cell gene expression. *Zygote* 1–13.

Cerny KL, Garrett E, Walton AJ, Anderson LH and Bridges PJ (2015) A transcriptomal analysis of bovine oviductal epithelial cells collected during the follicular phase versus the luteal phase of the estrous cycle. *Reproductive Biology and Endocrinology* **13** 84.

Chandonnet L, Roberts KD, Chapdelaine A and Manjunath P (1990) Identification of heparin-binding proteins in bovine seminal plasma. *Molecular Reproduction and Development* **26** 313–318.

Chang MC (1951) Fertilizing capacity of spermatozoa deposited into the fallopian tubes. *Nature* **168** 697–698.

Chang H and Suarez SS (2012) Unexpected flagellar movement patterns and epithelial binding behavior of mouse sperm in the oviduct. *Biology of Reproduction* **86**.

Chen S and Schoen J (2019) Air-liquid interface cell culture: from airway epithelium to the female reproductive tract. *Reproduction in Domestic Animals* **54** 38–45.

Chen S, Einspanier R and Schoen J (2013) In vitro mimicking of estrous cycle stages in porcine oviduct epithelium cells: estradiol and progesterone regulate differentiation, gene expression, and cellular function. *Biology of Reproduction* **89**.

Chen S, Palma-Vera SE, Langhammer M, Galuska SP, Braun BC, Krause E, Lucas-Hahn A and Schoen J (2017) An air-liquid interphase approach for modeling the early embryo-maternal contact zone. *Scientific Reports* **7** 42298.

Choudhary S, Kumaresan A, Kumar M, Chhillar S, Malik H, Kumar S, Kaushik JK, Datta TK and Mohanty AK (2017) Effect of recombinant and native buffalo OVGP1 on sperm functions and in vitro embryo development: a comparative study. *Journal of Animal Science and Biotechnology* **8**.

Coy P, Grullon L, Canovas S, Romar R, Matas C and Aviles M (2008) Hardening of the zona pellucida of unfertilized eggs can reduce polyspermic fertilization in the pig and cow. *Reproduction* **135** 19–27.

Coy P, García-Vázquez FA, Visconti PE and Avilés M (2012) Roles of the oviduct in mammalian fertilization. *Reproduction* **144** 649–660.

De Pauw IMC, Van Soom A, Laevens H, Verberckmoes S and de Kruif A (2002) Sperm binding to epithelial oviduct explants in bulls with different nonreturn rates investigated with a new in vitro model. *Biology of Reproduction* **67** 1073–1079.

Diskin MG (2018) Review: semen handling, time of insemination and insemination technique in cattle. *Animal* **12** s75–s84.

Dobrinski I (1996) Intracellular calcium concentration in equine spermatozoa attached to oviductal epithelial cells in vitro. *Biology of Reproduction* **54** 783–788.

Dobrowolski W and Hafez ESE (1970) Transport and distribution of spermatozoa in the reproductive tract of the cow. *Journal of Animal Science* **31** 940–943.

Druart X and de Graaf S (2018) Seminal plasma proteomes and sperm fertility. *Animal Reproduction Science* **194** 33–40.

Druart X, Cognié J, Baril G, Clément F, Dacheux J-L and Gatti J-L (2009) In vivo imaging of in situ motility of fresh and liquid stored ram spermatozoa in the ewe genital tract. *Reproduction* **138** 45–53.

Ealy AD, Wooldridge LK and McCoski SR (2019) BOARD INVITED REVIEW: Post-transfer consequences of in vitro-produced embryos in cattle. *Journal of Animal Science* **97** 2555–2568.

Ealy A, Drost M, Barros C and Hansen P (1992) Thermoprotection of preimplantation bovine embryos from heat shock by glutathione and taurine. *Cell Biology International Reports* **16** 125–131.

Ehrenwald E, Foote RH and Parks JE (1990) Bovine oviductal fluid components and their potential role in sperm cholesterol efflux. *Molecular Reproduction and Development* **25** 195–204.

Eichler J (2019) Protein glycosylation. *Current Biology: CB* **29** R229–R231.

Ellington JE, Evenson DP, Wright RW, Jones AE, Schneider CS, Hiss GA and Brisbois RS (1999) Higher-quality human sperm in a sample selectively attach to oviduct (fallopian tube) epithelial cells in vitro. *Fertility and Sterility* **71** 924–929.

Elliott RMA, Lloyd RE, Fazeli A, Sostaric E, Georgiou AS, Satake N, Watson PF and Holt WV (2009) Effects of HSPA8, an evolutionarily conserved oviductal protein, on boar and bull spermatozoa. *Reproduction* **137** 191–203.

Elweza AE, Ezz MA, Acosta TJ, Talukder AK, Shimizu T, Hayakawa H, Shimada M, Imakawa K, Zaghloul AH and Miyamoto A (2018) A proinflammatory response of bovine endometrial epithelial cells to active sperm in vitro. *Molecular Reproduction and Development* **85** 215–226.

Engle CC, Foley CW, Plotka ED and Witherspoon DM (1984) Free amino acids and protein concentrations in reproductive tract fluids of the mare. *Theriogenology* **21** 919–930.

Eriksen T, Terkelsen O, Hyttel P and Greve T (1994) Ultrastructural features of secretory cells in the bovine oviduct epithelium. *Anatomy and Embryology* **190**.

Fair S, Meade KG, Reynaud K, Druart X and de Graaf SP (2019) The biological mechanisms regulating sperm selection by the ovine cervix. *Reproduction* **158** R1–R13.

Faulkner S, Elia G, O'Boyle P, Dunn M and Morris D (2013) Composition of the bovine uterine proteome is associated with stage of cycle and concentration of systemic progesterone. *Proteomics* **13** 3333–3353.

Fernandez MC and O'Flaherty C (2018) Peroxiredoxin 6 is the primary antioxidant enzyme for the maintenance of viability and DNA integrity in human spermatozoa. *Human Reproduction* **33** 1394–1407.

Fernández-Hernández P, Marinaro F, Sánchez-Calabuig MJ, García-Marín LJ, Bragado MJ, González-Fernández L and Macías-García B (2021) The proteome of equine oviductal fluid varies before and after ovulation: a comparative study. *Frontiers in Veterinary Science* **8** 694247.

Ferramosca A and Zara V (2014) Bioenergetics of mammalian sperm capacitation. *BioMed Research International* **2014** 1–8.

Ferraz MAMM, Henning HHW, Costa PF, Malda J, Melchels FP, Wubbolts R, Stout TAE, Vos PLAM and Gadella BM (2017) Improved bovine embryo production in an oviduct-on-a-chip system: prevention of poly-spermic fertilization and parthenogenic activation. *Lab on a Chip* **17** 905–916.

Ferraz M de AMM, Carothers A, Dahal R, Noonan MJ and Songsasen N (2019) Oviductal extracellular vesicles interact with the spermatozoon's head and mid-piece and improves its motility and fertilizing ability in the domestic cat. *Scientific Reports* **9** 9484.

Ferré LB, Kjelland ME, Strøbech LB, Hyttel P, Mermillod P and Ross PJ (2020) Review: Recent advances in bovine in vitro embryo production: reproductive biotechnology history and methods. *Animal* **14** 991–1004.

First NL, Short RE, Peters JB and Stratman FW (1968) Transport and loss of boar spermatozoa in the reproductive tract of the sow. *Journal of Animal Science* **27** 1037–1040.

Ford MJ, Harwalkar K, Pacis AS, Maunsell H, Wang YC, Badescu D, Teng K, Yamanaka N, Bouchard M, Ragoussis J *et al.* (2021) Oviduct epithelial cells constitute two developmentally distinct lineages that are spatially separated along the distal-proximal axis. *Cell Reports* **36** 109677.

Forde N, McGettigan PA, Mehta JP, O'Hara L, Mamo S, Bazer FW, Spencer TE and Lonergan P (2014) Proteomic analysis of uterine fluid during the pre-implantation period of pregnancy in cattle. *Reproduction* **147** 575–587.

Franchi A, Moreno-Irusta A, Domínguez EM, Adre AJ and Giojalas LC (2019) Extracellular vesicles from oviductal isthmus and ampulla stimulate the induced acrosome reaction and signaling events associated with capacitation in bovine spermatozoa. *Journal of Cellular Biochemistry* **121** 2877–2888.

Fujihara Y, Miyata H and Ikawa M (2018) Factors controlling sperm migration through the oviduct revealed by gene-modified mouse models. *Experimental Animals* **67** 91–104.

Gad A, Hoelker M, Besenfelder U, Havlicek V, Cinar U, Rings F, Held E, Dufort I, Sirard M-A, Schellander K *et al.* (2012) Molecular mechanisms and pathways involved in bovine embryonic genome activation and their regulation by alternative in vivo and in vitro culture conditions. *Biology of Reproduction* **87**.

Gaddum-Rosse P (1981) Some observations on sperm transport through the uterotubal junction of the rat. *American Journal of Anatomy* **160** 333–341.

García-Vázquez FA, Hernández-Caravaca I, Matás C, Soriano-Úbeda C, Abril-Sánchez S and Izquierdo-Rico MJ (2015) Morphological study of boar sperm during their passage through the female genital tract. *Journal of Reproduction and Development* **61** 407–413.

Gatien J, Mermillod P, Tsikis G, Bernardi O, Janati Idrissi S, Uzbekov R, Le Bourhis D, Salvetti P, Almiñana C and Saint-Dizier M (2019) Metabolomic profile of oviductal extracellular vesicles across the estrous cycle in cattle. *International Journal of Molecular Sciences* **20** 6339.

Gegenfurtner K, Fröhlich T, Kösters M, Mermillod P, Locatelli Y, Fritz S, Salvetti P, Forde N, Lonergan P, Wolf E *et al.* (2019) Influence of metabolic status and genetic merit for fertility on proteomic composition of bovine oviduct fluid. *Biology of Reproduction* **101** 893–905.

Gegenfurtner K, Fröhlich T, Flenkenthaler F, Kösters M, Fritz S, Desnoës O, Le Bourhis D, Salvetti P, Sandra O, Charpigny G *et al.* (2020) Genetic merit for fertility alters the bovine uterine luminal fluid proteome. *Biology of Reproduction* **102** 730–739.

Glencross RG, Munro IB, Senior BE and Pope GS (1973) Concentrations of oestradiol-17 beta, oestrone and progesterone in jugular venous plasma of cows during the oestrous cycle and in early pregnancy. *Acta Endocrinologica* **73** 374–384.

Gonella-Diaza AM, da Silva Andrade SC, Sponchiado M, Pugliesi G, Mesquita FS, Van Hoeck V, de Francisco Strefezzi R, Gasparin GR, Coutinho LL and Binelli M (2015) Size of the ovulatory follicle dictates spatial differences in the oviductal transcriptome in cattle. *PLOS ONE* **10** e0145321.

Gonella-Diaza AM, Mesquita FS, da Silva KR, de Carvalho Balieiro JC, dos Santos NP, Pugliesi G, de Francisco Strefezzi R and Binelli M (2017) Sex steroids modulate morphological and functional features of the bovine oviduct. *Cell and Tissue Research* **370** 319–333.

González IM, Martin PM, Burdsal C, Sloan JL, Mager S, Harris T and Sutherland AE (2012) Leucine and arginine regulate trophoblast motility through mTOR-dependent and independent pathways in the preimplantation mouse embryo. *Developmental Biology* **361** 286–300.

Graña-Baumgartner A, Meikle A, Fernández-Foren A, Neimaur K, Barrera N, Cuadro F, Santos-Neto PC dos, Bosolasco D, Núñez-Olivera R, Crispo M *et al.* (2020) Local influence of the corpus luteum on the ipsilateral oviduct and early embryo development in the ewe. *Theriogenology* **151** 7–15.

Grippo AA, Henault MA, Anderson SH and Killian GJ (1992) Cation concentrations in fluid from the oviduct ampulla and isthmus of cows during the estrous cycle. *Journal of Dairy Science* **75** 58–65.

Gualtieri R and Talevi R (2000) In vitro-cultured bovine oviductal cells bind acrosome-intact sperm and retain this ability upon sperm release. *Biology of Reproduction* **62** 1754–1762.

Gualtieri R and Talevi R (2003) Selection of highly fertilization-competent bovine spermatozoa through adhesion to the Fallopian tube epithelium in vitro. *Reproduction (Cambridge, England)* **125** 251–258.

Hamdi M, Cañon-Beltrán K, Mazzarella R, Cajas YN, Leal CLV, Gutierrez-Adan A, González EM, Da Silveira JC and Rizos D (2021) Characterization and profiling analysis of bovine oviduct and uterine extracellular vesicles and their miRNA cargo through the estrous cycle. *The FASEB Journal* **35** e22000.

Hawk HW, Conley HH and Cooper BS (1978) Number of sperm in the oviducts, uterus, and cervix of the mated ewe as affected by exogenous estradiol. *Journal of Animal Science* **46** 1300–1308.

He Y, Zang X, Kuang J, Yang H, Gu T, Yang J, Li Z, Zheng E, Xu Z, Cai G *et al.* (2022) iTRAQ-based quantitative proteomic analysis of porcine uterine fluid during pre-implantation period of pregnancy. *Journal of Proteomics* **261** 104570.

Heyman Y and Levasseur M-C (1981) Transport des spermatozoïdes dans les voies génitales. In *L'utérus de La Vache. Anatomie, Physiologie, Pathologie*, pp 121–133.

Holt WV and Fazeli A (2015) Do sperm possess a molecular passport? Mechanistic insights into sperm selection in the female reproductive tract. *MHR: Basic Science of Reproductive Medicine* **21** 491–501.

Hugentobler S, Morris DG, Kane MT and Sreenan JM (2004) In situ oviduct and uterine pH in cattle. *Theriogenology* **61** 1419–1427.

Hugentobler SA, Humpherson PG, Leese HJ, Sreenan JM and Morris DG (2008) Energy substrates in bovine oviduct and uterine fluid and blood plasma during the oestrous cycle. *Molecular Reproduction and Development* **75** 496–503.

Hunter RH and Hall JP (1974) Capacitation of boar spermatozoa: synergism between uterine and tubal environments. *The Journal of Experimental Zoology* **188** 203–213.

Ignotz GG, Cho MY and Suarez SS (2007) Annexins are candidate oviductal receptors for bovine sperm surface proteins and thus may serve to hold bovine sperm in the oviductal reservoir. *Biology of Reproduction* **77** 906–913.

Ireland JJ, Murphee RL and Coulson PB (1980) Accuracy of predicting stages of bovine estrous cycle by gross appearance of the corpus luteum. *Journal of Dairy Science* **63** 155–160.

Iritani A, Sato E and Nishikawa Y (1974) Secretion rates and chemical composition of oviduct and uterine fluids in sows. *Journal of Animal Science* **39** 582–588.

Ito S, Kobayashi Y, Yamamoto Y, Kimura K and Okuda K (2016) Remodeling of bovine oviductal epithelium by mitosis of secretory cells. *Cell and Tissue Research* **366** 403–410.

Ito S, Yamamoto Y and Kimura K (2020) Analysis of ciliogenesis process in the bovine oviduct based on immunohistochemical classification. *Molecular Biology Reports* **47** 1003–1012.

Jalali BM, Bogacki M, Dietrich M, Likszo P and Wasielak M (2015) Proteomic analysis of porcine endometrial tissue during peri-implantation period reveals altered protein abundance. *Journal of Proteomics* **125** 76–88.

Jang M-J, Lim C, Lim B and Kim J-M (2022) Integrated multiple transcriptomes in oviductal tissue across the porcine estrous cycle reveal functional roles in oocyte maturation and transport. *Journal of Animal Science* **100** skab364.

Johnson GP, English A-M, Cronin S, Hoey DA, Meade KG and Fair S (2017) Genomic identification, expression profiling, and functional characterization of CatSper channels in the bovine†. *Biology of Reproduction* **97** 302–312.

Kanchev LN, Dobson H, Ward WR and Fitzpatrick RJ (1976) Concentration of steroids in bovine peripheral plasma during the oestrous cycle and the effect of betamethasone treatment. *Reproduction* **48** 341–345.

Katz DF, Morales P, Samuels SJ and Overstreet JW (1990) Mechanisms of filtration of morphologically abnormal human sperm by cervical mucus. *Fertility and Sterility* **54** 513–516.

Kawakami E, Arai T, Oishi I, Hori T and Tsutsui T (2000) Induction of dog sperm capacitation by glycosaminoglycans and glycosaminoglycan amounts of oviductal and uterine fluids in bitches. *The Journal of Veterinary Medical Science* **62** 65–68.

Khan FA, Diel de Amorim M and Chenier TS (2020) Qualitative analysis and functional classification of the uterine proteome of mares in oestrus and dioestrus. *Reproduction in Domestic Animals* **55** 1511–1519.

Kim B-J, Park D-R, Nam T-S, Lee SH and Kim U-H (2015) Seminal CD38 enhances human sperm capacitation through its interaction with CD31. *PLOS ONE* **10** e0139110.

King RS and Killian GJ (1994) Purification of bovine estrus-associated protein and localization of binding on sperm. *Biology of Reproduction* **51** 34–42.

Kowalik MK, Dobrzyn K, Rekawiecki R and Kotwica J (2019) Expression of membrane progestin receptors (mPRs) α, β and γ in the bovine uterus during the oestrous cycle and pregnancy. *Theriogenology* **140** 171–179.

Krzanowska H (1974) The passage of abnormal spermatozoa through the uterotubal junction of the mouse. *Reproduction* **38** 81–90.

Kumro FG, O'Neil EV, Ciernia LA, Moraes JGN, Spencer TE and Lucy MC (2020) Scanning electron microscopy of the surface epithelium of the bovine endometrium. *Journal of Dairy Science* **103** 12083–12090.

Kusama K, Nakamura K, Bai R, Nagaoka K, Sakurai T and Imakawa K (2018) Intrauterine exosomes are required for bovine conceptus implantation. *Biochemical and Biophysical Research Communications* **495** 1370–1375.

Kusters DHM, Chatrou ML, Willems BAG, De Saint-Hubert M, Bauwens M, van der Vorst E, Bena S, Biessen EAL, Perretti M, Schurgers LJ et al. (2015) Pharmacological treatment with Annexin A1 reduces atherosclerotic plaque burden in LDLR-/- mice on western type diet. PLOS ONE 10 e0130484.

Lachance C, Bailey JL and Leclerc P (2007) Expression of HSP60 and GRP78 in the human endometrium and oviduct, and their effect on sperm functions. *Human Reproduction* **22** 2606–2614.

La Spina FA, Puga Molina LC, Romarowski A, Vitale AM, Falzone TL, Krapf D, Hirohashi N and Buffone MG (2016) Mouse sperm begin to undergo acrosomal exocytosis in the upper isthmus of the oviduct. *Developmental Biology* **411** 172–182.

Laezer I, Palma-Vera SE, Liu F, Frank M, Trakooljul N, Vernunft A, Schoen J and Chen S (2020) Dynamic profile of EVs in porcine oviductal fluid during the periovulatory period. *Reproduction* **159** 371–382.

Lamy J, Liere P, Pianos A, Aprahamian F, Mermillod P and Saint-Dizier M (2016a) Steroid hormones in bovine oviductal fluid during the estrous cycle. *Theriogenology* **86** 1409–1420.

Lamy J, Labas V, Harichaux G, Tsikis G, Mermillod P and Saint-Dizier M (2016b) Regulation of the bovine oviductal fluid proteome. *Reproduction* **152** 629–644.

Lamy J, Corbin E, Blache M-C, Garanina AS, Uzbekov R, Mermillod P and Saint-Dizier M (2017) Steroid hormones regulate sperm–oviduct interactions in the bovine. *Reproduction* **154** 497–508.

Lamy J, Gatien J, Dubuisson F, Nadal-Desbarats L, Salvetti P, Mermillod P and Saint-Dizier M (2018) Metabolomic profiling of bovine oviductal fluid across the oestrous cycle using proton nuclear magnetic resonance spectroscopy. *Reproduction, Fertility and Development* **30** 1021.

Lange-Consiglio A, Capra E, Giuliani D, Canesi S, Funghi F, Bosi G, Cretich M, Frigerio R, Galbiati V and Cremonesi F (2022) Endometrial and oviduct extra-cellular vesicles for in vitro equine sperm hyperactivation and oocyte fertilization. *Theriogenology* **194** 35–45.

Lee CN and Ax RL (1984) Concentrations and composition of glycosaminoglycans in the female bovine reproductive tract. *Journal of Dairy Science* **67** 2006–2009.

Lee CN, Clayton MK, Bushmeyer SM, First NL and Ax RL (1986) Glycosaminoglycans in ewe reproductive tracts and their influence on acrosome reactions in bovine spermatozoa in vitro. *Journal of Animal Science* **63** 861–867.

Lee W-J, Jung E-J, Hwang J-M, Bae J-W and Kwon W-S (2022) GRP78 plays a key role in sperm function via the PI3K/PDK1/AKT pathway. *Reproductive Toxicology* **113** 103–109.

Leemans B, Stout TAE, De Schauwer C, Heras S, Nelis H, Hoogewijs M, Van Soom A and Gadella BM (2019) Update on mammalian sperm capacitation: how much does the horse differ from other species? *Reproduction* **157** R181–R197.

Leese H, Tay J, Reischl J and Downing S (2001) Formation of fallopian tubal fluid: role of a neglected epithelium. *Reproduction* 339–346.

Lefebvre R and Suarez SS (1996) Effect of capacitation on bull sperm binding to homologous oviductal epithelium. *Biology of Reproduction* **54** 575–582.

Li Z-H and Bresnick AR (2006) The S100A4 metastasis factor regulates cellular motility via a direct interaction with myosin-IIA. *Cancer Research* **66** 5173–5180.

Locatelli Y, Forde N, Blum H, Graf A, Piégu B, Mermillod P, Wolf E, Lonergan P and Saint-Dizier M (2019) Relative effects of location relative to the corpus luteum and lactation on the transcriptome of the bovine oviduct epithelium. *BMC Genomics* **20** 233.

López-Úbeda R, García-Vázquez FA, Gadea J and Matás C (2017) Oviductal epithelial cells selected boar sperm according to their functional characteristics. *Asian Journal of Andrology* **19** 396–403.

Lu C-H, Lee RK-K, Hwu Y-M, Chu S-L, Chen Y-J, Chang W-C, Lin S-P and Li S-H (2011) SERPINE2, a serine protease inhibitor extensively expressed in adult male mouse reproductive tissues, may serve as a murine sperm decapacitation factor. *Biology of Reproduction* **84** 514–525.

Lu DP, Chandrakanthan V, Cahana A, Ishii S and O'Neill C (2004) Trophic signals acting via phosphatidylinositol-3 kinase are required for normal pre-implantation mouse embryo development. *Journal of Cell Science* **117** 1567–1576.

Lusignan M-F, Bergeron A, Crête M-H, Lazure C and Manjunath P (2007) Induction of epididymal boar sperm capacitation by pB1 and BSP-A1/-A2 proteins, members of the BSP protein family. *Biology of Reproduction* **76** 424–432.

Machado SA, Sharif M, Wang H, Bovin N and Miller DJ (2019) Release of porcine sperm from oviduct cells is stimulated by progesterone and requires CatSper. *Scientific Reports* **9** 19546.

MacFarlane AJ, Perry CA, Girnary HH, Gao D, Allen RH, Stabler SP, Shane B and Stover PJ (2009) Mthfd1 is an essential gene in mice and alters biomarkers of impaired one-carbon metabolism. *Journal of Biological Chemistry* **284** 1533–1539.

Mahé C, Lavigne R, Com E, Pineau C, Locatelli Y, Zlotkowska AM, Almiñana C, Tsikis G, Mermillod P, Schoen J *et al.* (2022) Spatiotemporal profiling of the bovine oviduct fluid proteome around the time of ovulation. *Scientific Reports* **12** 4135.

Maillo V, de Frutos C, O'Gaora P, Forde N, Burns GW, Spencer TE, Gutierrez-Adan A, Lonergan P and Rizos D (2016) Spatial differences in gene expression in the bovine oviduct. *Reproduction* **152** 37–46.

Maloney S, Khan FA, Chenier TS, Diel de Amorim M, Anthony Hayes M and Scholtz EL (2019) A comparison of the uterine proteome of mares in oestrus and dioestrus. *Reproduction in Domestic Animals* **54** 473–479.

Manjunath P, Marcel YL, Uma J, Seidah NG, Chrétien M and Chapdelaine A (1989) Apolipoprotein A-I binds to a family of bovine seminal plasma proteins. *The Journal of Biological Chemistry* **264** 16853–16857.

Marín-Briggiler CI, González-Echeverría MF, Munuce MJ, Ghersevich S, Caille AM, Hellman U, Corrigall VM and Vazquez-Levin MH (2010) Glucose-regulated protein 78 (GRP78/BiP) is secreted by human oviduct epithelial cells and the recombinant protein modulates sperm–zona pellucida binding. *Fertility and Sterility* **93** 1574–1584.

Martin-DeLeon PA (2016) Uterosomes: exosomal cargo during the estrus cycle and interaction with sperm. *Frontiers in Bioscience (Scholar Edition)* **8** 115–122.

Mattner PE (1968) The distribution of spermatozoa and leucocytes in the female genital tract in goats and cattle. *Journal of Reproduction and Fertility* **17** 253–261.

Mattner P and Braden A (1969) Comparison of the distribution of motile and immotile spermatozoa in the ovine cervix. *Australian Journal of Biological Sciences* **22** 1069.

Menezo Y and Khatchadourian C (1986) Peptides bound to albumin. *Life Sciences* **39** 1751–1753.

Mitko K, Ulbrich SE, Wenigerkind H, Sinowatz F, Blum H, Wolf E and Bauersachs S (2008) Dynamic changes in messenger RNA profiles of bovine endometrium during the oestrous cycle. *Reproduction (Cambridge, England)* **135** 225–240.

Mondéjar I, Martínez-Martínez I, Avilés M and Coy P (2013) Identification of potential oviductal factors responsible for zona pellucida hardening and monospermy during fertilization in mammals. *Biology of Reproduction* **89**.

Mullen MP, Elia G, Hilliard M, Parr MH, Diskin MG, Evans ACO and Crowe MA (2012) Proteomic characterization of histotroph during the preimplantation phase of the estrous cycle in Cattle. *Journal of Proteome Research* **11** 3004–3018.

Muro Y, Hasuwa H, Isotani A, Miyata H, Yamagata K, Ikawa M, Yanagimachi R and Okabe M (2016) Behavior of mouse spermatozoa in the female reproductive tract from soon after mating to the beginning of fertilization. *Biology of Reproduction* **94** 80.

Nabors B (2021) Anatomy of the reproductive system of the cow. In *Bovine Reproduction*, 1st ed, pp 249–257. Ed RM Hopper. Wiley.

Navarro B, Kirichok Y and Clapham DE (2007) KSper, a pH-sensitive K^+ current that controls sperm membrane potential. *Proceedings of the National Academy of Sciences* **104** 7688–7692.

Nelis H, Vanden Bussche J, Wojciechowicz B, Franczak A, Vanhaecke L, Leemans B, Cornillie P, Peelman L, Van Soom A and Smits K (2016) Steroids in the equine oviduct: synthesis, local concentrations and receptor expression. *Reproduction, Fertility and Development* **28** 1390.

van Niel G, D'Angelo G and Raposo G (2018) Shedding light on the cell biology of extracellular vesicles. *Nature Reviews Molecular Cell Biology* **19** 213–228.

O'Neil EV, Burns GW, Ferreira CR and Spencer TE (2020) Characterization and regulation of extracellular vesicles in the lumen of the ovine uterus. *Biology of Reproduction* **102** 1020–1032.

Oren-Benaroya R, Kipnis J and Eisenbach M (2007) Phagocytosis of human post-capacitated spermatozoa by macrophages. *Human Reproduction* **22** 2947–2955.

Papp SM, Fröhlich T, Radefeld K, Havlicek V, Kösters M, Yu H, Mayrhofer C, Brem G, Arnold GJ and Besenfelder U (2019) A novel approach to study the bovine oviductal fluid proteome using transvaginal endoscopy. *Theriogenology* **132** 53–61.

Parrish JJ, Susko-Parrish J, Winer MA and First NL (1988) Capacitation of bovine sperm by heparin. *Biology of Reproduction* **38** 1171–1180.

Parrish JJ, Susko-Parrish JL, Handrow RR, Sims MM and First NL (1989) Capacitation of bovine spermatozoa by oviduct fluid. *Biology of Reproduction* **40** 1020–1025.

Parrish JJ, Krogenaes A and Susko-Parrish JL (1995) Effect of bovine sperm separation by either swim-up or Percoll method on success of in vitro fertilization and early embryonic development. *Theriogenology* **44** 859–869.

Petrunkina AM, Simon K, Günzel-Apel A-R and Töpfer-Petersen E (2004) Kinetics of protein tyrosine phosphorylation in sperm selected by binding to homologous and heterologous oviductal explants: how specific is the regulation by the oviduct? *Theriogenology* **61** 1617–1634.

Pillai VV, Weber DM, Phinney BS and Selvaraj V (2017) Profiling of proteins secreted in the bovine oviduct reveals diverse functions of this luminal microenvironment. *PLOS ONE* **12** e0188105.

Pini T, de Graaf SP, Druart X, Tsikis G, Labas V, Teixeira-Gomes AP, Gadella BM and Leahy T (2018) Binder of Sperm Proteins 1 and 5 have contrasting effects on the capacitation of ram spermatozoa. *Biology of Reproduction* **98** 765–775.

Plante G and Manjunath P (2014) Binder of sperm (BSP) proteins in the male reproductive tract of farm animals 9th Biennial Conference of the Association for Applied Animal Andrology Newcastle, Australia: International Veterinary Information Service (http://www.ivis.org) 103–118.

Plante G, Therien I, Lachance C, Leclerc P, Fan J and Manjunath P (2014) Implication of the human Binder of SPerm Homolog 1 (BSPH1) protein in capacitation. *Molecular Human Reproduction* **20** 409–421.

Plante G, Prud'homme B, Fan J, Lafleur M and Manjunath P (2016) Evolution and function of mammalian binder of sperm proteins. *Cell and Tissue Research* **363** 105–127.

Pollard JW, Plante C, Allan King W, Hansen PJ, Betteridge KJ and Suarez SS (1991) Fertilizing capacity of bovine sperm may be maintained by binding of oviductal epithelial cells. *Biology of Reproduction* **44** 102–107.

Pons-Rejraji H, Bailey JL and Leclerc P (2009) Cryopreservation affects bovine sperm intracellular parameters associated with capacitation and acrosome exocytosis. *Reproduction, Fertility and Development* **21** 525.

Quinlivan TD and Robinson TJ (1969) Number of spermatozoa in the genital tract after artificial insemination of progestagen-treated ewes. *Reproduction* **19** 73–86.

Rabouille C (2017) Pathways of unconventional protein secretion. *Trends in Cell Biology* **27** 230–240.

Rahban R and Nef S (2020) CatSper: The complex main gate of calcium entry in mammalian spermatozoa. *Molecular and Cellular Endocrinology* **518** 110951.

Rai A, Poh QH, Fatmous M, Fang H, Gurung S, Vollenhoven B, Salamonsen LA and Greening DW (2021) Proteomic profiling of human uterine extracellular vesicles reveal dynamic regulation of key players of embryo implantation and fertility during menstrual cycle. *PROTEOMICS* **21** 2000211.

Restall BJ and Wales RG (1966) The fallopian tube of the sheep. 3. The chemical composition of the fluid from the fallopian tube. *Australian Journal of Biological Sciences* **19** 687–698.

Rizos D, Fair T, Papadopoulos S, Boland MP and Lonergan P (2002) Developmental, qualitative, and ultrastructural differences between ovine and bovine embryos produced in vivo or in vitro. *Molecular Reproduction and Development* **62** 320–327.

Rizos D, Clemente M, Bermejo-Alvarez P, de La Fuente J, Lonergan P and Gutiérrez-Adán A (2008) Consequences of *in vitro* culture conditions on embryo development and quality. *Reproduction in Domestic Animals* **43** 44–50.

Rodríguez-Alonso B, Maillo V, Acuña OS, López-Úbeda R, Torrecillas A, Simintiras CA, Sturmey R, Avilés M, Lonergan P and Rizos D (2020) Spatial and pregnancy-related changes in the protein, amino acid, and carbohydrate composition of bovine oviduct fluid. *International Journal of Molecular Sciences* **21** 1681.

Rodriguez-Martinez H, McKenna D, Weston PG, Whitmore HL and Gustafsson BK (1987) Uterine motility in the cow during the estrous cycle. I. Spontaneous activity. *Theriogenology* **27** 337–348.

Romero-Aguirregomezcorta J, Cronin S, Donnellan E and Fair S (2019) Progesterone induces the release of bull spermatozoa from oviductal epithelial cells. *Reproduction, Fertility, and Development* **31** 1463–1472.

Rottmayer R, Ulbrich SE, Kölle S, Prelle K, Neumueller C, Sinowatz F, Meyer HHD, Wolf E and Hiendleder S (2006) A bovine oviduct epithelial cell suspension culture system suitable for studying embryo–maternal interactions: morphological and functional characterization. *Reproduction* **132** 637–648.

Rudolf Vegas A, Podico G, Canisso IF, Bollwein H, Almiñana C and Bauersachs S (2021) Spatiotemporal endometrial transcriptome analysis revealed the luminal epithelium as key player during initial maternal recognition of pregnancy in the mare. *Scientific Reports* **11** 22293.

Saccary L, She Y-M, Oko R and Kan FWK (2013) Hamster oviductin regulates tyrosine phosphorylation of sperm proteins during in vitro capacitation. *Biology of Reproduction* **89**.

Saint-Dizier M, Sandra O, Ployart S, Chebrout M and Constant F (2012) Expression of nuclear progesterone receptor and progesterone receptor membrane components 1 and 2 in the oviduct of cyclic and pregnant cows during the post-ovulation period. *Reproductive Biology and Endocrinology* **10** 76.

Saint-Dizier M, Marnier C, Tahir MZ, Grimard B, Thoumire S, Chastant-Maillard S and Reynaud K (2014) *OVGP1* is expressed in the canine oviduct at the time and place of oocyte maturation and fertilization. *Molecular Reproduction and Development* **81** 972–982.

Saint-Dizier M, Desnoes O, Lamy J, Le Berre L, Mermillod P, Tsikis G, Druart X and Salvetti P (2016) In vivo imaging of spermatozoa in the bovine genital tract. *International Congress of Animal Reproduction (ICAR)*

Saint-Dizier M, Schoen J, Chen S, Banliat C and Mermillod P (2020) Composing the early embryonic microenvironment: physiology and regulation of oviductal secretions. *International Journal of Molecular Sciences* **21** 223.

Sánchez JM, Passaro C, Forde N, Browne JA, Behura SK, Fernández-Fuertes B, Mathew DJ, Kelly AK, Butler ST, Spencer TE *et al.* (2019) Do differences in the endometrial transcriptome between uterine horns ipsilateral and contralateral to the corpus luteum influence conceptus growth to day 14 in cattle? *Biology of Reproduction* **100** 86–100.

Schmaltz-Panneau B, Locatelli Y, Uzbekova S, Perreau C and Mermillod P (2015) Bovine oviduct epithelial cells dedifferentiate partly in culture, while maintaining their ability to improve early embryo development rate and quality. *Reproduction in Domestic Animals* **50** 719–729.

Seytanoglu A, Georgiou AS, Sostaric E, Watson PF, Holt WV and Fazeli A (2008) Oviductal cell proteome alterations during the reproductive cycle in pigs. *Journal of Proteome Research* **7** 2825–2833.

Shalgi R, Smith TT and Yanagimachi R (1992) A quantitative comparison of the passage of capacitated and uncapacitated hamster spermatozoa through the uterotubal junction. *Biology of Reproduction* **46** 419–424.

Sirard MA and Blondin P (1996) Oocyte maturation and IVF in cattle. *Animal Reproduction Science* **42** 417–426.

Smits K, Nelis H, Van Steendam K, Govaere J, Roels K, Ververs C, Leemans B, Wydooghe E, Deforce D and Van Soom A (2017) Proteome of equine oviducal fluid: effects of ovulation and pregnancy. *Reproduction, Fertility and Development* **29** 1085.

Soleilhavoup C, Riou C, Tsikis G, Labas V, Harichaux G, Kohnke P, Reynaud K, de Graaf SP, Gerard N and Druart X (2016) Proteomes of the female genital tract during the oestrous cycle. *Molecular & Cellular Proteomics* **15** 93–108.

Sostaric E, Dieleman SJ, van de Lest CHA, Colenbrander B, Vos PLAM, Garcia-Gil N and Gadella BM (2008) Sperm binding properties and secretory activity of the bovine oviduct immediately before and after ovulation. *Molecular Reproduction and Development* **75** 60–74.

Suarez SS and Pacey AA (2006) Sperm transport in the female reproductive tract. *Human Reproduction Update* **12** 23–37.

Sumransap P, Tummaruk P and Kunavongkrit A (2007) Sperm distribution in the reproductive tract of sows after intrauterine insemination. *Reproduction in Domestic Animals* **42** 113–117.

Sung DC, Ahmad M, Lerma Cervantes CB, Zhang Y, Adelstein RS and Ma X (2021) Mutations in non-muscle myosin 2A disrupt the actomyosin cytoskeleton in Sertoli cells and cause male infertility. *Developmental Biology* **470** 49–61.

Taylor U, Rath D, Zerbe H and Schuberth H-J (2008) Interaction of intact porcine spermatozoa with epithelial cells and neutrophilic granulocytes during uterine passage. *Reproduction in Domestic Animals* **43** 166–175.

Thérien I, Soubeyrand S and Manjunath P (1997) Major proteins of bovine seminal plasma modulate sperm capacitation by high-density lipoprotein. *Biology of Reproduction* **57** 1080–1088.

Thérien I, Moreau R and Manjunath P (1998) Major proteins of bovine seminal plasma and high-density lipoprotein induce cholesterol efflux from epididymal sperm. *Biology of Reproduction* **59** 768–776.

Thérien I, Moreau R and Manjunath P (1999) Bovine seminal plasma phospholipid-binding proteins stimulate phospholipid efflux from epididymal sperm. *Biology of Reproduction* **61** 590–598.

Thérien I, Bergeron A, Bousquet D and Manjunath P (2005) Isolation and characterization of glycosaminoglycans from bovine follicular fluid and their effect on sperm capacitation. *Molecular Reproduction and Development* **71** 97–106.

Tienthai P, Kjellén L, Pertoft H, Suzuki K and Rodriguez-Martinez H (2000) Localization and quantitation of hyaluronan and sulfated glycosaminoglycans in the tissues and intraluminal fluid of the pig oviduct. *Reproduction, Fertility and Development* **12** 173.

Tríbulo P, Balzano-Nogueira L, Conesa A, Siqueira LG and Hansen PJ (2019) Changes in the uterine metabolome of the cow during the first 7 days after estrus. *Molecular Reproduction and Development* **86** 75–87.

Troedsson MHT, Desvousges A, Alghamdi AS, Dahms B, Dow CA, Hayna J, Valesco R, Collahan PT, Macpherson ML, Pozor M *et al.* (2005) Components in seminal plasma regulating sperm transport and elimination. *Animal Reproduction Science* **89** 171–186.

Tummaruk P, Sumransap P, Techakumphu M and Kunavongkrit A (2007) Distribution of Spermatozoa and Embryos in the Female Reproductive Tract after Unilateral Deep Intra Uterine Insemination in the Pig. *Reproduction in Domestic Animals* **42** 603–609.

Tunón A-M, Rodriguez-Martinez H, Hultén C, Nummijarvi A and Magnusson U (1998) Concentrations of total protein, albumin and immunoglobulins in undiluted uterine fluid of gynecologically healthy mares. *Theriogenology* **50** 821–831.

Varner DD, Bowen JA and Johnson L (1993) Effect of heparin on capacitation/acrosome reaction of equine sperm. *Archives of Andrology* **31** 199–207.

Velazquez MA, Parrilla I, Van Soom A, Verberckmoes S, Kues W and Niemann H (2010) Sampling techniques for oviductal and uterine luminal fluid in cattle. *Theriogenology* **73** 758–767.

Visconti PE, Westbrook VA, Chertihin O, Demarco I, Sleight S and Diekman AB (2002) Novel signaling pathways involved in sperm acquisition of fertilizing capacity. *Journal of Reproductive Immunology* **53** 133–150.

Visconti PE, Bailey JL, Moore GD, Pan D, Olds-Clarke P and Kopf GS (1995) Capacitation of mouse spermatozoa. I. Correlation between the capacitation state and protein tyrosine phosphorylation. *Development (Cambridge, England)* **121** 1129–1137.

Walter I (1995) Culture of bovine oviduct epithelial cells (BOEC). *The Anatomical Record* **243** 347–356.

Wang S and Larina IV (2018) *In vivo* three-dimensional tracking of sperm behaviors in the mouse oviduct. *Development* dev.157685.

Wang H, McGoldrick LL and Chung J-J (2021) Sperm ion channels and transporters in male fertility and infertility. *Nature Reviews Urology* **18** 46–66.

Wassarman PM (1999) Mammalian fertilization. *Cell* **96** 175–183.

Watanabe S, Tani T, Watanabe S and Seno¯ M (1991) Transport of steroid hormones facilitated by serum proteins. *Biochimica et Biophysica Acta (BBA) - General Subjects* **1073** 275–284.

Wrenzycki C (2022) Interaction of sperm cells with the female reproductive tract in cattle: Focus on neutrophil extracellular trap formation. *Animal Reproduction Science* 107056.

Xiong W, Wang Z and Shen C (2019) An update of the regulatory factors of sperm migration from the uterus into the oviduct by genetically manipulated mice. *Molecular Reproduction and Development* **86** 935–955.

Yang X, Zhao Y, Yang X and Kan FWK (2015) Recombinant hamster oviductin is biologically active and exerts positive effects on sperm functions and sperm-oocyte binding. *PLOS ONE* **10** e0123003.

Yániz JL, Lopez-Gatius F, Santolaria P and Mullins KJ (2000) Study of the functional anatomy of bovine oviductal mucosa. *The Anatomical Record* **260** 268–278.

Zhao Y, Yang X, Jia Z, Reid RL, Leclerc P and Kan FWK (2016) Recombinant human oviductin regulates protein tyrosine phosphorylation and acrosome reaction. *Reproduction* **152** 561–573.

Annexes

Annexe 1 : chapitre d'ouvrage : « Assessment of sperm binding capacity in the oviduct reservoir using an in vitro model of epithelial spheroids in cattle »

Assessment of sperm binding capacity in the reservoir using an *in vitro* model of oviduct epithelial spheroids in cattle

Coline Mahé[1,*], Ludivine Laffont[1], Thanya Pranomphon[1], Lorraine Schmaltz[1], Karine Reynaud[1], Pascal Mermillod[1] and Marie Saint-Dizier[1,2]

[1] *CNRS, IFCE, INRAE, Université de Tours, PRC, 37380, Nouzilly, France*

[2] *Tours University, Faculty of Sciences and Techniques, Tours, France*

[*] *Corresponding author : coline.mahe@inrae.fr*

Abstract

The sperm reservoir in the oviduct isthmus plays important roles in sperm survival, acquisition of sperm fertilization competence and sperm-oocyte interactions. Here we describe a bovine *in vitro* model of oviduct spheroids, easy to culture and normalize, and allowing robust quantification by confocal microscopy of sperm binding capacity to isthmic epithelial cells. This assay may be used to compare sperm binding capacity between males, evaluate sperm functionality and conduct studies on sperm-oviduct interactions. The method may be implemented in other species.

Keywords: oviduct, epithelial cell, isthmus, spheroids, spermatozoa, sperm reservoir

Running head: Sperm-oviduct binding test in cattle

1 Introduction

Out of millions of spermatozoa entering the uterus at insemination, a few hundred cross the utero-tubal junction and enter the oviduct, where a subpopulation binds to isthmic epithelial cells (IEC) in so called 'functional sperm reservoir'.

In vivo observations in cattle evidenced that only membrane-intact spermatozoa with normal morphology bind with their head to almost exclusively ciliated IEC [1]. Sperm binding to the isthmic reservoir is assumed to keep sperm alive before ovulation and release successive waves of fertilization-competent sperm toward the ampulla, where fertilization takes place [2]. The constitution of a sperm reservoir in mammals may thus be a prerequisite for successful sperm-oocyte interaction *in vivo*, while limiting the risk of polyspermy [3, 4]. Sperm-oviduct binding assay tests have been used to predict male fertility in cattle [5-7] and pigs [8], evaluate sperm chromatin quality [9] and plasma membrane functionality [10], to assess sperm injury after cryopreservation or sex sorting [11-13] and for physiological studies on sperm-oviduct interactions [14, 15]. Previous *in vitro* models used for sperm-oviduct binding assays include aggregates (or explants) of oviduct epithelial cells (OEC) [6, 7, 12, 16], OEC monolayers grown on plastic dish [15, 17] or on insert in an air/liquid interphase system [18], and mucosa explants [13]. However, OEC aggregates are heterogeneous in form and size and difficult to normalize between replicates [7, 16], whereas OEC monolayers grown on plastic rapidly dedifferentiate and lost cilia at confluence [1]. Furthermore, the air/liquid interphase system is technically challenging and takes 3 weeks before OEC differentiation [18], whereas mucosa explants can be used only for 24 hours [13]. Here we describe a new binding assay using spheroids cultured in suspension. The spheroid model is: i) easy to obtain after 3-4 days of culture; ii) composed with 25% of fully differentiated ciliated cells with the apical side of cells oriented outside, *i.e.* accessible to spermatozoa; iii) sortable by pipetting according to their diameter and shape, offering normalized and repeatable binding surface to a given sperm population; iv) stainable with the DNA-binding dye Hoechst for assessment of sperm density using confocal microscopy. Given the same pool of bull semen, the method was successfully used to obtain similar sperm density by spheroid surface between biological replicates. The method is applicable to other species.

2 Materials

2.1 Collection and preparation of oviducts

1. Clean pots.

2. Icebox with icepacks.

3. Razor blades.

4. Forceps.

5. Sterile compress.

6. NaCl 0.9%.

7. Ethanol 70%.

2.2 Cell culture

1. 15-mL sterile tubes.

2. 4-well plates suitable for cell culture.

3. 35-mm tissue culture dish.

4. Sterile 96-well plate.

5. Pasteur glass pipette.

6. Heating plate.

7. Vortex.

8. Culture medium: TCM 199 with L-glutamine, phenol red and HEPES (25 mM). Add 500 µL of gentamycin (10 mg/mL) and 5 mL of heat-decomplemented fetal bovine serum to 45 mL of TCM 199 under sterile conditions. Store at 4°C for maximum two weeks.

9. Cell culture incubator with a humidified atmosphere of 5% CO_2 in air.

2.3 Preparation of spermatozoa

1. Bull semen straws (2-15 million spermatozoa/0.25 mL straw).

2. Tyrode medium: mix 1 L of demineralized water with 6.666 mg NaCl (100 mM), 240 mg KCl (3.1 mM), 41 mg NaH_2PO_4 (2.1 mM) 300 mg $CaCl_2$ (2.1 mM) and 100 mg $MgCl_2$ (0.4 mM) (dissolve $CaCl_2$ and $MgCl_2$ separately). Aliquot in 50 mL and store at -20°C.

2. HEPES-buffered Tyrode's lactate pyruvate medium (TLP medium): mix 200 mL of Tyrode medium with 22.7 mg $NaHCO_3$ (1 mM), 480 mg HEPES (10 mM), 200 mg polyvinyl alcohol and 610 µL sodium DL-lactate (27.4 mM) with a 1 mL syringe. Adjust the pH to 7.4 with NaOH 1M and the osmolarity to 300 mOsm with NaCl (13.8 mM). Filter through a 0.22 µm filtration unit and store at 4°C for maximum 3 weeks.

3. Computer assisted sperm analysis (CASA) software and suitable slides or chamber for sperm observation.

4. Centrifuge allowing 300-700 ×g centrifugations of 1.5-mL and 15-mL tubes.

5. Percoll medium or equivalent media for density-gradient centrifugation procedure in cattle.

6. Thoma cell counting chamber or equivalent material for determination of sperm concentration.

7. 10-µL and 100-µL pipettes.

2.4 Confocal microscopy

1. Hoechst B2261.

2. Cacodylate 0.1 M: weigh 1.07 g sodium cacodylate and transfer to 50 mL of demineralized water. Store at -20°C or at 4°C for maximum 1 month.

3. Fixative solution: 2.5% glutaraldehyde. Add 500 µL of 25% glutaraldehyde to 5 mL of cacodylate 0.1 M. Filter through a 0.22 µm syringe filter.

4. PBS-BSA: phosphate buffer saline (PBS) supplemented with 1% bovine serum albumin (BSA): make stock solution at 10% BSA and store at -20°C. Add 1 mL of solution at 10% BSA in 9 mL of PBS. Filter through a 0.22 µm filtration unit. Store at 4°C for maximum 1 week.

5. Microscope slides treated to allow cell and tissue adherence, like Superfrost slides.

6. Hydrophobic marker pen like ImmEdge pens.

7. Coverslips 24 × 60 mm.

8. Nail polish.

9. Confocal microscope.

10. ImageJ software, free to download at https://imagej.net/software/fiji/downloads.

3 Methods

For the complete timeline of experiments, see **Fig. 1**.

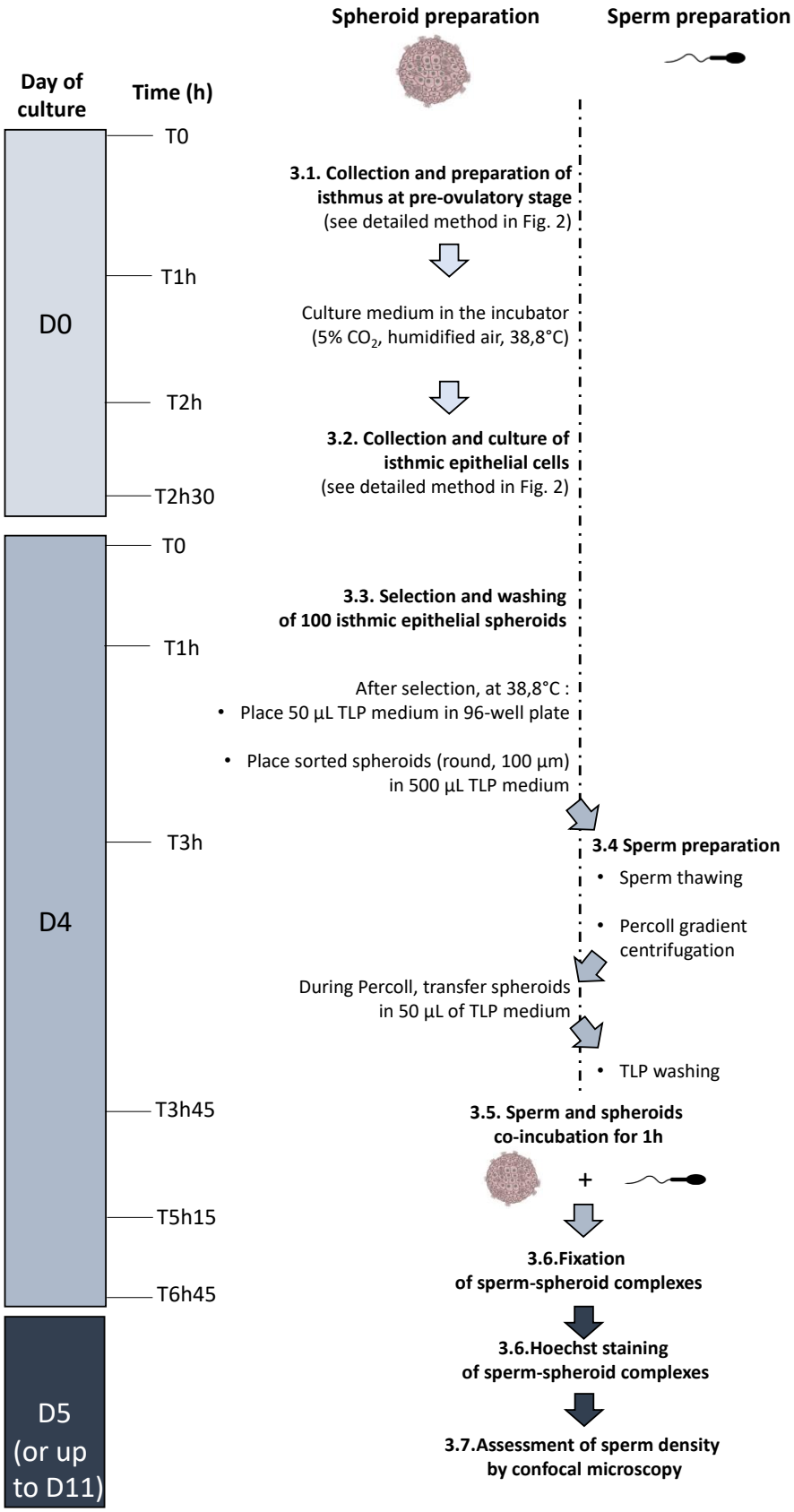

Fig. 1. Timeline of each step from the collection of oviducts up to assessment of bound sperm density on epithelial spheroids.

3.1 Collection and preparation of isthmus (1-2 hours)

1. Collect pairs of oviducts with ovaries at the slaughterhouse and transport to the laboratory at 4°C.

2. Exclude oviducts linked to ovaries with morphological abnormalities like ovarian cysts or signs of inflammation.

3.Select at least two pairs of oviducts at the pre-ovulatory phase of cycle according to ovarian morphology. In cattle, pre-ovulatory ovaries contain one follicle of 11 – 20 mm in diameter and one yellow, hard and small (<1 cm) *corpus albicans* from the previous ovulation (**Fig. 2**). (*see* **Note 1**).

4. Cut both isthmus at the utero-tubal and ampulla-isthmus junctions (*see* **Note 2**) and dissect them with a clean razor blade to remove surrounding vessels and fat (**Fig. 2**). Transfer the isthmus sections in a compress soaked in cold saline to the culture room for step 1 of § 3.2.

3.2 Culture of isthmic epithelial cells (30 min)

Next steps are carried out under a laminar flow hood. At least one hour before cell culture, put fresh culture medium in the incubator containing 5% CO_2 in humidified air at 38.8°C for equilibration.

1. Maintain both extremities of the isthmus closed with forceps and immerse 5 sec in 70% ethanol solution.

2. Rinse the isthmus 10 sec in saline then cut approximately 2 mm of both extremities with a sterile razor blade.

3. Place one isthmus above a 15-mL sterile tube containing 10 mL of culture medium and squeeze twice the section from one extremity to the other with two forceps. Repeat the procedure with the other isthmus (**Fig. 2**).

5. Mix the cells by vortexing for 1 min and let settle for 10 min at 38.8°C. Do not centrifuge.

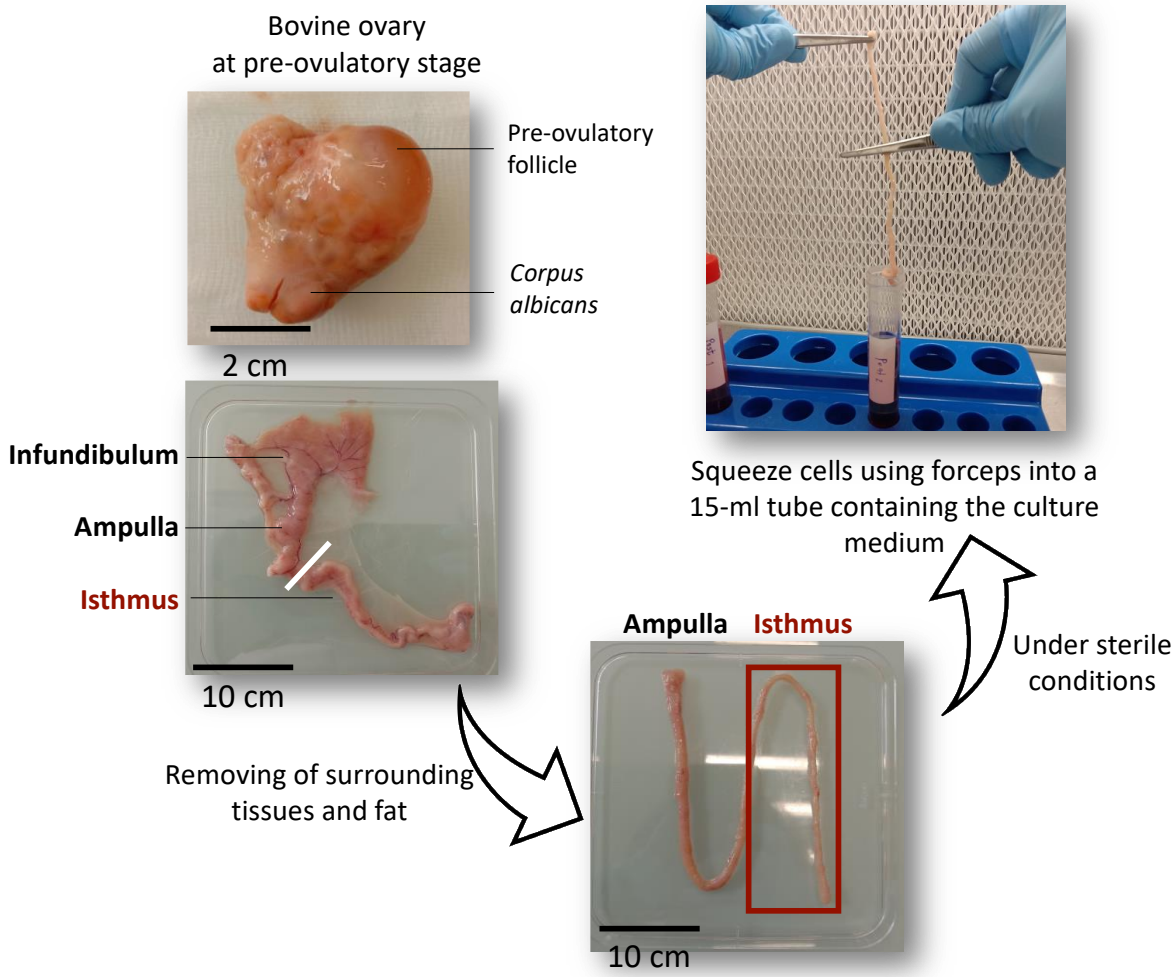

Fig. 2. Collection of isthmic cells from slaughterhouse oviducts. Oviducts and ovaries have to be collected together to sort animals at the pre-ovulatory stage of cycle.

6. Discard the supernatant and add 10 mL of fresh culture medium.

7. Mix the cells by vortexing for 1 min and let settle for 10 min at 38.8°C. Discard the supernatant and evaluate the volume of the cell pellet (*see* **Note 3)**.

8. Dilute the cell pellet at a 1:10 ratio in fresh culture medium (for a pellet of 0.1 mL of cells, add 0.9 mL of fresh culture medium).

9. Add 450 µL of fresh culture medium in a 4-well plate (*see* **Note 4**).

10. Add 50 µL of cells in each well containing 450 µL culture medium so that the final dilution of the cell pellet will be 1:100. Add 2 mL of sterile water between wells to avoid medium evaporation.

11. Leave the 4-well plate for 3-4 days in the incubator containing 5% CO_2 in humidified air at 38.8°C (*see* **Note 5**).

3.3 Selection and washing of isthmic epithelial spheroids (around 50 min for 100 spheroids, depending on the experience)

1. At the end of culture, add 1 mL of fresh culture medium in a 35-mm culture dish on a heating plate at 38.8°C.

2. Transfer the content of each well of the 4-well plates into the dish using a 1-mL pipette.

3. Sort the spheroids around 100 µm in diameter, having uniform circular shape and vigorous ciliary beating and gently transfer in a new petri dish containing fresh culture medium (**Fig. 3**) (*see* **Note 6**).

4. Transfer spheroids in 500 µL TLP medium in a 4-well plate for 2 h at 38.8°C in a humidified atmosphere without CO_2 (*see* **Note 7**).

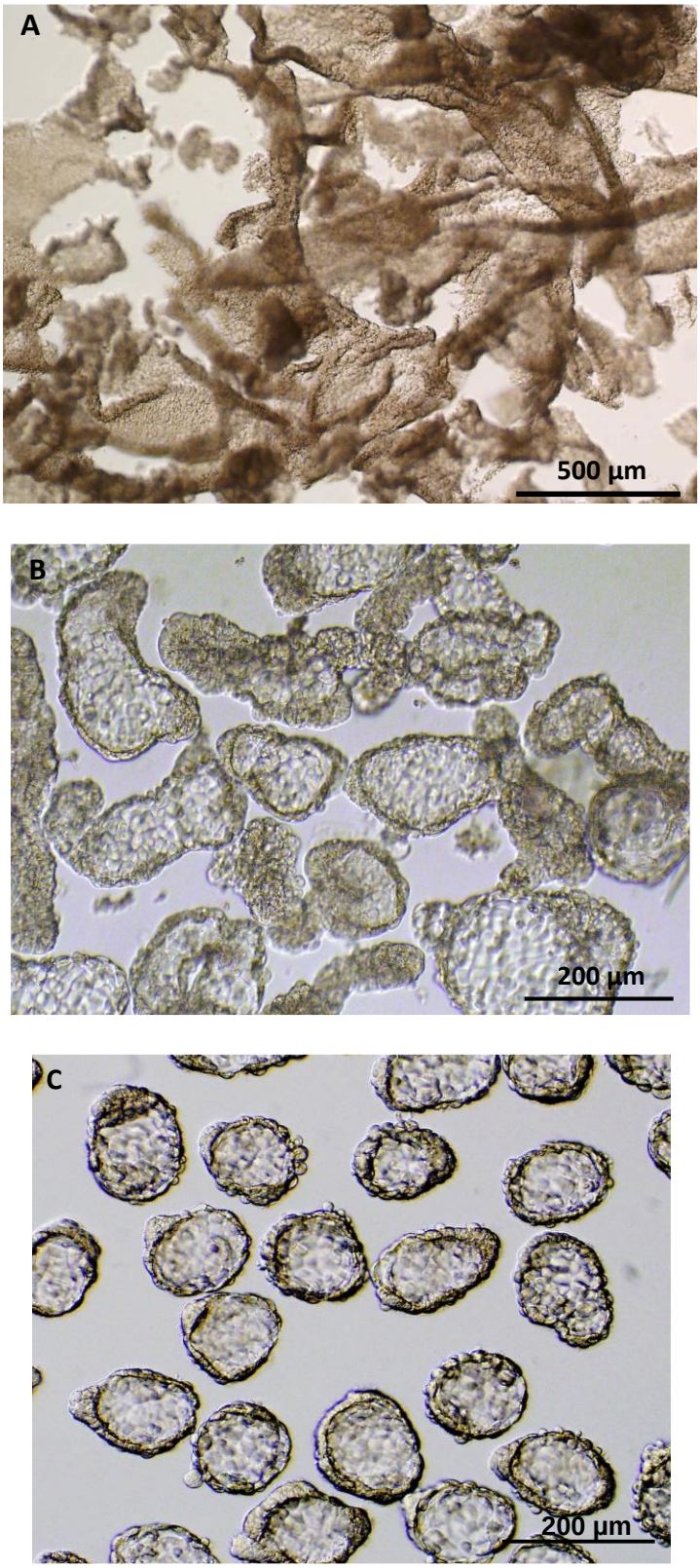

Fig 3. Bovine isthmic epithelial cells during four days of culture showing the mucosa fragments on the day of collection (A), the spheroids of various shape and size formed on day 4 (B), and 100-µm spheroids uniform in shape sorted for sperm co-incubation (C).

3.4 Sperm preparation (45 min)

1. Place 2 mL of TLP medium and the 45% and 90% Percoll solutions in a water bath at 38.5°C for at least 30 min before step 2 and put the 90% Percoll underneath the 45%.

2. Thaw the straw (or a pool of straws) in water at 37°C for 3 min then dry the straws with paper towels.

3. Cut the straw at the sealed end using scissors and directly put the open side of the straw on top of the Percoll gradient. Cut the straw below the cotton plug and centrifuge for 20 min at 700×*g* at 25°C.

4. Discard the supernatant and transfer 5 µL of the sperm pellet in 195 µL of demineralized water to assess sperm concentration

5. Dilute the sperm pellet in 1 mL TLP medium and centrifuge at 300×*g* at 25°C for 10 min. During this step, evaluate the sperm concentration using a Thoma cell counting chamber.

6. Discard the supernatant and adjust the sperm concentration with TLP medium to 10 million per mL (*see* **Note 8**).

7. Check sperm motility by computer assisted sperm analysis (CASA) (*see* **Note 9**).

3.5 Incubation of spermatozoa with spheroids (90 min)

1. Two hours before sperm thawing (step 2 of § 3.4 "Sperm preparation"), place 50 µL of TLP medium in a sterile 96-well culture plate at 38.8°C.

2. During density-gradient centrifugation (step 3 of § 3.4 "Sperm preparation"), transfer 20 spheroids with a glass pipette in 50 µL of TLP medium in a sterile 96-well culture plate at 38.8°C.

2. Add 5 µL of sperm in each well of 96-well plate containing 20 OES in 50 µL of TLP medium and/or other treatments

3. Incubate up to 60 min at 38.8°C in a humidified atmosphere (*see* **Note 10**).

4. During step 3, prepare the washing wells: 500 µL of TLP medium in three wells of a 4-well plate (3 wells per treatment) and put at 38.8°C. Prepare the fixative solution and put on the heating plate at 37°C under the hood.

5. Gently retrieve the content of each well from the 96-well plate with a 100 µL-pipette and transfer the sperm-spheroid complexes into the first washing well (500 µL of TLP medium), then wash twice more time to remove unbound and loosely bound spermatozoa (*see* **Note 11**). See sperm-spheroid complexes in **Fig. 4**.

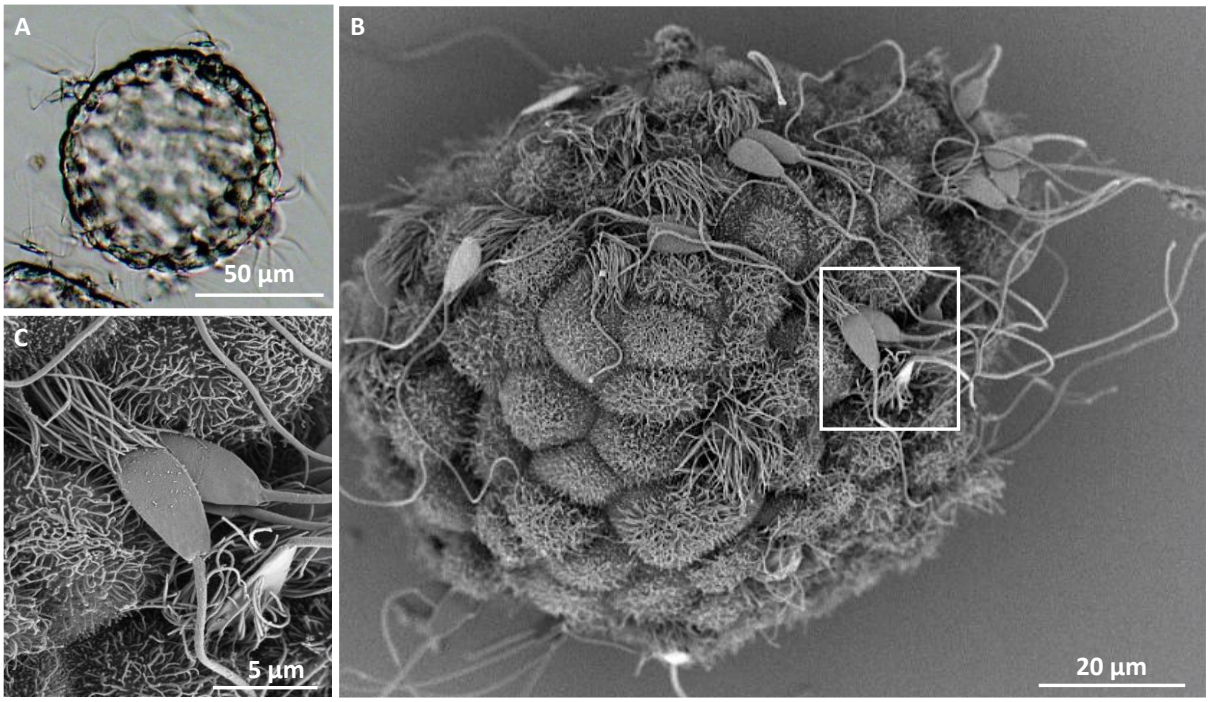

Fig 4. Sperm-spheroid complexes observed under light (A) and scanning electron microscopy (B, C) showing bull sperm firmly attached to cilia. The spheroids from isthmic cells at the pre-ovulatory stage are made with 25% ciliated cells on average.

3.6 Fixation and staining of sperm-spheroid complexes (120 min)

1. Transfer the sperm-spheroid complexes with a glass pipette in 500 µL of fixative solution (2.5% glutaraldehyde) at 37°C and leave for 1 h at 37°C under the hood.

2. Transfer the sperm-spheroid complexes in three successive baths of 500 µL PBS-BSA for washing. The complexes can be stored up to 7 days at 4°C (*see* **Note 12**).

3. Add 5 µL of staining solution at 10 µg/mL of Hoechst B2261 directly in each well containing sperm-spheroid complexes. Leave under agitation and in the dark for 15 min at room temperature.

4. Wash twice the complexes a few seconds in 500 µL PBS-BSA.

3. Add two drops of 10 spheroids with a glass pipette on a Superfrost slide and draw a circle around each drop with a hydrophobic marker pen.

5. Add a few drops of PBS-BSA around each circle and place delicately the coverslip from the left to the right of the slide: spheroids are flattened.

6. Add polish on each corner of the coverslip and keep the slides in a humid dark box until confocal analysis. The slides need to be analyzed by microscopy within max 1 day.

3.7 Assessment of sperm density by confocal microscopy (around 3 min per spheroid)

1. On the confocal microscope, select Hoechst as fluorochrome, a pinhole diameter of 1 Airy Unit (AU) and the transmitted photomultiplier tube (TPMT) option (*see* **Note 13**).

2. Observed each spheroid with at 20× magnification and take confocal pictures at each sides of the spheroid so that all bound sperm heads are visualized (**Fig. 5**). An extra picture in the middle of the spheroid could be helpful to visualize all spermatozoa.

3. Open confocal images in the ImageJ software.

4. Merge the Hoechst with the white light signal (in the Image menu, choose Color, then choose Make composite).

5. Use the polygon tool to measure the area (in µm^2) of each spheroid (in the Analyze menu, choose Measure).

6. Count the number of bound sperm on each image and note the number of sperm for each spheroid.

7. Calculate the mean sperm density per surface unit (in number of spz per µm^2) by dividing the total number of bound sperm with the total area of the spheroids (*see* **Note 14**).

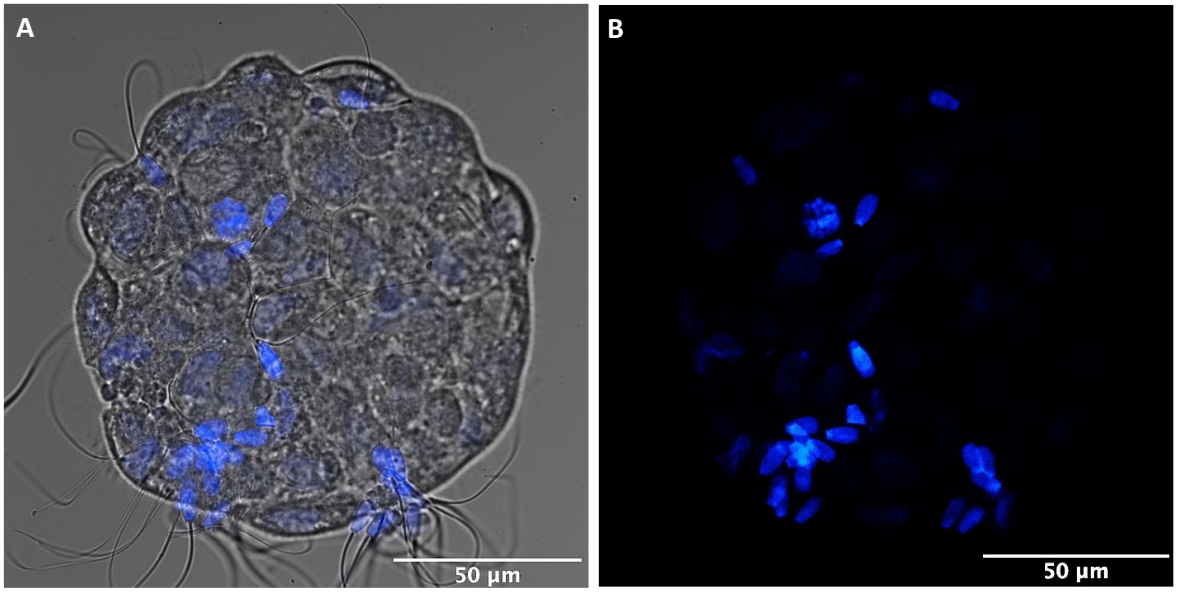

Fig 5. Confocal microscopy pictures of one sperm-spheroid complex with (A) and without (B) the TPMT option for sperm counting. The TPMT option (white light) helps to delineate the edge of the spheroid and count the sperm flagella.

4 Notes

1. Spheroids can form from other anatomical parts of the oviduct (ampulla or infundibulum) and from oviducts collected at other stages of the cycle; however, the pre-ovulatory isthmus is the time and location of sperm reservoir formation and is physiologically most relevant for sperm-oviduct binding assays.

2. In cattle, the ampulla-isthmus junction is not easy to identify. The isthmus is less vascularized, harder and more tortuous than the ampulla, and is not more than 10 cm in length starting from the utero-tubal junction.

3. Two isthmus sections will provide around 100 µL of cell pellet. Starting from 50 µL of diluted cells, between 10 and 50 spheroids circular in shape and 100 µm in diameter will form. This yield is indicative and may greatly vary between replicates. More pairs of oviducts may be used to obtain higher numbers of spheroids.

4. The 4-well plates may be replaced by 35-mm or 60-mm Petri dishes filled with 2 or 6 mL culture medium, respectively.

5. The first spheroids will appear after 2 days in culture and a maximum yield is obtained after 4 days in culture. Most spheroids on day 4 have a diameter ranging from 50 and 150 µm and contain on average 25% ciliated cells.

6. Sorting of spheroids may be achieved with a glass pipette or an equivalent material with an extremity diameter larger than 150 µm. The sorting time must not exceed 10 min. To avoid change in the medium pH and temperature, use several sorting plates and put back the plate in the incubator after 10 min.

7. As the TLP medium do not contain any bicarbonate, tubes and plates are placed in a humidified atmosphere without CO_2 to avoid any pH modification. Alternatively, tubes may be closed and wells covered with a plastic film in an incubator with 5% CO_2. Spheroids display vigorous ciliary beating, fluorescent live cell staining and no sign of membrane damage up to 4 h in the TLP medium.

8. Preliminary data showed that with 20 spheroids per condition, the density of bound sperm per spheroid reached a plateau at 1 million of spz/mL

9. After thawing and gradient-density centrifugation, bull sperm motility is usually greater than 70%. However, sperm motility may differ between bulls and influence sperm binding on spheroids.

10. Preliminary data showed that the density of bound sperm on spheroids increased from 5 to 60 min and decreased after 90 min.

11. The washing procedure of sperm-spheroid complexes is manipulator-dependent and may influence the final sperm density per spheroid. Be consistent with the washing procedure between replicates.

12. BSA is used to avoid any adhesion of sperm-spheroid complexes to the bottom of plates and may be replaced by polyvinyl alcohol (PVA) or pyrrolidone (PVP).

13. The TPMT option (white light) helps to delineate the edge of the spheroids and visualize the sperm flagella for sperm counting, as shown in **Fig. 5**.

14. The total area of spheroids may be approximated by doubling the surface of one side of each spheroid. In our conditions, the total area for 20 spheroids over 5 successive replicates was on average 0,628 mm^2. Using the same semen, the sperm density was on average 1500 spz per mm^2.

Ackowledgements

This work was supported by the ANR-18-CE92-0049 French grant to M.S.D. The authors thank Union Evolution, France for providing bull semen. The authors warmly thank the PIC platform of the PRC Unit for valuable assistance on confocal microscopy, and Albert Arnould for material collection at the slaughterhouse.

References

1. Sostaric E, Dieleman SJ, van de Lest CH, Colenbrander B, Vos PL, Garcia-Gil N, et al. Sperm binding properties and secretory activity of the bovine oviduct immediately before and after ovulation. Mol Reprod Dev. 2008;75(1):60-74.

2. Suarez SS. Mammalian sperm interactions with the female reproductive tract. Cell Tissue Res. 2016;363(1):185-94.

3. Coy P, Garcia-Vazquez FA, Visconti PE, Aviles M. Roles of the oviduct in mammalian fertilization. Reproduction. 2012;144(6):649-60.

4. Mahe C, Zlotkowska AM, Reynaud K, Tsikis G, Mermillod P, Druart X, et al. Sperm migration, selection, survival, and fertilizing ability in the mammalian oviductdagger. Biol Reprod. 2021;105(2):317-31.

5. Saraf KK, Singh RK, Kumaresan A, Nayak S, Chhillar S, Lathika S, et al. Sperm functional attributes and oviduct explant binding capacity differs between bulls with different fertility ratings in the water buffalo (Bubalus bubalis). Reprod Fertil Dev. 2019;31(2):395-403.

6. Donnellan EM, Lonergan P, Meade KG, Fair S. An ex-vivo assessment of differential sperm transport in the female reproductive tract between high and low fertility bulls. Theriogenology. 2022;181:42-9.

7. De pauw I, Van Soom A, Laevens H, Verberckmoes S, de Kruif A. Sperm binding to epithelial oviduct explants in bulls with different nonreturn rates investigated with a new in vitro model. Biol Reprod. 2002;67:1073-9.

8. Waberski D, Magnus F, Mendonca Ferreira F, Petrunkina AM, Weitze KF, Topfer-Petersen E. Importance of sperm-binding assays for fertility prognosis of porcine spermatozoa. Theriogenology. 2005;63(2):470-84.

9. Ardon F, Helms D, Sahin E, Bollwein H, Topfer-Petersen E, Waberski D. Chromatin-unstable boar spermatozoa have little chance of reaching oocytes in vivo. Reproduction. 2008;135(4):461-70.

10. Khalil AA, Petrunkina AM, Sahin E, Waberski D, Topfer-Petersen E. Enhanced binding of sperm with superior volume regulation to oviductal epithelium. J Androl. 2006;27(6):754-65.

11. Steele H, Makri D, Maalouf WE, Reese S, Kolle S. Bovine Sperm Sexing Alters Sperm Morphokinetics and Subsequent Early Embryonic Development. Sci Rep. 2020;10(1):6255.

12. Henning H, Franz J, Batz-Schott J, Le Thi X, Waberski D. Assessment of Chilling Injury in Boar Spermatozoa by Kinematic Patterns and Competitive Sperm-Oviduct Binding In Vitro. Animals (Basel). 2022;12(6).

13. Camara Pirez M, Steele H, Reese S, Kolle S. Bovine sperm-oviduct interactions are characterized by specific sperm behaviour, ultrastructure and tubal reactions which are impacted by sex sorting. Sci Rep. 2020;10(1):16522.

14. Ardon F, Markello RD, Hu L, Deutsch ZI, Tung CK, Wu M, et al. Dynamics of Bovine Sperm Interaction with Epithelium Differ Between Oviductal Isthmus and Ampulla. Biol Reprod. 2016;95(4):90.

15. Lamy J, Corbin E, Blache MC, Garanina AS, Uzbekov R, Mermillod P, et al. Steroid hormones regulate sperm-oviduct interactions in the bovine. Reproduction. 2017;154(4):497-508.

16. Saraf KK, Kumaresan A, Nayak S, Chhillar S, Sreela L, Kumar S, et al. Development of an in vitro oviduct epithelial explants model for studying sperm-oviduct binding in the buffalo. Reprod Domest Anim. 2017;52(4):687-91.

17. Gualtieri R, Talevi R. Selection of highly fertilization-competent bovine spermatozoa through adhesion to the Fallopian tube epithelium in vitro. Reproduction. 2003;125(2):251-8.

18. Chen S, Einspanier R, Schoen J. In vitro mimicking of estrous cycle stages in porcine oviduct epithelium cells: estradiol and progesterone regulate differentiation, gene expression, and cellular function. Biol Reprod. 2013;89(3):54.

Annexe 2 : revue : « Sperm interactions with the female reproductive tract: a key for successful fertilization in mammals »

Molecular and Cellular Endocrinology 516 (2020) 110956

Contents lists available at ScienceDirect

Molecular and Cellular Endocrinology

journal homepage: www.elsevier.com/locate/mce

Review

Sperm interactions with the female reproductive tract: A key for successful fertilization in mammals

Marie Saint-Dizier [a,b,*], Coline Mahé [a], Karine Reynaud [a], Guillaume Tsikis [a], Pascal Mermillod [a], Xavier Druart [a]

[a] INRAE, UMR PRC, 37380, Nouzilly, France
[b] University of Tours, Faculty of Sciences and Techniques, 37000, Tours, France

ARTICLE INFO

Keywords:
Spermatozoa
Oviduct
Uterus
Utero-tubal junction
Interaction
Protein
Progesterone
Extracellular vesicle
Exosome

ABSTRACT

Sperm migration through the female genital tract is not a quiet journey. Uterine contractions quickly operate a drastic selection, leading to a very restrictive number of sperm reaching the top of uterine horns and finally, provided the presence of key molecules on sperm, the oviduct, where fertilization takes place. During hours and sometimes days before fertilization, subpopulations of spermatozoa interact with dynamic and region-specific maternal components, including soluble proteins, extracellular vesicles and epithelial cells lining the lumen of the female tract. Interactions with uterine and oviductal cells play important roles for sperm survival as they modulate the maternal immune response and allow a transient storage before ovulation. The body of work reported here highlights the importance of sperm interactions with proteins originated from both the uterine and oviductal fluids, as well as hormonal signals around the time of ovulation for sperm acquisition of fertilizing competence.

1. Introduction

Ejaculated mammalian spermatozoa are not able to fertilize the oocyte; this ability is acquired following a series of molecular and physiological changes, collectively known as capacitation, which are accomplished during the transit of spermatozoa through the female genital tract. In addition to sperm acquisition of fertilizing competence, the maternal environment operates a dramatic sperm selection, resulting in a very low sperm:egg ratio in the site of fertilization (Hino et al., 2016). The maternal environment allows also long-term survival of a subpopulation of spermatozoa up to the time of ovulation. These crucial steps preceding fertilization imply sperm interactions with the complex and dynamic fluids present in the female reproductive tract and with epithelial cells lining its lumen, in addition to flows induced by muscular contractions of the female genital tract. Fertilization can occur *in vitro*, thus in the absence of these interactions, but the female tract may increase the efficiency and quality of fertilization. To illustrate, the rate of polyspermy and the incidence of chromosomal abnormalities in early embryos are generally much lower in vivo than under *in vitro* conditions (Coy and Aviles, 2010; Viuff et al., 2000, 2001). Therefore, the mechanisms involved in sperm interactions with somatic cells and region-specific secretions in vivo are of particular importance for the understanding of factors determining male and female fertility, but also for the improvement of assisted reproductive technologies (ART) and for better evaluation/prediction of male fertility in human and farm animals.

The objective of this review is to provide an update on the effects of interactions in the uterus, utero-tubal junction (UTJ) and the oviduct (known as the fallopian tube in human) on sperm physiology, with emphasis on the oviduct where fertilization takes place. Physical and biochemical interactions of spermatozoa in the cervix have been recently reviewed (Fair et al., 2019; Rickard et al., 2019) and were not included. In each region starting from the uterus, effects of interaction with secreted fluids, including extracellular vesicles, and luminal epithelial cells on sperm will be considered separately. Special attention will be given to sperm-interacting proteins identified in female secretions that modulate sperm physiology. However, details on the reorganization of specific sperm surface microdomains and proteins during capacitation were excluded as they are well described elsewhere (Baker, 2016; Brohi and Huo, 2017; Gadella, 2017). The changes induced by sperm interactions on female tract gene expression were also considered out of the scope of the present review. All mammals will be considered

* Corresponding author. INRAE, UMR PRC, 37380, Nouzilly, France.
E-mail address: marie.saint-dizier@univ-tours.fr (M. Saint-Dizier).

https://doi.org/10.1016/j.mce.2020.110956
Received 30 March 2020; Received in revised form 22 June 2020; Accepted 20 July 2020
Available online 23 July 2020
0303-7207/© 2020 Elsevier B.V. All rights reserved.

with a particular interest in farm animals, in which large amounts of data on sperm interactions were acquired thanks to the availability of the biological material and due to the economic importance of such research area for animal breeding and livestock production.

2. Sperm interactions with the uterus

The migration of spermatozoa through the uterus is associated with sperm interactions with the uterine fluid (UF) and with uterine (or endometrial) epithelial cells (UECs), each mediated by specific components and triggering different effects on sperm.

2.1. Sperm interactions with uterine fluid and extracellular vesicles

Changes in sperm physiology in contact with uterine fluid have been poorly investigated compared with oviductal fluid, and data lack consistency. Incubation of sperm with UF maintained higher sperm motility over time compared with untreated controls in cattle (Abe et al., 1995a) and human (Chirinos et al., 2017). Furthermore, a significant increase in protein tyrosine phosphorylation, a marker of sperm capacitation, without impact on sperm viability was observed when human sperm were incubated for 3 h with uterine flushing from women at the time of ovulation (Chirinos et al., 2017). However, adverse effects of UF on motility, viability and acrosome integrity of ejaculated boar sperm were observed in less than 2 h *in vitro* (Luongo et al., 2019). The negative effects of UF were reduced in the presence of seminal plasma, leading to the hypothesis that proteins in the seminal plasma have a protective effect against uterine attack by coating sperm surface (Luongo et al., 2019).

A comprehensive analysis of proteins present in the UF is now available in some mammals including cattle (Gegenfurtner et al., 2020), horses (Maloney et al., 2019) and humans (Kasvandik et al., 2020). However, specific proteins involved in sperm-UF interactions are poorly known (Fig. 1). Sperm Adhesion Molecule 1 (SPAM1 or PH-20 hyaluronidase), a well conserved sperm surface hyaluronidase involved in fertilization, is secreted in the male genital tract and already present at the surface of ejaculated spermatozoa (Martin-DeLeon, 2006). SPAM1 was also identified in the uterine and oviductal fluids of female mice in the absence of semen (Griffiths et al., 2008a). SPAM1 from estrous UF was shown to associate with sperm of *Spam1*-nul and wild-type mouse, predominantly to the acrosome and the mid-piece of the flagella (Griffiths et al., 2008a) (Fig. 1). Incubation of murine sperm with UF increased their ability to bind to hyaluronic acid, a compound abundantly secreted by cumulus cells surrounding the oocyte, and this effect was inhibited when spermatozoa were exposed to SPAM1 antiserum (Griffiths et al., 2008a). However, sperm lacking SPAM1 can fertilize murine oocytes under *in vitro* conditions, although with lower ability to disperse cumulus cells (Baba et al., 2002), suggesting that SPAM1 is not essential for *in vitro* fertilization in mice. But it is possible that the requirements for successful fertilization in vivo are different than *in vitro* and uterine SPAM1 may be required in vivo. Recently, cystatin-C (CST3), a cysteine protease inhibitor highly present in the human cervix, endometrium and UF near ovulation, was shown to interact with human sperm at the post-acrosomal head region and mid and principal piece of the tail (Lee et al., 2018). *In vitro*, recombinant CST3 enhanced sperm motility but inhibited the efflux of cholesterol from the sperm plasma membrane, an initiating step of sperm capacitation, and the subsequent increase in sperm protein tyrosine phosphorylation (Lee et al., 2018). It was suggested that CST3 may prevent precocious capacitation, thus preserving sperm fertilizing ability before reaching the oviduct.

Extracellular vesicles in the female reproductive tract secretions have raised attention due to their potential role in modulating sperm function (Fig. 2). Exosomes (40–100 nm) and microvesicles (100–1000 nm), collectively known as extracellular vesicles (EVs), are able to transfer a complex selection of molecules from one cell to another in a high variety of biological fluids (Yanez-Mo et al., 2015). While the involvement of EVs from epididymis (or epididymosomes) in sperm maturation is well established (Sullivan, 2016), few data are available on the molecular content and on the roles of uterine EVs, also known as uterosomes, on sperm physiology. The first report of the existence of uterine nanovesicles was made in 2008 in mice (Griffiths et al., 2008b). Since then, uterine EVs have been reported in several mammals including sheep (Burns et al., 2014), cattle (Qiao et al., 2018) and women (Franchi et al., 2016). Sperm analyzed after incubation with fluorescently labeled isolated uterine EVs revealed interactions with the acrosome and the midpiece of murine sperm (Griffiths et al., 2008b) (Fig. 1). Association of uterine EVs with human sperm head and tail was observed after only 15 min of incubation and reported to increase tyrosine phosphorylation of sperm proteins (Franchi et al., 2016). Murine spermatozoa were able to acquire SPAM1 during incubation with uterine EVs, suggesting vesicular docking to sperm via glycosylphosphatidylinositol (GPI)-linked mechanisms (Griffiths et al., 2008b). Recent data on sperm interaction with oviductal EVs support the idea that EVs carry proteins that are important for sperm maturation during their transit through the female reproductive tract (Alcântara-Neto et al., 2020c; Alcantara-Neto et al., 2020b; Ferraz et al., 2019; Franchi et al., 2020) (see below).

2.2. Sperm interaction with uterine epithelial cells and effects on local inflammatory response

Sperm interaction with UECs is linked to the integrity of sperm plasma membrane (Fig. 3). Most of the spermatozoa bound to the sow's endometrium showed normal ultrastructure, intact plasma membrane and high mitochondrial membrane potential whereas most of the spermatozoa collected in the uterine lumen had damaged membranes (Rath et al., 2008; Rodriguez-Martinez et al., 1990; Taylor et al., 2008). *In vitro* experiments of incubation of boar spermatozoa with porcine UECs in the presence of lectins indicate that sperm binding to UECs is mediated by N-acetyl-glucosamine (GlcNAc)/sialic acid and/or N-Acetylgalactosamine (GalNAc) moieties with corresponding lectins

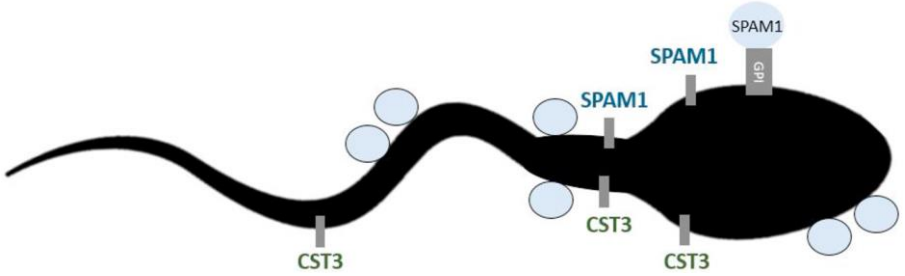

Fig. 1. Identification and localization of uterine proteins and extracellular vesicles interacting with spermatozoa. Sperm Adhesion Molecule 1 (SPAM1) interacts with mouse sperm acrosome and midpiece (Griffiths et al., 2008a). Cystatin-C (CST3) interacts with sperm post-acrosomal region, midpiece and tail of human sperm (Lee et al., 2018). Uterine extracellular vesicles (EVs, in blue) interact with sperm head, acrosome, midpiece and tail in mice (Griffiths et al., 2008b), human (Franchi et al., 2016) and pigs (Alcantara-Neto et al., 2020a). Murine uterine EVs deliver SPAM1 to sperm, possibly via glycosylphosphatidylinositol (GPI)--linked mechanisms (Griffiths et al., 2008b).

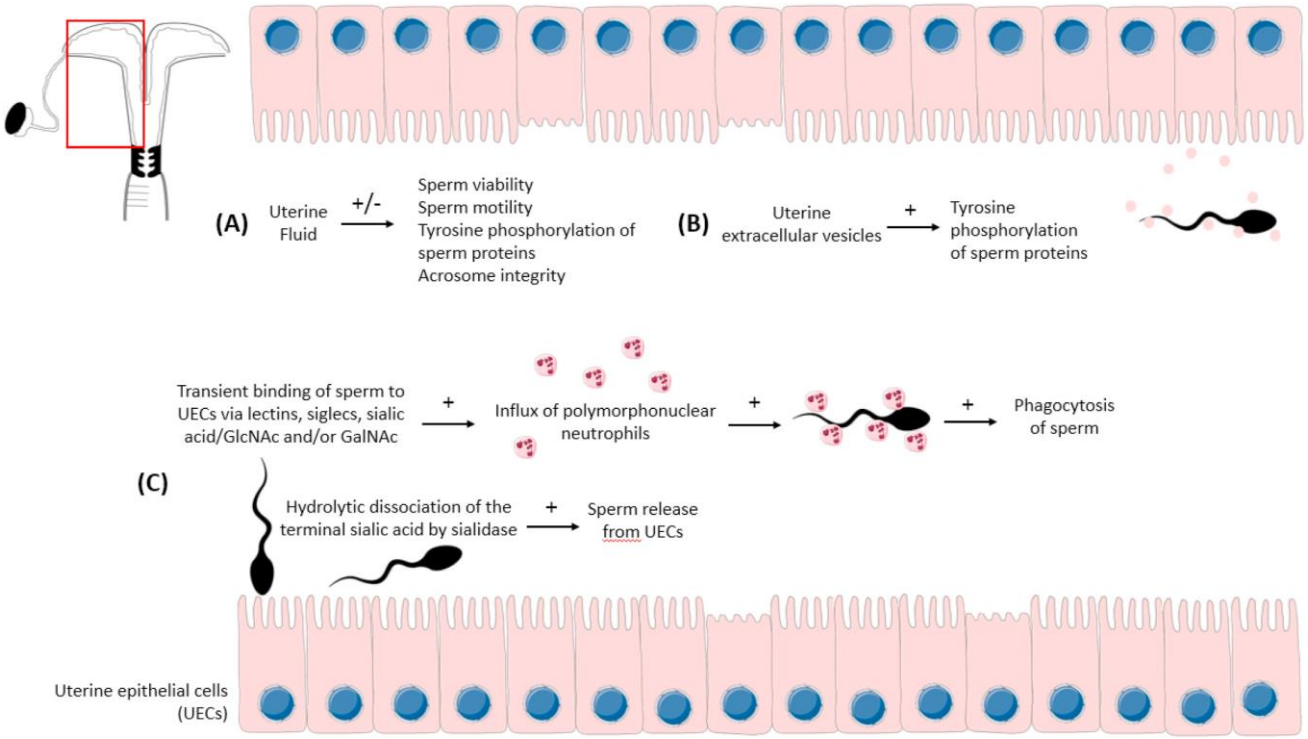

Fig. 2. Summarized effects of interactions with the uterus on sperm physiology. Sperm interact with uterine fluid (A), uterine extracellular vesicles (B) and uterine epithelial cells (UEC, C). Sperm-UEC interactions imply sialic acid-binding immunoglobulin-like lectins (Siglecs) as well as sialic acids, N-acetyl-glucosamine (GlcNAc), N-acetylgalactosamines (GalNAc) potentially present on both sperm and endometrial surfaces. See the text for corresponding references.

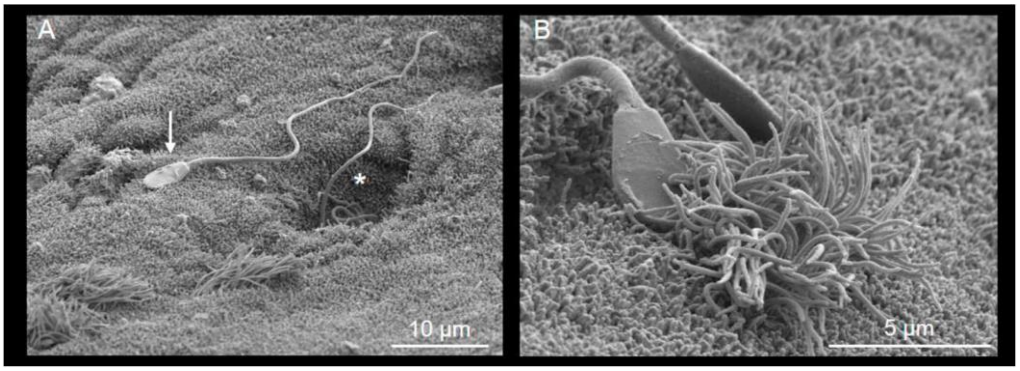

Fig. 3. Scanning electron microscopy (SEM) images of dog sperm interacting with uterine epithelial cells *in vivo*. Uterine epithelial cells at the luminal surface (A, white arrow) and in uterine gland (A, asterisk). B: higher magnification showing sperm heads with intact plasma membrane interacting with cilia at the UEC luminal surface. Source: K. Reynaud.

(Bergmann et al., 2012, 2013). Moreover, sperm sialic acids may interact with endometrial sialic acid-binding immunoglobulin-like lectins (Siglecs) detected at the endometrial surface in mice and women (Tecle et al., 2019). It was proposed that sperm binding may be transient with sperm detachment regulated by sialidase (Fig. 2). The sialidase might be liberated with follicular fluid at the time of ovulation and reach the uterine cavity where spermatozoa are released by hydrolytic dissociation of the terminal sialic acids (Rath et al., 2016).

Sperm binding to UECs induces transient endometrial inflammation followed by the entry of polymorphonuclear neutrophils (PMNs) in the lumen and their binding to spermatozoa (Schjenken and Robertson, 2014). One possible role of PMN binding to spermatozoa is to eliminate by phagocytosis the spermatozoa not previously removed by uterine contractions. Scanning electron microscopy of bovine endometrial explants incubated with spermatozoa revealed the presence of spermatozoa in the uterine glands along with PMNs (Akthar et al., 2019). Spermatozoa induce an acute inflammatory response and upregulation of mRNA expression of IL8 and TLR2 in endometrial explants (Akthar et al., 2019). *In vitro* models of sperm interaction with bovine UECs showed that sperm binding triggers innate immunity with induction of a pro-inflammatory response (Elweza et al., 2018) through the Toll-like receptor 2/4 (TLR2/4) signaling pathway (Ezz et al., 2019). In the horse, the influx of PMNs into the uterine lumen was previously shown to be triggered via complement activation (Troedsson et al., 1998). Another mechanism of sperm elimination in the uterus is the formation of neutrophils extracellular traps (NETs), previously described for bacteria elimination (Brinkmann et al., 2004), which ensnare spermatozoa and hinder their motility. Sperm entrapment by NETs has been reported

in horses (Alghamdi and Foster, 2005), cattle (Alghamdi et al., 2009; Fichtner et al., 2020) and humans (Zambrano et al., 2016). Spermatozoa might also be eliminated in the oviduct as PMNs were detected in the oviductal fluid of cyclic cows (Marey et al., 2014) and buffaloes (Yousef et al., 2019). However, *in vitro* data indicate that bovine oviduct epithelial cells around estrus secrete factors, including PGE_2, that suppress the phagocytic behavior of PMNs toward sperm but not toward bacteria (Marey et al., 2014, 2019; Yousef et al., 2019).

The site of sperm deposition, vagina or uterus, and therefore the absence or presence of seminal plasma in the uterus has an impact on mechanisms of sperm selection and survival (for reviews, see (Fair et al., 2019; Miller, 2018; Rickard et al., 2019)). In species with a deposit of semen in the vagina, most spermatozoa reach the uterus after elimination of seminal plasma by the cervix, whereas in species with a natural deposit of semen in the uterus such as the horse and pig, or after intrauterine insemination, both spermatozoa and seminal plasma interact with the endometrium. In addition to sperm, the seminal plasma is involved in the immune and inflammatory response of the endometrium after insemination (Schjenken and Robertson, 2015). In cattle after mating, the bulk of seminal plasma is expected to be eliminated by the cervix but *in vitro* experiments indicate a potential inhibitory impact of the seminal plasma on the viability and transmigration of PMNs through the endometrium and on their production of reactive oxygen species (Aloe et al., 2012). The seminal plasma of stallions was shown to increase the endometrial expression of IL-1 and IL-8 associated with inflammation in mares (Fedorka et al., 2016). In addition, the equine seminal plasma was reported to reduce sperm binding to neutrophils and the formation of NETs, which may allow more spermatozoa to reach the oviduct (Alghamdi and Foster, 2005). Contrary to horses, the bovine seminal plasma was shown to increase sperm-neutrophil binding, suggesting species-specific mechanisms (Alghamdi et al., 2009). In pigs, the regulation of endometrial immune and inflammatory response by seminal plasma was shown to be mediated by seminal exosomes (Bai et al., 2018a). When porcine UECs were treated with exosomes from seminal plasma, RNA transcripts related to immune and inflammatory response, such as CCL20 and interleukin 1, were up-regulated. Up-regulation of CCL20 was also demonstrated in the uterine endometrium from naturally mated pigs. As CCL20 recruits lymphocytes towards the epithelial tissue (Baba et al., 1997), it was suggested that seminal exosomes are involved in the recruitment and entry of lymphocytes in the porcine uterus (Bai et al., 2018b). Altogether, the results from *in vitro* and *in vivo* studies in several mammalian species suggest that the seminal plasma plays an important role in sperm survival in the female genital tract by protecting spermatozoa against negative effects of UF and controlling inflammatory and immune activation of the endometrium. Moreover, interactions between sperm sialic acids and uterine Siglecs activate downstream signaling pathways in endometrial cells, which may in turn modulate the immune response (Tecle et al., 2019). The innate immune response of the uterus may also be important for subsequent embryo development as it clears the uterine cavity and improves endometrial receptivity for implantation (Chastant and Saint-Dizier, 2019; Katila, 2012). Although spermatozoa are foreign cells for the female, an adaptive (or acquired) immune response toward spermatozoa has been reported only at low incidence in humans (2–3% of women with anti-sperm antibodies) (Clark and Schust, 2013). The mechanisms that allow this immune privilege for male gametes in the female reproductive tract are still poorly known. However, the unusual glycosylation signals on both spermatozoa and seminal plasma glycoproteins, namely the $Lewis^x$ or $Lewis^y$ sequences, may play important roles in the uterine tolerance toward spermatozoa (for review, see Clark and Schust, 2013).

To summarize, the uterine environment has both a negative effect on sperm number and viability, and a positive action on the regulation of sperm function, protecting them from premature capacitation and improving their ability to bind cumulus cells. This dual activity may result in the selection of the fittest sperm subpopulation and elimination of abnormal ones by immune cells recruited by the immune response induced by sperm binding to UEC and seminal plasma action. EVs might be interesting players in these complex interactions.

3. Sperm interactions with the utero-tubal junction

3.1. Factors involved in sperm migration up to the utero-tubal junction

The migration of spermatozoa up to the oviduct is the result of a combination of several male and female parameters. As spermatozoa swim in the uterine fluid to reach the UTJ, sperm mobility and morphology are expected to be limiting factors of sperm migration. After intrauterine insemination in sows, an increase in the proportion of morphologically abnormal sperm collected in the backflow from uterus to vagina was observed while this proportion was lower among sperm recovered in the UTJ (Garcia-Vazquez et al., 2015). Indeed, almost all spermatozoa that colonize the UTJ had a normal morphology. However, even if it is expected that normal morphology is required to transit in the female tract, it is not clear which mechanisms are actually involved in the selection of normal spermatozoa and which sperm morphological parameters, such as head size or flagella length, are of critical importance (Garcia-Vazquez et al., 2016). Furthermore, in some mammals including dogs in which a long interval can occur between mating and fertilization (up to 9 days), sperm storage seems to occur mainly within the uterine glands and in the UTJ (England and Burgess, 2003; Rijsselaere et al., 2004).

Beyond sperm mobility and morphology, the contractions of the uterus are also involved in the transit of the spermatozoa. In the sow after intrauterine insemination, spermatozoa can be found within minutes in the UTJ thanks to uterine contractions (Langendijk et al., 2005). The short duration of sperm transit from the uterus to the oviduct cannot be explained by the sole mobility of spermatozoa but rather by the existence of transporting waves induced by myometrial contractions (Langendijk et al., 2002). The uterine contractions do transport spermatozoa from the uterus to the UTJ but also remove lots of live and dead spermatozoa from the uterus by waves of contractions, also called fundo-cervical peristalsis in humans (Kunz and Leyendecker, 2002), in the opposite direction than those bringing sperm to the UTJ. In the mare within 4 h after intrauterine insemination, some spermatozoa were observed in the oviduct while most of them were eliminated in the vagina by uterine contractions (Katila et al., 2000).

3.2. Sperm molecules required to cross the utero-tubal junction

When spermatozoa reach the tip of the uterine horn, they have to cross the UTJ, connecting the uterus to the oviduct. The UTJ is a functional barrier between the uterus and the oviduct, selecting sperm with normal mobility and specific surface molecular properties. Indeed, null mouse mutants for more than 15 different genes are infertile because their sperm cannot pass through the UTJ despite normal sperm mobility and morphology (for reviews, see (Fujihara et al., 2018; Xiong et al., 2019); Fig. 4). Except *Ly6k*, *Pgap1* and *Lypd4*, these mutants share a common feature, the absence or the dislocation of sperm membrane protein A disintegrin and metallopeptidase domain 3 (ADAM3) in the detergent-rich membrane domain. Therefore, ADAM3 is suggested to be an important factor for sperm migration to the oviduct in the mouse. The precise mechanism by which ADAM3 facilitates the passage of sperm through the UTJ is unknown. Interestingly, all these mutants are not only unable to migrate to the oviduct but also to bind to the zona pellucida, suggesting that similar mechanisms might be involved in sperm transit and zona binding. The distribution of ADAM3 was not affected in spermatozoa from *Ly6K*, *Pgap1* and *Lypd4* KO mice, which suggests that mechanisms other than those involved in the correct distribution of ADAM3 on sperm surface are involved in sperm migration through the UTJ in mouse. So far similar mechanisms of sperm selection based on sperm surface proteins have not been evidenced in other species.

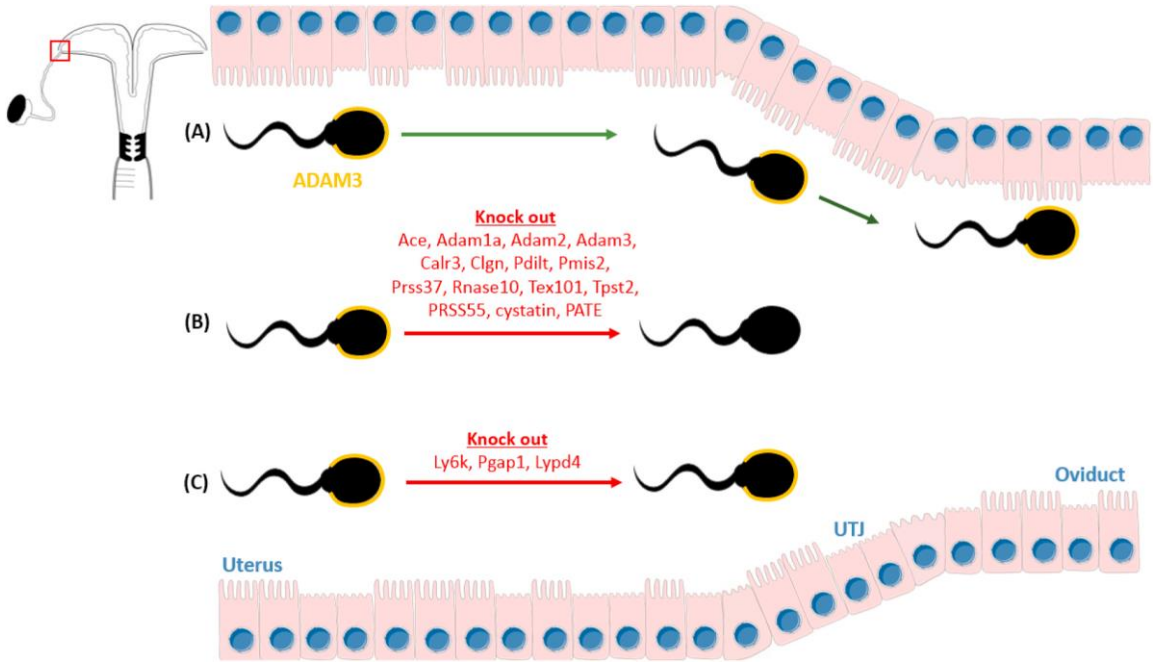

Fig. 4. Mechanisms of sperm transport through the utero-tubal junction (UTJ) identified in the mouse. (A) Spermatozoa with correct distribution of ADAM3 pass through the UTJ; (B) Genes involved in the correct distribution of ADAM3 on sperm surface and in sperm passage through the UTJ; (C) Genes involved in sperm passage through the UTJ without targeting ADAM3, assuming other potential mechanisms. References for corresponding null mutants: *Ace* (Krege et al., 1995), *Adam1a* (Nishimura et al., 2004), *Adam2* (Cho et al., 1998), *Adam3* (Shamsadin et al., 1999), *Calr3* (Ikawa et al., 2011), *Clgn* (Ikawa et al., 1997), *Ly6k* (Fujihara et al., 2014), *Pdilt* (Tokuhiro et al., 2012), *Pgap* (Ueda et al., 2007), *Pmis2* (Yamaguchi et al., 2012), *Prss37* (Shen et al., 2013), *Prss55* (Shang et al., 2018), *Rnase10* (Krutskikh et al., 2012), *Tex101* (Fujihara et al., 2013), *Tpst2* (Marcello et al., 2011), *Cystatin* (CST), Prostate and testis expressed proteins (PATE), lymphocyte antigen 6 (Ly6)/Plaur domain (*lypd*) (Fujihara et al., 2019).

4. Sperm interactions with the oviduct

After mating or insemination, a very small proportion of spermatozoa reach the oviduct. Genital tracts collected after insemination in cows and gilts evidenced no more than a few dozens to hundreds of sperm within the oviduct (Hunter, 1981; Hunter et al., 1991; Hunter and Wilmut, 1984; Sostaric et al., 2008). As oviducts are small intra-abdominal organs not accessible on animals without surgery or slaughter, exact information on oviductal sperm behavior in vivo is scarce and most data were obtained from in-vitro models using oviductal fluids collected post-mortem or from cell culture.

4.1. Effects of interactions with oviductal fluid and secreted proteins on sperm physiology

The oviductal fluid (OF) is a complex mixture of molecules originated from selective blood transudation and secretions of oviduct epithelial cells (OECs), and with possible participation of follicular and peritoneal fluids (for review, see (Saint-Dizier et al., 2019)). The composition of the OF differs from that of the UF in terms of ions (Hugentobler et al., 2007a), metabolites (Hugentobler et al., 2007b, 2008) and macromolecules (Soleilhavoup et al., 2016) and as such, has specific effect on sperm physiology. Many *in vitro* studies reported beneficial effects of OEC secretions on sperm viability, motility and capacitation in various mammals including cattle (Abe et al., 1995a; Bergqvist et al., 2006; Grippo et al., 1995; McNutt and Killian, 1991), pigs (Coy et al., 2010; Kumaresan et al., 2012), sheep (El-Shahat et al., 2018) and dogs (Kawakami et al., 1998). Fluctuating effects of the OF on sperm capacitation were observed depending on the time at which sperm parameters are measured and on the stage in the cycle. A 5-min exposure to pre-ovulatory OF was sufficient to increase significantly the proportion of sperm with phosphorylated tyrosine in pigs (Kumaresan et al., 2014). Bull sperm incubated with estrous OF displayed globally higher tyrosine phosphorylation levels (Kumaresan et al., 2019) and higher ability to undergo acrosome reaction (Grippo et al., 1995; Parrish et al., 1989) and to fertilize oocytes *in vitro* (Grippo et al., 1995) compared with fluids collected at other stages of cycle. Also, differences in sperm fertilizing ability were evidenced after incubation with isthmic and ampullary OF (Grippo et al., 1995), suggesting region-specific effects on sperm physiology. Interestingly, variation in terms of response to OF were observed between bulls with different fertility in the field (Kumaresan et al., 2016), which may explain differences in pregnancy rates between males with comparable semen quality.

Relatively high levels of bicarbonate, albumin, high-density lipoproteins (HDL) and phospholipids (leading to high phospholipid: cholesterol ratio) present in the peri-ovulatory OF have been proposed as effectors of sperm cholesterol efflux leading to capacitation and acrosome reaction (Bergqvist and Rodriguez-Martinez, 2006; Ehrenwald et al., 1990; Rodriguez-Martinez, 2007; Tienthai et al., 2004). Furthermore, incubation with OF protein extracts reproduced most beneficial effects of the OF on sperm viability, motility and acrosome integrity in cattle (Boquest et al., 1999; Kumaresan et al., 2005, 2006) and humans (Zumoffen et al., 2010), suggesting probable central roles played by OF proteins in the modulation of sperm functions. Antioxidant enzymes such as catalase and superoxyde dismutase present in the OF (Kobayashi et al., 2014; Lapointe et al., 1998) may protect spermatozoa from oxidative damages and promote their survival in the oviductal environment. Moreover, it was hypothesized that OF proteins maintain sperm membrane integrity by avoiding proteolytic damages, neutralizing toxic by-products of sperm metabolism and/or by reducing metabolism (Boquest et al., 1999). However, the exact mechanisms by which oviductal proteins affect sperm physiology are still unknown.

In order to obtain an exhaustive list of sperm-interacting proteins in

the OF, our group compared the proteomes (assessed by nanoLC-MS/MS) of bull sperm pre-incubated or not with cow OF collected at pre-ovulatory, post-ovulatory and luteal phases of the estrous cycle. A total of 27 sperm-interacting proteins ranging from 16 to 230 kDa were quantified on sperm, including the oviduct-specific glycoprotein OVGP1 as most abundant (Lamy et al., 2018). This was in accord with previous candidate-based approaches in which OVGP1 was immunolocalized on various mammalian spermatozoa (Abe et al., 1995b; King and Killian, 1994; Lippes and Wagh, 1989; Yang et al., 2015). In addition, new OF sperm-interacting proteins were identified including annexins (ANXA1, ANXA2), heat shock proteins (HSP27, GRP78), three myosins (MYH9, MYH14, MYO6) and proteins of the protein disulfide isomerase family (PDIA3, PDIA4, PDIA6) (Lamy et al., 2018) (Fig. 5). Annexins A1 and/or A2 were previously identified as sperm receptors on OEC apical side in cattle (Ignotz et al., 2007) and pigs (Teijeiro et al., 2009). Furthermore, MYH9 was previously identified as a binding partner of OVGP1 on monkey sperm (Kadam et al., 2006). Therefore, oviductal proteins may also interact with each other in the OF and form protein complexes competing with available interacting sites on sperm. Of interest, the abundance of interacting proteins on sperm differed according to the cycle stage and was not related to the initial abundance of specific proteins measured in the OF (Lamy et al., 2016a, 2018). This indicates that highly selective sperm-protein interactions take place in the oviduct and suggests specific (unknown) mechanisms of sperm binding depending on the protein environment. Furthermore, while OVGP1 was by far the most abundant protein on sperm before ovulation, a number of proteins including MYH9, MYH14, HSP27, ANXA1 and ANXA2 interacted with sperm only after ovulation or at higher abundance at post-ovulatory than at pre-ovulatory stage of cycle (Lamy et al., 2018), suggesting important role at the time of ovulation, possibly on sperm release from the oviductal sperm reservoir (see below).

The functional roles of OVGP1, a glycoprotein more abundant in the OF of various mammals during estrus than at other stages of cycle, has been given special attention (for review, see (Aviles et al., 2010)). The protein is not present in rats and megabats as *OVGP1* became a pseudogene in these two species (Moros-Nicolas et al., 2018). Female mice with a null mutation for OVGP1 displayed a slight decrease in litter size after mating (−14% with no statistical difference with controls), showing that OVGP1 is not essential for fertilization, at least in mice (Araki et al., 2003). The comparison of the amino acid sequences of various mammalian OVGP1 revealed significant differences between species, especially in the C-terminal region (Aviles et al., 2010), making it difficult to extrapolate the potential roles of OVGP1 on fertilization from one species to another. In cattle, spermatozoa incubated with purified OVGP1 displayed higher motility, viability (Abe et al., 1995b; Choudhary et al., 2017), membrane integrity and capacitation status (Choudhary et al., 2017) than untreated controls. Under capacitating conditions, OVGP1 enhanced sperm protein tyrosine phosphorylation and acrosome reaction in hamster (Saccary et al., 2013; Yang et al., 2015) and human (Zhao et al., 2016) in a time-dependent manner, with first stimulating effects observed after only 5 min (Saccary et al., 2013). Native OVGP1 was more effective than recombinant non-glycosylated OVGP1 on various buffalo sperm functions, inferring important roles played by OVGP1 glycosylation (Choudhary et al., 2017). Furthermore, pretreatment of either sperm or oocyte with recombinant hamster OVGP1 prior to co-incubation was shown to increase the number of sperm bound to the zona pellucida (Yang et al., 2015), indicating modulating roles on gamete interaction.

There is limited information on the role played by other oviductal proteins on sperm functions. Osteopontin (OPN), like OVGP1, is a glycoprotein present in the OF at highest abundance around ovulation time (Liu et al., 2015; Soleilhavoup et al., 2016). OPN was shown to bind on the post-equatorial region of bull ejaculated sperm, possibly via integrin and CD44 receptors (Souza et al., 2008), and promoted induced-acrosome reaction *in vitro* (Monaco et al., 2009) (Fig. 5). Since OPN is already present on ejaculated sperm, it was suggested that contact with OF changes OPN pattern on sperm heads and therefore facilitates sperm interactions with oocyte (Souza et al., 2008). In mice, anti-OPN antibody added *in vitro* reduced the rates of fertilization, cleavage and blastocyst formation (Liu et al., 2015), suggesting a beneficial role of OPN in these steps. In pigs, in which high incidence of polyspermy typically occurs during IVF, OPN reduced polyspermy and increased fertilization efficiency during IVF (Hao et al., 2006).

Heat shock proteins such as HSPA8 and GRP78 are present on the surface of OECs (Elliott et al., 2009; Marin-Briggiler et al., 2010) and as soluble proteins in the OF (Lamy et al., 2016a). The use of recombinant HSPA8 allowed to reproduce the beneficial effects of oviductal plasma membranes on long-term survival in cattle, pigs and sheep (Elliott et al., 2009; Lloyd et al., 2009; Moein-Vaziri et al., 2014) and improved post-freezing sperm survival in cattle (Holt et al., 2015). In addition, recombinant HSPA8 also enhanced boar sperm membrane fluidity after a 15-min exposure and improved monospermic fertilization compared to non-exposed controls *in vitro* (Moein-Vaziri et al., 2014). Furthermore, human spermatozoa incubated with recombinant HSP60 or GRP78 under capacitating conditions showed increased sperm intracellular calcium levels compared with controls (Lachance et al., 2007). Recombinant GRP78 was shown to bind to the acrosomal cap of human sperm and modulate zona pellucida interaction in a calcium-dependent manner (Marin-Briggiler et al., 2010).

4.2. *Effects of interactions with oviductal extracellular vesicles on sperm physiology*

Oviductal extracellular vesicles (oEVs), also called oviductosomes, have recently gained attention for their interactions with gametes/early embryos and potential effects on fertility (for review, see (Alminana and

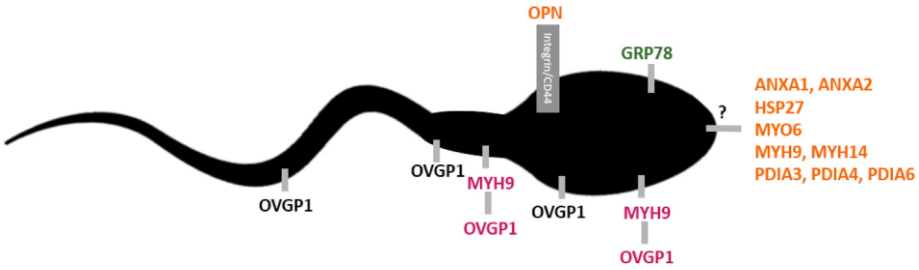

Fig. 5. Identification and localization of sperm-interacting proteins in the oviductal fluid. The heat shock protein GRP78 interacts with acrosomal cap of human sperm (Marin-Briggiler et al., 2010). OVGP1 was shown to associate with the sperm head region and midpiece in human (Lippes and Wagh, 1989; Zhao et al., 2016) and hamster (Yang et al., 2015) but with the whole surface of bull sperm (Abe et al., 1995b; King and Killian, 1994). MYH9 was proposed to be OVGP1 receptor on monkey sperm head and midpiece (Kadam et al., 2006). Osteopontin (OPN) interacts with bull sperm post-equatorial region probably via integrins and CD44 (Souza et al., 2008). Additional sperm-interacting proteins were identified in the bovine OF although their localization on sperm is still unknown (Lamy et al., 2018).

Bauersachs, 2019)). Observation of oEVs merging with the head, midpiece and tail of sperm was evidenced in mice (Al-Dossary et al., 2015), pigs (Alcantara-Neto et al., 2020a) and cats (Ferraz et al., 2019). A flow cytometry analysis of bull sperm co-incubated with fluorochrome-labeled oEVs showed a progressive sperm uptake starting after a single min of incubation (Franchi et al., 2020). As for sperm-OEC interactions, not all sperm appear able to interact with oEVs: a plateau was reached with 62% of sperm displaying oEV interactions after 2 h of co-incubation in cattle (Franchi et al., 2020), and 68% of sperm after 3 h of co-incubation in mice (Bathala et al., 2018).

Recent data in mammals evidenced important roles played by oEVs on sperm physiology. In pigs, our group showed that oEVs increased sperm motility and viability and reduced polyspermy without affecting the global fertilization rate, reproducing the beneficial effect of the OF on *in vitro* fertilization (Alcantara-Neto et al., 2020b). Incubation of cat sperm with oEVs sustained a greater percentage of motile sperm for 24 h and increased sperm fertilizing capacity *in vitro* (Ferraz et al., 2019). The effect of oEVs on sperm acrosome reaction appears species-specific. In cats, oEVs prevented premature acrosomal exocytosis (Ferraz et al., 2019). On the opposite, oEVs from bovine OF provoked a rise in bull sperm intracellular calcium, stimulated protein tyrosine phosphorylation and induced an acrosome reaction (Franchi et al., 2020). Interestingly, oEVs from the ampulla and isthmus showed similar but not identical effects on bull sperm calcium entry, suggesting that sperm physiology may be modulated differentially close to the fertilization site in the ampulla (Franchi et al., 2020).

The molecular content of oEVs includes a large number of proteins, small RNAs and metabolites that fluctuate throughout the reproductive cycle and especially around the time of ovulation, probably under hormonal influence (Alminana et al., 2017; Fereshteh et al., 2018; Gatien et al., 2019; Laezer et al., 2020). Among sperm proteins, plasma membrane calcium/calmodulin-dependent calcium ATPases (PMCA), in particular PMCA4, are important fertility-modulating proteins since they act as calcium efflux pump required for sperm hyperactivated motility and fertilizing ability (Schuh et al., 2004). PMCA1 and 4a were shown to be major forms of PMCAs in mice oEVs and detected at much higher abundance around the time of ovulation (at pro-estrus/estrus) than at other stages of the cycle (Al-Dossary et al., 2013; Bathala et al., 2018). Co-incubation assays indicated that mouse sperm are able to integrate PMCA4a from oEVs over the sperm head and midpiece (Al-Dossary et al., 2013, 2015). A fusion mechanism involving integrins (α5β1 and αvβ3) and CD9 tetraspanin expressed on sperm and oEVs was proposed (Al-Dossary et al., 2015). Further studies evidenced that oEVs can deliver enzymatically active PMCA1 and tyrosine-phosphorylated proteins to murine sperm and that this delivery was higher in capacitated than in uncapacitated sperm (Bathala et al., 2018). As PMCAs were also detected in human oEVs, it was proposed that the delivery of fertility-modulating proteins to sperm by oEVs was preserved in humans (Bathala et al., 2018). Moreover, oEVs seem able to deliver microRNAs in intracellular sperm subcompartments in mice (Fereshteh et al., 2018). Transferred microRNAs were mainly localized in sperm head while the microRNA *miR-34c-5p*, which is only sperm-derived in the embryo and crucial for the first embryo cleavage, was specifically concentrated near the centrosome (Fereshteh et al., 2018) (Fig. 6). These data identify oEVs as key components for sperm acquisition of fertilizing ability and for the quality of the early embryo. Further studies are needed to understand by which mechanisms oEV-derived molecules localize in specific sperm sub-compartments to perform their function.

4.3. Binding to oviduct epithelial cells: formation of a functional sperm reservoir

Mating or insemination in mammals occurs usually hours and up to a couple of days before ovulation, making sperm storage advantageous for successful fertilization. After passing the barrier of the UTJ, a subpopulation of spermatozoa adhere to the luminal epithelium of the caudal part of the oviduct, namely the isthmus, where they can be stored for hours to days (in most mammals), and even months (in bats), before their release around the time of ovulation to migrate toward the site of fertilization (Brussow et al., 2008; Holt and Fazeli, 2016; Hunter and Wilmut, 1984).

This 'functional sperm reservoir' forms approximately 8–12 h after insemination in cows (Wilmut and Hunter, 1984). Oviductal sperm reservoirs have been identified in a number of mammals including cattle (Hunter and Wilmut, 1984), sheep (Hunter and Nichol, 1983), pigs (Hunter, 1981), rabbits (Overstreet and Cooper, 1978), rodents (Smith and Yanagimachi, 1991; Suarez, 1987) and humans (Baillie et al., 1997). The oviduct epithelium contains both non-ciliated and ciliated cells. Microscopic observation of bovine oviducts after insemination evidenced that sperm bound by their head to OECs with a preference for ciliated cells (Ardon et al., 2016; Lefebvre et al., 1995; Sostaric et al., 2008) (Fig. 7).

In vitro, sperm bind in equivalent numbers to isthmic and ampullary explants in cattle and pigs (Fazeli et al., 2004; Lefebvre et al., 1995; Petrunkina et al., 2001; Sostaric et al., 2008) as well as in vivo, after surgical sperm infusion into the oviduct of pre-ovulatory cows (Lefebvre et al., 1995). It is thus likely that sperm form a reservoir in the isthmus because it is the first region encountered beyond the UTJ. However, sperm binding is not restricted to the caudal isthmus: in mice, in which very thin oviductal wall allowed direct observation of spermatozoa

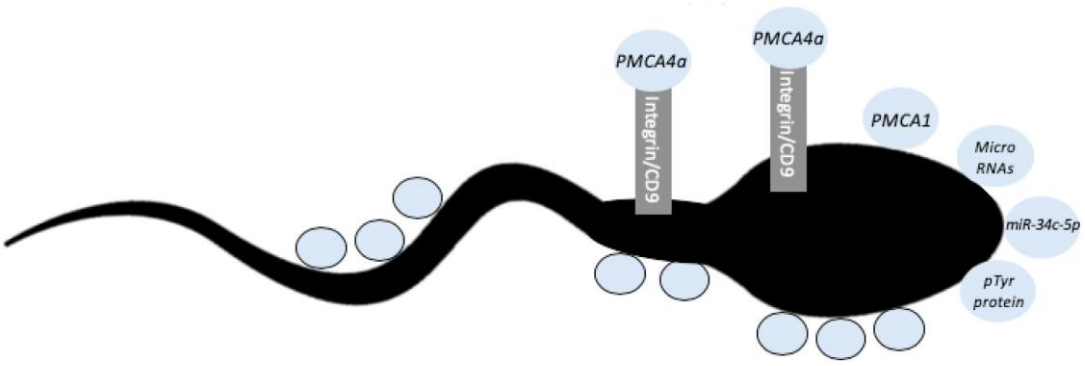

Fig. 6. Identification and localization of oviductal extracellular vesicles and intravesicular molecules interacting with spermatozoa. Oviductal EVs (in blue) were shown to merge with sperm head and midpiece in mice (Al-Dossary et al., 2015), and cats (Ferraz et al., 2019) but also with sperm tail in pigs (Alcantara-Neto et al., 2020a). Plasma membrane calcium ATPases (PMCA) 4a and tyrosine-phosphorylated proteins (pTyr protein) can be delivered to mouse sperm via oEVs through integrin and CD9 tetraspanin (Al-Dossary et al., 2013, 2015). PMCA1 and tyrosine phosphorylated proteins can also be delivered to sperm head via oEVs (Bathala et al., 2018). Intravesicular microRNAs can also be transferred to sperm head in mice (Fereshteh et al., 2018).

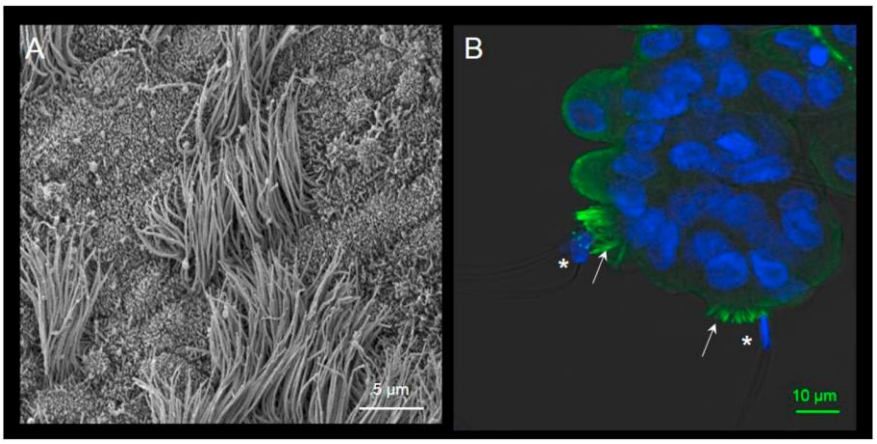

Fig. 7. Sperm interactions with oviduct epithelial cells (OECs) in cattle. (A) SEM picture of the luminal surface of oviduct epithelium composed of ciliated and non-ciliated cells. (B) Confocal microscopy picture of bull sperm interacting with bovine oviduct epithelial cells *in vitro*. Nuclei appeared in blue, cilia (acetylated α-tubulin) in green. Asterisks indicate sperm heads; arrows indicate cilia. Source: K. Reynaud. (For interpretation of the references to colour in this figure legend, the reader is referred to the Web version of this article.)

(from transgenic males) expressing green fluorescent protein (GFP) in their acrosome by live cell imaging, frequent detachment and reattachment were observed as sperm ascended toward the oocyte and most sperm located in the ampulla were found attached to the epithelium (Chang and Suarez, 2012).

There is evidence that not all sperm have the ability to bind to the oviduct epithelium (Fig. 8). Studies conducted in human and cattle showed that approximately 20%–50% of frozen-thawed and Percoll-washed spermatozoa were able to bind to OEC monolayers or oviduct explants *in vitro* (Ellington et al., 1999; Gualtieri and Talevi, 2003). It was shown that only motile, uncapacitated and acrosome-intact sperm with a normal phenotype selectively bound to OECs *in vitro* (Ellington et al., 1999; Fazeli et al., 1999; Gualtieri and Talevi, 2000; Leemans et al., 2014; Lefebvre and Suarez, 1996; Petrunkina et al., 2004; Thomas et al., 1994). In pigs, the ability to bind to OECs *in vitro* correlated with the ability of spermatozoa to swell in response to hypo-osmotic stress and to recover their initial volume after induced stress (Khalil et al., 2006). When bound and unbound boar sperm were compared during incubation with porcine OECs during 24 h, the percentage of viable and morphologically normal sperm was higher and increased over time in the bound population (Yeste et al., 2014). After sperm sex sorting in pigs, both X-and Y-bearing sperm bound at equivalent numbers to porcine oviduct aggregates (Winters et al., 2018). Furthermore, a high incidence of morphological abnormalities and cytoplasmic droplets, as well as abnormal or unstable chromatin, was shown to significantly reduce the ability of sperm to bind to OECs in human and pigs (Ardon et al., 2008; Ellington et al., 1999; Petrunkina et al., 2001; Waberski et al., 2006). This supports the general idea that after crossing of the UTJ, a functional sperm reservoir is formed with a highly selected population of top quality spermatozoa that are not (or not fully) capacitated.

Sperm binding to the oviduct epithelium is carbohydrate-dependent, as shown by extensive inhibition of sperm binding by competition assays in the presence of glycans (Cortes et al., 2004; Green et al., 2001; Lefebvre et al., 1997; Sostaric et al., 2005, 2008). The use of glycan arrays allowed to identify 6-sialylated biantennary N-acetyllactosamine

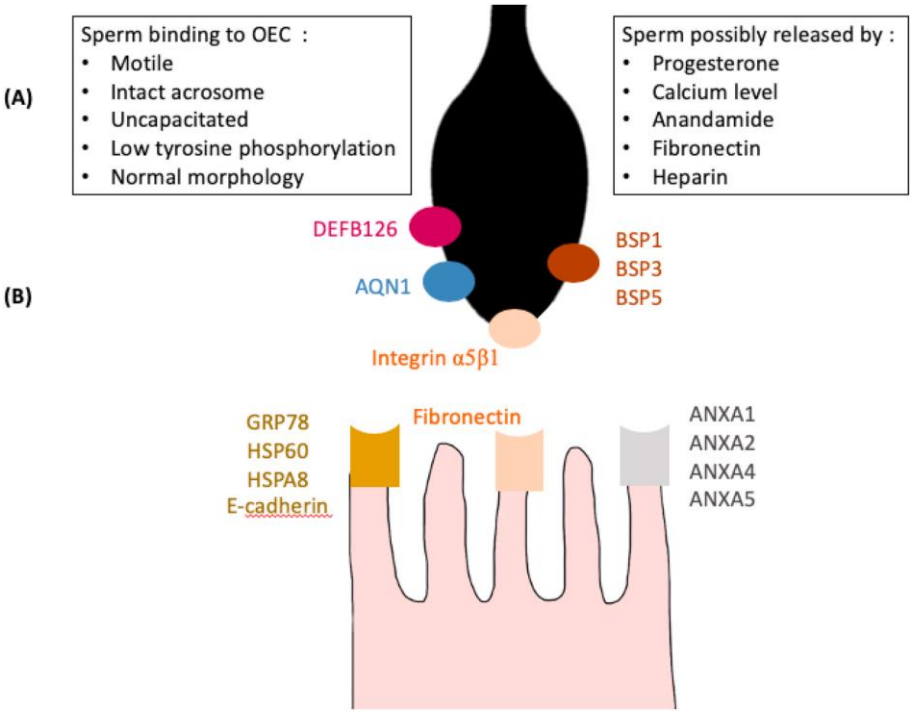

Fig. 8. Sperm interactions with oviduct epithelial cell and underlying mechanisms. (A) Sperm parameters for binding to OECs and candidates for the induction of sperm release around the time of ovulation are indicated in left and right squares, respectively. (B) Sperm surface proteins potentially involved in sperm binding to OECs include the spermadhesin AQN1, Binders of Sperm Proteins (BSPs) 1, 3 and 5, integrin α5β1 and beta defensin 126 (DEFB26). Sperm receptors identified at the luminal surface of OECs include the chaperones GRP78, HSP60 and HSPA8, E-cadherin, fibronectin (as specific partner of integrin α5β1) and various members of the annexin (ANX) family. Refer to the text for related species and references.

and Lewis X trisaccharide (Le^X) as the motifs that bind porcine sperm whereas bull sperm specifically bind the closely related isomere Lewis A motif (for review, see (Miller, 2018)). Various proteins that potentially contain the above carbohydrates have been identified as sperm receptors on the luminal surface of the oviduct epithelium (Fig. 8). The chaperones GRP78, HSP60 and HSPA8, a highly conserved member of the HSP70 family, are expressed at the luminal surface of the oviduct epithelium and were shown to bind spermatozoa in human (Lachance et al., 2007; Marin-Briggiler et al., 2010), cattle (Boilard et al., 2004; Elliott et al., 2009; Holt et al., 2015) and pigs (Elliott et al., 2009). Furthermore, affinity purification of proteins extracted from oviductal apical membranes identified annexins A1, A2, A4 and A5 as other sperm-interacting proteins in cattle (Ignotz et al., 2007) whereas annexin A2 (ANXA2) was also proposed as the main sperm binding isoform in pigs (Teijeiro et al., 2009). On the other hand, epithelial cadherin (E-cadherin), a protein involved in calcium-dependent somatic cell adhesion, was identified as a sperm receptor in the bovine oviduct (Caballero et al., 2014). Finally, fibronectin, a high molecular weight glycoprotein present at the apical surface of the oviduct epithelium in human and cattle (Inan et al., 2004; Osycka-Salut et al., 2017) was shown to interact with bovine sperm through α5β1, an integrin expressed in the sperm of several species (Osycka-Salut et al., 2017). It was proposed that an increase in fibronectin levels in the oviductal fluid during the pre-ovulatory period promotes sperm release in cattle (Osycka-Salut et al., 2017).

Epididymal sperm of various species were found to be able to bind to OECs, yet with a much lower binding capacity than ejaculated sperm (Gwathmey et al., 2003, 2006; Henry et al., 2015; Petrunkina et al., 2001; Silva et al., 2014). Beta-defensin 126 (DEFB126), a protein from the corpus epididymis and integral part of the sperm glycocalyx, was shown to be critical for sperm attachment to the macaque oviduct epithelium (Tollner et al., 2008). Removal or alteration of DEFB126 in primate sperm reduced the capacity of spermatozoa to bind to oviduct explants and treatment of explants with soluble DEFB126 demonstrated that DEFB126 associated predominantly with secretory non-ciliated cells (Tollner et al., 2008).

Spermatozoa from various species are able to bind to heterologous OECs (Ellington et al., 1998; Petrunkina et al., 2004), which is in favor of common mechanisms of oviduct-sperm interactions among species. Several families of seminal plasma proteins like the BSPs (Binder of Sperm Proteins) are adsorbed at the sperm surface at ejaculation and are involved in the establishment of sperm reservoir in cattle (Talevi and Gualtieri, 2010). BSPs consist of an N-terminal domain followed by two fibronectin type II domains possessing phospholipid and heparin binding sites (for review, see (Plante et al., 2016)). BSP1 (formerly called PDC-109), the most abundant protein in the bovine seminal plasma, as well as BSP3 and BSP5, were shown to promote binding of epididymal bull sperm to bovine oviductal explants (Gwathmey et al., 2003, 2006). In the pig, the most abundant proteins in the seminal plasma are members of the spermadhesin family (Topfer-Petersen et al., 1998). The spermadhesin AQN1was shown to recognize a wide range of glycans and to inhibit boar sperm binding to OECs when added in the culture medium (Ekhlasi-Hundrieser et al., 2005), suggesting a role in the formation of the oviductal sperm reservoir in pigs.

4.4. *Effects of interaction with oviduct epithelial cells on sperm physiology*

Binding to oviductal cells or OEC apical membrane preparations prolongs sperm lifespan, as shown *in vitro* in cattle (Boilard et al., 2002, 2004), pigs (Fazeli et al., 2003; Yeste et al., 2009) and humans (Morales et al., 1996; Murray and Smith, 1997) (Fig. 9). This beneficial effect on sperm viability was more pronounced with oviductal cells than with epithelial cells from mammary glands or kidney, showing oviduct-specific effects (Boilard et al., 2002; Moein-Vaziri et al., 2014;

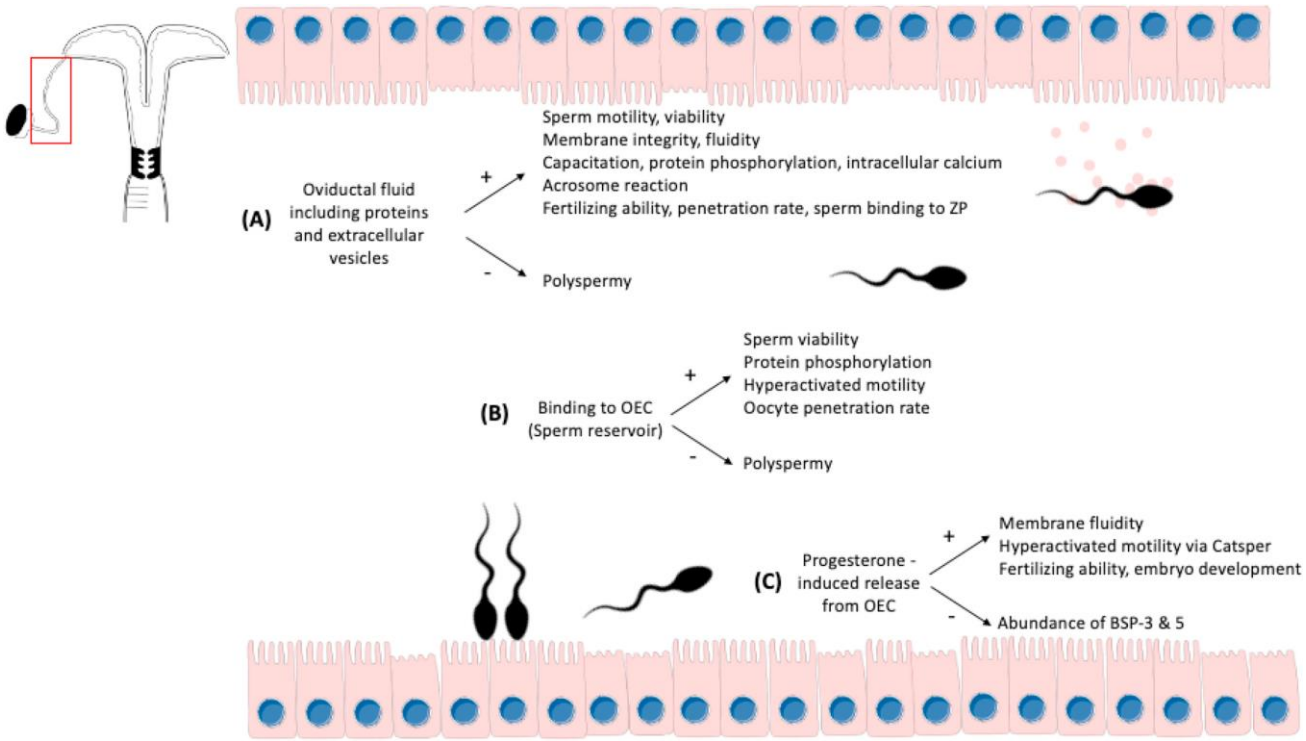

Fig. 9. Summarized effects of interactions with the oviduct on sperm physiology. (A) Effects of sperm interaction with the oviductal fluid including soluble proteins and oviductal extracellular vesicles (oEVs) on sperm physiology; (B) Effects of interactions with oviductal epithelial cells (OECs, formation of an oviductal sperm reservoir) on sperm physiology; (C) Effect of sequential binding to OECs then release by the action of progesterone on sperm physiology. See the text for corresponding references.

Yeste et al., 2009). Moreover, direct cell contact seems optimal for sperm survival as co-incubation with OEC-conditioned medium had much lower efficiency for maintaining boar sperm viability over time (Yeste et al., 2009).

Various factors fluctuating in the oviduct fluid around the time of ovulation have been proposed as sperm releasing factors, including calcium level (Bosch et al., 2001; Gervasi et al., 2016), anandamide (Gervasi et al., 2009, 2016; Kumar et al., 2017; Osycka-Salut et al., 2012), fibronectin (Osycka-Salut et al., 2017), sulfated glycosaminoglycans such as heparin (Ardon et al., 2016; Talevi and Gualtieri, 2001; Tienthai, 2015) and ovarian steroid hormones (Hunter, 2008; Lamy et al., 2016b). Using bovine OEC culture system, we showed that bull sperm bound to OECs can be released by physiological nanomolar concentrations of progesterone (Lamy et al., 2017).

Similarly, progesterone was recently shown to induce sperm release from OEC aggregates in pigs (Machado et al., 2019). Bull sperm detached from OECs by the action of progesterone displayed decreased levels of BSP-3 and BSP-5 (Ramal-Sanchez et al., 2020), supporting a role of BSPs in progesterone-induced sperm release. Furthermore, although œstradiol had no effect on bull sperm release from OECs *in vitro*, the releasing effect of progesterone was inhibited by œstradiol in a dose-dependent manner in cattle (Lamy et al., 2017), showing that both progesterone and œstradiol are likely to be involved in sperm release. It is worth noting that only 50–75% of bound sperm can be released through the action of progesterone (Lamy et al., 2017; Machado et al., 2019; Romero-Aguirregomezcorta et al., 2019), indicating that the ability of sperm to respond to the releasing signal, in addition to its ability to bind to OECs, are highly selective steps toward the oocyte.

Recent data in pigs and cattle indicate that sperm bound to OECs requires hyperactive motility to detach themselves from OECs, an action likely mediated by progesterone-triggered calcium influx through the cation channel of spermatozoa (CatSper) (Machado et al., 2019; Romero-Aguirregomezcorta et al., 2019). Hyperactivated motility is a particular asymmetrical flagellar movement that enhances the ability of sperm to penetrate the cumulus oophorus and the zona pellucida (Suarez, 2008). In mice, sperm hyperactive motility is typically observed each time sperm detach from the oviduct epithelium (Chang and Suarez, 2012; DeMott and Suarez, 1992). In accordance with data in cattle and pigs, murine sperm lacking CatSper are unable to display hyperactive motility and detach from the oviduct epithelium (Ho et al., 2009). Progesterone was shown to be able to induce or increase sperm hyperactive motility in the hamster (Noguchi et al., 2008), mouse (Perez-Cerezales et al., 2016) and macaque (Sumigama et al., 2015). However, the role of progesterone in sperm detachment from the sperm reservoir remains to be investigated in these species. It is however likely that sperm hyperactivated motility is initiated in the caudal isthmus, i.e. relatively far from the fertilization site, in order to detach from the sperm reservoir. In addition, although the cumulus cells and zona pellucida are known to induce the acrosome reaction, recent data in mice indicate that most spermatozoa begin to react in the isthmus, thus before reaching the site of fertilization in the ampulla (Hino et al., 2016; La Spina et al., 2016).

Sperm binding to the oviductal isthmus is not absolutely mandatory for sperm to acquire their fertilizing ability: when rabbits, sheep and pigs were surgically inseminated directly into the ampulla (via the infundibulum) or into the abdominal cavity, fertilization did take place (Hunter, 2011). Nonetheless, a large amount of data show that binding to OECs and subsequent release has beneficial effects not only on sperm viability and motility but also on sperm capacitation and fertilizing capacity (Fig. 9). Tyrosine phosphorylation of tail-associated protein was shown to increase over time in dog and stallion sperm bound to oviduct explants compared with unbound sperm (Leemans et al., 2014; Petrunkina et al., 2004). Specific patterns of protein phosphorylation located in the equatorial segment and tail were also observed in subpopulations of bound sperm in pigs (Lopez-Ubeda et al., 2017). Furthermore, bull sperm released from OECs by the action of progesterone showed increased membrane fluidity and displayed major lipidomic and proteomic changes, some of which related to sperm capacitation (Ramal-Sanchez et al., 2020). In addition, bull sperm submitted to the sequential binding and progesterone-induced or heparin-induced release from OECs showed higher *in vitro* fertilizing capacity compared to controls without OECs (Gualtieri and Talevi, 2003; Lamy et al., 2017). In pigs, pre-incubation of sperm with OECs reduced polyspermy and increased oocyte penetration rate compared with controls (Bureau et al., 2000). In another study, number of porcine zygotes and sperm nuclear decondensation were improved after sperm-OEC binding and release compared to unbound sperm (Lopez-Ubeda et al., 2017).

Finally, a positive relationship was evidenced between the capacity of sperm to bind to homologous oviduct explants and male fertility in pigs (Khalil et al., 2006; Waberski et al., 2005) and cattle (De pauw et al., 2002; Saraf et al., 2019). Further studies are now needed to determine if sperm-oviduct-binding *in vitro* tests may be used for accurate prediction of male fertility in the field.

5. Conclusions

The interactions taking place between spermatozoa and the female reproductive tract operate a drastic selection among male gametes, leading to a small subpopulation of top quality spermatozoa at the site of fertilization. Sperm selection involves uterine contractions to remove dead and abnormal spermatozoa from the uterus but also various mechanisms including sperm phagocytosis mediated by uterine inflammatory response, key molecules on sperm surface to cross the UTJ, binding to the oviductal sperm reservoir and then ability to respond to the releasing signal at the time of ovulation. Altogether, results show that the seminal plasma plays important roles in modulating the female immune response against sperm cells and protein interactions in female secretions. Effects of specific interactions between seminal proteins coating the sperm surface and female fluid components would bring new knowledge on the exact role of male secretions in sperm transit and survival in the route toward the oocyte. Although molecules involved in sperm transit to the oviduct have gained recent insights in mice, the mechanisms allowing sperm to cross the UTJ in other mammalian species remain unexplored. Furthermore, the mechanisms and functions of sperm interactions with genital tract secretions, especially in the uterine cavity, have been rather poorly investigated and deserve further studies. From *in vitro* studies, sperm interactions with oviductal cells appear to promote sperm survival and prevent precocious capacitation, but in some specific conditions to contribute to sperm capacitation and acquisition of fertilizing competence. Recent data highlight the dynamic hormone-regulated changes in the composition of uterine and oviductal fluids that may explain the lack of consistency recorded in *in vitro* studies. Finally, recent research suggest that EVs in the UF and OF act as natural cargos bringing key molecules from the female genital tract compartment onto male gametes for the success of fertilization. New knowledge in the cross-talk between spermatozoa and the female genital tract may provide new tools for a more accurate evaluation of fertility and to improve fertility in natural pregnancies as well as assisted reproductive technologies.

Acknowledgments

This work was funded by INRAe and Agence Nationale de la Recherche under the grant number ANR-18-CE92-0049. We thank Marc Chodkievicz for careful reading and edition of this manuscript. We thank Thierry Meylheuc, from the imaging facility at the microscopy and imaging platform MIMA2 (INRAe, Jouy-en-Josas, France), Maryse Meurisse and Marie-Claire Blache, from the microscopy and imaging platform PIC (INRAe, Nouzilly, France), for their help with scanning electronic and confocal microscopy images. MSD thanks the CNRS for full-time delegation in the PRC Unit during this year.

References

Abe, H., Sendai, Y., Satoh, T., Hoshi, H., 1995a. Secretory products of bovine oviductal epithelial cells support the viability and motility of bovine spermatozoa in culture in vitro. J. Exp. Zool. 272, 54–61.
Abe, H., Sendai, Y., Satoh, T., Hoshi, H., 1995b. Bovine oviduct-specific glycoprotein: a potent factor for maintenance of viability and motility of bovine spermatozoa in vitro. Mol. Reprod. Dev. 42, 226–232.
Akthar, I., Suarez, S., Morillo, V.A., Sasaki, M., Ezz, M.A., Takahashi, K.I., Shimada, M., Marey, M.A., Miyamoto, A., 2019. Sperm enter glands of preovulatory bovine endometrial explants and initiate inflammation. Reproduction 1, 19-0414.
Al-Dossary, A.A., Strehler, E.E., Martin-Deleon, P.A., 2013. Expression and secretion of plasma membrane Ca2+-ATPase 4a (PMCA4a) during murine estrus: association with oviductal exosomes and uptake in sperm. PloS One 8, e80181.
Al-Dossary, A.A., Bathala, P., Caplan, J.L., Martin-DeLeon, P.A., 2015. Oviductosome-sperm membrane interaction in cargo delivery: detection OF FUSION and underlying molecular players using three-dimensional super-resolution structured illumination microscopy (SR-SIM). J. Biol. Chem. 290, 17710–17723.
Alcantara-Neto, A., Schmaltz, L., Caldas, E., Blache, M.C., Mermillod, P., Alminana, C., 2020a. Porcine oviductal extracellular vesicles interact with gametes and regulate sperm motility and survival. Theriogenology (in press).
Alcantara-Neto, A.S., Fernandez-Rufete, M., Corbin, E., Tsikis, G., Uzbekov, R., Garanina, A.S., Coy, P., Alminana, C., Mermillod, P., 2020b. Oviduct fluid extracellular vesicles regulate polyspermy during porcine in vitro fertilisation. Reprod. Fertil. Dev. 32, 409–418.
Alcântara-Neto, A., Fernandez-Rufete, M., Corbin, E., Tsikis, G., Uzbekov, R., Garanina, A.S., Coy, P., Alminana, C., Mermillod, P., 2020c. Oviduct fluid extracellular vesicles regulate polyspermy during porcine in vitro fertilization. Reprod. Fertil. Dev. 32 (4), 409–418. RD19058.
Alghamdi, A.S., Foster, D.N., 2005. Seminal DNase frees spermatozoa entangled in neutrophil extracellular traps. Biol. Reprod. 73, 1174–1181.
Alghamdi, A.S., Lovaas, B.J., Bird, S.L., Lamb, G.C., Rendahl, A.K., Taube, P.C., Foster, D. N., 2009. Species-specific interaction of seminal plasma on sperm-neutrophil binding. Anim. Reprod. Sci. 114, 331–344.
Alminana, C., Bauersachs, S., 2019. Extracellular vesicles in the oviduct: progress, challenges and implications for the reproductive success. Bioengineering 6.
Alminana, C., Corbin, E., Tsikis, G., Alcantara-Neto, A.S., Labas, V., Reynaud, K., Galio, L., Uzbekov, R., Garanina, A.S., Druart, X., Mermillod, P., 2017. Oviduct extracellular vesicles protein content and their role during oviduct-embryo cross-talk. Reproduction 154, 153–168.
Aloe, S., Weber, F., Behr, B., Sauter-Louis, C., Zerbe, H., 2012. Modulatory effects of bovine seminal plasma on uterine inflammatory processes. Reprod. in domes. animals Zuchthygiene 47, 12–19.
Araki, Y., Nohara, M., Yoshida-Komiya, H., Kuramochi, T., Ito, M., Hoshi, H., Shinkai, Y., Sendai, Y., 2003. Effect of a null mutation of the oviduct-specific glycoprotein gene on mouse fertilization. Biochem. J. 374, 551–557.
Ardon, F., Helms, D., Sahin, E., Bollwein, H., Topfer-Petersen, E., Waberski, D., 2008. Chromatin-unstable boar spermatozoa have little chance of reaching oocytes in vivo. Reproduction 135, 461–470.
Ardon, F., Markello, R.D., Hu, L., Deutsch, Z.I., Tung, C.K., Wu, M., Suarez, S.S., 2016. Dynamics of bovine sperm interaction with epithelium differ between oviductal isthmus and ampulla. Biol. Reprod. 95, 90.
Aviles, M., Gutierrez-Adan, A., Coy, P., 2010. Oviductal secretions: will they be key factors for the future ARTs? Mol. Hum. Reprod. 16, 896–906.
Baba, D., Kashiwabara, S., Honda, A., Yamagata, K., Wu, Q., Ikawa, M., Okabe, M., Baba, T., 2002. Mouse sperm lacking cell surface hyaluronidase PH-20 can pass through the layer of cumulus cells and fertilize the egg. J. Biol. Chem. 277, 30310–30314.
Baba, M., Imai, T., Nishimura, M., Kakizaki, M., Takagi, S., Hieshima, K., Nomiyama, H., Yoshie, O., 1997. Identification of CCR6, the specific receptor for a novel lymphocyte-directed CC chemokine LARC. J. Biol. Chem. 272, 14893–14898.
Bai, R., Latifi, Z., Kusama, K., Nakamura, K., Shimada, M., Imakawa, K., 2018a. Induction of immune-related gene expression by seminal exosomes in the porcine endometrium. Biochem. Biophys. Res. Commun. 495, 1094–1101.
Bai, R., Latifi, Z., Kusama, K., Nakamura, K., Shimada, M., Imakawa, K., 2018b. Induction of immune-related gene expression by seminal exosomes in the porcine endometrium. Biochem. Biophys. Res. Commun. 495, 1094–1101.
Baillie, H.S., Pacey, A.A., Warren, M.A., Scudamore, I.W., Barratt, C.I.R., 1997. Greater numbers of human spermatozoa associate with endosalpingeal cells derived from the isthmus compared with those from the ampulla. Huamn Reprod. 12, 1985–1992.
Baker, M.A., 2016. Proteomics of post-translational modifications of mammalian spermatozoa. Cell Tissue Res. 363, 279–287.
Bathala, P., Fereshteh, Z., Li, K., Al-Dossary, A.A., Galileo, D.S., Martin-DeLeon, P.A., 2018. Oviductal extracellular vesicles (oviductosomes, OVS) are conserved in humans: murine OVS play a pivotal role in sperm capacitation and fertility. Mol. Hum. Reprod. 24, 143–157.
Bergmann, A., Taylor, U., Rath, D., 2012. Flow-cytometric evaluation of lectin binding moieties on porcine uterine epithelial cells. Reprod. Domest. Anim. 47, 77.
Bergmann, A., Taylor, U., Rath, D., 2013. Sperm binding to porcine uterine epithelial cells might be lectin mediated. Reprod. Fertil. Dev. 25, 152.
Bergqvist, A.S., Rodriguez-Martinez, H., 2006. Sulphated glycosaminoglycans (S-GAGs) and syndecans in the bovine oviduct. Anim. Reprod. Sci. 93, 46–60.
Bergqvist, A.S., Ballester, J., Johannisson, A., Hernandez, M., Lundeheim, N., Rodriguez-Martinez, H., 2006. In vitro capacitation of bull spermatozoa by oviductal fluid and its components. Zygote 14, 259–273.
Boilard, M., Bailey, J., Collin, S., Dufour, M., Sirard, M.A., 2002. Effect of bovine oviduct epithelial cell apical plasma membranes on sperm function assessed by a novel flow cytometric approach. Biol. Reprod. 67, 1125–1132.
Boilard, M., Reyes-Moreno, C., Lachance, C., Massicotte, L., Bailey, J.L., Sirard, M.A., Leclerc, P., 2004. Localization of the chaperone proteins GRP78 and HSP60 on the luminal surface of bovine oviduct epithelial cells and their association with spermatozoa. Biol. Reprod. 71, 1879–1889.
Boquest, A.C., Smith, J.F., Briggs, R.M., Duganzich, D.M., Summers, P.M., 1999. Effects of bovine oviductal proteins on bull spermatozoal function. Theriogenology 51, 583–595.
Bosch, P., de Avila, J.M., Ellington, J.E., Wright Jr., R.W., 2001. Heparin and Ca2+-free medium can enhance release of bull sperm attached to oviductal epithelial cell monolayers. Theriogenology 56, 247–260.
Brinkmann, V., Reichard, U., Goosmann, C., Fauler, B., Uhlemann, Y., Weiss, D.S., Weinrauch, Y., Zychlinsky, A., 2004. Neutrophil extracellular traps kill bacteria. Science 303, 1532–1535.
Brohi, R.D., Huo, L.J., 2017. Posttranslational modifications in spermatozoa and effects on male fertility and sperm viability. OMICS 21, 245–256.
Brussow, K.P., Ratky, J., Rodriguez-Martinez, H., 2008. Fertilization and early embryonic development in the porcine fallopian tube. Reprod. Domest. Anim. 43 (Suppl. 2), 245–251.
Bureau, M., Bailey, J.L., Sirard, M.A., 2000. Influence of oviductal cells and conditioned medium on porcine gametes. Zygote 8, 139–144.
Burns, G., Brooks, K., Wildung, M., Navakanitworakul, R., Christenson, L.K., Spencer, T. E., 2014. Extracellular vesicles in luminal fluid of the ovine uterus. PloS One 9, e90913.
Caballero, J.N., Gervasi, M.G., Veiga, M.F., Dalvit, G.C., Perez-Martinez, S., Cetica, P.D., Vazquez-Levin, M.H., 2014. Epithelial cadherin is present in bovine oviduct epithelial cells and gametes, and is involved in fertilization-related events. Theriogenology 81, 1189–1206.
Chang, H., Suarez, S.S., 2012. Unexpected flagellar movement patterns and epithelial binding behavior of mouse sperm in the oviduct. Biol. Reprod. 86 (140), 1–8.
Chastant, S., Saint-Dizier, M., 2019. Inflammation: friend or foe of bovine reproduction? Anim. Reprod. 16, 539–547.
Chirinos, M., Durand, M., Gonzalez-Gonzalez, M.E., Hernandez-Silva, G., Maldonado-Rosas, I., Lopez, P., Larrea, F., 2017. Uterine flushings from women treated with levonorgestrel affect sperm functionality in vitro. Reproduction 154, 607–614.
Cho, C., O'Dell Bunch, D., Faure, J.-E., Goulding, E.H., Eddy, E.M., Primakoff, P., Myles, D.G., 1998. Fertilization defects in sperm from mice lacking fertilin β. Science 281, 1857–1859.
Choudhary, S., Kumaresan, A., Kumar, M., Chhillar, S., Malik, H., Kumar, S., Kaushik, J. K., Datta, T.K., Mohanty, A.K., 2017. Effect of recombinant and native buffalo OVGP1 on sperm functions and in vitro embryo development: a comparative study. J. Anim. Sci. Biotechnol. 8, 69.
Clark, G.F., Schust, D.J., 2013. Manifestations of immune tolerance in the human female reproductive tract. Front. Immunol. 4, 26.
Cortes, P.P., Orihuela, P.A., Zuniga, L.M., Velasquez, L.A., Croxatto, H.B., 2004. Sperm binding to oviductal epithelial cells in the rat: role of sialic acid residues on the epithelial surface and sialic acid-binding sites on the sperm surface. Biol. Reprod. 71, 1262–1269.
Coy, P., Aviles, M., 2010. What controls polyspermy in mammals, the oviduct or the oocyte? Biol. Rev. Camb. Phil. Soc. 85, 593–605.
Coy, P., Lloyd, R., Romar, R., Satake, N., Matas, C., Gadea, J., Holt, W.V., 2010. Effects of porcine pre-ovulatory oviductal fluid on boar sperm function. Theriogenology 74, 632–642.
De pauw, I., Van Soom, A., Laevens, H., Verberckmoes, S., de Kruif, A., 2002. Sperm binding to epithelial oviduct explants in bulls with different nonreturn rates investigated with a new in vitro model. Biol. Reprod. 67, 1073–1079.
DeMott, R.P., Suarez, S.S., 1992. Hyperactivated sperm progress in the mouse oviduct. Biol. Reprod. 46, 779–785.
Ehrenwald, E., Foote, R.H., Parks, J.E., 1990. Bovine oviductal fluid components and their potential role in sperm cholesterol efflux. Mol. Reprod. Dev. 25, 195–204.
Ekhlasi-Hundrieser, M., Gohr, K., Wagner, A., Tsolova, M., Petrunkina, A., Topfer-Petersen, E., 2005. Spermadhesin AQN1 is a candidate receptor molecule involved in the formation of the oviductal sperm reservoir in the pig. Biol. Reprod. 73, 536–545.
El-Shahat, K.H., Taysser, M.I., Badr, M.R., Zaki, K.A., 2018. Effect of oviduct and follicular fluids on ram sperm capacitation and acrosome reaction in vitro. Int. J. Vet. Sci. Med. 6, S57–S62.
Ellington, J.E., Jones, A.E., Davitt, C.M., Schneider, C.S., Brisbois, R.S., Hiss, G.A., Wright Jr., R.W., 1998. Human sperm function in co-culture with human, macaque or bovine oviduct epithelial cell monolayers. Hum. Reprod. 13, 2797–2804.
Ellington, J.E., Evenson, D.P., Wright Jr., R.W., Jones, A.E., Schneider, C.S., Hiss, G.A., Brisbois, R.S., 1999. Higher-quality human sperm in a sample selectively attach to oviduct (fallopian tube) epithelial cells in vitro. Fertil. Steril. 71, 924–929.
Elliott, R.M., Lloyd, R.E., Fazeli, A., Sostaric, E., Georgiou, A.S., Satake, N., Watson, P.F., Holt, W.V., 2009. Effects of HSPA8, an evolutionarily conserved oviductal protein, on boar and bull spermatozoa. Reproduction 137, 191–203.
Elweza, A.E., Ezz, M.A., Acosta, T.J., Talukder, A.K., Shimizu, T., Hayakawa, H., Shimada, M., Imakawa, K., Zaghloul, A.H., Miyamoto, A., 2018. A proinflammatory response of bovine endometrial epithelial cells to active sperm in vitro. Mol. Reprod. Dev. 85, 215–226.
England, G.C., Burgess, C.M., 2003. Survival of dog spermatozoa within the reproductive tract of the bitch. Reprod. Domest. Anim. 38, 325–326.
Ezz, M.A., Marey, M.A., Elweza, A.E., Kawai, T., Heppelmann, M., Pfarrer, C., Balboula, A.Z., Montaser, A., Imakawa, K., Zaabel, S.M., Shimada, M., Miyamoto, A.,

2019. TLR2/4 signaling pathway mediates sperm-induced inflammation in bovine endometrial epithelial cells in vitro. PloS One 14.
Fair, S., Meade, K., Reynaud, K., Druart, X., de Graaf, S.P., 2019. The biological mechanisms regulating sperm selection by the ovine cervix. Reproduction 1, 18-0595.
Fazeli, A., Duncan, A.E., Watson, P.F., Holt, W.V., 1999. Sperm-oviduct interaction: induction of capacitation and preferential binding of uncapacitated spermatozoa to oviductal epithelial cells in porcine species. Biol. Reprod. 60, 879–886.
Fazeli, A., Affara, N.A., Hubank, M., Holt, W.V., 2004. Sperm-induced modification of the oviductal gene expression profile after natural insemination in mice. Biol. Reprod. 71, 60–65.
Fazeli, A., Elliott, R.M., Duncan, A.E., Moore, A., Watson, P.F., Holt, W.V., 2003. In vitro maintenance of boar sperm viability by a soluble fraction obtained from oviductal apical plasma membrane preparations. Reproduction 125, 509–517.
Fedorka, C.E., Scoggin, K.E., Woodward, E.M., Squires, E.L., Ball, B.A., Troedsson, M., 2016. The effect of select seminal plasma proteins on endometrial mRNA cytokine expression in mares susceptible to persistent mating-induced endometritis. Reprod. in domes. animals Zuchthygiene 30, 12813.
Fereshteh, Z., Schmidt, S.A., Al-Dossary, A.A., Accerbi, M., Arighi, C., Cowart, J., Song, J. L., Green, P.J., Choi, K., Yoo, S., Martin-DeLeon, P.A., 2018. Murine Oviductosomes (OVS) microRNA profiling during the estrous cycle: delivery of OVS-borne microRNAs to sperm where miR-34c-5p localizes at the centrosome. Sci. Rep. 8, 16094.
Ferraz, M., Carothers, A., Dahal, R., Noonan, M.J., Songsasen, N., 2019. Oviductal extracellular vesicles interact with the spermatozoon's head and mid-piece and improves its motility and fertilizing ability in the domestic cat. Sci. Rep. 9, 9484.
Fichtner, T., Kotarski, F., Gartner, U., Conejeros, I., Hermosilla, C., Wrenzycki, C., Taubert, A., 2020. Bovine sperm samples induce different NET phenotypes in a NADPH oxidase-, PAD4-, and Ca++-dependent processdagger. Biol. Reprod. 102, 902–914.
Franchi, A., Cubilla, M., Guidobaldi, H.A., Bravo, A.A., Giojalas, L.C., 2016. Uterosome-like vesicles prompt human sperm fertilizing capability. Mol. Hum. Reprod. 22, 833–841.
Franchi, A., Moreno-Irusta, A., Dominguez, E.M., Adre, A.J., Giojalas, L.C., 2020. Extracellular vesicles from oviductal isthmus and ampulla stimulate the induced acrosome reaction and signaling events associated with capacitation in bovine spermatozoa. J. Cell. Biochem. 121, 2877–2888.
Fujihara, Y., Okabe, M., Ikawa, M., 2014. GPI-anchored protein complex, LY6K/TEX101, is required for sperm migration into the oviduct and male fertility in mice. Biol. Reprod. 90.
Fujihara, Y., Miyata, H., Ikawa, M., 2018. Factors controlling sperm migration through the oviduct revealed by gene-modified mouse models. Exp. Anim. 67, 91–104.
Fujihara, Y., Tokuhiro, K., Muro, Y., Kondoh, G., Araki, Y., Ikawa, M., Okabe, M., 2013. Expression of TEX101, regulated by ACE, is essential for the production of fertile mouse spermatozoa. Proc. Natl. Acad. Sci. U. S. A. 110, 8111–8116.
Fujihara, Y., Noda, T., Kobayashi, K., Oji, A., Kobayashi, S., Matsumura, T., Larasati, T., Oura, S., Kojima-Kita, K., Yu, Z., Matzuk, M.M., Ikawa, M., 2019. Identification of multiple male reproductive tract-specific proteins that regulate sperm migration through the oviduct in mice. Proc. Natl. Acad. Sci. U. S. A. 116, 18498–18506.
Gadella, B.M., 2017. Reproductive tract modifications of the boar sperm surface. Mol. Reprod. Dev. 84, 822–831.
Garcia-Vazquez, F.A., Gadea, J., Matas, C., Holt, W.V., 2016. Importance of sperm morphology during sperm transport and fertilization in mammals. Asian J. Androl. 18, 844–850.
Garcia-Vazquez, F.A., Hernandez-Caravaca, I., Matas, C., Soriano-Ubeda, C., Abril-Sanchez, S., Izquierdo-Rico, M.J., 2015. Morphological study of boar sperm during their passage through the female genital tract. J. Reprod. Dev. 61, 407–413.
Gatien, J., Mermillod, P., Tsikis, G., Bernardi, O., Janati Idrissi, S., Uzbekov, R., Le Bourhis, D., Salvetti, P., Alminana, C., Saint-Dizier, M., 2019. Metabolomic profile of oviductal extracellular vesicles across the estrous cycle in cattle. Int. J. Mol. Sci. 20.
Gegenfurtner, K., Frohlich, T., Flenkenthaler, F., Kosters, M., Fritz, S., Desnoes, O., Le Bourhis, D., Salvetti, P., Sandra, O., Charpigny, G., Mermillod, P., Lonergan, P., Wolf, E., Arnold, G.J., 2020. Genetic merit for fertility alters the bovine uterine luminal fluid proteome. Biol. Reprod. 102, 730–739.
Gervasi, M.G., Rapanelli, M., Ribeiro, M.L., Farina, M., Billi, S., Franchi, A.M., Perez Martinez, S., 2009. The endocannabinoid system in bull sperm and bovine oviductal epithelium: role of anandamide in sperm-oviduct interaction. Reproduction 137, 403–414.
Gervasi, M.G., Osycka-Salut, C., Sanchez, T., Alonso, C.A., Llados, C., Castellano, L., Franchi, A.M., Villalon, M., Perez-Martinez, S., 2016. Sperm release from the oviductal epithelium depends on Ca(2+) influx upon activation of CB1 and TRPV1 by anandamide. J. Cell. Biochem. 117, 320–333.
Green, C.E., Bredl, J., Holt, W.V., Watson, P.F., Fazeli, A., 2001. Carbohydrate mediation of boar sperm binding to oviductal epithelial cells in vitro. Reproduction 122, 305–315.
Griffiths, G.S., Miller, K.A., Galileo, D.S., Martin-DeLeon, P.A., 2008a. Murine SPAM1 is secreted by the estrous uterus and oviduct in a form that can bind to sperm during capacitation: acquisition enhances hyaluronic acid-binding ability and cumulus dispersal efficiency. Reproduction 135, 293–301.
Griffiths, G.S., Galileo, D.S., Reese, K., Martin-Deleon, P.A., 2008b. Investigating the role of murine epididymosomes and uterosomes in GPI-linked protein transfer to sperm using SPAM1 as a model. Mol. Reprod. Dev. 75, 1627–1636.
Grippo, A.A., Way, A.L., Killian, G.J., 1995. Effect of bovine ampullary and isthmic oviductal fluid on motility, acrosome reaction and fertility of bull spermatozoa. J. Reprod. Fertil. 105, 57–64.
Gualtieri, R., Talevi, R., 2000. In vitro cultured bovine oviductal cells bind acrosome-intact sperm and retain this ability upon sperm release. Biol. Reprod. 62, 1754–1762.
Gualtieri, R., Talevi, R., 2003. Selection of highly fertilization-competent bovine spermatozoa through adhesion to the Fallopian tube epithelium in vitro. Reproduction 125, 251–258.
Gwathmey, T.M., Ignotz, G.G., Suarez, S.S., 2003. PDC-109 (BSP-A1/A2) promotes bull sperm binding to oviductal epithelium in vitro and may be involved in forming the oviductal sperm reservoir. Biol. Reprod. 69, 809–815.
Gwathmey, T.M., Ignotz, G.G., Mueller, J.L., Manjunath, P., Suarez, S.S., 2006. Bovine seminal plasma proteins PDC-109, BSP-A3, and BSP-30-kDa share functional roles in storing sperm in the oviduct. Biol. Reprod. 75, 501–507.
Hao, Y., Mathialagan, N., Walters, E., Mao, J., Lai, L., Becker, D., Li, W., Critser, J., Prather, R.S., 2006. Osteopontin reduces polyspermy during in vitro fertilization of porcine oocytes. Biol. Reprod. 75, 726–733.
Henry, F., Eder, S., Reynaud, K., Schon, J., Wibbelt, G., Fontbonne, A., Muller, K., 2015. Seminal fluid promotes in vitro sperm-oviduct binding in the domestic cat (Felis catus). Theriogenology 83, 1373–1380.
Hino, T., Muro, Y., Tamura-Nakano, M., Okabe, M., Tateno, H., Yanagimachi, R., 2016. The behavior and acrosomal status of mouse spermatozoa in vitro, and within the oviduct during fertilization after natural mating. Biol. Reprod. 95, 50.
Ho, K., Wolff, C.A., Suarez, S.S., 2009. CatSper-null mutant spermatozoa are unable to ascend beyond the oviductal reservoir. Reprod. Fertil. Dev. 21, 345–350.
Holt, W.V., Fazeli, A., 2016. Sperm selection in the female mammalian reproductive tract. Focus on the Oviduct: Hypo. Mech. Opport. Theriogenol. 85, 105–112.
Holt, W.V., Del Valle, I., Fazeli, A., 2015. Heat shock protein A8 stabilizes the bull sperm plasma membrane during cryopreservation: effects of breed, protein concentration, and mode of use. Theriogenology 84, 693–701.
Hugentobler, S.A., Morris, D.G., Sreenan, J.M., Diskin, M.G., 2007a. Ion concentrations in oviduct and uterine fluid and blood serum during the estrous cycle in the bovine. Theriogenology 68, 538–548.
Hugentobler, S.A., Humpherson, P.G., Leese, H.J., Sreenan, J.M., Morris, D.G., 2008. Energy substrates in bovine oviduct and uterine fluid and blood plasma during the oestrous cycle. Mol. Reprod. Dev. 75, 496–503.
Hugentobler, S.A., Diskin, M.G., Leese, H.J., Humpherson, P.G., Watson, T., Sreenan, J. M., Morris, D.G., 2007b. Amino acids in oviduct and uterine fluid and blood plasma during the estrous cycle in the bovine. Mol. Reprod. Dev. 74, 445–454.
Hunter, R.H., 1981. Sperm transport and reservoirs in the pig oviduct in relation to the time of ovulation. J. Reprod. Fertil. 63, 109–117.
Hunter, R.H., 2008. Sperm release from oviduct epithelial binding is controlled hormonally by peri-ovulatory graafian follicles. Mol. Reprod. Dev. 75, 167–174.
Hunter, R.H., 2011. Sperm head binding to epithelium of the oviduct isthmus is not an essential preliminary to mammalian fertilization - review. Zygote 19, 265–269.
Hunter, R.H., Nichol, R., 1983. Transport of spermatozoa in the sheep oviduct: preovulatory sequestering of cells in the caudal isthmus. J. Exp. Zool. 228, 121–128.
Hunter, R.H., Wilmut, I., 1984. Sperm transport in the cow: peri-ovulatory redistribution of viable cells within the oviduct. Reprod. Nutr. Dev. 24, 597–608.
Hunter, R.H., Flechon, B., Flechon, J.E., 1991. Distribution, morphology and epithelial interactions of bovine spermatozoa in the oviduct before and after ovulation: a scanning electron microscope study. Tissue Cell 23, 641–656.
Ignotz, G.G., Cho, M.Y., Suarez, S.S., 2007. Annexins are candidate oviductal receptors for bovine sperm surface proteins and thus may serve to hold bovine sperm in the oviductal reservoir. Biol. Reprod. 77, 906–913.
Ikawa, M., Wada, I., Kominami, K., Watanabe, D., Toshimori, K., Nishimune, Y., Okabe, M., 1997. The putative chaperone calmegin is required for sperm fertility. Nature 387, 607–611.
Ikawa, M., Tokuhiro, K., Yamaguchi, R., Benham, A.M., Tamura, T., Wada, I., Satouh, Y., Inoue, N., Okabe, M., 2011. Calsperin is a testis-specific chaperone required for sperm fertility. J. Biol. Chem. 286, 5639–5646.
Inan, S., Giray, G., Vatansever, H.S., Ozbilgin, K., Kuscu, N.K., Sayhan, S., 2004. Immunolocalization of integrins and fibronectin in tubal pregnancy. Acta Histochem. 106, 235–243.
Kadam, K.M., D'Souza, S.J., Bandivdekar, A.H., Natraj, U., 2006. Identification and characterization of oviductal glycoprotein-binding protein partner on gametes: epitopic similarity to non-muscle myosin IIA, MYH 9. Mol. Hum. Reprod. 12, 275–282.
Kasvandik, S., Saarma, M., Kaart, T., Rooda, I., Velthut-Meikas, A., Ehrenberg, A., Gemzell, K., Lalitkumar, P.G., Salumets, A., Peters, M., 2020. Uterine fluid proteins for minimally invasive assessment of endometrial receptivity. J. Clin. Endocrinol. Metab. 105.
Katila, T., 2012. Post-mating inflammatory responses of the uterus. Reprod. Domest. Anim. 47 (Suppl. 5), 31–41.
Katila, T., Sankari, S., Makela, O., 2000. Transport of spermatozoa in the reproductive tracts of mares. J. Reprod. Fertil. 56 (Suppl. ment), 571–578.
Kawakami, E., Hori, T., Tsutsui, T., 1998. Induction of dog sperm capacitation by oviductal fluid. J. Vet. Med. Sci. 60, 197–202.
Khalil, A.A., Petrunkina, A.M., Sahin, E., Waberski, D., Topfer-Petersen, E., 2006. Enhanced binding of sperm with superior volume regulation to oviductal epithelium. J. Androl. 27, 754–765.
King, R.S., Killian, G.J., 1994. Purification of bovine estrus-associated protein and localization of binding on sperm. Biol. Reprod. 51, 34–42.
Kobayashi, M., Wada, M., Hori, T., Kawakami, E., 2014. Superoxide dismutase activity in the oviductal and uterine fluid of the bitch and the effects of the enzyme on viability, motility and hyperactivation of canine sperm in vitro. J. Vet. Med. Sci. 76, 741–743.
Krege, J.H., John, S.W., Langenbach, L.L., Hodgin, J.B., Hagaman, J.R., Bachman, E.S., Jennette, J.C., O'Brien, D.A., Smithies, O., 1995. Male-female differences in fertility and blood pressure in ACE-deficient mice. Nature 375, 146–148.

Krutskikh, A., Poliandri, A., Cabrera-Sharp, V., Dacheux, J.L., Poutanen, M., Huhtaniemi, I., 2012. Epididymal protein Rnase10 is required for post-testicular sperm maturation and male fertility. Faseb. J. 26, 4198–4209.
Kumar, V., Kumaresan, A., Kumar, D.S.P., Lathika, S., Nayak, S., Kishor Saraf, K., Nag, B. S.P., Chhillar, S., Kumar Datta, T., Kumar Mohanty, T., 2017. Anandamide exerts a suppressive effect on sperm binding to oviduct explants through CB1 receptors in the water buffalo (Bubalus bubalis). Anim. Reprod. Sci. 185, 188–194.
Kumaresan, A., Ansari, M.R., Garg, A., 2005. Modulation of post-thaw sperm functions with oviductal proteins in buffaloes. Anim. Reprod. Sci. 90, 73–84.
Kumaresan, A., Johannisson, A., Bergqvist, A.S., 2016. Sperm function during incubation with oestrus oviductal fluid differs in bulls with different fertility. Reprod. Fertil. Dev. 29, 1096–1106.
Kumaresan, A., Ansari, M.R., Garg, A., Kataria, M., 2006. Effect of oviductal proteins on sperm functions and lipid peroxidation levels during cryopreservation in buffaloes. Anim. Reprod. Sci. 93, 246–257.
Kumaresan, A., Johannisson, A., Saravia, F., Bergqvist, A.S., 2012. The effect of oviductal fluid on protein tyrosine phosphorylation in cryopreserved boar spermatozoa differs with the freezing method. Theriogenology 77, 588–599.
Kumaresan, A., Gonzalez, R., Johannisson, A., Berqvist, A.S., 2014. Dynamic quantification of intracellular calcium and protein tyrosine phosphorylation in cryopreserved boar spermatozoa during short-time incubation with oviductal fluid. Theriogenology 82, 1145–1153.
Kumaresan, A., Johannisson, A., Humblot, P., Bergqvist, A.S., 2019. Effect of bovine oviductal fluid on motility, tyrosine phosphorylation, and acrosome reaction in cryopreserved bull spermatozoa. Theriogenology 124, 48–56.
Kunz, G., Leyendecker, G., 2002. Uterine peristaltic activity during the menstrual cycle: characterization, regulation, function and dysfunction. Reprod. Biomed. Online 4 (Suppl. 3), 5–9.
La Spina, F.A., Puga Molina, L.C., Romarowski, A., Vitale, A.M., Falzone, T.L., Krapf, D., Hirohashi, N., Buffone, M.G., 2016. Mouse sperm begin to undergo acrosomal exocytosis in the upper isthmus of the oviduct. Dev. Biol. 411, 172–182.
Lachance, C., Bailey, J.L., Leclerc, P., 2007. Expression of Hsp60 and Grp78 in the human endometrium and oviduct, and their effect on sperm functions. Hum. Reprod. 22, 2606–2614.
Laezer, I., Palma-Vera, S.E., Liu, F., Frank, M., Trakooljul, N., Vernunft, A., Schoen, J., Chen, S., 2020. Dynamic profile of EVs in porcine oviductal fluid during the periovulatory period. Reproduction 159, 371–382.
Lamy, J., Labas, V., Harichaux, G., Tsikis, G., Mermillod, P., Saint-Dizier, M., 2016a. Regulation of the bovine oviductal fluid proteome. Reproduction 152, 629–644.
Lamy, J., Liere, P., Pianos, A., Aprahamian, F., Mermillod, P., Saint-Dizier, M., 2016b. Steroid hormones in bovine oviductal fluid during the estrous cycle. Theriogenology 86, 1409–1420.
Lamy, J., Corbin, E., Blache, M.C., Garanina, A.S., Uzbekov, R., Mermillod, P., Saint-Dizier, M., 2017. Steroid hormones regulate sperm-oviduct interactions in the bovine. Reproduction 154, 497–508.
Lamy, J., Nogues, P., Combes-Soia, L., Tsikis, G., Labas, V., Mermillod, P., Druart, X., Saint-Dizier, M., 2018. Identification by proteomics of oviductal sperm-interacting proteins. Reproduction 155 (5), 457–466.
Langendijk, P., Soede, N.M., Kemp, B., 2005. Uterine activity, sperm transport, and the role of boar stimuli around insemination in sows. Theriogenology 63, 500–513.
Langendijk, P., Bouwman, E., Kidson, A., Kirkwood, R., Soede, N., Kemp, B., 2002. Role of myometrial activity in sperm transport through the genital tract and in fertilization in sows. Reproduction 123, 683–690.
Lapointe, S., Sullivan, R., Sirard, M.A., 1998. Binding of a bovine oviductal fluid catalase to mammalian spermatozoa. Biol. Reprod. 58, 747–753.
Lee, R.K., Tseng, H.C., Hwu, Y.M., Fan, C.C., Lin, M.H., Yu, J.J., Yeh, L.Y., Li, S.H., 2018. Expression of cystatin C in the female reproductive tract and its effect on human sperm capacitation. Reprod. Biol. Endocrinol. 16, 8.
Leemans, B., Gadella, B.M., Sostaric, E., Nelis, H., Stout, T.A., Hoogewijs, M., Van Soom, A., 2014. Oviduct binding and elevated environmental ph induce protein tyrosine phosphorylation in stallion spermatozoa. Biol. Reprod. 91, 13.
Lefebvre, R., Suarez, S.S., 1996. Effect of capacitation on bull sperm binding to homologous oviductal epithelium. Biol. Reprod. 54, 575–582.
Lefebvre, R., Lo, M.C., Suarez, S.S., 1997. Bovine sperm binding to oviductal epithelium involves fucose recognition. Biol. Reprod. 56, 1198–1204.
Lefebvre, R., Chenoweth, P.J., Drost, M., Leclear, C.T., MacCubbin, M., Dutton, J.T., Suarez, S.S., 1995. Characterization of oviductal sperm reservoir in cattle. Biol. Reprod. 53, 1066–1074.
Lippes, J., Wagh, P.V., 1989. Human oviductal fluid (hOF) proteins. IV. Evidence for hOF proteins binding to human sperm. Fertil. Steril. 51, 89–94.
Liu, Q., Xie, Q.Z., Zhou, Y., Yang, J., 2015. Osteopontin is expressed in the oviduct and promotes fertilization and preimplantation embryo development of mouse. Zygote 23, 622–630.
Lloyd, R.E., Elliott, R.M., Fazeli, A., Watson, P.F., Holt, W.V., 2009. Effects of oviductal proteins, including heat shock 70 kDa protein 8, on survival of ram spermatozoa over 48 h in vitro. Reprod. Fertil. Dev. 21, 408–418.
Lopez-Ubeda, R., Garcia-Vazquez, F.A., Gadea, J., Matas, C., 2017. Oviductal epithelial cells selected boar sperm according to their functional characteristics. Asian J. Androl. 19, 396–403.
Luongo, C., Abril-Sanchez, S., Hernandez, J.G., Garcia-Vazquez, F.A., 2019. Seminal plasma mitigates the adverse effect of uterine fluid on boar spermatozoa. Theriogenology 136, 28–35.
Machado, S.A., Sharif, M., Wang, H., Bovin, N., Miller, D.J., 2019. Release of porcine sperm from oviduct cells is stimulated by progesterone and requires CatSper. Sci. Rep. 9, 19546.
Maloney, S.E., Khan, F.A., Chenier, T.S., Diel de Amorim, M., Anthony Hayes, M., Scholtz, E.L., 2019. A comparison of the uterine proteome of mares in oestrus and dioestrus. Reprod. Domest. Anim. 54, 473–479.
Marcello, M.R., Jia, W., Leary, J.A., Moore, K.L., Evans, J.P., 2011. Lack of tyrosylprotein sulfotransferase-2 activity results in altered sperm-egg interactions and loss of ADAM3 and ADAM6 in epididymal sperm. J. Biol. Chem. 286, 13060–13070.
Marey, M.A., Matsukawa, H., Sasaki, M., Ezz, M.A., Yousef, M.S., Takahashi, K.I., Miyamoto, A., 2019. Bovine oviduct epithelial cells suppress the phagocytic activity of neutrophils towards sperm but not for bacteria in vitro: immunofluorescence and electron microscopic observations. Histol. Histopathol. 18172.
Marey, M.A., Liu, J., Kowsar, R., Haneda, S., Matsui, M., Sasaki, M., Takashi, S., Hayakawa, H., Wijayagunawardane, M.P., Hussein, F.M., Miyamoto, A., 2014. Bovine oviduct epithelial cells downregulate phagocytosis of sperm by neutrophils: prostaglandin E2 as a major physiological regulator. Reproduction 147, 211–219.
Marin-Briggiler, C.I., Gonzalez-Echeverria, M.F., Munuce, M.J., Ghersevich, S., Caille, A. M., Hellman, U., Corrigall, V.M., Vazquez-Levin, M.H., 2010. Glucose-regulated protein 78 (Grp78/BiP) is secreted by human oviduct epithelial cells and the recombinant protein modulates sperm-zona pellucida binding. Fertil. Steril. 93, 1574–1584.
Martin-DeLeon, P.A., 2006. Epididymal SPAM1 and its impact on sperm function. Mol. Cell. Endocrinol. 250, 114–121.
McNutt, T.L., Killian, G.J., 1991. Influence of bovine follicular and oviduct fluids on sperm capacitation in vitro. J. Androl. 12, 244–252.
Miller, D.J., 2018. Review: the epic journey of sperm through the female reproductive tract. Animal 12, s110–s120.
Moein-Vaziri, N., Phillips, I., Smith, S., Alminana, C., Maside, C., Gil, M.A., Roca, J., Martinez, E.A., Holt, W.V., Pockley, A.G., Fazeli, A., 2014. Heat-shock protein A8 restores sperm membrane integrity by increasing plasma membrane fluidity. Reproduction 147, 719–732.
Monaco, E., Gasparrini, B., Boccia, L., De Rosa, A., Attanasio, L., Zicarelli, L., Killian, G., 2009. Effect of osteopontin (OPN) on in vitro embryo development in cattle. Theriogenology 71, 450–457.
Morales, P., Palma, V., Salgado, A.M., Villalon, M., 1996. Sperm interaction with human oviductal cells in vitro. Hum. Reprod. 11, 1504–1509.
Moros-Nicolas, C., Fouchecourt, S., Goudet, G., Monget, P., 2018. Genes encoding mammalian oviductal proteins involved in fertilization are subjected to gene death and positive selection. J. Mol. Evol. 86, 655–667.
Murray, S.C., Smith, T.T., 1997. Sperm interaction with fallopian tube apical membrane enhances sperm motility and delays capacitation. Fertil. Steril. 68, 351–357.
Nishimura, H., Kim, E., Nakanishi, T., Baba, T., 2004. Possible function of the ADAM1a/ADAM2 Fertilin complex in the appearance of ADAM3 on the sperm surface. J. Biol. Chem. 279, 34957–34962.
Noguchi, T., Fujinoki, M., Kitazawa, M., Inaba, N., 2008. Regulation of hyperactivation of hamster spermatozoa by progesterone. Reprod. Med. Biol. 7, 63–74.
Osycka-Salut, C., Gervasi, M.G., Pereyra, E., Cella, M., Ribeiro, M.L., Franchi, A.M., Perez-Martinez, S., 2012. Anandamide induces sperm release from oviductal epithelia through nitric oxide pathway in bovines. PloS One 7, e30671.
Osycka-Salut, C.E., Castellano, L., Fornes, D., Beltrame, J.S., Alonso, C., Jawerbaum, A., Franchi, A., Diaz, E.S., Perez Martinez, S., 2017. Fibronectin from oviductal cells fluctuates during the estrous cycle and contributes to sperm-oviduct interaction in cattle. J. Cell. Biochem. 118 (11), 4095–4108.
Overstreet, J.W., Cooper, G.W., 1978. Sperm transport in the reproductive tract of the female rabbit: II. The sustained phase of transport. Biol. Reprod. 19, 115–132.
Parrish, J.J., Susko-Parrish, J.L., Handrow, R.R., Sims, M.M., First, N.L., 1989. Capacitation of bovine spermatozoa by oviduct fluid. Biol. Reprod. 40, 1020–1025.
Perez-Cerezales, S., Lopez-Cardona, A.P., Gutierrez-Adan, A., 2016. Progesterone effects on mouse sperm kinetics in conditions of viscosity. Reproduction 151, 501–507.
Petrunkina, A.M., Simon, K., Gunzel-Apel, A.R., Topfer-Petersen, E., 2004. Kinetics of protein tyrosine phosphorylation in sperm selected by binding to homologous and heterologous oviductal explants: how specific is the regulation by the oviduct? Theriogenology 61, 1617–1634.
Petrunkina, A.M., Gehlhaar, R., Drommer, W., Waberski, D., Topfer-Petersen, E., 2001. Selective sperm binding to pig oviductal epithelium in vitro. Reproduction 121, 889–896.
Plante, G., Prud'homme, B., Fan, J., Lafleur, M., Manjunath, P., 2016. Evolution and function of mammalian binder of sperm proteins. Cell Tissue Res. 363, 105–127.
Qiao, F., Ge, H., Ma, X., Zhang, Y., Zuo, Z., Wang, M., Wang, Y., 2018. Bovine uterus-derived exosomes improve developmental competence of somatic cell nuclear transfer embryos. Theriogenology 114, 199–205.
Ramal-Sanchez, M., Bernabo, N., Tsikis, G., Blache, M.C., Labas, V., Druart, X., Mermillod, P., Saint-Dizier, M., 2020. Progesterone induces sperm release from oviductal epithelial cells by modifying sperm proteomics, lipidomics and membrane fluidity. Mol. Cell. Endocrinol. 504, 110723.
Rath, D., Knorr, C., Taylor, U., 2016. Communication requested: boar semen transport through the uterus and possible consequences for insemination. Theriogenology 85, 94–104.
Rath, D., Schuberth, H.J., Coy, P., Taylor, U., 2008. Sperm interactions from insemination to fertilization. Reprod. in domes. animals Zuchthygiene 5, 2–11.
Rickard, J.P., Pool, K.R., Druart, X., de Graaf, S.P., 2019. The fate of spermatozoa in the female reproductive tract: a comparative review. Theriogenology 137, 104–112.
Rijsselaere, T., Van Soom, A., Van Cruchten, S., Coryn, M., Gortz, K., Maes, D., de Kruif, A., 2004. Sperm distribution in the genital tract of the bitch following artificial insemination in relation to the time of ovulation. Reproduction 128, 801–811.
Rodriguez-Martinez, H., 2007. Role of the oviduct in sperm capacitation. Theriogenology 68, S138–S146.

Rodriguez-Martinez, H., Nicander, L., Viring, S., Einarsson, S., Larsson, K., 1990. Ultrastructure of the uterotubal junction in preovulatory pigs. Anat. Histol. Embryol. 19, 16–36.
Romero-Aguirregomezcorta, J., Cronin, S., Donnellan, E., Fair, S., 2019. Progesterone induces the release of bull spermatozoa from oviductal epithelial cells. Reprod. Fertil. Dev. 31 (9), 1463–1472.
Saccary, L., She, Y.M., Oko, R., Kan, F.W., 2013. Hamster oviductin regulates tyrosine phosphorylation of sperm proteins during in vitro capacitation. Biol. Reprod. 89, 38.
Saint-Dizier, M., Schoen, J., Chen, S., Banliat, C., Mermillod, P., 2019. Composing the early embryonic microenvironment: physiology and regulation of oviductal secretions. Int. J. Mol. Sci. 21.
Saraf, K.K., Singh, R.K., Kumaresan, A., Nayak, S., Chhillar, S., Lathika, S., Datta, T.K., Mohanty, T.K., 2019. Sperm functional attributes and oviduct explant binding capacity differs between bulls with different fertility ratings in the water buffalo (Bubalus bubalis). Reprod. Fertil. Dev. 31, 395–403.
Schjenken, J.E., Robertson, S.A., 2014. Seminal fluid and immune adaptation for pregnancy-comparative biology in mammalian species. Reprod. in domes. animals Zuchthygiene 3, 27–36.
Schjenken, J.E., Robertson, S.A., 2015. Seminal fluid signalling in the female reproductive tract: implications for reproductive success and offspring health. Adv. Exp. Med. Biol. 868, 127–158.
Schuh, K., Cartwright, E.J., Jankevics, E., Bundschu, K., Liebermann, J., Williams, J.C., Armesilla, A.L., Emerson, M., Oceandy, D., Knobeloch, K.P., Neyses, L., 2004. Plasma membrane Ca2+ ATPase 4 is required for sperm motility and male fertility. J. Biol. Chem. 279, 28220–28226.
Shamsadin, R., Adham, I.M., Nayernia, K., Heinlein, U.A., Oberwinkler, H., Engel, W., 1999. Male mice deficient for germ-cell cyritestin are infertile. Biol. Reprod. 61, 1445–1451.
Shang, X., Shen, C., Liu, J., Tang, L., Zhang, H., Wang, Y., Wu, W., Chi, J., Zhuang, H., Fei, J., Wang, Z., 2018. Serine protease PRSS55 is crucial for male mouse fertility via affecting sperm migration and sperm-egg binding. Cell. Mol. Life Sci. 75, 4371–4384.
Shen, C., Kuang, Y., Liu, J., Feng, J., Chen, X., Wu, W., Chi, J., Tang, L., Wang, Y., Fei, J., Wang, Z., 2013. Prss37 is required for male fertility in the mouse. Biol. Reprod. 88 (5), 123.
Silva, E., Kadirvel, G., Jiang, R., Bovin, N., Miller, D., 2014. Multiple proteins from ejaculated and epididymal porcine spermatozoa bind glycan motifs found in the oviduct. Andrology 2, 763–771.
Smith, T.T., Yanagimachi, R., 1991. Attachment and release of spermatozoa from the caudal isthmus of the hamster oviduct. J. Reprod. Fertil. 91, 567–573.
Soleilhavoup, C., Riou, C., Tsikis, G., Labas, V., Harichaux, G., Kohnke, P., Reynaud, K., de Graaf, S.P., Gerard, N., Druart, X., 2016. Proteomes of the female genital tract during the oestrous cycle. Mol. Cell. Proteomics 15, 93–108.
Sostaric, E., van de Lest, C.H., Colenbrander, B., Gadella, B.M., 2005. Dynamics of carbohydrate affinities at the cell surface of capacitating bovine sperm cells. Biol. Reprod. 72, 346–357.
Sostaric, E., Dieleman, S.J., van de Lest, C.H., Colenbrander, B., Vos, P.L., Garcia-Gil, N., Gadella, B.M., 2008. Sperm binding properties and secretory activity of the bovine oviduct immediately before and after ovulation. Mol. Reprod. Dev. 75, 60–74.
Souza, C.E., Moura, A.A., Monaco, E., Killian, G.J., 2008. Binding patterns of bovine seminal plasma proteins A1/A2, 30 kDa and osteopontin on ejaculated sperm before and after incubation with isthmic and ampullary oviductal fluid. Anim. Reprod. Sci. 105, 72–89.
Suarez, S.S., 1987. Sperm transport and motility in the mouse oviduct: observations in situ. Biol. Reprod. 36, 203–210.
Suarez, S.S., 2008. Control of hyperactivation in sperm. Hum. Reprod. Update 14, 647–657.
Sullivan, R., 2016. Epididymosomes: role of extracellular microvesicles in sperm maturation. Front. Biosci. 8, 106–114.
Sumigama, S., Mansell, S., Miller, M., Lishko, P.V., Cherr, G.N., Meyers, S.A., Tollner, T., 2015. Progesterone accelerates the completion of sperm capacitation and activates CatSper channel in spermatozoa from the rhesus macaque. Biol. Reprod. 93, 130.
Talevi, R., Gualtieri, R., 2001. Sulfated glycoconjugates are powerful modulators of bovine sperm adhesion and release from the oviductal epithelium in vitro. Biol. Reprod. 64, 491–498.
Talevi, R., Gualtieri, R., 2010. Molecules involved in sperm-oviduct adhesion and release. Theriogenology 73, 796–801.
Taylor, U., Rath, D., Zerbe, H., Schuberth, H.J., 2008. Interaction of intact porcine spermatozoa with epithelial cells and neutrophilic granulocytes during uterine passage. Reprod. in domes. animals Zuchthygiene 43, 166–175.
Tecle, E., Reynoso, H.S., Wang, R., Gagneux, P., 2019. The female reproductive tract contains multiple innate sialic acid-binding immunoglobulin-like lectins (Siglecs) that facilitate sperm survival. J. Biol. Chem. 294, 11910–11919.
Teijeiro, J.M., Ignotz, G.G., Marini, P.E., 2009. Annexin A2 is involved in pig (Sus scrofa) sperm-oviduct interaction. Mol. Reprod. Dev. 76, 334–341.
Thomas, P.G.A., Ball, B.A., Brinsko, S.P., 1994. Interaction of equine spermatozoa with oviduct epithelial cell explants is affected by estrous cycle and anatomic origin of explant. Biol. Reprod. 51.
Tienthai, P., 2015. The porcine sperm reservoir in relation to the function of hyaluronan. J. Reprod. Dev. 61, 245–250.
Tienthai, P., Johannisson, A., Rodriguez-Martinez, H., 2004. Sperm capacitation in the porcine oviduct. Anim. Reprod. Sci. 80, 131–146.
Tokuhiro, K., Ikawa, M., Benham, A.M., Okabe, M., 2012. Protein disulfide isomerase homolog PDILT is required for quality control of sperm membrane protein ADAM3 and male infertility. Proc. Natl. Acad. Sci. Unit. States Am. 109 (10), 3850–3855.
Tollner, T.L., Yudin, A.I., Tarantal, A.F., Treece, C.A., Overstreet, J.W., Cherr, G.N., 2008. Beta-defensin 126 on the surface of macaque sperm mediates attachment of sperm to oviductal epithelia. Biol. Reprod. 78, 400–412.
Topfer-Petersen, E., Romero, A., Varela, P.F., Ekhlasi-Hundrieser, M., Dostalova, Z., Sanz, L., Calvete, J.J., 1998. Spermadhesins: a new protein family. Facts, hypotheses and perspectives. Andrologia 30, 217–224.
Troedsson, M.H., Liu, I.K., Crabo, B.G., 1998. Sperm transport and survival in the mare: a review. Theriogenology 50, 807–818.
Ueda, Y., Yamaguchi, R., Ikawa, M., Okabe, M., Morii, E., Maeda, Y., Kinoshita, T., 2007. PGAP1 knock-out mice show otocephaly and male infertility. J. Biol. Chem. 282, 30373–30380.
Viuff, D., Greve, T., Avery, B., Hyttel, P., Brockhoff, P.B., Thomsen, P.D., 2000. Chromosome aberrations in in vitro-produced bovine embryos at days 2-5 post-insemination. Biol. Reprod. 63, 1143–1148.
Viuff, D., Hendriksen, P.J., Vos, P.L., Dieleman, S.J., Bibby, B.M., Greve, T., Hyttel, P., Thomsen, P.D., 2001. Chromosomal abnormalities and developmental kinetics in in vivo-developed cattle embryos at days 2 to 5 after ovulation. Biol. Reprod. 65, 204–208.
Waberski, D., Magnus, F., Mendonca Ferreira, F., Petrunkina, A.M., Weitze, K.F., Topfer-Petersen, E., 2005. Importance of sperm-binding assays for fertility prognosis of porcine spermatozoa. Theriogenology 63, 470–484.
Waberski, D., Magnus, F., Ardon, F., Petrunkina, A.M., Weitze, K.F., Topfer-Petersen, E., 2006. Binding of boar spermatozoa to oviductal epithelium in vitro in relation to sperm morphology and storage time. Reproduction 131, 311–318.
Wilmut, I., Hunter, R.H.F., 1984. Sperm transport into the oviducts of heifers mated early in estrus. Reprod. Nutr. Dev. 24, 461–468.
Winters, R.A., Nettenstrom, L.M., Lopez, D.G., Willenburg, K.L., Vishwanath, R., Bovin, N.V., Miller, D.J., 2018. Effect of sorting boar spermatozoa by sex chromosomes on oviduct cell binding. Theriogenology 108, 22–28.
Xiong, W., Wang, Z., Shen, C., 2019. An update of the regulatory factors of sperm migration from the uterus into the oviduct by genetically manipulated mice. Mol. Reprod. Dev. 86, 935–955.
Yamaguchi, R., Fujihara, Y., Ikawa, M., Okabe, M., 2012. Mice expressing aberrant sperm-specific protein PMIS2 produce normal-looking but fertilization-incompetent spermatozoa. Mol. Biol. Cell 23, 2671–2679.
Yanez-Mo, M., Siljander, P.R., Andreu, Z., Zavec, A.B., Borras, F.E., Buzas, E.I., Buzas, K., Casal, E., Cappello, F., Carvalho, J., Colas, E., Cordeiro-da Silva, A., Fais, S., Falcon-Perez, J.M., Ghobrial, I.M., Giebel, B., Gimona, M., Graner, M., Gursel, I., Gursel, M., Heegaard, N.H., Hendrix, A., Kierulf, P., Kokubun, K., Kosanovic, M., Kralj-Iglic, V., Kramer-Albers, E.M., Laitinen, S., Lasser, C., Lener, T., Ligeti, E., Line, A., Lipps, G., Llorente, A., Lotvall, J., Mancek-Keber, M., Marcilla, A., Mittelbrunn, M., Nazarenko, I., Nolte-'t Hoen, E.N., Nyman, T.A., O'Driscoll, L., Olivan, M., Oliveira, C., Pallinger, E., Del Portillo, H.A., Reventos, J., Rigau, M., Rohde, E., Sammar, M., Sanchez-Madrid, F., Santarem, N., Schallmoser, K., Ostenfeld, M.S., Stoorvogel, W., Stukelj, R., Van der Grein, S.G., Vasconcelos, M.H., Wauben, M.H., De Wever, O., 2015. Biological properties of extracellular vesicles and their physiological functions. J. Extracell. Vesicles 4, 27066.
Yang, X., Zhao, Y., Kan, F.W., 2015. Recombinant hamster oviductin is biologically active and exerts positive effects on sperm functions and sperm-oocyte binding. PloS One 10, e0123003.
Yeste, M., Holt, W.V., Bonet, S., Rodriguez-Gil, J.E., Lloyd, R.E., 2014. Viable and morphologically normal boar spermatozoa alter the expression of heat-shock protein genes in oviductal epithelial cells during co-culture in vitro. Mol. Reprod. Dev. 81, 805–819.
Yeste, M., Lloyd, R.E., Badia, E., Briz, M., Bonet, S., Holt, W.V., 2009. Direct contact between boar spermatozoa and porcine oviductal epithelial cell (OEC) cultures is needed for optimal sperm survival in vitro. Anim. Reprod. Sci. 113, 263–278.
Yousef, M.S., Abd-Elhafeez, H.H., Talukder, A.K., Miyamoto, A., 2019. Ovulatory follicular fluid induces sperm phagocytosis by neutrophils, but oviductal fluid around oestrus suppresses its inflammatory effect in the buffalo oviduct in vitro. Mol. Reprod. Dev. 86, 835–846.
Zambrano, F., Carrau, T., Gartner, U., Seipp, A., Taubert, A., Felmer, R., Sanchez, R., Hermosilla, C., 2016. Leukocytes coincubated with human sperm trigger classic neutrophil extracellular traps formation, reducing sperm motility. Fertil. Steril. 106, 1053–1060 e1.
Zhao, Y., Yang, X., Jia, Z., Reid, R.L., Leclerc, P., Kan, F.W., 2016. Recombinant human oviductin regulates protein tyrosine phosphorylation and acrosome reaction. Reproduction 152, 561–573.
Zumoffen, C.M., Caille, A.M., Munuce, M.J., Cabada, M.O., Ghersevich, S.A., 2010. Proteins from human oviductal tissue-conditioned medium modulate sperm capacitation. Hum. Reprod. 25, 1504–1512.

Annexe 3 : communication (poster) : « Spatiotemporal regulation of sperm-interacting proteins in the bovine oviduct fluid », *International Congress on Animal Reproduction (ICAR), 2022*

Spatiotemporal regulation of sperm-interacting proteins in the bovine oviduct fluid

Coline Mahé[1], Régis Lavigne[2,3], Emmanuelle Com[2,3], Charles Pineau[2,3], Aleksandra Maria Zlotkowska[4,#], Guillaume Tsikis[1], Pascal Mermillod[1], Jennifer Schoen[4,#], Marie Saint-Dizier[1]

[1]CNRS, IFCE, INRAE, Université de Tours, UMR PRC, Nouzilly, France
[2]Univ Rennes, Inserm, EHESP, Irset (Institut de recherche en santé, environnement et travail) - UMR-S 1085, F-35000 Rennes, France
[3]Protim, Univ Rennes, Biosit – UMS 3480 CNRS, US 018 Inserm, F-35000 Rennes, France
[4]Institute of Reproductive Biology, Leibniz Institute for Farm Animal Biology, FBN, Dummerstorf, Germany
#Current address: Department of Reproduction Biology, Leibniz Institute for Zoo and Wildlife Research (IZW), Berlin, Germany

INTRODUCTION

Spermatozoa (spz) interact with the oviduct fluid (OF) before fertilization *in vivo*. Purified OF proteins have been shown to modulate sperm physiology *in vitro* and may have a central role in the well-timed acquisition of sperm fertilizing ability. However, very few **sperm-interacting proteins (SIPs)** in the female tract have been identified so far.
The aim of the study was to identify an exhaustive list of SIPs in the bovine OF and to assess the impact of two female factors : **the oviduct anatomical region** (isthmus vs ampulla) and **the ovulation time** (pre-ovulatory vs. post-ovulatory), on SIPs numbers and abundance.

MATERIAL & METHODS

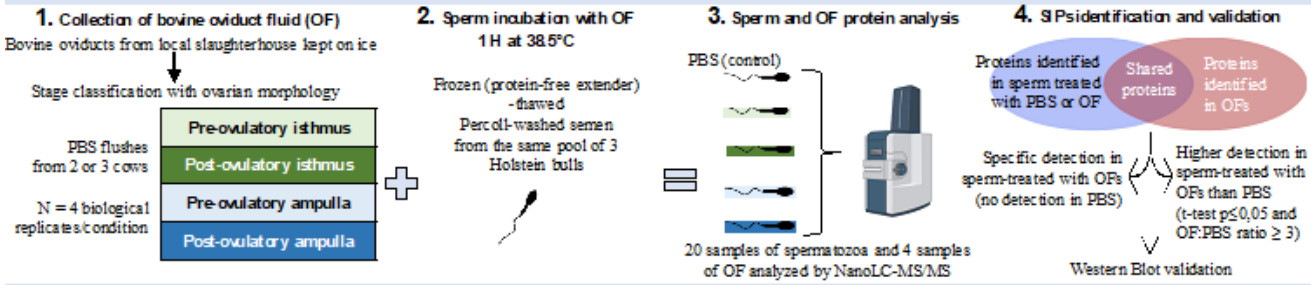

RESULTS

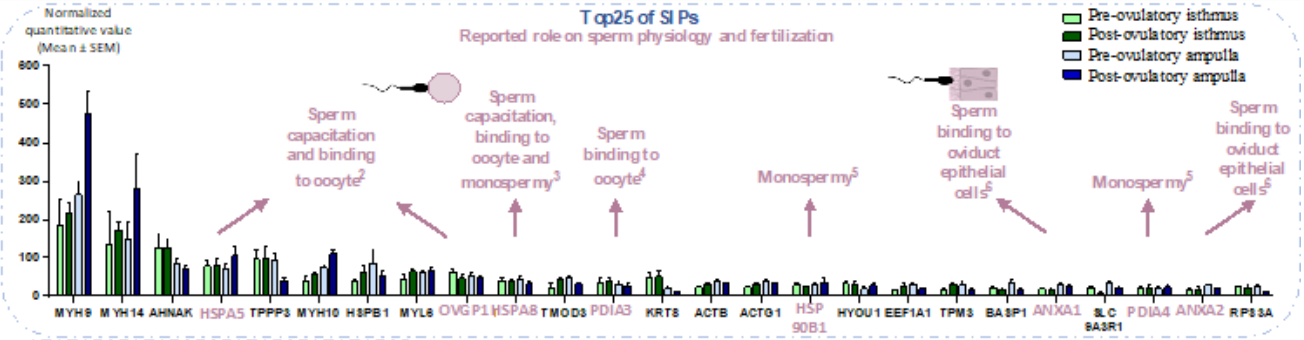

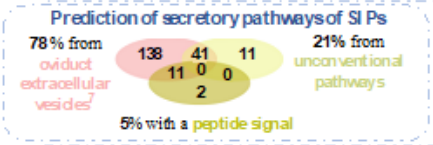

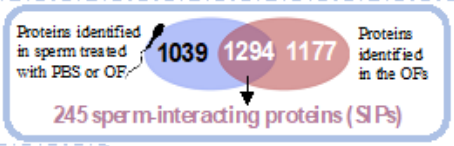

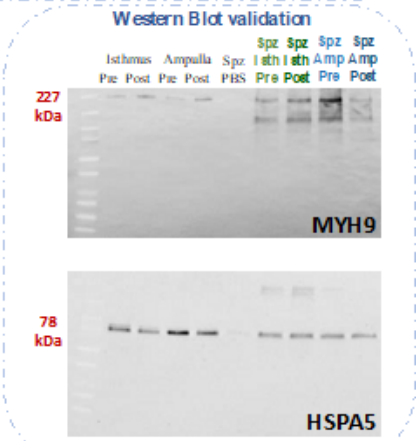

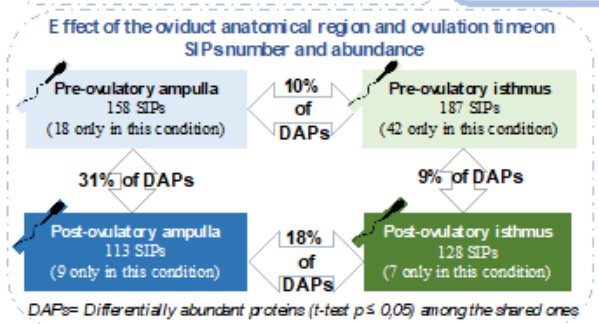

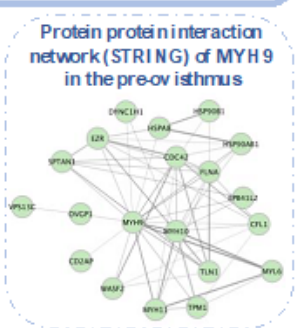

CONCLUSIONS & PERSPECTIVES

Using a new quantitative proteomic approach, **245 proteins in the OF were identified as interacting with spermatozoa**, some of which with reported **roles in fertilization** and mostly predicted to originate from oviduct extracellular vesicles. Up to 31% of SIPs fluctuated in numbers and abundance according to the time of ovulation and the region. Overall, these data suggest dynamic sperm-protein interactions in the periconception period. Furthermore, most SIPs were previously identified in oviduct extracellular vesicles but the exact origin of SIPs in the OF remain to be determined. These data provide new candidates to be tested on sperm motility, capacitation and maintenance of viability after cryopreservation.

UMR Physiologie de la Reproduction et des Comportements 37380 Nouzilly, France

References
1 Boquest et al., 1999; Kumaresan et al., 2005, 2006; Imam et al., 2010
2 Lachance et al. 2007 ; Marin-Briggiler et al., 2010 ; Choudhary et al. 2017 ; Coy et al. 2008
3 Elliott et al. 2009
4 Wong et al. 2017
5 Mondéjar et al. 2013
6 Ignotz et al. 2007
7 Almiñana et al. 2017 ; Jeanz et al. 2019 ; Lazzer et al. 2020

Fundings
This work was funded by INRAE, Agence Nationale de la Recherche, Biogenouest, Infrastructures en Biologie Santé et Agronomie (IBiSA) and Conseil Régional de Bretagne

Annexe 4 : communication (orale et poster) : « Role of secreted proteins and heparan sulfate on sperm binding to oviduct epithelial cells in cattle », *Association of Embryo Technology in Europe (AETE), 2022*

Role of secreted proteins and heparan sulfate on sperm binding to oviduct epithelial cells in cattle

Coline Mahé[1], Karine Reynaud[1], Ludivine Laffont[1], Pascal Mermillod[1], Marie Saint-Dizier[1]

[1]CNRS, IFCE, INRAE, Université de Tours, UMR PRC, Nouzilly, France

Introduction

During the pre-ovulatory (**Pre-ov**) period, a subpopulation of spermatozoa (**spz**) reaches the first part of the oviduct (isthmus) where they can bind to oviduct epithelial cells (**OEC**) to form a sperm reservoir (1). This reservoir may provide capacitated spermatozoa right on time for fertilization to occur. In cattle, sperm–binding glycoproteins on OEC surface are also secreted in the oviduct fluid (**OF**) and interact with sperm (2). Sulfated glycosaminoglycans are other macromolecules secreted in the OF and known to interact with sperm surface (3). Moreover, heparin, a sGAG which is not present in the bovine OF, was shown to release bovine sperm from OEC (4). The **aim of the study** was to assess the roles of soluble proteins and heparan sulfate, one of the most abundant sGAG in the bovine OF, on the binding of sperm to OEC by using an *in vitro* model of oviduct spheroids.

Material and methods

I. Culture of bovine oviduct epithelial cells

Pool of cells from pre-ov isthmus of 2 – 3 cows from slaughterhouse

4 days of culture in TCM 199 10% FBS

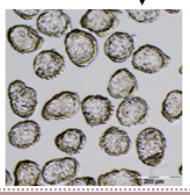

Bovine oviduct epithelial spheroids (bOES)

II. Incubation of bOES and spz 1h 38,8°C 5%CO_2

20 uniform circular 100 µm bOES + 1 millions/mL of frozen-thawed Percoll-washed sperm from 3 Holstein bulls

in

Control : TALP-HEPES + Pyruvate, Lactate, PVA

1. Pre-ov OF from 0,06 to 4 mg/mL of proteins

2. OF fractions (Vivaspin cut-off 3 kDa)

3. OF after protein denaturation (10' 100°C) or digestion (Proteinase K)

4. OF after heparan sulfate digestion (Heparinases)

Heparan sulfate 10, 100, 1000 µg/mL

III. Fixation and confocal microscopy



Fixation 1 H at 37°C with 2,5% glutaraldehyde

↓

Hoechst staining

↓

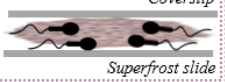

IV. Assessment of sperm density

Sperm density = Number of spz per spheroid area / Spheroids area

V. Assessment of sperm motility by CASA and viability by flow cytometry (propidium iodide)

VI. Statistical analysis

Mean ± SEM (N = 3-5)

ANOVA and Tukey post test

c : p<0,01

e : p<0,0001

Results

Effect of the OF

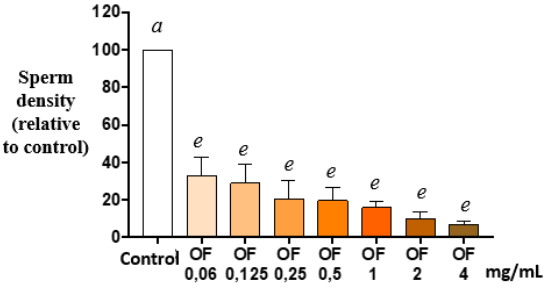

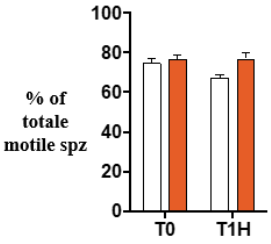

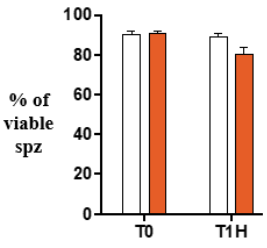

The OF decreased sperm density in a protein dose dependent manner without affecting sperm motility and membrane integrity

Sperm density on bovine oviduct spheroids

Effect of the OF components

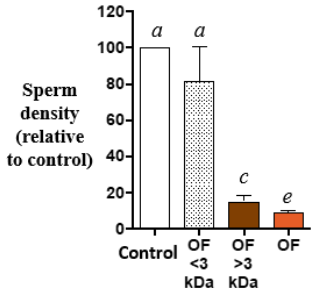

- **OF fraction > 3 kDa reproduced the effect of OF on sperm density**

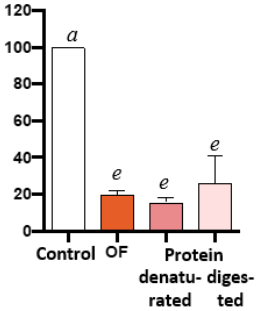

- **OF in which proteins were denaturated or digested reproduced the effect of the OF on sperm density**

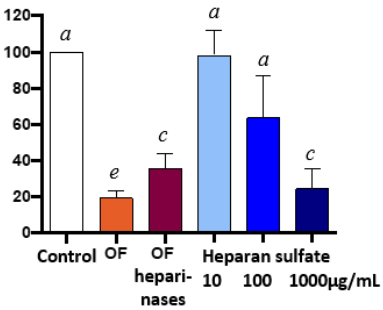

- **OF in which heparan sulfate was digested decreased sperm density (to a lower extent than the native OF)**
- **Heparan sulfate decreased sperm density in a dose dependant manner**

Conclusions and perspectives

The pre-ovulatory OF decreased sperm density bound to OEC without affecting their motility. This effect of the OF on sperm binding may be a way to select best sperm for fertilization during the periconception period. Heparan sulfate and probably other macromolecules in the OF seem responsible of the OF selective effect. The impact of sperm binding and subsequent release from spheroids on fertilizing ability and embryo quality remain to be tested.

UMR Physiologie de la Reproduction et des Comportements 37380 Nouzilly, France

Fundings

This work was funded by INRAE and Region Centre-Val de Loire

References

(1) Lefebvre et al., Biol Reprod, 1995
(2) Lamy et al., Reproduction, 2018
(3) Plante et al., Cell Tissue Res, 2015
(4) Talevi and Gualteri, Biol Reprod, 2001

Annexe 5 : article de recherche (collaboration au cours de la thèse) : « Metabolomic analysis of oviduct fluid on day 3 post-estrus in Holstein heifers »

Reproductive Biology 21 (2021) 100512

Contents lists available at ScienceDirect

Reproductive Biology

journal homepage: www.elsevier.com/locate/repbio

Short communication

Metabolomic analysis of oviduct fluid on day 3 post-estrus in Holstein heifers

Coline Mahé[a,1], Julie Gatien[b,1], Olivier Desnoes[b], Daniel Le Bourhis[b], Pascal Mermillod[a], Pascal Salvetti[b], Marie Saint-Dizier[a,c,*]

[a] Physiologie de la Reproduction et des Comportements, INRAE, CNRS, IFCE, University of Tours, 37380, Nouzilly, France
[b] Allice, 37380, Nouzilly, France
[c] Faculty of Sciences and Techniques, Tours University, 37200, Tours, France

ARTICLE INFO

Article history:
Received 23 March 2021
Received in revised form 30 April 2021
Accepted 5 May 2021
Available online xxx

Keywords:
Oviduct
Fallopian tube
Metabolomics
Embryo
Cattle

ABSTRACT

The metabolites in the oviduct fluid (OF) of both oviducts were analyzed by proton nuclear magnetic resonance (^{1}H-NMR) in Holstein heifers on day 3 after synchronized estrus. Twenty-six metabolites were quantified, among which lactate, glycine and myoinositol were the most abundant. Six metabolites including glycine and myoinositol varied in amount according to the proximity to the corpus luteum. Glucose and histidine were among the most variable metabolites among heifers while threonine and lactate were among the most stable ones, suggesting different mechanisms of homeostasis in the OF.
© 2021 Society for Biology of Reproduction & the Institute of Animal Reproduction and Food Research of Polish Academy of Sciences in Olsztyn. Published by Elsevier B.V. All rights reserved.

1. Introduction

In cattle breeding, the transfer of embryos into the uterus of female recipients is widely used for genetic purposes in North America, South America and Europe. Since 2016, the number of *in-vitro* produced (IVP) embryos exceeds that of their *in vivo* conceived counterparts [1]. However, cattle embryos developed *in vitro, i.e.* by bypassing the oviduct, are of lower quality than *in-vivo* conceived embryos in terms of morphology, gene expression, methylation profiles and developmental competence [2]. In order to meet the requirements of the embryo and improve the quality of IVP blastocysts, a precise knowledge of the early oviduct microenvironment and its individual variation is highly desirable.

The bovine embryo develops in the oviduct fluid (OF) ipsilateral to the ovulation for approximately 4–5 days after estrus [3]. A crucial step for embryo development is the major activation of the embryonic genome at the 8- to 16-cell stage that occurs around day 3 post-estrus [3,4]. The OF is a complex and dynamic fluid made of proteins, lipids, hormones, electrolytes and metabolites [5]. In a previous study, proton nuclear magnetic resonance spectroscopy (^{1}H-NMR) was used successfully to monitor the metabolome of the bovine OF across the estrous cycle [6]. However, the OF samples collected at the post-ovulatory phase of cycle were pooled in groups of 3–10 cows on days 1–5 post-ovulation, precluding any evaluation of individual variability on a specific day in the cycle. We hypothesized that various mechanisms of homeostasis in the oviduct may lead to individual changes in OF metabolite concentrations despite similar genetics, age and breeding conditions. Therefore, the objective of this study was to compare the metabolome of the bovine OF between Holstein heifers on day 3 post-estrus.

2. Materials and methods

The protocol of this study was approved by the regional 'Centre-Val-de-Loire' ethics committee (agreement number #22926-2019112513501450 v4). All animals were housed indoors in straw bedded pens and were fed a diet consisting of straw *ad libitum* supplemented with 5 kg of concentrate per day distributed in 2 meals. The estrous cycles of nulliparous Holstein heifers (n = 7) of similar age (average 32.4 ± 0.7 months) and live weight (average 609 ± 17 kg) were synchronized using a 9-day progesterone-releasing intravaginal insert (PRID delta, Ceva Santé Animale, Libourne, France) combined with an injection of 0.5 mg of a prostaglandin analog (cloprostenol, Estrumate, MSD Animal Health, Beaucouzé, France) the day before removal of the vaginal

* Corresponding author at: CNRS, IFCE, INRAE, Université de Tours, PRC, 37380, Nouzilly, France.
E-mail address: marie.saint-dizier@univ-tours.fr (M. Saint-Dizier).
[1] These authors contributed equally to this work.

http://dx.doi.org/10.1016/j.repbio.2021.100512
1642-431X/© 2021 Society for Biology of Reproduction & the Institute of Animal Reproduction and Food Research of Polish Academy of Sciences in Olsztyn. Published by Elsevier B.V. All rights reserved.

insert. Behavioral signs of estrus were monitored using the automated neck-mounted Heatime HR system (SCR Engineers Ltd., Netanya, Israël). Heatime HR is an accelerometer which translates each female's activity into index values representing weighted standard deviations from the female's own basal activity and transfers data wirelessly to a registering station every 2 h. The maximal index value (or peak of activity) observed after PRID removal was considered as the time of estrus (Day 0) [7]. Heifers were slaughtered 6 days after PRID removal in a local slaughterhouse (Vendôme, France). The time interval (h) between estrus (Day 0) and oviduct collection was calculated retrospectively.

The OF samples were collected and prepared as described earlier [6]. Briefly, both oviducts and ovaries from individual cows were placed on ice within less than 15 min after death and transported to the laboratory within 3 h after the first cow. One early hemorrhagic corpus luteum (in the side of ovulation) was observed in all animals. The entire oviducts ipsilateral and contralateral to ovulation were cleaned of surrounding tissues and vessels and after elimination of the infundibulum, their content (OF + mucosa cells) was collected by a single evenly gentle squeeze with a glass slide. Then the OF was separated from oviductal cells and cell debris by two successive centrifugations (2000*g*, 5 min then 12 000*g*, 10 min) at 4 °C. The OF samples (30−50 μL/oviduct) were stored at −80 °C until analyzed.

Metabolites were quantified in OF samples using proton nuclear magnetic resonance (^{1}H-NMR) as previously described [6]. Briefly, 10 μL of OF were diluted in 190 μL of 0.2 M potassium phosphate buffer in deuterium oxide (D2O) (pH 7.4 ± 0.5). The

Table 1
Mean concentrations, coefficients of variation (CV) and biological functions of metabolites quantified in the oviductal fluid of Holstein heifers on day 3 post-estrus (n = 7). Metabolites are classified in decreasing order of abundance.

		Ipsilateral side		*Contralateral side*		
	Chemical class	Mean ± SD (μM)	CV (%)	Mean ± SD (μM)	CV (%)	Biological function
Lactate	Alpha hydroxy acids and derivatives Energy substrate	34,498.0 ± 4,970.2	14.4	35,843.4 ± 4,616.4	12.9	Biochemical processes. Produced by the muscle during intense activity.
Glycine	Amino acids, peptides, and analogues Non-essential amino acids Proteinogenic	21,399.9 ± 6210.7	29.0	15,009.6 ± 2,726.2	18.2	Participate in metabolic pathways and production of DNA, phospholipids and collagen.
Myoinositol	Alcohols and polyols	10,998.3 ± 1,715.4	15.6	12,431.6 ± 1,963.3	15.8	Involved in the inositol and galactose metabolism.
Alanine	Amino acids, peptides, and analogues Non-essential amino acids Proteinogenic	5,911.2 ± 735.2	12.4	5,647.4 ± 921.0	16.3	Protein biosynthesis. Source of energy.
Threonine	Amino acids, peptides, and analogues Essential amino acids Proteinogenic	4,491.5 ± 556.8	12.4	4,591.3 ± 500.7	10.9	Protein biosynthesis.
Phosphocholine	Quaternary ammonium salts	3,742.0 ± 367.5	9.8	3,843.6 ± 310.6	8.1	Phosphatidylcholine biosynthesis. Metabolic pathways.
Creatine	Amino acids, peptides, and analogues Endogenous amino acid	3,741.9 ± 541.6	14.5	4,232.0 ± 755.4	17.8	Participate in energy metabolism for muscle contractions
Isoleucine	Amino acids, peptides, and analogues Essential amino acids Proteinogenic	3,155.0 ± 728.4	23.1	3,026.0 ± 473.9	15.7	Protein synthesis. Stress, energy and muscle metaboslim.
Glucose	Carbohydrates and carbohydrate conjugates Energy substrate	1,921.0 ± 905.0	47.1	1,781.4 ± 815.6	45.8	Primary source of energy.
Carnitine	Quaternary ammonium salts Non-proteinogenic	1,501.8 ± 268.0	17.8	1,856.5 ± 429.0	23.1	Provide energy for muscles. Vitamin.
Citrate	Tricarboxylic acids and derivatives	1,180.8 ± 175.1	14.8	1,140.5 ± 166.8	14.6	Energy production. Precursor of ROS and prostaglandins.
Aspartate	Amino acids, peptides, and analogues Proteinogenic	1,169.7 ± 211.2	18.1	1,279.1 ± 322.8	25.2	Precursor of cell signaling compound. Involved in gluconeogenesis. Neurotransmitter.
Acetate	Carboxylic acids	1,152.7 ± 183.4	15.9	1,111.6 ± 136.2	12.3	Participate in the metabolism of carbohydrates and fats when associated with coenzyme A.
Malonate	Dicarboxylic acids and derivatives	931.2 ± 113.9	12.2	928.5 ± 108.2	11.7	Fatty acid biosynthesis pathway.
Leucine	Amino acids, peptides, and analogues Essential amino acids Proteinogenic	906.8 ± 176.4	19.5	869.6 ± 123.5	14.2	Protein synthesis. Stress, energy and muscle metaboslim. Stimulation on insulin signaling.
Valine	Amino acids, peptides, and analogues Essential amino acids Proteinogenic	749.5 ± 133.3	17.8	715.4 ± 98.5	13.8	Stress, energy and muscle metabolism.
Mannose	Carbohydrates and carbohydrate conjugates	541.3 ± 119.3	22.0	604.6 ± 172.6	28.5	Protein quality control. Involved in the innate immune system.
Acetylcarnitine	Fatty acid esters Acyl carnitines	494.5 ± 89.5	18.1	546.4 ± 109.7	20.1	Involved in the oxidation of fatty acids.
Choline	Quaternary ammonium salts Essential vitamin	494.5 ± 89.5	18.1	546.4 ± 109.7	20.1	Phospholipids biosynthesis. Converted into the neurotransmitter Acetylcholine
Creatine phosphate	Amino acids, peptides, and analogues	466.9 ± 81.7	17.5	468.7 ± 49.7	10.6	Participate in energy metabolism for muscle contractions
Histamine	Amines	386.5 ± 53.5	13.8	380.4 ± 58.3	15.3	Involved in several metabolic and enzymatic pathway and gastric acid secretion. Neurotransmitter.
Histidine	Amino acids, peptides, and analogues Proteinogenic	227.0 ± 107.4	47.3	250.6 ± 81.1	32.3	Protein biosynthesis. Metabolic pathways. Ammonia recycling.
Pyruvate	Alpha-keto acids and derivatives	178.8 ± 35.2	19.7	167.0 ± 24.5	14.7	Participate in the gluconeogenesis, glycolyse and several metabolic pathways.
Fumarate	Dicarboxylic acids and derivatives	113.4 ± 17.9	15.8	118.1 ± 18.0	15.2	Energy production (TCA cycle). Metabolic pathways.
Succinate	Dicarboxylic acids and derivatives	75.0 ± 36.8	49.1	73.2 ± 31.6	43.2	Involved in the TCA cycle, respiratory chain, metabolic pathways and signal during inflammation.
Glucose-1-phosphate	Carbohydrates and carbohydrate conjugates Energy substrate	65.9 ± 91.1	138.4	114.5 ± 112.3	98.1	Converted into Glucose-6-phosphate in the glycolyse and gluconeogenesis.

resulting solution was transferred to conventional 3-mm NMR tubes and ^{1}H-NMR spectra were then recorded at 298 K on a Bruker Ascend 600-MHz spectrometer (Bruker, Sadis, Wissembourg, France), equipped with a TCI cryoprobe. The intra-assay (sample-to-sample variations) and inter-assay (assay-to-assay variations) coefficients of variation were 6.0 % and 4.6 %, respectively. Metabolite quantifications using the Electronic Reference To access *in vivo* Concentrations (ERETIC) peak as a quantitative reference were obtained using the Bruker TopSpin 3.2 program (Bruker daltonik, Karlsruhe, Germany). Spiking experiments were used to validate metabolite assignments. Spectral assignments were done using the free version of ChenomX 7.1 software (ChenomX, Edmonton, Canada) and based on the human metabolome database (HMDB).

To obtain an overview of metabolomic data across the various animals, a principal component analysis of all data was performed using the FactoMineR package (version 1.34) of the RStudio software (version 1.1.456). A statistical analysis of data was then performed using the GraphPad software (Prism 7.0; GraphPad Software Inc., San Diego, CA, USA). Comparisons between sides relative to ovulation were assessed using the non-parametric Wilcoxon test for paired comparisons. The variability between individuals was assessed by the coefficients of variation (CV) expressed as percentages (SD/Mean × 100). The correlation between metabolite concentrations and CV on each side was assessed by Pearson tests. A P-value lower than 0.05 was considered significant. Chemical classes and biological functions of metabolites were obtained from "The bovine metabolome database" (www.bovinedb.ca/) [8]. All data are presented as means ± SD.

3. Results and discussion

The Heatime system was reported previously as highly accurate for estrus detection (positive predictive value ≥ 84 %) [7]. Coupled with estrus synchronization, this monitoring system allowed us to time precisely the collection of oviducts between 72 h (3.0 days) and 88 h (3.7 days) after the peak of estrous activity (average: 79.1 ± 2.2 h *i.e.* 3.3 ± 0.1 days after the peak of estrus), *i.e.* at the time when cattle embryos reach the 8-cell or early morula stage after fertilization [3].

This is the first time ^{1}H-NMR was used to exhaustively identify OF metabolites in Holstein heifers on day 3 post-estrus. A total of 39 metabolites, including 14 amino acids, were identified in the OF. Of those, 13 metabolites could not be quantified: 10 (3-hydroxybutyrate, creatinine, ethanolamine, isobutyrate, methionine, niacinamide, nicotinurate, phenylalanine, proline and tyrosine) due to low signals and three of them (acetylcholine,

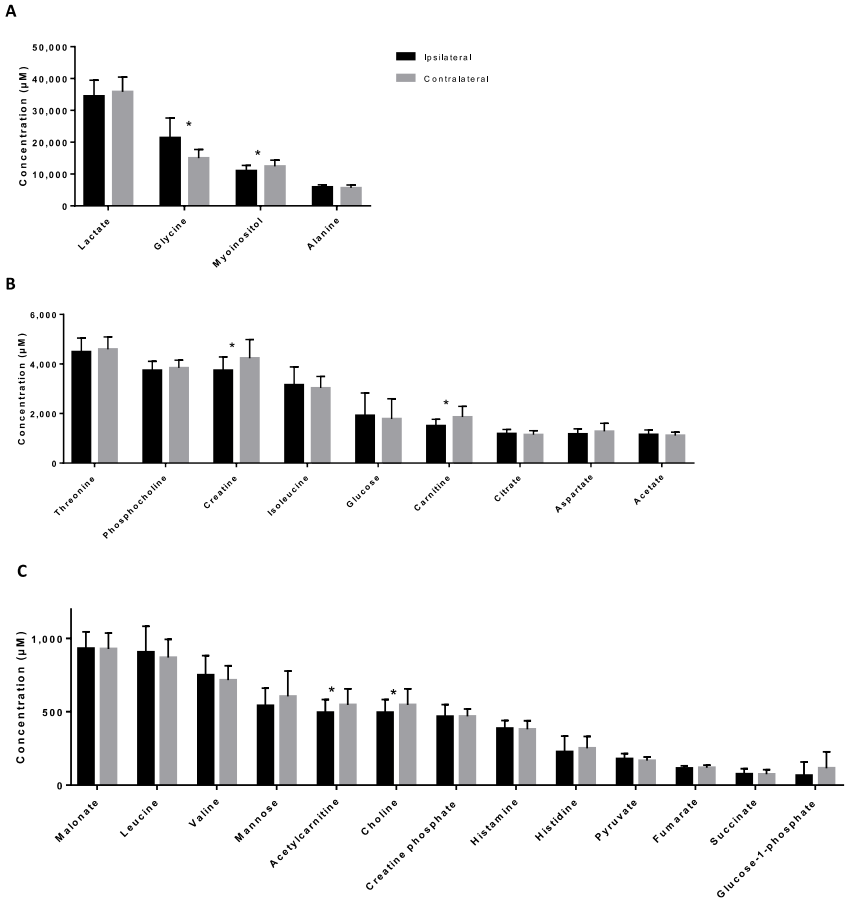

Fig. 1. Metabolites in the oviductal fluid of cyclic Holstein heifers on day 3 post-estrus with average concentrations above 5 mM (A), between 1 and 5 mM (B) and below 1 mM (C). Data are indicated as means ± SD. Asterisks indicate significant differences between ipsilateral and contralateral sides relative to ovulation. *P < 0.05.

glutamate and glutamine) due to a large overlap of their signals with others.

Table 1 shows the average concentrations and CV of the 26 metabolites quantified in both sides relative to ovulation. Principal component analysis of metabolomic data did not evidence any separation between animals or ipsilateral *vs*. contralateral sides of ovulation (see supplementary material). Overall, the amino acids glycine and alanine and the energy substrates lactate and myoinositol were the most abundant metabolites, with concentrations above 5 mM (Fig. 1A). The concentration of other metabolites ranged from less than 100 μM (succinate) up to 4500 μM (Fig. 1B–C). This is in accordance with earlier reports of amino acid detection using high performance liquid chromatography (HPLC) or ^{1}H-NMR in the post-ovulatory bovine OF [6,9–11]. Lactate was also the most abundant energy substrate in previous studies quantifying glucose, pyruvate and lactate in the post-ovulatory OF of cyclic cows [9–11]. However, absolute concentrations of metabolites vary between studies which may be due to differences in animal breed, nutrition, parity and/or in methods of OF collection (post-mortem *vs*. after oviduct cannulation) and quantification. These metabolites are known to be involved in a wide range of biological functions (Table 1). Furthermore, important roles of lactate, pyruvate, glucose, succinate and various amino acids in the development of the early bovine embryo have been reported (reviewed in [4]).

A significant effect of the proximity to the corpus luteum was evidenced for glycine, which was more abundant in the side of ovulation compared to the other side (Fig. 1A). On the opposite, myoinositol, creatine, carnitine, acetylcarnitine and choline were less abundant on the side of ovulation compared to the contralateral oviduct (Fig. 1A–C). These data are in keeping with those from Lamy et al. [6] who reported the same patterns of differences between sides during the post-ovulatory period. Significantly higher concentrations of progesterone were measured in the oviduct ipsilateral to ovulation compared to the contralateral one [12,13]. Furthermore, a systemic supplementation of progesterone on day 3 of the cycle led to an increase in glycine concentrations in the OF of cows [11], in line with the present results. These data highlight the local regulatory role of ovarian steroid hormones in the metabolome of the oviduct.

In this study, OF samples were collected at the same amount of time post-estrus from animals of similar genetics, age, weight with identical diet and living conditions, which were assumed to limit the individual variability in OF metabolites. A very high CV was recorded for G1P due to its non-detection in 4 out of 14 samples (138.4 % and 98.1 % in ipsilateral and contralateral oviducts, respectively). The average CVs for the remaining 25 metabolites were 20.6 % (range: 9.8 %–49.1 %) and 19.1 % (range: 8.1 %–43.2 %) in the ipsilateral and contralateral OF, respectively, with no correlation between CV and metabolite abundance (Pearson's test not significant). In the ipsilateral side of ovulation, the most stable metabolites included phosphocholine, malonate, threonine and alanine (CVs between 9.8 and 12.4 %) while the most variable metabolites included glucose, glycine, histidine and succinate (CV between 29.0 and 49.1 %; see Table 1). This is in accordance with previous studies in which a high individual variability (high SEM values) was reported for glucose, lactate and many amino acids in the OF from crossbred heifers [9,10,14]. These data have to be taken with caution due to the low number of animals in previous studies as well as in this one. It is likely that metabolites with low CV are essential for oviduct homeostasis and for support of vital functions in gametes and embryos. On the other hand, metabolites with high CV may vary in the circulating blood and OF in response to environmental factors. For instance, blood concentrations of glucose were shown to increase in stress-related situations like surgery [15], which could explain differences in the response of animals to the stress of transport and slaughterhouse environment prior to collection of oviducts.

In conclusion, 26 metabolites were quantified in the bovine OF at the time of early embryo development, giving new insights into the embryonic maternal environment. The mechanisms underlying a relative homeostasis for some OF metabolites and on the opposite a high individual variability for some others including glucose and glycine, remain to be elucidated.

Author contributions

MSD and PS conceived and designed the experiments; PS and OD managed the animals and the collection of biological material; PS, MSD, OD and DLB collected and prepared the materials; JG performed the metabolomic analyses; CM and MSD performed the analysis of metabolomic data; PM provided guidance and resources; MSD and PS managed the project; MSD and CM wrote the paper; all authors read and approved the manuscript.

Funding

This work was funded by APIS-GENE (Embryomimetisme project) and INRAE. Coline Mahé was funded by the Region Centre Val-de-Loire.

Declaration of Competing Interest

The authors report no declarations of interest.

Acknowledgments

The authors are grateful to Marc Chodkiewicz for critical review of this paper.

Appendix A. Supplementary data

Supplementary material related to this article can be found, in the online version, at doi:https://doi.org/10.1016/j.repbio.2021.100512.

References

[1] Ferre LB, Kjelland ME, Strobech LB, Hyttel P, Mermillod P, Ross PJ. Review: recent advances in bovine in vitro embryo production: reproductive biotechnology history and methods. Animal 2020;14:991–1004.
[2] Besenfelder U, Brem G, Havlicek V. Review: Environmental impact on early embryonic development in the bovine species. Animal 2020;14:s103–12.
[3] Hamilton WJ, Laing JA. Development of the egg of the cow up to the stage of blastocyst formation. J Anat 1946;80:194–204.
[4] Milazzotto MP, de Lima CB, da Fonseca AM, Dos Santos EC, Ispada J. Erasing gametes to write blastocysts: metabolism as the new player in epigenetic reprogramming. Anim Reprod 2020;17:e20200015.
[5] Saint-Dizier M, Schoen J, Chen S, Banliat C, Mermillod P. Composing the early embryonic microenvironment: physiology and regulation of oviductal secretions. Int J Mol Sci 2019;21:.
[6] Lamy J, Gatien J, Dubuisson F, Nadal-Desbarats L, Salvetti P, Mermillod P, et al. Metabolomic profiling of bovine oviductal fluid across the oestrous cycle using proton nuclear magnetic resonance spectroscopy. Reprod Fertil Dev 2018;30:1021–8.
[7] Silper BF, Madureira AM, Kaur M, Burnett TA, Cerri RL. Short communication: comparison of estrus characteristics in Holstein heifers by 2 activity monitoring systems. J Dairy Sci 2015;98:3158–65.
[8] Foroutan A, Fitzsimmons C, Mandal R, Piri-Moghadam H, Zheng J, Guo A, et al. The bovine metabolome. Metabolites 2020;10:.
[9] Rodriguez-Alonso B, Maillo V, Acuna OS, Lopez-Ubeda R, Torrecillas A, Simintiras CA, et al. Spatial and pregnancy-related changes in the protein, amino acid, and carbohydrate composition of bovine oviduct fluid. Int J Mol Sci 2020;21:.
[10] Hugentobler SA, Humpherson PG, Leese HJ, Sreenan JM, Morris DG. Energy substrates in bovine oviduct and uterine fluid and blood plasma during the oestrous cycle. Mol Reprod Dev 2008;75:496–503.
[11] Hugentobler SA, Sreenan JM, Humpherson PG, Leese HJ, Diskin MG, Morris DG. Effects of changes in the concentration of systemic progesterone on ions, amino acids and energy substrates in cattle oviduct and uterine fluid and blood. Reprod Fertil Dev 2010;22:684–94.
[12] Lamy J, Liere P, Pianos A, Aprahamian F, Mermillod P, Saint-Dizier M. Steroid hormones in bovine oviductal fluid during the estrous cycle. Theriogenology 2016;86:1409–20.
[13] Wijayagunawardane MPB, Miyamoto A, Cerbito WA, Acosta TJ, Takagi M, Sato K. Local distributions of oviductal estradiol, progesterone, prostaglandins, oxytocin and endothelin-1 in the cyclic cow. Theriogenology 1998;49:607–18.
[14] Hugentobler SA, Diskin MG, Leese HJ, Humpherson PG, Watson T, Sreenan JM, et al. Amino acids in oviduct and uterine fluid and blood plasma during the estrous cycle in the bovine. Mol Reprod Dev 2007;74:445–54.
[15] Mudron P, Rehage J, Sallman HP, Höltershinken M, Scholz H. Stress response in dairy cows related to blood glucose. Acta Vet Brno. 2005;74:37–42.

Annexe 6 : article de recherche (collaboration au cours de la thèse) : « Dynamic changes in the proteome of early bovine embryos developed *in vivo* »

frontiers in Cell and Developmental Biology

ORIGINAL RESEARCH
published: 21 March 2022
doi: 10.3389/fcell.2022.863700

Dynamic Changes in the Proteome of Early Bovine Embryos Developed *In Vivo*

Charles Banliat[1,2†], Coline Mahé[1†], Régis Lavigne[3,4], Emmanuelle Com[3,4], Charles Pineau[3,4], Valérie Labas[1,5], Benoit Guyonnet[2], Pascal Mermillod[1] and Marie Saint-Dizier[1]*

[1]CNRS, INRAE, Université de Tours, IFCE, UMR PRC, Nouzilly, France, [2]Union Evolution, Noyal-sur-Vilaine, France, [3]Irset–UMRS 1085, Inserm, University of Rennes, Rennes, France, [4]Protim, Univ Rennes, Biosit–UMS 3480, US-S 018, Rennes, France, [5]Pixanim, INRAE, Université de Tours, CHU de Tours, Nouzilly, France

OPEN ACCESS

Edited by:
João Ramalho-Santos,
University of Coimbra,Portugal

Reviewed by:
Bernard Roelen,
Utrecht University, Netherlands
Il-Keun Kong,
Gyeongsang National University, South Korea
Anette Kristine Krogenæs,
Norwegian University of Life Sciences, Norway
Sofia Diaz-Lundahl,
Norwegian University of Life Sciences, Norway, in collaboration with reviewer AK

***Correspondence:**
Marie Saint-Dizier
marie.saint-dizier@univ-tours.fr

[†]These authors have contributed equally to this work and share first authorship

Specialty section:
This article was submitted to Molecular and Cellular Reproduction, a section of the journal Frontiers in Cell and Developmental Biology

Received: 27 January 2022
Accepted: 07 March 2022
Published: 21 March 2022

Citation:
Banliat C, Mahé C, Lavigne R, Com E, Pineau C, Labas V, Guyonnet B, Mermillod P and Saint-Dizier M (2022) Dynamic Changes in the Proteome of Early Bovine Embryos Developed In Vivo. Front. Cell Dev. Biol. 10:863700. doi: 10.3389/fcell.2022.863700

Early embryo development is a dynamic process involving important molecular and structural changes leading to the embryonic genome activation (EGA) and early cell lineage differentiation. Our aim was to elucidate proteomic changes in bovine embryos developed *in vivo*. Eleven females were used as embryo donors and pools of embryos at the 4–6 cell, 8–12 cell, morula, compact morula and blastocyst stages were analyzed by nanoliquid chromatography coupled with label free quantitative mass spectrometry. A total of 2,757 proteins were identified, of which 1,950 were quantitatively analyzed. Principal component analysis of data showed a clear separation of embryo pools according to their developmental stage. The hierarchical clustering of differentially abundant proteins evidenced a first cluster of 626 proteins that increased in abundance during development and a second cluster of 400 proteins that decreased in abundance during development, with most significant changes at the time of EGA and blastocyst formation. The main pathways and processes overrepresented among upregulated proteins were RNA metabolism, protein translation and ribosome biogenesis, whereas Golgi vesicle transport and protein processing in endoplasmic reticulum were overrepresented among downregulated proteins. The pairwise comparison between stages allowed us to identify specific protein interaction networks and metabolic pathways at the time of EGA, morula compaction and blastocyst formation. This is the first comprehensive study of proteome dynamics in non-rodent mammalian embryos developed *in vivo*. These data provide a number of protein candidates that will be useful for further mechanistic and functional studies.

Keywords: embryo, proteomics, mass spectrometry, morula, blastocyst, cattle, development

1 INTRODUCTION

Mammalian embryo development starts after fertilization in the oviduct where the zygote undergoes its mitotic divisions while progressing toward the uterus. Bovine embryos stay in the oviduct for 3.5–4 days before they pass into the uterus, between the 8-cell and morula stages (Hamilton and Laing, 1946). During the first cleavage divisions, the embryo is transcriptionally quiescent, as its development is mainly controlled by oocyte-derived RNAs and proteins (Schulz and Harrison, 2019). Then, the zygotic genome is activated, leading to a progressive replacement of maternal and sperm supply by embryonic gene products (Lee et al., 2014). The major embryonic genome activation (EGA) event, also called maternal to zygotic transition (MZT), occurs between the 4-cell and 8-cell

stages in humans (Braude et al., 1988) and around the 8-cell stage in cattle (Gad et al., 2012; Graf et al., 2014b; Jiang et al., 2014). Thereafter, the embryo becomes a morula, in which the blastomeres start to differentiate and bind firmly together in a process called compaction (Van Soom et al., 1997). In the compact morula, two distinct cell lineages differentiate to form a blastocyst: the inner cell mass, which will give rise to the embryo and the trophectoderm cells which will participate in the embryonic part of the placenta (Watson and Barcroft, 2001).

The molecular mechanisms governing mammalian embryo development are still poorly understood and, so far, very few studies have explored the dynamics in the proteome of the early embryo (Jensen et al., 2014a; Jensen et al., 2014b; Deutsch et al., 2014; Demant et al., 2015; Gao et al., 2017). The mouse model has been most widely used to study mammalian embryo development. However, bovine and human early embryos seem to be more similar in terms of biochemical regulatory processes, transcriptomic dynamics and the kinetics of development up to the blastocyst stage (Menezo and Herubel, 2002; Jiang et al., 2014; Schulz and Harrison, 2019), reinforcing interest in cattle embryos as models to study early development. Proteomic studies on cattle embryos have focused on a few developmental stages and were exclusively conducted with embryos produced *in vitro* (Jensen et al., 2014a; Jensen et al., 2014b; Deutsch et al., 2014; Demant et al., 2015), which are well-known to have divergent gene expression patterns (Lonergan et al., 2003; Gutierrez-Adan et al., 2004; Wrenzycki et al., 2005) and less developmental competence (Enright et al., 2000; Rizos et al., 2017) than their *in vivo* counterparts. The main reasons for this lack of information are the difficulty of accessing oviducts in live animals and the scarcity of the required material (Saint-Dizier et al., 2019).

Transcriptomic studies conducted on bovine embryos developed *in vivo* (Kues et al., 2008; Gad et al., 2012; Jiang et al., 2014; Diaz-Lundahl et al., 2021) or *in vitro* (Gad et al., 2012; Graf et al., 2014b; Kropp et al., 2017; Wei et al., 2017) have greatly expanded our comprehension of the regulatory mechanisms underlying the EGA, cell lineage specification and metabolic requirements during pre-implantation development. However, data on proteomic dynamics during early development *in vivo* are currently lacking in non-rodent mammals. The objectives of the present study were to identify for the first time dynamic changes in the proteome of bovine embryos developed *in vivo* from the 4–6 cell to blastocyst stages and to predict functional implication of differentially abundant proteins.

2 RESULTS

In this study, we used nanoliquid chromatography coupled with tandem mass spectrometry (nanoLC-MS/MS) to elucidate dynamic changes in the proteome of bovine embryos developed *in vivo*. A total of 2,757 proteins were identified in embryos (see **Supplementary Table S1** for the complete list of proteins with their accession number, gene symbol and normalized quantification). Overall, 1,627 identified proteins were shared between stages. The blastocyst stage displayed the highest number of specific proteins (138 specific proteins; **Figure 1**).

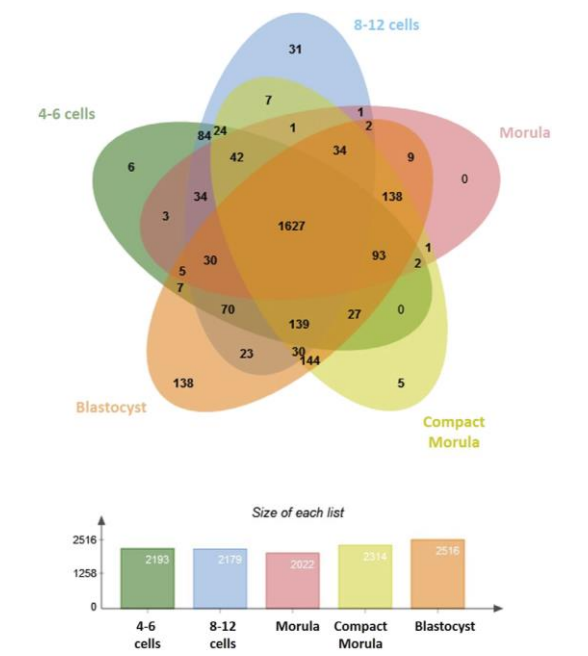

FIGURE 1 | Comparative analysis of proteins identified in bovine early embryos. Venn diagram showing the overlap among developmental stages and histogram showing numbers of proteins identified in each stage.

2.1 Global Analysis of Differentially Abundant Proteins Across Development

A total of 1,950 proteins quantified with ≥2 normalized weighted spectra (NWS) in at least one condition were retained for statistical analysis (**Supplementary Table S1**). Oviduct-specific glycoprotein (OVGP1) was detected with high abundance (>100 NWS) at all stages. Principal component analysis (PCA) of all data showed a clear segregation of embryo pools according to their developmental stage, except between the 4–6 and 8–12 cell stages, which clustered together (**Figure 2**).

The heatmap representation of differentially abundant proteins (DAPs) between stages (ANOVA p-value ≤ 0.05) evidenced that the biggest changes in protein abundance occurred between the 8–12 cell and morula stages then between the compact morula and blastocyst stages (vertical arrows in **Figure 3**).

The hierarchical clustering of DAPs allowed us to identity four clusters: a first cluster of 626 proteins that increased in abundance during development (upregulated proteins) and a second cluster of 400 proteins that decreased in abundance during development (downregulated proteins). Two other small clusters of 26 and 6 proteins, respectively, presented bimodal evolutions (see the lists of proteins in each cluster in **Supplementary Table S2**).

2.2 Functional Analysis of Differentially Abundant Proteins Across Development

The two first clusters were retained for functional analysis using Metascape. The enrichment analysis showed that pathways and

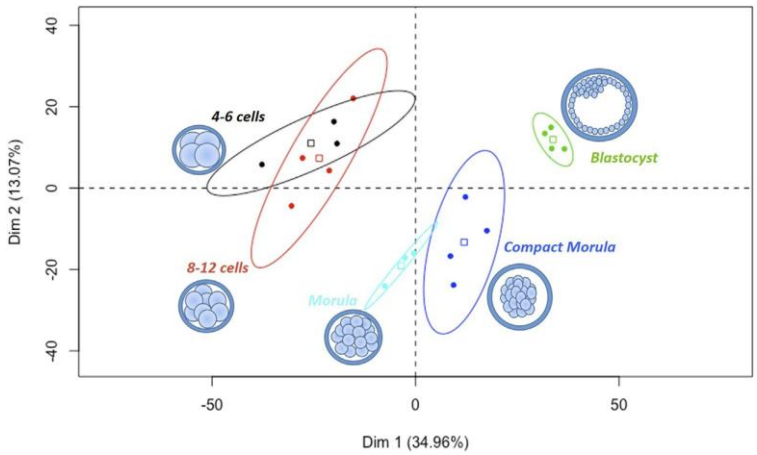

FIGURE 2 | Principal component analysis of all *in vivo* embryos pools from the 4–6 cell to blastocyst stages. All proteins quantified with min 2 NWS in at least one stage were considered. Scatter plots represent the position of each pool of embryos along the first two dimensions of PCA. The variability between pools was mainly explained by their stage of development on the first horizontal dimension (Dim 1, 35% of variance). The square in each ellipse represents the mean of data for a given stage and colored ellipses represent the 95% confidence intervals.

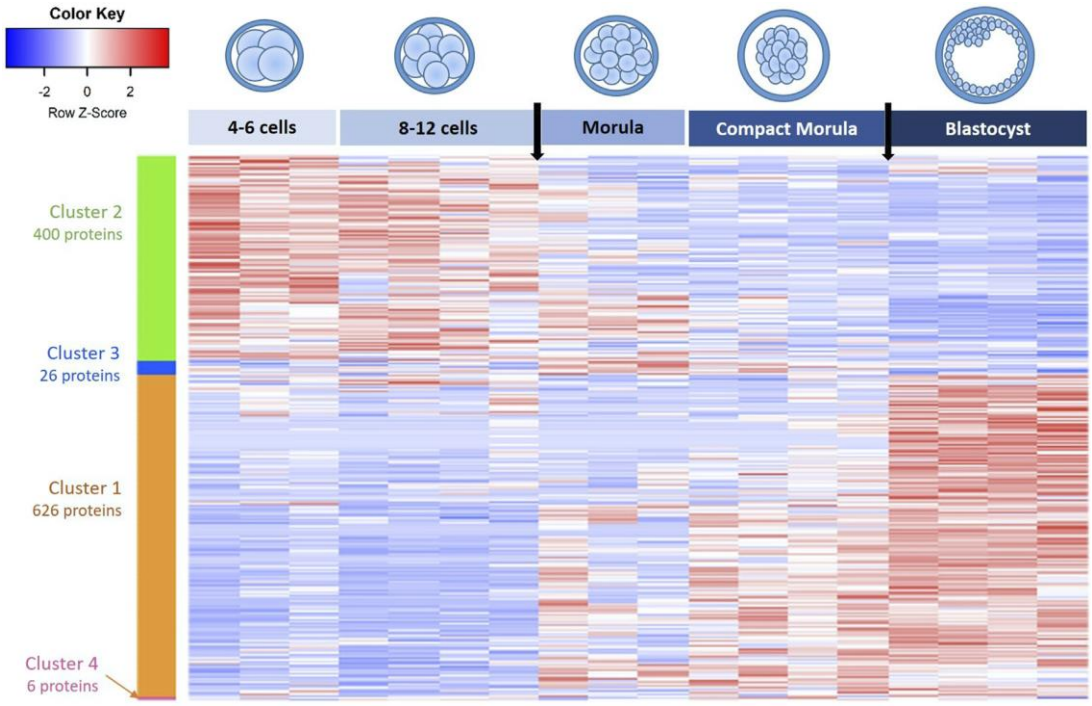

FIGURE 3 | Heatmap and hierarchical clustering of differentially abundant proteins (DAPs) in *in vivo* embryos from the 4–6 cell to blastocyst stages. Each line corresponds to one protein and each row to the abundance values of one embryo pool. Red indicates higher abundance while blue indicates lower abundance compared with other conditions. Clusters of proteins are indicated by colored vertical bars and are numbered in the decreasing order of protein numbers. Black arrows on the top indicate biggest changes in protein abundance at the time of 8-12-cell-to morula and compact morula-to-blastocyst transitions.

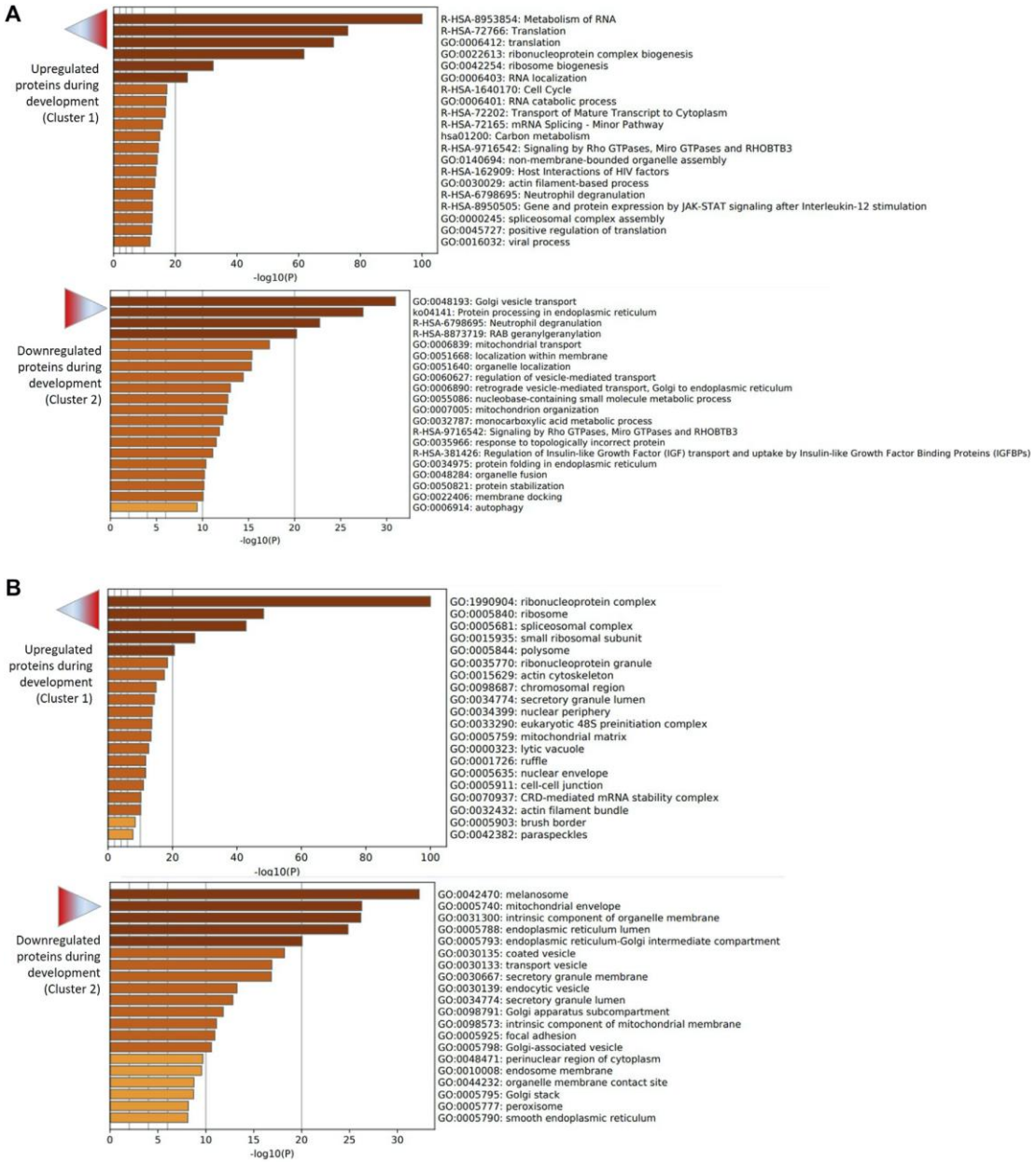

FIGURE 4 | Functional enrichment analysis of upregulated (cluster 1) and downregulated (cluster 2) proteins during embryo development. The analysis was performed using Metascape. **(A)** Bar graph of enriched pathway and process terms for upregulated (top graph) and downregulated (bottom graph) proteins. **(B)** Bar graph of enriched cellular component terms for upregulated (top graph) and downregulated (bottom graph) proteins. Darker color of bars indicates higher significance (lower p-value).

processes related to the metabolism of RNA, protein translation (ribonucleoprotein complex biogenesis, ribosome biogenesis, RNA localization, RNA catabolic process) and carbon metabolism were overrepresented among upregulated proteins, whereas Golgi vesicle transport, protein processing in endoplasmic reticulum and neutrophil degranulation were overrepresented among downregulated proteins (**Figure 4A** and **Supplementary Table S2** for all enriched GO terms according to Metascape). Furthermore, the enrichment analysis for cellular components (CC) showed that components of the protein translation machinery (ribonucleoprotein complex, ribosome, spliceosome complex, small ribosomal subunit, polysome …) were overrepresented among

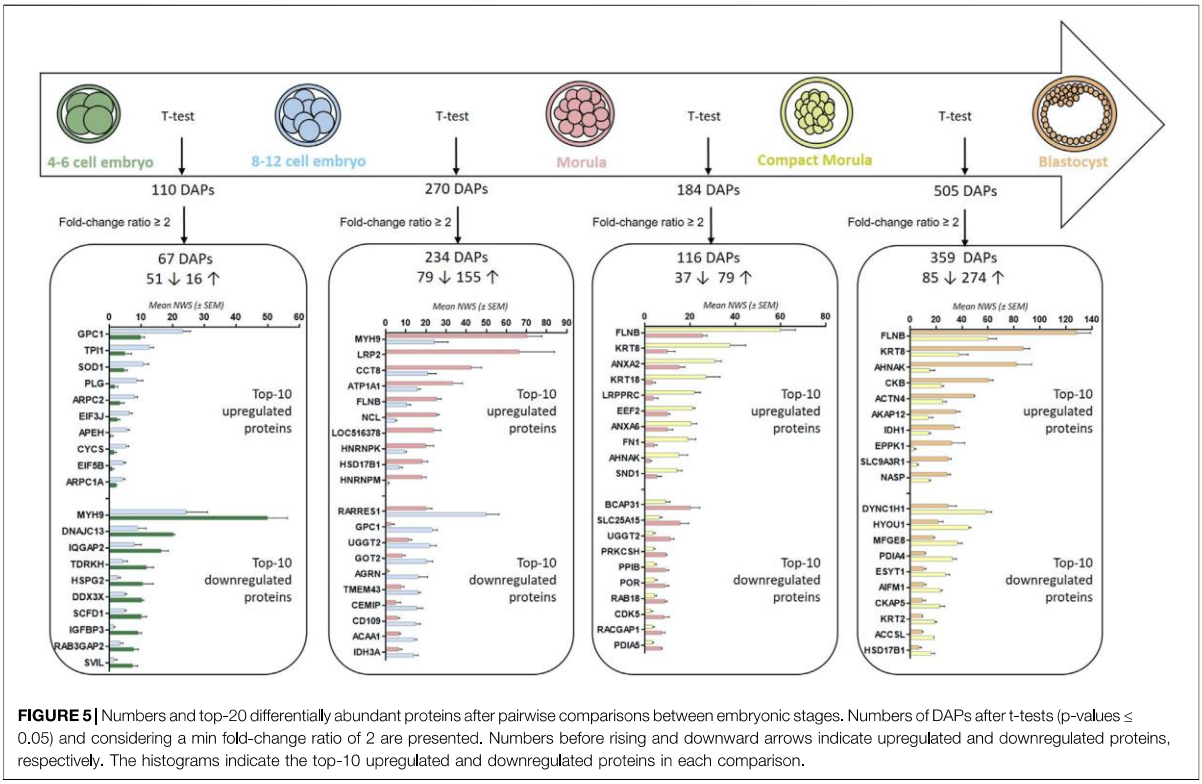

FIGURE 5 | Numbers and top-20 differentially abundant proteins after pairwise comparisons between embryonic stages. Numbers of DAPs after t-tests (p-values ≤ 0.05) and considering a min fold-change ratio of 2 are presented. Numbers before rising and downward arrows indicate upregulated and downregulated proteins, respectively. The histograms indicate the top-10 upregulated and downregulated proteins in each comparison.

upregulated proteins. On the other side, proteins of the melanosome, mitochondrial envelope and intrinsic component of organelle membrane were overrepresented among downregulated proteins (**Figure 4B**; **Supplementary Table S2**).

2.3 Pair-Wise Comparisons Between Stages and Functional Implication

Pairwise comparisons (t-test p-value ≤ 0.05) between stages evidenced between 110 and 505 DAPs in total and between 67 and 359 DAPs considering a minimal fold-change of 2 (**Figure 5**; see **Supplementary Table S3** for complete lists of DAPs after t-tests). In accordance with the heatmap on **Figure 3**, the highest numbers of DAPs were observed at the 8–12 cell-to-morula and compact morula-to-blastocyst transitions.

DAPs with a fold-change ratio ≥2 were further studied for their functional involvement and interaction networks. Between the 4–6 and 8–12 cell stages, due to the relatively low number of DAPs, no PPI network and only two enriched KEGG pathways were identified (RNA transport and regulation of actin cytoskeleton; p-values ≤ 0.05; see enriched terms during the 4–6-to-8–12 cell transition in **Supplementary Table S4**).

2.3.1 From 8–12 Cell to Morula Stages

From the 8–12 cell to morula stages, the Proteomaps of DAPs showed that upregulated proteins were mainly involved in the transcription and translation pathways (ribosome, RNA transport, spliceosome) and to a lesser extent in cellular processes (cellular community, cytoskeleton) and biosynthesis (**Figure 6A**). On the other hand, downregulated proteins were overrepresented among the environmental information processing category (ECM-receptor interactions, CD molecules, GTP-signaling molecules) and metabolic pathways (amino acid metabolism, lipid and steroid biosynthesis, cofactor biosynthesis and carbon metabolism) (**Figure 6B**).

The STRING (Search Tool for the Retrieval of Interacting Genes/proteins) functional analysis of DAPs during the 8–12 cell-to-morula transition confirmed the highly significant enrichment in the ribosome, spliceosome and RNA transport pathways (p-values < 10^{-5}; see all enriched terms during the 8–12 cell-to-morula transition in **Supplementary Table S5**). In addition, numerous protein interactions were identified, including two dense PPI networks encompassing several ribosomal proteins and proteins involved in RNA transport and the spliceosome that were all upregulated (**Figure 7**; see network details in **Supplementary Table S5**).

2.3.2 From Morula to Compact Morula Stages

Between the morula and compact morula stages, Proteomaps of DAPs showed that upregulated proteins were mainly involved in the cytoskeleton and vesicular transport pathways, whereas

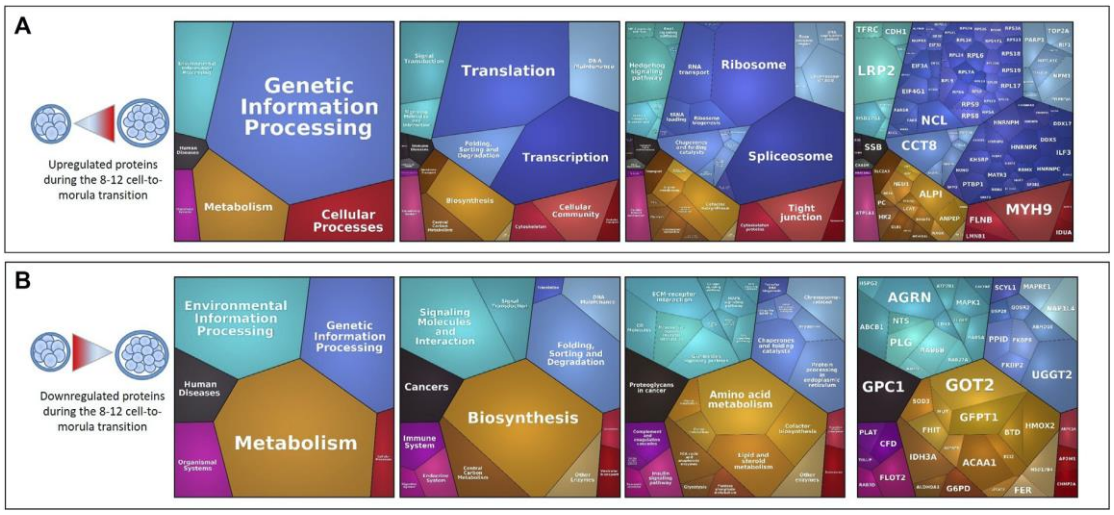

FIGURE 6 | Proteomaps of differentially abundant proteins (DAPs) during the 8–12 cell-to-morula transition. Proteomaps were carried out using the lists of gene names of proteins increasing [**(A)**, upper panels] or decreasing [**(B)**, down panels] in abundance (t-test p-value ≤ 0.05; min fold-change of 2) between the 8–12 cell and morula stages and based on the KEGG Pathway gene classification. Functional categories (left and middle panels) and related proteins (right panel) are shown by polygons. Areas of polygons illustrate protein abundance, weighted by protein size. Functionally related functions/proteins are arranged in common regions and coded using similar colors.

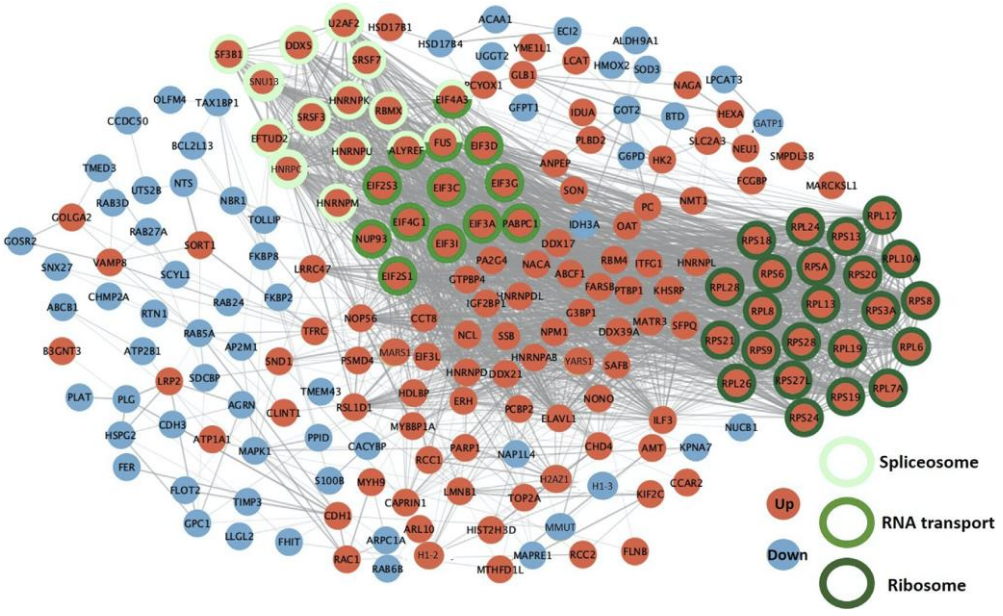

FIGURE 7 | Protein-protein interaction networks between differentially abundant proteins (DAPs) during the 8–12-cell-to-morula transition. The PPI network was built using STRING and Cytoscape. DAPs increased in abundance between the 8–12 cell and morula stages are in red while proteins decreased in abundance are in blue. The DAPs involved in the three most significant KEGG pathways are indicated by colored circles in green.

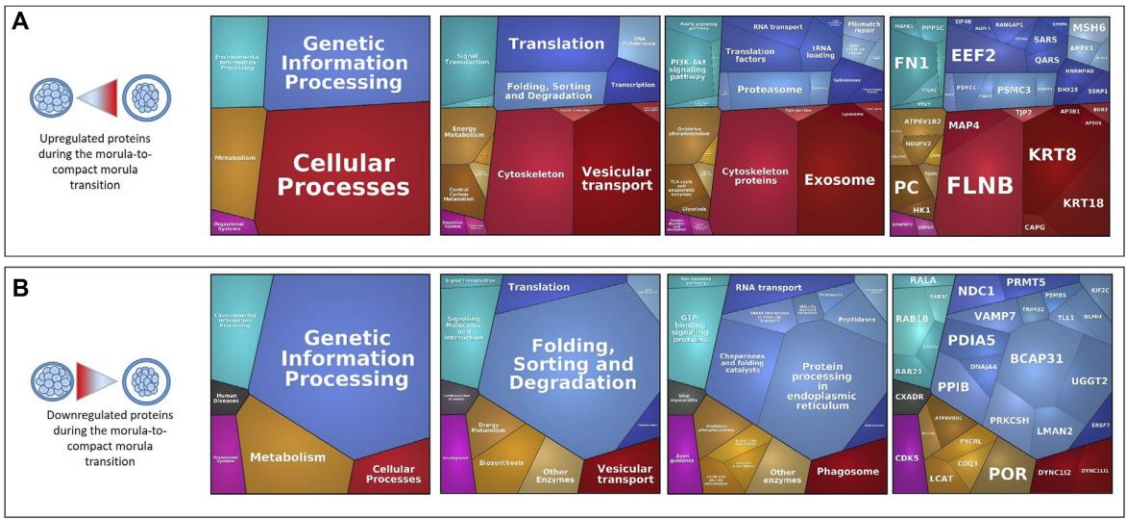

FIGURE 8 | Proteomaps of differentially abundant proteins (DAPs) during the morula-to-compact morula transition. Proteomaps were carried out using the lists of gene names of proteins increasing [**(A)**, upper panels] or decreasing [**(B)**, down panels] in abundance (t-test p-value ≤ 0.05; min fold-change of 2) between the morula and compact stages and based on the KEGG Pathway gene classification. Functional categories (left and middle panels) and related proteins (right panel) are shown by polygons. Areas of polygons illustrate protein abundance, weighted by protein size. Functionally related functions/proteins are arranged in common regions and coded using similar colors.

downregulated proteins were largely involved in protein folding, sorting and degradation (**Figure 8**). The STRING analysis did not identify enriched pathways but several enriched molecular functions (MF) and biological process (BP) terms including developmental process and multicellular organism development (see all enriched terms and the PPI network during morula compaction in **Supplementary Table S6**).

2.3.3 From Compact Morula to Blastocyst Stages

Between the compact morula and blastocyst stages, upregulated proteins related to cellular processes were involved in the cytoskeleton, vesicular transport and cellular community pathways whereas downregulated proteins were more specifically involved in the apoptosis, exosome and phagosome pathways. Concerning genetic information processing pathways, upregulated proteins were involved in transcription, translation and DNA maintenance while downregulated proteins were mainly involved in protein folding, sorting and degradation. In addition, both up and downregulated proteins were involved in metabolic pathways such as amino acid metabolism and lipid and steroid metabolism, however upregulated proteins were more specifically involved in glycolysis and tricarboxylic acid (TCA) cycle (**Figure 9**). The STRING enrichment analysis of DAPs at the time of blastocyst formation confirmed highly significant enrichment in metabolic pathway, carbon metabolism, biosynthesis of amino acids (p-values $< 10^{-4}$) and TCA cycle ($p = 0.003$; see all enriched terms during blastocyst formation in **Supplementary Table S7**). Finally, numerous interactions between DAPs were identified including proteins implied in the above metabolic pathways (**Figure 10**; see network details in **Supplementary Table S7**).

3 DISCUSSION

Very few studies on embryonic proteomes have been reported, and the large majority of them used *in vitro* embryos (Jensen et al., 2014a; Jensen et al., 2014b; Deutsch et al., 2014; Demant et al., 2015; Gao et al., 2017), which may give a biased picture of embryo protein dynamics due to divergent gene expression (Lonergan et al., 2003; Gutierrez-Adan et al., 2004; Wrenzycki et al., 2005). The present study identified 2,757 proteins in bovine embryos developed *in vivo*, representing the most comprehensive embryo proteome identified in non-rodent mammals so far.

Interestingly, oviduct-specific glycoprotein (OVGP1), also known as oviductin, was detected among the most abundant proteins at all stages. Oviductin was identified in the proteomic profile of ovine blastocyst developed *in vivo* (Sanchez et al., 2021) and as a major embryo-interacting protein in the bovine oviduct fluid (Banliat et al., 2020). Oviductin has been reported to interact with embryos in various mammalian species (Aviles et al., 2010) and improves the quality of *in vitro* produced cattle embryos when added as a recombinant protein in culture medium (Algarra et al., 2018).

3.1 Proteomic Dynamics During Embryonic Genome Activation

The number of proteins identified per embryo slightly decreased from the 4–6 cell to morula (2,193 to 2,022) then increased from compact morula to blastocyst stages (2,314 to 2,516). Upregulated proteins (cluster 1) from the 4–6 cell to the blastocyst stages

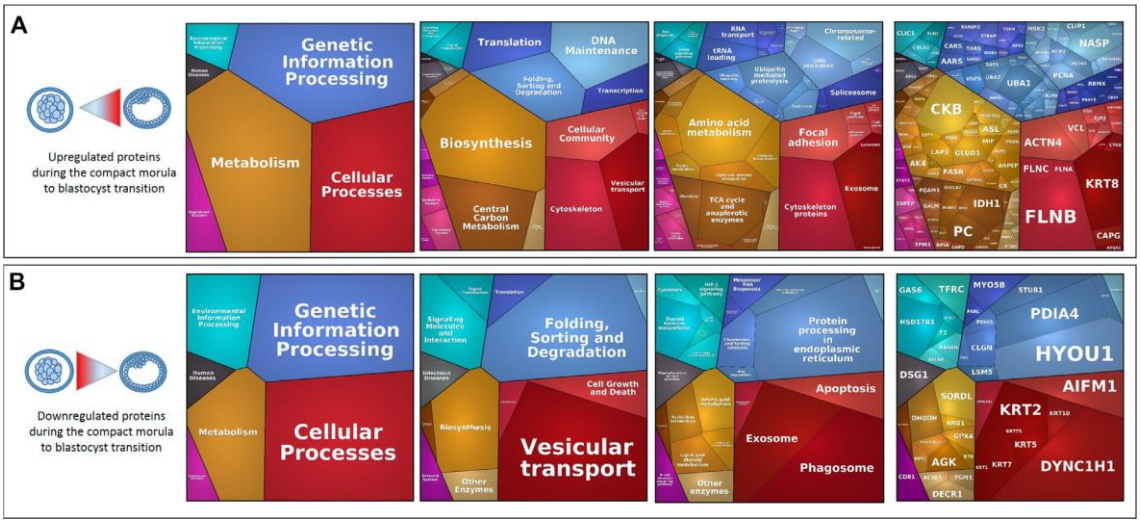

FIGURE 9 | Proteomaps of differentially abundant proteins (DAPs) during the compact morula-to-blastocyst transition. Proteomaps were carried out using the lists of gene names of proteins increasing [**(A)**, upper panels] or decreasing [**(B)**, down panels] in abundance (t-test p-value ≤ 0.05; min fold-change of 2) between the compact morula and blastocyst stages and based on the KEGG Pathway gene classification. Functional categories (left and middle panels) and related proteins (right panel) are shown by polygons. Areas of polygons illustrate protein abundance, weighted by protein size. Functionally related functions/proteins are arranged in common regions and coded using similar colors.

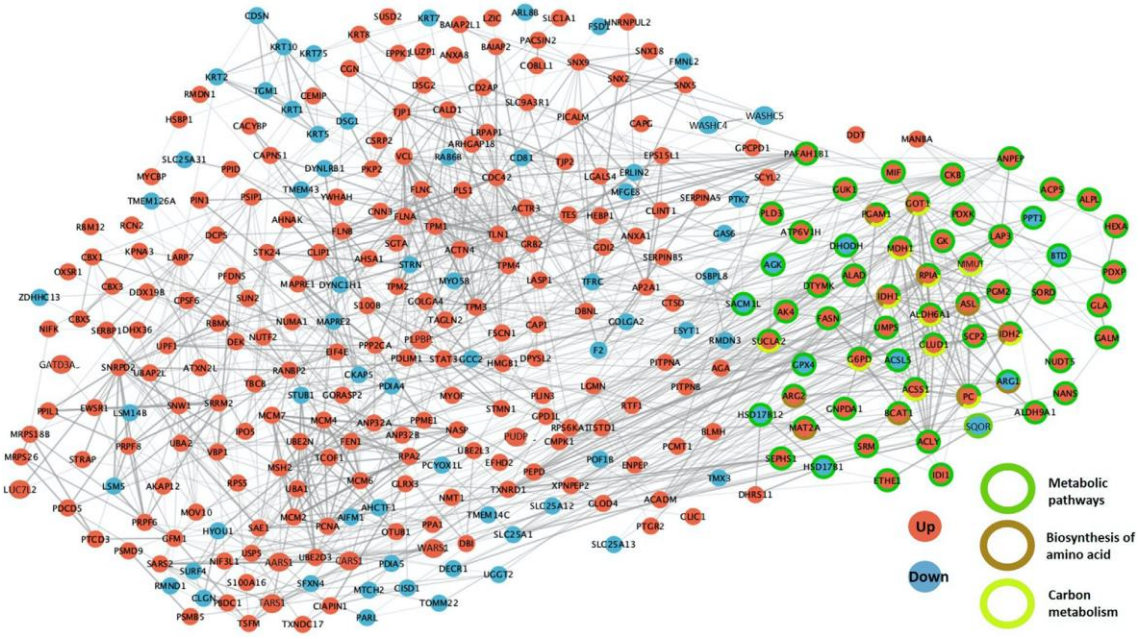

FIGURE 10 | Protein-protein interaction networks between differentially abundant proteins (DAPs) during the compact morula-to-blastocyst transition. The PPI network was built using STRING and Cytoscape. DAPs increased in abundance between the compact morula and blastocyst stages are in red while proteins decreased in abundance are in blue. The DAPs involved in the three most significant KEGG pathways are indicated by colored circles in green, brown and yellow.

evidenced a significant enrichment in RNA metabolism and protein translation, presumably to provide enough materials to support further development. This is globally in accordance with previous data on protein synthesis in bovine embryo that indicated a higher rate of protein degradation than that of synthesis in early stages, the net protein growth per embryo starting only after morula compaction (Thompson et al., 1998). In line with our data, upregulated proteins during *in vivo* development of mouse embryos tended to execute protein translation and RNA metabolism while downregulated proteins were mostly involved in protein transport, protein localization and cell cycle (Gao et al., 2017). This is also concordant with the timing of EGA during which maternal proteins, and to a lesser extent paternal proteins, are progressively replaced by embryonic gene products (Graf et al., 2014a).

The onset of EGA in cattle embryos was established according to transcriptomic data with some discrepancies between studies. Using *in vitro* embryos, the onset of major EGA was timed between the 8 and 16-cell stages (Memili and First, 1998; Graf et al., 2014b); however, transcriptomic analyses of *in vivo* embryos reported an EGA just before the 8-cell stage (Kues et al., 2008; Jiang et al., 2014). Our results provide for the first time a comprehensive picture of proteomic dynamics during the EGA. Major changes in the dynamics of protein synthesis were first evidenced after the 8–12 cell stage, which is consistent with a major EGA at the 8-cell stage. Due to the collection method, the donor cows of morulas differed from those of 8–12 cell embryos, which may account for changes in proteomic dynamics. Nevertheless, upregulated proteins during the 8–12-cell-to-morula transition evidenced a significant enrichment in functional pathways and protein-protein interaction networks related to transcription, RNA transport, RNA splicing and protein translation, which are assumed to underlie the EGA.

3.2 Proteomic Dynamics and Functional Candidates During Morula Compaction

To the best of our knowledge, this is the first proteomic study to separately analyze morulas and compact morulas in mammals, providing insights into the molecular mechanisms underlying the compaction process. Compaction marks the start of important cell differentiation events: the outer blastomeres of the morula adhere firmly to each other and give rise to the trophectoderm, while the inner blastomeres of the compact morula form the inner cell mass of the blastocyst (Van Soom et al., 1997; Watson and Barcroft, 2001). A total of 184 DAPs were identified at the time of morula compaction, of which 116 DAPs with a minimal fold-change ratio of 2. In contrast to the 8-cell-to-morula transition, during which genetic information processing pathways were predominant, the Proteomaps of DAPs during morula compaction showed that upregulated proteins were largely involved in cellular processes, in line with important cell differentiation events during this process.

The cellular process-related proteins fibronectin 1 (FN1), filamin B (FLNB), keratins 8 (KRT8) and 18 (KRT18) were particularly increased during compaction (fold-changes of 4.6, 2.4, 3.8 and 7.9, respectively). Fibronectin 1 is a large glycoprotein of the extracellular matrix that binds cell surfaces and is involved in a variety of biological processes including cell adhesion, cell migration and the maintenance of cell shape (Humphries et al., 1989). Previous transcriptomic data on bovine *in vivo* embryos reported a marked increase in FN1 transcripts between the 8-cell and blastocyst stages (Goossens et al., 2007; Goossens et al., 2009) and immunolabelling for FN1 on *in vitro* produced embryos was first observed in late morulas (Goossens et al., 2007), in accordance with our results. The assembly of FN1 with integrin partners on neighboring cells were shown to play important roles in tissue differentiation during mouse and chicken embryo development (de Almeida et al., 2016). In cattle embryos, several potential integrin partners were reported to have similar or overlapping RNA expression patterns as compared to FN1 (Goossens et al., 2009); however, the exact candidate receptors of FN1 in morulas remain to be identified.

The filamin family of cytoplasmic actin-binding proteins exert crucial signaling functions in cell cytoskeleton dynamics and tissue morphogenesis during embryo development (Baldassarre et al., 2009; Baudier et al., 2018). In mice with a targeted disruption of the *Flnb* gene, less than 3% of homozygous embryos reached term, and the migration of primary fibroblasts was reduced, indicating a pivotal role of filamin B in embryonic development (Zhou et al., 2007). In various human cell lines, filamin B was also identified as a key regulator of cell migration (Baldassarre et al., 2009; Del Valle-Perez et al., 2010). The exact roles of fibronectin 1 and filamin B in cattle early embryo development remain to be determined but their abundance pattern together with previous published data strengthen the idea that those proteins are involved in the compaction of morula leading to cell lineage differentiation.

Other interesting candidates are keratin 8 and 18. Keratin proteins constitute the intermediate filaments of epithelial cells and were expressed by preimplantation embryos in several species (Oshima et al., 1983; Sun et al., 2010). In our analysis, we excluded human keratin contaminants by comparing the sequences of the MS peptides identified with their homologous in *Homo sapien*s. Upregulation of KRT8 and 18 during compaction were in line with previous transcriptomic data on bovine embryos, in which gene expression of *KRT8* and *KRT18* was greatly increased between morula and blastocyst stages (Goossens et al., 2007; Wei et al., 2017). Using single cell gene expression analysis, *KRT8* was reported to display a bimodal distribution among cells in bovine morulas, suggesting that KRT8 is an early marker of trophectoderm cells during early lineage specification (Wei et al., 2017). In addition, the protein expression of KRT18 has been reported to start at the morula stage and to be specific to the trophectoderm in bovine embryos produced *in vitro* (Goossens et al., 2007). Suppression of *KRT18* gene expression in bovine zygotes led to an associated reduction in *KRT8* expression and a 41-% reduction in blastocyst formation (Goossens et al., 2010). Our results, together with those of previous studies, suggest important roles for KRT8 and KRT18 in preimplantation bovine embryos.

Another upregulated protein during morula compaction and blastocyst formation (with fold-changes of 2.1 and 1.8, respectively) was elongation factor 2 (EEF2). EEF2 catalyzes

the GTP-dependent ribosomal translocation step during translation elongation and is an essential factor for protein synthesis. *EEF2* was previously identified in a transcriptomic study in bovine *in vivo* blastocysts as a hub gene, i.e. central and highly connected with other stage-specific regulated genes, and as such was proposed as a master regulator of gene expression during pre-implantation development (Jiang et al., 2014).

3.3 Proteomic Dynamics and Functional Candidates During Blastocyst Formation

Another major change in protein dynamics was evidenced at the compact morula-to-blastocyst transition, which demonstrated the highest number of DAPs: among these, 359 had fold-change ratios greater than 2. Donors of blastocysts partly differed from those of compact morulas and included both Holstein cows and heifers. Furthermore, three bulls of different breeds (one Normande and two Holsteins) were used for blastocysts while only the Normande bull was the progenitor of all other embryos, which may account for the specificities of blastocysts in the present study. It has been shown that the father has an impact on gene expression and epigenomics in bovine blastocysts (Kropp et al., 2017; Diaz-Lundahl et al., 2021). However, the fertility of the bulls used, as previously assessed on a large population of heifers and cows, was high and homogeneous (59–62% and 45–49% of non-return rates at 90 days after insemination, respectively). Furthermore, the different pools of blastocysts had very similar proteomic profiles, pointing out a major effect of the developmental stage rather than the genetic origin of progenitors or female parity on the embryo proteome. In a previous proteomic study comparing six stages of *in vivo* mice embryos derived from a much higher number of progenitors (8000 embryos per stage), the most significant changes in protein abundance were similarly observed between morulas and blastocysts (Gao et al., 2017). These data highlight the specificity of the protein expression profiles in blastocysts compared to earlier developmental stages.

Considering a minimal fold-change ratio of two, 274 proteins were found at significantly higher abundance in blastocysts compared to compact morulas, which represented 76% of the total number of DAPs. Similarly, 102 proteins out of 140 DAPs (73%) were found to be increased in abundance between cattle *in vitro* morulas and blastocysts (Demant et al., 2015). This high proportion of upregulated proteins is in line with the overrepresented translation-related pathways observed in earlier stages and the increasing need for materials during embryo development.

The most abundant upregulated proteins included annexins A2 and A6 (ANXA2, ANXA6), AHNAK nucleoprotein (AHNAK), creatine kinase B (CKB), alpha-actin-1 and 4 (ACTN1, ACTN4), LIM and SH3 domain protein 1 (LASP1), and fibronectin 1 (FN1), whereas hypoxia up-regulated protein 1 (HYOU1), lactadherin (MFGE8), and protein disulfide-isomerase A4 and A5 (PDIA4, PDIA5) were at lower abundance in blastocysts compared to compact morulas. Our results are partially consistent with a previous proteomic study that compared cattle *in vitro* morulas and blastocysts, in which ANXA2, ANXA6, CKB, ACTN1 and LASP1 were upregulated while HYOU1, PDIA4 and PDIA5, among others, were downregulated (Demant et al., 2015). In addition, some upregulated proteins (cluster 1) like the transketolase (TKT), myosin light polypeptide 6 (MYL6), 60S ribosomal protein L13 (RPL13) and D-dopachrome decarboxylase (DDT) increased also in abundance in a study by Demant et al. (2015). However, some discrepancies between both studies were also found. For instance, phosphoglycerate mutase (BPGM), L-lactate dehydrogenase A (LDHA), glutathione S-transferase mu 3 (GSTM3), ubiquitin carboxyl-terminal hydrolase isozyme L1 (UCHL1) and peroxiredoxin-1 (PRDX1) were stable in abundance during embryo development in the present study, but were identified among the top-25 downregulated proteins during blastocyst formation in the study by Demant et al. (2015). The *in vitro* or *in vivo* origin of embryos and the methods of analysis (iTRAQ *vs*. label-free MS approaches) may account for those discrepancies.

DAPs during blastocyst formation may be considered as early markers of cell lineage differentiation and important functional candidates for the regulation of key developmental processes. Keratin 8 and filamin B were both upregulated (fold change >2) during morula compaction and in blastocysts, in which they were among the most abundant DAPs. Another interesting candidate protein is AHNAK, with fold-changes of 6.5 and 5.8 during morula-to-compact morula and compact morula-to-blastocyst transitions, respectively. AHNAKs are a class of unusually large proteins (600–700 kDa) that associate with calcium channel proteins and have various subcellular localization depending on the cell type and cell cycle progression (Komuro et al., 2004). During mouse development, AHNAK protein expression was found in derivatives of trophectoderm and in several major sites of placentation and neurulation, suggesting multiple developmental roles (Downs et al., 2002). However, functional studies on AHNAK during earlier stages of embryo development are currently lacking.

Annexins 1, 2, 6 and 8 are other potential stage-specific markers of embryonic cell differentiation: ANXA2 and ANXA6 were detected at increased abundance during morula compaction (with fold-changes of 2.0 and 2.1, respectively), while ANXA1, ANXA6, and ANXA8 were increased during blastocyst formation (with fold-changes of 3.4, 1.8 and 5.3, respectively). Annexins are a family of calcium- and phospholipid-binding proteins bearing multiple functions and that could play important roles during the process of blastocyst differentiation. Annexins 1 and 2 have been previously reported in the blastocyst cells and blastocoel fluid of *in vitro* produced bovine embryos (Jensen et al., 2014b). Annexin 1 is involved in cell adhesion and promotes the rearrangement of the actin cytoskeleton, cell polarization and cell migration in immune cells (Moraes et al., 2017). ANXA1 has been linked to pregnancy in mice: *AnxA1*-deficient females presented increased numbers of blastocysts, implantation sites and pups delivered (Hebeda et al., 2018). In humans and mice, ANXA2 is transiently expressed at the embryo-uterine luminal interface and has been implicated as an important adhesion molecule in the process of embryo implantation (Garrido-Gomez et al., 2012; Wang and Shao,

TABLE 1 | Pools of *in vivo* produced bovine embryos used for nanoLC-MS/MS analysis (*n* = 4 embryos per pool).

Embryonic stage	Interval of embryo collection after first insemination	Female donor[a]	Bull semen[b]	Number of pools
4–6 cells	Days 1.7–3.8	A, B, C, D	X	3
8–12 cells	Days 3.6–3.8	A, B	X	4
Morula (>16 cells)	Days 5.7–6.7	E, F, G	X	3
Compact morula	Days 5.7–6.8	E, F, H	X	4
Blastocyst	Days 6.8–7.5	H, I, J, K	X, Y, Z	4

[a]*A total of 9 Holstein cows (called A to I) and 2 Holstein heifers (called J and K) were used as female donors.*
[b]*A total of 3 bulls of proven fertility, one Normand (called X) and two Holstein (called Y and Z), were used for the insemination of female donors.*

2020). The development of cattle embryos differs from that of humans and mice in that their trophectoderm elongates in the uterine lumen before they finally attach to the endometrium, and such roles of annexin A2 in embryo attachment lacks evidence so far in this species.

3.4 Metabolic Pathways Activated During Early Embryo Development

The GO analysis of DAPs at the time of blastocyst formation evidenced a significant enrichment in metabolic pathways, carbon metabolism, biosynthesis of amino acids and the TCA cycle. The well-orchestrated activation of metabolic pathways is required during early embryo development. During the first cleavage divisions, mammalian embryos, including bovine, use mostly pyruvate and amino acids as preferred substrates, which are metabolized through the TCA cycle and oxidative phosphorylation to produce energy (Khurana and Niemann, 2000; Li and Winuthayanon, 2017). At the time of compaction, the demand for energy and biomass increases and glucose is metabolized with greater efficiency through the pentose phosphate pathway (PPP), important for the biosynthesis of nucleotides, and the glycolysis pathway in addition to the TCA cycle (Milazzotto et al., 2020). Furthermore, substrates generated by metabolism seem to be important players in epigenetic modifications in preimplantation embryos (Ispada et al., 2020; Milazzotto et al., 2020).

Based on biochemical studies in cattle embryos developed *in vivo*, there is evidence that compaction and blastocyst formation are accompanied by marked increases in the consumption of glucose (Khurana and Niemann, 2000). This is globally in line with the proteomic dynamics observed in our results. Several enzymes implied in the production of energy and biomass from glucose were upregulated and identified in the first cluster of DAPs across development. This was the case for glucose-6-phosphate 1-dehydrogenase (G6PD), which catalyzes the first rate-limiting step of the PPP, 6-phosphogluconate dehydrogenase (PGD), ribose-5-phosphate isomerase (RPIA), transketolase (TKT) and transaldolase (TALDO1) in the PPP. This was also the case for hexokinase (HK2), implied in the first step of glycolysis, phosphoglycerate kinase 1 (PGK1) and phosphoglycerate mutase 1 (PGAM1) in the glycolysis pathway. In particular, the protein abundance of HK1 and HK2 significantly increased during morula compaction with fold-changes of 10.4 and 1.6, respectively, while after compaction during blastocyst formation, G6PD, TALDO1, PGAM1 and PGK1 increased with fold-changes of 5.0, 1.9, 2.8, and 1.8, respectively. However, some other glycolytic enzymes like fructose-bisphosphate aldolase (ALDOC) and glyceraldehyde-3-phosphate dehydrogenase (GAPDH) decreased in abundance, although with lower fold-changes (1.7 and 1.4, respectively), during blastocyst formation. These data confirm a global switch in the energy requirements of the embryo toward more glucose after the major EGA and constitute an important step forward for the comprehension of embryo metabolism and regulation during *in vivo* mammalian development.

3.5 Limitations of the Study

One limitation of the present study is that the embryos were collected after estrus synchronization and superovulation treatment. This was done for evident ethical, technical and economic reasons. Superovulation represents the primary tool for the production of cattle embryos and has been commercially practiced for embryo transfer on a wide scale for more than 40 years (Seidel, 1981). However, circulating concentrations of reproductive hormones such as progesterone can be modified in superovulated cows and heifers (Lamond and Gaddy, 1972), and an effect of this particular endocrine environment on the embryo proteome cannot be excluded. As discussed earlier, another weakness compared to studies in mice is the relative low number of animals and higher heterogeneity between progenitors.

Another limitation is that, due to the required materials for MS analysis, the use of extra *in vivo* embryos to explore changes in candidate proteins by complementary methods was not possible. Due to the divergence in gene expression reported between bovine embryos developed *in vivo* or *in vitro* (Lonergan et al., 2003; Gutierrez-Adan et al., 2004; Wrenzycki et al., 2005), the use of *in vitro* embryos for protein validation was not judged to be suitable.

4 CONCLUSION

This is the first comprehensive evaluation of proteome dynamics during early bovine development *in vivo*. Our results indicate significant changes in protein dynamics at the time of EGA and during first cell lineage differentiation during morula compaction

and blastocyst formation. Here, we provide a large database of new protein markers of these processes and valuable candidates that make possible further functional studies on embryo development. These data may also be used to evaluate the impact of various *in vitro* conditions on the embryo proteomics and improve the safety and yield of embryo culture media.

5 MATERIALS AND METHODS

5.1 Collection and Preparation of *In Vivo* Embryos From Synchronized Donors

All experimental protocols were conducted following the European directive 2010/63/EU on the protection of animals used for scientific purposes and approved by the French Ministry of National Education, Higher Education, Research and Innovation after ethical assessment by the local ethics committee "Comité d'Ethique en Experimentation Animale Val de Loire (CEEA VdL)" (protocol registered under the number CE19-2021-0402-1).

A total of 11 Holstein females (9 dried off cows and 2 heifers, aged 1–5 years) housed at the INRAE Experimental Unit of Animal Physiology of the Orfrasière (Nouzilly, France) were used as donor animals. The estrus cycles of the donors were synchronized with the prostaglandin analog cloprostenol (0.5 mg, i.m.; Estrumate, MSD Animal Health, Beaucouzé, France) and all females showing normal estrus, following an ovarian corpus luteum 1 week later (as checked by ultrasonography), received a progesterone releasing intravaginal device (PRID DELTA, Ceva Santé animale, Libourne, France). Ovarian stimulation treatment started 12 days after estrus and consisted of eigth intramuscular injections of decreasing pFSH/pLH doses every 12 h over 4 days (Stimufol, Reprobiol, Liège, Belgique; 500 µg pFSH and 100 µg LH in total in cows; 350 µg pFSH and 70 µg pLH in total in heifers). Luteolysis was induced with 2 ml cloprostenol (0.5 mg, i.m; Estrumate, MSD Animal Health, Beaucouzé, France) and the PRID DELTA device was withdrawn together with the fourth and sixth FSH administrations, respectively.

For embryo collection, donor females were inseminated with frozen-thawed semen from one bull of proven fertility 12 and 24 h after standing estrus. The same ejaculate from one Normande bull (bull X) was used for most embryos while two extra Holstein bulls (Y and Z) were used for blastocysts (**Table 1**). The fertility of the bulls was previously estimated by the 90-day non-return rate after artificial insemination on a large population of dairy females and ranged from 59 to 62% in heifers (3,241–8,587 AI per bull) and from 45 to 49% in lactating cows (22,864–26,623 AI per bull). Early stages (from 4–6 cell to compact morula) and 6 blastocysts were recovered after the slaughter of donor cows between days 1.7 and 7.5 after the first AI (AI1) in a local experimental slaughterhouse. The genital tracts were immediately processed on site. Oviducts and uterine horns were flushed with 5 and 35 ml, respectively, of prewarmed PBS+0.1% polyvinyl alcohol (PVA) at 38.5°C. Additional blastocysts were collected by non-invasive cervical flushing of the uterine horns of heifers on day 7 after AI1, as previously described (Janati Idrissi et al., 2021). Recovered fluids were carefully observed for the presence of embryos under a stereomicroscope and all embryos were classified for quality grade and stage of development according to the International Embryo Technology Society recommendations (Wright, 1998). Representative pictures of embryos are shown in **Supplementary Figure S1**.

All embryos were thoroughly washed three times in 20 mM Tris-HCl buffer (pH 6.8) supplemented with 8.9% sucrose (Tris-sucrose), minimizing contamination from oviduct ad uterine fluids, then individually frozen at −80°C. Typically, the time period between animal death and genital tract flushing and between flushing and embryo freezing was less than 15 and 30 min, respectively. For proteomic analyses, only grade-1 embryos, i.e., embryos consistent with their expected stage of development, with blastomeres uniform in size, color and density, few irregularities or excluded cells and an intact and smooth zona pellucida were used. All embryos (with no sex determination) were thawed on ice and pools of 4 embryos at the same stage were prepared under a stereomicrosope (**Table 1**). Tubes containing embryos were manipulated for no more than 10 min at ambient temperature. After brief pelleting, the Tris-sucrose in excess was eliminated and tubes were stored at—80°C until proteomic analysis.

5.2 Nanoliquid Chromatography Coupled With Tandem Mass Spectrometry (nanoLC-MS/MS) Analysis

Proteins from pools of embryos were extracted and digested using the PreOmics iST-BCT kit following the manufacturer's instructions. Briefly, samples were thawed and lysed (denatured, reduced and alkylated) for 10 min at 95°C then Trypsin/LysC digested for 60 min at 37°C. Purification of peptides was then carried out at room temperature on spin cartridge and peptides were finally eluted in 10 µL of LC-load buffer. The volume corresponding to one equivalent-embryo (corresponding to approximately 300 ng proteins) was then loaded on a 75 µm × 250 mm IonOpticks Aurora 2 C18 column (Ion Opticks Pty Ltd., Bundoora, Australia). Peptide analysis was performed as previously described (Banliat et al., 2020). A gradient of basic reversed-phase buffers (Buffer A: 0.1% formic acid, 98% H_2O MilliQ, 2% acetonitrile; Buffer B: 0.1% formic acid, 100% acetonitrile) was run on a NanoElute HPLC System (Bruker Daltonik GmbH, Bremen, Germany) at a flow rate of 400 nL/min at 50°C. The liquid chromatography (LC) run lasted for 120 min (2–15% of buffer B during 60 min; up to 25% at 90 min; up to 37% at 100 min; up to 95% at 110 min and finally 95% for 10 min to wash the column). The column was coupled online to a TIMS TOF Pro (Bruker Daltonik GmbH, Bremen, Germany) with a CaptiveSpray ion source (Bruker Daltonik). The temperature of the ion transfer capillary was set at 180°C. Ions were accumulated for 114 ms, and mobility separation was achieved by ramping the entrance potential from −160 V to −20 V within 114 ms. The acquisition of the MS and MS/MS mass spectra was done with average resolutions of 60,000 and 50,000 full width at half maximum (mass range 100–1700 m/z), respectively. To enable the PASEF method, precursor m/z and mobility information was first derived from full scan TIMS-MS experiments (with a mass range of m/z 100–1700). The quadrupole isolation width was set to 2 and 3 Th and,

for fragmentation, the collision energies varied between 31 and 52 eV depending on the precursor mass and charge. TIMS, MS operation and PASEF were controlled and synchronized using the control instrument software OtofControl 5.1 (Bruker Daltonik). LC-MS/MS data were acquired using the PASEF method with a total cycle time of 1.31 s, including 1 TIMS MS scan and 10 PASEF MS/MA scans. The 10 PASEF scans (100 ms each) containing, on average, 12 MS/MS scans per PASEF scan. Ion mobility-resolved mass spectra, nested ion mobility vs. m/z distributions, as well as summed fragment ion intensities were extracted from the raw data file with DataAnalysis 5.1 (Bruker Daltonik GmbH, Bremen, Germany).

5.3 Protein Identification and Data Validation

Peptides were identified using the MASCOT software (version 2.5.1; Matrix Science, 454 London, United Kingdom) against the UniProt *Bos taurus* database (May 2019; 23523 sequences) using its automatic decoy database search to calculate a false discovery rate (FDR). The parameters used for database searches included trypsin as enzyme (one missed cleavage allowed), carbamidomethylcysteine as fixed modification, oxidation of methionine and N-terminal protein acetylation as variable modifications. Monoisotopic mass was considered and mass tolerance was set at 15 ppm for MS ions and 0,05 Da for MS/MS ions. Mascot results from the target and decoy databases were incorporated to Scaffold Q+ software (version 5.0.1, Proteome Software, Portland, United States, www.proteomesoftware.com) for data validation. Threshold for peptide and protein identification were set to 95.0% as specified by the Peptide Prophet algorithm (Keller et al., 2002) and the Protein Prophet algorithm (Nesvizhskii et al., 2003). To exclude potential human contaminants from the pool of keratin proteins (KRT 1, 2, 5, 6A, 7, 8, 10, 14, 18, 19, 24, 28, and 75), the peptides identified in the *Bos taurus* database were blasted against the *Homo sapiens* homologous sequences. For all keratins except KRT14, the peptide sequences were specific to *Bos taurus*, meaning that except for KRT14, we were able to exclude human contaminants.

5.3 Label-Free Protein Quantification and Statistical Analysis

All proteins containing at least two unique peptides (FDR <0.01%) were considered for protein quantification. Protein quantification was based on a label-free approach using the spectral counting method, as previously described (Liu et al., 2004; Old et al., 2005). Scaffold Q+ software (Proteome Software, version 5.0.1) was used using the Spectral Count quantitative module. The normalization of spectra among samples was realized in Scaffold by adjusting the sum of the selected quantitative values for all proteins within each MS sample to a common value, which was the average of the sums of all MS samples present in the experiment. This was achieved by applying a scaling factor for each sample to each protein or protein group. Thus, numbers of normalized weighted spectra (NWS) were tabulated using experiment-wide protein clusters.

Statistical analysis was performed on proteins quantified with minimum 2 NWS on average in at least one stage. To obtain an overview of proteomic data, principal component analysis (PCA) of all samples was carried out using RStudio software (version 1.4.1106) and the FactoMineR and ggplot2 packages. Analysis of variance (ANOVA) on biological replicates was done using RStudio. The hierarchical clustering of differentially abundant proteins (DAPs; ANOVA's p-value ≤ 0.05) were done using Spearman correlations and the gplots package of RStudio. Finally, pairwise comparisons in protein abundance were evaluated by Student's t-tests using R. Proteins were considered as differentially abundant with a t-test p-value ≤ 0.05. A fold-change ratio ≥2 was retained for the functional analysis.

5.4 Functional Analysis of Differentially Abundant Proteins

The overlap of identified proteins between stages was visualized using the jvenn online tool (http://jvenn.toulouse.inra.fr) (Bardou et al., 2014). The functional analysis of DAPs in the two main clusters (ANOVA p-value ≤ 0.05) was performed using the Metascape online tool (metascape.org) (Zhou et al., 2019). The *Bos taurus* taxonomy is not available in Metascape therefore orthologs between *Bos taurus* and *Homo sapiens* were first searched using the HCOP orthology prediction tool (www.genenames.org/tools/hcop/). Human orthologs were found for all *Bos taurus* genes. The resulting gene lists without redundancy were used in the Metascape enrichment analysis using the *Homo sapiens* genome as background and the following ontology sources: KEGG (Kyoto Encyclopedia of Genes and Genomes) Functional Sets, KEGG Pathway, GO Biological Processes and Reactome Gene Sets. The cellular component enrichment analysis was carried out with the GO Cellular components source. Terms with a p-value < 0.01, a minimum count of 3, and an enrichment factor >1.5 (the enrichment factor is the ratio between the observed counts and the counts expected by chance) were collected and grouped into clusters based on their membership similarities. In histograms presenting the enriched terms, the most statistically significant term within a cluster is chosen by Metascape to represent the cluster.

The functions of DAPs in pairwise comparisons between stages (t-test p-value ≤ 0.05) considering a fold-change ratio ≥2 were further analyzed using the Proteomaps (proteomaps.net) and STRING (string-db.org, version 11.5) online tools (Liebermeister et al., 2014; Szklarczyk et al., 2015). Proteomaps graphics were generated from the gene lists of DAPs and related NWS values and using the *Homo sapiens* database as background, which is better annotated that those of *Bos Taurus* in Proteomaps. Proteomaps are built automatically from proteome quantitative data and based on the KEGG pathways gene classification. To create a Proteomap, the total area is first divided into polygons representing the top-level functional categories. These polygons are constructed from a Voronoi diagram, where the polygons' areas were chosen to represent copy numbers weighted by protein chain lengths (the investment in terms of amino acids, also termed the mass fraction). The top-level

areas are then subdivided into subcategories and the procedure is repeated down to the level of individual proteins. In the Proteomaps, functionally related proteins are arranged in common regions with similar colors. In addition, an enrichment analysis and protein-protein interaction (PPI) network were generated from each gene list of DAPs using STRING and the *Bos taurus* as organism background (which is well annotated in STRING). The settings for PPI networks were the full STRING network (in which the edges indicate both functional and physical protein interaction) as network type; a minimum required interaction score of 0.4; and the experiments, databases, co-expression, neighborhood, gene fusion and co-occurrence as interaction sources. The disconnected nodes in the network were discarded and only PPI networks with an enrichment p-value < 0.01, indicating that the proteins were at least partially biologically connected as a group, were retained. Finally, the STRING networks of DAPs together with their regulation pattern (up or downregulated) were imported into Cytoscape (version 3.9.0) in order to build interactions networks integrating those data (Shannon et al., 2003). The three most enriched KEGG pathways (with lowest FDR) identified by STRING were finally added in the networks.

DATA AVAILABILITY STATEMENT

The datasets presented in this study can be found in online repositories. The names of the repository/repositories and accession number(s) can be found below: The datasets PXD030994 and 10.6019/PXD030994 for this study can be found in the ProteomeXchange Consortium *via* the PRIDE (Perez-Riverol et al., 2022) partner repository (www.ebi.ac.uk/pride/archive/login).

ETHICS STATEMENT

The animal study was reviewed and approved by Comité d'Ethique en Experimentation Animale Val de Loire.

AUTHOR CONTRIBUTIONS

MS-D and PM designed the research. CB and MS-D collected the materials. CM, CB, EC, RL, and VL analyzed the data. MS-D and CM wrote the original draft. MS-D, BG, and CP acquired and administrated the funding. All authors read and approved the manuscript.

FUNDING

This research was funded by Union Evolution and INRAE. CB was funded by ANRT, grant number 2017/0684. This work was also supported by grants from Biogenouest, Infrastructures en Biologie Santé et Agronomie (IBiSA) and Conseil Régional de Bretagne awarded to CP.

ACKNOWLEDGMENTS

The authors acknowledge Union Evolution and Allice, France, for providing frozen semen samples required for this study. The authors are grateful to Eric Briant, Damien Capo, Jean-Philippe Dubois, Sylvan Bourgeois and Tiphaine Aguirre-Lavin (UEPAO) for the management and sacrifice of embryo donors.

SUPPLEMENTARY MATERIAL

The Supplementary Material for this article can be found online at: https://www.frontiersin.org/articles/10.3389/fcell.2022.863700/full#supplementary-material

Supplementary Figure S1 | Representative pictures of the bovine embryos collected at the 4–6 cell, 8–12 cell, morula, compact morula and blastcyst stages.

Supplementary Table S1 | Lists of proteins identified and quantified with at least two normalized weighed spectra (NWS) in pools of cattle embryos developed *in vivo*.

Supplementary Table S2 | Classification of differentially abundant proteins (DAPs) according to the hierarchical clustering (ANOVA p-value ≤ 0.05) and Metascape enrichment analysis of upregulated (cluster 1) and downregulated (cluster 2) proteins during development.

Supplementary Table S3 | Lists of differentially abundant proteins (DAPs) in each pairwise comparisons between stages (t-test p-value ≤ 0.05). The DAPs with fold-change ratios ≤0.5 or ≥2 are highlighted.

Supplementary Table S4 | Functional enrichment analysis of DAPs between the 4–6 cell and 8–12 cell stages. The analysis was performed using STRING.

Supplementary Table S5 | Functional enrichment analysis of DAPs between the 8–12 cell and morula stages. The analysis was performed using STRING.

Supplementary Table S6 | Functional enrichment analysis of DAPs between morula and compact morula stages. The analysis was performed using STRING.

Supplementary Table S7 | Functional enrichment analysis of DAPs between compact morula and blastocyst stages. The analysis was performed using STRING.

REFERENCES

Algarra, B., Maillo, V., Avilés, M., Gutiérrez-adán, A., Rizos, D., and Jiménez-movilla, M. (2018). Effects of Recombinant OVGP1 Protein on *In Vitro* Bovine Embryo Development. *J. Reprod. Development* 64 (5), 433–443. doi:10.1262/jrd.2018-058

Avilés, M., Gutiérrez-Adán, A., and Coy, P. (2010). Oviductal Secretions: Will They Be Key Factors for the Future ARTs? *Mol. Hum. Reprod.* 16 (12), 896–906. doi:10.1093/molehr/gaq056

Baldassarre, M., Razinia, Z., Burande, C. F., Lamsoul, I., Lutz, P. G., and Calderwood, D. A. (2009). Filamins Regulate Cell Spreading and Initiation of Cell Migration. *PLoS One* 4 (11), e7830. doi:10.1371/journal.pone.0007830

Banliat, C., Tsikis, G., Labas, V., Teixeira-Gomes, A.-P., Com, E., Lavigne, R., et al. (2020). Identification of 56 Proteins Involved in Embryo-Maternal Interactions in the Bovine Oviduct. *Ijms* 21 (2), 466. doi:10.3390/ijms21020466

Bardou, P., Mariette, J., Escudié, F., Djemiel, C., and Klopp, C. (2014). Jvenn: an Interactive Venn Diagram Viewer. *BMC Bioinformatics* 15, 293. doi:10.1186/1471-2105-15-293

Baudier, J., Jenkins, Z. A., and Robertson, S. P. (2018). The Filamin-B-Refilin axis - Spatiotemporal Regulators of the Actin-Cytoskeleton in Development and Disease. *J. Cel Sci* 131 (8). doi:10.1242/jcs.213959

Braude, P., Bolton, V., and Moore, S. (1988). Human Gene Expression First Occurs between the Four- and Eight-Cell Stages of Preimplantation Development. *Nature* 332 (6163), 459–461. doi:10.1038/332459a0

de Almeida, P. G., Pinheiro, G. G., Nunes, A. M., Gonçalves, A. B., and Thorsteinsdóttir, S. (2016). Fibronectin Assembly during Early Embryo Development: A Versatile Communication System between Cells and Tissues. *Dev. Dyn.* 245 (4), 520–535. doi:10.1002/dvdy.24391

del Valle-Pérez, B., Martínez, V. G., Lacasa-Salavert, C., Figueras, A., Shapiro, S. S., Takafuta, T., et al. (2010). Filamin B Plays a Key Role in Vascular Endothelial Growth Factor-Induced Endothelial Cell Motility through its Interaction with Rac-1 and Vav-2. *J. Biol. Chem.* 285 (14), 10748–10760. doi:10.1074/jbc.m109.062984

Demant, M., Deutsch, D. R., Fröhlich, T., Wolf, E., and Arnold, G. J. (2015). Proteome Analysis of Early Lineage Specification in Bovine Embryos. *Proteomics* 15 (4), 688–701. doi:10.1002/pmic.201400251

Deutsch, D. R., Fröhlich, T., Otte, K. A., Beck, A., Habermann, F. A., Wolf, E., et al. (2014). Stage-specific Proteome Signatures in Early Bovine Embryo Development. *J. Proteome Res.* 13 (10), 4363–4376. doi:10.1021/pr500550t

Diaz-Lundahl, S., Sundaram, A. Y. M., Gillund, P., Gilfillan, G. D., Olsaker, I., and Krogenæs, A. (2021). Gene Expression in Embryos from Norwegian Red Bulls with High or Low Non Return Rate: An RNA-Seq Study of In Vivo-Produced Single Embryos. *Front. Genet.* 12, 780113. doi:10.3389/fgene.2021.780113

Downs, K. M., McHugh, J., Copp, A. J., and Shtivelman, E. (2002). Multiple Developmental Roles of Ahnak Are Suggested by Localization to Sites of Placentation and Neural Plate Fusion in the Mouse Conceptus. *Mech. Development* 119 (Suppl. 1), S31–S38. doi:10.1016/s0925-4773(03)00088-1

Enright, B. P., Lonergan, P., Dinnyes, A., Fair, T., Ward, F. A., Yang, X., et al. (2000). Culture of *In Vitro* Produced Bovine Zygotes *In Vitro* vs *In Vivo*: Implications for Early Embryo Development and Quality. *Theriogenology* 54 (5), 659–673. doi:10.1016/s0093-691x(00)00381-2

Gad, A., Hoelker, M., Besenfelder, U., Havlicek, V., Cinar, U., Rings, F., et al. (2012). Molecular Mechanisms and Pathways Involved in Bovine Embryonic Genome Activation and Their Regulation by Alternative *In Vivo* and *In Vitro* Culture Conditions. *Biol. Reprod.* 87 (4), 100. doi:10.1095/biolreprod.112.099697

Gao, Y., Liu, X., Tang, B., Li, C., Kou, Z., Li, L., et al. (2017). Protein Expression Landscape of Mouse Embryos during Pre-implantation Development. *Cel Rep.* 21 (13), 3957–3969. doi:10.1016/j.celrep.2017.11.111

Garrido-Gómez, T., Dominguez, F., Quiñonero, A., Estella, C., Vilella, F., Pellicer, A., et al. (2012). Annexin A2 Is Critical for Embryo Adhesiveness to the Human Endometrium by RhoA Activation through F-Actin Regulation. *FASEB J.* 26 (9), 3715–3727. doi:10.1096/fj.12-204008

Goossens, K., Tesfaye, D., Rings, F., Schellander, K., Hölker, M., Van Poucke, M., et al. (2010). Suppression of Keratin 18 Gene Expression in Bovine Blastocysts by RNA Interference. *Reprod. Fertil. Dev.* 22 (2), 395–404. doi:10.1071/rd09080

Goossens, K., Van Soom, A., Van Poucke, M., Vandaele, L., Vandesompele, J., Van Zeveren, A., et al. (2007). Identification and Expression Analysis of Genes Associated with Bovine Blastocyst Formation. *BMC Dev. Biol.* 7, 64. doi:10.1186/1471-213x-7-64

Goossens, K., Van Soom, A., Van Zeveren, A., Favoreel, H., and Peelman, L. J. (2009). Quantification of Fibronectin 1 (FN1) Splice Variants, Including Two Novel Ones, and Analysis of Integrins as Candidate FN1 Receptors in Bovine Preimplantation Embryos. *BMC Dev. Biol.* 9, 1. doi:10.1186/1471-213x-9-1

Graf, A., Krebs, S., Heininen-Brown, M., Zakhartchenko, V., Blum, H., and Wolf, E. (2014a). Genome Activation in Bovine Embryos: Review of the Literature and New Insights from RNA Sequencing Experiments. *Anim. Reprod. Sci.* 149 (1-2), 46–58. doi:10.1016/j.anireprosci.2014.05.016

Graf, A., Krebs, S., Zakhartchenko, V., Schwalb, B., Blum, H., and Wolf, E. (2014b). Fine Mapping of Genome Activation in Bovine Embryos by RNA Sequencing. *Proc. Natl. Acad. Sci. U.S.A.* 111 (11), 4139–4144. doi:10.1073/pnas.1321569111

Gutiérrez-Adán, A., Rizos, D., Fair, T., Moreira, P. N., Pintado, B., de la Fuente, J., et al. (2004). Effect of Speed of Development on mRNA Expression Pattern in Early Bovine Embryos Cultured *In Vivo* or *In Vitro*. *Mol. Reprod. Dev.* 68 (4), 441–448. doi:10.1002/mrd.20113

Hamilton, W. J., and Laing, J. A. (1946). Development of the Egg of the Cow up to the Stage of Blastocyst Formation. *J. Anat.* 80 (4), 194–195.

Hebeda, C. B., Machado, I. D., Reif-Silva, I., Moreli, J. B., Oliani, S. M., Nadkarni, S., et al. (2018). Endogenous Annexin A1 (AnxA1) Modulates Early-phase Gestation and Offspring Sex-ratio Skewing. *J. Cel Physiol* 233 (9), 6591–6603. doi:10.1002/jcp.26258

Humphries, M. J., Obara, M., Olden, K., and Yamada, K. M. (1989). Role of Fibronectin in Adhesion, Migration, and Metastasis. *Cancer Invest.* 7 (4), 373–393. doi:10.3109/07357908909039866

Ispada, J., da Fonseca Junior, A. M., de Lima, C. B., Dos Santos, E. C., Fontes, P. K., Nogueira, M. F. G., et al. (2020). Tricarboxylic Acid Cycle Metabolites as Mediators of DNA Methylation Reprogramming in Bovine Preimplantation Embryos. *Int. J. Mol. Sci.* 21 (18). doi:10.3390/ijms21186868

Janati Idrissi, S., Le Bourhis, D., Lefevre, A., Emond, P., Le Berre, L., Desnoës, O., et al. (2021). Lipid Profile of Bovine Grade-1 Blastocysts Produced Either *In Vivo* or *In Vitro* before and after Slow Freezing Process. *Sci. Rep.* 11 (1), 11618. doi:10.1038/s41598-021-90870-8

Jensen, P. L., Beck, H. C., Petersen, T. S., Stroebech, L., Schmidt, M., Rasmussen, L. M., et al. (2014a). Proteomic Analysis of the Early Bovine Yolk Sac Fluid and Cells from the Day 13 Ovoid and Elongated Preimplantation Embryos. *Theriogenology* 82 (5), 657–667. doi:10.1016/j.theriogenology.2014.04.028

Jensen, P. L., Grøndahl, M. L., Beck, H. C., Petersen, J., Stroebech, L., Christensen, S. T., et al. (2014b). Proteomic Analysis of Bovine Blastocoel Fluid and Blastocyst Cells. *Syst. Biol. Reprod. Med.* 60 (3), 127–135. doi:10.3109/19396368.2014.894152

Jiang, Z., Sun, J., Dong, H., Luo, O., Zheng, X., Obergfell, C., et al. (2014). Transcriptional Profiles of Bovine *In Vivo* Pre-implantation Development. *BMC Genomics* 15, 756. doi:10.1186/1471-2164-15-756

Keller, A., Nesvizhskii, A. I., Kolker, E., and Aebersold, R. (2002). Empirical Statistical Model to Estimate the Accuracy of Peptide Identifications Made by MS/MS and Database Search. *Anal. Chem.* 74 (20), 5383–5392. doi:10.1021/ac025747h

Khurana, N. K., and Niemann, H. (2000). Energy Metabolism in Preimplantation Bovine Embryos Derived *In Vitro* or *In Vivo*1. *Biol. Reprod.* 62 (4), 847–856. doi:10.1095/biolreprod62.4.847

Komuro, A., Masuda, Y., Kobayashi, K., Babbitt, R., Gunel, M., Flavell, R. A., et al. (2004). The AHNAKs Are a Class of Giant Propeller-like Proteins that Associate with Calcium Channel Proteins of Cardiomyocytes and Other Cells. *Proc. Natl. Acad. Sci.* 101 (12), 4053–4058. doi:10.1073/pnas.0308619101

Kropp, J., Carrillo, J. A., Namous, H., Daniels, A., Salih, S. M., Song, J., et al. (2017). Male Fertility Status Is Associated with DNA Methylation Signatures in Sperm and Transcriptomic Profiles of Bovine Preimplantation Embryos. *BMC Genomics* 18 (1), 280. doi:10.1186/s12864-017-3673-y

Kues, W. A., Sudheer, S., Herrmann, D., Carnwath, J. W., Havlicek, V., Besenfelder, U., et al. (2008). Genome-wide Expression Profiling Reveals Distinct Clusters of Transcriptional Regulation during Bovine Preimplantation Development *In Vivo*. *Proc. Natl. Acad. Sci. U.S.A.* 105 (50), 19768–19773. doi:10.1073/pnas.0805616105

Lamond, D. R., and Gaddy, R. G. (1972). Plasma Progesterone in Cows with Multiple Ovulations. *Reproduction* 29 (2), 307–311. doi:10.1530/jrf.0.0290307

Lee, M. T., Bonneau, A. R., and Giraldez, A. J. (2014). Zygotic Genome Activation during the Maternal-To-Zygotic Transition. *Annu. Rev. Cel Dev. Biol.* 30, 581–613. doi:10.1146/annurev-cellbio-100913-013027

Li, S., and Winuthayanon, W. (2017). Oviduct: Roles in Fertilization and Early Embryo Development. *J. Endocrinol.* 232 (1), R1–R26. doi:10.1530/joe-16-0302

Liebermeister, W., Noor, E., Flamholz, A., Davidi, D., Bernhardt, J., and Milo, R. (2014). Visual Account of Protein Investment in Cellular Functions. *Proc. Natl. Acad. Sci. U.S.A.* 111 (23), 8488–8493. doi:10.1073/pnas.1314810111

Liu, H., Sadygov, R. G., and Yates, J. R., 3rd (2004). A Model for Random Sampling and Estimation of Relative Protein Abundance in Shotgun Proteomics. *Anal. Chem.* 76 (14), 4193–4201. doi:10.1021/ac0498563

Lonergan, P., Rizos, D., Gutierrez-Adan, A., Moreira, P. M., Pintado, B., de la Fuente, J., et al. (2003). Temporal Divergence in the Pattern of Messenger RNA Expression in Bovine Embryos Cultured from the Zygote to Blastocyst Stage *In Vitro* or *In Vivo*. *Biol. Reprod.* 69 (4), 1424–1431. doi:10.1095/biolreprod.103.018168

Memili, E., and First, N. L. (1998). Developmental Changes in RNA Polymerase II in Bovine Oocytes, Early Embryos, and Effect of α-amanitin on Embryo Development. *Mol. Reprod. Dev.* 51 (4), 381–389. doi:10.1002/(sici)1098-2795(199812)51:4<381::aid-mrd4>3.0.co;2-g

Ménézo, Y. J., and Hérubel, F. (2002). Mouse and Bovine Models for Human IVF. *Reprod. BioMedicine Online* 4 (2), 170–175. doi:10.1016/s1472-6483(10)61936-0

Milazzotto, M. P., de Lima, C. B., da Fonseca, A. M., Dos Santos, E. C., and Ispada, J. (2020). Erasing Gametes to Write Blastocysts: Metabolism as the New Player in Epigenetic Reprogramming. *Anim. Reprod.* 17 (3), e20200015. doi:10.1590/1984-3143-AR2020-0015

Moraes, L. A., Kar, S., Foo, S. L., Gu, T., Toh, Y. Q., Ampomah, P. B., et al. (2017). Annexin-A1 Enhances Breast Cancer Growth and Migration by Promoting Alternative Macrophage Polarization in the Tumour Microenvironment. *Sci. Rep.* 7 (1), 17925. doi:10.1038/s41598-017-17622-5

Nesvizhskii, A. I., Keller, A., Kolker, E., and Aebersold, R. (2003). A Statistical Model for Identifying Proteins by Tandem Mass Spectrometry. *Anal. Chem.* 75 (17), 4646–4658. doi:10.1021/ac0341261

Old, W. M., Meyer-Arendt, K., Aveline-Wolf, L., Pierce, K. G., Mendoza, A., Sevinsky, J. R., et al. (2005). Comparison of Label-free Methods for Quantifying Human Proteins by Shotgun Proteomics. *Mol. Cell Proteomics* 4 (10), 1487–1502. doi:10.1074/mcp.m500084-mcp200

Oshima, R. G., Howe, W. E., Klier, F. G., Adamson, E. D., and Shevinsky, L. H. (1983). Intermediate Filament Protein Synthesis in Preimplantation Murine Embryos. *Developmental Biol.* 99 (2), 447–455. doi:10.1016/0012-1606(83)90294-4

Perez-Riverol, Y., Bai, J., Bandla, C., García-Seisdedos, D., Hewapathirana, S., Kamatchinathan, S., et al. (2022). The PRIDE Database Resources in 2022: a Hub for Mass Spectrometry-Based Proteomics Evidences. *Nucleic Acids Res.* 50 (D1), D543–D552. doi:10.1093/nar/gkab1038

Rizos, D., Maillo, V., Sánchez-Calabuig, M.-J., and Lonergan, P. (2017). The Consequences of Maternal-Embryonic Cross Talk during the Periconception Period on Subsequent Embryonic Development. *Adv. Exp. Med. Biol.* 1014, 69–86. doi:10.1007/978-3-319-62414-3_4

Saint-Dizier, M., Schoen, J., Chen, S., Banliat, C., and Mermillod, P. (2019). Composing the Early Embryonic Microenvironment: Physiology and Regulation of Oviductal Secretions. *Int. J. Mol. Sci.* 21 (1). doi:10.3390/ijms21010223

Sanchez, D. J. D., Vasconcelos, F. R., Teles-Filho, A. C. A., Viana, A. G. A., Martins, A. M. A., Sousa, M. V., et al. (2021). Proteomic Profile of Pre-implantational Ovine Embryos Produced *In Vivo*. *Reprod. Dom Anim.* 56 (4), 586–603. doi:10.1111/rda.13897

Schulz, K. N., and Harrison, M. M. (2019). Mechanisms Regulating Zygotic Genome Activation. *Nat. Rev. Genet.* 20 (4), 221–234. doi:10.1038/s41576-018-0087-x

Seger, C., and Salzmann, L. (2020). After Another Decade: LC-MS/MS Became Routine in Clinical Diagnostics. *Clin. Biochem.* 82, 2–11. doi:10.1016/j.clinbiochem.2020.03.004

Seidel, G. E., Jr. (1981). Superovulation and Embryo Transfer in Cattle. *Science* 211 (4480), 351–358. doi:10.1126/science.7194504

Shannon, P., Markiel, A., Ozier, O., Baliga, N. S., Wang, J. T., Ramage, D., et al. (2003). Cytoscape: a Software Environment for Integrated Models of Biomolecular Interaction Networks. *Genome Res.* 13 (11), 2498–2504. doi:10.1101/gr.1239303

Soom, A. V., Boerjan, M. L., Bols, P. E. J., Vanroose, G., Lein, A., Coryn, M., et al. (1997). Timing of Compaction and Inner Cell Allocation in Bovine Embryos Produced *In Vivo* after Superovulation1. *Biol. Reprod.* 57 (5), 1041–1049. doi:10.1095/biolreprod57.5.1041

Sun, P., Yuan, Y., Li, A., Li, B., and Dai, X. (2010). Cytokeratin Expression during Mouse Embryonic and Early Postnatal Mammary Gland Development. *Histochem. Cel Biol* 133 (2), 213–221. doi:10.1007/s00418-009-0662-5

Szklarczyk, D., Franceschini, A., Wyder, S., Forslund, K., Heller, D., Huerta-Cepas, J., et al. (2015). STRING V10: Protein-Protein Interaction Networks, Integrated over the Tree of Life. *Nucleic Acids Res.* 43 (Database issue), D447–D452. doi:10.1093/nar/gku1003

Thompson, J. G., Sherman, A. N. M., Allen, N. W., McGowan, L. T., and Tervit, H. R. (1998). Total Protein Content and Protein Synthesis within Pre-elongation Stage Bovine Embryos. *Mol. Reprod. Dev.* 50 (2), 139–145. doi:10.1002/(sici)1098-2795(199806)50:2<139::aid-mrd3>3.0.co;2-l

Wang, B., and Shao, Y. (2020). Annexin A2 Acts as an Adherent Molecule under the Regulation of Steroids during Embryo Implantation. *Mol. Hum. Reprod.* 26 (11), 825–836. doi:10.1093/molehr/gaaa065

Watson, A. J., and Barcroft, L. C. (2001). Regulation of Blastocyst Formation. *Front. Biosci.* 6, D708–D730. doi:10.2741/watson

Wei, Q., Zhong, L., Zhang, S., Mu, H., Xiang, J., Yue, L., et al. (2017). Bovine Lineage Specification Revealed by Single-Cell Gene Expression Analysis from Zygote to Blastocyst†. *Biol. Reprod.* 97 (1), 5–17. doi:10.1093/biolre/iox071

Wrenzycki, C., Herrmann, D., Lucas-Hahn, A., Korsawe, K., Lemme, E., and Niemann, H. (2005). Messenger RNA Expression Patterns in Bovine Embryos Derived from *In Vitro* Procedures and Their Implications for Development. *Reprod. Fertil. Dev.* 17 (1-2), 23–35. doi:10.1071/rd04109

Wright, J. M. (1998). "Photographic Illustrations of Embryo Developmental Stage and Quality Codes," in *Manual of the International Embryo Transfer Society*. Editors D. A. Stringfellow and S. M. Seidel. 3rd ed. (Savoy, Illinois), 167–170.

Zhou, X., Tian, F., Sandzén, J., Cao, R., Flaberg, E., Szekely, L., et al. (2007). Filamin B Deficiency in Mice Results in Skeletal Malformations and Impaired Microvascular Development. *Proc. Natl. Acad. Sci. U.S.A.* 104 (10), 3919–3924. doi:10.1073/pnas.0608360104

Zhou, Y., Zhou, B., Pache, L., Chang, M., Khodabakhshi, A. H., Tanaseichuk, O., et al. (2019). Metascape Provides a Biologist-Oriented Resource for the Analysis of Systems-Level Datasets. *Nat. Commun.* 10 (1), 1523. doi:10.1038/s41467-019-09234-6

Conflict of Interest: Authors CB and BG were employed by the company Union Evolution.

The remaining authors declare that the research was conducted in the absence of any commercial or financial relationships that could be construed as a potential conflict of interest.

Publisher's Note: All claims expressed in this article are solely those of the authors and do not necessarily represent those of their affiliated organizations, or those of the publisher, the editors and the reviewers. Any product that may be evaluated in this article, or claim that may be made by its manufacturer, is not guaranteed or endorsed by the publisher.

Copyright © 2022 Banliat, Mahé, Lavigne, Com, Pineau, Labas, Guyonnet, Mermillod and Saint-Dizier. This is an open-access article distributed under the terms of the Creative Commons Attribution License (CC BY). The use, distribution or reproduction in other forums is permitted, provided the original author(s) and the copyright owner(s) are credited and that the original publication in this journal is cited, in accordance with accepted academic practice. No use, distribution or reproduction is permitted which does not comply with these terms.

Annexe 7 : article de recherche (collaboration au cours de la thèse) : « The proteomic analysis of bovine embryos developed in vivo or in vitro reveals the contribution of the maternal environment to early embryo»

Banliat *et al. BMC Genomics* (2022) 23:839
https://doi.org/10.1186/s12864-022-09076-5

BMC Genomics

RESEARCH Open Access

The proteomic analysis of bovine embryos developed *in vivo* or *in vitro* reveals the contribution of the maternal environment to early embryo

Charles Banliat[1,2†], Coline Mahé[1†], Régis Lavigne[3,4], Emmanuelle Com[3,4], Charles Pineau[3,4], Valérie Labas[1,5], Benoit Guyonnet[2], Pascal Mermillod[1] and Marie Saint-Dizier[1*]

Abstract

Background: Despite many improvements with *in vitro* culture systems, the quality and developmental ability of mammalian embryos produced *in vitro* are still lower than their *in vivo* counterparts. Though previous studies have evidenced differences in gene expression between *in vivo*- and *in vitro*-derived bovine embryos, there is no comparison at the protein expression level.

Results: A total of 38 pools of grade-1 quality bovine embryos at the 4–6 cell, 8–12 cell, morula, compact morula, and blastocyst stages developed either *in vivo* or *in vitro* were analyzed by nano-liquid chromatography coupled with label-free quantitative mass spectrometry, allowing for the identification of 3,028 proteins. Multivariate analysis of quantified proteins showed a clear separation of embryo pools according to their *in vivo* or *in vitro* origin at all stages. Three clusters of differentially abundant proteins (DAPs) were evidenced according to embryo origin, including 463 proteins more abundant *in vivo* than *in vitro* across development and 314 and 222 proteins more abundant *in vitro* than *in vivo* before and after the morula stage, respectively. The functional analysis of proteins found more abundant *in vivo* showed an enrichment in carbohydrate metabolism and cytoplasmic cellular components. Proteins found more abundant *in vitro* before the morula stage were mostly localized in mitochondrial matrix and involved in ATP-dependent activity, while those overabundant after the morula stage were mostly localized in the ribonucleoprotein complex and involved in protein synthesis. Oviductin and other oviductal proteins, previously shown to interact with early embryos, were among the most overabundant proteins after *in vivo* development.

Conclusions: The maternal environment led to higher degradation of mitochondrial proteins at early developmental stages, lower abundance of proteins involved in protein synthesis at the time of embryonic genome activation, and a global upregulation of carbohydrate metabolic pathways compared to *in vitro* production. Furthermore, embryos developed *in vivo* internalized large amounts of oviductin and other proteins probably originated in the oviduct as

†Charles Banliat and Coline Mahé contributed equally to this work and share first authorship.

*Correspondence: marie.saint-dizier@univ-tours.fr

[1] INRAE, CNRS, Tours University, IFCE, UMR PRC, Nouzilly, France
Full list of author information is available at the end of the article

© The Author(s) 2022. **Open Access** This article is licensed under a Creative Commons Attribution 4.0 International License, which permits use, sharing, adaptation, distribution and reproduction in any medium or format, as long as you give appropriate credit to the original author(s) and the source, provide a link to the Creative Commons licence, and indicate if changes were made. The images or other third party material in this article are included in the article's Creative Commons licence, unless indicated otherwise in a credit line to the material. If material is not included in the article's Creative Commons licence and your intended use is not permitted by statutory regulation or exceeds the permitted use, you will need to obtain permission directly from the copyright holder. To view a copy of this licence, visit http://creativecommons.org/licenses/by/4.0/. The Creative Commons Public Domain Dedication waiver (http://creativecommons.org/publicdomain/zero/1.0/) applies to the data made available in this article, unless otherwise stated in a credit line to the data.

soon as the 4–6 cell stage. These data provide new insight into the molecular contribution of the mother to the developmental ability of early embryos and will help design better *in vitro* culture systems.

Keywords: Embryo, Proteomics, Mass spectrometry, Morula, Blastocyst, Cattle, Oviduct, Development

Background

The high frequency of embryo demise after *in vitro* development is a general feature in mammalian species. Recent data registered by the European Society of Human Reproduction and Embryology (ESHRE) indicate that the rate of clinical pregnancy after transfer of *in vitro*-fertilized human embryos averages 35% over 39 countries [1]. In cattle, the number of *in vitro*-produced embryos that are transferred worldwide is continuously growing and has overpassed that of *in vivo*-produced embryos since 2016 [2]. The main objectives of embryo production and transfer in cattle is to disseminate genetically superior females and optimize animal breeding for milk and meat production. Data collected by the International Embryo Transfer Society (IETS) indicate that more than 1.2 million cattle embryos are transferred worldwide each year, 80% of which are produced *in vitro* [3]. However, despite many improvements in *in vitro* systems and embryo culture media, the blastocyst yield and embryo quality did not significantly progress over the past decades. On average, 20% to 40% of cultured presumptive zygotes reach the blastocyst stage, and many of these are unable to sustain development following embryo transfer [2, 4]. Based on studies reported over the past 25 years, the pregnancy rates of recipient cows carrying *in vitro*-produced (IVP) embryos are 10 to 40% lower when compared with *in vivo*-derived embryos generated by superovulation, and only 27% of cows receiving IVP embryos will produce a living calf [5]. Furthermore, the ability of cattle embryos to survive after cryopreservation is much lower after *in vitro* development than *in vivo* development [2, 4]. Bovine and human early embryos are similar in terms of biochemical regulatory processes, transcriptomic dynamics, and the kinetics of development up to the blastocyst stage [6–8], reinforcing interest in cattle embryos as models to study the contribution of the maternal environment to embryo quality.

Earlier studies comparing bovine embryos developed *in vitro* or *in vivo* have reported differences in morphology and ultrastructure [9–12], lipid profiles [13], and energy metabolism [14–16]. Furthermore, transcriptomic studies comparing bovine embryos developed *in vitro* or *in vivo* have reported differences in gene expression [17–20] and methylation patterns [21], revealing molecular mechanisms underlying the higher developmental ability of *in vivo*-developed embryos. Based on the previously reported "quiet embryo" theory, it was hypothesized that at the time of embryonic genome activation (between the 8-cell and 16-cell stages), *in vivo*-derived embryos may have a lower activation of protein synthesis and slightly lower metabolic activity compared to their *in vitro* counterparts, increasing their chance to pursue development [22–24]. In addition, based on our previous work, 56 proteins, including oviduct-specific glycoprotein 1, were internalized by *in vitro*-produced embryos during incubation with oviduct fluid [25] so we hypothesized that those proteins would be at higher abundance in *in vivo*- compared to *in vitro*- derived embryos. However, due to the difficulty to access early embryos *in vivo* and scarcity of materials, the proteomic comparison between *in vivo*- and *in vitro*-derived embryos in mammals remained unexplored. In a previous study, we analyzed the proteomic dynamics of bovine *in vivo*-derived embryos from the 4–6 cell to blastocyst stages [26]. In the present study, the same pools of *in vivo*-developed embryos were compared to contemporary pools of bovine embryos produced *in vitro*. All embryos were analyzed in the same analysis batch by nanoliquid chromatography coupled with tandem mass spectrometry (nanoLC-MS/MS) and label-free quantification.

Results

Only embryos of grade-1 quality, i.e., of high morphological quality, with no sex sorting, were included in the analysis. Although not systematically observed, *in vitro*-produced embryos tended to appear darker than those collected *in vivo* (see representative pictures in Figure S1).

Distribution of proteins identified between *in vivo* and *in vitro*-derived embryos

A total of 3,028 proteins were identified by at least two unique peptides in embryos (false discovery rate < 0.01%; see Table S1 for the complete list of proteins with their accession number, gene symbol, and normalized quantification). Figure 1 shows the number and distribution of identified proteins between *in vivo* and *in vitro*-derived embryos at each stage. An increase in the number of identified proteins was observed from the 4–6 cell to blastocyst stages in both groups of embryos (+16.6% and +19.3% in *in vivo* and *in vitro*-derived embryos, respectively). Overall, more than 85% of proteins were shared between *in vivo* and *in vitro*-derived embryos (see Table S1 for the list of specific proteins at each stage).

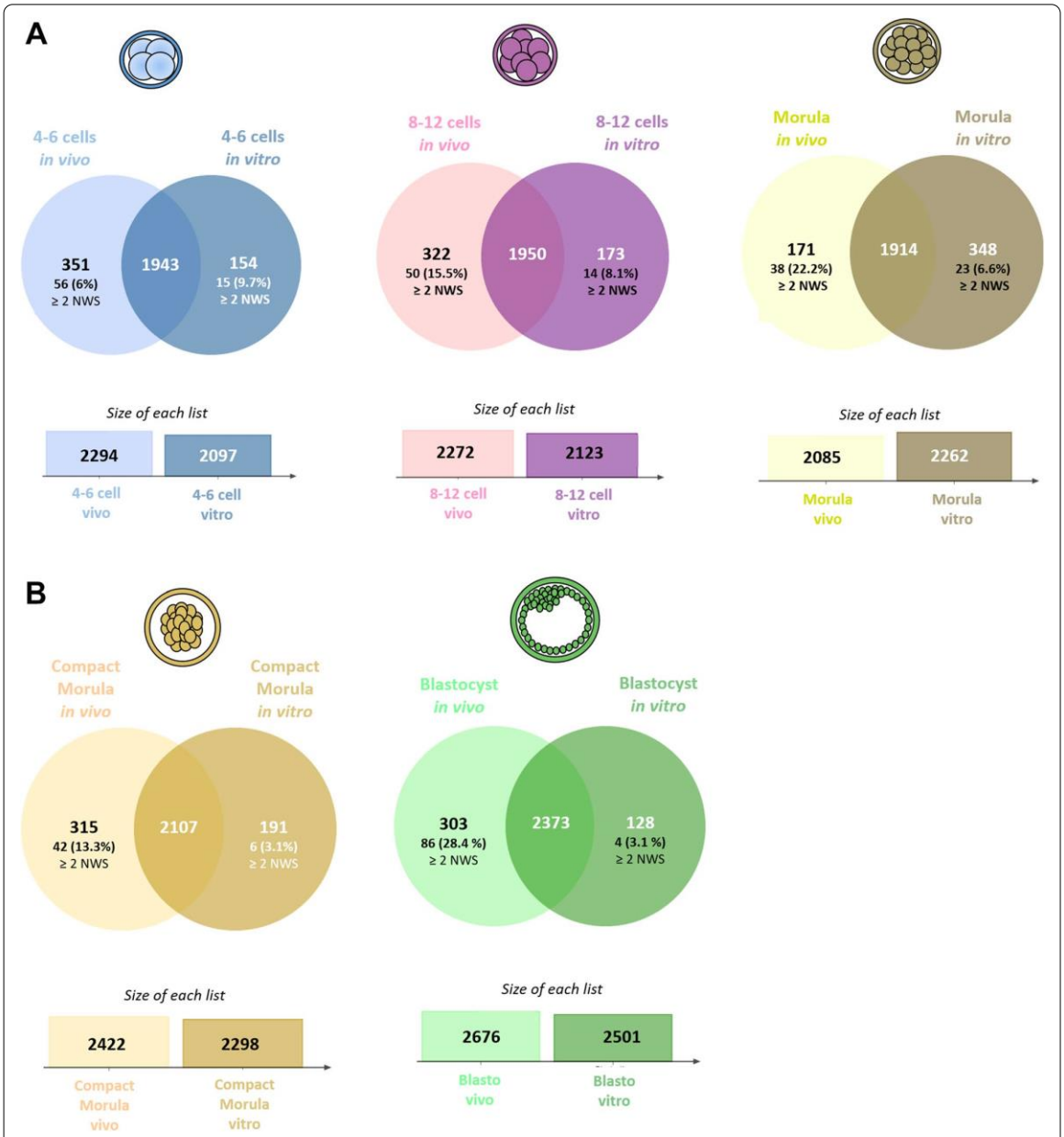

Fig. 1 Comparative analysis of proteins identified in bovine early embryos produced *in vivo* or *in vitro*. The Venn diagram indicates the overlap between origins at each stage, and the histograms in the bottom indicate the number of proteins identified in each pool of embryos

Most of proteins detected exclusively *in vivo* or *in vitro* were at low abundance as only 3%–28% were quantified with more than two normalized weighted spectra (NWS; Fig. 1).

Global analysis of differentially abundant proteins between *in vivo* and *in vitro*-derived embryos across development

A total of 2,184 proteins quantified with a minimum of 2 NWS in at least one condition were retained for

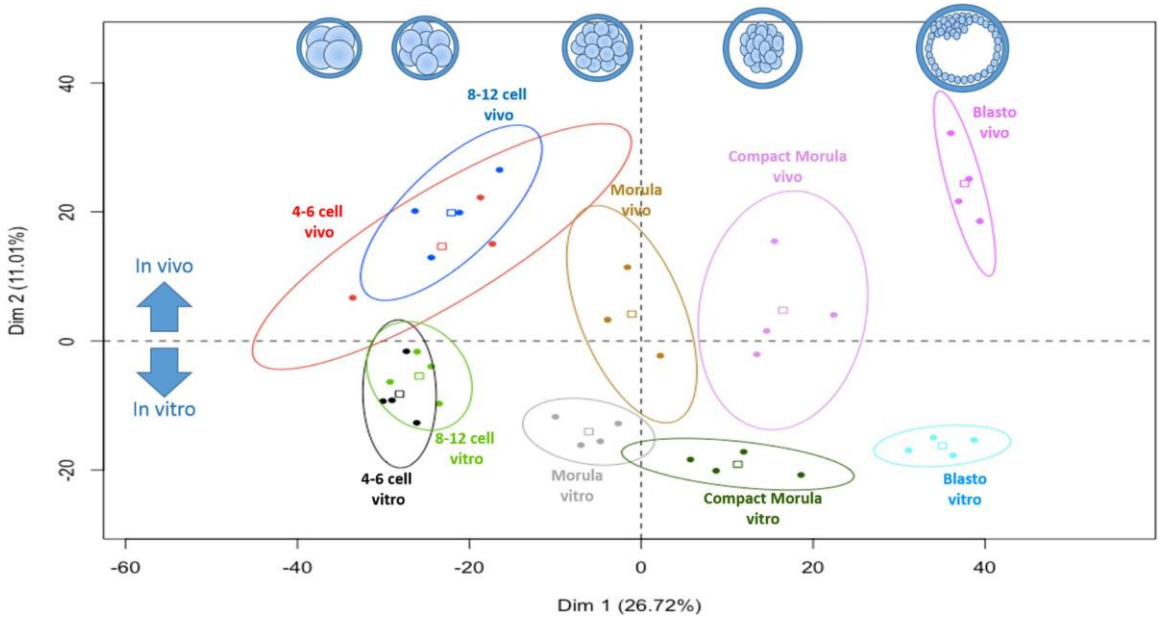

Fig. 2 Principal component analysis of all embryo pools from the 4–6 cell to blastocyst stages. The 2,186 proteins quantified with a minimum of 2 normalized weighted spectra in at least one condition were considered. Scatter plots represent the position of each pool of embryos along the first two principal components. The variability between pools was mainly explained by their stage of development on the first horizontal dimension (Dim 1; 26.7% of variance) then by their origin (*in vivo* vs. *in vitro*) on the second vertical dimension (Dim 2; 11.0% of variance). The square in each ellipse represents the mean of data for a given condition, and colored ellipses represent the 95% confidence intervals

statistical analysis (Table S1). Figure 2 shows the principal component analysis (PCA) of all quantified proteins. The first dimension of PCA on the horizontal axis separated embryo pools according to their stage of development, except between the 4–6 cell and 8–12 cell stages, which clustered together. The second dimension of PCA on the vertical axis showed a clear separation of embryo pools according to their origin, starting at the 4–6 cell stage, with maximal gap at the blastocyst stage (Fig. 2).

The hierarchical clustering of differentially abundant proteins (DAPs) according to embryo origin allowed us to identify three clusters of DAPs illustrated in Fig. 3 (ANOVA p-value ≤ 0.050; see the list of DAPs in Table S2). Cluster 1 contained 463 proteins with higher abundance *in vivo* than *in vitro* across development. Cluster 2 contained 222 proteins that increased in abundance from the morula to blastocyst stages but displayed higher abundance in embryos developed *in vitro* compared to *in vivo*. Cluster 3 contained 314 proteins that decreased in abundance from the 4–6 cell to morula stages but displayed higher abundance *in vitro* than *in vivo*.

The gene lists of the three clusters of DAPs were used for gene ontology (GO) enrichment analysis using the Metascape tool. The DAPs in cluster 1 were overrepresented in biological processes and pathways related to energy metabolism (carbohydrate metabolic and biosynthesis processes, small molecule biosynthetic process, pentose phosphate pathway, glycosyl compound metabolic process; see Fig. 4A and list of all enriched terms with related DAPs and p-values in Table S3). Another group of enriched processes and pathways was related to cellular detoxification (lysosome pathway, glutathione metabolism, regulation of proteolysis, cellular detoxification), while cadherin binding was the most enriched molecular function (Fig. 4B). The top enriched cellular components of cluster 1 included cytoplasmic components (cytoplasmic vesicle lumen, vacuolar lumen) and the extracellular compartment (focal adhesion, extracellular matrix) as the most significant terms (Fig. 4C and Table S3).

The DAPs in cluster 2 were largely involved in protein synthesis; the most significant terms among the biological processes included cytoplasmic translation, translational initiation, ribosome biogenesis, ribosome assembly, and regulation of translation, among others (see Fig. 5A and Table S4 for details). In accordance, the enriched molecular functions were related to protein synthesis, including structural constituents of ribosomes, translation initiation factor activity,

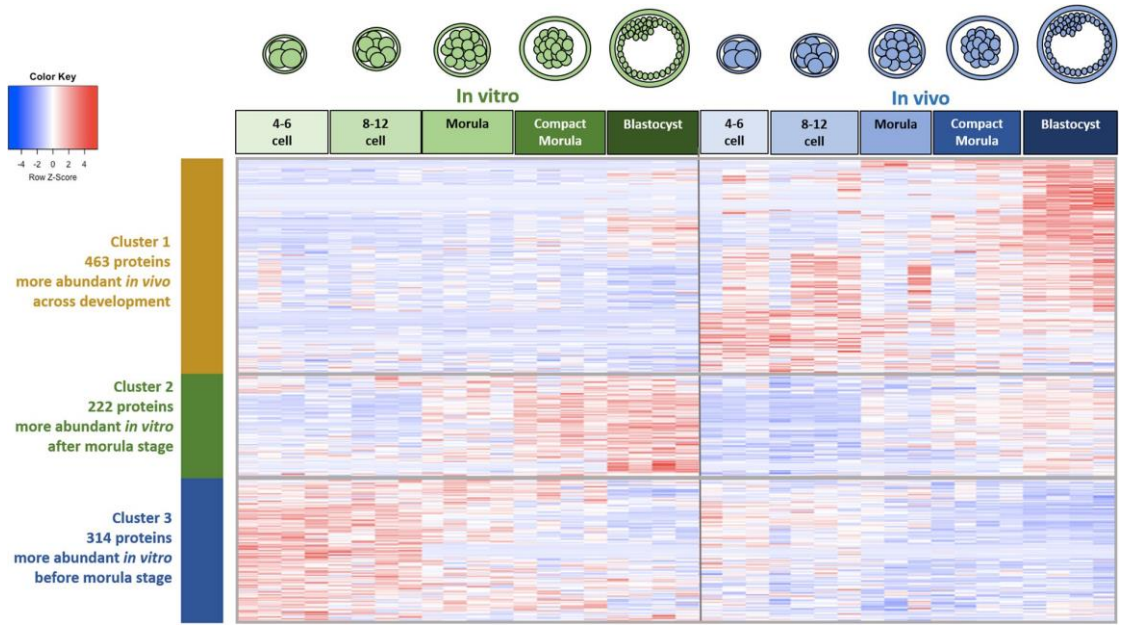

Fig. 3 Heatmap and hierarchical clustering of differentially abundant proteins (DAPs) according to the origin of embryos. The 999 proteins with a *p*-value ≤ 0.050 after analysis of variance (ANOVA) were considered. Each line corresponds to one protein and each column to the normalized quantitative values of one embryo pool. The vertical grey line delimitates *in vitro*-derived embryos on the left from *in vivo*-derived embryos on the right. Red indicates higher abundance while blue indicates lower abundance compared with other conditions. Clusters of proteins identified after hierarchical clustering of data are delimited by colored vertical bars on the left and horizontal grey lines

and ribonucleoprotein complex binding (Fig. 5B). The cell adhesion molecule binding was the second most enriched molecular function. The top cellular components of cluster 2 were involved in the translation machinery (ribonucleoprotein complex, cytosolic small ribosomal subunit, polysome, eukaryotic translation initiation factor 3 complex, among others; Fig. 5C).

The DAPs in cluster 3 were overrepresented in biological processes and pathways related to intracellular organization and protein processing, including organelle localization, Golgi vesicle transport, protein folding, actin filament-based processes, microtubule cytoskeleton organization, and intracellular protein transport (Fig. 6A; see details in Table S5). The most significantly enriched molecular functions were ATP-dependent activity followed by cell adhesion molecule binding (Fig. 6B). The most significantly enriched cellular component of cluster 3 was the mitochondrial matrix (Fig. 6C).

Pairwise comparisons between *in vivo* and *in vitro*-derived embryos at each stage

Pairwise comparisons between *in vivo* and *in vitro*-derived embryos retrieved between 211 and 541 DAPs at each stage (t-test *p*-value ≤ 0.05; fold-change ratios ≥ 1.5; overabundant protein ≥ 2 NWS). Figure 7 shows the total number of DAPs and those increased in abundance at each developmental stage and for each origin (see Table S6 for complete lists of DAPs with fold-change ratios and *p*-values).

The comparative analysis of DAPs across all stages evidenced nine proteins always more abundant *in vivo* than *in vitro*, including oviduct-specific glycoprotein 1 (also called oviductin, OVGP1), clusterin (CLU), CD109 molecule (CD109), retinoic acid receptor responder 1 (RARRES), and tissue alpha-L fucosidase (FUCA1; Fig. 8A). On the other hand, four proteins, including cochlin (COCH), kinesin family member 23 (KIF23), insulin like growth factor 2 mRNA binding protein 3 (IGF2BP3), and dynein cytoplasmic 1 heavy chain 1 (DYNC1H1), were always less abundant *in vivo* than *in vitro* (Fig. 8B; see Table S6 for the list of stage-specific DAPs after pair-wise comparisons).

The gene lists of DAPs in each *in vivo* vs. *in vivo* comparison were used for functional enrichment analysis using the Metascape tool. Figure 9A, B, and C show the

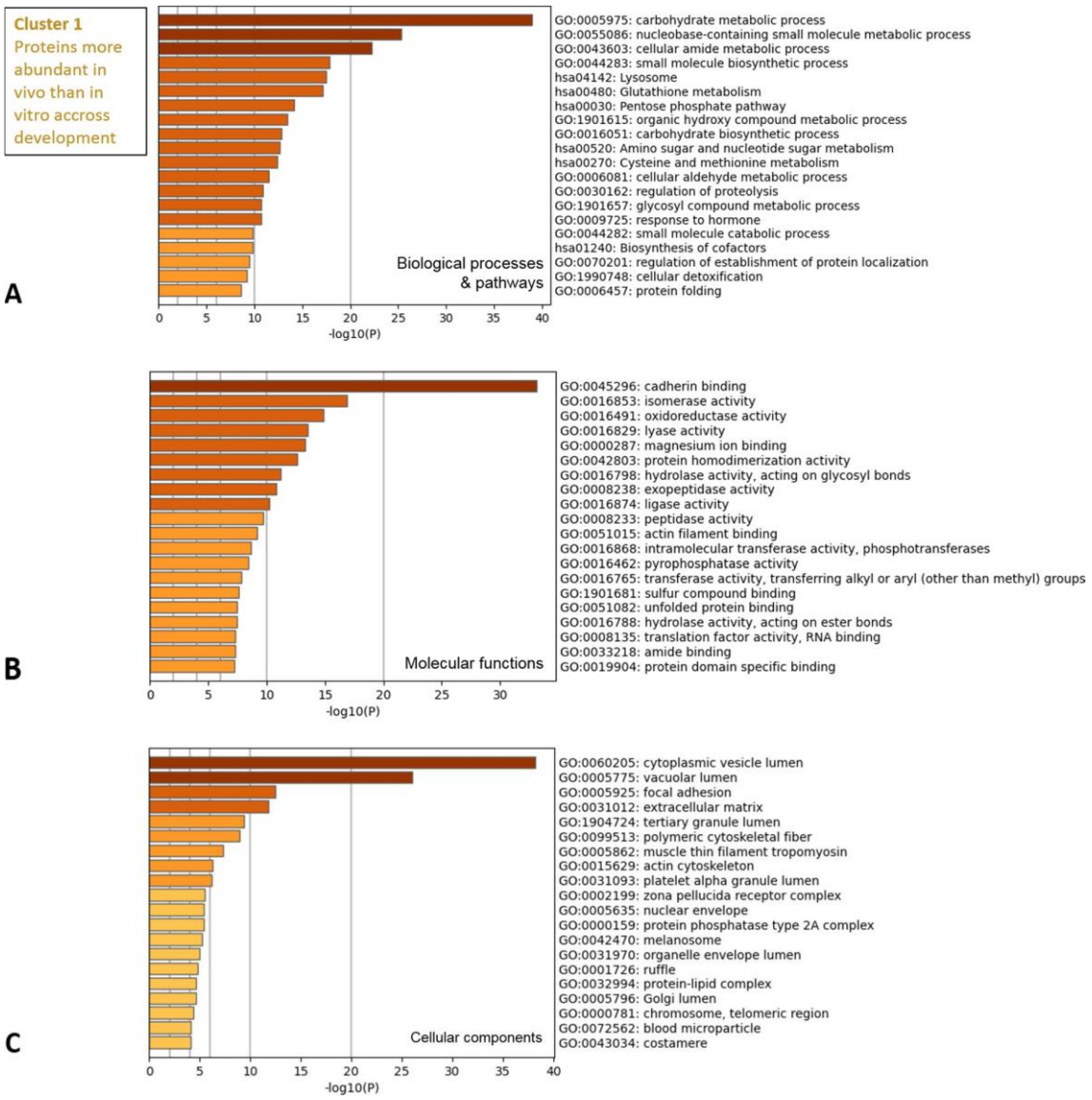

Fig. 4 Functional enrichment analysis of proteins found more abundant *in vivo* than *in vitro* across development (cluster 1). The Metascape bar graphs represent the top 20 clusters of enriched gene ontology (GO) terms for biological processes and KEGG pathways (**A**), molecular functions (**B**), and cellular components (**C**). Each row represents one enriched cluster, and the darker color of the bars indicates higher significance (lower *p*-value). A -log10(P) of 20 corresponds to a *P*-value of 10^{-20}. See Table S3 for the complete list of GO terms with corresponding gene names and *p*-values

significantly enriched GO terms of biological processes and pathways, molecular functions, and cellular components, respectively, for proteins more abundant *in vivo* than *in vitro* at each stage (see Table S7 for complete list of enriched terms). The most enriched processes/pathways were the carbohydrate derivative catabolic process and cellular amide metabolic process for all stages and carbohydrate metabolic process and carbon metabolism for all stages except the 4–6 cell stage. The blastocyst stage retrieved numerous highly significant processes, including small molecule catabolic processes and cellular detoxification. Enriched molecular functions at the

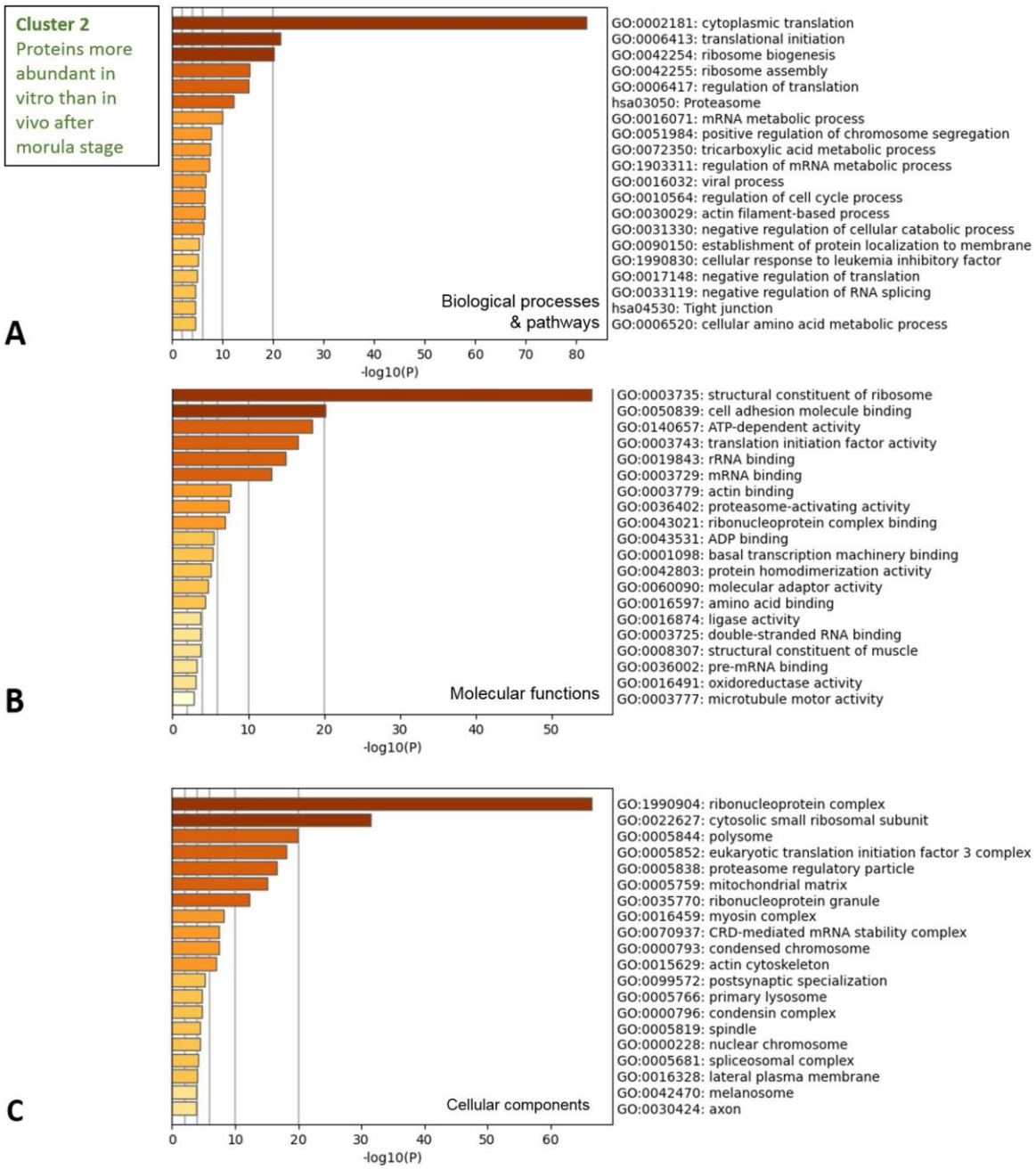

Fig. 5 Functional analysis of proteins more abundant *in vitro* than *in vivo* after the morula stage (cluster 2). The Metascape bar graphs represent the top 20 clusters of enriched GO terms for biological processes and KEGG pathways (**A**), molecular functions (**B**), and cellular components (**C**). Each row represents one enriched cluster, and the darker color of the bars indicates higher significance (lower p-value). A -log10(P) of 20 corresponds to a *P*-value of 10^{-20}. See Table S4 for the complete list of GO terms with corresponding gene names and *p*-values

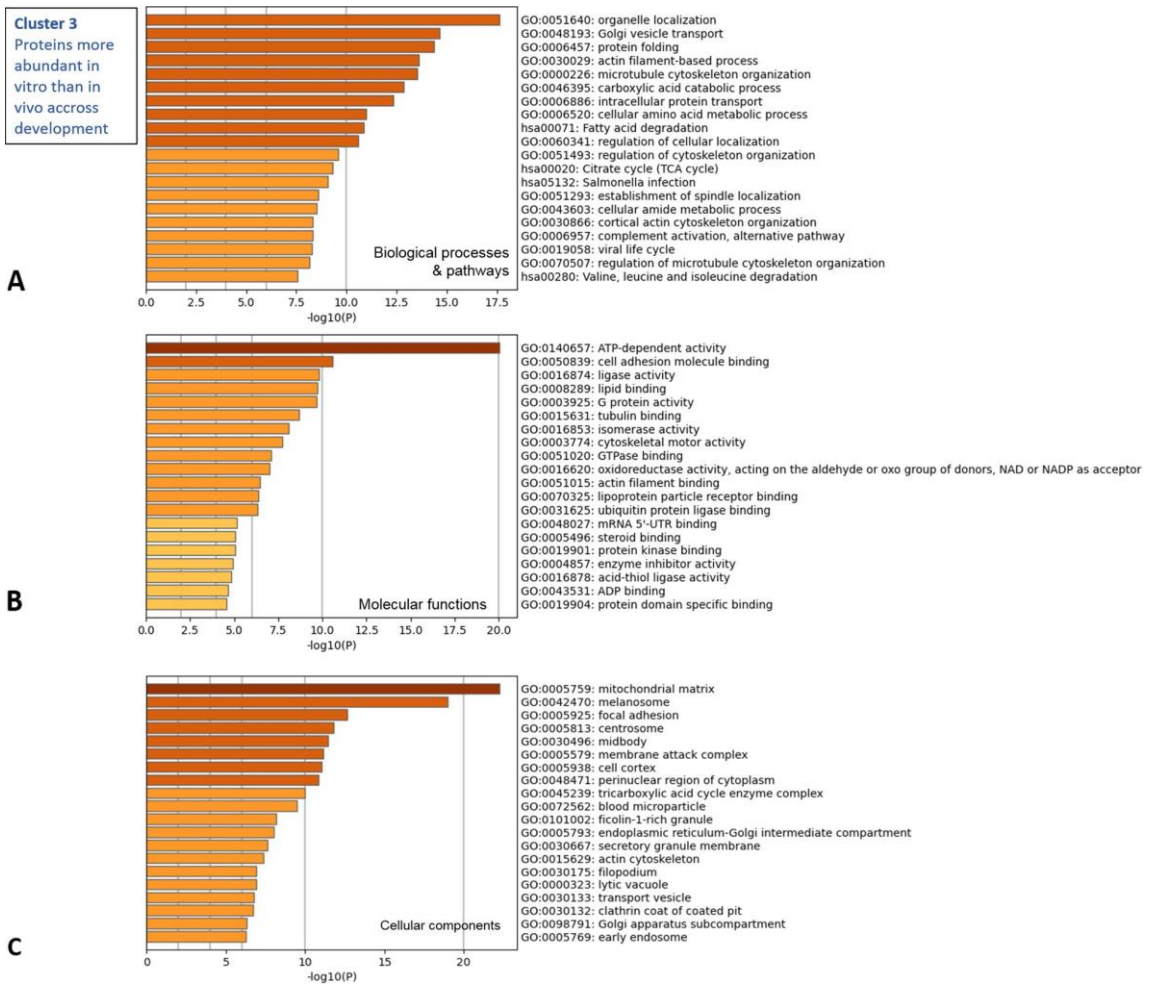

Fig. 6 Functional analysis of proteins more abundant *in vitro* than *in vivo* before the morula stage (cluster 3). The Metascape bar graphs represent the top 20 clusters of enriched GO terms for biological processes and KEGG pathways (**A**), molecular functions (**B**), and cellular components (**C**). Each row represents one enriched cluster, and the darker color of the bars indicates higher significance (lower *p*-value). A -log10(P) of 10 corresponds to a *P*-value of 10^{-10}. See Table S5 for the complete list of GO terms with corresponding gene names and *p*-values

blastocyst stage included cadherin binding, antioxidant activity, and intramolecular oxidoreductase activity. The most enriched cellular components for proteins found overabundant *in vivo* at all stages were the cytoplasmic vesicle lumen and vacuolar lumen.

Figure 10A, B, and C show significantly enriched GO terms of biological processes/pathways, molecular functions, and cellular components, respectively, for proteins found less abundant *in vivo* than *in vitro* at each developmental stage (see Table S8 for complete list of enriched terms). Here, most enriched clusters were common to all stages. The most enriched processes/pathways were translation, cell division, organelle localization, and actin filament-based processes with high significance. Other biological processes included non-coding RNA metabolic process, translational initiation, and ribonucleoprotein complex biogenesis. The most enriched molecular functions for proteins found overabundant *in vitro* were ATP-dependent activity, cytoskeletal motor activity, and structural molecule activity. The most enriched cellular components were the mitochondrial matrix (all stages except blastocyst), ribonucleoprotein complex (all stages except morula), focal adhesion, and microtubule associated complex (all stages).

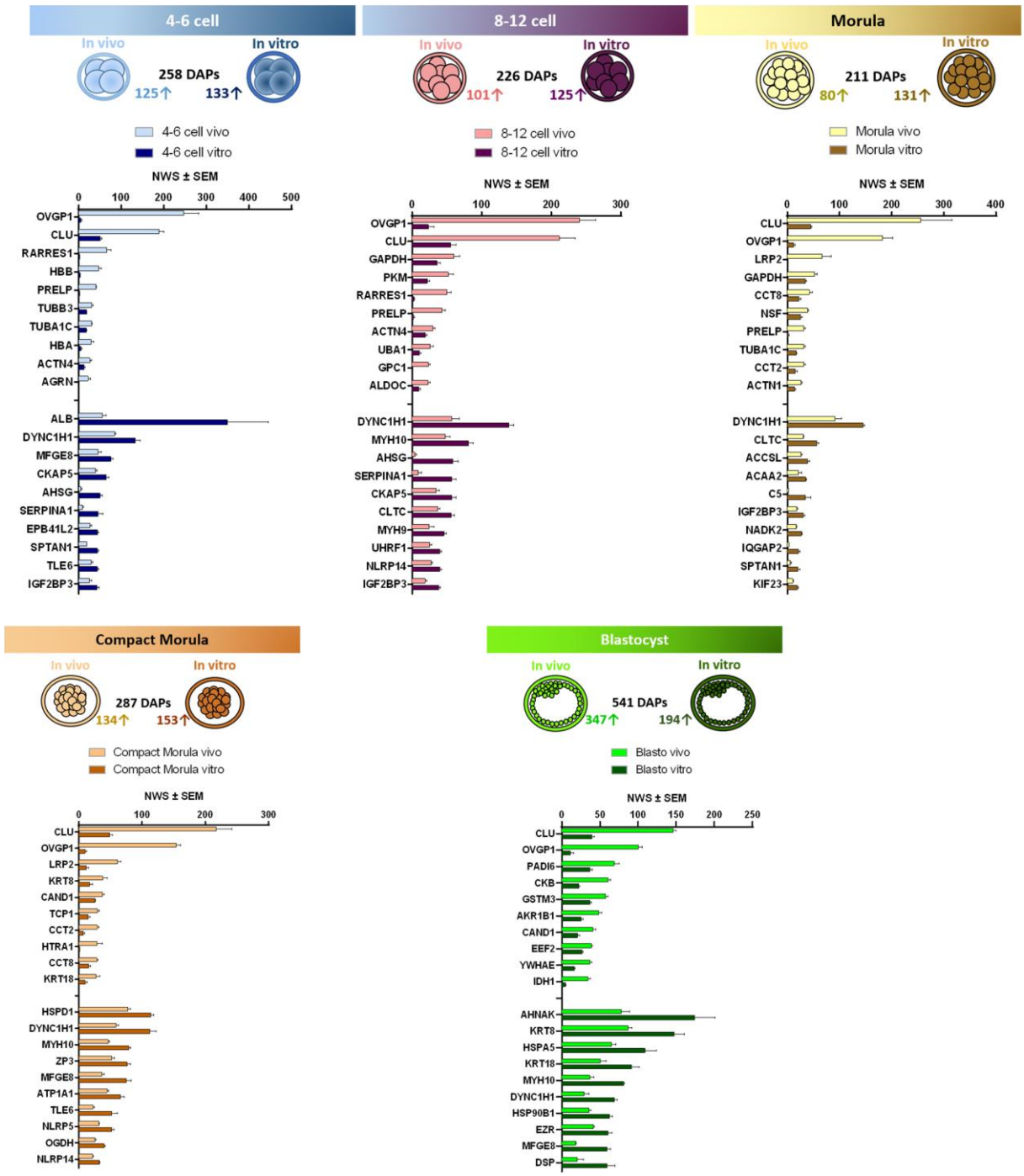

Fig. 7 Top 20 DAPs after pairwise comparisons between *in vivo* and *in vitro*-derived embryos at each stage. Numbers of overabundant DAPs *in vivo* and *in vitro* (or less abundant DAPs *in vitro* and *in vivo*) are indicated beside the upward arrows. The histograms indicate the top 10 DAPs in each comparison. DAPs with a t-test *p*-value ≤ 0.05 and fold-change ratio ≥ 1.5 were considered

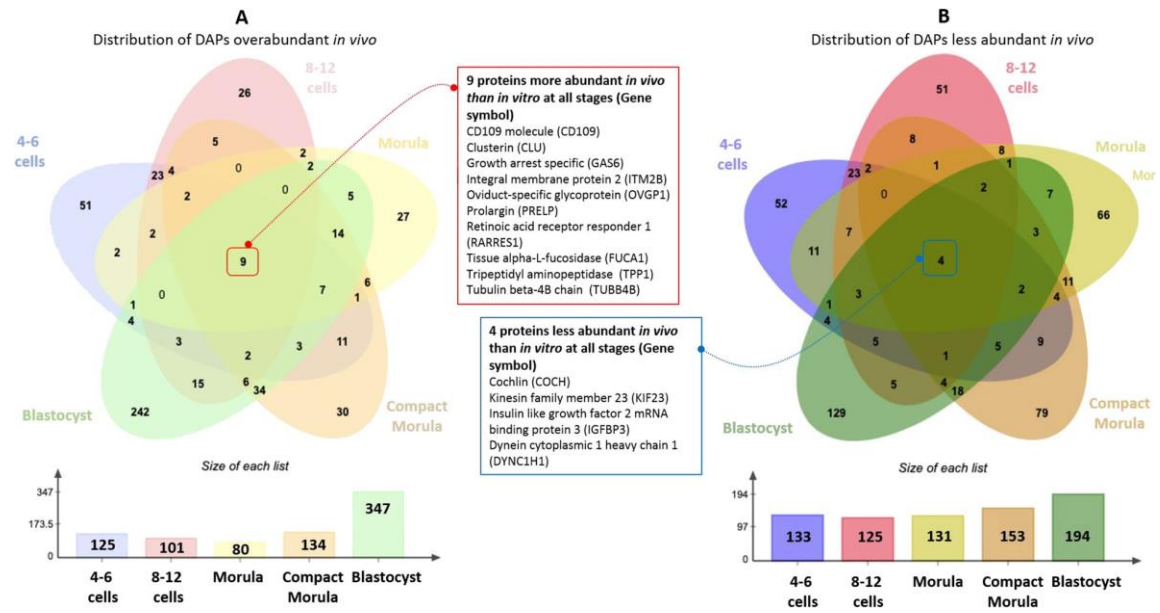

Fig. 8 Distribution of proteins more (**A**) or less (**B**) abundant *in vivo* than *in vitro*. The Venn diagram indicates the overlap of DAPs between stages, and the histograms in the bottom indicate the number of DAPs at each stage. The frames indicate overabundant and less abundant DAPs, respectively, shared between all stages. DAPs with a t-test *p*-value ≤ 0.05 and fold-change ratio ≥ 1.5 were considered

Discussion

This study aimed at identifying the global contribution of the maternal environment to the embryo proteome and pointing out the alterations induced by *in vitro* embryo production. Previous studies have shown that the *in vivo* or *in vitro* maturation of oocytes is determinant for the developmental rate up to the blastocyst stage, while the culture environment of embryos is determinant for their quality in terms of gene expression, cryotolerance, and developmental ability [12, 20, 27–29]. The present data identify the global impact of *in vitro* oocyte maturation, fertilization, and culture conditions on the embryo proteome. To our knowledge, this is the first comparative proteomic analysis of preimplantation embryos developed either *in vivo* or *in vitro* in mammals. A total of 3,028 proteins were identified, representing the most comprehensive proteomic database in early embryos so far. Although the developmental stage was the first discriminating factor, the PCA of quantified proteins clearly differentiated embryos according to their origin as soon as the 4–6 cell stage. Overall, 46% of embryo proteins (999 of 2,184) were differentially abundant according to their origin, highlighting the great contribution of the maternal environment to the embryo proteome, in accordance with previous transcriptomic studies [17–21].

Functional implication of proteins found less abundant *in vivo* than *in vitro* at early stages of development

Proteins in cluster 3 were more abundant in *in vitro*- than *in vivo*-derived embryos before the morula stage, as observed on the heatmap of DAPs. The mitochondrial matrix was the most significantly enriched cellular component in cluster 3 and included 38 proteins, including aconitate hydratase, mitochondrial (ACO2), fumarate hydratase, mitochondrial (FH), 3-ketoacyl-CoA thiolase, mitochondrial (ACAA2), ATP synthase subunit alpha, mitochondrial (ATP5F1A) and 2-oxoglutarate dehydrogenase, mitochondrial (OGDH) among the most abundant ones in 8–12 cell embryos produced *in vitro*. This indicates that although the cell numbers were the same, 4–6 cell and 8–12 cell embryos produced *in vitro* had higher abundance or lower degradation of mitochondrial

(See figure on next page.)
Fig. 9 Functional analysis of proteins more abundant *in vivo* than *in vitro* at each developmental stage. The Metascape heatmap plots represent the top 20 clusters of enriched GO terms of biological processes and KEGG pathways (**A**), molecular functions (**B**), and cellular components (**C**). Each row represents one enriched cluster, and the orange gradation reflects statistical significance (the darker the color, the more significant the *p*-value is). Gray color indicates a lack of significance. DAPs with a t-test *p*-value ≤ 0.05 and fold-change ratio ≥ 1.5 were considered

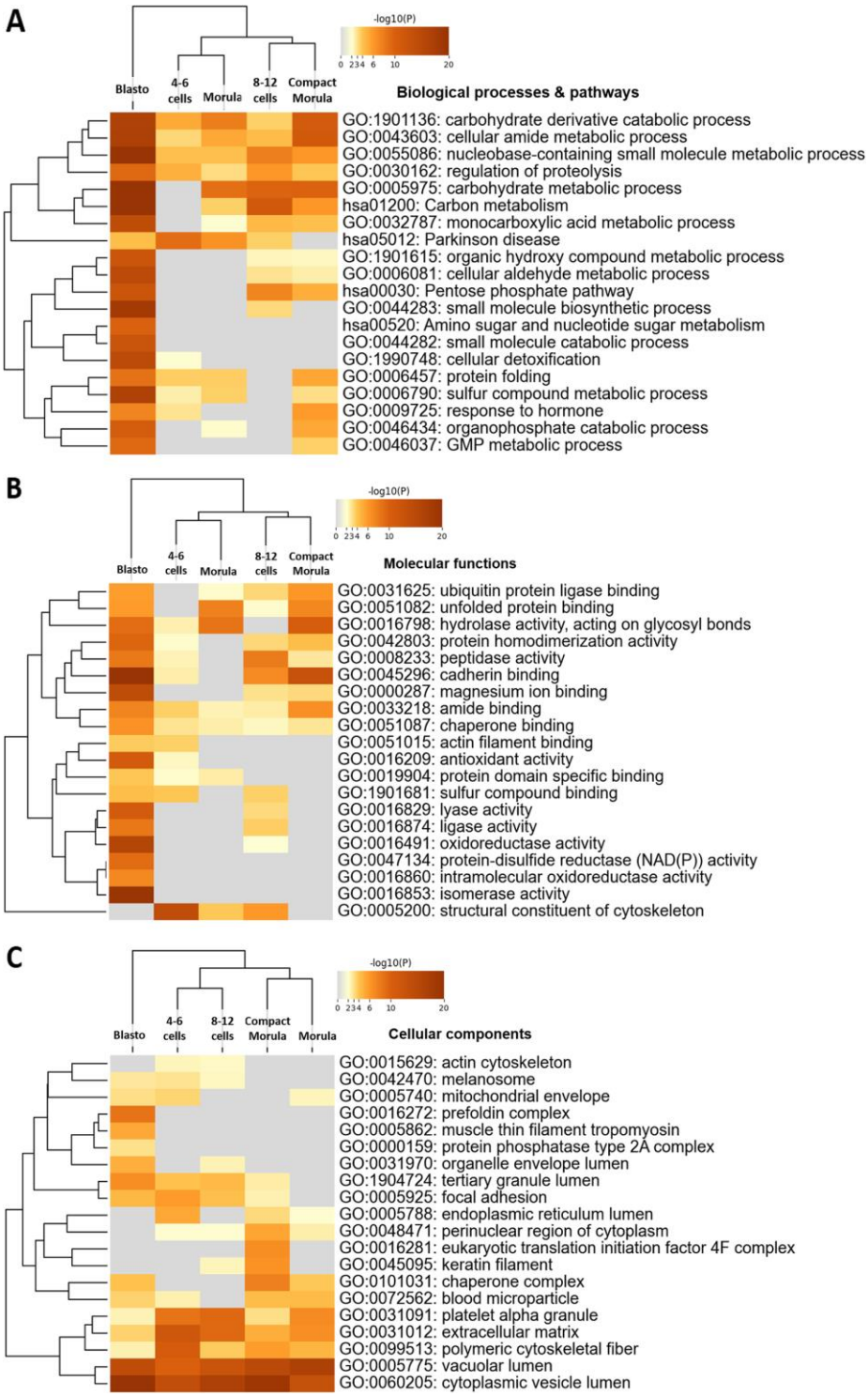

Fig. 9 (See legend on previous page.)

proteins than their *in vivo* counterparts. Mitochondria are maternally inherited in embryos and do not replicate until embryonic differentiation at the morula stage, leading to a progressive decrease of mitochondrial copies per blastomere at each cell division [30]. In accordance, ATP-dependent activity, a mitochondrial activity, was the most enriched molecular function for proteins in cluster 3 and also significantly enriched in proteins found overabundant *in vitro* at all stages. The mitochondrial content of bovine oocytes lacks data; however, in humans, the number and ultrastructure of mitochondria do not differ between *in vivo*- and *in vitro*-matured oocytes [31]. Furthermore, the general ATP content per oocyte did not differ according to *in vivo* vs. *in vitro* origin in pigs [32]. Thus, it is likely that bovine *in vitro*-derived embryos had initially similar content in mitochondrial proteins but slower decrease in these proteins over time. These results suggest that *in vitro* culture conditions impaired the capacity of embryos to properly use the oocyte-derived mitochondrial proteins. Consistent with this hypothesis, previous studies on bovine blastocysts observed a larger amount of mitochondrial debris [10] and DNA copy numbers [33] in *in vitro*- compared to *in vivo*-derived embryos. ATP is an important energy source for protein synthesis and all cellular functions. Further studies would be necessary to see if this slower decrease in mitochondrial proteins *in vitro* is associated with dysregulation of ATP synthesis.

Other proteins in cluster 3 may be the result of higher initial abundance and/or slower use of oocyte-derived proteins in *in vitro*-derived embryos. For instance, metalloendopeptidase (ASTL), cochlin (COCH), enoyl-CoA delta isomerase 2 (ECI2), endoplasmic reticulum resident protein 44 (ERP44), SLC3A2 protein (SLC3A2), Tudor and KH domain containing protein (TDRKH) and the uncharacterized protein LSM14B were all included in cluster 3 and previously identified in a cluster of proteins that gradually decreased in abundance from metaphase II oocytes to 4-cell embryos in cattle [34].

Proteins in cluster 3 were overrepresented in pathways related to intracytoplasmic organelle localization and actin filament-based processes. In accordance, at early stages of development, proteins overabundant *in vitro* were involved in cell division, actin filament-based process, cytoskeletal motor activity, and structural molecule activity as the most enriched pathways and functions. These pathways included numerous proteins including annexins (ANXA11), myosins (MYO1B, MYH9, MYH10, MYH11, MYO1C…), and spectrins (SPTAN1, SPTBN1). This indicates that pathways related to cellular organization and cell division were dysregulated in *in vitro*-derived embryos, which could impair embryo morphology and kinetics of development. Morphological evaluation is widely used to evaluate embryo quality, and only embryos of grade-1 quality, i.e., consistent with their expected stage of development, with uniform blastomeres and few irregularities, were used for the present study. Furthermore, although the timing of fertilization is impossible to determine *in vivo*, the time of embryo collection after insemination was similar to the time of embryo collection after *in vitro* fertilization (Table 1), indicating globally similar rates of development. Although their morphology was similar to those developed *in vivo*, some embryos developed *in vitro* tended to appear darker than *in vivo*-developed embryos, probably due to the accumulation of lipid droplets and increased debris in the perivtelline space and intercellular cavities [9–12, 17]. Therefore, proteomic differences may in part explain the reported ultrastructural alterations in bovine *in vitro*-produced embryos, which are associated with lower tolerance to cryopreservation and developmental ability.

Differences in embryo genome activation between *in vivo*- and *in vitro*-derived embryos

The switch from mRNA and proteins derived from the oocyte to those resulting from embryonic genome activation (EGA) is a critical step during embryo development. Based on previous transcriptomic data, the onset of EGA in cattle was timed between the 8-cell and 16-cell stages [8, 35–37]. Our previous proteomic analysis of *in vivo*-derived embryos evidenced a significant increase in proteins involved in protein synthesis between the 8–12 cell and morula stages, consistent with a major EGA starting around the 8-cell stage [26]. The present results confirm that EGA occurred approximately at the same time in *in vitro*-derived embryos; a marked increase in the abundance of proteins involved in protein synthesis was clearly seen after the 8–12 cell stage, resulting in increased numbers of proteins identified per embryo up to the blastocyst stage. This is in line with previous data that showed an increase in the uptake of ^{35}S-methionine to measure de novo protein synthesis in embryos starting from the 8- to 16-cell stage in both *in vivo*- and *in vitro*-derived bovine embryos [22].

(See figure on next page.)

Fig. 10 Functional analysis of proteins less abundant *in vivo* than *in vitro* at each developmental stage. The Metascape heatmap plots represent the top 20 clusters of enriched GO terms of biological processes and KEGG pathways (**A**), molecular functions (**B**), and cellular components (**C**). Each row represents one enriched cluster and the orange gradation reflects statistical significance (the darker the color, the more significant the *p*-value is). Gray color indicates a lack of significance. DAPs with a t-test *p*-value ≤ 0.05 and fold-change ratio ≥ 1.5 were considered

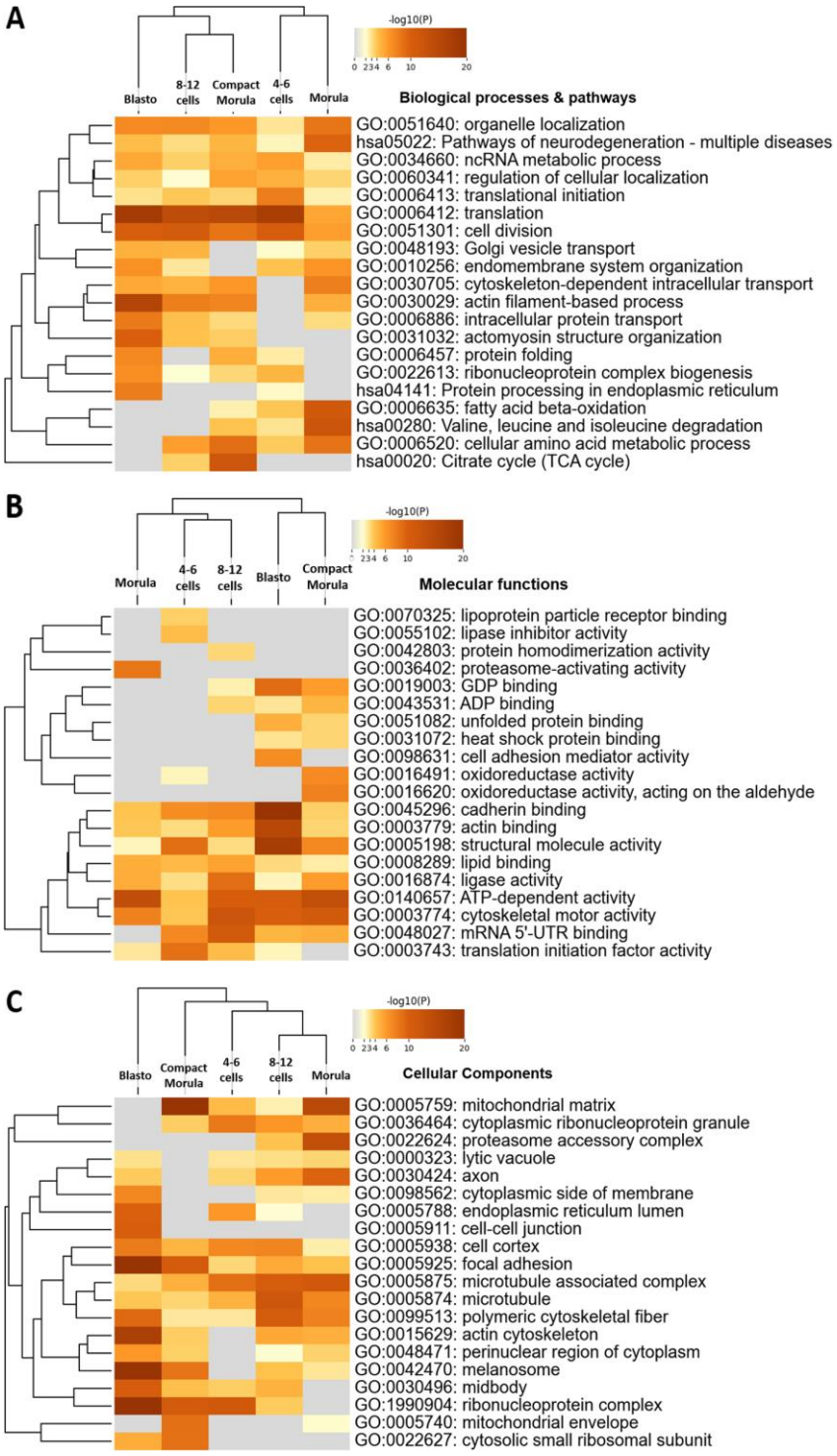

Fig. 10 (See legend on previous page.)

Table 1 Pools of *in vivo*- and *in vitro*-derived bovine embryos used for nanoLC-MS/MS analysis ($n = 4$ embryos per pool)

Embryonic stage	Origin	Time of embryo collection after AI1 or IVF[a]	Female donors[b]	Bull semen[c]	Number of pools
4–6 cells	*In vivo*	Days 1.7–3.8	A, B, C, D	X	3
	In vitro	Day 2		X	4
8–12 cells	*In vivo*	Days 3.6–3.8	A, B	X	4
	In vitro	Day 3		X	4
Morula (> 16 cells)	*In vivo*	Days 5.7–6.7	E, F, G	X	3
	In vitro	Days 5–6		X	4
Compact morula	*In vivo*	Days 5.7–6.8	E, F, H	X	4
	In vitro	Day 6		X	4
Blastocyst	*In vivo*	Days 6.8–7.5	H, I, J, K	X, Y, Z	4
	In vitro	Days 7–8		X	4

[a] *IA1* first artificial insemination of donor cows for *in vivo*-derived embryos, *IVF in vitro* fertilization

[b] A total of 9 Holstein cows (called A to I) and 2 Holstein heifers (called J and K) were used as female donors for *in vivo*-derived embryos. *In vitro*-derived embryos were produced from ovaries collected at a commercial slaughterhouse

[c] A total of 3 bulls of proven fertility, one Normande (called X) and two Holstein (called Y and Z), were used for the production of *in vivo*-derived embryos; the X bull was used for *in vitro*-produced embryos

However, dynamics in total numbers of proteins identified slightly differed between *in vivo* and *in vitro*-derived embryos around EGA. While protein numbers reached a nadir in *in vivo*-derived embryos at the morula stage then increased again up to the blastocyst stage, *in vitro*-derived embryos had constantly increased numbers of proteins. Furthermore, the increase in proteins involved in protein synthesis was much stronger and faster in *in vitro*-derived embryos compared to their *in vivo* counterparts, resulting in the identification of cluster 2 regrouping proteins largely involved in protein synthesis.

The most significant enriched GO terms in cluster 2 were related to cytoplasmic translation and included multiple ribosomal proteins (of the small 40S and large 60S ribosomal subunits, RPSs and RPLs, respectively) as well as eukaryotic translation initiation factors (EIF4G1, EIF4G2, EIF3E…) and proteins involved in positive regulation of protein translation (DDX3X, HNRNPU, HSPB1…). In accordance, translation and other biological processes related to RNA metabolism were among the most significantly enriched pathways for proteins found more abundant *in vitro* at each stage. In accordance with our results, the uptake of ^{35}S-methionine was significantly higher in *in vitro*-produced bovine embryos as compared to *in vivo*-derived embryos from the 8–16 cell to the blastocyst stages [22]. A culture effect on the expression of genes involved in gene expression was also observed by comparing the transcriptomic profiles of bovine blastocysts fertilized *in vitro* or *in vivo* [19].

The present results indicate that *in vitro* fertilization and culture conditions led to a higher abundance of proteins involved in RNA metabolism and translation at the time of EGA. Although spending more resources for protein synthesis, the blastocysts produced *in vitro* did not display a higher number of proteins compared to *in vivo*-developed blastocysts, in line with previous data reporting similar total protein contents in bovine blastocysts of both origins [38]. The higher abundance of translation-related proteins in *in vitro*-derived embryos may be due to an upregulation of genes coding for those proteins coupled or not with a lower turn-over of those proteins, as compared to *in vivo*. These results are globally in accordance with the "quiet embryo" hypothesis, in which a premature or an excessive activation of the embryonic genome, in response to an unfavorable environment, decreases the ability of an embryo to pursue development [22]. In the "quiet embryo" hypothesis, it was suggested that the embryos possessing a greater ability to recycle endogenous proteins via specific degradation pathways before EGA has an advantage to pursue development [22]. We speculate that the upregulation of proteins involved in protein synthesis in embryos produced *in vitro* may compensate for their lower consumption of oocyte-derived proteins before EGA.

Specificity of the blastocyst stage

The blastocyst stage retrieved several particularities in the present study. The number of proteins identified were highest in both groups of blastocysts compared with earlier stages. This was expected as protein synthesis has been reported to overcome protein degradation after EGA, leading to an increased amount of proteins per embryo [38]. The PCA of all quantified proteins

evidenced gaps between blastocysts and compact morulas in both groups of embryos and also between *in vivo* and *in vitro* blastocysts. This was confirmed after pair-wise comparison of proteins at each stage, which retrieved the highest number of DAPs in blastocysts. In accordance, the functional analysis of DAPs at the blastocyst stage evidenced several processes and pathways overrepresented only at this stage.

In order to decrease genetic heterogeneity between embryos, only one Normande bull was used for the production of all embryos produced *in vitro* and most embryos produced *in vivo*. While all embryos developed *in vivo* up to the compact morula stage had the same bull as *in vitro*-fertilized embryos as progenitor, 10 out of 16 *in vivo*-derived blastocysts were obtained with two additional Holstein bulls. This was needed for technical, economical, and ethical reasons as donor cows did not provide enough blastocysts. As a result, *in vivo* blastocysts originated from three fathers, whereas all other embryos had one father out of the three previous ones. However, the three bulls used had very similar fertility, as assessed on a large population of cows and heifers (59%–62% and 45%–49% of non-return rates at 90 days after insemination on more than 3,200 and 22,800 heifers and cows, respectively). It has been shown that the father has an impact on gene expression and epigenomics in bovine blastocysts [39, 40], which may account for differences in protein abundance between blastocysts in this study.

Higher abundance of proteins involved in carbohydrate metabolism in *in vivo*-derived embryos

The most crucial nutrients for early developing embryos are carbohydrates and amino acids, which not only provide energy and substrates for protein synthesis but act as players of epigenetic programming [41]. The DAPs found more abundant in the *in vivo*-derived embryos compared to *in vitro*-derived embryos were largely involved in energy metabolism. For proteins overabundant *in vivo* across development (cluster 1) and at each stage (after pair-wise comparisons), the most significantly enriched GO terms were related to carbohydrate metabolism. In accordance, previous transcriptomic studies evidenced that the most significant GO terms of differentially expressed genes between bovine *in vivo*- and *in vitro*-derived blastocysts were related to metabolic processes, including carbohydrate metabolism but also lipid, nucleic acid, and amino acid metabolism [17, 18]. Similarly, a high proportion of genes related to metabolism was dysregulated when porcine *in vivo*- or *in vitro*-derived blastocysts were compared, most of which were upregulated *in vivo* [42].

When considering *in vivo*-derived embryos, the enrichment in the carbohydrate metabolic and catabolic processes started at the 8–12 cell stage and reached highest significance at the compact morula and blastocyst stages. Our results indicate that *in vivo*-derived embryos allocated more resources toward the synthesis of key glycolytic enzymes compared to their *in vitro* counterparts as soon as the 8–12 cell stage. Around this stage, bovine embryos enter the uterus, where concentrations of glucose are higher than in the oviduct fluid [43]. Our results are in accordance with previous reports on bovine embryos that observed the first increase in pyruvate and glucose utilization between the 8- and 16-cell stages, i.e., around the time of EGA, and significant increases in the oxidation of pyruvate, glucose, and lactose at the time of morula compaction [14, 15]. The proteins found more abundant in the *in vivo*-derived embryos of this study regrouped proteins of the pyruvate metabolic pathway (fructose bisphosphate aldolase, ALDOA; phosphoglycerate mutase, BPGM; galactokinase, GALK1; L-lactate dehydrogenase A and B chains, LDHA and LDHB; phosphoglycerate mutase 1, PGAM1; phosphoglycerate kinase 1, PGK1; phosphoglucomutase-1, PGM1…) as well as many proteins involved in the glycolytic (GAPDH, GPI, HK2, PGK1, PGM1 and alpha-enolase, ENO1) and pentose phosphate (glucose-6-phosphate 1-dehydrogenase, G6PD; 6-phosphogluconate dehydrogenase, decarboxylating, PGD; ribose-5-phosphate isomerase, RPIA; transketolase, TKT; transaldolase, TALDO1) pathways. It is well established that early mammalian embryos use mostly pyruvate as the preferred carbohydrate, which is metabolized through the tricarboxylic acid (TCA) cycle and oxidative phosphorylation to produce ATP, then when the demand for energy increases, glucose is metabolized through the pentose phosphate pathway and the glycolysis pathway, in addition to the TCA cycle [44].

While the large majority of studies on embryo metabolism used *in vitro*-derived embryos, there are few comparing carbohydrate metabolism of *in vivo*- and *in vitro*-derived embryos at the same stages of development and within the same experiments [14, 45]. Globally similar patterns of glucose, pyruvate, and lactate consumption were observed in bovine early embryos of both origins, except a lower carbon uptake and higher rate of lactate conversion from glucose (i.e. higher glycolysis) after the 16-cell stage in *in vitro*-derived embryos as compared to their *in vivo* counterparts [14]. In the present study, most enzymes involved in glucose-to-lactate conversion were found more abundant in *in vivo*-derived embryos after the 8–12 cell stage (hexokinase HK2; glyceraldehyde-3-phosphate dehydrogenase, GAPDH; phosphoglycerate kinase 1, PGK1) or at all stages (glucose-6-phosphate isomerase, GPI; phosphoglucomutase-1, PGM1; alpha-enolase, ENO1; L-lactate dehydrogenase, LDHA). This is suggestive of a higher glycolytic rate in *in vivo*-derived

embryos. Proteins of the pentose phosphate pathway were also more abundant in *in vivo*-derived embryos, suggesting that glucose may also be converted into NADPH and pentoses at a higher rate as compared to *in vitro*-derived embryos.

Although *in vivo*-derived embryos had low abundance of proteins dedicated to protein synthesis suggestive of a "quiet EGA", their carbohydrate metabolism seemed more active as compared to *in vitro*-produced embryos. According to our results, the allocation of resources toward carbohydrate metabolism rather than protein synthesis at the time of EGA may be predictive of higher developmental ability. This does not support the hypothesis of the "quiet metabolism", that is a low rather than active metabolism could support better embryo viability and further development [22, 23]. Interestingly, intermediate, but not low, levels of pyruvate consumption have been identified to be predictive of bovine embryo quality and the ability to develop up to the blastocyst stage *in vitro* [24]. Although the "quiet embryo" hypothesis has been recently reworked to propose an optimal range of metabolic activity depending on individual embryos [46], our results are more in favor of an active carbohydrate metabolism to pursue development.

Oviduct origin of proteins found more abundant in *in vivo*-derived embryos

Overabundant proteins in *in vivo*-derived embryos may result from higher protein synthesis, lower protein degradation, and/or internalization from the maternal tract fluids. As discussed above, higher protein synthesis in *in vivo*-derived embryos is unlikely, especially after EGA, as there was no increase in the total amount of proteins identified. Furthermore, contrary to cluster 2, proteins in cluster 1 were not functionally implied in protein synthesis. It is probable that some proteins present in the post-ovulatory oviduct fluid and able to cross the zona pellucida were internalized by *in vivo*-derived embryos. It is to note that *in vivo*-derived embryos were extensively washed before analysis to avoid contamination with oviduct/uterine fluids at the surface of the zona pellucida.

Many studies using various culture conditions mimicking the maternal environment have shown that the secretions of the oviduct are determinant for early embryo quality [28, 47–49]. However, very few oviductal proteins involved in embryo development have been identified to date, and most studies used *in vitro*-derived embryos [25, 50–53], which gives a biased picture of this issue. It has been well established that OVGP1, a glycoprotein of around 100 kDa secreted in the oviduct fluid, has the ability to cross the zona pellucida and be internalized by developing mammalian embryos [25, 54–57]. From *in vitro* studies, positive effects of purified or recombinant OVGP1 on embryo development have been evidenced in mice [53], goats [52], and cattle [51]. It appears from our data that OVGP1 is not strictly speaking an oviduct-specific protein since OVGP1 was detected in all *in vitro*-developed embryos (at 6 to 23 NWS on average), in accord with a previous study that detected low levels of OVGP1 mRNAs in bovine 8-cell embryos produced *in vitro* without oviduct cells or fluid [58]. Nevertheless, OVGP1 was on average 9- to 44-fold more abundant in embryos developed *in vivo* as compared to those produced *in vitro* (mean fold-change ratios of 44, 10, 16, 16, and 9 at the 4–6 cell, 8–12 cell, morula, compact morula, and blastocyst stages, respectively), confirming that this protein is internalized by embryos from the start of development. In accordance, previous observation using immunolabelling of OVGP1 in embryos collected *in vivo* revealed that this protein localized in the perivitelline space and inside embryo blastomeres in baboons [55], golden hamsters [56], pigs [57], and cattle [25, 54].

Some other proteins found overabundant in the *in vivo*-derived embryos were previously identified as interacting with *in vitro*-produced embryos after incubation with post-ovulatory oviduct fluid, including retinal dehydrogenase 1 (ALDH1A1) and alpha isoform of regulatory subunit A protein phosphatase 2 (PPP2R1A) at the 4–6 cell stage, cytoplasmic aconitate hydratase (ACO1), hemoglobin subunit beta (HBB) and purine nucleoside phosphorylase (PNP) at the morula stage, and annexin A8 (ANXA8), creatine kinase B-type (CKB), chloride intracellular channel protein 1 (CLIC1), cytosolic non-specific dipeptidase (CNDP2), hemoglobin subunit alpha (HBA), ribonuclease inhibitor (RNH1), tubulin polymerization-promoting protein family member 3 (TPPP3), and CD109 at both stages [25]. A comparison between proteins in cluster 1 and those identified by MS in the isthmic part of the oviduct fluid just after ovulation [59], i.e., place and time of early embryo development, indicates that 341 (75%) are also present in the oviduct fluid (data not shown). Among those, OVGP1, CD109, CLU, RARRES1, and tubulin beta-4B chain (TUBB4B) were quantified at high abundance in the postovulatory oviduct fluid (36 to 121 NWS, [59]) and were found overabundant in *in vivo*-derived embryos from the 4–6 cell up to blastocyst stages, making them good candidates for embryo-interacting proteins originated in the oviduct.

The present database is valuable for further functional studies on embryo-maternal interactions and may allow us to exclude some hypotheses, at least in the bovine species. For instance, complement C3 was previously reported as an oviductal cell-derived protein with embryotropic activity in rodents [60, 61] and shown to be internalized by rat embryos just after implantation [61]. In this study, C3 was more abundant *in vitro* than *in vivo*

from the 4–6 cell to compact morula stages and identified in cluster 3. Therefore, although C3 was reported at high abundance in the bovine post-ovulatory OF [59], the present data do not support any internalization by cattle embryos *in vivo*.

Limitations of the study

For technical and ethical reasons, female donors were synchronized for estrus and treated for superovulation, which may modify the endocrine environment of *in vivo*-developed embryos compared to classical insemination [62] and have consequences on their proteome. In addition, the number of bulls used as progenitors was voluntarily low, which probably helped identify differences between *in vivo* and *in vitro*-derived embryos by decreasing genetic heterogeneity but does not reflect the proteomic diversity of bovine embryos.

In vitro-produced embryos were cultured without any protein or serum supplementation to avoid protein contaminant. The absence of proteins in the culture medium may have induced specific pathways compared with embryos developed in the presence of serum or proteins in the culture medium.

Conclusions

The maternal environment led to higher degradation of mitochondrial proteins at early developmental stages, lower abundance of proteins involved in protein synthesis at the time of embryonic genome activation, and a global upregulation of carbohydrate and small molecule metabolic pathways compared to *in vitro* production. Furthermore, our data confirm that embryos developed *in vivo* uptake large amounts of OVGP1 and probably other oviduct fluid-derived proteins as soon as the 4–6 cell stage. These data provide new insight into the molecular contribution of the maternal environment to the developmental ability of early embryos. Moreover, the DAPs identified constitute valuable markers of embryo quality and target pathways for the assessment of new *in vitro* systems, closer to *in vivo* conditions.

Methods

Collection of embryos developed *in vivo* from synchronized donors

The protocol used for embryo collection was reported previously [26]. A total of 11 Holstein females (9 dried off cows and 2 heifers, aged 1–5 years) housed at the INRAE Experimental Unit of Animal Physiology of the Orfrasière (Nouzilly, France) were used as donor animals. The estrus cycles of the donors were synchronized with the prostaglandin analog cloprostenol (0.5 mg, i.m.; Estrumate, MSD Animal Health, Beaucouzé, France) and all females showing normal estrus and an ovarian corpus luteum 7 days after estrus (checked by ultrasonography) received a progesterone-releasing intravaginal device (PRID DELTA, Ceva Santé animale, Libourne, France). Ovarian stimulation treatment started 12 days after estrus and consisted of eight intramuscular injections of decreasing porcine Follicle stimulating hormone (pFSH)/porcine Luteinizing hormone (pLH) doses every 12 h over 4 days (Stimufol, Reprobiol, Liège, Belgique; 500 µg pFSH and 100 µg pLH in total in cows; 350 µg pFSH and 70 µg pLH in total in heifers). Luteolysis was induced with 2 mL of cloprostenol (0.5 mg, i.m; Estrumate, MSD Animal Health, Beaucouzé, France) and the PRID DELTA device was withdrawn together with the fourth and sixth FSH administrations, respectively.

For embryo collection, donor females were inseminated twice with frozen-thawed semen from one bull of proven fertility 12 and 24 h after standing estrus. The same ejaculate from one Normande bull (called X) was used for all embryos except 10 blastocysts for which two extra Holstein bulls (called Y and Z) were used (Table 1). Bulls' fertility was previously estimated by the 90-day non-return rate after artificial insemination (AI) on a large population of dairy females and ranged from 59 to 62% in heifers (3,241–8,587 AI per bull) and from 45 to 49% in lactating cows (22,864–26,623 AI per bull). The 10 blastocysts from bulls Y and Z were collected by non-invasive cervical flushing of the uterine horns of heifers (one flushing session per heifer) on day 7 after the first AI, as previously described [26]. All other *in vivo*-derived embryos were recovered after the slaughter of donor cows between days 1.7 and 7.5 after the first AI in the local experimental slaughterhouse. The genital tracts were immediately processed on site. Oviducts and uterine horns were flushed with 5 mL and 35 mL, respectively, of prewarmed phosphate buffered saline (PBS) and 0.1% polyvinyl alcohol (PVA) at 38.5 °C. Recovered fluids were carefully observed for the presence of embryos under a stereomicroscope, and all embryos were classified for quality grade and stage of development according to the IETS recommendations [63]. Only grade-1 embryos, i.e., embryos consistent with their expected stage of development, with blastomeres uniform in size, color, and density, with few irregularities or excluded cells, and an intact and smooth zona pellucida, were used.

All embryos were thoroughly washed three times in 20 mM Tris–HCl buffer (pH 6.8) supplemented with 8.9% sucrose (Tris-sucrose), minimizing contamination from oviduct and uterine fluids, then individually frozen at -80 °C. Typically, the time period between animal death and genital tract flushing and between flushing and embryo freezing was less than 15 and 30 min, respectively.

Production of embryos developed *in vitro*

Bovine embryos were produced *in vitro* as previously described [25] in parallel with the flushing sessions. Bovine ovaries were collected from a local slaughterhouse (slaughtering mostly Holstein cows) and transported at 36 °C to the laboratory. Cumulus-oocyte complexes (COCs) were recovered using HEPES-buffered TCM-199 supplemented with 0.4 g/L bovine serum albumin (BSA) and 0.25% gentamicin. Groups of 30–60 COCs were matured in TCM-199 supplemented with 10 ng/mL EGF, 19 ng/mL IGF-1, 2.2 ng/mL FGF, 5 UI/mL hCG, 10 UI/mL PMSG, 4 µg/mL transferrin, 4 µg/mL insulin, 5 ng/mL sodium selenite, 1% PG-600, 90 µg/mL L-cysteine, 0.1 mM beta-mercaptoethanol, 75 µg/mL ascorbic acid, 720 µg/mL glycine, 0.1 mg/mL glutamine, and 110 µg/mL pyruvate at 38.8 °C (5% CO2) for 22 h. After maturation, COCs were transferred in 250 µL of fertilization medium (Tyrode medium supplemented with 25 mM bicarbonate, 10 mM lactate, 1 mM pyruvate, 6 mg/mL fatty-acid free BSA, 10 µg/ml heparin, and 40 µg/ml gentamicin). To minimize variability between embryos, the Normande bull X used for most *in vivo*-derived embryos was used for all *in vitro* fertilization (IVF) (Table 1). Motile spermatozoa were recovered by Percoll washing and added to the fertilization medium (day 0) at a final concentration of 10^6 spermatozoa/mL for 22 h. At day 1, all presumptive zygotes were cultured in 25 µL of synthetic oviductal fluid (SOF) medium [64] supplemented with 0.01% of polyvinyl alcohol (SOF-PVA) under mineral oil (M8410) at 38.8 °C with 5% CO_2 and 5% O_2. To avoid protein contamination, embryos were cultured without any serum or protein supplementation. Only grade-1 embryos according to the IETS classification were retained for analysis. As for *in vivo*-derived embryos, all *in vitro*-produced embryos were washed three times in Tris-sucrose then stored individually in 1.5 mL tubes at -80 °C. A total of 9 IVF replicates were done and embryos at a given stage were originated from at least three IVF replicates.

Analysis of embryo proteins by nanoLC-MS/MS

All embryos (with no sex determination) were thawed on ice and pools of 4 embryos at the same stage after *in vivo* or *in vitro* development were prepared under a stereomicroscope for a total of 3–4 pools per origin × stage (Table 1). Tubes containing embryos were manipulated for no more than 10 min at ambient temperature. After brief pelleting, the excess Tris-sucrose was eliminated and tubes were stored at -80 °C until proteomic analysis. Proteins from pools of embryos were extracted and digested using the PreOmics iST-BCT kit following the manufacturer's instructions. Briefly, samples were thawed and lysed (denatured, reduced, and alkylated) for 10 min at 95 °C then trypsin/LysC digested for 60 min at 37 °C. Purification of peptides was then carried out at room temperature on spin cartridges and peptides were finally eluted in 10 µL of LC-load buffer. The volume corresponding to one equivalent-embryo (corresponding to approximately 300 ng proteins) was then loaded on a 75 µm × 250 mm IonOpticks Aurora 2 C18 column (Ion Opticks Pty Ltd., Bundoora, Australia). Peptide analysis was performed as previously described [25]. A gradient of basic reversed-phase buffers (Buffer A: 0.1% formic acid, 98% H_2O MilliQ, 2% acetonitrile; Buffer B: 0.1% formic acid, 100% acetonitrile) was run on a NanoElute high performance liquid chromatography (HPLC) System (Bruker Daltonik GmbH, Bremen, Germany) at a flow rate of 400 nL/min at 50 °C. The liquid chromatography (LC) run lasted for 120 min (2% to 15% of buffer B during 60 min; up to 25% at 90 min; up to 37% at 100 min; up to 95% at 110 min, and finally 95% for 10 min to wash the column). The column was coupled online to a trapped ion motility spectrometry-time of flight (TIMS-TOF) Pro (Bruker Daltonik GmbH, Bremen, Germany) with a CaptiveSpray ion source (Bruker Daltonik). The temperature of the ion transfer capillary was set at 180 °C. Ions were accumulated for 114 ms, and mobility separation was achieved by ramping the entrance potential from -160 V to -20 V within 114 ms. The acquisition of the MS and MS/MS mass spectra was done with average resolutions of 60,000 and 50,000 full width at half maximum (mass range 100–1,700 m/*z*), respectively. To enable the parallel accumulation-serial fragmentation (PASEF) method, precursor *m/z* and mobility information was first derived from full scan TIMS-MS experiments (with a mass range of 100–1,700 m/*z*). The quadrupole isolation width was set to 2 and 3 Th, and for fragmentation, the collision energies varied between 31 and 52 eV depending on the precursor mass and charge. TIMS, MS operation, and PASEF were controlled and synchronized using the control instrument software OtofControl 5.1 (Bruker Daltonik). LC–MS/MS data were acquired using the PASEF method with a total cycle time of 1.31 s, including 1 TIMS MS scan and 10 PASEF MS/MA scans. The 10 PASEF scans (100 ms each) contained, on average, 12 MS/MS scans per PASEF scan. Ion mobility-resolved mass spectra, nested ion mobility, *m/z* distributions, and summed fragment ion intensities were extracted from the raw data file with DataAnalysis 5.1 (Bruker Daltonik GmbH, Bremen, Germany).

Protein identification and data validation

Peptides were identified using the Mascot software (version 2.5.1; Matrix Science, 454 London, UK) against the UniProt *Bos taurus* database (May 2019; 23,523 sequences) using its automatic decoy database search to

calculate a false discovery rate (FDR). The parameters used for database searches included trypsin as enzyme (one missed cleavage allowed), carbamidomethylcysteine as fixed modification, oxidation of methionine, and N-terminal protein acetylation as variable modifications. Monoisotopic mass was considered, and mass tolerance was set at 15 ppm for MS ions and 0.05 Da for MS/MS ions. Mascot results from the target and decoy databases were incorporated to Scaffold Q+software (version 5.0.1, Proteome Software, Portland, USA, www.proteomesoftware.com) for data validation. Threshold for peptide and protein identification were set to 95.0% as specified by the Peptide Prophet algorithm [65] and the Protein Prophet algorithm [66]. To exclude potential human contaminants from the pool of keratin proteins (KRT 1, 2, 5, 7, 8, 10, 14, 18, 19, 24, 28, 71, and 75), the peptides identified in the *Bos taurus* database were blasted against the *Homo sapiens* homologous sequences. For all keratins, the peptide sequences were specific to *Bos Taurus*, excluding human contaminants.

Label-free protein quantification and statistical analysis

All proteins containing at least two unique peptides (FDR < 0.01%) were considered for protein quantification. Protein quantification was based on a label-free approach using the spectral counting method, as previously described [67, 68]. The "Spectral Count" quantitative module of Scaffold Q+software (Proteome Software, version 5.0.1) was used. The normalization of spectra among samples was realized in "Scaffold" by adjusting the sum of the selected quantitative values for all proteins within each MS sample to a common value, which was the average of the sums of all MS samples present in the experiment. This was achieved by applying a scaling factor for each sample to each protein or protein group. Thus, the number of NWS were tabulated using experiment-wide protein clusters.

Statistical analysis was performed on proteins quantified with a minimum of 2.0 NWS (mean value of biological replicates) in at least one origin × stage. To obtain an overview of proteomic data, PCA of all samples was carried out using RStudio software (version 1.4.1106) and the FactoMineR package. Analysis of variance (ANOVA) on biological replicates was done using RStudio. The hierarchical clustering of DAPs (ANOVA p-value ≤ 0.050) were done using Spearman correlations and the "gplots" package of RStudio. Finally, pairwise comparisons of protein abundance between *in vitro* and *in vivo*-derived embryos at a given stage were evaluated by Student's t-tests using RStudio. Proteins were considered as differentially abundant with a t-test p-value ≤ 0.050, fold-change ratio > 1.5, and a minimum of 2.0 NWS (mean value of biological replicates) for higher abundance.

Functional analysis of differentially abundant proteins

The overlap of identified proteins between stages and origins was visualized using the jvenn online tool (http://jvenn.toulouse.inra.fr) [69]. Functional analysis of DAPs in the three clusters (ANOVA p-value ≤ 0.050) and in pairwise comparisons between origins at a given stage (t-test p-value ≤ 0.050) was performed using the corresponding gene lists and Metascape online tool (metascape.org) [70]. Since the *Bos taurus* taxonomy was unavailable in Metascape, the *Homo sapiens* genome was used as background, and the gene list was converted in *Homo sapiens* orthologs. For individual and combined gene lists, three successive enrichment analyses were undertaken: 1) pathway enrichment using the GO biological processes and the Kyoto Encyclopedia of Genes and Genomes (KEGG) pathways; 2) functional enrichment using the GO molecular functions; and 3) structural enrichment using the GO cellular components. Terms with a p-value < 0.01, a minimum count of 3, and an enrichment factor > 1.5 (the enrichment factor is the ratio between the observed counts and the counts expected by chance) were collected and grouped by Metascape into clusters based on their membership similarities. In histograms presenting the enriched terms, the most statistically significant term within a cluster is chosen by Metascape to represent the cluster.

Abbreviations

DAP: Differentially abundant protein; EGA: Embryonic Genome Activation; GO: Gene Ontology; IVF: *in vitro* Fertilization; NWS: Normalized Weighted Spectra; PCA: Principal Component Analysis.

Supplementary Information

The online version contains supplementary material available at https://doi.org/10.1186/s12864-022-09076-5.

Additional file 1: Figure S1.

Additional file 2: Tables S1–S8.

Acknowledgements

The authors acknowledge Union Evolution and Allice, France, for providing bull semen required for this study. The authors are grateful to Eric Briant, Damien Capo, Jean-Philippe Dubois, Sylvan Bourgeois, and Tiphaine Aguirre-Lavin (UEPAO) for the management and sacrifice of embryo donors.

Authors' contributions

M.S.D., B.G., and P.M. initiated the project and designed the study; C.B. and M.S.D. collected the materials; C.B. prepared the materials for analysis; E.C. and R.L. did the MS analysis under the supervision of C.P.; C.B., V.L., and C.M. analyzed the data; M.S.D. and C.M. wrote the original draft; M.S.D., B.G., and C.P. acquired and administrated the funding; all authors read and approved the manuscript.

Funding

This work was funded by Union Evolution and INRAE. C.B. was funded by the National Association of Research and Technology (ANRT), grant number 2017/0684. This work was also supported by grants from Biogenouest,

Infrastructures in Biology, Health and Agronomy (IBiSA), and Regional Council of Brittany (France) awarded to C.P.

Availability of data and materials
The datasets generated during the current study are available in the ProteomeXchange Consortium via the PRIDE [71] partner repository (www.ebi.ac.uk/pride/archive/login) with the dataset identifier PXD035294 and https://doi.org/10.6019/PXD035294.

Declarations

Ethics approval and consent to participate
All experimental protocols were conducted following the European directive 2010/63/EU on the protection of animals used for scientific purposes and approved by the French Ministry of National Education, Higher Education, Research, and Innovation after ethical assessment by the local ethics committee "Comité d'Ethique en Experimentation Animale Val de Loire (CEEA VdL)". The protocol was registered under the number CE19-2021–0402-1. The study was conducted in accordance with the ARRIVE guidelines (https://arriveguidelines.org).

Consent for publication
Not applicable.

Competing interests
The authors declare that that they have no competing interests.

Author details
[1]INRAE, CNRS, Tours University, IFCE, UMR PRC, Nouzilly, France. [2]Union Evolution, Rue Eric Tabarly, Noyal-Sur-Vilaine, France. [3]Univ Rennes, Inserm, EHESP, Irset (Institut de Recherche en Santé, Environnement et Travail), UMR_S 1085, Rennes, France. [4]Univ Rennes, CNRS, Inserm, Biosit UAR 3480 US_S 018, Protim Core Facility, Rennes, France. [5]Pixanim, INRAE, Tours University, CHU of Tours, Nouzilly, France.

Received: 26 September 2022 Accepted: 8 December 2022
Published online: 19 December 2022

References

1. Wyns C, De Geyter C, Calhaz-Jorge C, Kupka MS, Motrenko T, Smeenk J, Bergh C, Tandler-Schneider A, Rugescu IA, Vidakovic S, et al. ART in Europe, 2017: results generated from European registries by ESHRE. Hum Reprod Open. 2021;2021(3):1–17.
2. Ferre LB, Kjelland ME, Strobech LB, Hyttel P, Mermillod P, Ross PJ. Review: Recent advances in bovine *in vitro* embryo production: reproductive biotechnology history and methods. Animal. 2020;14(5):991–1004.
3. Viana JHM. 2020 Statistics of embryo production and transfer in domestic farm animals. Embryo Technol Newsletter. 2021;39(4):1–14.
4. Rizos D, Clemente M, Bermejo-Alvarez P, de La Fuente J, Lonergan P, Gutierrez-Adan A. Consequences of *in vitro* culture conditions on embryo development and quality. Reprod Domest Anim. 2008;43(Suppl 4):44–50.
5. Ealy AD, Wooldridge LK, McCoski SR. BOARD INVITED REVIEW: Post-transfer consequences of *in vitro*-produced embryos in cattle. J Anim Sci. 2019;97(6):2555–68.
6. Menezo YJ, Herubel F. Mouse and bovine models for human IVF. Reprod Biomed Online. 2002;4(2):170–5.
7. Schulz KN, Harrison MM. Mechanisms regulating zygotic genome activation. Nat Rev Genet. 2019;20(4):221–34.
8. Jiang Z, Sun J, Dong H, Luo O, Zheng X, Obergfell C, Tang Y, Bi J, O'Neill R, Ruan Y, et al. Transcriptional profiles of bovine *in vivo* pre-implantation development. BMC Genomics. 2014;15:756.
9. Fair T, Lonergan P, Dinnyes A, Cottell DC, Hyttel P, Ward FA, Boland MP. Ultrastructure of bovine blastocysts following cryopreservation: effect of method of blastocyst production. Mol Reprod Dev. 2001;58(2):186–95.
10. Rizos D, Fair T, Papadopoulos S, Boland MP, Lonergan P. Developmental, qualitative, and ultrastructural differences between ovine and bovine embryos produced *in vivo* or *in vitro*. Mol Reprod Dev. 2002;62(3):320–7.
11. Abe H, Yamashita S, Satoh T, Hoshi H. Accumulation of cytoplasmic lipid droplets in bovine embryos and cryotolerance of embryos developed in different culture systems using serum-free or serum-containing media. Mol Reprod Dev. 2002;61(1):57–66.
12. Rizos D, Ward F, Duffy P, Boland MP, Lonergan P. Consequences of bovine oocyte maturation, fertilization or early embryo development *in vitro* versus *in vivo*: implications for blastocyst yield and blastocyst quality. Mol Reprod Dev. 2002;61(2):234–48.
13. Janati Idrissi S, Le Bourhis D, Lefevre A, Emond P, Le Berre L, Desnoes O, Joly T, Buff S, Maillard V, Schibler L, et al. Lipid profile of bovine grade-1 blastocysts produced either *in vivo* or *in vitro* before and after slow freezing process. Sci Rep. 2021;11(1):11618.
14. Khurana NK, Niemann H. Energy metabolism in preimplantation bovine embryos derived *in vitro* or *in vivo*. Biol Reprod. 2000;62(4):847–56.
15. Gardner DK. Changes in requirements and utilization of nutrients during mammalian preimplantation embryo development and their significance in embryo culture. Theriogenology. 1998;49(1):83–102.
16. de Andrade Melo-Sterza F, Poehland R. Lipid Metabolism in Bovine Oocytes and Early Embryos under *In vivo*, *In vitro*, and Stress Conditions. Int J Mol Sci. 2021;22(7):3421.
17. Gad A, Hoelker M, Besenfelder U, Havlicek V, Cinar U, Rings F, Held E, Dufort I, Sirard MA, Schellander K, et al. Molecular mechanisms and pathways involved in bovine embryonic genome activation and their regulation by alternative *in vivo* and *in vitro* culture conditions. Biol Reprod. 2012;87(4):100.
18. Driver AM, Penagaricano F, Huang W, Ahmad KR, Hackbart KS, Wiltbank MC, Khatib H. RNA-Seq analysis uncovers transcriptomic variations between morphologically similar *in vivo*- and *in vitro*-derived bovine blastocysts. BMC Genomics. 2012;13:118.
19. Smith SL, Everts RE, Sung LY, Du F, Page RL, Henderson B, Rodriguez-Zas SL, Nedambale TL, Renard JP, Lewin HA, et al. Gene expression profiling of single bovine embryos uncovers significant effects of *in vitro* maturation, fertilization and culture. Mol Reprod Dev. 2009;76(1):38–47.
20. Knijn HM, Wrenzycki C, Hendriksen PJ, Vos PL, Zeinstra EC, van der Weijden GC, Niemann H, Dieleman SJ. *In vitro* and *in vivo* culture effects on mRNA expression of genes involved in metabolism and apoptosis in bovine embryos. Reprod Fertil Dev. 2005;17(8):775–84.
21. Salilew-Wondim D, Saeed-Zidane M, Hoelker M, Gebremedhn S, Poirier M, Pandey HO, Tholen E, Neuhoff C, Held E, Besenfelder U, et al. Genome-wide DNA methylation patterns of bovine blastocysts derived from *in vivo* embryos subjected to *in vitro* culture before, during or after embryonic genome activation. BMC Genomics. 2018;19(1):424.
22. Baumann CG, Morris DG, Sreenan JM, Leese HJ. The quiet embryo hypothesis: molecular characteristics favoring viability. Mol Reprod Dev. 2007;74(10):1345–53.
23. Leese HJ. Quiet please, do not disturb: a hypothesis of embryo metabolism and viability. BioEssays. 2002;24(9):845–9.
24. Guerif F, McKeegan P, Leese HJ, Sturmey RG. A simple approach for COnsumption and RElease (CORE) analysis of metabolic activity in single mammalian embryos. PLoS ONE. 2013;8(8):e67834.
25. Banliat C, Tsikis G, Labas V, Teixeira-Gomes AP, Com E, Lavigne R, Pineau C, Guyonnet B, Mermillod P, Saint-Dizier M. Identification of 56 Proteins Involved in Embryo-Maternal Interactions in the Bovine Oviduct. Int J Mol Sci. 2020;21(2):466.
26. Banliat C, Mahe C, Lavigne R, Com E, Pineau C, Labas V, Guyonnet B, Mermillod P, Saint-Dizier M. Dynamic Changes in the Proteome of Early Bovine Embryos Developed *In vivo*. Front Cell Dev Biol. 2022;10:863700.
27. Rizos D, Lonergan P, Boland MP, Arroyo-Garcia R, Pintado B, de la Fuente J, Gutierrez-Adan A. Analysis of differential messenger RNA expression between bovine blastocysts produced in different culture systems: implications for blastocyst quality. Biol Reprod. 2002;66(3):589–95.
28. Rizos D, Carter F, Besenfelder U, Havlicek V, Lonergan P. Contribution of the female reproductive tract to low fertility in postpartum lactating dairy cows. J Dairy Sci. 2010;93(3):1022–9.
29. Rizos D, Ramirez MA, Pintado B, Lonergan P, Gutierrez-Adan A. Culture of bovine embryos in intermediate host oviducts with emphasis on the isolated mouse oviduct. Theriogenology. 2010;73(6):777–85.
30. St John JC, Facucho-Oliveira J, Jiang Y, Kelly R, Salah R. Mitochondrial DNA transmission, replication and inheritance: a journey from the gamete through the embryo and into offspring and embryonic stem cells. Hum Reprod Update. 2010;16(5):488–509.

31. Coticchio G, Dal Canto M, Fadini R, Mignini Renzini M, Guglielmo MC, Miglietta S, Palmerini MG, Macchiarelli G, Nottola SA. Ultrastructure of human oocytes after *in vitro* maturation. Mol Hum Reprod. 2016;22(2):110–8.
32. Brad AM, Bormann CL, Swain JE, Durkin RE, Johnson AE, Clifford AL, Krisher RL. Glutathione and adenosine triphosphate content of *in vivo* and *in vitro* matured porcine oocytes. Mol Reprod Dev. 2003;64(4):492–8.
33. Noguchi T, Aizawa T, Munakata Y, Iwata H. Comparison of gene expression and mitochondria number between bovine blastocysts obtained *in vitro* and *in vivo*. J Reprod Dev. 2020;66(1):35–9.
34. Deutsch DR, Frohlich T, Otte KA, Beck A, Habermann FA, Wolf E, Arnold GJ. Stage-specific proteome signatures in early bovine embryo development. J Proteome Res. 2014;13(10):4363–76.
35. Kues WA, Sudheer S, Herrmann D, Carnwath JW, Havlicek V, Besenfelder U, Lehrach H, Adjaye J, Niemann H. Genome-wide expression profiling reveals distinct clusters of transcriptional regulation during bovine preimplantation development *in vivo*. Proc Natl Acad Sci U S A. 2008;105(50):19768–73.
36. Memili E, First NL. Developmental changes in RNA polymerase II in bovine oocytes, early embryos, and effect of alpha-amanitin on embryo development. Mol Reprod Dev. 1998;51(4):381–9.
37. Graf A, Krebs S, Heininen-Brown M, Zakhartchenko V, Blum H, Wolf E. Genome activation in bovine embryos: review of the literature and new insights from RNA sequencing experiments. Anim Reprod Sci. 2014;149(1–2):46–58.
38. Thompson JG, Sherman AN, Allen NW, McGowan LT, Tervit HR. Total protein content and protein synthesis within pre-elongation stage bovine embryos. Mol Reprod Dev. 1998;50(2):139–45.
39. Kropp J, Carrillo JA, Namous H, Daniels A, Salih SM, Song J, Khatib H. Male fertility status is associated with DNA methylation signatures in sperm and transcriptomic profiles of bovine preimplantation embryos. BMC Genomics. 2017;18(1):280.
40. Diaz-Lundahl S, Sundaram AYM, Gillund P, Gilfillan GD, Olsaker I, Krogenaes A. Gene Expression in Embryos From Norwegian Red Bulls With High or Low Non Return Rate: An RNA-Seq Study of *in vivo*-Produced Single Embryos. Front Genet. 2021;12:780113.
41. Milazzotto MP, de Lima CB, da Fonseca AM, Dos Santos EC, Ispada J. Erasing gametes to write blastocysts: metabolism as the new player in epigenetic reprogramming. Anim Reprod. 2020;17(3):e20200015.
42. Miles JR, Blomberg LA, Krisher RL, Everts RE, Sonstegard TS, Van Tassell CP, Zuelke KA. Comparative transcriptome analysis of *in vivo*- and *in vitro*-produced porcine blastocysts by small amplified RNA-serial analysis of gene expression (SAR-SAGE). Mol Reprod Dev. 2008;75(6):976–88.
43. Hugentobler SA, Humpherson PG, Leese HJ, Sreenan JM, Morris DG. Energy substrates in bovine oviduct and uterine fluid and blood plasma during the oestrous cycle. Mol Reprod Dev. 2008;75(3):496–503.
44. Li S, Winuthayanon W. Oviduct: roles in fertilization and early embryo development. J Endocrinol. 2017;232(1):R1–26.
45. Azizi-Moghadam A. Metabolism of energy substrates of *in vitro* and *in vivo* derived embryos from ewes synchronized and super ovulated with norgestomet and porcine follicle stimulating hormone. J Anim Sci Biotechnol. 2012;3(1):37.
46. Leese HJ, Brison DR, Sturmey RG. The Quiet Embryo Hypothesis: 20 years on. Front Physiol. 2022;13:899485.
47. Lopera-Vasquez R, Hamdi M, Maillo V, Lloreda V, Coy P, Gutierrez-Adan A, Bermejo-Alvarez P, Rizos D. Effect of bovine oviductal fluid on development and quality of bovine embryos produced *in vitro*. Reprod Fertil Dev. 2017;29(3):621–9.
48. Lopera-Vasquez R, Hamdi M, Maillo V, Gutierrez-Adan A, Bermejo-Alvarez P, Ramirez MA, Yanez-Mo M, Rizos D. Effect of bovine oviductal extracellular vesicles on embryo development and quality *in vitro*. Reproduction. 2017;153(4):461–70.
49. Alminana C, Corbin E, Tsikis G, Alcantara-Neto AS, Labas V, Reynaud K, Galio L, Uzbekov R, Garanina AS, Druart X, et al. Oviduct extracellular vesicles protein content and their role during oviduct-embryo cross-talk. Reproduction. 2017;154(3):153–68.
50. Goncalves RF, Staros AL, Killian GJ. Oviductal fluid proteins associated with the bovine zona pellucida and the effect on *in vitro* sperm-egg binding, fertilization and embryo development. Reprod Domest Anim. 2008;43(6):720–9.
51. Choudhary S, Kumaresan A, Kumar M, Chhillar S, Malik H, Kumar S, Kaushik JK, Datta TK, Mohanty AK. Effect of recombinant and native buffalo OVGP1 on sperm functions and *in vitro* embryo development: a comparative study. J Anim Sci Biotechnol. 2017;8:69.
52. Pradeep MA, Jagadeesh J, De AK, Kaushik JK, Malakar D, Kumar S, Dang AK, Das SK, Mohanty AK. Purification, sequence characterization and effect of goat oviduct-specific glycoprotein on *in vitro* embryo development. Theriogenology. 2011;75(6):1005–15.
53. Yong P, Gu Z, Luo JP, Wang JR, Tso JK. Antibodies against the C-terminal peptide of rabbit oviductin inhibit mouse early embryo development to pass 2-cell stage. Cell Res. 2002;12(1):69–78.
54. Boice ML, Mavrogianis PA, Murphy CN, Prather RS, Day BN. Immunocytochemical analysis of the association of bovine oviduct-specific glycoproteins with early embryos. J Exp Zool. 1992;263(2):225–9.
55. Boice ML, McCarthy TJ, Mavrogianis PA, Fazlebas AT, Verhage HG. Localization of oviductal glycoproteins within the zona pellucida and perivitelline space of ovulated ova and early embryos in baboons (Papio anubis). Biol Reprod. 1990;43(2):340–6.
56. Kan FW, Roux E, Bleau G. Immunolocalization of oviductin in endocytic compartments in the blastomeres of developing embryos in the golden hamster. Biol Reprod. 1993;48(1):77–88.
57. Buhi WC, O'Brien B, Alvarez IM, Erdos G, Dubois D. Immunogold localization of porcine oviductal secretory proteins within the zona pellucida, perivitelline space, and plasma membrane of oviductal and uterine oocytes and early embryos. Biol Reprod. 1993;48(6):1274–83.
58. van der Weijden VA, Chen S, Bauersachs S, Ulbrich SE, Schoen J. Gene expression of bovine embryos developing at the air-liquid interface on oviductal epithelial cells (ALI-BOEC). Reprod Biol Endocrinol. 2017;15(1):91.
59. Mahe C, Lavigne R, Com E, Pineau C, Locatelli Y, Zlotkowska AM, Alminana C, Tsikis G, Mermillod P, Schoen J, et al. Spatiotemporal profiling of the bovine oviduct fluid proteome around the time of ovulation. Sci Rep. 2022;12(1):4135.
60. Tse PK, Lee YL, Chow WN, Luk JM, Lee KF, Yeung WS. Preimplantation embryos cooperate with oviductal cells to produce embryotrophic inactivated complement-3b. Endocrinology. 2008;149(3):1268–76.
61. Usami M, Mitsunaga K, Miyajima A, Sunouchi M, Doi O. Complement component C3 functions as an embryotrophic factor in early postimplantation rat embryos. Int J Dev Biol. 2010;54(8–9):1277–85.
62. Lamond DR, Gaddy RG. Plasma progesterone in cows with multiple ovulations. J Reprod Fertil. 1972;29(2):307–11.
63. Wright JM. Photographic illustrations of embryo developmental stage and quality codes. In: Stringfellow DA, Seidel SM, editor. Manual of the International Embryo Transfer Society. 3rd edn. Savoy: The Society; 1998. p. 167–70.
64. Holm P, Booth PJ, Schmidt MH, Greve T, Callesen H. High bovine blastocyst development in a static *in vitro* production system using SOFaa medium supplemented with sodium citrate and myo-inositol with or without serum-proteins. Theriogenology. 1999;52(4):683–700.
65. Keller A, Nesvizhskii AI, Kolker E, Aebersold R. Empirical statistical model to estimate the accuracy of peptide identifications made by MS/MS and database search. Anal Chem. 2002;74(20):5383–92.
66. Nesvizhskii AI, Keller A, Kolker E, Aebersold R. A statistical model for identifying proteins by tandem mass spectrometry. Anal Chem. 2003;75(17):4646–58.
67. Liu H, Sadygov RG, Yates JR 3rd. A model for random sampling and estimation of relative protein abundance in shotgun proteomics. Anal Chem. 2004;76(14):4193–201.
68. Old WM, Meyer-Arendt K, Aveline-Wolf L, Pierce KG, Mendoza A, Sevinsky JR, Resing KA, Ahn NG. Comparison of label-free methods for quantifying human proteins by shotgun proteomics. Mol Cell Proteomics. 2005;4(10):1487–502.
69. Bardou P, Mariette J, Escudie F, Djemiel C, Klopp C. jvenn: an interactive Venn diagram viewer. BMC Bioinformatics. 2014;15:293.
70. Zhou Y, Zhou B, Pache L, Chang M, Khodabakhshi AH, Tanaseichuk O, Benner C, Chanda SK. Metascape provides a biologist-oriented resource for the analysis of systems-level datasets. Nat Commun. 2019;10(1):1523.
71. Perez-Riverol Y, Bai J, Bandla C, Garcia-Seisdedos D, Hewapathirana S, Kamatchinathan S, Kundu DJ, Prakash A, Frericks-Zipper A, Eisenacher M, et al. The PRIDE database resources in 2022: a hub for mass spectrometry-based proteomics evidences. Nucleic Acids Res. 2022;50(D1):D543–52.

Publisher's Note

Springer Nature remains neutral with regard to jurisdictional claims in published maps and institutional affiliations.

Coline MAHÉ

Migration spermatique dans les voies génitales femelles : interactions fonctionnelles chez le bovin

Résumé en français :

La migration des spermatozoïdes dans les voies génitales femelles conditionne la réussite de la fécondation dans l'oviducte. Au cours de cette migration, les spermatozoïdes interagissent avec les fluides issus des cellules épithéliales luminales et se lient à ces cellules, notamment dans la première partie de l'oviducte, pour former un « réservoir spermatique ». Les objectifs de cette thèse étaient de (1) caractériser la composition protéique des fluides femelles traversés par les spermatozoïdes bovins ; (2) identifier dans l'oviducte les protéines interagissant avec les spermatozoïdes ; (3) comprendre les effets de ces interactions sur la physiologie et la liaison des spermatozoïdes aux cellules épithéliales de l'oviducte. Les résultats montrent que les protéomes luminaux de l'utérus et de l'oviducte bovins sont modulés en fonction de la région anatomique, du stade péri-ovulatoire et de la proximité de l'ovaire ovulant. Par une analyse protéomique des spermatozoïdes, 245 protéines du fluide d'oviducte interagissant avec les spermatozoïdes de manière différentielle en fonction de la région anatomique et du stade ont pu être identifiées. A l'aide d'un nouveau modèle d'organoïdes d'oviducte reproduisant les propriétés biologiques du réservoir spermatique, un effet inhibiteur du fluide tubaire sur la liaison des spermatozoïdes aux cellules épithéliales, sans altération de leur mobilité ni de l'intégrité de leur membrane, a été mis en évidence. Les N-glycanes liées aux glycoprotéines solubles et l'héparane sulfate semblent en partie responsables de cet effet du fluide sur la liaison spermatique. Ces résultats ouvrent le pas vers l'amélioration des milieux utilisés pour conserver, sélectionner et utiliser les spermatozoïdes en insémination animale, pour la fécondation *in vitro* et la conservation de la biodiversité animale.

Mots clés : Spermatozoïde, interaction, protéomique, utérus, oviducte, réservoir spermatique

Summary :

Sperm migration in the female genital tract is critical for successful fertilization in the oviduct. During this migration, spermatozoa interact with fluids from luminal epithelial cells and bind to these cells, especially in the first part of the oviduct, to form a "sperm reservoir". The objectives of this thesis were to (1) characterize the protein composition of female fluids crossed by bull sperm; (2) identify proteins in the oviduct fluid that interact with sperm; and (3) understand the effects of these interactions on the physiology and binding of sperm to epithelial cells of the oviduct. Results show that the luminal proteomes of the bovine uterus and oviduct are modulated by anatomical region, peri-ovulatory stage, and proximity of the the ovulating ovary. By proteomic analysis of spermatozoa, 245 oviduct fluid proteins interacting with spermatozoa in a differential manner depending on anatomical region and stage could be identified. Using a new oviduct organoid model reproducing the biological properties of the sperm reservoir, an inhibitory effect of the tubal fluid on sperm binding to epithelial cells, without altering their motility or membrane integrity, was demonstrated. The N-glycans bound to soluble glycoproteins and heparan sulfate appear to be partly responsible for this effect of fluid on sperm binding. These results open the way to the improvement of media used to preserve, select and use spermatozoa in animal insemination, in vitro fertilization and conservation of animal biodiversity.

Keywords : spermatozoa, interaction, proteomic, uterus, oviduct, sperm reservoir